

**A multi-model approach for
examining cross-reactive antibody-
mediated alphavirus immunity
following infection and vaccination**

Whitney C. Weber

A DISSERTATION

Thesis submitted to the Department of Molecular Microbiology and Immunology
Oregon Health and Science University
School of Medicine

In Partial Fulfillment of the Requirements for the Degree of Doctor of Philosophy

October 11th, 2024

Dissertation Advisory Committee

Advisor: Daniel N. Streblow, Professor, Ph.D.

Chair: Mark K. Slifka, Professor, Ph.D.

Member: Nancy L. Haigwood, Professor, Ph.D.

Member: William B. Messer, Professor, M.D., Ph.D.

External Reviewer: Lark L. Coffey, Professor, Ph.D.

I. Table of Contents

I. TABLE OF CONTENTS	III
II. COMMON ABBREVIATIONS	X
III. ACKNOWLEDGEMENTS	XI
IV. ABSTRACT	XVI
CHAPTER 1: INTRODUCTION	1
SECTION 1.1. PREFACE	1
SECTION 1.2. INTRODUCTION TO ALPHAVIRUS CLASSIFICATION, DISTRIBUTION, AND TRANSMISSION.....	1
Figure 1.2.1. The distribution of alphaviruses of clinical importance.	2
Figure 1.2.2. Alphavirus phylogeny.....	3
Figure 1.2.3. Alphavirus antigenic complexes.	4
SECTION 1.3. HUMAN DISEASE AND DIAGNOSIS	4
1.3.1 <i>Arthritogenic alphavirus infection</i>	4
1.3.2 <i>Encephalitic alphavirus infection</i>	5
SECTION 1.4. HOST IMMUNE RESPONSE TO INFECTION.....	6
1.4.1 <i>Innate immunity</i>	6
1.4.2 <i>Cellular immunity</i>	6
1.4.3 <i>Humoral immunity</i>	8
1.4.4 <i>Cross-reactive immunity</i>	10
Figure 1.4.1. The E2B domain is highly conserved amongst the alphaviruses.....	12
1.4.5 <i>Correlates of protection</i>	12
1.4.6 <i>Antibody-dependent enhancement of infection</i>	13
SECTION 1.5. ALPHAVIRUS GENOME AND REPLICATION.....	15
1.5.1 <i>Genome organization and replication</i>	15
1.5.2 <i>Alphavirus infectious clones</i>	16
SECTION 1.6. VIRUS-SPECIFIC EPIDEMIOLOGY, DISTRIBUTION, AND TRANSMISSION.....	16
1.6.1a <i>Chikungunya virus (CHIKV) epidemiology</i>	16
1.6.1b <i>CHIKV transmission – vectors, hosts, and cycle</i>	18
1.6.2a <i>O'nyong-nyong virus (ONNV) epidemiology</i>	19
1.6.2b <i>ONNV transmission – vectors, hosts, and cycle</i>	20
1.6.3a <i>Mayaro virus (MAYV) epidemiology</i>	20
1.6.3b <i>MAYV transmission – vectors, hosts, and cycle</i>	21
1.6.4a <i>Ross River virus (RRV)</i>	22
1.6.4b <i>RRV transmission – vectors, hosts, and cycle</i>	22
1.6.5a <i>Encephalitic alphaviruses epidemiology</i>	22
1.6.5b <i>Encephalitic alphaviruses transmission – vectors, hosts, and cycle</i>	23
SECTION 1.7. ANIMAL MODELS OF INFECTION	23
1.7.1 <i>Early non-human primate (NHP) disease models for arthritogenic alphaviruses</i>	23
1.7.2 <i>Development of CHIKV NHP models of infection</i>	23
1.7.3 <i>Utilization of the CHIKV NHP model to evaluate vaccine efficacy and immunogenicity</i>	25
1.7.4 <i>Utilization of the CHIKV NHP model to evaluate mAbs and antivirals</i>	26
1.7.5 <i>MAYV NHP models of infection</i>	27
1.7.6 <i>Mouse models of arthritogenic alphavirus disease</i>	28
1.7.7 <i>NHP disease models for encephalitic alphaviruses</i>	29
SECTION 1.8: ALPHAVIRUS VACCINE APPROACHES.....	30
1.8.1 <i>Vaccines for chikungunya virus</i>	30
Figure 1.8.1. Landscape of CHIKV vaccines in the clinical development pipeline.	31
1.8.1a <i>The first licensed CHIKV vaccine: IXCHIQ</i>	31
1.8.1b <i>Phase III vaccine candidates: PXVX0317 and BBV87</i>	32
1.8.1c <i>Phase II vaccine candidates</i>	33
1.8.1d <i>Phase I vaccine candidates</i>	34
1.8.2 <i>Vaccines for Mayaro virus</i>	35

1.8.3	<i>Vaccines for Ross River virus</i>	35
1.8.4	<i>Vaccines for other alphaviruses</i>	36
1.8.5	<i>Vaccines for the encephalitic alphaviruses</i>	36
1.8.6	<i>Cross-protective vaccines, multivalent vaccines, and pan-alphavirus vaccine potential</i>	36
1.8.7	<i>Vaccine-elicited versus infection-elicited immunity</i>	38

CHAPTER 2: INFECTION WITH CHIKUNGUNYA VIRUS CONFERS HETEROTYPIC CROSS-NEUTRALIZING ANTIBODIES AND MEMORY B CELLS AGAINST OTHER ARTHRITOGENIC ALPHAVIRUSES PREDOMINANTLY THROUGH THE B DOMAIN OF THE E2 GLYCOPROTEIN 40

SECTION 2.1.1:	ABSTRACT	41
SECTION 2.1.2:	AUTHOR SUMMARY	42
SECTION 2.2:	INTRODUCTION	42
SECTION 2.3:	RESULTS	45
2.3.1	<i>Study subjects</i>	45
	Table 2.1. Summary of subject data.....	46
2.3.2	<i>Alphavirus specific neutralization and antigenic relationship by subject</i>	46
	Figure 2.1. Longitudinal serology for endemic and non-endemic patients.....	48
	Table 2.S1. Compiled PRNT ₅₀ values for each subject against the six alphaviruses serologically profiled in this study.....	49
	Figure 2.2. Antigenic cartography to map human subject alphavirus cross-neutralization by human sera.....	51
2.3.3	<i>Dissecting the role of E2 B domain in homotypic and heterotypic neutralization</i>	52
	Figure 2.3. Comparison of Alphavirus E2 B domains.	53
	Figure 2.S1. MAYV and CHIKV E2 B domain protein detection.	53
	Figure 2.4. Impact of depletion of E2B-binding antibodies on CHIKV and MAYV neutralization.	54
	Figure 2.5. Analysis of changes in CHIKV and MAYV neutralizing antibody titers following E2 B domain depletion.	55
	Table 2.S2. PRNT ₅₀ values and fold change of MAYV E2 B domain depleted serum samples relative to controls.	56
	Table 2.S3. PRNT ₅₀ values and fold change of CHIKV E2 B domain depleted serum samples relative to controls.	57
2.3.4	<i>Homotypic and cross-reactive alphavirus-specific MBC frequency in immune subjects 1 to 24 years post-infection</i>	58
	Figure 2.6. Antigen-specific MBC frequency per 10 ⁶ PBMC over time in non-endemic cohort (blue n = 6), endemic (orange n = 5), and naïve subjects (black n = 3).	59
	Table 2.2. Antigen-specific MBC frequency for non-endemic and endemic cohorts.....	59
	Figure 2.S2. Relationship between CHIKV or MAYV MBC frequency and PRNT ₅₀	60
	Figure 2.S3. Relationship between antigen-specific MBC frequencies.	60
SECTION 2.4:	DISCUSSION	60
SECTION 2.5:	MATERIALS & METHODS	62
2.5.1	<i>Human research ethics</i>	62
2.5.2	<i>Non-endemic human cohort population (n = 7)</i>	62
2.5.3	<i>Endemic Human-cohort population (n = 5)</i>	63
2.5.4	<i>Sample collection and storage</i>	63
2.5.5	<i>Viruses</i>	63
2.5.6	<i>Neutralization assays—fifty percent plaque reduction neutralization test (PRNT₅₀)</i>	64
2.5.7	<i>E2 B domain cloning and synthesis</i>	64
2.5.8	<i>E2 B domain expression and binding to Ni-NTA magnetic beads</i>	65
2.5.9	<i>Human serum antibody absorption to Ni-NTA magnetic bead absorbed human serum</i>	66
2.5.10	<i>Neutralization assays with Ni-NTA magnetic bead absorbed human serum</i>	66
2.5.11	<i>Protein modeling of MAYV structural glycoproteins and alphavirus E2 B domain alignment</i>	66
2.5.12	<i>Memory B cell frequency</i>	67
2.5.13	<i>Antigen-specific ELISAs</i>	67
2.5.14	<i>Antigenic cartography</i>	68
2.5.15	<i>Statistical analysis</i>	68
SECTION 2.6:	ACKNOWLEDGEMENTS	69

CHAPTER 3: THE APPROVED LIVE-ATTENUATED CHIKUNGUNYA VIRUS VACCINE (IXCHIQ®) ELICITS CROSS-NEUTRALIZING ANTIBODY BREADTH EXTENDING TO MULTIPLE ARTHRITOGENIC ALPHAVIRUSES SIMILAR TO THE ANTIBODY BREADTH FOLLOWING NATURAL INFECTION 70

SECTION 3.1: ABSTRACT	71
SECTION 3.2: INTRODUCTION	71
SECTION 3.3: RESULTS	73
3.3.1 <i>IXCHIQ</i> elicits broad alphavirus immunity against CHIKV strains as well as related ONNV, MAYV, and RRV.	73
Table 3.1. Participant demographics for IXCHIQ adult vaccinees and CHIKV-immune individuals. ..	74
Table 3.S1. Viral stock sequencing analysis summary for the alphaviruses used in this study.....	75
Figure 3.1. IXCHIQ immunization of human participants elicits antibodies that neutralize multiple CHIKV strains and cross-neutralize related arthritogenic alphaviruses.	77
Table 3.2. Summary of alphavirus neutralizing antibody responses in all participants.....	78
Table 3.S2. Compiled raw neutralization titers for vaccinee participants.	79
3.3.2 <i>The potency of alphavirus neutralizing antibodies for IXCHIQ vaccinees decreases with decreasing genetic similarity of viral antigens.</i>	81
Figure 3.2. Cross-neutralizing antibodies decrease in potency with increasing phylogenetic and Dayhoff distance from the CHIKV _{LR2006} parental vaccine strain.....	82
Table 3.S3. Amino acid sequences (E1/6K/E2/E3) used for phylogenetic and Dayhoff distance analyses to compare the genetic relatedness of the alphaviruses under investigation in this study.	84
3.3.3 <i>IXCHIQ</i> vaccinees develop alphavirus cross-neutralizing antibody potency and breadth similar to individuals who were naturally infected with CHIKV.	86
Figure 3.3. Neutralizing antibody breadth of human serum collected in Puerto Rico 8-9 years following 2014 CHIKV infections.	87
Table 3.S4. Compiled raw neutralization titers from CHIKV infection participants.	88
Figure 3.4. The neutralizing antibody breadth elicited by vaccination is comparable to CHIKV infection-induced cross-reactivity.	89
Figure 3. S1. Correlating age and antibody titer after vaccination or infection.....	91
Figure 3.5. Vaccinee sera cluster antigenically with infection sera.	93
SECTION 3.4: DISCUSSION	93
SECTION 3.5: MATERIALS & METHODS	96
3.5.1 <i>Ethics Statement</i>	96
3.5.2 <i>Study participants</i>	96
3.5.3 <i>Cells and viruses</i>	97
3.5.4 <i>Construction of the CHIKV Brazil infectious clone</i>	98
3.5.5 <i>Next generation sequencing of viral stocks</i>	99
3.5.6 <i>Neutralization assays (50% plaque reduction neutralization test, PRNT₅₀)</i>	99
3.5.7 <i>Antigenic cartography</i>	100
3.5.8 <i>Statistical analysis</i>	101
SECTION 3.6: ACKNOWLEDGEMENTS	101

CHAPTER 4: NON-RECIPROCITY IN CHIKV AND MAYV VACCINE-ELICITED PROTECTION..... 102

SECTION 4.1: ABSTRACT	103
SECTION 4.2: INTRODUCTION	103
SECTION 4.3: RESULTS	106
4.3.1 <i>Adenovirus-vectored alphavirus vaccines elicit virus-specific neutralizing antibodies and T cells in mice</i>	106
Figure 4.S1. Preliminary immunogenicity analysis.	107
Figure 4.1. Immunogenicity of adenovirus-vectored alphavirus vaccines in C57BL/6 mice.....	109
Table 4.1. Summary of alphavirus neutralizing antibody titer responses (n=8) and <i>in vitro</i> antibody-dependent enhancement activity in RAW264.7 at 58 days post-prime.	110
4.3.2 <i>All vaccine regimens cross-protect against MAYV and CHIKV-induced disease.</i>	111
Figure 4.2. All CHIKV and MAYV vaccination strategies cross-protect against disease but protection is not sterilizing.	113
Figure 4.S2. Vaccine cross-protection at 5 dpi.	115
4.3.3 <i>Passive antibody transfer demonstrates that robust cross-neutralizing antibody responses are not sufficient to provide sterilizing cross-protection against infection or disease.</i>	116

Figure 4.3. Passive transfer of vaccine immune sera demonstrates that antibodies are not sufficient for sterilizing cross-protection against viral replication in tissues.....	118
Figure 4.4. Differential disease outcomes elicited by passive antibody transfer.	120
4.3.4 <i>Serum from immunized mice exhibits antibody-dependent enhancement activity of MAYV and UNAV replication in vitro.</i>	121
Figure 4.5. Vaccine sera enhance MAYV but not CHIKV replication in mouse macrophages.	122
Figure 4.S3. Raw titer data for MAYV and CHIKV ADE assays.	123
Figure 4.6. Vaccine sera enhance UNAV replication in mouse macrophages.	125
Figure 4.S4. Raw titer data for UNAV and RRV ADE assays.	126
SECTION 4.4: DISCUSSION.....	126
SECTION 4.5: MATERIALS & METHODS.....	129
4.5.1 <i>Ethics statement</i>	129
4.5.2 <i>Cells, viruses, and viral vaccine vectors</i>	129
4.5.3 <i>Mouse experiments</i>	130
4.5.4 <i>Neutralization assays</i>	131
4.5.5 <i>Viral RNA detection</i>	131
4.5.6 <i>Quantification of infectious virus</i>	132
4.5.7 <i>ELISPOT</i>	132
4.5.8 <i>Western blot analysis</i>	132
4.5.9 <i>Antibody-dependent enhancement assays</i>	133
4.5.10 <i>Statistical analysis</i>	133
SECTION 4.6: ACKNOWLEDGEMENTS.....	133
CHAPTER 5: DEVELOPMENT OF A VIRULENT O'NYONG'NYONG CHALLENGE MODEL TO EVALUATE HETEROLOGOUS PROTECTION MEDIATED BY A HYDROGEN PEROXIDE-INACTIVATED CHIKUNGUNYA VIRUS VACCINE.....	135
SECTION 5.1: ABSTRACT.....	136
SECTION 5.2: INTRODUCTION.....	136
SECTION 5.3: RESULTS.....	138
5.3.1 <i>Genetics and replication comparison of ONNV strains</i>	138
Figure 5.1. ONNV strain genetic comparison and growth characteristics in four cell lines.....	140
5.3.2 <i>ONNV₀₈₀₄ is more pathogenic than ONNV_{UgMP30} in immunocompetent mice</i>	141
Figure 5.2. ONNV pathogenesis, disease, and viral persistence in immunocompetent mice.	142
Figure 5.S1. ONNV pathogenesis in C57BL/6 mice between 1 and 5 days after viral challenge.....	143
5.3.3 <i>ONNV₀₈₀₄ infection leads to persistence of viral RNA in muscle and joint tissues and potent neutralizing antibody levels and breadth</i>	144
Figure 5.3. ONNV RNA persistence at 43 dpi and the development of neutralizing antibodies in immunocompetent mice.	145
5.3.4 <i>ONNV₀₈₀₄ is more pathogenic than ONNV_{UgMP30} in immunodeficient AG129 mice</i>	145
Figure 5.4. ONNV ₀₈₀₄ is more virulent than ONNV _{UgMP30} in AG129 immunodeficient mice.	147
5.3.5 <i>HydroVax-CHIKV immunization elicits antibodies that cross-neutralize ONNV₀₈₀₄ and cross-protect against lethal arthritogenic disease in AG129 mice</i>	148
Figure 5.5. HydroVax-CHIKV immunization elicits antibodies that cross-neutralize ONNV ₀₈₀₄ and cross-protect against lethal arthritogenic disease in AG129 mice.	150
Figure 5.6. HydroVax-CHIKV vaccination partially cross-protects against 170,000 HE ₅₀ of ONNV ₀₈₀₄ in AG129 mice.	153
Figure 5.S2. Viral loads in surviving animals at 14 dpi.	154
SECTION 5.4: DISCUSSION.....	154
SECTION 5.5: MATERIALS & METHODS.....	157
5.5.1 <i>Ethics Statement</i>	157
5.5.2 <i>Cells</i>	157
5.5.3 <i>Viruses and the HydroVax-CHIKV Vaccine</i>	158
5.5.4 <i>Cloning Strategy</i>	159
5.5.5 <i>Growth Curves</i>	159
5.5.6 <i>Mouse Experiments</i>	160
5.5.7 <i>Histopathological Analysis</i>	160
5.5.8 <i>Viral RNA Detection</i>	161
5.5.9 <i>Quantification and Isolation of Infectious Virus</i>	161

5.5.10 Neutralization Assays	161
5.5.11 Statistical Analysis	162
SECTION 5.6: ACKNOWLEDGEMENTS	162
CHAPTER 6: MAYARO VIRUS PATHOGENESIS AND IMMUNITY IN RHESUS MACAQUES	163
SECTION 6.1.1: ABSTRACT	164
SECTION 6.1.2: AUTHOR SUMMARY	164
SECTION 6.2: INTRODUCTION	165
SECTION 6.3: RESULTS	168
6.3.1 <i>Infection of mice with the MAYV BeAr505411 strain results in robust replication and viral dissemination</i>	168
Figure 6.1. Evaluation of MAYV strain pathogenesis in C57BL/6 mice.	169
Figure 6.S1. MAYV strains in IFN α R $^{-/-}$ mice	170
6.3.2 <i>Kinetics of MAYV replication in rhesus macaques reveals peak viremia at 2 dpi</i>	171
Figure 6.2. Study overview of MAYV infection of NHPs.....	172
Table 6.1. Isolation of infectious MAYV from RM plasma and tissue.	173
Figure 6.S2. Complete blood count (CBC) data for macaques over the duration of the study.....	174
Figure 6.S3. Serum chemistry panel analytes for macaques during the study.....	175
Figure 6.3. Dermatologic pathology in MAYV-infected rhesus macaques.	176
Table 6.2. Perivascular lymphocytic inflammation in the musculoskeletal, nervous, cardiovascular, and integumentary tissues of MAYV-infected rhesus macaques at 10 dpi.	177
Figure 6.4. Detection of MAYV RNA in NHP tissues at 10 dpi.	178
6.3.3 <i>MAYV infects joint, muscle, lymphoid, cardiac, and nervous system tissues of rhesus macaques.</i> ..	178
6.3.4 <i>Immunopathologic changes associated with MAYV infection in rhesus macaques highlight variable tissue inflammation in joints, muscles, heart, and central nervous tissues</i>	180
Figure 6.5. Lymphocytic inflammation in the musculoskeletal, cardiac, and nervous system of MAYV-infected rhesus macaques.	181
Figure 6.S4. Lymphoid pathology of MAYV-infected rhesus macaques.....	182
Table 6.S1. Presence or absence of perivascular lymphocytic inflammation in endocrine, respiratory, alimentary, hepatobiliary and pancreatic, and genitourinary tissues in MAYV-infected rhesus macaques at 10 dpi.	182
Figure 6.S5. Lymphocytic inflammation in the nervous system of a MAYV-infected rhesus macaque.	184
Table 6.S2. Hematopoietic pathology in MAYV-infected rhesus macaques at 10 dpi.	184
6.3.5 <i>Cytokine and cellular innate immune signatures peak with MAYV viremia in rhesus macaques.</i> ..	185
Figure 6.6. Cytokine and chemokine profile following MAYV infection.....	187
Figure 6.S6. Cytokine and chemokine profile following MAYV infection.....	188
Figure 6.7. Longitudinal peripheral blood and lymphoid tissue cell phenotype activation of monocytes, dendritic cells, and NK cells following MAYV infection.	189
Figure 6.S7. Flow cytometry gating strategy for monocyte/DC/NK panel.	190
6.3.6 <i>Proliferating T and B cell subsets dominate the early adaptive immune response to MAYV infection in rhesus macaques</i>	190
Figure 6.8. Kinetics of T cell proliferation and granzyme B expression in peripheral blood and phenotype comparisons in lymphoid tissues pre- and post-MAYV infection.	192
Figure 6.S8. Flow cytometry gating strategy for T and B cell panels.....	193
Figure 6.S9. B cell phenotype and proliferation in longitudinal peripheral blood and lymphoid tissues following MAYV infection.	194
Figure 6.9. Transcriptional analysis of changes following MAYV infection and pathway analysis between 0 and 2 dpi.....	195
Figure 6.S10. Transcriptional analysis of changes following MAYV infection and pathway analysis between 0 and 3 dpi.....	197
6.3.7 <i>Virus-specific antibodies are present as early as 5 dpi and expand in neutralization breadth by 10 dpi</i>	198
Figure 6.10. Characterization of MAYV-specific antibodies and analysis of cross-reactive breadth. .	199
SECTION 6.4: DISCUSSION	200
SECTION 6.5: MATERIALS & METHODS	205
6.5.1 <i>Ethics statement</i>	205
6.5.2 <i>Cells and viruses</i>	205
6.5.3 <i>Mouse experiments</i>	206

6.5.4 Nonhuman primate experiments	206
6.5.5 Histopathological analysis	207
6.5.6 Viral RNA detection	207
6.5.7 Quantification and isolation of infectious virus	208
6.5.8 Transcriptomic analysis.....	209
6.5.9 Neutralization assays.....	210
6.5.10 Antigenic cartography	210
6.5.11 Enzyme-linked immunoassays (ELISA)	211
6.5.12 Limiting dilution assay for quantification of MAYV antibody-secreting cell frequency	211
6.5.13 Plasma cytokine and chemokine analysis	212
6.5.14 Lymphocyte phenotypic analysis	212
6.5.15 Western blot analysis.....	213
6.5.16 Statistical analysis	213
SECTION 6.6: ACKNOWLEDGEMENTS	214
APPENDIX I: THE ALPHAVIRUS NEUTRALIZING ANTIBODY BREADTH IS SHAPED BY PRIMARY ANTIGEN EXPOSURE	215
SECTION A1.1: ABSTRACT	215
Figure A1.1. Alphavirus infection in mice shapes the cross-neutralizing antibody breadth.	216
Figure A1.2. Evidence of infection-elicited neutralizing antibodies against VEEV and MAYV and cross-neutralizing antibodies against related alphaviruses in an individual residing in Iquitos, Peru. .	216
SECTION A1.2: ACKNOWLEDGEMENTS	217
APPENDIX II: DEVELOPMENT OF MOUSE MODELS OF LETHAL ARTHRITOGENIC ALPHAVIRUS INFECTION FOR EVALUATION OF VACCINE-ELICITED PROTECTION	218
SECTION A2.1: ABSTRACT	218
Figure A2.1. AG129 model of lethal RRV infection.	219
Figure A2.2. AG129 model of lethal UNAV infection.....	220
SECTION A2.2: ACKNOWLEDGEMENTS	220
APPENDIX III: CHIKUNGUNYA VIRUS VACCINES: A REVIEW OF IXCHIQ AND PXVX0317 FROM PRE-CLINICAL EVALUATION TO LICENSURE	221
SECTION A3.1: ABSTRACT	221
SECTION A3.2.1: CHIKUNGUNYA VIRUS	222
SECTION A3.2.2: CHIKUNGUNYA DISEASE AND MANAGEMENT	222
SECTION A3.2.3: UNMET NEED FOR CHIKV VACCINE.....	223
SECTION A3.2.4: CHIKV VACCINES IN DEVELOPMENT	224
SECTION A3.2.5: CHIKV-SPECIFIC NEUTRALIZING ANTIBODY AS A TARGET FOR CHIKV VACCINE DEVELOPMENT	224
SECTION A3.2.6: IXCHIQ	224
Figure A3.2.6 Design of the IXCHIQ live attenuated vaccine (LAV).	225
SECTION A3.2.7: PXVX0317	232
Figure A3.2.7 Design of the PXVX0317 virus-like particle (VLP) vaccine.	232
SECTION A3.2.8: COMPARING IXCHIQ AND PXVX0317	239
SECTION A3.2.9: OUTSTANDING UNKNOWNNS.....	241
SECTION A3.2.10: CONCLUSIONS	245
SECTION A3.3: ACKNOWLEDGEMENTS	245
CHAPTER 7: SUMMARY AND FINAL PERSPECTIVES	246
SECTION 7.1: HIGHLIGHTS AND FUTURE DIRECTIONS	246
7.1.1 Chapter 1 highlights: Alphaviruses	246
7.1.2 Chapter 2 highlights: Infection with chikungunya virus confers heterotypic cross-neutralizing antibodies and memory B cells against other arthritogenic alphaviruses predominantly through the B domain of the E2 glycoprotein.....	246

7.1.3	<i>Chapter 3 highlights: The approved live-attenuated chikungunya virus vaccine (IXCHIQ®) elicits cross-neutralizing antibody breadth extending to multiple arthritogenic alphaviruses similar to the antibody breadth following natural infection</i>	247
7.1.4	<i>Chapter 4 highlights: Nonreciprocity in CHIKV and MAYV vaccine-elicited protection</i>	248
7.1.5	<i>Chapter 5 highlights: Heterologous protection of contemporary O'nyong-nyong virus strain UVR10804 by a hydrogen peroxide inactivated chikungunya virus vaccine</i>	249
7.1.6	<i>Chapter 6 highlights: Mayaro virus pathogenesis and immunity in rhesus macaques</i>	250
7.1.7	<i>Appendix I highlights: The alphavirus neutralizing antibody breadth is shaped by the primary antigen exposure</i>	251
7.1.8	<i>Appendix II highlights: Development of mouse models of lethal arthritogenic alphavirus infection for evaluation of vaccine-elicited protection</i>	251
SECTION 7.2:	CROSS-REACTIVE ALPHAVIRUS IMMUNITY	252
SECTION 7.3:	STRATEGIES FOR DEVELOPING CROSS-PROTECTIVE ALPHAVIRUS VACCINES	253
SECTION 7.4:	DEVELOPING NEW INFECTION AND DISEASE ANIMAL MODELS	254
SECTION 7.5:	FINAL THOUGHTS	255
REFERENCES		256

II. Common Abbreviations

Abv	Abbreviation		Abv	Abbreviation
CHIKV	chikungunya virus			
MAYV	Mayaro virus			
RRV	Ross river virus			
UNAV	Una virus			
SFV	Semliki Forest virus			
ONNV	O'nyong-nyong virus			
VEEV	Venezuelan equine encephalitis virus			
WEEV	Western equine encephalitis virus			
EEEV	Eastern equine encephalitis virus			
GETV	Getah virus			
NHP	Non-human primate			
nAb	Neutralizing antibodies			
ADE	Antibody-dependent enhancement			
PBMC	Peripheral blood mononucleated cells			
PFU	Plaque forming units			
dpi	days post-infection			
mAb	Monoclonal antibody			
LAV	Live-attenuated vaccine			
VLP	Virus-like particle			
i.m.	intramuscular			
PRNT₅₀	50% plaque reduction neutralization test			
IC₅₀	Half maximal inhibitory concentration			
i.v.	intravenous			

III. Acknowledgements

Graduate school has tested me in ways I could not have ever imagined as well as every relationship in my life. I have to thank everyone who was patient with me and believed in me during this journey, especially when it was hard to understand why this is the path I have chosen. Thank you to my friends and family who took care of me outside of the lab. Thank you to my mentor, lab mates, and dissertation advisory committee mentors who were committed to my success in the lab and in my career.

To my mentor Dr. Daniel Streblow, thank you for all of the freedom you have given me during my PhD. When I joined your lab, you said I could work on whatever I wanted; this held true until the very end of my PhD. You let me work on mostly unfunded studies and pursue projects that interested me. You never made demands of me in the projects or experiments that I had to do—you gave me guidance but let me do things my own way. When I made mistakes, you were calm, forgiving, and patient with me. Thank you for your flexibility in me taking weeks off at a time for my wild adventures and having trust that I would come back and continue working hard (ideally more motivated). I chose you as my mentor not only because I knew I would have a lot of freedom in your lab, but also because I could tell you respected me and my thoughts and opinions in our conversations. You treated me unlike from the position of a boss but more of like an equal colleague which I always appreciated. You inspire me with the breadth of projects and pathogens you can take on, while somehow remaining passionate and engaged in them all. When I think of the characteristics of really who makes a virologist, it's you. Thank you for providing the resources and opportunities for me to be successful and grow as a scientist in your lab. I believe that together we have accomplished a tremendous amount and have made significant contributions to the alphavirus field. I hope that your research program only continues to grow in this area and I am happy to know I have contributed to that. The last six months have been a blast working more closely together, passing back and forth and pumping out several manuscripts. We all thought it couldn't be done. You've been supportive and encouraging during this phase where I continue to question my adequacy and worthiness of a PhD, and I really needed this. I didn't know if I'd make it, but we made it. Thanks for everything, Dan.

To my friends and family, thanks for bearing with me and supporting me during these last four years. Thanks for understanding when I cancelled/postponed plans or didn't show up as my best self. Your support was invaluable to me and promoted such a rich and fulfilled life for me outside of the lab. If everything else failed, at least I knew I'd have you all. Thank you for doing your best to be engaged and ask me about my research, even when you didn't understand, and listening to me yap on about viruses all the time (especially looking at Alli). Apologies, but that won't be ending here. To my friends who have supported me from across the state, country, or across the world, you mean so much to me (Alli, Brie, Abby, Hannah, Mike, Yoni). To my Portland gals, thank you for making life fun and for your support through good and bad times (Hailey, Ariana, Jenn, Kate, Reggie, Michelle, Lauren). To my parents, thank you for raising me in a safe and stable home and supporting me in furthering my education (Valerie, Kevin, Mike, Lynda). To my local Portland family, thank you for feeding me and taking me in when I break a foot (Uncle Ron, Aunt Patti, Aunt Wendy, Uncle Greg). To my grandma Katie, although you no longer remember me, thanks for asking me about how life is going.

Flic, my mentor turned friend, my jungle girl, it has been an honor to take on a PhD alongside you. We traveled to Peru together to present our research on viruses that circulate there. How many people can say they got to write their dissertation at the same time as a good friend? I have learned so much about life and science from you. We have shared so many adventures and wonderful moments together. Our friendship will undoubtedly persist in our new adventures.

To my colleagues in the Streblov Lab, I couldn't have done any of this without you. You all provided experimental assistance, comradery, and sometimes emotional support that was instrumental in my success. Mike Denton helped me get started in the lab on day one and was a tremendous source of knowledge and support every day. For my first year, we spent many long days in the lab where it was just the two of us. Mike taught me nearly everything I know about protein expression and purification as well as cloning, which are such fundamental skills. More than this though, I felt comfortable approaching Mike with all of my "dumb" questions in the lab and never had to worry about embarrassing myself or any judgement. Mike was always my go to person when I had "lost" something in the freezer and needed to go freezer diving, couldn't find something in the lab, or needed to figure out how to perform a new assay. He's the type of person that will drop everything to help you. We have shared a lot of laughs and fun days, also some hard

days, and I will miss his daily support and comradery from our corner of the lab. Craig and Takeshi in the lab significantly contributed to several of my projects. Takeshi, thank you for your contributions to the mouse studies we conducted and your patience with me in learning mouse handling. Craig, thank you for all of the viral RNA quantification you contributed and thank you for your patience with me as well. Zach contributed significant time to helping me with the cross-neutralization assays for the IXCHIQ human sera, and I think we broke a lab record for number of neut plates in a day- 121! Sam and Hannah, thank you for commiserating with me over the challenges of graduate school and PhD struggles. Sam, thanks for telling me “we’re gonna make it” at least weekly, I needed this! I’ve learned a lot from my colleagues in the lab. I value my relationships with you and highly respect each of you. I have also been thinking a lot about the way I have watched our laboratory scientifically evolve over the last four years. Scientists have both joined and left the lab, we’ve expanded viruses and models, adopted new techniques, secured new funding sources, and made several discoveries. I feel that I have played a role in the future directions of our lab and have seen the way one result can shift future directions and research pursuits. That is something that I love and will miss about academic research, that it almost feels spontaneous at times, or at least this has been my experience.

To my dissertation advisory committee, thank you all for pushing me in my development as an independent researcher. Thank you for all of the time you have dedicated to my training. I chose each of you to be part of my committee for the unique perspectives, wisdom, and expertise I thought you could bring to my projects. You all pushed me and refused to except anything but my very best work and held me to the highest standards. While our discussions challenged me, they also encouraged and motivated me. I wanted to show you all that I was capable of whatever you asked of me and I have done my very best to meet your expectations. Each of you deeply inspire me. I highly respect each of you as people and as scientists and hope to remain connected to you all throughout my career.

Mark, thank you for taking on the responsibility of chairing my committee. You have dedicated a lot of your time to my success and I appreciate your wisdom and guidance. I have enjoyed all of the collaborations with your lab and wish I would be around to see more of these studies through. Your knowledge breadth of vaccine-elicited immunity and vaccine history inspires me and pushes me understand the significance of historical discoveries. I feel honored that

you have been able to contribute some of your expertise to my training and development as a viral immunologist and vaccinologist.

Bill, it has been a pleasure to be mentored by you. I was interested in joining your lab after my rotation, but I think I got the best of both worlds with your outside mentorship throughout my time in the Streblov Lab. My rotation in your lab was my very first exposure to hands-on research with arboviruses and I was immediately entranced with the concepts of cross-reactive immunity and antibody-dependent enhancement. I have enjoyed getting to know you on a more personal level at the three conferences we have attended together and always felt adopted by your lab when invited to stay with your lab for these travels as far as Lima, Peru. Thanks for the last-minute pep talks for my conference presentations when Dan wasn't present and for doing your best to help me grow my professional network during these meetings. I feel like you have unspokenly gone out of your way to support me in my development as a scientist throughout my PhD, and it has not gone unnoticed. Thank you for all of your help with R for antigenic cartography, the intricate stats discussions, for being an active influence in the direction of my projects (even outside of DAC meetings), and so much more. Your passion for science is infectious and deeply inspires me.

Nancy, you've been a source of inspiration and support as a woman in science. I strive to emulate your qualities of grace, strength and perseverance in all that I pursue. Thank you for your support and encouragement in these final months leading up to my defense. You have always been an engaged member of my committee and I value all of your contributions to my training.

Lark, thank you for the refreshing perspective and energy you bring to my science and my life. I was terrified of you when I first met you at ASTMH 2022 because I thought your lab was going to scoop my first (first) author publication, the MAYV NHP study. But this lit a fire in me and let's be honest, the more NHP studies with MAYV, the better. I'm grateful that I met you and only wish we had started collaborating sooner in my graduate career. Thank you for checking in on me these last few months, empathizing with my feelings of imposter syndrome, and your dedication to my success.

Thank you to all of our scientific collaborators at ONPRC, the Messer Lab, the Slifka Lab, Ponce Health Sciences in Puerto Rico, Valneva, and Washington University. Without you, completion of these studies would not have been possible. Thank you to my research/student communities in the PBMS program, MMI department and at VGTI. Finally, thank you to the individuals who volunteered their time and gave a part of themselves to science and disease

prevention through participation in our studies. Your invaluable contribution advances our knowledge of human health and disease.

IV. Abstract

My dissertation research has focused on characterizing cross-reactive immunity following emerging alphavirus infection or vaccination in humans, and in non-human primate (NHP) or mouse models. These studies also involved optimizing alphavirus infection models including Mayaro virus (MAYV) infection in rhesus macaques and lethal arthritogenic alphavirus infection models in immunodeficient mice. Alphaviruses are predominantly mosquito-transmitted emerging viruses with the capacity to cause acute and chronic human disease, for which there are no currently licensed therapeutics. A vaccine was recently approved for chikungunya virus (CHIKV), the most epidemic alphavirus, which offers promise for disease prevention yet presents many new scientific questions to be pursued in the alphavirus immune landscape, some of which are probed in this dissertation.

My dissertation covers research that further characterizes antibody responses to alphavirus following infection and vaccination using a balance of human cohort studies, mouse infection and vaccine studies, and an NHP study. These studies reveal that similar alphavirus cross-neutralizing antibody potency and breadth is induced by CHIKV infection or vaccination with a recently licensed human vaccine. In mouse studies, we demonstrated inequity in reciprocal cross-protection afforded by adenovirus-vectored vaccines against CHIKV and MAYV and provide evidence of *in vitro* ADE. We explore different vaccine administration strategies like heterologous prime-boost and coadministration as strategies to improve cross-reactive immunity. Using the HydroVax-CHIKV vaccine with previously characterized homotypic efficacy, we interrogated the protective efficacy against the related alphavirus, ONNV, using our newly characterized lethal challenge model. Finally, we characterized MAYV pathogenesis and immunity in rhesus macaques as a new alphavirus disease model. Altogether, these studies provide examples of the way primary alphavirus exposure by infection or vaccination shapes the cross-neutralizing antibody breadth. This dissertation encompasses studies that expand the understanding of antibody-mediated alphavirus immunity after infection and vaccination in a multi-model approach to ultimately reduce the human disease burden of these emerging viruses around the globe.

Chapter 1: Introduction

Section 1.1. Preface

Currently an estimated 3.9 billion at risk individuals are living in tropical climates where arboviruses thrive [1]. Alphaviruses are emerging and re-emerging arboviruses with global distribution. Infection in humans has the ability to cause serious acute disease symptoms that may last weeks to months following infection and can be potentially lethal, posing a major public health threat. Infection with many alphaviruses can cause long-term disease symptoms because these pathogens are capable of long-term persistence. Due to the climate and vector circulation, alphaviruses disproportionately impact tropical regions of the world where populations of lower socioeconomic status reside.

Section 1.2. Introduction to alphavirus classification, distribution, and transmission

Alphaviruses belong to the *Togaviridae* family and make up a genus of 32 identified viruses that have been studied over the last ~70 years. At least a third of these recognized alphaviruses are known to infect humans while many other alphaviruses infect fish, birds, non-human mammals, or other non-mosquito insects. Alphaviruses are broadly classified as Old World or New World viruses which was first designated by geographical distribution (**Figure 1.2.1**), but these groups also have differences in clinical presentation. For example, Old World alphaviruses originated in the eastern hemisphere and are typically characterized by their presentation of arthritogenic disease. New World alphaviruses originated in the western hemisphere and typically cause encephalitic disease but they can also cause arthritogenic disease. Notably, Old and New World alphaviruses distinctly cluster both phylogenetically (**Figure 1.2.2**) and antigenically (**Figure 1.2.3**). Antigenically, alphaviruses are grouped into seven main serological complexes: Barmah Forest, Ndumu, Middleburg, Semliki Forest, Western, Eastern and Venezuelan equine encephalitis (**Figure 1.2.3**) [2]. This dissertation focuses on viruses in the Semliki Forest virus (SFV) complex, specifically CHIKV, ONNV, MAYV, UNA, and RRV. Alphaviruses have global distribution and have been detected on each of seven continents including Antarctica [3]. Due to similarity of disease symptoms, overlapping circulation, limited testing, and absence of specific diagnostics,

the overall global burden of alphavirus infections is predicted to be vastly underestimated. Alphavirus transmission occurs following the bite of a viremic mosquito, at the interface of mosquito saliva and contact with host blood; mosquito vectors vary by alphavirus species and geographic distribution. Host restriction factors of transmission involve innate immune responses and pathways [4, 5]. Research studies have indicated that climate shift has the potential to expand the distribution of CHIKV to regions such as North America, parts of China, and sub-Saharan Africa in the future [6-9]. Expansion of urbanization and climate changes are two factors that continue to impact alphavirus distribution and promote viral emergence.

Figure 1.2.1. The distribution of alphaviruses of clinical importance.

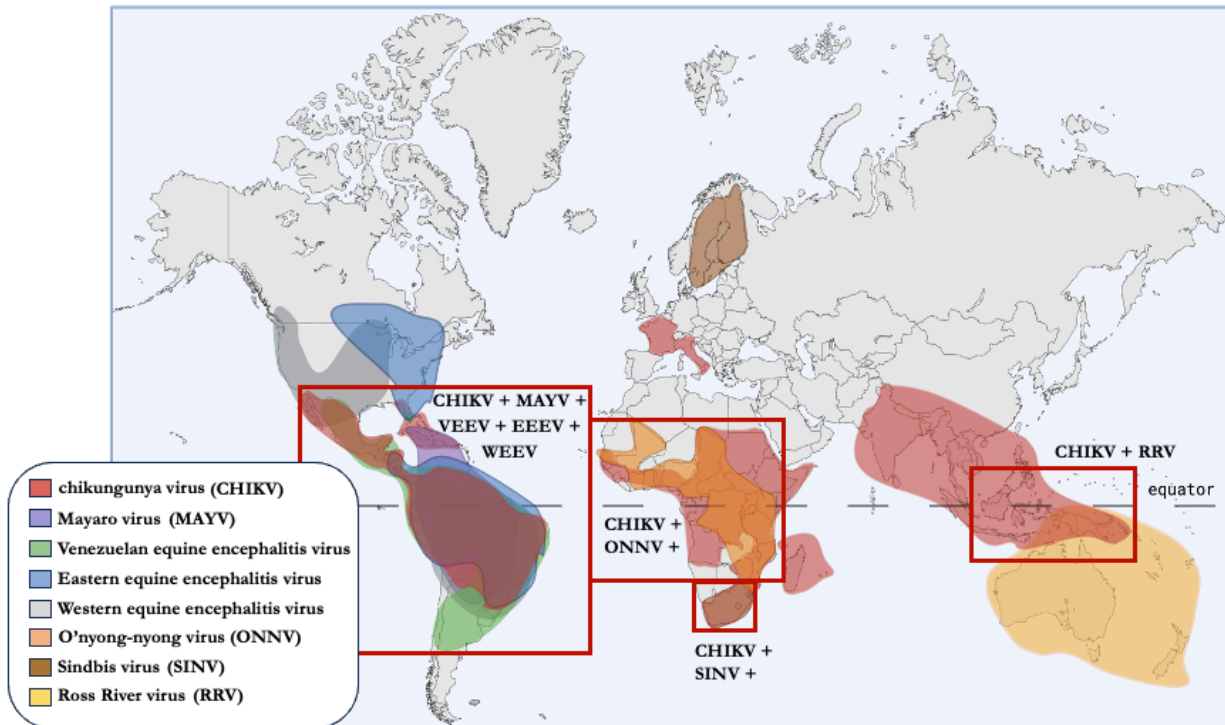
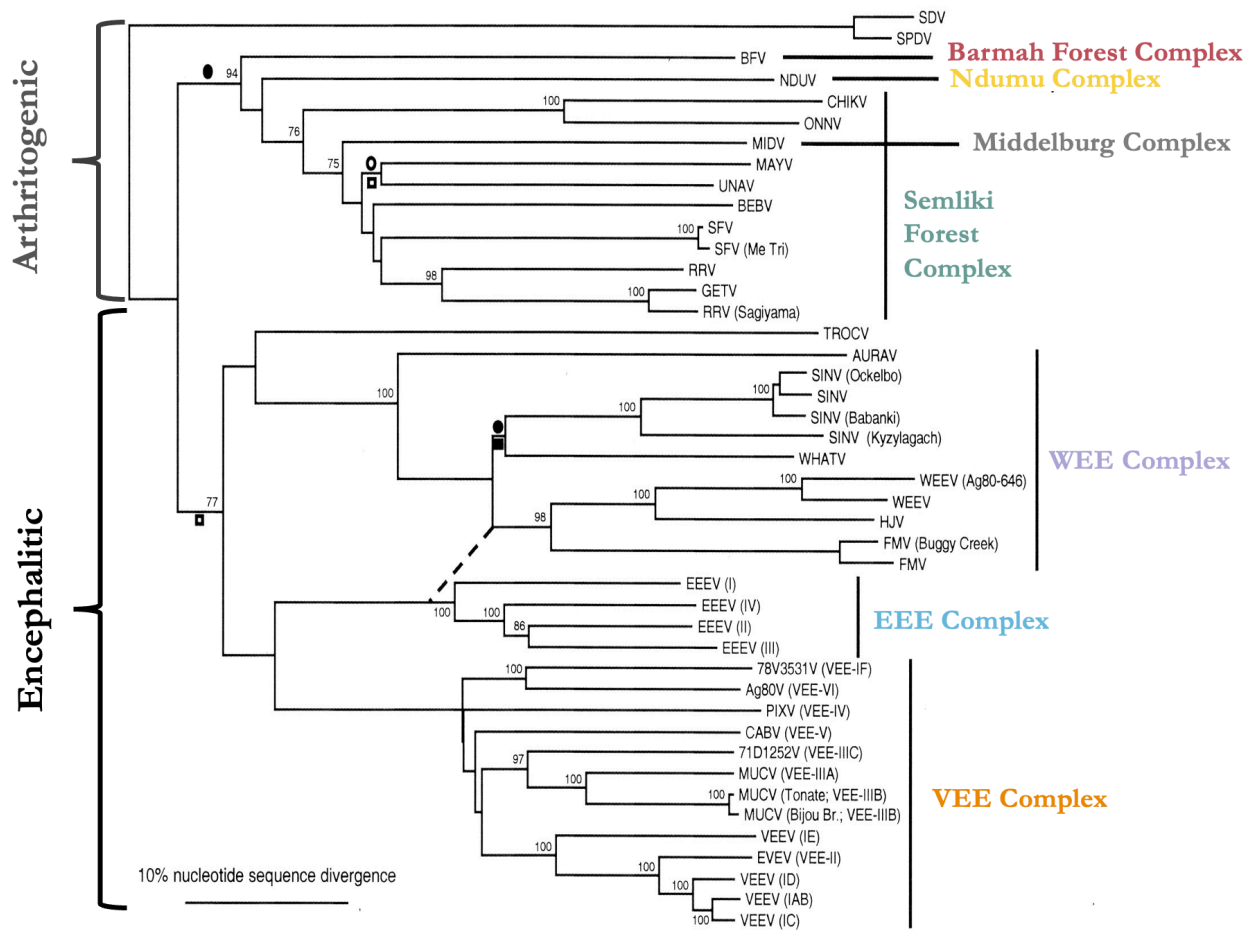


Figure 1.2.1. Map depicting the geographical distribution of clinically relevant arthritogenic and encephalitic alphaviruses. Graphic created by Whitney Weber; adapted from figure published in Weber *et al.* in *BioDrugs* (**Appendix III**) [10]. The distribution is estimated using several references and areas of cocirculation are outlined in red [11-13].

Figure 1.2.2. Alphavirus phylogeny.



Adapted from Powers *et al.*, 2001

Figure 1.2.2. Alphavirus phylogenetic organization constructed using partial E1 sequences with labeled antigenic complexes. Adapted from Powers *et al.* [14]. Abbreviations: MUCV, Mucambo virus; TONV, Tonate virus; PIXV, pixuna virus; CABV, Cabassou virus; FMV, Fort Morgan virus; HJV, Highlands virus; WHATV, Whataroa virus; SINV, Sindbis virus; KZLV, Kyzylagach virus; MIDV, Middelburg virus; MAYV, Mayaro virus; SFV, Semliki Forest virus; RRV, Ross River virus; CHIKV, chikungunya virus; ONNV, o'nyong nyong virus; BFV, Barmah Forest virus; SAGV, Sagiama virus; GETV, getah virus; NDUV, Ndumu virus; BEBV, Bebaru virus; TROCV, Trocara virus.

Figure 1.2.3. Alphavirus antigenic complexes.

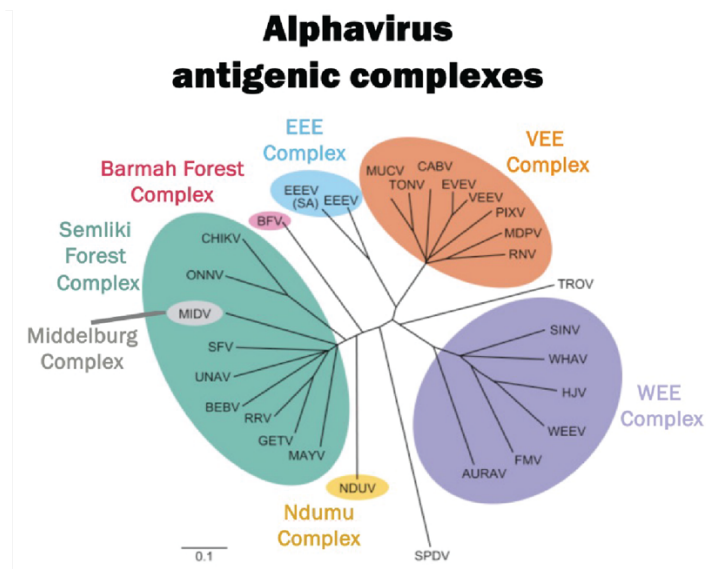


Figure 1.2.3. Alphavirus antigenic organization, adapted from Fenner’s Veterinary Virology (Fifth Edition) [2].

Section 1.3. Human disease and diagnosis

1.3.1 Arthritogenic alphavirus infection

Following the bite of an infected mosquito, arthritogenic alphaviruses replicate in the skin, then disseminate to the liver, joints, lymphoid tissues, brain, and throughout the body by blood circulation; cellular tropism includes fibroblasts, macrophages, dendritic cells, endothelial, and epithelial cells [15]. Alphavirus infection generally presents with a fever during the acute viremic phase following the 7-to-10-day incubation period. Typical accompanying acute symptoms often include maculopapular rash, headache and joint or muscle pain, which can persist for weeks to years following infection [16-20]. Rash, fever, and peripheral joint pain present within the first five days of infection, concurrent with viremia [21, 22]. Rash can be coupled with other mucocutaneous manifestations and result in longer lasting skin pigmentation lesions. Viremia duration is typically 5-8 days and peaks between 1-3 days-post infection (dpi) [22, 23]. Additional symptoms can include fatigue, nausea, diarrhea, conjunctivitis, and retroorbital pain. Although less common, disease can also progress to neurological manifestations, which is more common in cases of fatal infection [24]. Although there are no specific antiviral treatments available, symptoms are typically self-resolving. However infection can lead to mortality in about 1-1.3 out of 1,000

individuals [25, 26]. The working case definition for arthritogenic alphavirus infection has three major criteria: fever with muscle/joint pain of acute onset and visit to an area with active or historical viral transmission or detection of virus-specific antibodies or genomes [27, 28].

Arthritogenic alphavirus symptoms are clinically indistinguishable from each other and are also highly similar to infection with other cocirculating arboviruses such as flaviviruses, which can lead to frequent misdiagnosis. The limitation of using antibody detection as a laboratory test to diagnose specific alphavirus infection is that humoral responses directed against viruses within the Semliki Forest complex are highly cross-reactive, so a positive antisera test may be a result of a heterotypic rather than homotypic infection. The only way to definitively identify the type of alphavirus infection is by amplification of specific viral RNA sequences through qRT-PCR, but this requires that the patient is in the acute (viremic) phase of infection, which is reliably only a ~4 to 6 day period within the first ~12 days of infection. Detection of neutralizing antibodies (nAb) can also be used for diagnosis, but it is important to quantify nAb to related viruses to again conclude that the nAb are not simply cross-reactive. In the alphavirus literature, misinformed conclusions are often made about viral outbreaks and distribution based on host seroprevalence to a single alphavirus alone, which can be misleading when alphaviruses overlap in circulation and cross-reactivity. These limitations of the current diagnostics emphasize why a more standardized approach is warranted but is a complicated issue to address given the circulation of these viruses in often resource-limited regions.

1.3.2 Encephalitic alphavirus infection

Encephalitic alphaviruses are transmitted to humans and horses through the bite of infected mosquitoes, and symptoms typically develop after an incubation period ranging from 1-14 days. Infection may include the previously discussed symptoms for arthritogenic alphavirus infection, with the accompaniment of neurologic symptoms. Neurologic sequelae can include seizures, paralysis, behavioral changes, altered mental status, and convulsions. Survivors often have long lasting neurological deficits [29]. Of the encephalitic alphaviruses, the mortality rate is highest for EEEV, occurring in 50-75% of symptomatic human cases and in 70-90% of infected horses [30]. The case fatality rate for VEEV and WEEV is much lower (1%, 3-7%, respectively), however, lasting neurological sequelae is expected in 4-14% and 15-30% of cases, respectively [29].

Treatment is limited to supportive care and no vaccines to prevent EEEV or WEEV are available for humans. A vaccine for VEEV is available but administration is limited due to vaccine safety concerns in vulnerable populations (VEEV TC-83 vaccine discussed in **section 1.8.5**). A formalin-inactivated vaccine is available for use in horses to prevent infections of WEEV and EEEV.

Section 1.4. Host immune response to infection

1.4.1 Innate immunity

Upon viral entry to a target cell, alphaviruses are greeted by pattern recognition receptors (PRRs) such as toll-like receptors TLR3, TLR7, and TLR8 or RIG-I-like receptors [31]. These PRRs activate the production of IFN-stimulated genes and pro-inflammatory cytokines/chemokines through transcription by NF- κ B and IRF transcription factors [32, 33]. Mice deficient in IRF3 and IRF7 (C57BL/6 background) are highly susceptible to lethal infection, underscoring their role in protective innate immunity [34]. The alphavirus replication complex compartmentalizes RNA synthesis in membrane spherules to evade the host innate immune response by limiting the recognition of double stranded viral RNA intermediates by pathogen associated molecular patterns (PAMPs) [35].

Inflammatory cytokines and chemokines are secreted rapidly during the acute phase of alphavirus infection and include IL-6, IL-7, IL-12, IP-10, RANTES (CCL5), MCP-1 (CCL2), G-CSF, GM-CSF, IFN- α , and IFN- γ as well as others [36-38]. Inflammatory cytokine and chemokine secretion in the host generally peaks at 2-3 dpi, which is concurrent with peak viremia [39, 40]. The elevation of pro-inflammatory cytokines and chemokines such as IL-6, IL-8, IFN- α , TNF- α , GM-CSF, and CCL-2 have been associated with CHIKV infections that progressed to death in humans in comparison to CHIKV infection survivors [26]. Chemokines like MCP-1, or IL-8 recruit monocytes/macrophages and neutrophils to the site of infection, and the cytokine TNF- α recruits NK cells and CD8⁺ T cells, initiating the next phase of the antiviral immune response.

1.4.2 Cellular immunity

T-cells and NK cells

T-cells are a key component of the cellular adaptive immune response to alphavirus infection. Activated antiviral T-cells and NK cells generally develop a few days after alphavirus infection symptom onset, and these cells play an important role in viral clearance and repair of infected tissues [21, 37]. Activated CD8⁺ T-cells expand first after infection to target and kill infected cells followed by CD4⁺ T-cells, which stimulate B- and T-cell help [37]. Both CD4⁺ and CD8⁺ T-cells can secrete the cytokine IFN- γ , which can act directly on the target cells and stimulate macrophages, dendritic cells, and other T-cells. Activated CD8⁺ T-cells present during acute infection also express granzyme B and perforin, indicative of their cytotoxic function [41]. CD4⁺ T-cells, particularly follicular helper CD4⁺ T-cells, are required for B-cell differentiation, IgG class switching, affinity maturation, and therefore enhancing the production of antiviral IgG antibodies [42]. Antiviral CD4⁺ (but not CD8⁺) T-cells, due to their inability to mediate inflammation via the IFN- γ pathway, have also been linked to the development of joint disease in mice but did not impact viral replication, implicating their role in promoting early inflammation [43]. In mice, T cells educated by exposure to CD8-specific CHIKV peptides can reprogram the normal inflammatory process and reduce virus-mediated disease, but the presence of CD4⁺ epitopes negate this effect [44]. Following infection, the CD8⁺ antiviral T-cell response is greater than the CD4⁺ T-cell response and is predominantly directed against E2, nsP1, and the capsid proteins [45, 46]. Overall, the role of T-cells in response to alphavirus infection is complex [47].

Monocytes, macrophages, and dendritic cells

Monocytes, macrophages, and dendritic cells are key participants in the antiviral response and in repair of tissue destruction and inflammation after infection [48]. Chemokines recruit these cells to the site of infection and are highly activated during acute infection, concurrent with peak viremia [39, 40]. Activation of these cells usually declines with the same kinetics of viremia clearance, implicating their role in this process. While these macrophages have a positive role in antiviral immunity, they are also implicated in arthritogenic pathology as alphavirus persistence manifesting as chronic arthralgia has been linked to viral replication in macrophages and persistence of these cells in infected tissues, as shown for CHIKV [36, 49]. Dendritic cells are antigen presenting cells activated early after alphavirus infection that process and present antigens to lymphocytes to stimulate adaptive immunity, while plasmacytoid dendritic cells also secrete type 1 interferons and pro-inflammatory cytokines and chemokines to stimulate innate immune

activation [50-52]. The contribution of monocytes, macrophages, and dendritic cells examples of the complex antiviral immune response for their roles in both protection and pathology.

1.4.3 Humoral immunity

B-cells

B-cells are derived from hematopoietic cells in the bone marrow, and once mature, they secrete antibodies, which are a dominant player in the humoral immune response to alphavirus infection by their direct involvement in viral clearance and mitigation of viral pathogenesis. The importance of the humoral response is highlighted by the findings that mice lacking B-cells develop persistent viremia after CHIKV infection and develop more severe disease, underscoring the role of antibody-secreting cells in the resolution of disease [53]. During the acute viremic phase of alphavirus infection, B cell activation is stimulated through the detection of viral antigens by B-cell receptors. Marginal zone and B1 cells are the first B-cell responders to infection that give rise to the first antibody-secreting plasma cells, but these are generally low affinity IgM antibodies [54] but they have shown long term persistence [55]. We have shown that proliferating marginal zone-like B cells expand early after MAYV infection in macaques [39]. The activated B-cells release stimulatory cytokines and chemokines that trigger B-cell proliferation and differentiation into plasma cells which secrete antiviral antibodies [56]. Antigen primed, activated follicular B-cells enter germinal center reactions with the help of T cells and follicular dendritic cells in lymphoid tissues [57]. Within germinal centers, proliferation, somatic hypermutation, isotype-switching, and apoptosis promote the emergence of B-cells that produce high affinity antibodies (which takes time and antigen stimulation) [58]. Key to adaptive antiviral immunity, long-lived plasma cells (LLPCs) and memory B-cells exit germinal centers. LLPCs are B-cells that have terminally differentiated and are poised to secrete antibodies throughout their lifespan upon antigen exposure. Memory B-cells proliferate and differentiate into new populations of antibody-secreting cells upon antigen exposure but do not secrete antibodies themselves, thus playing an important role in humoral immunity. Our group has identified CHIKV-specific memory B-cells detectable up to 24 years post-infection in CHIKV-immune individuals in Puerto Rico (**Chapter 2**) [59]. Additionally, one study demonstrated comparable vaccine-elicited memory B-cells for an Eilat alphavirus chimeric CHIKV vaccine as well as for the 181/25 CHIKV vaccine [60]. With improved high-throughput screening of memory B-cells, it is possible to clone antibodies from

infected people with relative ease. As for other viral diseases, it is now appreciated that the number of B cells responsive to any given antigen or virus is far greater than had been previously estimated and hence the B cell repertoire is immense [61].

Antibodies

Alphavirus infections elicit very potent antibody responses, often to higher titer than other viruses such as flaviviruses like dengue virus, Zika virus, and yellow fever virus. Antibodies come in many flavors- they can prevent virion entry to a target cell, activate complement, promote cellular phagocytosis (opsonization), and neutralize virus. Antibody diversity occurs through V(D)J recombination, junctional diversification, somatic hypermutation, and affinity maturation. Following alphavirus infection, the IgM response develops between 4-5 dpi and lasts 1-3 months [62, 63], and the IgG response develops between 4-10 dpi, persisting for years after infection [64-66]. Although the IgM response is classically thought to be short lived, persistence of alphavirus-specific IgM antibodies have been detected in patients for years after infection, potentially due to continuous antigenic stimulation by persisting viral replication in macrophages and tissues [16, 67, 68]. The major targets of the host antibody response to alphavirus infection are within the E1 and E2 glycoproteins, as these proteins are antigenically accessible at the virion surface.

Neutralizing antibodies are detectable as early as 4 dpi and persist for years following infection [59, 69]. It is important to note that the neutralizing activity of the polyclonal response is composed of individual monoclonals, and these individual antibodies may differ considerably in their antigen binding, neutralizing capacity, and potency and that all these activities will differ in each host. Neutralizing antibodies play a critical role in clearing viruses from circulation but are less effective at eliminating infection at the tissue level. Targets of neutralizing antibodies are identified using epitope mapping, alanine scanning mutagenesis, competition assays, and other mechanistic studies. Virus neutralization occurs when an antibody binds and blocks cell entry at the surface of a target cell. Neutralizing antibodies can block viral fusion mediated by the E1 glycoprotein [70] or receptor-mediated endocytosis for viral entry to a target host cell [71]. To achieve this, an antibody needs to have high avidity and affinity for its target epitope and be present in a high enough concentration to defend against circulating virus. Although neutralizing antibodies are best described for prevention of alphavirus infection, non-neutralizing antibodies have also been shown

to protect against infection [72]. Antiviral antibodies target the viral envelope proteins, predominantly the E2 glycoprotein and even more specifically, the E2B domain [59, 73-77]. Neutralizing antibodies targeting the E2B domain have been identified for CHIKV, MAYV, RRV, Sindbis virus (SINV), EEEV, and VEEV but not for ONNV, UNA, or WEEV [74]. Other important neutralizing epitopes have also been identified in the E2A and E2C domains, the ASR1 and ASR2 connecting domains of E2, and E1 [75-79]. The E1 glycoprotein also contains epitopes for many non-neutralizing antibodies.

Antibodies with Fc-effector functions allow monocyte and neutrophil-dependent phagocytosis (opsonization), which have been shown to be important for protection against alphavirus infection and can orchestrate additional immune responses [77]. Protective mAbs administered to anti-Ifnar1 mAb-treated FcγR deficient mice lost their protective phenotype, implicating the role of Fc-effector functions in protection. Another mechanism of opsonization is labeling of an antigen with complement, which activates the innate immune pathway ultimately promoting phagocytosis. CHIKV [80], ONNV [81], and RRV [82, 83] have been shown to activate host complement activation or downregulate expression of molecules (CD55 or CD59) that regulate complement, which has been linked to arthralgia. On the vector side of the equation, mosquitoes have adapted to prevent human complement activation in the gut after taking a human bloodmeal, protecting the vector [84]. Antibodies can also signal for killing of infected cells by NK cells. Tremendous antibody diversity is implicated in seemingly infinite functions through interaction with cellular and molecular components of the immune system, with just a few of them described here.

1.4.4 Cross-reactive immunity

There is considerable antigenic conservation within each antigenic complex (**Figure 1.2.3**), affording both cross-reactive antibodies and T-cells. For each arthritogenic alphavirus, there is little antigenic variation between strains, implicating them generally as a single serotype.

Cross-neutralizing antibodies

Both the genetic and antigenic similarity of alphaviruses within an antigenic complex allows for antibodies to bind and neutralize antigenically conserved epitopes, such as the E2 envelope glycoprotein, which is the most immunodominant antigen and primary neutralizing antibody target due to antigenic accessibility on the virion surface. The E2B domain of E2, a 62 amino acid region,

is a dominant target of cross-neutralizing antibodies (**Figure 1.4.1**) [59, 74]. Alphavirus cross-reactivity largely refers to viruses positioned within the same antigenic complex. For example, numerous studies have described that human CHIKV infection-elicited antibodies can cross-neutralize related alphaviruses from the Semliki Forest virus (SFV) complex (**Figure 1.2.3**), which includes SFV, CHIKV, ONNV, MAYV, UNA, RRV, Bebaru virus (BEBV), and Getah virus (GETV) [59, 75, 85]. In mouse studies, MAYV infection has been shown to elicit antibodies that cross-neutralize other related alphaviruses [86]. While we have successfully quantified cross-neutralizing antibodies after CHIKV and MAYV infection in humans by 50% plaque reduction neutralization tests (PRNT₅₀) (**Chapter 2/3, Appendix I**), other studies have failed to detect these antibodies with PRNT₈₀ assays, underscoring the importance of the appropriate assay for detection [87, 88]. A few studies have also demonstrated that human ONNV infection-elicited antibodies neutralize CHIKV. However, one study demonstrated that ONNV infection resulted in cross-reactivity against CHIKV in only 22% of cases, whereas CHIKV infection resulted in the development of antibodies against ONNV in 80% of cases [89]. This inequity underscores the complexity of cross-reactive immunity within the SFV antigenic complex. We [90, 91] and others [92-94] have shown partial cross-protection phenotypes elicited by alphavirus vaccines, implicating complex dynamics in reciprocity in cross-protection. This concept is discussed in more detail in **Chapter 4**. Missing antigenic relationships of antibody potency and breadth that remain to be demonstrated for human alphavirus infection of circulating human pathogens are for ONNV, MAYV and RRV infection. The encephalitic alphaviruses conform to their respective antigenic complexes, but some cross-reactivity has been described between complexes [95]. Defining these antigenic relationships has important translational impact for potential immune protection of individuals susceptible to circulation of diverse alphaviruses and relevance for alphavirus vaccine development.

translation to other studies. Numerous studies in mice and NHP [99] have demonstrated the ability of passively transferred vaccine or infection-elicited antibodies to protect against disease and or infection [91, 102-106], and other studies have shown only partial protection in context of heterologous challenge [90, 105] or even the lack of protection. Some studies have also illustrated some protection from infection through transfer of polyclonal or monoclonal antibodies shortly after infection, although the window of efficacy for this is very narrow and successful implementation would be a challenge clinically [40, 107-110]. These studies imply that protection is indeed antibody-mediated as protection from infection is achieved in the absence of cellular immunity.

Neutralizing antibodies are the most well studied and accepted correlate of protection, but numerous studies have shown protective roles of T-cells as well. Most alphavirus vaccine development that occurs focuses on the development of virus neutralizing antibodies and vaccine-elicited antiviral T-cells are not often characterized. However, a measles virus-vectored CHIKV vaccine in clinical development reportedly elicits antiviral T-cells targeting capsid and the E1/E2 envelope proteins in humans [111]. Our lab published a study of an MHC Class I T-cell-biased CHIKV vaccine approach using an adenovirus-vectored vaccine with no neutralizing epitopes that demonstrated protection against infection and virus-induced footpad swelling implying an important role for T-cell mediated immunity in shaping the inflammatory disease process [112]. In contrast, another study reported a MAYV DNA vaccine that elicits both humoral and cellular antiviral T-cell immunity, but found that the vaccine-elicited protection was mediated by humoral immunity [113]. Other studies have shown that transfer of vaccine-elicited, virus-specific T-cells failed to protect against infection [104], thus the evidence for T-cell mediated protection is unclear.

1.4.6 Antibody-dependent enhancement of infection

Antibody-dependent enhancement (ADE) of infection is a mechanism by which viral replication is increased in Fc receptor bearing myeloid cells in the presence of preexisting sub-neutralizing homotypic or heterotypic antibody levels, translating to potential for enhanced infection and/or disease [114, 115]. ADE was first reported in 1964 showing increased viral infectivity of fibroblasts in presence of antisera of domestic fowls infected with a variety of flaviviruses or the alphavirus, Getah virus (GETV) [116]. This report describes ADE as a new antibody functionality and even reports cross-enhancing activity between viruses. In 1982, enhancing activity was

described in macrophages infected with SFV and Sindbis virus (SINV) in presence of homotypic antibody [117]. This report also demonstrated the absence of enhancing activity between alphaviruses and flaviviruses, which has been corroborated by subsequent reports [118]. There have been only a handful of reports of *in vitro* ADE that have been limited to CHIKV and RRV. We explore this antibody-mediated effect for vaccine-elicited antibodies in **Chapter 4**. One finding for RRV *in vitro* ADE demonstrated that dilution of anti-RRV human sera enhances RRV titers in four monocyte/macrophage cell lines by up to three logs, and the authors hypothesized that this was due to persistent, productive infection of macrophages [119]. Two additional reports have demonstrated *in vitro* ADE due to the ability of RRV to target transcription of antiviral genes in macrophages to achieve uninhibited replication in these cells [120, 121]. One study developed a formaldehyde-inactivated RRV vaccine (which later completed a Phase III clinical trial) and evaluated risk for ADE in context of both homotypic RRV and heterotypic CHIKV challenge, finding no evidence of ADE in mice [105]. For CHIKV infection, Lum *et al* revealed that dilution of anti-CHIKV human sera enhanced viral replication in monocytes/macrophages as well as B cells, however, this was only evident when examining viral titers and not viral RNA levels [122]. Further, Lum *et al* presented that mice display CHIKV viremia (RNA) enhanced by one log after passive transfer of anti-CHIKV mouse sera for 1-7 dpi, the first *in vivo* evidence of alphavirus ADE. The consensus has been that evidence of *in vivo* alphavirus ADE is only speculative in research settings and has not been observed clinically in humans to date for any alphavirus. The CHIKV VLP vaccine in Phase III clinical development (PXVX0317) [123] as well as the recently licensed IXCHIQ vaccine [124] have now been administered to CHIKV seropositive individuals and were generally immunogenic, safe and well tolerated, representing the aversion of one context that could have promoted ADE. However, compelling evidence for the risk or absence of risk of ADE in alphavirus seropositive individuals following exposure by infection or vaccination to a heterologous alphavirus has not been demonstrated. These are scientific questions of potentially great consequence to public health and warrant further exploration both *in vitro* and in animal infection models.

Section 1.5. Alphavirus genome and replication

1.5.1 Genome organization and replication

Alphaviruses have small, single-stranded positive sense RNA genomes that are 11,000-12,000 nucleotides in length. The genome encodes two open reading frames composed of four nonstructural proteins (NSP1-4) and five structural proteins (C, E3, E2, 6K, E1) and the genome length RNA contains a 5' cap and 3' poly-A tail. The nonstructural proteins form the replication complex that contributes to viral genome replication by synthesizing the negative strand viral RNA, which is the template that gives rise to additional positive sense genomic length RNA as well as the 26S subgenomic RNA, which is translated into the structural polyproteins. The structural proteins make up the virion infrastructure and are synthesized as a single polyprotein, which includes capsid, three envelope proteins, and 6K. The envelope proteins engage in viral attachment and entry into host cells, making them accessible neutralizing antibody targets. To enter a target cell, alphavirus virions engage with a variety of host attachment factors and receptors with usage specific to the virus [125]. The major attachment factors for CHIKV are heparan sulfate and phosphatidylserine receptors and the major entry receptor for the arthritogenic alphavirus is MXRA8, which binds the E2 glycoprotein [126, 127]. The encephalitic alphaviruses utilize different key entry receptors. Following attachment, host cell entry is mediated by clathrin-mediated endocytosis. After membrane fusion in the endosome, the acidic pH promotes capsid disassembly and release of viral RNA into the cytoplasm. The non-structural polyprotein is translated and nonstructural protein 2 (nsP2) cleaves the polyprotein to assemble the replicative complex, made up of nsP1-nsP4. nsP1 participates in 5' cap synthesis, plasma membrane anchoring, and acts as a scaffold for the replication complex [128]. Functions of nsP3 are not completely defined, but nsP3 is known to be essential for replication, as the protein co-localizes with double-stranded RNA, and interacts with multiple host factors [129, 130]. Additionally, nsP3 contains an N-terminal macrodomain that hydrolyzes ADP-ribosylation. There are non-essential regions of nsP3 including the hypervariable domain that make nsP3 an ideal attenuation site for the development of live-attenuated vaccines [131] [132]. nsP4 is the RNA-dependent RNA polymerase which catalyzes RNA replication [133], as described above. The structural polyprotein is processed in the Golgi complex of the cell. Virions are transported to the plasma membrane where they assemble and bud from the infected cell. Mature alphavirus virions are about 70nm in

size, spherical, and are enveloped with 80 trimeric E2-E1 heterodimer spikes with icosahedral symmetry (T= 4) [70].

1.5.2 Alphavirus infectious clones

Alphavirus infectious clones are a critical tool for the study of the molecular determinants of alphavirus replication, transmission, antigenicity/immunity, and vaccine development. Alphavirus RNA replication is error prone with approximately one mutation per genome, thus infectious clones reduce viral sequence mutation rates by freezing the genome in time, which is ideal for their use in research settings. The ability to repeatedly recover viruses with a known genetic sequence increases experimental reproducibility and allows for the usage of lower passage stocks. The process of constructing an infectious clone is well described for CHIKV [134-138] and other alphaviruses. In **Chapter 3**, we describe the construction of an infectious clone based on the sequence of a CHIKV strain isolated from a febrile patient in Brazil and use the virus to assess heterotypic CHIKV neutralization by IXCHIQ vaccinee sera. In **Chapter 5**, we describe the construction of an infectious clone based on a recent ONNV clinical isolate to study the pathogenesis of a contemporary strain compared to a well characterized isolate in a susceptible mouse model, and to develop a stringent model of heterologous ONNV challenge following CHIKV vaccination.

Section 1.6. Virus-specific epidemiology, distribution, and transmission

1.6.1a Chikungunya virus (CHIKV) epidemiology

Early detection and outbreaks 1820s to 1970s

Chikungunya virus (CHIKV) is thought to have caused the first human illnesses from 1827-1828 in Zanzibar and St. Thomas in the Caribbean and was mistaken for dengue fever at that time [139-142], according to medical observer Henry Dickson and physician James Christie [143]. Defined CHIKV cases were reported for the first time in 1952, impacting the Newala and Masasi Districts in Tanganyika (now known as Tanzania), but the virus was originally isolated and characterized in 1953 from a febrile patient [144, 145]. In the Kimakonde language, chikungunya means “that

which bends up” referring to the painful joint and muscle pain caused by infection. The first isolated viral strain conformed to what later became named the East/Central/South Africa (ECSA) genotype. CHIKV was next documented in Thailand in 1958 and 1960 [146, 147] giving rise to the Asian lineage. The outbreaks in Thailand were massive (one estimate was 44,000 cases in Bangkok alone) and they occurred concurrently with a large dengue virus (DENV) outbreak, which has substantial symptom similarity to CHIKV, making it difficult to accurately estimate the incidence of infections. CHIKV then spread to India and caused prolonged outbreaks between 1963-1973. Strikingly, the morbidity rate in India was reported to be 37.5% [148] and there was generally a higher incidence of more severe disease, including encephalitis [149]. Following the outbreaks in India in the early 1970s, CHIKV vanished from detection for 32 years before resurfacing again in 2004 [150]. Notably, these early outbreaks of CHIKV in India were caused by the Asian lineage and when the virus returned 32 years later, it was again the ECSA lineage.

Explosive epidemics 2004-present

CHIKV started causing explosive epidemics in 2004, beginning in Lamu Island of coastal Kenya, resulting in an estimated 13,500 cases [151]. In 2005, an outbreak involving an estimated 215,000 individuals occurred in Grande Comore Island (Comoros) off the coast of Tanzania [152]. These outbreaks were much larger than historical outbreaks and were caused by strains of the ECSA genotype. An initially small outbreak spread to La Reunión Island in the Indian Ocean in 2005 but grew to one of the largest outbreaks to date, causing about 260,000 cases at a speed of 40,000 new cases per week [153, 154]. The island was known for having a limited *Aedes aegypti* mosquito population, the main urban transmission vector for CHIKV at the time. Viral sequencing of isolates collected once the outbreak had escalated revealed a single amino acid mutation in E1 (A226V) that was later shown to confer transmission capability in the mosquito species *Aedes albopictus*, which extends the potential range for CHIKV significantly [155, 156]. The La Reunión outbreak is famous not only for its case count but also for the way that selective pressure led to a viral mutation that conferred transmissibility to an entirely new vector, which has implications for further viral emergence in new climates and new transmission cycles. After La Reunión, CHIKV swept through islands in the Indian Ocean and eventually made its way to India in 2006, resulting

in over 1.5 million cases according to the WHO and an estimated loss in 25,588 disability adjusted life years (DALY) in India in 2006 alone [157]. This outbreak gave rise to the Indian Ocean Lineage (IOL) which continued spread to Southeast Asia and northern Italy [158]. The outbreak in Italy resulted in an estimated 300 infections and is notable in that it was the first outbreak to date to occur in a temperate region paired with the absence of the *Aedes aegypti* vector.

The introduction of CHIKV as the Asian genotype to the Americas came in 2013 to Saint Martin Island [159] and then as the ECSA genotype to Brazil in 2014 [160]. These initial outbreaks led to the explosion of CHIKV cases in Latin America, with over 1 million cases reported in the first year alone on 26 islands and 14 mainland countries [161]. CHIKV outbreaks are ongoing in 2024, which has been termed a pandemic due to detection in over 110 countries [21]. The majority of the case burden is currently in the South American countries Brazil and Paraguay. Since 2016, there have been 1,659,167 CHIKV infections in Brazil, more cases than anywhere else in the region [162]. As of July 2024, according to the European Centre for Disease Prevention and Control (ECDC), there had been approximately 350,000 cases and over 140 deaths reported due to CHIKV in the first six months of the year alone. While the Asian and ECSA lineages of CHIKV have each circulated in the Americas before, the Asian lineage has not been detected in the Americas since 2018, and current outbreaks in Brazil and Paraguay are caused by an ECSA lineage genotype [162].

1.6.1b CHIKV transmission – vectors, hosts, and cycle

CHIKV is transmitted by daytime biting *Aedes aegypti* and *Aedes albopictus* mosquitos when human amplification is involved, but the virus has been detected in other mosquito species including additional *Aedes* species, *Culex* and *Anopheles* mosquitos [163]. Remarkably, a single amino acid mutation (A226V) in the E1 glycoprotein conferred transmission capability to *Aedes albopictus* and this mutation was implicated in the promotion of the CHIKV epidemic in La Réunion from 2005-2006 [155, 156]. Unlike other emerging alphaviruses, CHIKV has established transmission in both urban and sylvatic transmission cycles. CHIKV causes explosive epidemics and maintains transmission between mosquitos and humans in the urban transmission cycle without the contribution of additional reservoir hosts. In the sylvatic or zoonotic transmission cycle, viral transmission is maintained between mosquitos and NHPs or other vertebrate hosts. Humans and NHPs are the only recognized amplifying hosts; CHIKV has been isolated from

African green monkeys, patas monkeys, guinea baboons, guenons, bats, squirrels, and a bushbaby [164-166]. Additional hosts have been infected experimentally, demonstrating replication competence even if the role as a natural reservoir host has yet to be shown [167]. Seroprevalence has been detected in additional NHP species as well as birds, bats, rodents, and other species, implicating a role in the enzootic cycle [164, 168, 169]. Occasional spillover of viruses in the sylvatic cycle into humans occurs with assistance from what are referred to as “bridge vectors” like *Aedes furcifer*, which are promiscuous mosquitos that feed on NHP and humans [170]. The evolutionary success of CHKV adaptation to *Aedes albopictus* mosquitos has led viral entomologists to hypothesize that additional transmission landscape-shaping mutations are to be expected and that variants have not yet reached maximum fitness in *Aedes albopictus*, posing a significant threat to further viral expansion [171]. Given these transmission dynamics, ongoing surveillance of CHIKV in both sylvatic and urban settings within endemic and non-endemic regions will always be warranted to elucidate the role of various hosts in transmission.

1.6.2a O’nyong-nyong virus (ONNV) epidemiology

O’nyong-nyong virus (ONNV) caused its first recognized epidemic contributing to an estimated 2 million cases beginning in northwest Uganda in 1959 [172] and was isolated for the first time in 1961 [173, 174]. The virus name came from the Acholi tribe residing in Uganda who’s community was impacted in the outbreak and means “very painful weakening of joints” [172]. ONNV and CHIKV share nearly indistinguishable disease symptoms and very high genetic and antigenic similarity. Since its drastic emergence in 1959 then ~34 year disappearance from detection, ONNV has caused two other smaller outbreaks, one epidemic in 1996 contributing to 21,000 cases in south-central Uganda [175-177] and a single reported case in 2004 in Chad [178]. Modern day seroprevalence of ONNV is difficult to enumerate with existing diagnostics due to antigenic cross-reactivity with CHIKV; CHIKV infection elicits antibodies that cross-neutralize ONNV and vice versa. Phylogenetically, CHIKV and ONNV are highly related, indicating some synchrony in evolution. Despite genetic and antigenic similarity and overlap in circulation with CHIKV, ONNV has yet to emerge outside of Africa and has yet to reach north African countries bordering the Mediterranean Sea [13].

1.6.2b ONNV transmission – vectors, hosts, and cycle

The transmission cycles of ONNV have yet to be defined and virus has not been isolated from any animal, but serological evidence suggests some kind of enzootic cycle. A reservoir host for ONNV has not been identified, but antibodies have been detected in buffalo, duikers, and mandrills (non-human primates) within the Congo basin (Gabon, Democratic Republic of the Congo) [179]. ONNV is transmitted by nighttime biting *Anopheles funestus* and *Anopheles gambiae* mosquitos, which are also vectors for *Plasmodium* that cause malaria [173, 180]. ONNV-malaria co-infection has not been reported but during heightened ONNV transmission there was an observed reduction in malaria prevalence [181]. CHIKV and malaria coinfection has been documented [182], but CHIKV is transmitted by other mosquito vectors.

1.6.3a Mayaro virus (MAYV) epidemiology

Mayaro virus (MAYV) was first isolated from forest workers in Mayaro County in Trinidad and Tobago in 1954 [183, 184]. Viral distribution is generally confined to South America, primarily within and surrounding the Amazon Basin, but MAYV cases have been detected as distantly as Haiti in both 2014 and 2015 [185-187] and Mexico [188]. MAYV cases have been reported in Trinidad & Tobago, Brazil, Peru, Mexico, Venezuela, Panama, Haiti, Ecuador, Bolivia, Surinam, and French Guiana [65, 189, 190]. A total of 901 confirmed cases have been reported as of 2020 [191], although the majority of the literature that exists reporting MAYV outbreaks often does not include confirmed case counts. MAYV strains have diverged into three main genotypes with about 17% nucleotide divergence across them: D (dispersed), L (limited) and N (new). Genotype D has the most widespread distribution across South America and the Caribbean, genotype L is confined to Brazil, and genotype N viruses are confined to the Madre de Dios / Puerto Maldonado region of Peru [192]. Since original detection 70 years ago, human outbreaks have been sporadic but have occurred every decade since 1954 and are increasing in frequency. Outbreaks are typically on the order of dozens of cases rather than hundreds. The largest recorded outbreak occurred in 1977-1978 in Belterra, Brazil, where an estimated 20% of a 4000 person community were infected, equivalent to ~800 cases [193]. The second largest outbreak to date occurred in La Estación village, Venezuela, in 2010 where about 70 individuals were reportedly infected [194]. Present day seroprevalence of MAYV is very high in Iquitos, Peru, one of the largest urban centers in the Amazon basin, as well as in communities in this region [195]. MAYV detection often goes under

the radar as the disease and antiviral immunity can be mistaken for CHIKV infection at diagnosis, or individuals who are infected don't seek treatment. Overall, surveillance is more limited for MAYV compared to CHIKV and further expansion of surveillance efforts is warranted.

1.6.3b MAYV transmission – vectors, hosts, and cycle

MAYV is mainly transmitted by upper canopy-dwelling *Haemagogus janthinomys* mosquitos but has shown replication competence in both *Aedes aegypti* and *Aedes albopictus* vectors in experimental settings [196-198]. Viral genomes have been detected in additional endemic mosquito species as well, including *Culex*, *Aedes*, *Mansonia*, *Sabethes*, and *Psorophora*, implicating these mosquitos as potential secondary vectors [65]. MAYV maintains amplification in sylvatic transmission cycles between mosquitos and primates where humans are only sporadically infected upon entrance to forested areas [65]. Being transmitted by upper canopy-dwelling mosquitos, MAYV is largely thought to be transmitted in the treetops of the jungle to monkeys inhabiting that space. The virus has yet to consistently establish an urban transmission cycle, although outbreaks have occasionally occurred in Brazilian cities or peri-urban settings [199-202]. It is hypothesized that additional animal reservoirs like reptiles, birds, and rodents play a role in transmission, but the role has yet to be defined. Like other alphaviruses, additional mosquito vectors are also hypothesized to play a role in transmission maintenance. MAYV has been successfully isolated from marmosets [193], lizards [203], and oriole birds [204] but evidence of additional amplifying hosts is currently absent. Seroprevalence has been detected in several NHP species including howler monkeys, marmosets, and tamarins (*Alouatta*, *Cebidae*, *Callithricidae*, *Saguinus*), implicating these animals as the primary hosts maintaining viral transmission [193, 205, 206]. Evidence of seroprevalence has also been identified in other animals like sloths, opossums, porcupines, rodents, armadillos, dogs, horses, and cattle [207, 208]. MAYV is very much an emerging virus at the moment, showing evidence of broad host range, but somehow maintaining transmission exclusively in the jungle. As observed with CHIKV, small changes in viral evolution may adapt the virus to new vectors with wider distribution, easily impacting the transmission landscape and opening the door for emergence. As such, a single amino acid substitution in the MAYV E2 protein can increase viral infection and replication in *Aedes* mosquitoes, which predicts eventual urban transmission cycle possibility for MAYV [209].

1.6.4a Ross River virus (RRV)

Ross River virus (RRV) was first identified in 1959 in Ross River, Townsville, Queensland, Australia [210]. RRV is now the most prevalent arbovirus in Australia, contributing to 2,942 cases so far in 2024 (as of June) [211]. To date, RRV has been geographically confined to Australia and some South Pacific islands and territories. The virus is endemic in Australia, Papua New Guinea [212], and the Solomon islands [213]. RRV has also been isolated following 1979-1980 epidemics in Fiji [214], American Samoa [215], the Cook Islands [216], and New Caledonia [217]. It is typical for Australia to have 5,000 cases of RRV per year on average. In 2015 there were 9800 cases in Australia, and in 2017, a larger outbreak occurred in Victoria, Australia, where 1200 cases were reported in a two month period [218].

1.6.4b RRV transmission – vectors, hosts, and cycle

RRV is transmitted by over 40 *Aedes* and *Culex* mosquito species to primary reservoir hosts that include kangaroos and wallabies. Enzootic transmission is maintained in this marsupial-mosquito vector cycle where humans and horses are occasionally infected. The role of horses in the transmission cycle is unclear but they are susceptible to disease [219]. Additional suspected spillover hosts in urban or peri-urban environments, evidenced by seroprevalence data, include brushtail possums, flying foxes, dogs, and cats [220]. A human-mosquito transmission cycle has also been hypothesized for an outbreak in northeastern Australia in 2016 [221]. Outbreaks usually occur temporally from February to May or surrounding periods of rainfall.

1.6.5a Encephalitic alphaviruses epidemiology

The most well studied New World alphaviruses are Venezuelan equine encephalitis virus (VEEV) and Eastern and Western equine encephalitis viruses (EEEV and WEEV), all of which were originally isolated in the 1930s [30]. The encephalitic alphaviruses are particularly threatening to human health for their ability to cause more serious and potentially lethal infections, and also for their potential as bioterrorism agents. EEEV and WEEV have geographical distribution ranging from North to South America whereas VEEV distribution is more confined to Central and South America (**Figure 1.2.1**). EEEV and WEEV generally cause outbreaks that are smaller in case counts. In contrast, VEEV has caused a number of large outbreaks, with one of the largest reported outbreaks occurring in the 1960s in Columbia involving more than 200,000 human cases and

100,000 deaths in horses [222]. A more recent explosive outbreak in Columbia and Venezuela occurred in 1995 and involved an estimated 75,000-100,000 human infections with 300 deaths [30].

1.6.5b Encephalitic alphaviruses transmission – vectors, hosts, and cycle

The encephalitic alphaviruses are transmitted by *Aedes*, *Culex*, *Psorophora* or *Culex* mosquitoes to rodents (VEEV) or birds (WEEV and (EEEV) in the enzootic cycle and humans or horses are occasionally infected in the epizootic cycle.

Section 1.7. Animal models of infection

1.7.1 Early non-human primate (NHP) disease models for arthritogenic alphaviruses

The first experiment seeking to study CHIKV in non-human primate hosts was published in 1953 by RW Ross and demonstrated that three rhesus macaques developed anti-CHIKV nAb responses to inoculation with viremic human sera [223]. Years later in 1967, Binn *et al.* conducted seminal experiments with additional alphaviruses MAYV and ONNV as well as two strains of CHIKV in rhesus macaques [224]. These studies revealed that upon subcutaneous challenge, macaques developed CHIKV and MAYV viremia lasting 4-5 days but the strain of ONNV used in these studies did not cause detectable viremia in these animals. Binn *et al.* also demonstrated that these macaques developed homotypic neutralizing antibodies upon infection as well as antibodies that cross-neutralized CHIKV, ONNV, and MAYV that conferred protection against heterotypic challenge with CHIKV or MAYV. These early experiments laid groundwork for understanding alphavirus pathogenesis with translational application to human infection and showed early evidence of cross-protective alphavirus immunity, which is a central theme of this dissertation.

1.7.2 Development of CHIKV NHP models of infection

Later experiments sought to further characterize CHIKV infection in aged or pregnant rhesus macaques as well as cynomolgus macaques [225]. CHIKV infection is not typically lethal in any of these models, but aspects of human disease are displayed such as fever, rash, and arthralgia. These three models are similar but have slight variations in approach that result in subtleties in

pathogenesis and antiviral immunity. These studies present applicable models for the evaluation of CHIKV-specific therapeutics.

The first comprehensive analysis of CHIKV pathogenesis in NHP was reported in 2010 by Labadie *et al.* in cynomolgus macaques following intravenous or intradermal challenge with 10^1 - 10^8 PFU of CHIKV_{LR2006} [49]. An understated finding of the study was that challenge with only 10 PFU resulted in peak viremia of 10^8 vRNA copies/mL in one macaque, indicating that a low challenge dose could result in robust viral amplification. The observed clinical signs of disease included fever, rash, joint effusion, subcutaneous edema, and even meningoencephalitis in one animal which succumbed to infection. A key finding of this study was the challenge dose-dependent escalation of clinical outcomes. Persistent infectious virus at 44 dpi and CHIKV RNA at three months after infection was detected in the spleen of animals challenged with 10^6 PFU (i.v.) and viral persistence was identified in macrophages. This model recapitulated viral, pathological, immunological, and several clinical features of CHIKV infection in humans, but the observance of arthritogenic disease was absent. Notably, this study provided strong evidence of the ability of CHIKV to persist in lymphoid tissues and more descriptively, in macrophages.

The next study of CHIKV infection in NHP was also published in 2010 by Chen CI *et al.*, presenting data demonstrating East African epidemic or West African enzootic (CHIKV₃₇₉₉₇) infection in six pregnant rhesus macaques [226]. Following subcutaneous challenge (10^3 - 10^4 PFU), viremia was detectable at 1 dpi, peaked at 2 dpi, and had subsided by 5 dpi, regardless of strain. Slightly higher viremia was observed in animals after challenge with the enzootic strain from 2-4 dpi. Some animals developed muscle/joint swelling (short-lived, self-resolving), fever, and/or rash. Lower heart rates for the fetuses were observed at 1 dpi but fetal demise was not observed and all six pregnant macaques survived infection. At necropsy at 21 dpi, viral RNA was detected in several maternal tissues, including the spleen, joints, and spinal cord, providing additional evidence of wide tissue distribution and viral persistence even after the resolution of viremia. CHIKV RNA was not detected in any of the assayed fetal tissues. This study successfully recapitulated the key pillars of CHIKV infection in humans with respect to viral replication and tropism, antiviral immunity, and pathology.

In the study by Messaoudi *et al.*, CHIKV infection with 10^7 - 10^9 PFU of CHIKV₃₇₉₉₇ or CHIKV_{LR2006} was compared in aged and adult rhesus macaques [227]. The kinetics of viremia were similar for both strains: five-day duration with peak viremia occurring at 1-2 dpi. However, CHIKV_{LR2006} generally replicated to higher titers. Some of the animals developed fever, rash, and lymphadenopathy. One of the aged macaques displayed viremia detectable at 10 dpi when all other animals were undetectable, and two animals had higher viral loads in the spleen at 35 dpi compared to six adult animals which were undetectable. The authors concluded that the aged macaques had higher and more persistent CHIKV_{LR2006} replication than the adult macaques due to defects in antiviral immunity. The conclusions of the study were limited in that only two rhesus macaques per viral strain were challenged for comparison to the adult macaques, however, the overall kinetics of viremia and antiviral immune activation were consistent with prior studies of CHIKV infection in NHP.

One recent study published in 2024 by Chen H *et al.* utilized the rhesus macaque model of CHIKV infection to study the contribution of gut microbiota to CHIKV-induced rheumatoid arthritis and characterized changes in the gastrointestinal microbiome in response to CHIKV infection [228]. This study demonstrated the reproducibility of infection and disease in the NHP model and shows applicability for multidisciplinary studies.

1.7.3 Utilization of the CHIKV NHP model to evaluate vaccine efficacy and immunogenicity

Models of cynomolgus (*Macaca fascicularis*) or rhesus macaque (*Macaca mulatta*) CHIKV infection have been utilized to evaluate the efficacy of three CHIKV vaccines that were described in six studies. The first study conducted in 1985 by Levitt *et al.* demonstrated vaccine-elicited protection induced by the first live-attenuated CHIKV vaccine, 181/25, in rhesus macaques [229]. Animals were challenged at 37 days after immunization with $5.0 \log_{10}$ PFU of the parental virus, CHIKV-AF15561, and all vaccinated animals had undetectable viremia. This vaccine advanced to clinical evaluation but further advancement was discontinued due to high rates of arthralgia in vaccinees in a Phase II trial [230]. In Akahata *et al.*, a virus-like particle vaccine, PXVX0317, was evaluated in rhesus macaques [231]. Immunized macaques developed robust CHIKV nAb responses $>10^4$ IC₅₀ titer, which compared to controls, protected them from intravenous challenge with 10^{10} PFU of a heterotypic strain of CHIKV. In this established model, naïve animals

developed viremia lasting 5-6 days, peaking at 1 dpi. The PXVX0317 vaccine advanced to clinical evaluation and recently completed a Phase III trial; licensure is anticipated in 2025. In Rossi *et al.*, a measles virus-vectored CHIKV vaccine, MV-CHIK-202/V-184, was evaluated in cynomolgus macaques [232]. MV-CHIK-202 immunization resulted in 100% CHIKV seroconversion and was shown to protect against viremia and fever after viral challenge with the La Reunión CHIKV strain. In two studies by Roques *et al.* in cynomolgus macaques, the protective efficacy of the IXCHIQ (VLA1553) vaccine is directly evaluated [233] and later a serological surrogate of protection was established for the vaccine through passive transfer of human sera to macaques prior to challenge [99]. Progression of these vaccines in the clinical pipeline is further described in **section 1.8.1**.

Two studies have evaluated the immunogenicity alone of CHIKV vaccine candidates in NHPs. One study evaluated the immunogenicity of a DNA CHIKV vaccine construct in rhesus macaques [234] and another study evaluated the immunogenicity of an mRNA vaccine expressing a CHIKV mAb in cynomolgus macaques [235], but protective efficacy against CHIKV infection was not evaluated in either study. These vaccines were shown to be immunogenic in the NHP model, and the mRNA vaccine, mRNA-1944, advanced to a Phase I clinical trial but further development has yet to be reported.

1.7.4 Utilization of the CHIKV NHP model to evaluate mAbs and antivirals

Two studies have evaluated CHIKV mAb therapies in NHP. Broeckel *et al.* utilized the CHIKV NHP challenge model to evaluate the therapeutic potential of a human monoclonal antibody therapy in rhesus macaques, finding that the therapy had the capacity to eliminate viremia and reduce disease [40]. One additional study evaluated the immunogenicity of mRNA encoding a CHIKV-neutralizing human mAb in cynomolgus macaques, showing antibody persistence in the sera out to 90 days after infection, but did not present data for challenge of the animals to evaluate therapeutic efficacy [235].

Antiviral evaluation in NHPs has been limited to just one study to date. In 2018, Roques *et al.* prophylactically evaluated the malaria antiviral drug, chloroquine, against CHIKV infection in cynomolgus macaques [236]. Despite observations of *in vitro* antiviral activity, chloroquine paradoxically enhanced CHIKV replication in the macaques through inhibition of antiviral humoral and cellular immunity.

1.7.5 MAYV NHP models of infection

There have been four published studies focused on experimentally characterizing MAYV infection in NHP including the 1967 Binn *et al* study in rhesus macaques [224], the 1981 Hoch *et al.* study demonstrating viremia in marmosets (*Callithrix argentata*)[193], our recent rhesus macaque study published in November of 2023 (Weber *et al.*) [39], and a recent study in cynomolgus macaques published in July of 2024 (Hamilton *et al.*) [237]. In our study, although we did not observe the same severity of pathology and clinical manifestation as reported for the CHIKV NHP model, we observed many similarities in immunity and pathogenesis of MAYV infection compared to CHIKV infection in rhesus macaques. MAYV infection is also non-lethal in macaques. Our results are described in our published manuscript included in **Chapter 6** of this dissertation. In the recent Hamilton *et al.* study, cynomolgus macaques were intravenously challenged with 10^6 PFU of one of three strains, one from each of the genotypes. The D and N strains were clinical isolates whereas the L genotype strain was isolated from a *Haemagogus* mosquito and was the same isolate used in our study: MAYV_{BeAr505411}. Hamilton *et al.* observed viremia that peaked at 2 dpi at 10^6 - 10^7 RNA copies/mL and was detectable 1-7dpi for all strains but reached nearly undetectable levels by 11 dpi; these kinetics were consistent with our study in rhesus macaques although our route of challenge was subcutaneous with 10^5 PFU. Notably, Hamilton *et al.* observed peak viremia that was about 2 logs lower for the genotype L strain compared to the other two strains, which could be attributable to the mosquito-isolated rather than human-isolated strain or due to the intravenous route of infection. Both studies reported a robust MAYV-specific nAb response, peak in antiviral pro-inflammatory cytokines/chemokines correlating with viremia, and similar viral tissue tropism. The animals in the Hamilton *et al.* study were euthanized at one month post-infection (in comparison to 10 dpi for our study) so comparison of these viral loads is not appropriate, but intriguingly high levels of virus persisted in the muscle and joints associated with the knee and in lymphoid and reproductive tissues at one month post-infection. Quantification of virus in additional muscles and joints was absent from this study as was determination of cross-nAb responses or other antiviral immune characterization. Overall, these two key studies investigating MAYV pathogenesis and immunity in two macaque models expand our translational knowledge of MAYV disease in humans and provide physiologically relevant models for the future evaluation of MAYV-specific countermeasures.

1.7.6 Mouse models of arthritogenic alphavirus disease

An abundance of lethal and non-lethal mouse models exist to study pathogenesis and immunity of arthritogenic alphavirus infection and to evaluate therapeutics. Lethal models of arthritogenic alphavirus infection have been developed in AG129 and IFNAR^{-/-} mice, while non-lethal models of disease and/or infection exist in RAG1^{-/-}, BALB/c, C57BL/6 and CD-1 mice. In all mouse models, age is an important factor as it has been linked to higher susceptibility to infection [238]. Some of the viral strains commonly used in alphavirus mouse challenge models are described in Lucas *et al.* [239]. Models have been developed for CHIKV [240], MAYV [241], RRV [242], and ONNV [13].

In the immunodeficient lethal models, mice exhibit footpad swelling and weight loss causing them to succumb to infection or reach humane endpoint in experimental studies. IFNAR^{-/-} mice are deficient in alpha and beta interferon receptors and AG129 mice are deficient in alpha, beta, and gamma interferon receptors. These mouse models succumb to infection because interferon signaling is essential for the control and protection from alphavirus infection [37, 243, 244]. Immunodeficient mouse models are useful for evaluating the ability of a vaccine or therapeutic agent to protect against disease (i.e. footpad swelling, weight loss, survival) and provide opportunities to characterize the contribution of different immune responses to protection, which can be interrogated using gene-specific knockout mice. Immunodeficient lethal models are generally not used for examining therapeutic impact on viral pathogenesis (i.e. viral tissue burden) because animals rapidly succumb to infection. Overall, immunodeficient mouse models recapitulate aspects of human infection but the type 1 interferon response is essential to control of infection in humans, so the model relies on an artificial immune environment. This can lead to overestimation of vaccine efficacy which is why it is necessary for vaccines to be evaluated in different models.

Immunocompetent mice do not lose weight following infection but they do develop footpad swelling as a proxy for arthritogenic disease. The kinetics of footpad swelling and viremia in all of these models vary with challenge route, dose, and viral strain. For example, CHIKV infection in C57BL/6 mice following subcutaneous footpad challenge (but not by intramuscular injection) results in biphasic contralateral footpad swelling, which is first detectable at 3-4 dpi, decreases at 5 dpi, and generally peaks again at 7-9 dpi [90, 102, 112]. In contrast, MAYV infection in C57BL/6

mice following subcutaneous footpad challenge results in contralateral footpad swelling that is not detectable until 6 dpi and generally peaks at 7 dpi [90, 91, 93]. RRV infection also causes footpad swelling that peaks at 6 or 7 dpi depending on the strain in C57BL/6 mice [94]. Histological analysis is another method that reliably shows evidence of arthritis and myositis in this model at the cellular level in infected tissues [245]. In addition to the development of arthritogenic disease, C57BL/6 mice exhibit viral tissue tropism that is indicative of arthritogenic disease and have detectable viral RNA and infectious virus in muscle, joint, spleen, and heart tissues after infection. Studies have also identified viral RNA in the brain, providing evidence of the neurotropic ability of alphaviruses and their ability to cross the blood-brain barrier [246, 247]. Mice deficient in T and B lymphocytes (RAG1^{-/-}) develop persistent MAYV viremia but do not develop muscle damage or succumb to infection, but pathogenesis (i.e. viral tissue burden) can still be characterized [248]. These qualities combined establish what are widely used and accepted models for the assessment of vaccine-elicited protection from infection and characterization of viral pathogenesis including viral persistence.

Mouse models of ONNV disease are more complicated due to the limited availability of low passage virulent isolates and limited studies to date have shown ONNV to replicate or be pathogenic in wild type mice [249, 250]. Susceptible models like IFNAR^{-/-} mice are used to study ONNV-induced disease [251]. ONNV mouse models are discussed further in our study in **Chapter 5** where we present lethal and non-lethal challenge models in AG129 and C57BL/6 mice that model ONNV disease following challenge with a highly virulent contemporary isolate from a febrile patient.

1.7.7 NHP disease models for encephalitic alphaviruses

NHP models have been developed for the encephalitic alphaviruses. EEEV is lethal in cynomolgus macaques following subcutaneous or aerosol challenge [252-255]. VEEV is non-lethal in macaques but macaques develop disease similar to humans [253, 256-258]. Following subcutaneous challenge with WEEV, cynomolgus macaques develop non-lethal disease that is more limited than disease following aerosol challenge which is lethal in some macaques [253, 259]. These models are generally more characterized in context of aerosol challenge, however, subcutaneous challenge more closely resembles natural mosquito transmission and this route has

been characterized in more detail recently [253]. NHP models have been utilized to evaluate vaccines for encephalitic alphaviruses [260].

Section 1.8: Alphavirus vaccine approaches

1.8.1 Vaccines for chikungunya virus

The landscape of vaccines targeting CHIKV in the clinical pipeline are briefly reviewed in this section and are represented in **Figure 1.8.1**. These vaccine approaches contrast in their platform design and there are advantages and disadvantages to each. Live attenuated virus (LAV) vaccine platforms are advantageous for their ease of production and replication to high titers yet require use of cell culture methods which can introduce challenges like contamination or challenges in scalability. LAV vaccines have the capacity to cause vaccine viremia in vaccinees which stimulates a robust immune response yet can cause more side effects especially in susceptible individuals. Viral vectored vaccines are advantageous for their association with both potent antibody and cellular immunity and have had success against CHIKV. A disadvantage is that pre-existing vector immunity can dampen the immune response and there is also a risk to genomic integration. In general, LAV and viral vaccines are best at mimicking the antigen presentation of natural infection through preservation of viral antigens in the most natural form. This makes for better immune responses upon virus exposure. Virus-like particle (VLP) and mRNA vaccines are also great immunogenic vaccine approaches and the platforms can be designed to naturally present target antigens, preserving antigenic structure and epitope recognition. Another factor that should be considered for platform design is the vaccine storage condition, which depending on the requirements, has the capacity to impact global vaccine access. Altogether, there are pros and cons to every vaccine platform that must be carefully weighed depending on the target population.

Figure 1.8.1. Landscape of CHIKV vaccines in the clinical development pipeline.

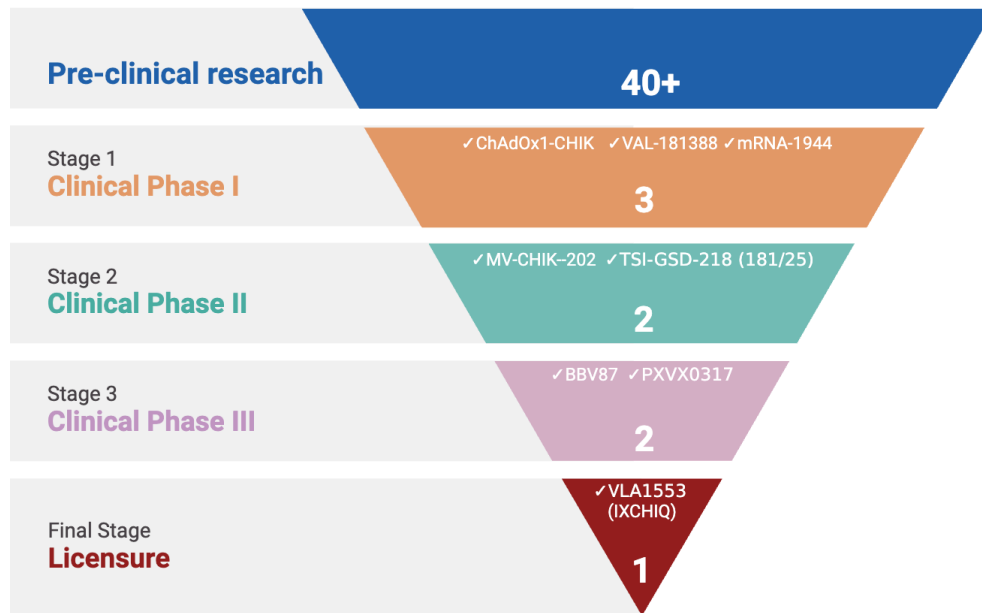


Figure 1.8.1. Vaccines targeting CHIKV in various phases of clinical development: pre-clinical research to licensure. Graphic generated by Whitney Weber.

1.8.1a The first licensed CHIKV vaccine: IXCHIQ

Prior to 2023, there were no vaccines or therapeutics approved for any alphavirus infection. In November 2023, the first vaccine targeting CHIKV was approved by the U.S. Food and Drug Administration (FDA) [261] and by additional regulators in 2024 including the European Medicines Agency [262] and Health Canada. The vaccine, referred to as IXCHIQ also known as VLA1553, is a live-attenuated vaccine (LAV) platform based upon the CHIKV_{LR2006-OPY1} backbone containing a large genetic deletion in nsP3 that attenuates but does not ablate viral replication [101]. The vaccine is delivered as a single intramuscular injection. IXCHIQ was evaluated in mice and cynomolgus macaques to establish a protective neutralizing antibody threshold due to the challenges of conducting an efficacy trial with the sporadic nature of CHIKV outbreaks [99, 101, 233, 263]. IXCHIQ has now been administered to over 4,000 individuals in non-endemic settings and is generally immunogenic and well tolerated although viremia and some side effects including headache, fever, arthralgia, and myalgia have been noted [264-267]. Antibody persistence at 2 years post-vaccination for participants in a Phase 3b trial was recently

reported [268]. Additional trials are ongoing to evaluate IXCHIQ in endemic settings and in adolescents. Interim results for a Phase III trial in adolescents in Brazil were very recently reported, indicating the vaccine was safe and immunogenic in individuals who were either seropositive or seronegative for CHIKV at baseline [124], which has been shown to be a vaccine hurdle in licensure of other vaccines such as Dengvaxia [269, 270].

1.8.1b Phase III vaccine candidates: PXVX0317 and BBV87

An aluminum hydroxide-adjuvanted virus-like particle (VLP) CHIKV vaccine candidate approaching licensure is PXVX0317 (also VRC-CHKVLP059-00-VP), which contrasts with IXCHIQ in structure, platform, dose, and storage conditions (**Figure 1.8.2**). PXVX0317 has been evaluated in BALB/c mice [231], NHPs [231], a Phase I trial [271, 272], two Phase II trials [123, 273-275], and in a Phase III trial (unpublished). The vaccine was produced by Bavarian Nordic. The immunogenicity profile in terms of neutralizing antibody potency and breadth is comparable for PXVX0317 and IXCHIQ, which are compared in Weber *et al.* (*BioDrugs*) (**Appendix III**) [10] and independently analyzed for IXCHIQ in Weber *et al.* (*Vaccines*) [69] in **Chapter 3** and for PXVX0317 in Raju *et al.* [274]. Importantly, PXVX0317 is the first CHIKV vaccine reported to be administered to baseline CHIKV seropositive individuals, which was unintentional but was revealed after the fact [123]. The VLP vaccine was well tolerated and immunogenic in individuals with pre-existing immunity, although vaccinees did experience a higher incidence of swelling at injection site compared with baseline seronegative individuals.

A second Phase III vaccine candidate approaching licensure is BBV87, a whole virus (ECSA strain), formalin-inactivated platform produced by Bharat Biotech International and the International Vaccine Institute. The vaccine is two intramuscular doses, 4 weeks apart, and was shown to be immunogenic and sterilely protected against viral tissue dissemination in BALB/c mice [276]. BBV87 completed Phase II and III trials at the end of 2023 in Latin America and Thailand (Columbia, Guatemala, Panama, Costa Rica, and Thailand). Publication of clinical trial results or evaluation in NHPs is currently absent in the literature as of September 2024.

TSI-GSD-218, also known as 181/25, was the first CHIKV live attenuated vaccine developed using serial plaque to plaque passaging of the Asian lineage AF15561 strain isolated in Thailand in 1962 in primary grivet kidney cells and human lung MRC-5 cells [229]. The candidate was evaluated in suckling mice as well as rhesus macaques and was found to be both immunogenic and protective against lethal CHIKV challenge in mice and protective against viremia in the macaques [229]. The vaccine was evaluated in a Phase II study and was found to be immunogenic but was considered insufficiently attenuated when it caused transient arthralgia in vaccinees [230]. Later studies showed that the strain was attenuated by only two amino acid changes in the E2 glycoprotein, explaining its instability and ability to cause disease in vaccinees [277].

The live-attenuated measles virus-vectored CHIKV vaccine, MV-CHIK-202, completed Phase I and Phase II trials but further advancement was put on hold in February of 2023 [278, 279]. This vaccine was shown to confer cross-nAb against ONNV, MAYV, RRV, and other arthritogenic alphaviruses[75]. The vaccine was initially tested in mice and a single dose conferred protection against lethal challenge [103]. MV-CHIK-202 immunization of cynomolgus macaques resulted in 100% CHIKV seroconversion and was shown to protect against viremia and fever after viral challenge with the La Reunión CHIKV strain [232].

1.8.1d Phase I vaccine candidates

There are three CHIKV vaccines that have reached Phase I clinical trials but their development has not continued to date: ChAdOx1 Chik (CHIK001), mRNA-1944, and mRNA-1388 (VAL-181388).

ChAdOx1 Chik is a chimpanzee adenovirus-vectored vaccine expressing the CHIKV structural proteins to form a VLP. ChAdOx1 Chik was found to be immunogenic in BALB/c mice [280] and protected against lethal challenge in AG129 mice [281]. This vaccine also partially cross-protected against MAYV [92], which we explore in a similar study in **Chapter 4**. In a Phase I study, a single dose of ChAdOx1 Chik immunization resulted in 100% CHIKV seroconversion in just 14 days [282]. In an additional Phase 1b trial, ChAdOx1 Chik was evaluated in participants in Monterrey, Mexico; the results have yet to be published (as of September 2024) but the study concluded in 2022.

The first CHIKV mRNA vaccine developed, mRNA-1944, was formulated with a lipid nanoparticle and encodes the heavy and light chains of a human, neutralizing monoclonal antibody (CHKV-24). This vaccine was evaluated in AG129 mice and protected against lethal challenge and was immunogenic in cynomolgus macaques but no efficacy data was presented [235]. The mRNA-1944 vaccine was evaluated in a Phase I proof of concept clinical trial and was generally safe and immunogenic with limited reactogenicity in participants [283]. There have been no additional trials initiated.

A second CHIKV mRNA vaccine, mRNA-1388 (VAL-181388), was constructed to encode the entire CHIKV structural polyprotein. Preclinical reports evaluating the vaccine candidate in mouse or NHP animal models are absent from the literature as of September 2024. The vaccine was evaluated in a Phase I clinical trial dose-ranging study and although it was safe and generally well tolerated, the neutralizing antibody response waned significantly (100% seroconversion to 79%) after one-year post-vaccination [284, 285]. Additional clinical trials to advance the candidate have not been reported as of September 2024.

1.8.2 Vaccines for Mayaro virus

A number of vaccines have now been developed for MAYV [190], but the market is limited for this due to viral distribution being restricted to Latin America with smaller outbreaks. Thus, none of the vaccines that have been developed for MAYV have entered clinical development. MAYV vaccine approaches have included inactivated [286], live-attenuated [93, 287, 288], viral vectors [91, 92], VLP [289], and DNA/RNA [290] platforms. None of the vaccines developed for MAYV have yet to be evaluated in an NHP model of infection. Select cross-reactive vaccines targeting MAYV are discussed in **Chapter 4** and an approach to administer an adenovirus-vectored MAYV vaccine in combination with a CHIKV vaccine to improve cross-reactive immunity is described [90].

1.8.3 Vaccines for Ross River virus

RRV is another major arthritogenic alphavirus for which vaccines are actively being developed. One RRV vaccine has even had success in a Phase III clinical trial [291]. This vaccine candidate

is a formaldehyde-inactivated vaccine that was first shown to be efficacious in mice [105, 292] and immunogenic in a Phase I/II dose-escalation clinical trial [293]. There are no additional vaccines in the clinical pipeline targeting RRV.

1.8.4 Vaccines for other alphaviruses

A vaccine was recently developed for Getah virus (GETV), which is very similar antigenically to RRV and primarily infects livestock animals like pigs, horses, cattle, sheep, and goats [294]. GETV has not yet been identified as a human pathogen.

1.8.5 Vaccines for the encephalitic alphaviruses

The most well known and most clinically advanced vaccine for any of the encephalitic alphaviruses is TC-83, the live attenuated vaccine for VEEV. TC-83 is administered to military personnel and laboratory workers at risk of infection. The vaccine was shown to protect mice from subcutaneous challenge with homotypic and heterotypic strains, but mice remained susceptible to breakthrough infection following aerosol challenge [295]. Despite being a live attenuated viral vaccine, TC-83 vaccinees do not reliably seroconvert, and vaccination is associated with serious adverse events including myalgia, respiratory symptoms, heart issues, and even spontaneous abortion [296-298]. The development and approval of additional vaccines targeting VEEV is warranted, and is ongoing with several vaccines in clinical trials [74].

1.8.6 Cross-protective vaccines, multivalent vaccines, and pan-alphavirus vaccine potential

A number of vaccines with cross-protective efficacy have been developed and evaluated against alphavirus challenge in mice. No studies to date have evaluated vaccine-elicited immunity against a heterotypic alphavirus in NHP, although challenge with heterotypic CHIKV strains has been demonstrated. Vaccines are predominantly developed against CHIKV and thus cross-protective immunity is typically assessed against MAYV, ONNV, UNAV, or RRV. Several candidates have demonstrated heterologous protection from infection. Vaccines have been developed against MAYV and evaluated against CHIKV and/or UNAV [90-93]. We (**Chapter 5**) and others [94, 106] have also evaluated CHIKV vaccines against ONNV. A number of studies have explored this concept of cross-protection, but a key study by Nguyen *et al.* elegantly demonstrated clear inequities in cross-protection mediated by infection or vaccine-elicited immunity in a matrixed

fashion for multiple arthritogenic alphaviruses [94]. This study showed that one-way antigenic relationships can exist or at least imbalances in reciprocal immunity, this concept is expanded on in **Chapter 4**.

A potential strategy to improve partial cross-protection due to lower cross-reactivity is to develop multivalent vaccines. Multivalent vaccines can be a single construct encoding multiple antigens or multiple constructs mixed into a single formulation. Multivalent antigen presentation is known to elicit durable protective immunity that is superior to monovalent vaccine antigen presentation due to improved B-cell cross-linking and activation, CD4⁺ T-cell help, and therefore B-cell imprinting and differentiation into long-lived, antibody-secreting plasma cells [299]. This leads to multivalent antigen exposure to a single B-cell, thus secretion of a repertoire of antibodies with specificity to shared and diverse epitopes [300]. The virus structure lends itself to multimeric antigen presentation, as numerous proteins are antigenically accessible on the virion surface to antibody recognition, which is why whole virus and virus-like particle vaccine platforms are effective. Successful use of multivalent vaccines has been demonstrated for influenza virus, human papilloma virus, SARS-CoV-2, arenaviruses, and other pathogens. A bivalent trans-amplifying RNA vaccine for CHIKV and RRV has been reported, but only immunogenicity and no protective data was shown [301]. In **Chapter 4**, we describe a coadministration approach for adenovirus-vectored vaccines against CHIKV and MAYV as well as heterologous prime-boost with these constructs and illustrate that cross-protection from disease can be achieved using these strategies [90]. There is potential that these adenovirus-vectored alphavirus vaccine constructs could be combined with additional constructs for a multivalent approach. A multivalent VLP vaccine against CHIKV, ZIKV, yellow fever virus, and Japanese encephalitis virus has been developed but no efficacy data was presented [302]. Additional multivalent vaccines targeting more than two arthritogenic alphaviruses have not been reported to date.

For the encephalitic alphaviruses, a trivalent VLP vaccine was developed targeting VEEV, EEEV, and WEEV and was shown to protect against lethal disease in mice and NHPs; this vaccine is currently in Phase I clinical trials [260, 303]. An additional trivalent DNA vaccine targeting VEEV, EEEV, and WEEV was shown to be immunogenic in mice and rabbits and efficacious in mice but has yet to enter clinical development [304]. These trivalent approaches targeting the

encephalitic alphaviruses could also be paired with arthritogenic alphavirus antigens to produce a pan-alphavirus vaccine.

1.8.7 Vaccine-elicited versus infection-elicited immunity

Direct comparison of vaccine-elicited versus infection-elicited alphavirus immunity is rarely made side by side in a study, at least for alphaviruses. Vaccine design is inherently outpaced by viral evolution due to the length of time it takes for vaccine evaluation and the approval process, which is especially relevant for rapidly evolving pathogens like influenza and HIV. Therefore, immune evasion is more likely in context of vaccine-elicited versus infection-elicited immunity as viral antigens evolve over time. In contrast to these pathogens, alphaviruses are known for their antigenic stability between strains, despite genetic evolution, the emergence of new genotypes, and the expansion of circulation of new strains. It has been continuously demonstrated throughout the history of CHIKV emergence and expansion that the genotypes conform to a single serogroup [69, 274, 305]. Even with antigenic stability throughout the evolution of these viruses, the vaccine platform type and antigenic target are probably the biggest contributors to the differences in vaccine versus infection-elicited immunity. Some vaccine platforms display their antigens in a similar fashion to the virus structure (i.e. live-attenuated, inactivated, viral-vectored, VLP) while other platforms (i.e. subunit, mRNA) may only encode the most immunogenic protein of the virus. Indeed, antigen presentation due to vaccine design can result in the development of immunity that is very different from immunity developed in response to natural infection, which can be for better or worse depending on the correlate(s) of protection from infection. For example, vaccines can be developed using consensus viral sequences across strains with the aim to create more broad immune responses with antigenic breadth against different strains as they emerge or evolve. This is currently a common approach for influenza and coronavirus vaccines. However, this approach may result in the development of antibodies targeting epitopes that contrast to epitopes targeted by infection-elicited antibodies and could lead to infection due to neutralization escape mechanisms. There are also instances where vaccines target conserved epitopes that generally don't change significantly with viral evolution, leading to more efficacious, durable immunity against emerging variants. In our study in **Chapter 3**, we analyzed the cross-neutralizing antibody breadth elicited by LAV IXCHIQ (VLA1553) vaccination and directly compared these responses to the cross-neutralizing antibody breadth induced by natural CHIKV infection [69]. We found that the potency

and breadth of these antibodies in these groups were nearly equivalent, which is the first reported comparison of this human antibody comparison for vaccine to wildtype infection-elicited CHIKV immunity.

A first example of CHIKV hybrid immunity, a combination of infection and vaccine-elicited immunity, now exists in CHIKV seropositive individuals (who were seronegative by ELISA at baseline) who were vaccinated with CHIKV VLP PXVX0317 [123]. These individuals developed higher neutralizing antibody levels than seronegative individuals and the vaccine was generally well tolerated, with the exception of the incidence of higher injection site pain. Hybrid immunity is well described for coronaviruses and influenza, but this was the first example in context of alphavirus immunity in humans. More recently, IXCHIQ was evaluated in an endemic area in adolescents with pre-existing CHIKV immunity and was found to be safe, immunogenic, and well tolerated [306].

Chapter 2: Infection with chikungunya virus confers heterotypic cross-neutralizing antibodies and memory B cells against other arthritogenic alphaviruses predominantly through the B domain of the E2 glycoprotein

Status: Published March 13th, 2023, in PLoS Neglected Tropical Diseases.

Note: Data appears in Drs. John M Powers & Zoe L. Lyski's dissertations, final published data included here

John M. Powers ^{1*#}, Zoe L. Lyski ^{2*##}, **Whitney C. Weber** ^{1,2*}, Michael Denton ¹, Magdalene M. Streblow ¹, Adam T. Mayo ¹, Nicole N. Haese ¹, Chad D. Nix ², Rachel Rodríguez-Santiago ³, Luisa I. Alvarado ³, Vanessa Rivera-Amill ³, William B. Messer ^{2,4,5}, Daniel N. Streblow ^{1,6}

¹ Vaccine and Gene Therapy Institute, Oregon Health and Science University, Beaverton, Oregon, USA

² Department of Molecular Microbiology and Immunology, Oregon Health and Science University, Portland, Oregon, USA

³ Ponce Health Sciences University/ Ponce Research Institute, Ponce, Puerto Rico

⁴ Department of Medicine, Division of Infectious Disease Oregon Health and Science University, Portland, Oregon, USA

⁵ OHSU-PSU School of Public Health, Program in Epidemiology, Oregon Health and Science University, Portland, Oregon, USA

⁶ Division of Pathobiology and Immunology, Oregon National Primate Research Center, Beaverton, Oregon, USA

* Contributed equally to this manuscript

Current Address: Department of Epidemiology, University of North Carolina at Chapel Hill, Chapel Hill, NC, USA

Current address: Department of Immunobiology, University of Arizona, Tucson, AZ, USA.

PLoS Neglected Tropical Diseases 17(3):e0011154. March 13th, 2023.

Doi: [10.1371/journal.pntd.0011154](https://doi.org/10.1371/journal.pntd.0011154)

Author contributions

Conceptualization: J.M.P, Z.L.L., N.N.H, W.B.M, D.N.S; Data curation: J.M.P, Z.L.L., W.C.W, W.B.M.; Formal analysis: J.M.P, Z.L.L., W.C.W, D.N.S; Investigation: J.M.P, Z.L.L., W.C.W, M.D., M.M.S., A.T.M., N.N.H, C.D.N., D.N.S; Methodology: J.M.P, Z.L.L., W.C.W, C.D.N, M.D., N.N.H, D.N.S; Visualization: D.N.S.; Writing – original draft: J.M.P, Z.L.L., W.C.W, N.N.H, W.B.M, D.N.S; Writing – review & editing: J.M.P, Z.L.L., W.C.W, N.N.H, R.R., L.I.A, V.R., W.B.M, D.N.S; Resources: R.R., L.I.A, V.R., W.B.M., D.N.S.; Funding acquisition: V.R., W.B.M, D.N.S; Project administration: W.B.M., D.N.S; Supervision: W.B.M., D.N.S.

Section 2.1.1: Abstract

Infections with Chikungunya virus, a mosquito-borne alphavirus, cause an acute febrile syndrome often followed by chronic arthritis that persists for months to years post-infection. Neutralizing antibodies are the primary immune correlate of protection elicited by infection, and the major goal of vaccinations in development. Using convalescent blood samples collected from both endemic and non-endemic human subjects at multiple timepoints following suspected or confirmed chikungunya infection, we identified antibodies with broad neutralizing properties against other alphaviruses within the Semliki Forest complex. Cross-neutralization generally did not extend to the Venezuelan Equine Encephalitis virus (VEEV) complex, although some subjects had low levels of VEEV-neutralizing antibodies. This suggests that broadly neutralizing antibodies elicited following natural infection are largely complex restricted. In addition to serology, we also performed memory B-cell analysis, finding chikungunya-specific memory B-cells in all subjects in this study as remotely as 24 years post-infection. We functionally assessed the ability of memory B-cell derived antibodies to bind to chikungunya virus, and related Mayaro virus, as well as the highly conserved B domain of the E2 glycoprotein thought to contribute to cross-reactivity between related Old-World alphaviruses. To specifically assess the role of the E2 B domain in cross-neutralization, we depleted Mayaro and Chikungunya virus E2 B domain specific antibodies from convalescent sera, finding E2B depletion significantly decreases Mayaro virus specific cross-neutralizing antibody titers with no significant effect on chikungunya virus neutralization, indicating that the E2 B domain is a key target of cross-neutralizing and potentially cross-protective neutralizing antibodies.

Section 2.1.2: Author summary

The emergence and re-emergence of alphaviruses as important human pathogens raises questions about the durability and breadth of alphavirus immunity following natural infection in humans. In this study, we examine human immune sera from twelve individuals infected (up to 24 years) previously with chikungunya virus and test the sera against a panel of five Old-World arthritogenic alphaviruses and one New-World encephalitic alphavirus. Both homotypic and cross-reactive memory B-cells were identified in subjects out to 24 years post infection. Our results indicate that infection with chikungunya virus results in a robust and durable cross-reactive humoral immune response. Such a response could potentially provide immunity against repeat infection with chikungunya as well as related alphaviruses for years to decades after initial infection. This cross-reactivity might contribute to restricted transmission of closely related alphaviruses and indicates the potential for chikungunya candidate vaccines to elicit broad protection against other alphaviruses in the Semliki Forest complex.

Section 2.2: Introduction

Alphaviruses, members of the family *Togaviridae*, are a large group of arthropod-borne viruses with worldwide distribution that cause both sporadic outbreaks and epidemics. These predominantly mosquito-borne viruses have a wide host range and can replicate in a variety of cell types [3, 307, 308]. Alphaviruses are broadly grouped in seven distinct antigenic complexes—Barmah Forest, Eastern Equine Encephalitis, Middleburg, Ndumu, Semliki Forest, Venezuelan Equine Encephalitis, and Western Equine Encephalitis [309]. These viruses can be broadly divided into two categories, New and Old World, based on phylogenetic relatedness and clinical manifestations of disease. While infections with Old World alphaviruses, such as chikungunya virus (CHIKV) and Mayaro virus (MAYV) predominantly cause myalgia and arthralgia, New World alphaviruses such as Venezuelan equine encephalitis virus (VEEV) and Eastern equine encephalitis virus (EEEV) infections can cause life-threatening encephalitis.

Of the alphavirus members, CHIKV has the widest global distribution, with CHIKV transmission reported in over 100 countries worldwide [11, 310]. Before 2013, CHIKV had not yet been locally acquired or transmitted within the Americas [311]. Historically, circulating

predominantly in regions of Africa and Asia, CHIKV emerged on a global scale in the mid-2000s, resulting in outbreaks in Africa, Asia, as well as the Caribbean and North, Central, and South Americas, leading to almost 2 million reported infections [161]. At the time of the writing of this manuscript (October 27th 2022), there have been 338,592 cases with 70 deaths in 2022, with the majority of the cases occurring in Brazil (ECDC). In the current investigation, we characterize samples from an endemic human cohort in Puerto Rico. The island of Puerto Rico experienced a CHIKV epidemic starting in May 2014 with official surveillance reporting 28,327 suspected cases and 31 deaths by the epidemic's end [312].

Other related Old-World alphaviruses include O'nyong nyong virus (ONNV), which forms a monophyletic group with CHIKV. ONNV is endemic in sub-Saharan Africa and periodically causes outbreaks in West and East Africa [313, 314]. Mayaro (MAYV) and Una (UNAV) viruses are closely related alphaviruses that commonly cause disease outbreaks in Central and South America [315]. The most distant member of the SFV complex that we included in our alphavirus panel is Ross River virus (RRV), which is endemic to Australia and several neighboring Pacific Islands [316]. Outside of the SFV complex are the distantly related New World encephalitic alphaviruses that circulate in North, South, and Central America.

In general, alphaviruses are ~70 nm enveloped viruses with an icosahedral capsid of $T = 4$ symmetry that is composed of 240 capsid monomers. Each virus particle contains ~10–12 kb single-stranded, positive sense RNA genome that contains two open reading frames, both translated with a 5' cap and 3' poly-A tail [316-318]. The viral genome encodes four nonstructural proteins (nsP1 –nsP4) involved in RNA replication, and five structural proteins (Capsid, E3, E2, 6K, E1) required for viral encapsidation and budding [3, 319, 320]. Structural E1-E2 heterodimers trimerize to form the surface spikes of the virus envelope responsible for attachment and entry into host cells. Specifically, E2 is responsible for cellular receptor binding, and E1 mediates membrane fusion [320]. The structural proteins E1 and E2 are key targets of the host antibody response. In humans and mice, the antibody response is primarily generated against E2 [73, 321-323]. Previous studies have reported the development of cross-neutralizing antibodies (Abs) in model organisms and humans following infection with SFV complex alphavirus members, and the B domain of the E2 (E2 B) glycoprotein has been implicated as a potential target for broadly cross-neutralizing antibodies due to the disruption of the trimeric spike [323-326].

Virus-specific Abs are initially secreted by short-lived plasma cells to help combat the current infection. Virus-specific B-cells further differentiate in germinal centers of peripheral lymph nodes where they undergo affinity maturation and exit the lymph node as one of two types of long-lived memory cells. One cell type, long-lived plasma cells (LLPCs), traffic to bone marrow where they secrete large amounts of antigen-specific Abs that circulate in the serum for months to years post-exposure [55]. LLPC-derived Abs are thought to protect against repeat infections with homologous or closely related pathogens and are often regarded as the first line of defense. Memory B-cells (MBCs) also differentiate in germinal centers and circulate in low numbers in peripheral blood. MBCs do not secrete Abs, but instead patrol peripheral circulation for invading pathogens, poised to quickly respond to repeat infections by proliferating and differentiating into Ab secreting cells. It has been reported that MBCs respond to related but antigenically distinct pathogens that evade preexisting serum Abs [327, 328]. Consequently, MBCs have the potential to play a critical role in developing broad immunity especially in the face of waning Ab titers and the emergence of new closely related alphaviruses.

To further characterize the durability and breadth of cross-reactive anti-alphavirus Abs and MBCs, we evaluated a panel of convalescent samples from subjects enrolled in one of two larger human arbovirus cohorts. The first, a non-endemic (travelers) cohort based in Portland, Oregon and the second, an endemic cohort based in Ponce, Puerto Rico. Subjects had suspected or confirmed CHIKV infection, further confirmed by serology (CHIKV 50% neutralization titer > 1:20) and samples from three alphavirus naïve subjects (CHIKV 50% neutralization titer < 1:20) were included as controls (Table 2.1). We evaluated study participants for the presence of CHIKV neutralizing antibodies, cross-alphavirus neutralizing antibodies, and CHIKV-specific and cross-reactive memory B cells. We observed that subjects have varying levels of neutralizing antibodies against other SFV-complex members, but this breadth generally did not extend to distantly related VEEV, with the majority of subjects exhibiting VEEV plaque reduction neutralizing titer (PRNT) values below the limit of detection. Similarly, interrogation of the MBC compartment following natural infection identified MBCs capable of recognizing both CHIKV and MAYV. Additionally, we looked for the presence of antibodies and MBCs that recognize the E2 B domain, which has previously been implicated as a potential target for broadly cross-neutralizing antibodies [324, 326]. The results of this study indicate that natural infection with CHIKV elicits a robust and durable immune response that would ostensibly be protective against repeat infection with CHIKV

as well as related Semliki Forest complex alphaviruses for years to decades after initial infection. This cross-reactivity might contribute to the restriction of transmission of closely related alphaviruses in arbovirus endemic regions.

Section 2.3: Results

2.3.1 Study subjects

Twelve subjects with a confirmed or suspected history of CHIKV infection that occurred between 1992 and 2016 were used for this study (**Table 2.1**). Individual subject sera and peripheral blood mononuclear cells (PBMC) were obtained from timepoints ranging from 1–24 years post-infection. Five of the subjects are from a larger endemic cohort of arbovirus immune subjects in Ponce, Puerto Rico (color coded in orange), these infections were PCR confirmed. Seven subjects are from a larger non-endemic (travelers) cohort of arbovirus exposed individuals based in Portland, Oregon (color coded in blue) who were identified through clinical and travel history as well as serology testing (**Table 2.1**). Each of these subjects reported the incidence of at least one symptom consistent with alphavirus infection (**Table 2.1**). Based on initial screening, subjects with 50% plaque reduction neutralization titers (PRNT₅₀) of >1:20 against CHIKV were presumed to be CHIKV-immune.

Table 2.1. Summary of subject data

Subject ID	Age at time of infection	Country of birth	Country of infection	Range of time post-infection for serum collection (Years)	CHIKV PRNT ₅₀	Symptoms
1	45	Puerto Rico	Puerto Rico	2.8–6	12673	fever, muscle/joint pain, headache
3	13	Puerto Rico	Puerto Rico	4.3–5.1	8464	fever, muscle/joint pain, rash
8	17	Puerto Rico	Puerto Rico	2.8–5.3	11834	fever, muscle/joint pain, rash, malaise
13	12	Puerto Rico	Puerto Rico	3.4–4	59931	rash
14	13	Puerto Rico	Puerto Rico	3.4	14347	fever, joint/muscle pain, rash, malaise
16	26	United States	El Salvador	1.1–6.9	17552	fever, muscle/joint pain, rash, headache, malaise
17	48	United States	Papua New Guinea	24.3	81.8	fever, headache, malaise
18	26	India	India	9.3–12.4	1202	fever, muscle/joint pain, malaise
19	30	India	India	8.7–11.4	1130	fever, muscle/joint pain, rash, headache, malaise
20	27	India	India	7.9	12565	fever, muscle/joint pain, rash, headache, malaise
21	24	United States	Haiti	3.5–7.4	5996	fever, muscle/joint pain, rash, headache, malaise
22	23	United States	Haiti	4–8.2	17924	fever, muscle/joint pain, rash, headache, malaise
Naïve 1	N/A	United States	N/A	N/A	<1:20	N/A
Naïve 2	N/A	United States	N/A	N/A	<1:20	N/A
Naïve 3	N/A	United States	N/A	N/A	<1:20	N/A

<https://doi.org/10.1371/journal.pntd.0011154.t001>

Table 2.1. Subjects with confirmed or suspected CHIKV infection were enrolled in either an endemic cohort (Ponce, Puerto Rico; color coded in orange), a non-endemic cohort (Portland, Oregon; color coded in blue), or an alphavirus naïve cohort (Portland, Oregon; color coded in black). Subjects are assigned an ID with age, country of birth, country of infection, range of time-post infection for serum collection, CHIKV PRNT₅₀ at time of primary blood draw, and reported symptoms displayed.

2.3.2 Alphavirus specific neutralization and antigenic relationship by subject

Immune serum from twelve subjects with presumed or confirmed CHIKV infection history and three naïve subjects (**Table 2.1**) were used in neutralization assays against a panel of five alphaviruses of the SFV antigenic complex including CHIKV, ONNV, MAYV, UNAV, and RRV, as well as VEEV, which is a representative virus from the VEEV antigenic complex. Amino acid sequences for E1, 6K, and E2 were used to generate the phylogenetic tree (**Fig 2.1A**) to demonstrate the genetic relatedness of the viruses used in this study. We conducted 50% plaque reduction neutralization tests (PRNT₅₀) for each of the sera against the panel of alphaviruses to determine antigenic breadth and durability following alphavirus infection (**Fig 2.1B, 2.1C** and **2.1D** and **2.S1 Table**). Serum samples from five endemic subjects, 4 longitudinal and 1 single time-point, (**Fig 2.1B**) and seven non-endemic subjects, 5 longitudinal and 2 single time-points, (**Fig 2.1C**) were tested for serum neutralization. All 12 subjects had anti-CHIKV neutralizing

antibodies with the highest levels of detection observed for endemic Subject 13 (V2) and non-endemic Subject 16 (V2), which were 4.0 and 6.9 years out from initial infection, respectively, indicating the presence of anti-CHIKV immunity lasting for greater than 20 years following natural infection in both endemic and non-endemic transmission settings (**Fig 2.1B and 2.1C**). Anti-CHIKV neutralizing antibody levels were lowest for non-endemic Subject 17, which demonstrated the highest level of neutralizing antibodies against RRV with a PRNT₅₀ of 1120. This result leads us to suspect subject 17, who was infected in Papua New Guinea, may have experienced a primary RRV infection with cross-reactive antibodies against CHIKV (**Table 2.1 and Fig 2.1C**). Interestingly, this person still had durable heterotypic immunity even at >20 years post infection or as an alternative this person may have undergone infection with the same or a related virus. When quantifying cross-neutralizing antibodies against the other five alphaviruses, we found that neutralizing antibody levels were highest for ONNV, which is the closest related of the five viruses to CHIKV; and cross-neutralizing antibody levels decreased the more phylogenetically divergent the virus is from CHIKV (**Fig 2.1D**). Not surprisingly, high levels of CHIKV-neutralizing antibodies correlate with higher levels of cross-neutralizing antibodies. Our statistical analysis showed CHIKV neutralizing antibody titers were significantly higher than cross-neutralizing antibody titers against MAYV, UNA, RRV, and VEEV but not ONNV, which is expected given the phylogenetic similarity of CHIKV and ONNV (***p* = 0.0001, *****p* = <0.0001) (**Fig 2.1D**). Overall, for 9 of the 12 subjects that we serologically profiled at more than one time point post-infection, we found longitudinal changes in both homotypic and heterotypic neutralization over time to be variable compared to the original blood draw but overall antibodies remained stable overtime (**Fig 2.1B and 2.1C**).

Figure 2.1. Longitudinal serology for endemic and non-endemic patients.

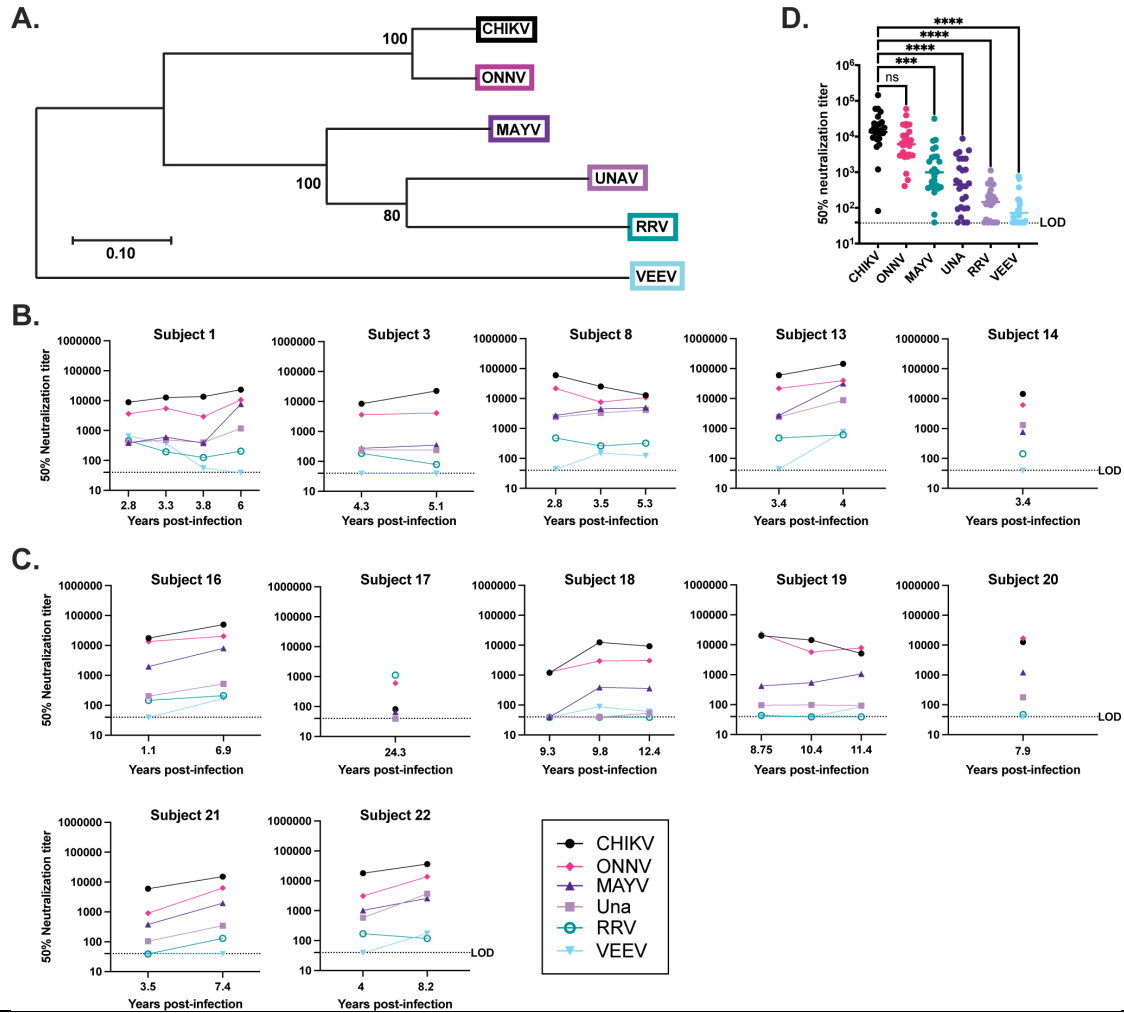


Figure 2.1. (A) Phylogenetic tree produced using the E1, 6k, and E2 amino acid sequences for the six alphaviruses under investigation; viruses are color coded to match serology graphs. (B, C) Sera samples from each subject were tested for neutralization activity against CHIKV, ONNV, RRV, MAYV, Una, and VEEV by plaque reduction neutralization titer assays (PRNT) performed on confluent monolayers of Vero cells. Shown are the average 50% reduction titer values (PRNT₅₀) calculated by variable slope non-linear regression using Prism software. Longitudinal serology is shown for 9/12 human subjects. Additional samples for the other human subjects were unavailable. Endemic subject serologic profiles are shown in (B). Serology for non-endemic subjects is shown in (C). (D) Summarizes the breadth of cross-neutralization data for both endemic and non-endemic subjects at all time points presented in (B) and (C). The statistical analysis to compare grouped cross-neutralizing PRNT₅₀ values to CHIKV PRNT₅₀ was completed using an ANOVA and Friedman's test ***p = 0.0001, ****p = <0.0001. Limit of detection (LOD) is 40, samples below the LOD were assigned an arbitrary value of 39.

Table 2.S1. Compiled PRNT₅₀ values for each subject against the six alphaviruses serologically profiled in this study.

	Subject	Years post-infection	CHIKV PRNT ₅₀	Una PRNT ₅₀	MAYV PRNT ₅₀	VEEV PRNT ₅₀	ONNV PRNT ₅₀	RRV PRNT ₅₀
Endemic	1 V1	2.8	8865	404	383	650	3648	458
	1 V2	3.3	12673	488	601	376	5486	195
	1 V3	3.8	13612	403	379	56	2925	126
	1 V4	6	23301	1181	7661	<1:40	10649	204
	3 V1	4.3	8464	2400	2737	43	21704	479
	3 V2	5.1	28414	ND	1080	<1:40	7863	ND
	8	2.8	11834	1124	519	<1:40	2679	182
	8 V2	3.5	25193	3300	4498	150	7582	261
	8 V3	5.3	12830	4119	4972	122	10836	322
	13	3.4	59931	2400	2737	43	21704	479
	13 V2	4	144824	8750	31764	772	39498	611
	14	3.4	14347	1302	775	<1:40	6157	143
Non-endemic	16	1.1	17552	203	1977	<1:40	2727	147
	16 V2	6.9	49758	521	8056	171	20356	210
	17	24.3	82	<1:40	65	<1:40	602	1122
	18	9.3	1202	<1:40	<1:40	<1:40	409.8	<1:40
	18 V2	9.8	12523	<1:40	387	88	2963	<1:40
	18 V3	12.4	9293	54	361	61	3067	<1:40
	19	8.75	20034	96	422	<1:40	22546	43
	19 V2	10.4	14426	98	540	<1:40	5683	<1:40
	19 V3	11.4	5146	93	1055	86	7850	<1:40
	20	7.9	12565	178	1223	<1:40	59589	47
	21	3.5	5996	105	380	<1:40	907	<1:40
	21 V2	7.4	15244	345	1974	<1:40	6332	130
	22	4	17924	588	1025	<1:40	3125	171
22 V2	8.2	36278	3698	2594	173	13700	119	

Table 2.S1. Plaque reduction neutralization titer assays were performed to calculate the 50% neutralization titer against a panel of SFV complex alphaviruses and the encephalitic alphavirus VEEV from the endemic cohort (n = 5) and non-endemic cohort (n = 7) at multiple timepoints. The limit of detection was a 1:40 serum dilution and values not determined are denoted with ND due to insufficient serum volume.

We next characterized the antigenic relationship between distinct alphaviruses using antigenic cartography, which has previously been implemented to describe the antigenic relatedness of dengue and influenza viruses [329, 330]. Antigenic maps provide an alternate means of using neutralization titers to evaluate antigenic rather than genetic similarities between viruses. We found that CHIKV and ONNV are the most antigenically similar, consistent with the phylogenetic relationship between these two viruses (**Fig 2.1A**), suggesting that antibody responses against these viruses share antigenically conserved epitopes; whereas VEEV and RRV are placed at a greater distance from CHIKV, again consistent with the phylogenetic relationships between the viruses (**Fig 2.1A**). All sera tested cluster around CHIKV and the closely related ONNV, except for Subject 17, which clusters most closely to RRV (**Fig 2.2A**). We next plotted sera and viruses for subjects for who we have serial serum samples, finding that for most subjects, relative antigenic distances between sera and viruses shifted little over time, with the exception of subject 1, who, on their third blood draw, shifted to a position on the map much farther from the other alphaviruses apart from CHIKV. This pattern is consistent with increased virus specificity and narrowed neutralization breadth over time. This finding was either not evident or less prominent for the remaining subject sera. Longitudinal samples (**Fig 2.2B**) continue to cluster most closely to CHIKV suggesting maintenance of CHIKV-specific and cross-reactive antibodies over time (**Fig 2.2B**).

Figure 2.2. Antigenic cartography to map human subject alphavirus cross-neutralization by human sera.

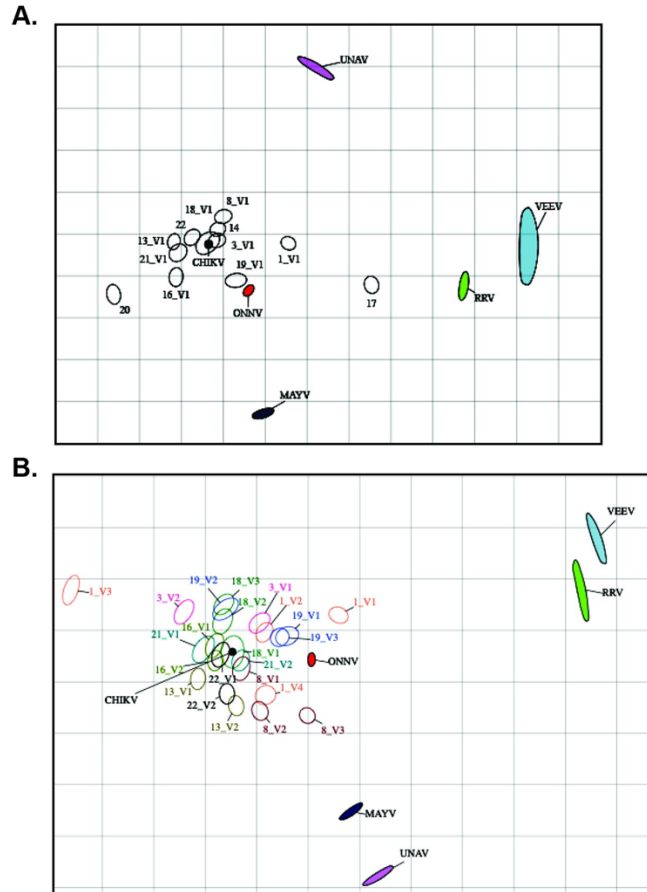


Figure 2.2. Antigenic map shows the relative antigenic relatedness between CHIKV, ONNV, RRV, MAYV, UNAV, and VEEV. Each unit of antigenic distance (AU), the length of one side of a grid square, is equivalent to a two-fold dilution in a neutralization assay. Sera are shown as open ellipses and labeled by subject number. Each virus is shown as a color filled ellipses and is colored according to virus strain (**Fig 2.1A**). The size and shape of each ellipse is the confidence area of its position. In making the map, each sera is initially plotted on top of the virus it most potently neutralizes and then pairwise distances between each sera:virus combination are calculated as a fold-difference in titer between the most potently neutralized virus and each other virus. The map is then optimized to place each virus relative to the serum samples in a manner that minimizes error between pairwise fold-differences. The closer a virus is to another virus, the more antigenically related the two are. Sera are initially plotted nearest to the virus they most potently neutralize with subsequently increasing distance to other viruses in descending neutralization potency against each virus. The antigenic map in (**A**) reflects each human subject at the primary blood draw, and (**B**) is representative of longitudinal sampling.

2.3.3 Dissecting the role of E2 B domain in homotypic and heterotypic neutralization

Conservation of the E2 B domain among members of the SFV complex has been shown to correlate with antibody cross-reactivity [251, 324]. The E2 B domain amino acid sequences for CHIKV, ONNV, MAYV, UNAV, and RRV are highly conserved (ranging from 56 to 88% sequence identity) sharing clusters of amino acids distributed across this region of E2, while VEEV shares only 27% sequence identity (**Fig 2.3A** and **2.3B**). When viewed in a structural model, the organization of the E1-E2 monomer and arrangement in the spike trimer demonstrates the accessibility of antibody binding to the E2B domain (**Fig 2.3C** and **2.3D**). To explore the cross-neutralizing potential of E2 B domain specific antibodies, we first depleted MAYV E2B-specific antibodies by adsorbing subject immune sera against magnetic beads coated with purified MAYV E2 B domain polypeptide (**2.S1A** and **2.S1B Fig**). Serum samples were incubated with MAYV E2 B domain bound beads, beads alone, or in the absence of beads. Following depletion, sera were evaluated for changes in neutralizing antibody titers against both CHIKV and MAYV relative to controls (**Fig 2.4**). Depletion with recombinant MAYV E2 B domain protein did not alter homotypic CHIKV neutralization titers (**Fig 2.5B** and **2.5E**), where no significant difference in CHIKV neutralization titer was observed between control and E2 B depletion. However, MAYV neutralization titers significantly decreased compared to control beads (** $p = 0.0045$) for all subjects except for Subject 17, which was excluded from statistical analyses due to the uncertainty of infection history (**Fig 2.5F**). Specifically, heterotypic PRNT₅₀ titers against MAYV dropped nearly five-fold (0.208 ± 0.071 -fold change) whereas control depleted sera PRNT₅₀ titers did not change significantly (0.937 ± 0.275 -fold change) (**2.S2 Table**). Conversely, homotypic CHIKV neutralization assays following MAYV-E2B bead depletion showed no significant impact on neutralizing antibody titers under either condition compared to the non-adsorbed serum (0.88 ± 0.251 and 1.028 ± 0.415 -fold change, respectively) (**Fig 2.5B** and **2.5E**).

Figure 2.3. Comparison of Alphavirus E2 B domains.

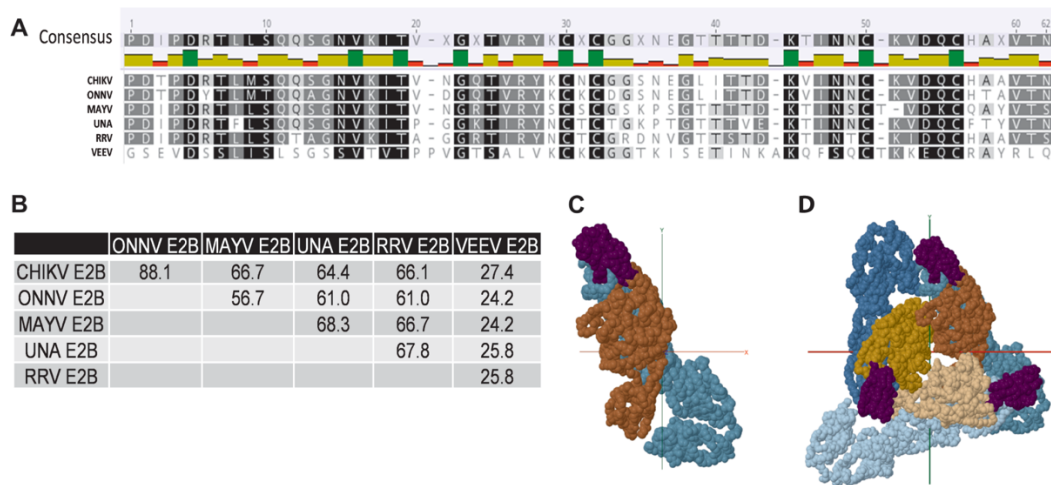


Figure 2.3. (A) Amino acid sequence alignment was performed using Geneious software for the E2 B domains of the alphaviruses examined in this study. Regions of 100% homology are highlighted in black, 80–100% similarity is dark grey, 60–80% similarity is light grey, and less than 60% similarity is in white. (B) Matrix depicts the amino acid sequence identity as a percentage. (C) Top-down view of the organization of the Mayaro Virus E1:E2 monomer (Teal:Brown) shown with the E2 B domain annotated in purple. (D) E1:E2 trimer spike organization depicted with the E2 B domain annotated in purple, E1 in shades of teal, and E2 in shades of brown.

Figure 2.S1. MAYV and CHIKV E2 B domain protein detection.

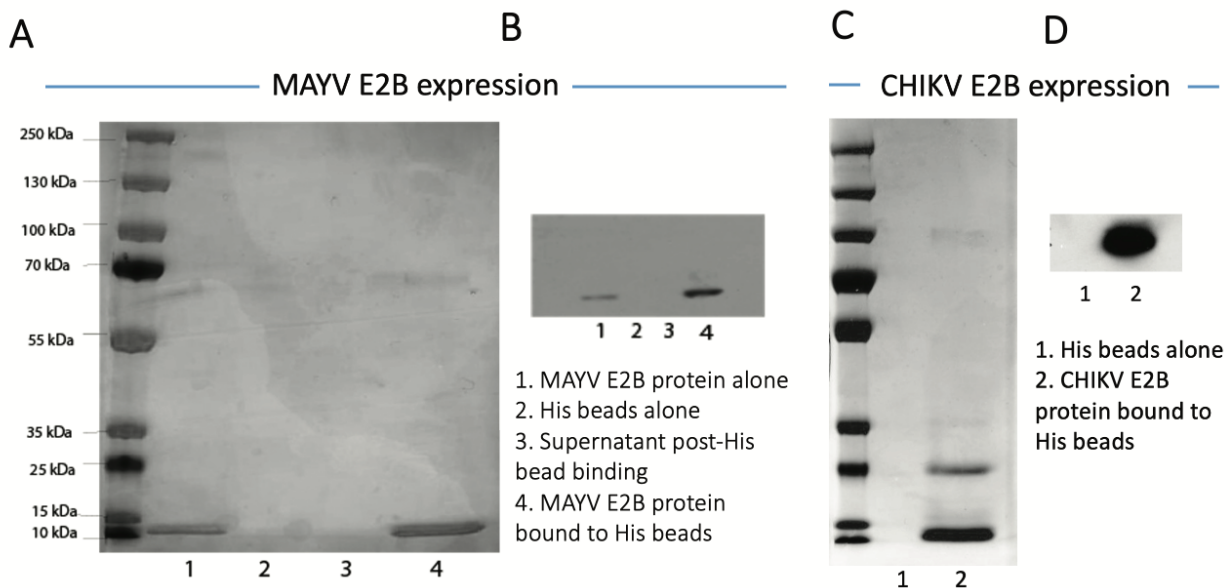


Figure 2.S1. Purified E2 B domain detection by (A, C) SDS-PAGE and (B, D) western blot for HiBit-tagged proteins (~8kDa) to confirm that the MAYV and CHIKV E2B proteins were indeed bound to the His beads before use in subsequent assays. In (A, C), samples were heated to 95°C for 5 minutes then electrophoresed on a 4–12% Bis-Tris gel for 40min at 160V. Gels in (A, B) were loaded with the same samples to detect MAYV E2B and gels

in (C,D) were loaded with the same set of samples to detect CHIKV E2B. Gels in (A, C) were stained using the Coomassie Brilliant Blue Staining Solutions Kit to visualize the proteins and confirm the correct protein sizes of 8 kDa. For western blots in (B,D), the gels were transferred to polyvinylidene fluoride (PVDF) membranes using a semi-dry transfer system and probed for HiBit using a 1:200 dilution of LgBiT, according to a HiBit Blotting System protocol and luminescence was visualized. For (A, B), lane 1 is MAYV E2B protein before His bead binding, lane 2 is control His beads only without protein, lane 3 is unbound protein, and lane 4 is MAYV E2B protein bound to His beads. For (C, D), lane 1 is control His beads only without protein and lane 2 is CHIKV E2B protein bound to His beads.

Figure 2.4. Impact of depletion of E2B-binding antibodies on CHIKV and MAYV neutralization.

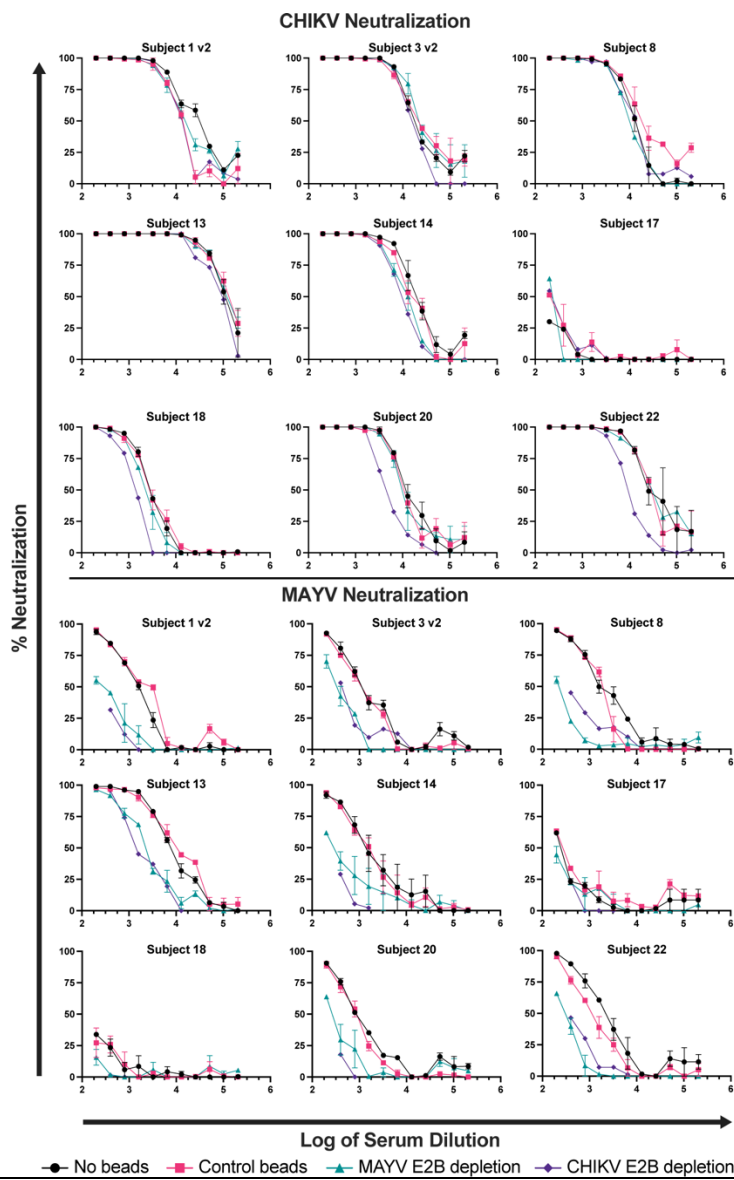


Figure 2.4. His-tagged CHIKV or MAYV E2 B domain bound to magnetic beads (or control beads alone) was adsorbed by diluted human serum for 4 hours and the beads were pulled off with a magnet. Following depletion, the sera was used in both CHIKV and MAYV neutralization assays. Human sera samples from the first blood draw were diluted 1:2 from 1:100 to 1:102,400. "No beads" is diluted serum only in black, CHIKV E2B absorbed human sera is in purple, MAYV E2B absorbed human sera is in teal, and control beads bound to diluted human sera is in pink. The data are representative of 3 biological experiments completed with duplicate samples.

Figure 2.5. Analysis of changes in CHIKV and MAYV neutralizing antibody titers following E2 B domain depletion.

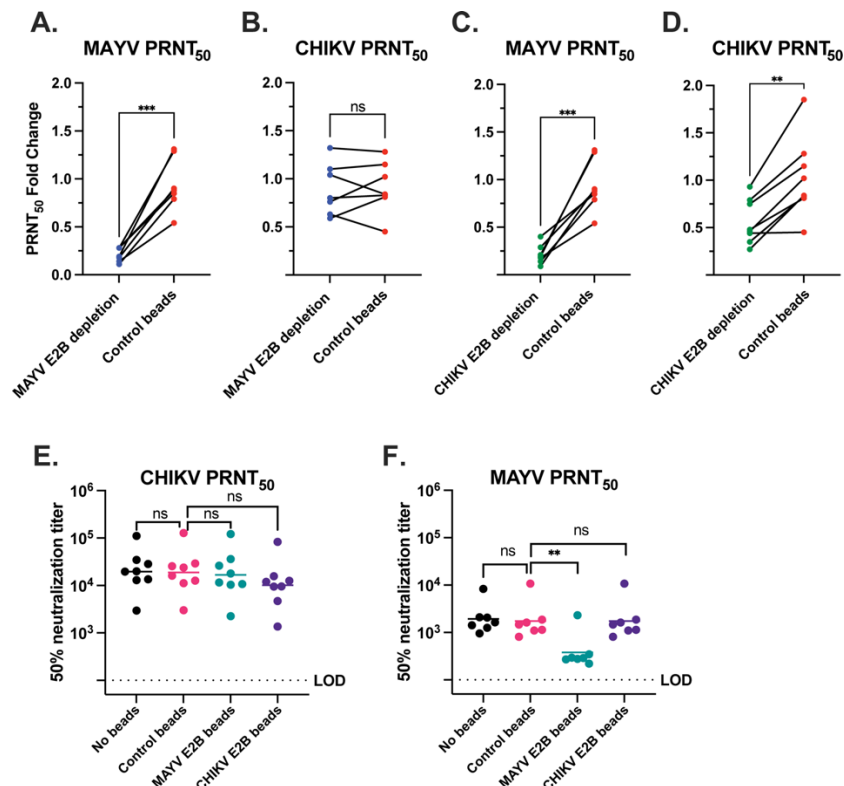


Figure 2.5. Fold change in neutralizing antibody titers (nAb) of subject serum samples following adsorption against E2B domain coated Ni-NTA or control beads was calculated against non-bead-treated serum samples. Depletion of MAYV E2 B domain-specific antibodies and impact on (A) MAYV or (B) CHIKV neutralizing antibody titer fold change compared to serum with control beads. A paired t-test for comparison of fold change heterotypic MAYV neutralization following MAYV E2B depletion yielded a p value *** = 0.0003 and 0.3276 (ns) for homotypic CHIKV neutralization. Depletion of CHIKV E2 B domain-specific antibodies and impact on (C) MAYV or (D) CHIKV neutralizing antibody titer fold change compared to serum with control beads. A paired t-test for comparison of fold change in heterotypic MAYV neutralization following CHIKV E2B depletion yielded a p value *** = 0.0006 and ** 0.0013 for homotypic CHIKV neutralization. Comparison of changes in (E) CHIKV PRNT₅₀ or (F) MAYV PRNT₅₀ following E2B depletion relative to no beads or control samples. LOD = 100 with values below the limit of detection graphed as 99. Data were analyzed using a one-way ANOVA with the significant

comparison in (F) being ** p = 0.0045. Note Subject 17 was excluded from this statistical analysis as the MAYV neutralization in this subject was low, therefore, the impact on E2B depletion was not detectable.

Table 2.S2. PRNT₅₀ values and fold change of MAYV E2 B domain depleted serum samples relative to controls.

	MAYV PRNT ₅₀					CHIKV PRNT ₅₀			
	No Beads	E2B Beads	Control Beads	Δ1	Δ2	No Beads	E2B Beads	Control Beads	Δ1
Subject 1 v2	1424	276.8	1862	0.19	1.31	28382	17945	12679	0.63
Subject 3 v2	1253	347.1	1102	0.28	0.88	19932	26258	25483	1.32
Subject 8	2056	219.9	1621	0.11	0.79	12928	10368	23924	0.80
Subject 13	8319	2304	10768	0.28	1.29	110426	121750	127457	1.10
Subject 14	1636	288.3	1470	0.18	0.90	19667	11520	16025	0.59
Subject 20	958.8	270.2	810.6	0.28	0.85	13466	10759	11192	0.80
Subject 22	2089	294.8	1134	0.14	0.54	34750	36086	29079	1.04
Subject 17	244.6	137.7	256.9	0.56	1.05	112.5	203.4	205.7	1.81
Subject 18	110.8	<100	85.8	N/A	0.77	2961	2258	3020	0.76

Table 2.S2. PRNT assays were performed on serum samples incubated with beads alone or beads coupled with E2 B domain protein. PRNT₅₀ values were calculated for each sample using Prism software. Fold change was calculated in Excel and is relative to the appropriate control (Δ1: Fold change in PRNT₅₀ titer following E2B bead treatment relative to non-bead treated serum; Δ2: Fold change in PRNT₅₀ titer following control bead treatment relative to non-bead treated serum).

To ensure that our MAYV E2B depletion experiment was not resulting in simply the depletion of MAYV-specific antibodies and strengthen our conclusion for a role of E2B-specific antibodies in cross-neutralization, we next depleted CHIKV E2B-specific antibodies from human sera with the same experimental framework as the MAYV depletion experiment (**Fig 2.4**). Indeed, we found that depletion of CHIKV E2B-specific antibodies resulted in significant reduction (0.214 ± 0.102 fold change) of MAYV cross-neutralization compared to control depleted sera ($0.937 \pm$

0.275 fold change) (Figs 2.4, 2.5C and 2.5F and 2.S3 Table), while homotypic CHIKV neutralizing antibody titers were only minimally reduced by CHIKV E2B depletion (0.558 ± 0.234 fold change) compared to control depleted sera (1.02 ± 0.415 fold change) (Figs 2.4, 2.5D and 2.5E and 2.S3 Table). These data support that antibodies induced following CHIKV natural infection target epitopes in addition to E2B but underscores that MAYV cross-neutralizing antibodies induced following CHIKV exposure are predominantly mediated by the E2 B domain.

Table 2.S3. PRNT₅₀ values and fold change of CHIKV E2 B domain depleted serum samples relative to controls.

	MAYV PRNT ₅₀					CHIKV PRNT ₅₀				
	No Beads	E2B Beads	Control Beads	Δ1	Δ2	No Beads	E2B Beads	Control Beads	Δ1	Δ2
Subject 1 v2	1424	275.8	1862	0.19	1.31	28382	12502	12679	0.44	0.45
Subject 3 v2	1253	367.4	1102	0.29	0.88	19932	15713	25483	0.79	1.28
Subject 8	2056	292.7	1621	0.14	0.79	12928	11978	23924	0.93	1.85
Subject 13	8319	1781	10768	0.21	1.29	110426	82965	127457	0.75	1.15
Subject 14	1636	144.3	1470	0.09	0.90	19667	9497	16025	0.48	0.81
Subject 20	958.8	380.7	810.6	0.40	0.85	13466	4704	11192	0.35	0.83
Subject 22	2089	374.9	1134	0.18	0.54	34750	9541	29079	0.27	0.84
Subject 17	244.6	385.8	256.9	1.58	1.05	112.5	219.9	205.7	1.95	1.83
Subject 18	110.8	<100	85.8	N/A	0.77	2961	1359	3020	0.46	1.02

Table 2.S3. PRNT assays were performed on serum samples incubated with beads alone or beads coupled with CHIKV E2 B domain protein. PRNT₅₀ values were calculated for each sample using Prism software. Fold change was calculated in Excel and is relative to the appropriate control (Δ1: Fold change in PRNT₅₀ titer following E2 B bead treatment relative to non-bead treated serum; Δ2: Fold change in PRNT₅₀ titer following control bead treatment relative to non-bead treated serum).

2.3.4 Homotypic and cross-reactive alphavirus-specific MBC frequency in immune subjects 1 to 24 years post-infection

To further characterize homotypic and cross-specific immune response in CHIKV immune subjects, memory B-cell (MBC) limiting dilution assays were performed. PBMCs were serially diluted in 96 well plates and stimulated to expand and secrete Abs. These Abs were then analyzed for antigen specificity by ELISA using whole CHIKV and MAYV virions as bait. All subjects had CHIKV-specific MBCs, as remotely as 24 years post-infection (**Fig 2.6A**). Cross-reactive MAYV-specific MBCs were present in 10/11 (91%) subjects, with only subject 17 falling below the limit of detection (**Fig 2.6B**). We next looked for MAYV E2B domain binding MBCs, finding 9 out of 11 (82%) subjects had MBCs encoding E2B cross-reactive Abs as remotely as 8.7 years post-infection (**Fig 2.6C**). When grouping the endemic and non-endemic cohorts for geometric mean MBC frequency analysis, the CHIKV MBC frequency was highest at 9.35 per 10^6 PBMC compared to 2.5 per 10^6 PBMC for MAYV and 0.892 per 10^6 PBMC for MAYV E2B MBCs (**Fig 2.6D**). The variability of cross-reactive MBCs attributable to E2B varied by subject (**Table 6.2**), ranging from 1.7% to 98% of MAYV-binding MBCs. We explored the relationship between MBC frequency and PRNT₅₀ titer finding only a very weak correlation (Spearman $R^2 = 0.126$) between the CHIKV-specific MBC frequency and CHIKV PRNT₅₀ titer (P value = 0.2862) (**2.S2A Fig**). A similar trend was observed for the relationship between MAYV-specific MBC frequency and MAYV PRNT₅₀ titer (Spearman $R^2 = 0.318$, P value = 0.0739) (**2.S2B Fig**). This indicates that PRNT₅₀ titer is not predictive of MBC response, as the two are distinct and independent B-cell populations. Finally, we found that CHIKV and MAYV-MBC frequencies were highly correlated (Spearman $R^2 = 0.747$, P value = 0.0006) with a ratio of CHIKV:MAYV of about 4:1 overall (**Table 2.2** and **2.S3A Fig**). MAYV binding MBC frequency was also highly correlated with MAYV E2B MBC frequency (Spearman $R^2 = 0.656$, P value = 0.002) with approximately 1 in 10 MAYV MBCs also being E2B specific (**Table 2.2** and **2.S3B Fig**). Overall, we have shown that similar to serum antibody profiles, CHIKV-infection results in a robust and durable MBC response in both endemic and non-endemic transmission settings, with CHIKV-specific and cross-reactive MBCs detected in 91% of subjects out to 24 years post infection.

Figure 2.6. Antigen-specific MBC frequency per 10^6 PBMC over time in non-endemic cohort (blue n = 6), endemic (orange n = 5), and naïve subjects (black n = 3).

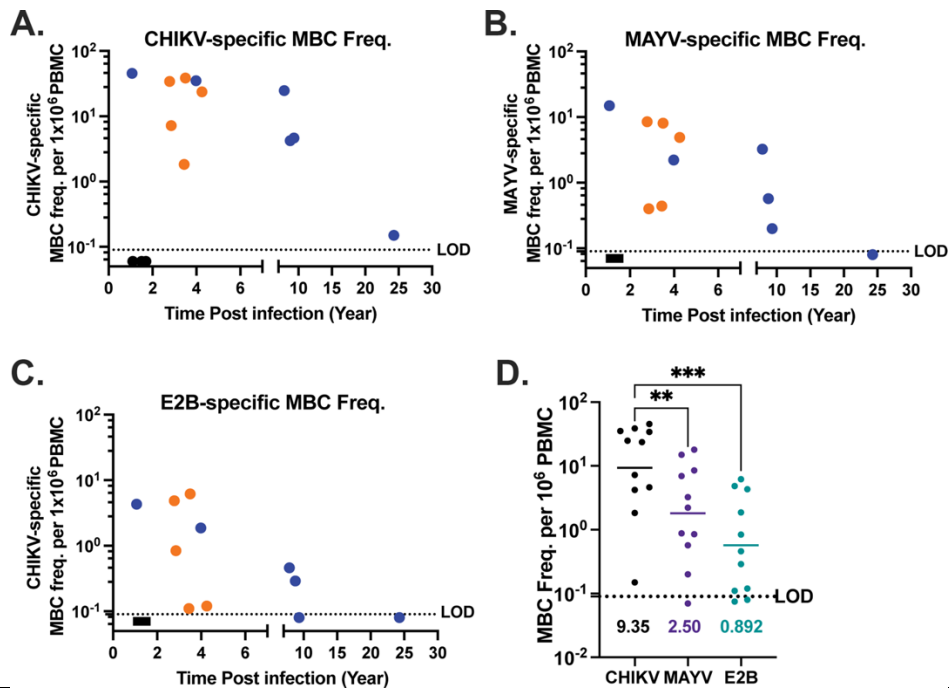


Figure 2.6. (A) CHIKV-specific MBC frequency as determined by whole CHIKV-ELISA. (B) MAYV-specific MBC frequency determined by whole MAYV-ELISA. (C) E2B-specific MBC frequency determined by MAYV-E2B ELISA. Negative samples and those below the limit of detection were assigned an arbitrary value between 0.05 and 0.09 (LOD = 0.1). (D) Summary of antigen-specific MBC frequency for CHIKV, MAYV, and MAYV E2B with subjects grouped together. Geometric mean frequencies are reported on the graph. P values are the result of a one-way ANOVA ** $p = 0.0044$, *** $p = 0.006$.

Table 2.2. Antigen-specific MBC frequency for non-endemic and endemic cohorts.

	Subject ID	Time Post Infection at primary draw (Years)	CHIKV MBC Freq.	MAYV MBC Freq.	E2B MBC Freq.	% MAYV MBC attributable to E2B
Endemic	1	4.5	34.15	8.50	4.85	57.0
	3	4.7	23.62	6.93	0.12	1.7
	8	4.8	10.37	0.85	0.84	98.1
	13	4.7	1.83	0.88	0.11	12.2
	14	4.7	38.63	17.99	6.18	34.4
Non-endemic	16	1.1	45.36	14.92	4.31	28.9
	17	24.3	0.15	ND	ND	N/A
	18	9.3	4.64	0.20	ND	N/A
	19	8.7	4.22	0.57	0.29	50.0
	20	7.9	24.81	3.24	0.46	14.2
	22	4.0	35.15	2.21	1.87	84.7

<https://doi.org/10.1371/journal.pntd.0011154.t002>

Table 2.2. Table summarizes subject sampling time post-infection, MBC frequencies for the three antigens tested, and % MAYV MBC attributable to E2B, determined by E2B MBC frequency divided by total MAYV-MBC frequency. ND = not detected, N/A = not applicable.

Figure 2.S2. Relationship between CHIKV or MAYV MBC frequency and PRNT₅₀.

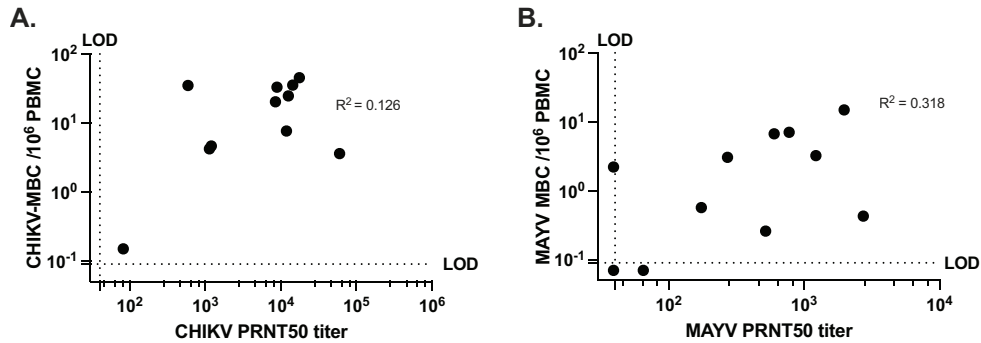


Figure 2.S2. (A) CHIKV MBC frequency compared to CHIKV neutralization titer at primary blood draw, non-parametric Spearman correlation $R^2 = 0.126$. (B) MAYV MBC frequency compared to MAYV neutralization titer at primary blood draw, non-parametric Spearman correlation $R^2 = 0.318$.

Figure 2.S3. Relationship between antigen-specific MBC frequencies.

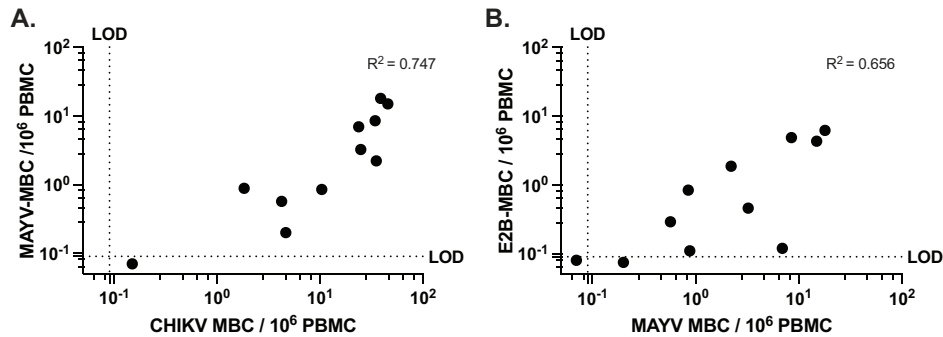


Figure 2.S3. (A) Relationship between MAYV-MBC frequency and CHIKV-MBC frequency non-parametric Spearman correlation $R^2 = 0.747$. (B) E2B-MBC frequency compared to MAYV-MBC frequency non-parametric Spearman correlation $R^2 = 0.656$.

Section 2.4: Discussion

Previous characterization of the durability and breadth of CHIKV specific neutralizing antibodies and virus specific MBCs in humans [75, 85, 331] and mice [77] have been quite limited, but have shown broad serum cross-reactivity. Our data highlight that infection with CHIKV not only elicits durable long-term homotypic neutralizing antibodies years after infection, but also induces neutralizing antibody breadth that extends across multiple SFV complex alphaviruses. Broad neutralization was observed in both endemic and non-endemic subjects with antibody breadth against antigenically distinct viruses remaining stable over time (**Fig 2.1**); although we also recognize that the subjects could have been infected, even subclinically, with CHIKV or

another alphavirus and this might impact Ab responses to CHIKV or other alphaviruses. Cross-neutralizing antibody responses of a PRNT₅₀ of 80 have been suggested to be protective against MAYV [93]. Our data imply that human primary infection with CHIKV has the potential to confer protection against other alphaviruses with the ability to emerge in these same regions. This immunity could reduce patient susceptibility to alphavirus infection and, therefore, has substantial public health relevance as herd immunity could contribute to mitigation of the emergence of closely related arthritogenic alphaviruses. The majority of characterized cross-neutralizing antibodies recognize E2, with many mapping to the linear epitope E2 B domain. There have also been reports of non-neutralizing alphavirus antibodies playing a role in protection, but that was not explored in this investigation [72, 78].

We further determined that much of the cross-neutralization and heterologous binding of both LLPC and MBC-derived Abs was attributed to antibodies that recognize the E2 B domain. When serum was depleted of CHIKV or MAYV E2 B domain binding antibodies, cross-neutralization was significantly ablated without significantly reducing neutralization against CHIKV. As such, this further implicates the E2 B domain as an important vaccine antigen for the development of broadly neutralizing alphavirus antibodies and indicates that other antigenic sites are responsible for robust type-specific neutralization. The subjects with the highest percentage of MAYV-specific MBC frequency attributed to the E2 B domain are also the subjects that have the highest fold-change differences in PRNT₅₀ following E2B serum depletion. The representation of specific Abs that bind the E2 B domain in the LLPC and MBC compartments varies greatly by subject; however, it is unclear what mechanisms mediate this difference and warrants further investigation.

Further differences were observed between homotypic and heterotypic antibodies in the MBC and LLPC compartments. Geometric mean titers between CHIKV and MAYV differed by 13-fold, compared to differences in MBC frequencies, which differed by less than 4-fold. This difference observed between serum Abs (a product of long-lived plasma cells) and MBC has been shown before in mice and humans where serum Abs are highly specific for the original antigen of infection, while MBCs recognize a greater breadth of antigens, those that are similar but antigenically distinct from the original invading pathogen [327, 328, 332]. Our study provides additional evidence of the importance of antibody specificity targeting the E2 B domain following

natural CHIKV infection in humans [75, 326]. During this investigation we hypothesized that one of our alphavirus immune subjects (Subject 17) had a serum neutralization profile more consistent with prior RRV instead of CHIKV infection. This conclusion is consistent with travel history (infected in Papua New Guinea) and by antigenic cartography (**Fig 2.2A**) where the subject antigenically clustered most closely to RRV. This subject was initially identified through a CHIKV-specific neutralization assay screen, and we chose to retain the subject in our analyses because their infection history adds information about the breadth of Ab responses within the SFV-complex and illustrates the importance of specific serological tests to determine infection history. The durability and breadth of the B-cell mediated immune response to CHIKV indicates that regions with high CHIKV seroprevalence may have a constricted range for closely related alphaviruses as well as point out the importance of specific serologic assays to determine alphavirus infection histories.

Section 2.5: Materials & Methods

2.5.1 Human research ethics

The study has been reviewed and approved by the Oregon Health & Science University Institutional Review Board (IRB#10212) for the non-endemic cohort and Ponce Medical School Foundation Review Board (IRB #180321-VR) for the endemic cohort. Informed written consent was obtained from subjects upon initiation of their participation in the study. Written formal consent for child participants was obtained from the parent/guardian.

2.5.2 Non-endemic human cohort population (n = 7)

CHIKV immune individuals in this study were enrolled in a larger study of long-term immunity following infection with the arthropod-borne viruses including DENVs, and ZIKV, as well as for those receiving yellow fever virus (YFV) vaccination. Study subjects with suspected arbovirus infection contacted the long-term immunity study and were offered participation in the study, and following informed consent, provided extensive additional history including other known and suspected arboviral infections, lifetime travel histories, and YFV and Japanese encephalitis virus (JEV) vaccination histories.

2.5.3 Endemic Human-cohort population (n = 5)

CHIKV immune individuals in this study were enrolled in a larger study of long-term immunity following infection with the arthropod-borne viruses. Study subjects that came to the ER with fever seeking medical attention were approached to enroll in Sentinel Enhanced Dengue Surveillance System (SEDSS). Subjects with PCR confirmed CHIKV infections were offered to participate in the long-term immunity study and following informed consent, provided additional history including other known and suspected arboviral infections, lifetime travel histories, and vaccination histories. Samples were collected, processed and shipped to Oregon Health & Science University for further analysis.

2.5.4 Sample collection and storage

On enrollment, subjects provided approximately 80 mL of blood, with 30 mL collected in BD serum vacutainers (Becton-Dickson) for serologic studies and stored at -80°C until used for assays. PBMCs were isolated from 50 mL of whole blood collected in BD EDTA or Heparin vacutainers (Becton-Dickson) and stored in liquid nitrogen.

2.5.5 Viruses

MAYV_{CH} was generated from an infectious clone received from Dr. Thomas E. Morrison (UC-Denver). Mayaro virus_{BeAr505411} (NR-49910); Una virus_{MAC150} (NR-49912); RRV_{T-48} (NR-51457); ONNV_{UgMP30} (NR-51661); and VEEV_{TC-83} (NR-63) were obtained through BEI. CHIKV_{181/25} was generated from infectious clones as previously described [112]. Alphaviruses were grown in C6/36 cells and viral stocks were prepared from clarified supernatants at 72 hours post-infection (hpi) by ultracentrifugation over 10% sucrose (SW32Ti, 70 min at 82,70055 x g). The virus pellets were resuspended in 1X PBS (Corning) and stored at -80°C. Viral limiting dilution plaque assays using Vero cells were performed on 10-fold serial dilutions of virus stocks. The infected cells were rocked continuously in an incubator at 37°C for 2 hours, and then DMEM (Corning) containing 5% FBS (HyClone), 1x Penicillin, Streptomycin, and Glutamine (PSG) (Gibco), 0.3% high viscosity carboxymethyl cellulose (CMC) (Sigma) and 0.3% low viscosity CMC (Sigma) was added to the cells. At 2 dpi, cells were fixed with 3.7% formaldehyde (Fisher) and stained with 0.2% methylene blue (Fisher). Plaques were visualized under a light microscope and counted.

2.5.6 Neutralization assays—fifty percent plaque reduction neutralization test (PRNT₅₀)

PRNT₅₀ titers were used to characterize subject sera. Assays were prepared in duplicate (for CHIKV_{181/25}). Subject sera were heat-inactivated at 56°C for 30 minutes, then diluted four-fold in MEM supplemented with 2% FBS from a starting dilution of 1:10 for CHIKV_{181/25}, 1:20 for assessment against the other viruses (MAYV_{CH}, MAYV_{BeAr505411}, Una_{Mac150}, RRV_{T-48}, ONNV_{UgMP30}, or VEEV_{TC-83}.) 2-fold dilutions were performed in DMEM supplemented with 5% FBS and 1% PSG. Serum dilutions were mixed with an equal volume of 50–100 plaque forming units (PFU) of virus giving a final starting serum dilution of 1:20 for CHIKV_{181/25} and 1:40 for the other viruses evaluated (MAYV_{CH}, MAYV_{BeAr505411}, Una_{Mac150}, RRV_{T-48}, ONNV_{UgMP30}, or VEEV_{TC-83}.) Virus-dilution mixes without sera were prepared simultaneously as controls for input virus PFUs. After incubation at 37°C for 2 hours, virus mixtures were inoculated into individual wells of 24-well plates (CHIKV_{181/25}) or 12-well plates seeded with Vero cells, incubated for 2 hours at 37°C 5% CO₂, and overlaid with 1% methylcellulose in Opti-MEM (Gibco) supplemented with NEAA, anti-anti, amphotericin B, and 2% FBS (CHIKV_{181/25}) or 5% FBS/DMEM/CMC. Plates were incubated for 2 days (MAYV_{CH}, MAYV_{BeAr505411}, Una_{Mac150}, RRV_{T48}, or VEEV_{TC-83}) or 3 days (CHIKV_{181/25} and ONNV_{UgMP30}) at 37°C and 5% CO₂. The overlay was then removed, monolayers were fixed with 80% methanol (CHIKV_{181/25}) or 3.7% formaldehyde and stained with 2% crystal violet (CHIKV_{181/25}) or 0.2% methylene blue dye, and plaques were enumerated by visual review of each well. Proportion of virus neutralized per well was calculated, and the serum dilution that neutralizes 50% of control input virus (PRNT₅₀) was determined by non-linear regression using GraphPad Prism, version 7.0.

2.5.7 E2 B domain cloning and synthesis

RNA was isolated from the supernatant of MAYV_{BeAr505411} infected C6/36 cells (Quick RNA Viral Kit, Zymo), then purified with RNeasy Mini Kit (Qiagen). cDNA was synthesized using SuperScript IV Reverse Transcriptase (Invitrogen) and the MAYV E2 B domain was amplified with

	Forward	primer:
TGAATTCCATATGGTGAGCGGCTGGCGGCTGTTCAAGAAGATTAGC-		
CCGGACATTCCGGATAGAAC	and	Reverse primer:
AAGCTTTTAGTGATGGTGATGGTGATGGCTCGTGACGTAAGCCTGACATTTG		and

cloned into pcDNA3.1. The CHIKV E2 B domain was codon optimized for bacteria with NdeI and HindIII restriction sites, and synthesized by Twist Biosciences: (ATGGGCGTAAGTGGTTGGCGTCTGTTTAAGAAAATCTCGCCGGATACACCAGATCGCACGTTAATGTCCCAACAGTCTGGGAATGTGAAAATTACCGTCAATGGCCAGACTGTTCGCTATAAATGCAACTGTGGAGGTAGCAATGAAGGCCTGATTACGACCGACAAAGTGATCAACAAGTGGATCAGTGTTCATGCGGCCGTTACCAACCACCATCACCACCATCATTA). Both amplicons were cloned into pRSET-B bacterial expression vector with NdeI and HindIII restriction enzymes and transformed into Rosetta (DE3) Competent Cells (Novagen).

2.5.8 E2 B domain expression and binding to Ni-NTA magnetic beads

Rosetta (DE3) *E.coli* containing the plasmid pRSET-B MAYV or CHIKV E2 B domain were grown in 2X YT broth at 37°C until the OD₆₀₀ reached ~0.6 and then induced with 1 mM final concentration isopropyl β-D-1-thiogalactopyranoside (IPTG) for 10 hours at 37°C. Cells were pelleted at 10,000 x g for 10 min. Pellets were resuspended in buffer containing 50 mM NaPO₄³⁻ and 300 mM NaCl with 1mg/mL lysozyme and DNase (5ug/mL) pH 8.0 and sonicated for three thirty second cycles at 84W. Cell lysates were centrifuged at 10,000 x g for 10 min, and inclusion body-containing pellets were resuspended with denaturing buffer (8M urea, 30 mM NaPO₄, 300 mM NaCl, and 3mM β-mercaptoethanol). Resuspended pellets were rocked for 10 minutes and then incubated at 65°C for 30 minutes. Supernatants were clarified by centrifugation at 416,000 x g for 30 minutes. Supernatant was added to 1 mL of Superflow Ni-NTA resin beads (Qiagen) equilibrated in denaturing buffer. The bead slurry was rocked for 1 hour at RT and then pelleted at 700 x g for 2 minutes. Beads were loaded into a gravity flow column. The beads were washed with 1 mL 20 mM imidazole to remove non-specific binding proteins. The bound protein was eluted with 4 mL of 250 mM imidazole in denaturing buffer, then concentrated to ~750 μL using an Amicon Ultra-15 Centrifugal Filter Unit with 3 kDa cut-off (Amicon), and filtered through a 0.22 μm filter. Filtered elute was loaded onto a Sephacryl S-100HR column that was equilibrated with gel filtration buffer (8M Urea, 100mM Tris pH 8) and separated using an AKTA Start Liquid Chromatograph (GE Lifesciences). Fractions were analyzed for mobility on a NuPAGE 4–12% Bis-Tris gel visualized following staining with Coomassie Brilliant Blue R-250 (Bio-Rad). Fractions containing purified E2 B monomers were combined and then dialyzed in 2-

fold steps from 8M urea to PBS using a 3.5K MWCO Slide-A-Lyzer Dialysis Cassette (Pierce). Proteins were quantified using the Nano-Glo HiBiT Lytic Detection System (Promega). Dialyzed fractions were then mixed with 300 μ L of PBS equilibrated Ni-NTA Magnetic Beads (Pierce) and rocked overnight at 4°C. Control PBS equilibrated Ni-NTA Magnetic Beads were rocked overnight at 4°C in an equivalent volume of 1X PBS.

2.5.9 Human serum antibody absorption to Ni-NTA magnetic bead absorbed human serum

E2 B domain loaded or control Ni-NTA magnetic beads were washed 3 times with PBS, followed by a blocking wash with DMEM supplemented with 10% human serum (Sigma Human AB serum #H4522). Beads were resuspended homogeneously in 2.1 mL of serum-free DMEM and aliquoted evenly between 2 mL centrifuge tubes for each patient and supernatant was removed. Subject serum samples were diluted 1:100 in serum-free DMEM and 1 mL of diluted serum was incubated with E2 B loaded Ni-NTA magnetic beads, control Ni-NTA magnetic beads, or no beads for 4 hours at 4°C. Following incubation, supernatant was removed to new 2 mL tubes and further diluted for use in neutralization assays.

2.5.10 Neutralization assays with Ni-NTA magnetic bead absorbed human serum

Diluted human serum supernatant following Ni-NTA magnetic bead binding was used in neutralization assays with MAYV_{BeAr} and CHIKV_{181/25}. Serum was diluted 1:2 from 1:100 to 1:102,400 and mixed with media containing 50 PFU of either MAYV_{BeAr} or CHIKV_{181/25}. Neutralization assays were then carried out as previously described [91].

2.5.11 Protein modeling of MAYV structural glycoproteins and alphavirus E2 B domain alignment

MAYV 3D structural model 6W2U, deposited by Powell *et al.*, was downloaded from protein data bank [326, 333]. Chains A & E were modeled for Fig 2.3A, and chains A–C & E–G were modeled for Fig 2.3B. Chains A and E and A–C & E–G were modeled for monomer and trimer orientations, respectively, using Jmol: an open-source Java viewer for chemical structures in 3D (<http://www.jmol.org/>). E2 B domain alignment was constructed in Geneious Prime version 11, using the following GenBank accession numbers: CHIKV (SL15649), ONNV (AF079456),

MAYV (KT754168), Una (HM147992), RRV (AEC497521), and VEEV (NC001449). Aligned residues were scored using the BLOSUM62 matrix to compare similarity.

2.5.12 Memory B cell frequency

PBMCs were thawed and resuspended in LDA media (RPMI 1640 medium (Gibco), 1×Antibiotic-Antimycotic (Corning), 1X non-essential amino acids (HyClone), 20 mM HEPES (Thermo Scientific), 50 μM β-ME, and 10% heat-inactivated fetal bovine serum (VWR)). Cells were serially 2-fold diluted (10 wells per cell sample) starting with 3–5 x 10⁵ PBMCs per well at the highest concentration and cultured in 96-well round-bottom plates in a final volume of 200 μL per well. Cells were stimulated with IL-2 (Prospec) 1000U/mL and R848 (InvivoGen) 2.5μg/mL [334]. To determine background absorbance values, supernatants were used from 8 wells of unstimulated PBMCs only. Plates were incubated at 37°C and 5% CO₂ for 7 days. B cell stimulation and expansion was determined by performing ELISAs detecting total IgG.

MBC precursor frequencies were calculated by the semi-logarithmic plot of the percent of negative cultures versus the cell dose per culture, as previously described [335]. Frequencies were calculated as the reciprocal of the cell dilution at which 37% of the cultures were negative for antigen-specific IgG production. Rows which yielded 0% negative wells were excluded, since this typically resides outside of the linear range of the curve and artificially reduced the MBC precursor frequency. For subjects with low frequency of antigen-specific antibody secreting cells frequency was determined by number of positive wells divided by the total number of IgG positive secreting wells, multiplied by one million, giving a frequency per million PBMCs stimulated.

2.5.13 Antigen-specific ELISAs

Antigen-specific MBC frequencies were calculated by assaying LDA supernatants by antigen-specific ELISAs [335]. Ninety-six half-well ELISA plates (Greiner Bio-one) were coated with 5 x 10⁷ PFU/mL CHIKV or 1 x 10⁷ PFU/mL MAYV in PBS. Plates were incubated for four days at 4°C, washed with PBS-T (0.05% Tween) and blocked for 1 hour with 5% milk prepared in PBS-T and then 20 μL of LDA supernatants were added to each well and incubated at RT for 1 hour. Plates were washed 4 times with wash buffer, and 50 μL of 1:3,000 dilution of donkey anti-human IgG-HRP (H + L) (Novusbio, NBP1-73319) detection antibody was added and incubated at RT for 1 hour. Plates were washed 4 times with wash buffer, 50 μL of colorimetric detection reagent

containing 0.4mg/mL o-phenylenediamine and 0.01% hydrogen peroxide in 0.05M citrate buffer (pH 5) were added and the reaction was stopped after 20 minutes by the addition of 1M HCl. Optical density (OD) at 492nm was measured using a CLARIOstar ELISA plate reader. LDA wells were scored positive at ODs at least 2-fold above background (unstimulated PBMC wells).

2.5.14 Antigenic cartography

The CHIKV antigenic map was constructed as previously described [329, 336] and implemented using the Acmacs Web Cherry platform (<https://acmacs-web.antigenic-cartography.org/>). Briefly, antigenic maps are constructed by first generating a table of antigenic distances (D_{ij}) between each individual virus (i) and serum (j) using serum titers for each serum-titer pair (N_{ij}). To calculate table distance, the titer against the best neutralized virus for that serum is defined as b_i and the distances for that serum are calculated as $D_{ij} = \log_2(b_i) - \log(N_{ij})$. For the best neutralized virus for that serum, $N_{ij} = b_i$, and this distance will be equal to 0. For the remaining serum-virus pairs, table distance D_{ij} is equivalent to the fold-difference in titer between b_{ij} and N_{ij} . Euclidean map distance (d_{ij}) for each serum-virus pair is found by minimizing the error between the table distance D_{ij} and map distance, d_{ij} , using the error function $E = \sum_{ij} e(D_{ij}, d_{ij})$, where $e(D_{ij}, d_{ij}) = (D_{ij} - d_{ij})^2$ when the neutralization titer is above 1:20. For viruses with neutralization titers <1:20, the error was defined as $e(D_{ij}, d_{ij}) = (D_{ij} - 1 - d_{ij})^2 / (1 + e^{-10(D_{ij} - 1 - d_{ij})})$. To make a map and derive d_{ij} for each serum-virus pair, viruses and sera are assigned random starting coordinates and the error function is minimized using the conjugate gradient optimization method.

2.5.15 Statistical analysis

Statistics and graphs were created with GraphPad Prism 8. Normalized variable slope non-linear regression using upper and lower limits of 100 and 0, respectively, was used to calculate neutralizing antibody titers. Data from Subject 17 was not included in the analysis represented in Figs 2.5 and 2.6D because it is unclear which alphavirus the patient was infected with based upon serology.

Section 2.6: Acknowledgements

The work presented in this manuscript was supported by grants from the National Institutes of Health 1U19AI142790 (DNS), R01AI153434 (WBM), R21AI135537(WBM), UL1TR002369 (WBM), Takeda IISR 2016-101586 (WBM), and the Sunlin and Priscilla Chou foundation (WBM). Centers for Disease Control and Prevention U01CK000437 (VRA) and U01CK000580 (VRA) and T32GM142619 (WCW). The funders had no role in study design, data collection and analysis, decision to publish, or preparation of this manuscript.

Chapter 3: The approved live-attenuated chikungunya virus vaccine (IXCHIQ[®]) elicits cross-neutralizing antibody breadth extending to multiple arthritogenic alphaviruses similar to the antibody breadth following natural infection

Status: Published in Vaccines on August 7th, 2024.

Whitney C. Weber^{1,2}, Zachary J. Streblov¹, Craig N. Kreklywich¹, Michael Denton¹, Gauthami Sulgey¹, Magdalene M. Streblov¹, Dorca Marcano³, Paola N. Flores³, Rachel Rodriguez-Santiago³, Luisa Alvarado³, Vanessa Rivera-Amill³, William B. Messer², Romana Hochreiter⁴, Karin Kosulin⁴, Katrin Dubischar⁴, Vera Buerger⁴, and Daniel N. Streblov^{1,5*}

¹Vaccine and Gene Therapy Institute, Oregon Health and Science University, Beaverton, Oregon, USA

²Department of Molecular Microbiology and Immunology, Oregon Health and Science University, Portland, Oregon, USA

³Ponce Health Sciences University, Ponce Research Institute, Ponce, Puerto Rico

⁴Valneva Austria GmbH, 1030 Vienna, Austria

⁵Division of Pathobiology and Immunology, Oregon National Primate Research Center, Beaverton, Oregon, USA

Publication info: *Vaccines* **2024**, *12*(8), 893

DOI: <https://doi.org/10.3390/vaccines12080893>

Author Contributions: Conceptualization, W.C.W., R.H., K.K., K.D., V.B., and D.N.S.; methodology, W.C.W., D.N.S. and W.B.M.; validation, W.C.W. and D.N.S.; formal analysis, W.C.W.; investigation, W.C.W., Z.J.S., C.N.K., M.D., G.S., M.M.S., D.M., and P.N.F.; resources, D.N.S, W.B.M., L.A., V.R.A.; data curation, W.C.W. and W.B.M.; writing—original draft preparation, W.C.W. and D.N.S.; writing—review and editing, W.C.W., W.B.M., R.H., K.K., K.D., V.B., and D.N.S.; visualization, W.C.W.; supervision, W.C.W. and D.N.S.; project administration, D.N.S.; funding acquisition, D.N.S., W.B.M., V.R.A. R.H. and K.K. All authors have read and agreed to the published version of the manuscript.

Section 3.1: Abstract

The first vaccine against chikungunya virus (CHIKV) was recently licensed in the U.S., Europe, and Canada (brand IXCHIQ®, referred to as VLA1553). Other pathogenic alphaviruses co-circulate with CHIKV and major questions remain regarding the potential of IXCHIQ to confer cross-protection for populations that are exposed to them. Here, we characterized the cross-neutralizing antibody (nAb) responses against heterotypic CHIKV and additional arthritogenic alphaviruses in individuals at one month, six months, and one year post-IXCHIQ vaccination. We characterized nAbs against CHIKV strains LR2006, 181/25, and a 2021 isolate from Tocantins, Brazil, as well as O'nyong-nyong virus (ONNV), Mayaro virus (MAYV) and Ross River virus (RRV). IXCHIQ elicited 100% seroconversion to each virus, with exception of RRV at 83.3% seroconversion of vaccinees and cross-neutralizing antibody potency decreased with increasing genetic distance from CHIKV. We compared vaccinee responses to cross-nAbs elicited by natural CHIKV infection in individuals living in the endemic setting of Puerto Rico at 8-9 years post-infection. These data suggest that IXCHIQ efficiently and potently elicits cross-nAb breadth that extends to related alphaviruses, in a manner similar to natural CHIKV infection, which may have important implications for individuals that are susceptible to alphavirus co-circulation in regions of potential vaccine rollout.

Section 3.2: Introduction

Chikungunya virus (CHIKV) is a human pathogenic alphavirus responsible for sporadic epidemics that have burdened 100+ countries over 50 years. From 2013-2023, there were over 3.68 million suspected and confirmed cases in 50 countries in the Americas [162]. Alphaviruses are part of the *Togaviridae* family composing a number of additional emerging human pathogenic viruses that are predominantly mosquito transmitted. CHIKV belongs to the Semliki Forest antigenic complex, which includes seven additional viruses with varying degrees of cross-reactivity due to shared antigenicity. While there are three distinct lineages of CHIKV, Asian lineage, East Central South African (ECSA) lineage, and West African lineage, a fourth Indian Ocean lineage (IOL) has been proposed to exist. Immunologically these lineages conform to a single serotype [305, 337]. It has been observed that even decades after large CHIKV outbreaks, herd immunity limits additional outbreaks or emergence of new CHIKV strains in that region, further supporting a single serotype [305]. Predominantly circulating CHIKV strains have yet to

accumulate mutations to confer host antibody-neutralization escape but the viral evolution of CHIKV continues to be cause for concern after single mutations have conferred transmissibility in new mosquito vectors [155]. This warrants investigation to identify differences in CHIKV antibody potency against diverse strains. Notable emerging viruses that have contributed to sporadic outbreaks within the Semliki Forest antigenic complex include O'nyong-nyong virus (ONNV), Mayaro virus (MAYV) and Ross River virus (RRV). Each of these viruses have been shown to co-circulate with CHIKV [338-340], and are transmitted by similar vectors as several flaviviruses such as dengue and Zika viruses [341]. This leads to co-circulation of diverse human pathogenic arbovirus infections, presenting urgent public health concern.

Vaccines to counter CHIKV have been in development for decades based upon virus like particle, viral vector, live-attenuated virus, nucleic acid, subunit, and inactivated viral vaccine platforms. The primary goal of these vaccine platforms has been to elicit high levels of neutralizing antibodies, which are generally accepted as the main correlate of protection, although protective roles of T cells have also been established [46, 112]. There are several CHIKV vaccines currently in clinical trials with two vaccines in Phase I, two vaccines in Phase II, and two vaccines in Phase III trials [342]. In November of 2023, the U.S. Food and Drug Administration (FDA) approved the CHIKV vaccine IXCHIQ (VLA1553), which was a huge step for the alphavirus field, especially amidst a year with over 500,000 CHIKV cases with epicenter in Brazil where many additional arboviruses burden the community. The European Medicines Agency has also now officially approved marketing authorization of IXCHIQ in the European Union [262]. Under the OPEN regulatory procedure, this review was joined by other regulators including Brazilian ANVISA, marking the first endemic country reviews [343]. The IXCHIQ vaccine is a single dose, live-attenuated vaccine (LAV) platform based upon the CHIKV_{LR2006-OPY1} backbone containing a large genetic deletion in nsP3 [101]. IXCHIQ was tested in mice and cynomolgus macaques to establish a protective antibody threshold due to the challenges of conducting an efficacy trial given the sporadic nature of CHIKV outbreaks [99, 101, 233, 263]. IXCHIQ has now been tested in over 4,000 individuals in non-endemic settings and is generally immunogenic and well tolerated although viremia and some side effects including headache, fever, arthralgia, and myalgia have been noted [264-266]. Additional trials are ongoing to evaluate IXCHIQ in endemic settings, in adolescents, and to examine long-term antibody persistence. A study is planned in moderately immunocompromised individuals living with HIV.

IXCHIQ approval brings forward many scientific questions regarding the breadth of cross-reactive immunity and the implications this may have in communities with the potential of alphavirus co-circulation. It is well established that primary CHIKV infection in humans has the ability to elicit cross-neutralizing immune responses that extend to related alphaviruses within the Semliki Forest virus (SFV) complex, which is driven, in large part, by antibodies recognizing the envelope protein E2 domain B region [59, 75, 325]. Although live-attenuated vaccines are capable of causing symptoms similar to infection, there is a clear benefit to eliciting robust immune responses with potency similar to a natural infection. For the purposes of this study, we sought to quantify neutralizing antibody responses in IXCHIQ vaccinees and CHIKV-infected participants across CHIKV genotypes and to other members of the SFV complex including ONNV, MAYV, and RRV. We anticipated that the neutralizing antibody potency and breadth would be similar to the immunity elicited by natural CHIKV infection due to the live-attenuated nature of the vaccine. Our data demonstrate a comparable antigenic profile induced by IXCHIQ immunization and natural CHIKV infection offering promising implications for alphavirus cross-protection.

Section 3.3: Results

3.3.1 IXCHIQ elicits broad alphavirus immunity against CHIKV strains as well as related ONNV, MAYV, and RRV.

We sought to assess the presence of alphavirus cross-neutralizing antibodies at day 1 (baseline), day 29 (expected peak of response), day 180 (expected setpoint level), and day 365 (durability assessment) post-vaccination in human sera from 30 adult vaccinees aged 19 to 71 who were immunized with IXCHIQ (VLA1553 prior to approval) in clinical trial NCT04546724 and included in the follow up trial NCT04838444 (**Table 3.1**). Samples from 17 females and 13 males with an age range of 19 to 76 with a median of 42.5 were tested (**Table 3.1**). We propagated a panel of six viruses within the Semliki Forest antigenic complex including three CHIKV strains (LR2006, 181/25, Brazil-7124), ONNV_{UgMP30}, MAYV_{BeAr505411}, and RRV_{T-48}. The panel of alphaviruses were propagated from viral stocks provided by BEI or infectious clones provided by generous collaborators. CHIKV Brazil strain 7124 of the ESCA genotype, a contemporary 2021 Brazilian isolate, was generated using Gibson assembly methods based on the sequence of sample

TO-UFT-7124 collected in 2021 in Tocantins, Brazil [344]. We included CHIKV_{LR2006} because the IXCHIQ live-attenuated vaccine was derived from the CHIKV LR2006-OPY1 strain from the ECSA genotype. We also included the attenuated CHIKV_{181/25} strain of the Asian genotype derived from the strain AF15561 as 181/25 is a previously characterized vaccine virus that was discontinued after Phase II clinical trials [230]. Additionally, the 181/25 strain was used in neutralization assays performed during Phase III clinical trials of VLA1553. ONNV_{UgMP30} is both phylogenetically and antigenically highly similar to CHIKV and has caused sporadic human outbreaks in sub-Saharan Africa. MAYV_{BeAr505411} and RRV_{T-48} are pathogenic, clinically relevant alphaviruses with the ability to cause outbreaks and human disease and circulate in South America and Australia, respectively. The alphavirus stocks were sequence verified using next generation sequencing of the viral genomes and the mutations are listed in **Supplemental Table 3.S1**. The detected mutation levels are considered low and because most of the mutations were in the non-structural proteins, they are not predicted to impact antibody neutralization epitopes that are dominantly located in the structural proteins.

Table 3.1. Participant demographics for IXCHIQ adult vaccinees and CHIKV-immune individuals.

	IXCHIQ vaccinees	CHIKV-immune
<i>Total participants</i>	30	9
<i>Sex</i>		
Female	17 (56.7%)	5 (55.5%)
Male	13 (43.3%)	4 (44.4%)
<i>Country of birth</i>	Not available	Puerto Rico
<i>Country of vaccination or infection</i>	Continental U.S.	Puerto Rico
<i>Age min-max¹</i>	19-76	19.5-81.5
<i>Age median¹</i>	42.5	38.9
<i>Age standard deviation¹</i>	16.12	19.58
<i>Age at vaccination or infection</i>	19-76	12-73
<i>Race</i>		
Hispanic	1 (3.3%)	9 (100%)
Non-Hispanic	29 (96.7%)	0
Not reported	0	0
Unknown	0	0
<i>Ethnicity</i>		
Caucasian / white	25 (83.3%)	2 (22.2%)
Native Hawaiian or Pacific Islander	2 (6.7%)	0
Black or African American	3 (10%)	0
Asian	0	0
Multiracial	0	2 (22.2%)
Other	0	5 (55.5%)
<i>Time points for blood draws</i>	Day 1 (baseline), 1 month, 6 months, 1 year post-vaccination	~8 and ~9 years post-infection

<i>Infection symptoms reported</i>		
Asymptomatic		1 (11.1%)
Muscle/joint/bone pain (severe)		6 (66.6%)
Fever		5 (55.5%)
Headache		4 (44.4%)
Sensitivity to light		5 (55.5%)
Eye pain		3 (33.3%)
Rash		7 (77.7%)
Cough		1 (11.1%)
Runny nose		2 (22.2%)
Malaise		4 (44.4%)
Shortness of breath		1 (11.1%)
Loss of appetite		4 (44.4%)
Diarrhea		1 (11.1%)

¹ age in this context refers to participant age at first blood draw when the study was initiated.

Table 3.S1. Viral stock sequencing analysis summary for the alphaviruses used in this study.

Virus	Position		Variant		Region	# of Virus Reads / Total Reads	Virus Reference Sequence
	Nucleotide Change	A.A. Change	Change	Frequency			
CHIKV Brazil 7124	688	G -> K	Arg -> Met	55.80%	NSP 1	1,354,589 of 4,624,952	CHIKV TO-UFT-7124
	691	A -> G	No Change	35.60%	NSP 1		
	1361	G -> A	No Change	54.40%	NSP 1		
	9083	A -> C	No Change	56.30%	E2B domain		Accession: ON586955.1
CHIKV 181/25	3706	G -> A	Arg -> His	98.70%	NSP 1	344,119 of 5,133,734	CHIKV 181/25
	8345	A -> G	No Change	39.10%	NSP 2		Accession: MW473668.1
CHIKV LR2006 OPY1	561	A -> G	Gln -> Arg	98.40%	NSP 1	2,800,692 of 3,517,670	CHIKV LR2006 OPY1
	1025	G -> A	Val -> Met	95.50%	NSP 1		
	4140	A -> G	Asp -> Gly	93.10%	NSP 3		Accession: KY575571.1
MAYV BeAr505411	1362	G -> C	Lys -> Asn	85.9	NSP 1-3	2,007,089 of 2,857,853	MAYV BeAr505411
	3980	C -> A	Pro -> Gln	99.8	NSP 1-3		
	9501-9503	Deletion of CAG	Gln	100	E2		Accession: KP842818.1
ONNV UGMP30	173	G -> A	Val -> Ile	25.00%	NSP 1	38,028 of 2,635,751	ONNV UGMP30
	957	G -> A	Ser -> Asn	100.00%	NSP 1		
	1008	G -> A	Gly -> Asp	100.00%	NSP 1		Accession: M20303.1
RRV T-48	314	T -> A	Cys -> Ser	99.80%	NSP 1	748,882 of 4,585,162	RRV T48
	413	T -> G	Ser -> Ala	99.50%	NSP 1		Accession: GQ433359.1
	1138	T -> C	No Change	99.80%	NSP 1		
	1466	A -> C	Ile -> Leu	99.70%	NSP 1		
	5085	G -> T	Ser -> Ile	97.90%	NSP 3		
	5263	T -> C	No Change	99.40%	NSP 3		

7736	Y -> C	No Change or Ser -> Phe	97.10%	Capsid
8585	A -> T	No Change	25.40%	E2
8623	Y -> T	No Change	97.70%	E2
8766	R -> G	Gln -> Arg or No Change	98.80%	E2

To assess the neutralizing antibody potency and breadth of the vaccinee sera, we performed 50% plaque reduction neutralization tests (PRNT₅₀) on confluent monolayers of Vero cells for serum samples collected at day 1, 29, 180, and 365 post-vaccinations from 30 vaccinees (**Figure 3.1, Table 3.2, Supplemental Table 3.S2**). Overall, seroconversion status (PRNT₅₀ ≥ 20) was reached for 100% of vaccinees for each of the three CHIKV strains, ONNV_{UgMP30}, and MAYV_{BeAr505411} as early as day 29 post-vaccination and was maintained at day 180 and day 365 post-vaccination (**Table 3.2**). RRV_{T-48} was the only virus where seroconversion was not reached in all vaccinees, with seroconversion rates reduced to 66.6% at day 29, 83.3% at day 180, and 83.3% at day 365 post-vaccination (**Table 3.2**). The neutralization titers against RRV are considered very low. Consistent with IXCHIQ (VLA1553) clinical trial immunogenicity findings where μ PRNT testing was performed using attenuated heterologous strain CHIKV_{181/25} [264], we found that the homotypic PRNT₅₀ geometric mean titer (GMT) against CHIKV_{LR2006} peaked at day 29 post-vaccination at 16,022 and gradually leveled off at a titer of 5,147 at day 365 post-vaccination (**Figure 3.1A, Table 3.2**) [264, 266]. Vaccinee GMT declined significantly between day 29 and 180 post-vaccination (***P* = 0.0018) (**Figure 3.1A**). The kinetics of the antibody potency against CHIKV_{181/25} were similar with peak GMT at day 29 post-vaccination of 10,879 with a significant reduction to 3,714 at day 180 (***P* = 0.0054) and 3,440 by day 365 post-vaccination (***P* = 0.0048 compared to d29) (**Figure 3.1B, Table 3.2**). For the contemporary CHIKV_{Brazil-7124} strain, GMTs peaked at day 29 post-vaccination at 6,491 and declined to 3,881 by day 180 and 3,792 by day 365; only the comparison between day 29 and day 365 reached statistical significance (**P* = 0.0177) (**Figure 3.1C, Table 3.2**). This finding indicated that IXCHIQ immunization elicits neutralizing responses against a recently circulating CHIKV isolate. The IXCHIQ vaccine also elicited heterotypic neutralizing antibodies against ONNV_{UgMP30} that did not change significantly over time with a peak GMT at day 29 of 1,676, 1,102 at day 180 and 1,156 at day 365 post-vaccination (**Figure 3.1D, Table 3.2**). In contrast to the GMTs against CHIKV strains and ONNV_{UgMP30} that peaked at day 29 post-vaccination, the MAYV_{BeAr505411} GMT

gradually increased over time from 374 at day 29, to 417 at day 180, and 652 at day 365; this gradual increase was not statistically significant (**Figure 3.1E, Table 3.2**). Finally, RRV_{T-48}, which is the most distantly related Semliki Forest antigenic complex member included in our investigation, the GMT was 32 at day 29, 33 at day 180, and 39 at day 365 post-vaccination; there was consistency of these low-level responses over time and these changes did not reach statistical significance (**Figure 3.1F, Table 3.2**). Altogether, these data demonstrate that IXCHIQ immunization elicits both homotypic and heterotypic cross-neutralizing immunity extending to related arthritogenic alphaviruses in vaccine recipients. Importantly, both the homotypic and heterotypic neutralizing responses retained durability up to one-year post-vaccination.

Figure 3.1. IXCHIQ immunization of human participants elicits antibodies that neutralize multiple CHIKV strains and cross-neutralize related arthritogenic alphaviruses.

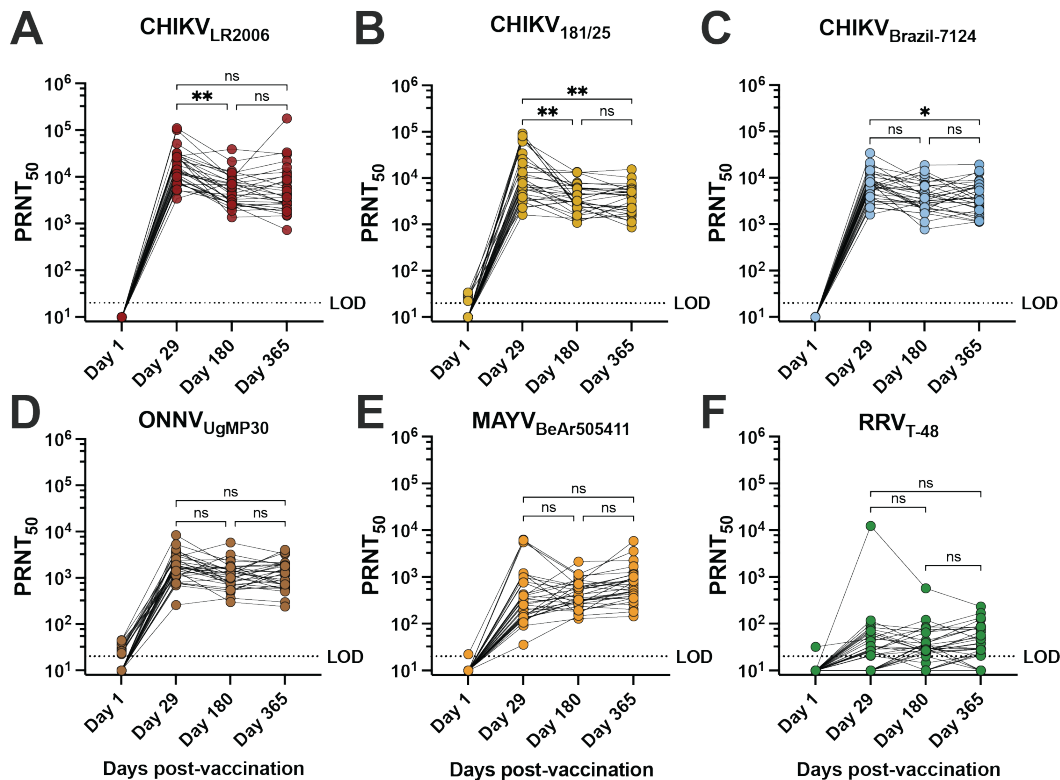


Figure 3.1. Serum from 30 human vaccinees was collected at day 1, 29, 180, and 365 after administration of the IXCHIQ vaccine and used in 50% plaque reduction neutralization titer assays (PRNT₅₀) performed on Vero cells. Neutralizing antibody titers calculated using variable slope non-linear regressions in Prism software are shown in logarithmic scale for neutralization against (A) CHIKV_{LR2006}, (B) CHIKV_{181/25}, (C) CHIKV_{Brazil-7124}, (D) ONNV_{UgMP30}, (E) MAYV_{BeAr505411}, and (F) RRV_{T-48}. Repeated measures one-way ANOVA with Geisser-

Greenhouse correction was used to compare PRNT₅₀ values among day 29, 180, and 365 timepoints. A Bonferroni test to correct for multiple comparisons was performed where ns $P > 0.05$, * $P = 0.0177$, and ** $P < 0.001$. The limit of detection for the assay was 20 and sera falling below the limit of detection were assigned a titer of 10.

Table 3.2. Summary of alphavirus neutralizing antibody responses in all participants.

PRNT ₅₀	IXCHIQ vaccinees			CHIKV-immune (Puerto Rican cohort)	
	1 month	6 months	1 year	~8 years	~9 years post-infection
CHIKV_{LR2006}					
Min - Max	34,333 – 109,913	1,363 – 38,895	728 – 177,237	4,091 – 64,794	4,297 – 50,825
Geometric mean	16,022	5,197	5,147	17,317	12,530
Mean	23,181	7,140	12,983	25,901	16,863
Standard deviation	24,954	7,379	32,100	21,826	15,639
<i>Participants that seroconverted (PRNT₅₀ ≥ 20)</i>	30 (100%)	30 (100%)	30 (100%)	9 (100%)	9 (100%)
CHIKV_{181/25}					
Min - Max	1,619 – 91,693	1,078 – 13,632	859 – 15,395	3,578 – 52,100	2,766 – 30,003
Geometric mean	10,879	3,714	3,440	12,522	10,146
Mean	22,489	4,681	4,370	17,850	13,126
Standard deviation	28,393	3,492	3,131	16,069	9,664
<i>Participants that seroconverted (PRNT₅₀ ≥ 20)</i>	30 (100%)	30 (100%)	30 (100%)	9 (100%)	9 (100%)
CHIKV_{Brazil-7124}					
Min - Max	1,619 – 34,109	774 – 18,838	1,124 – 19,412	3,552 – 35,772	4,504 – 47,026
Geometric mean	6,491	3,881	3,792	11,639	14,138
Mean	8,305	5,110	5,085	15,039	19,465
Standard deviation	6,728	4,188	4,266	11,202	15,978
<i>Participants that seroconverted (PRNT₅₀ ≥ 20)</i>	30 (100%)	30 (100%)	30 (100%)	9 (100%)	9 (100%)
ONNV_{UgMP30}					
Min - Max	259 – 8,395	299 – 5,800	240 – 4,026	3,771 – 30,296	3505 – 75,454
Geometric mean	1,676	1,102	1,156	10,370	10,360
Mean	2,122	1,361	1,435	13,206	19,300
Standard deviation	1,648	1,067	946	9,751	24,097
<i>Participants that seroconverted (PRNT₅₀ ≥ 20)</i>	30 (100%)	30 (100%)	30 (100%)	9 (100%)	9 (100%)
MAYV_{BeAr505411}					
Min - Max	35.5 – 6,259	128 – 2110	145 – 5,863	194 – 14,652	470 – 40,903
Geometric mean	374	417	652	1,462	2,471
Mean	954	524	967	2,860	6,797
Standard deviation	1,737	410	1,158	4,491	12,926
<i>Participants that seroconverted (PRNT₅₀ ≥ 20)</i>	30 (100%)	30 (100%)	30 (100%)	9 (100%)	9 (100%)
RRV_{T-48}					
Min - Max	10 – 12,271	10 – 571	10 – 232.5	25.4 – 675	29.9–651
Geometric mean	31.7	32.5	39.25	135	112
Mean	444	54.7	56.6	206	166
Standard deviation	2,234	101	51.9	198	190
<i>Participants that seroconverted</i>	20 (66.6%)	25 (83.3%)	25 (83.3%)	9 (100%)	9 (100%)

($PRNT_{50} \geq 20$)

note: undetectable $PRNT_{50}$ is recorded as 10

Table 3.S2. Compiled raw neutralization titers for vaccinee participants.

Participant	CHIKV _{LR2006}				CHIKV _{181/25}			
	Day 1	Day 29	Day 180	Day 365	Day 1	Day 29	Day 180	Day 365
1	10	101155	9166	177237	10	34109	3316	7191
2	10	29029	10538	12578	10	12484	6201	4867
3	10	9402	2611	2611	10	9960	2123	1194
4	10	12627	7373	10248	10	3651	3001	4542
5	10	11561	2450	728.9	27.02	2328	3266	1113
6	10	14237	5155	10876	10	5967	2827	2367
7	10	25999	4086	4388	10	4485	2928	2148
8	10	27816	38895	30689	10	66596	13244	15395
9	10	109913	21270	33314	22.66	17445	13642	10241
10	10	51572	9610	3540	10	10538	7917	6585
11	10	22011	13297	6094	10	13351	13392	5170
12	10	31911	4393	7825	10	6935	3312	7229
13	10	16756	3053	2828	10	25713	5846	3908
14	10	5001	4205	2910	10	5386	7500	7590
15	10	7467	2629	1794	10	3092	4635	4363
16	10	3433	7574	5736	10	5599	4431	4915
17	10	6863	6846	3857	30.67	6392	5913	5901
18	10	28583	1363	1480	10	78606	2432	859.2
19	10	27071	7609	2543	10	75997	2524	1654
20	10	7801	2209	2785	10	1619	1342	1523
21	10	8220	1894	2073	10	8467	1587	4096
22	10	32292	12139	21936	33.95	21182	6191	5544
23	10	12327	6022	2706	10	61193	5936	5005
24	10	17793	8194	15923	10	7696	4297	5069
25	10	26534	2739	1533	10	91693	3216	1118
26	10	14219	3274	8661	22.23	80449	2288	2454
27	10	11465	6993	5019	10	4427	1258	1739
28	10	6967	3285	3673	10	3139	1078	3176
29	10	5339	2804	2076	10	2298	3220	1870
30	10	10053	2532	1816	10	3879	1571	2269

Participant	CHIKV _{Brazil-7124}				ONNV _{UgMP30}			
	Day 1	Day 29	Day 180	Day 365	Day 1	Day 29	Day 180	Day 365
1	10	34109	8015	12962	10	3477	1149	2070

2	10	12484	8448	8771	10	690.4	495.2	1671
3	10	9960	2135	1670	22.45	1677	1118	564
4	10	3651	2830	3002	10	796.7	973.9	1978
5	10	2328	1714	1124	10	259.3	365.3	300.6
6	10	5967	2845	3874	10	769.9	538.3	690.6
7	10	4485	2314	1451	10	1928	838.9	1155
8	10	6659	18838	19412	25.84	2828	5800	3307
9	10	17445	10480	6273	29.3	3814	1422	1357
10	10	10538	7041	3029	30.03	1533	1645	1266
11	10	13351	4325	14015	27.82	3023	1464	811.6
12	10	6935	3306	6711	35.44	1673	1271	915.1
13	10	2571	3261	3616	44.96	8395	1784	1982
14	10	5386	12094	3203	10	2383	2492	2033
15	10	3092	3122	3831	10	1165	706.7	889.9
16	10	5599	6913	5740	10	1073	1404	3514
17	10	6392	5227	2714	41.22	1089	3206	1873
18	10	7860	774.1	1140	10	1418	299.1	240.4
19	10	7599	4246	2245	10	2260	1492	684.4
20	10	1619	2959	1260	10	792.9	602.9	594.1
21	10	8467	4808	2092	10	4142	746.5	606.5
22	10	21182	4018	7400	10	5291	2276	2114
23	10	6119	14147	3750	25.71	1140	1819	691.2
24	10	14387	6644	8373	10	2091	1193	4026
25	10	9169	2018	1168	44.45	2519	695.3	510.3
26	10	8044	2001	7193	10	1624	791.8	1505
27	10	4427	3658	6111	10	1716	1705	1874
28	10	3139	2302	5240	10	757.6	544.8	1288
29	10	2298	1711	3171	23.5	1910	978.2	720.5
30	10	3879	1112	2013	10	1413	1016	1807

Participant	MAYV _{BeAr505411}				RRV _{T-48}			
	Day 1	Day 29	Day 180	Day 365	Day 1	Day 29	Day 180	Day 365
1	10	791.4	528.4	862.3	10	83.56	65.03	87.96
2	10	276.1	401.1	880	10	32.81	23.02	28.57
3	10	90.82	128.1	144.6	10	27.37	10	10
4	10	134.5	237	200.4	10	10	10	21.18
5	10	6295	625.2	507.5	10	12271	571.1	232.5
6	10	210.8	184.7	357.6	10	10	10	10
7	10	164.2	271.7	256	10	20.52	14.48	21.66
8	10	427.1	871.2	575.9	10	48.16	120.6	45.11

9	10	1128	163.6	792.3	10	97.43	75.81	76.37
10	10	387.9	2110	2269	10	24.93	85.05	83.43
11	10	193	294.6	485	31.81	47.7	37.62	10
12	10	147.4	346.6	481.3	10	10	10	22.85
13	10	1147	633.9	692.6	10	76.45	43.21	84.71
14	10	152.4	533.6	910.8	10	64.73	25.35	28.92
15	10	121.7	308.4	388.9	10	28.52	30.21	29.34
16	10	254.7	423.2	572.6	10	10	23.75	67.28
17	10	126.4	308.2	504.8	10	20.88	34.28	29.16
18	10	1205	324.9	438.1	10	56.1	25.91	37.33
19	10	343.4	266.3	398	10	10	20.18	10
20	10	35.56	147.6	180.4	10	10	30.67	20.65
21	10	5521	1070	1260	10	117.4	35.34	50.73
22	10	395.5	754	5863	10	42.01	79.29	167.9
23	10	138.1	985.4	1679	10	10	26.01	38.34
24	22.26	6115	1149	3553	10	10	37.42	124.6
25	10	326.3	555.9	1148	10	33.32	29.03	10
26	10	978.5	604.4	1115	10	10	38.98	85.57
27	10	106.7	710.1	821	10	25.98	64.86	133.1
28	10	761.8	266.1	1012	10	10	10	27.69
29	10	254.9	193.3	298	10	69.74	28.08	47.4
30	10	398	324.1	353.3	10	20.97	26.86	56.17

3.3.2 The potency of alphavirus neutralizing antibodies for IXCHIQ vaccinees decreases with decreasing genetic similarity of viral antigens.

Next, we compared vaccinee serum homotypic and heterotypic neutralization titer results with the genetic relatedness of the viruses neutralized (**Figure 3.2**). To compare phylogenetic distances, we constructed a maximum likelihood phylogenetic tree based on the sequences of the structural proteins E1/6K/E2/E3 of the viruses included in our study (**Figure 3.2A**). We next grouped the neutralization data for IXCHIQ vaccinees by virus strain at 1 month (**Figure 3.2B**), 6 months (**Figure 3.2C**), and 1 year post-vaccination (**Figure 3.2D**) and found that the potency of neutralizing antibodies gradually decreased with increasing phylogenetic distance from the parental vaccine strain virus, CHIKV_{LR2006} (**Figure 3.2A**). At 1 month post-vaccination, compared to CHIKV_{LR2006}, the GMT for CHIKV_{181/25} was ~1.4-fold lower (ns), ~2.4-fold lower for CHIKV_{Brazil-7124} (*P = 0.0289), ~9.6-fold lower for ONNV_{UgMP30} (****P < 0.0001), ~43-fold lower for MAYV_{BeAr505411} (****P < 0.0001), and ~505-fold lower for RRV_{T-48} (****P < 0.0001) (**Figure**

3.2B). At 6 months post-vaccination, compared to CHIKV_{LR2006}, the GMT for CHIKV_{181/25} was ~1.4-fold lower (ns), ~1.3-fold lower for CHIKV_{Brazil-7124} (ns), ~4.7-fold lower for ONNV_{UgMP30} (****P < 0.0001), ~12.5-fold lower for MAYV_{BeAr505411} (****P < 0.0001), and ~160-fold lower for RRVT_{T-48} (****P < 0.0001) (**Figure 3.2C**). At 1 year post-vaccination in comparison to CHIKV_{LR2006}, the GMT against CHIKV strains and ONNV were nearly identical: CHIKV_{181/25} was ~1.2-fold lower (ns), CHIKV_{Brazil-7124} ~1.2-fold higher (ns), ONNV_{UgMP30} ~1.2-fold lower (****P < 0.0001); greater differences were observed for MAYV_{BeAr505411} at ~5.1-fold lower GMT (****P < 0.0001) and ~112-fold lower for RRVT_{T-48} (****P < 0.0001) (**Figure 3.2D**). These data affirm the durability of cross-neutralizing antibodies up to one year post-vaccination (**Figure 3.2B-D**). The E1/6K/E2/E3 amino acid sequences were used to calculate Dayhoff distances (MEGA software) to compare the amino acid relatedness of our panel of viruses with respect to the most antigenic viral proteins in terms of antibody responses (**Supplemental Table 3**). The vaccinee neutralization data was grouped in the same manner by time post-vaccination but now compared with the Dayhoff distance, revealing that decreasing cross-neutralizing antibody potency was related to increasing Dayhoff distance of the viruses neutralized (**Figure 3.2E-G**). Neutralizing antibody titer and Dayhoff distance were significantly negatively correlated by Spearman correlation (P < 0.0001, r = -0.7165) (**Figure 3.2G**). For example, RRVT_{T-48} is the most genetically and antigenically divergent virus from CHIKV_{LR2006}, resulting in the lowest sera neutralization capability. Indeed, this highlights that antibody epitope profiles induced by vaccination are dominantly located in the amino acids of these viral structural proteins and that small changes in Dayhoff distance have a significant impact on the neutralization titer (**Figure 3.2E-G**). Overall, by analyzing the vaccinee neutralization titers with respect to genetic relatedness, we were able to discern that the neutralizing antibody potency and breadth was related to genetic similarity of the Semliki Forest antigenic complex viruses included in our investigation (**Figure 3.2**).

Figure 3.2. Cross-neutralizing antibodies decrease in potency with increasing phylogenetic and Dayhoff distance from the CHIKV_{LR2006} parental vaccine strain.

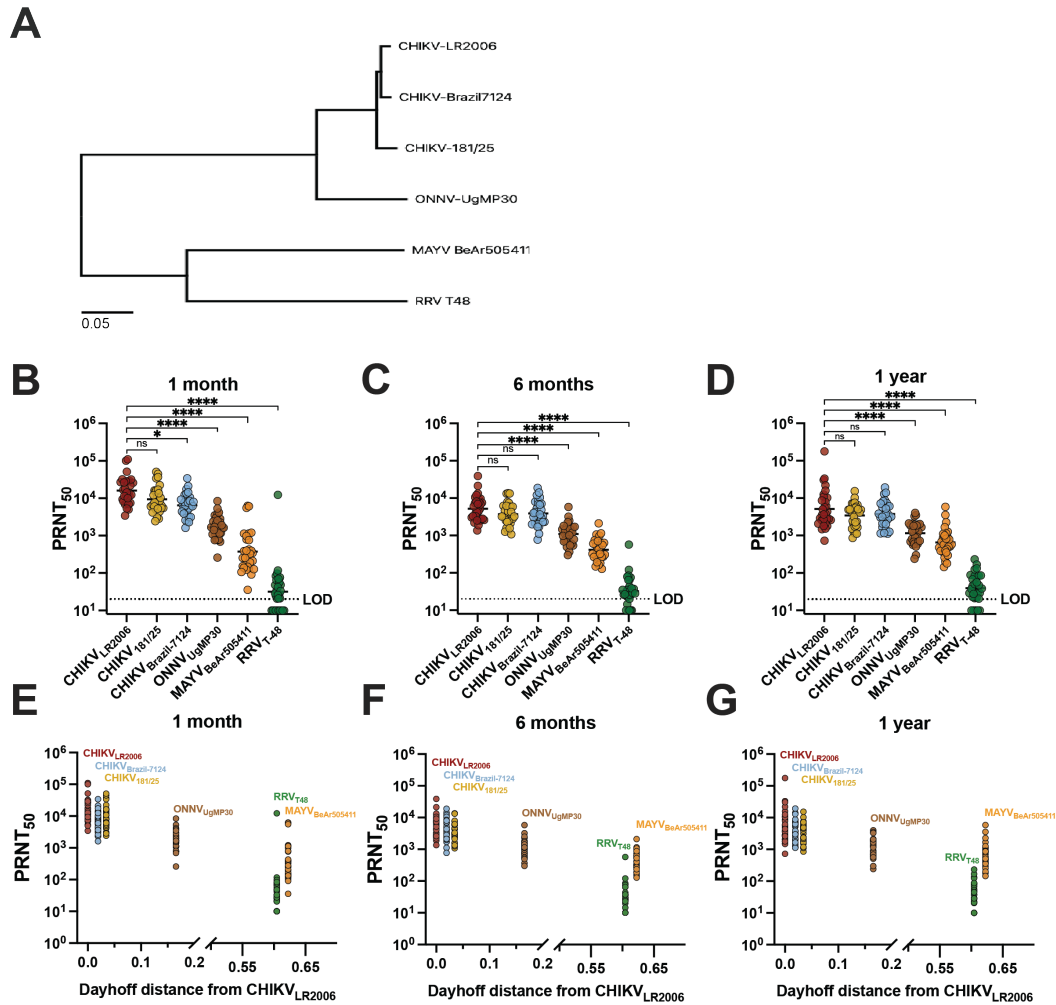


Figure 3.2. The maximum likelihood phylogenetic tree shown in (A) for the viruses used in this study represents viral stock sequencing consensus data aligned and trimmed to E1/6K/E2/E3 in Geneious Prime software with phylogeny constructed in MEGA software using the Dayhoff model with uniform rates and nearest-neighbor interchange. Neutralizing antibody titers for each virus by 50% plaque reduction neutralization test (PRNT₅₀) are grouped on logarithmic scale by (B) 1 month, (C) 6 months, and (D) 1-year post-vaccination timepoints. Variable slope, non-linear regressions in Prism software were used to calculate PRNT₅₀. Neutralizing activity is compared to the parental vaccine strain CHIKV_{LR2006} and data are analyzed by one-way ANOVA (Friedman's test) with Dunn's multiple comparisons where ns $P > 0.05$, $*P = 0.0289$, and $P^{****} < 0.0001$. Panels E-G represent analysis of serology data with Dayhoff distance of amino acid relatedness between each virus and the parental CHIKV_{LR2006} strain. Dayhoff distances were calculated using viral stock sequences trimmed to E1/6K/E2/E3 in MEGA software. The limit of detection for the neutralization assays was 20 and sera falling below the limit of detection were assigned a value of 10 for graphing and calculations of antigenic distances.

Table 3.S3. Amino acid sequences (E1/6K/E2/E3) used for phylogenetic and Dayhoff distance analyses to compare the genetic relatedness of the alphaviruses under investigation in this study.

<p>CHIKV LR2006-OPY1</p> <p>SLAIPVMCLLANTTFPCSQPPCTPCCYEKEPEETLRMLEDNVMRPGYYQLLQASLTCSPHRQRRSTKDNFN VYKATRPYLAHCPDCGEGHSCHSPVALERIRNEATDGTLKIQVSLQIGIKTDDSHDWTCLRYMDNHMPAD AERAGLFVRTSAPCTITGTMGHFILARCPKGETLTVGFTDSRKISHSCTHPFHHDPPVIGREKFHSRPQHGKE LPCSTYVQSTAATTEEIEVHMPPDTPDRTLMSQQSGNVKITVNGQTVRYKCNCGGSNEGLTTTDDKVINNCK VDQCHAAVTNHKKWQYNSPLVPRNAELGDRKGKIHIPFLANVTCRVPKARNPTVTVYGNQVIMLLYPD HPTLLSYRNMGEEPNYQEEWVMHKKEVVLTPTEGLEVTWGNNEPYKYWPQLSTNGTAHGHPHEIILYY YELYPTMTVVVSVATFILLSMVGMAGMCMCARRRCITPYELTPGATVPFLLSLICCIRTAKAATYQEA IYLWNEQQPLFWLQALIPLAALIVLCNCLRLLPCCCKTLAFLAVMSVGAHTVSAYEHVTVIPNTVGVVYKT LVNRPGYSPMVLEMELLSVTLEPTLSLDYITCEYKTVIPSPYVKCCGTAECKDKNLPDYCKVFTGVYPFM WGGAYCFDAENTQLSEAHVEKSECKTEFASAYRAHTASASAKLRVLYQGNNITVTAYANGDHAHTVK DAKFIVGPMSSAWTPFDNKIVVYKGDVYNMDYPPFGAGRPGQFGDIQSRTPESKDVYANTQLVLRPAVG TVHVPYSQAPSGFKYWLKERGASLQHTAPFGCQIATNPVRAVNCAVGNMPISIDIPEAAFRVVDAPSLTD MSCEVPACTHSSDFGGVAIIKYAASKKKGKCAVHSMTNAVITIREAEIEVEGNSQLQISFSTALASAEFRVQV STQVHCAAACHPPKDHIVNYPASHTTLGVQDISATAMSWVQKITGGVGLVVAVAALILIVVLCVSFSRH</p>
<p>CHIKV 181/25</p> <p>SLAIPVMCLLANTTFPCSQPPCTPCCYEKEPEKTLRMLEDNVMSPGYYQLLQASLTCSPRRQRSSIKDNFN YKAIRPYLAHCPDCGEGHSCHSPVALERIRNEATDGTLKIQVSLQIGIKTDDSHDWTCLRYMDNHMPADA ERARLFVRTSAPCTITGTMGHFILARCPKGETLTVGFTDGRKISHSCTHPFHHDPPVIGREKFHSRPQHGREL PCSTYAQSTAATAEEIEVHMPPDTPDRTLMSQQSGNVKITVNSQTVRYKCNCGDSNEGLTTTDDKVINNCK VDQCHAAVTNHKKWQYNSPLVPRNAELGDRKGKVHIPPFLANVTCRVPKARNPTVTVYGNQVIMLLYPD HPTLLSYRNMGEEPNYQEEWVTHKKEIRLTPTEGLEVTWGNNEPYKYWPQLSTNGTAHGHPHEIILYYY ELYPTMTVVVSVASFVLLSMVGVAVGMCMCARRRCITPYELTPGATVPFLLSLICCIRTAKAATYQEA VYLWNEQQPLFWLQALIPLAALIVLCNCLRLLPCFCKTLTFLAVMSVGAHTVSAYEHVTVIPNTVGVVYKT LVNRPGYSPMVLEMELLSVTLEPTLSLDYITCEYKTVIPSPYVKCCGTAECKDKSLPDYCKVFTGVYPFM WGGAYCFDENTQLSEAHVEKSECKTEFASAYRAHTASASAKLRVLYQGNNITVTSAYANGDHAHTV KDAKFIVGPMSSAWTPFDNKIVVYKGDVYNMDYPPFGAGRPGQFGDIQSRTPESKDVYANTQLVLRPSA GTVHVPYSQAPSGFKYWLKERGASLQHTAPFGCQIATNPVRAMNCAVGNMPISIDIPDAAFTRVVDAPSLT DMSCEVPACTHSSDFGGVAIIKYAASKKKGKCAVHSMTNAVITIREAEIEVEGNSQLQISFSTALASAEFRVQV CSTQVHCAAACHPPKDHIVNYPASHTTLGVQDISVTAMSWVQKITGGVGLVVAVAALILIVVLCVSFSRH</p>
<p>CHIKV Brazil-7124</p> <p>SLAIPVMCLLANTTFPCSQPPCTPCCYEREPEETLRMLEDNVMRPGYYQLLQASLTCSPHRQRRSTKDNFN VYKATRPYLAHCPDCGEGHSCHSPVALERIRNEATDGTLKIQVSLQIGIKTDDSHDWTCLRYMDNHMPAD AERAGLFVRTSAPCTITGTMGHFILTRCPKGETLTVGFTDSRKISHSCTHPFHHDPPVIGREKFHSRPQHGKE LPCSTYVQSTAATTEEIEVHMPPDTPDRTLMSQQSGNVKITVNGQTVRYKCNCGGSNEGLITDDKVINNCK VDQCHAAVTNHKKWQYNSPLVPRNAELGDRKGKIHIPFLANVTCRVPKARNPTVTVYGNQVIMLLYPD HPTLLSYRNMGEEPNYQEEWVTHKKEVVLTPTEGLEVTWGNNEPYKYWPQLSTNGTAHGHPHEIILYY YELYPTMTVVVSVASFVLLSMVGVAVGMCMCARRRCITPYELTPGATVPFLLSLICCIRTAKAATYQEA AVYLWNEQQPLFWLQALIPLAALIVLCNCLRLLPCCCKTLAFLAVMSVGAHTVSAYEHVTVIPNTVGVVY KTLVNRPGYSPMVLEMELLSVTLEPTLSLDYITCEYKTVIPSPYVKCCGTAECKDKNLPDYCKVFTGVY FMWGGAYCFDAENTQLSEAHVEKSECKTEFASAYRAHTASASAKLRVLYQGNNITVTAYANGDHAHT VKDAKFIVGPMSSAWTPFDNKIVVYKGDVYNMDYPPFGAGRPGQFGDIQSRTPESTDVYANTQLVLRPA AGTVHVPYSQAPSGFKYWLKERGASLQHTAPFGCQIATNPVRAMNCAVGNMPISIDIPDAAFIRVVDAPSL TDMSCVPTCTHSSDFGGVAIIKYAASKKKGKCAVHSMTNAVITIREAEIEVEGNSQLQISFSTALASAEFRVQ VCSTQVHCAAACHPPKDHIVNYPASHTTLGVQDISATALSWSVQKITGGVGLVVAVAALILIVVLCVSFSRR</p>

ONNV-UgMP30

SLALPVMCLLANTTFPCSQPPCAPCCYEKKPEETLRMLEDNVMQPGYYQLLDSALACSQRRQKRNARENF
NVYKVTRPYLAHCPDCGEGHSCHSPIALERIRSEATDGLTKIQVSLQIGIKTDDSHDWTCLRYMDSHTPVD
ADRSGLFVRTSAPCTITGTMGHFILARCPKGETLTVGFVDSRRISHTCMHPPFRHEPPLIGREKFHSRPQHGKE
LPCSTYVHTTAATAEEIEVHMPPDTPDYTLMTQQAGNVKITVDGQTVRYKCKCDGSNEGLITADKVINNC
KVDQCHTAVTNHKKWQYNSPLTPRNSEQGDRKGKIHIPPLVNTTCRVPKARNPTVTYGKNRVTLHHPD
HPTLLSYRAMGRIPDYHEEWITNKKEISITVPAEGLEVTWGNNDPYKYWPQLSTNGTAHGHPHEIILYYYE
LYPTTTIAVLAASIVITSLVGLSLGMCICARRRCITPYELTPGATIPFLGLVCCARTAKAASYEEAATYLW
NEQQPLFWLQLLIPLSAAIVVCNCLKLLPCCCKTLTFLAVMSIGARTVTAYEHATVIPNTVGVPCCTLVSRP
GYSPMVLEMELQSVTLEPALSLDYITCEYKTIPTSPYVKCCGTAECKAKNLPDYNCKVFTGVYPPFMWGG
YCFDAENTQLSEAHVEKSESKTEFASAYRAHTASVSAKLRVIFYQGNNTVSAAYANGDHAVTVEDAKFV
IGPLSSAWSPFDNKIVVYKGEVYNMDYPPFGAGRPGQFGDIQSRTDPSKDVYANTQLILQRPAAAGAIHVPY
SQAPSGFKYWLKEKGASLQHTAPFGCQIATNPVRAVNCAVGNIPVSIDIPDAAFTRVTDAPSITDMSCEVAS
CTHSSDFGGAAVIKYTASKKKGKCAVHVSNTAVTIREPNVDVKGTAQLQIAFSTALASAEFKVQICSTLVHC
SATCHPPKDHIVNYPSPHTLGVQDISTAMSWWQKITGGVGLVVAIAALILIIIVLCVSFSRH

MAYV-BeAr505411

ASTVTAMCLLNTNISFPCFPQSCAPCCYEKGPEPTLRMLEENVNSEGYYDLLHAAVYCRNSSRSKRSTANHF
NAYKLTRPYVAYCADCGMGHSCHSPIAMIENIQADATDGLTKIQFASQIGLTKTDTHDHTKIRYAEGHDIAE
AARSTLKVHSSSECTVTGTMGHFILAKCPPGEAISVSFVDSKNEHRTCRIAYHHEQRLIGRERFTVRPHHGIE
LPCTTYQLTTAETSEEIDMHMPPDIPDRITLSQQSGNVKITVNGRTVRYSCSCGSKPSGTTTTDKTINSCTVD
KCQAYVTSHTKWQFNPFVPRAEQAERKGVHIPPPLINTTCRVPLAPEALVRSGKREATLSLHPIHPTLLS
YRTLGAEPVFDEQWITAQTEVTIPVPEVEYQWGNHQPQLWSQLTTEGKAHGWPHEIIEYYYGLHPTIT
IVVVIAVSVVLLSLAASVVMCVARNKCLTPYALTPGAVVPVTIGVLCCAPKAHAASFAEGMAYLWDN
NQSMFWMELTGPLALLILTTCCARSLSCCKGSFLVAMSIGSAVASAYEHTAIIPNQVGFYKAHVAREGY
SPLTLQMQVVETSLEPTLNLEYITCDYKTKVSPYVKCCGTAECRTQDKPEYKCAVFTGVYPPFMWGGAYC
FCDSSENTQMSEAYVERADVCKHDHAAAYRAHTASLRAQIKVTYGTVNQTVEAYVNGDHAVTIAGTKFIF
GPVSTAWTPFDKIVVYKGEVYNQDFPPYAGQPRFGDIQSRTLDSRDLYANTGLKLARPAAGNIHVPY
TQTPSGFKTWQKDRDSPLNAKAPFGCVIQTNPVRAMNCAVGNIPVSMADIADSAFTRLTDAPVISELTCTVS
TCTHSSDFGGIAVLSYKVEKPGRCDIHSHSNVAVLQEVSIETEGRSVIHFSTASAAPSFVSVCSSRATCTAK
CEPPKDHVVTPANHNGVTLPLDLSSTAMTWAQHLAGGVLLIVLAVLILVIVTCVTLRR

RRV-T-48

WSAALMMCILANTSFPCCSSPPCYPCYEKQPEQTLRMLEDNVNRPGYELLEASMTCRNRSRHRRSVTEH
FNVYKATRPYLAAYCADCGDGYFCYSPVAIEKIRDEASDGLMKIQVSAQIGLKDAGTHAHTKIRYMAGHDV
QESKRDSLRYVYTSAAACSIHGTMGHFIVAHCPPGDYLVKVSFEDADSHVKACKVQYKHDPLVPGREKFVVRP
HFGVELPCTSYQLTTAPTDEEIDMHTPPDIPDRITLSQTAGNVKITAGGRTIRYNCTCGRDNVGTSTDKTI
NTCKIDQCHAAVTSHDKWQFTSPFVPRADQTARRGKVHVPFPLTNVTCRVPLARAPDVTYGKKEVTLRLH
PDHPTLFSYRSLGAEPHPYEEWVDKFSERIIPVTEEGIEYQWGNPPVRLWAQLTTEGKPHGWPHEIQQYYY
GLYPAATIAAVSGASLMALLTLAATCCMLATARRKCLTPYALTPGAVVPLTLGLLCCAPRANAASFAETM
AYLWDENKTLFWMEFAAPAAALALLACCIKSLICCKPFSFLVLLSLGASAKAYEHTATIPNVVGFYKAH
IERNGFSPMTLQLEVVETSLEPTLNLEYITCEYKTVVPSPIKCCGTSECSSEKQPDYQCKVYTGVPFMWG
GAYCFDSSENTQLSEAYVDRSDVCKHDHASAYKAHTASLKATIRISYGTINQTTEAFVNGEHAVNVGGSK
FIFPISTAWSPFDNKIVVYKDDVYNQDFPPYGSQPRFGDIQSRTVESKDLANTALKLSRSPGVVHVP
YTQTPSGFKYWLKEKSSLNKAPFGCKIKTNPVRAMNCAVGSIPVSMIPDSAFTRVVDAPAVTDLSCQV
VVCTHSSDFGGVATLSYKTDKPGKCAVHSHSNVAVLQEAATVDVKEDGKVTVHFSTASAPAFKVSVCDA
KTTCTAACPPKDHIVPYGASHNNQVFPDMSGTAMTWVQRLASGLGLALIAVVVLVLTCTMRR

3.3.3 IXCHIQ vaccinees develop alphavirus cross-neutralizing antibody potency and breadth similar to individuals who were naturally infected with CHIKV.

The cross-neutralizing antibody potency and breadth of vaccinee sera was compared to the sera of individuals who had experienced natural CHIKV infection during the 2014-2015 outbreak in Puerto Rico [345]. Serum samples were collected from nine adults aged 19-81 who had documented CHIKV infections in 2014 (**Table 3.1**). This group is composed of five female and four male participants who identify as hispanic and were all born in Puerto Rico; the ethnicities of this group were caucasian/white (n=2), multiracial (n=2), and other (n=5) (**Table 3.1**). Although one individual was asymptomatic, the most common symptoms during infection were rash (77.7%), severe muscle/joint pain (66.6%), sensitivity to light (55.5%), and fever (55.5%) (**Table 3.1**). We determined the alphavirus cross-neutralizing antibody profiles for human sera from this cohort collected between June of 2022 and November of 2023 (**Figure 3.3, Table 3.2, Supplemental Table 3.S4**). There is no confirmation of which CHIKV strain was responsible for infection in these individuals but the Asian genotype is known to have circulated in Puerto Rico at the time the patients were reportedly infected [346, 347]. We detected potent neutralizing activity for all three CHIKV strains with no significant change in GMTs between the two timepoints (**Figure 3.3A-C**). GMTs of the cohort were observed for CHIKV_{LR2006} at 17,317 and 12,530 at ~8 and ~9 years post-infection, respectively (**Figure 3.3A, Table 3.2**). The GMTs for CHIKV_{181/25} were 12,522 and 10,146 at ~8 and ~9 years post-infection (**Figure 3.3B, Table 3.2**), and for CHIKV_{Brazil-7124} they were 11,639 and 14,138 at ~8 and ~9 years post-infection, respectively (**Figure 3.3C, Table 3.2**). Robust cross-neutralization was also observed for ONNV_{UgMP30} with GMTs of 10,370 at ~8 years post-infection and 10,360 at ~9 years post-infection with no significant change between the two time points (**Figure 3.3D, Table 3.2**). The cross-neutralizing antibody titers against MAYV_{BeAr505411} were 1,462 at ~8 years post-infection and 2,471 at ~9 years post-infection (**Figure 3.3E, Table 3.2**). The GMT for RRV_{T-48} was 135 at ~8 years post-infection and 112 at ~9 years post-infection (**Figure 3.3F, Table 3.2**). Importantly, 100% seroconversion against each alphavirus in this investigation was observed for these CHIKV immune sera (**Figure 3.3A-F, Table 3.2**). At ~8 years post-infection, there were no significant differences when comparing the CHIKV_{LR2006} PRNT₅₀ to CHIKV_{181/25}, CHIKV_{Brazil-7124}, and ONNV_{UgMP30} (**Figure 3.3G**). For the cross-neutralizing responses at ~8 years post-infection compared to CHIKV_{LR2006}, the GMTs were ~11.8-fold lower against MAYV_{BeAr505411} (**P = 0.0053), and ~128-fold lower

against RRV_{T-48} (****P < 0.0001), (Figure 3.3G). At ~9 years post-infection, there were no significant changes when comparing the CHIKV_{LR2006} PRNT₅₀ to CHIKV_{181/25}, CHIKV_{Brazil-7124}, ONNV_{UgMP30}, and MAYV_{BeAr505411} (Figure 3.3H). The GMT was a significant ~112-fold lower for RRV_{T-48} at ~9 years post-infection (**P = 0.002) (Figure 3.3H). Together, these data highlight that CHIKV infection induces cross-neutralizing breadth with no significant reduction in potency against the recently and potentially actively circulating contemporary CHIKV_{Brazil-7124} strain (Figure 3.3C). These findings also indicate the extension of neutralizing responses against the Semliki Forest antigenic complex which remain stable for nearly a decade after infection (Figure 3.3).

Figure 3.3. Neutralizing antibody breadth of human serum collected in Puerto Rico 8-9 years following 2014 CHIKV infections.

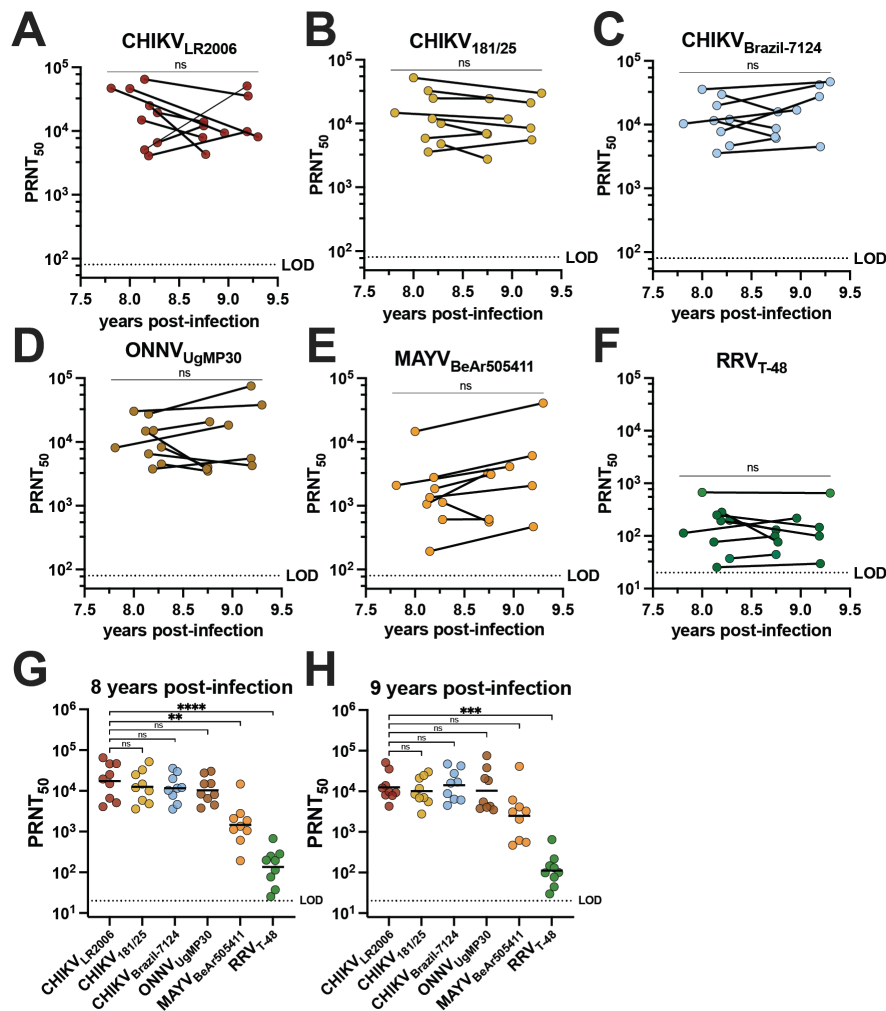


Figure 3.3. Sera collected from nine human participants in Puerto Rico between June 2022 and November 2023 following diagnosed CHIKV infections in 2014 were used in virus neutralization assays against the six alphaviruses included in this study: (A) CHIKV_{LR2006}, (B) CHIKV_{181/25}, (C) CHIKV_{Brazil-7124}, (D) ONNV_{UgMP30}, (E) MAYV_{BeAr505411}, and (F) RRV_{T-48}. The PRNT₅₀ data are plotted against year post-infection for each participant and the two timepoints (~8 and ~9 years post-infection) were compared by paired t tests in (A-F). Neutralizing activity is also grouped by virus and strain at (G) ~8 years post-infection and (H) ~9 years post-infection. GMTs are shown in (G) and (H) where PRNT₅₀ for CHIKV_{LR2006} is compared to PRNT₅₀ for each other virus through analysis by one-way ANOVA (Freidman’s test) with Dunn’s multiple comparisons where ns $P > 0.05$, ** $P = 0.0053$, *** $P = 0.002$, and $P **** < 0.0001$. Variable slope, non-linear regressions in Prism software were used to calculate PRNT₅₀. The limit of detection for neutralization assays was 20.

Table 3.S4. Compiled raw neutralization titers from CHIKV infection participants.

Years post-infection	Participant, visit	CHIKV _{LR2006-OPY1}	CHIKV _{181/25}	CHIKV _{Brazil-7124}	ONNV _{UgMP30}	MAYV _{BeAr505411}	RRV _{T-48}
8	70001 v1	46285	52100	35772	30296	14652	674.6
9.3	70001 v2	8114	30003	47026	37990	40903	651.4
8.15	70003 v1	64794	3578	3552	6496	193.6	25.4
9.2	70003 v2	35561	5546	4504	4266	469	29.92
8.15	70005 v1	5093	32735	19960	27464	1355	250.1
9.19	70005 v2	50825	21174	42058	75454	2061	146.4
8.19	70008 v1	4091	11932	7765	3771	2787	194.0
9.19	70008 v2	9785	8458	27542	5498	6095	99.95
7.81	70011 v1	46829	24822	10302	8132	2092	113.9
8.96	70011 v2	9322	11792	16920	18421	4114	218.0
8.2	70012 v1	25074	14730	29663	15089	1860	283.6
8.77	70012 v2	4297	24603	15878	20747	3101	76.86
8.12	70013 v1	14929	5881	11602	14772	1059	76.86
8.74	70013 v2	7897	6958	6418	3769	3261	98.63
8.28	70015 v1	19441	4800	4642	4516	609.5	37.34
8.75	70015 v2	13890	2766	6118	3505	615.6	44.51
8.28	70016 v1	6576	10075	12091	8315	1131	198.4
8.75	70016 v2	12072	6848	8718	4050	556.3	130.5

The neutralizing antibody potency and breadth profiles were analyzed for CHIKV vaccinees and CHIKV-immune participants by comparing the neutralizing antibody responses at 1-year post-vaccination for 30 participants with responses at ~8 and ~9 years post-infection for the nine individuals (**Figure 3.4**). We found no significant difference in GMT for CHIKV_{LR2006},

MAYV_{BeAr505411}, and RRV_{T-48} (**Figure 3.4A**). For CHIKV_{181/25}, the GMT trended ~3.6-fold higher for infection participants compared to vaccinees ($*P = 0.0361$) (**Figure 3.4A**). For CHIKV_{Brazil-7124}, the GMT trended ~3.1-fold higher for infected participants compared to vaccinees ($*P = 0.0290$) (**Figure 3.4A**). For ONNV_{UgMP30}, the GMT trended ~9.0-fold higher for infected participants compared to vaccinees ($**P = 0.0067$) (**Figure 3.4A**), and we found no significant difference in GMT for CHIKV_{LR2006}, ONNV_{UgMP30}, MAYV_{BeAr505411}, and RRV_{T-48} (**Figure 3.4B**). For neutralization against CHIKV_{181/25}, the GMT was ~3.0-fold higher for infected participants compared to vaccinees ($*P = 0.0265$) (**Figure 3.4B**). The CHIKV_{Brazil-7124} GMT for naturally infected participants was ~3.7-fold higher compared to vaccinees ($*P = 0.0272$) (**Figure 3.4B**). Additionally, we examined the Pearson correlation between neutralizing antibody potency and age post-vaccination or post-infection (**Supplementary Figure 3.S1**). We found no significant correlation between neutralizing antibody titers and age for vaccinees; however, we did detect significant but weak negative correlations between neutralizing antibody titer and age for CHIKV-immune individuals (**Supplementary Figure 3.S1**). Although neutralization titers were slightly higher in CHIKV-immune individuals for some viruses, we can conclude that IXCHIQ vaccination elicits similar alphavirus neutralizing antibody potency and breadth to CHIKV infection by 1-year post-vaccination.

Figure 3.4. The neutralizing antibody breadth elicited by vaccination is comparable to CHIKV infection-induced cross-reactivity.

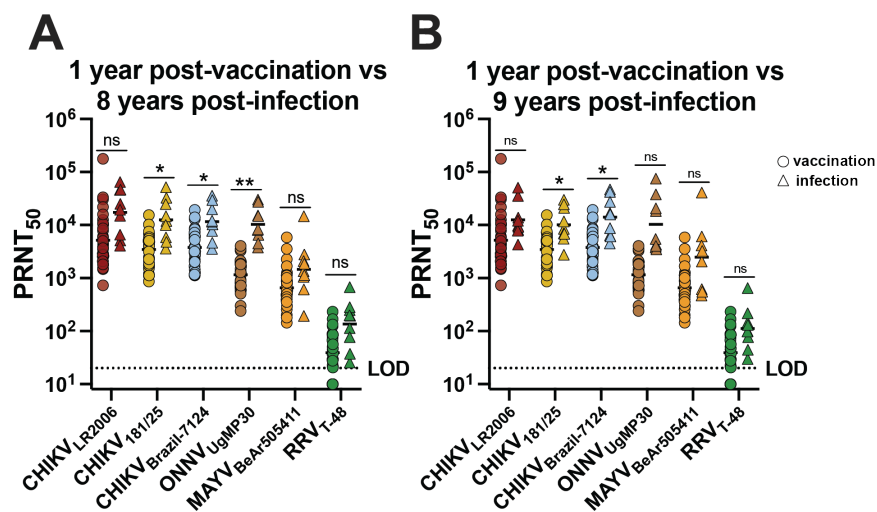


Figure 3.4. Serum from vaccinees and from patients following CHIKV infection in Puerto Rico were used in virus plaque reduction neutralization assays against CHIKV_{LR2006}, CHIKV_{181/25}, CHIKV_{Brazil-7124}, ONNV_{UgMP30}, MAYV_{BeAr505411}, and RRV_{T-48}. The 50% plaque reduction neutralization titers (PRNT₅₀) were compared at 1-year post-vaccination with (A) ~8 years post-infection and (B) ~9 years post-infection. Variable slope, non-linear regressions in Prism software were used to calculate PRNT₅₀. GMT in logarithmic scale is shown for each group. Data are analyzed by multiple unpaired t tests with Welch correction on each row where ns $P > 0.05$, * $P < 0.05$ and ** $P < 0.001$. The limit of detection for neutralization assays was 20 and sera falling below the limit of detection were assigned a value of 10.

Figure 3. S1. Correlating age and antibody titer after vaccination or infection.

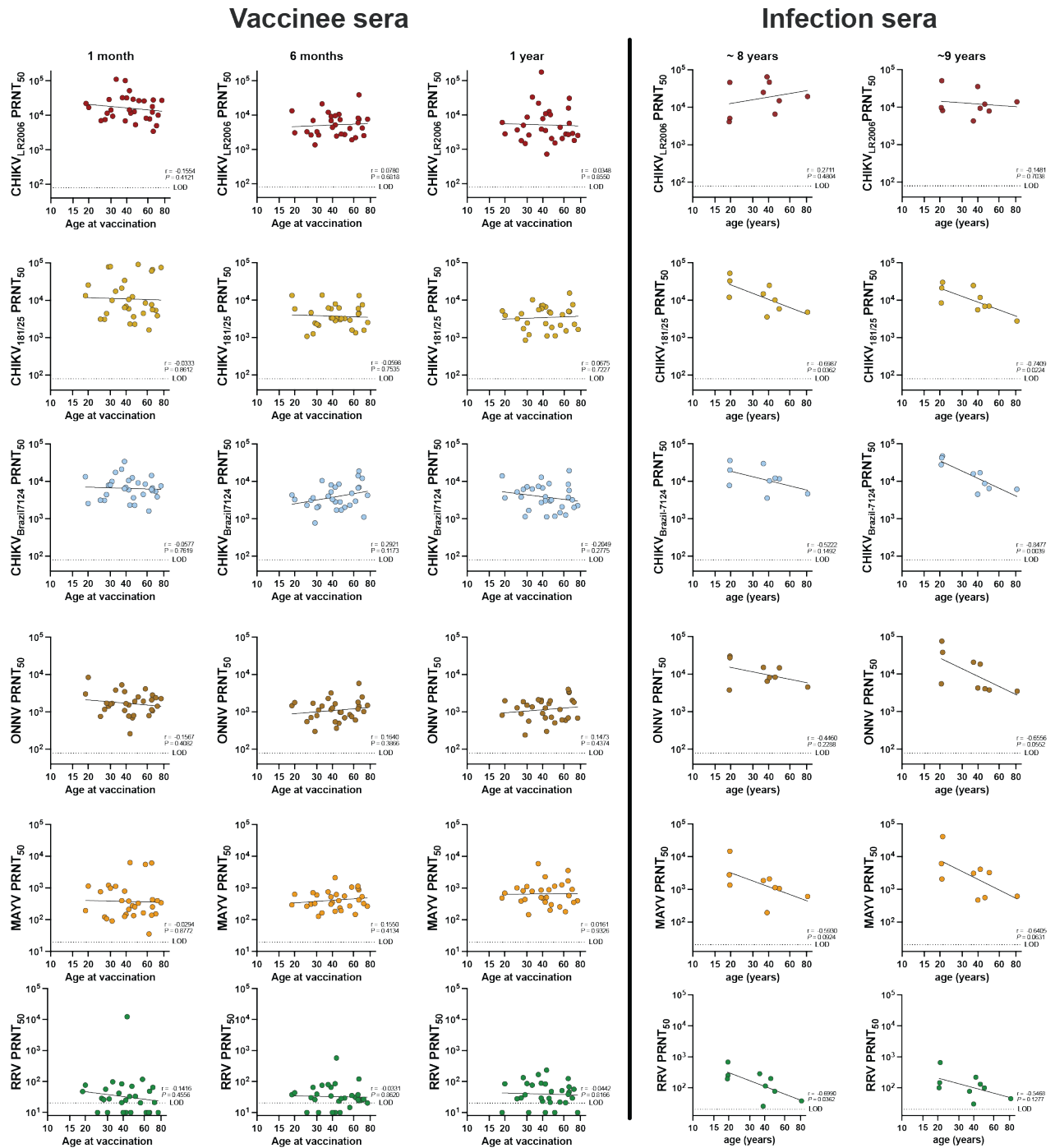


Figure 3.S1. Virus-specific 50% plaque reduction neutralization titer (PRNT₅₀) and age at vaccination or age at blood draw after infection are plotted. Age and PRNT₅₀ are log-transformed and analyzed by Pearson correlation. Pearson correlation coefficients (r) and corresponding P values are shown with a simple linear regression fit to the log-transformed data. Variable slope, non-linear regressions in Prism software were used to calculate PRNT₅₀. The

limit of detection for neutralization assays was 20 and sera falling below the limit of detection are assigned a value of 10.

We next used neutralization titers from vaccine- and CHIKV infection-immune sera to resolve the antigenic relationships between the alphaviruses using antigenic cartography (**Figure 3.5**). Antigenic cartography provides a means to use neutralization titers to graphically visualize antigenic distances between viruses and sera. For this analysis, we utilized the neutralization titers of the vaccinee sera at 1 month, 6 months, and 1 year post-vaccination (**Supplemental Table 3.S2**), and compared them to the CHIKV natural infection neutralization titers at 8 years post-infection (**Supplemental Table 3.S4**). In general, neutralization titers placed the vaccine and CHIKV infection-immune sera in a cluster around the three CHIKV viral strains, comprising a single serogroup with very little difference in antigenic distances between vaccinee and infected samples (**Figure 3.5**). Lower neutralization titers against the heterotypic alphaviruses led to more distant placement from all the sera samples with ONNV_{UgMP30} being the closest followed by MAYV_{BeAr505411}, and then RRV_{T-48}, against which all sera had the lowest neutralizing activity (**Figure 3.5**). When comparing these antigenic relationships at 1 month post-vaccination and 8 years post-infection, we found that there was about an 8-fold range in antigenic units across the map for all vaccinee and CHIKV infection sera (**Figure 3.5A**). When comparing these antigenic relationships at 6 months post-vaccination and 8 years post-infection, the two serum groups clustered even more tightly with about a 6-fold range across the map except for one outlier (**Figure 3.5B**). At 1 year post-vaccination, an average of a 6-fold change in antigenic units was also observed with the exception of two outlying sera (**Figure 3.5C**). Intriguingly, over time the viral antigens MAYV and RRV became positioned more closely to the vaccinee sera suggesting the broadening of cross-neutralizing immunity over time throughout the first year after vaccination (8 to 14-fold change vs 4 to 12-fold change at 1 year post-vaccination) (**Figure 3.5**). Perhaps most importantly, at all timepoint comparisons, we found that the vaccinee sera clustered antigenically with the CHIKV infection immune sera, suggesting that the IXCHIQ vaccine elicits antibody responses similar to natural CHIKV infection. This conclusion is consistent with our comparative analysis of neutralization titers alone (**Figure 3.4**) and supports our conclusion that IXCHIQ vaccination elicits similar cross-neutralizing antibody potency and breadth to CHIKV infection.

Figure 3.5. Vaccinee sera cluster antigenically with infection sera.

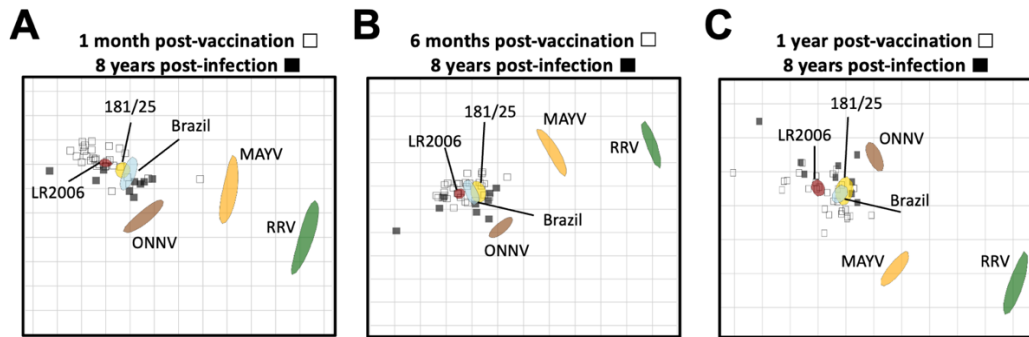


Figure 3.5. Antigenic cartography was utilized to make an antigenic map to illustrate the relationship between sera and viruses neutralized as well as relative antigen relatedness of the viral antigens compared in this study based on PRNT₅₀. The vaccinee sera are represented by unfilled squares and the infection sera at 8 years post-infection are the black filled squares. The viral antigens are plotted as larger blob shapes based on the confidence area of its position. The grid of the antigenic map are units of antigenic distance and represent a 2-fold change in serum dilution in the neutralization assay. The map is constructed using 50% plaque reduction neutralization titers (PRNT₅₀) of each sera sample for each virus which position the sera closest to the viral antigen best neutralized, with viruses with lower neutralization potency positioned further away based on calculated pairwise distances between the sera and virus. Antigenic maps are shown comparing sera collected at 8 years post-CHIKV infection to vaccinee serum collected at (A) 1 month post-vaccination, (B) 6 months post-vaccination, or (C) 1 year post-vaccination. The limit of detection for neutralization assays was a PRNT₅₀ of 20 and sera falling below the limit of detection are recorded as 10 for calculations of antigenic distances.

Section 3.4: Discussion

Investigators have previously described the alphavirus antibody breadth elicited by CHIKV infection in humans, demonstrating cross-neutralization within the Semliki Forest virus antigenic complex, which is mediated by recognition of similar domains within the envelope proteins [59, 75-78, 85, 348]. Additionally, the breadth of neutralizing antibodies elicited by other CHIKV vaccines has also been examined in humans [75, 274] and mice [86, 102, 301], but not previously for IXCHIQ (VLA1553, attenuated based on the La Reunion strain of ECSA genotype). Here, we characterized the alphavirus cross-neutralizing antibody responses in humans elicited by the recently approved IXCHIQ vaccine. While Asian genotype CHIKV_{181/25} neutralizing antibody responses elicited by IXCHIQ had been previously reported following NHP studies and phase 3 trials, this is the first characterization of the human neutralizing antibody response against

additional CHIKV strains as well as to other related alphaviruses including ONNV_{UgMP30}, MAYV_{BeAr505411}, and RRV_{T-48} elicited by IXCHIQ.

We found that IXCHIQ vaccination elicits both homotypic and heterotypic neutralizing responses against three strains of CHIKV, ONNV_{UgMP30}, MAYV_{BeAr505411}, and RRV_{T-48}. These responses were durable, with only modest reduction in neutralization titer between one month and one year post-vaccination. This is important for the populations living in areas with not only CHIKV transmission but also potential for circulation of additional alphaviruses. Given that neutralizing antibodies are a correlate of protection for alphavirus infection in humans [98, 349, 350], these cross-neutralizing responses have potential to provide cross-protection to populations vulnerable to heterotypic alphavirus infection, although increasing antigenic differences between CHIKV and heterotypic alphaviruses may ultimately limit such cross-protective breadth. We found that cross-neutralization decreased in potency with increased phylogenetic distance and Dayhoff distance of amino acid relatedness. Cross-reactive neutralization strongly supports the presence of shared key neutralizing antibody epitopes among the viruses included in our investigation, which we and others have shown to be linked, at least in part, to antibodies targeting the B domain of E2 [59, 73, 75, 79, 251, 274, 326, 331]. The small differences in neutralizing activity between the CHIKV strains at all timepoints and a small reduction in PRNT₅₀ compared to ONNV_{UgMP30} for the vaccinees and CHIKV-immune participants over all time points supports the conclusion that all CHIKV strains cluster as a single serotype [305, 337]. Although CHIKV strains cluster antigenically, in some cases, unique amino acid mutations have been demonstrated to contribute to antigenic variation [351], which is why we included a contemporary CHIKV isolate from 2021 in Brazil [344] in this analysis. Ultimately, we found the mutations in the CHIKV_{Brazil-7124} strain relative to the other CHIKV strains did not greatly impact neutralization activity of vaccinees or CHIKV-immune individuals against the Brazilian strain. One intriguing result from our study was the modest increases in MAYV_{BeAr505411} and RRV_{T-48} neutralizing activity over time for vaccinees, suggesting that vaccine-elicited cross-reactive immunity broadens over one year post-vaccination; this finding would be consistent with previous work demonstrating that human antibody breadth broadens over time after natural CHIKV infection [59, 75]. CHIKV VLP vaccine-elicited (PXVX0317) cross-neutralizing antibodies against ONNV, MAYV, and RRV in humans have been identified by Raju *et al.* and some of these isolated monoclonal antibodies were shown to partially cross-protect against viral pathogenesis and disease in mice

[274]. Our work builds upon these findings of CHIKV vaccine-elicited alphavirus cross-neutralization in humans and reveals the first report of cross-neutralizing antibodies induced by the licensed vaccine IXCHIQ paired with evidence that these antibodies persist at one year post-vaccination and share potency and breadth features consistent with what is seen following natural infection. Additionally, our study directly compares these vaccinee responses to the cross-neutralizing antibodies generated in response to CHIKV infection and shows that IXCHIQ elicits neutralizing antibody populations similar in potency and breadth to antibodies elicited by natural CHIKV infection.

While cross-neutralization against other alphaviruses was detected, a limitation of this study is the translational impact that IXCHIQ will have on infection and disease outcomes for these antigenically related alphaviruses. Additionally, future studies are needed to examine the impact of pre-existing alphavirus immunity on the immune response to IXCHIQ when administered to CHIKV pre-immune vaccinees including the manner in which prior infection can shape the cross-neutralizing antibody breadth. It is possible that prior CHIKV immunity could impact IXCHIQ vaccine efficacy or in positive or negative ways. As a live attenuated virus vaccine, IXCHIQ may be neutralized by pre-existing CHIKV antibodies in CHIKV infected vaccinees – a victim of so called “sterilizing immunity.” It is also possible that IXCHIQ vaccination may stimulate expansion and diversification of latent memory cells from prior infection, giving rise to plasmablasts that may exhibit greater potency and/or breadth than pre-vaccination neutralizing antibodies in vaccinees. These studies have not been carried out to date, rather phase III trial participants were screened to select immunologically CHIKV-naïve vaccinees. There is an ongoing trial in adolescent participants in endemic Brazil that will begin to address these questions. Reciprocally, the way that IXCHIQ vaccination can shape the potency and breadth of cross-reactive alphavirus immunity, should also be addressed empirically. CHIKV outbreaks have the capacity to be explosive in immunologically naïve populations and then disappear for decades at a time, but it is not known whether CHIKV infection-elicited cross-reactive alphavirus immunity is sufficient to prevent infection with related alphaviruses. While no clinical or epidemiological reports suggest that cross-reactive alphavirus immunity would enhance infection as has been seen with dengue virus vaccines and earlier RSV vaccine candidates, this question will warrant monitoring as for all new viral vaccines. It is not yet understood how CHIKV seroconversion of endemic populations through immunization could shape transmission of

CHIKV and other alphaviruses. It is also not yet understood how immunization programs will be shaped (universal or targeted) and what the resulting impact on alphavirus transmission will be. To address these open questions, it will be important to characterize the alphavirus cross-neutralizing antibody breadth in individuals with diverse alphavirus exposure histories (vaccinated and unvaccinated) and conduct surveillance for emerging alphaviruses in these regions, especially with related sylvatic transmission cycles. Vaccine rollout in a new population inevitably invites many scientific questions and it is important that these are urgently addressed to avoid public health risks and ensure that the benefits of vaccination outweigh disease and public health risks. The implementation of the IXCHIQ vaccine and potentially other future approved CHIKV vaccines represents a step forward for prevention of CHIKV-induced disease burden impacting millions of people and has the potential to shape the emergence of additional alphaviruses over the coming years due to cross-reactive immunity.

Section 3.5: Materials & Methods

3.5.1 Ethics Statement

All participants gave their informed consent for inclusion before they participated in the study. The study was conducted in accordance with the Declaration of Helsinki and approved by the central Institutional Review Board (Advarra IRB #Pro00045587, approved August 6th, 2020, and #Pro00050546, approved March 24th, 2021) for the human IXCHIQ vaccinees in NCT04546724 and NCT04838444 clinical trials. The study has been reviewed and approved by the Oregon Health and Science University (OHSU) IRB (IRB #10212, November 6th, 2015) for the CHIKV endemic cohort.

3.5.2 Study participants

IXCHIQ recipient vaccinee cohort

A total of 120 samples from 30 adult participants that were part of VLA1553 clinical trials in the continental U.S., NCT04546724 and NCT04838444, were included in this exploratory analysis. Samples were selected based on availability and based on neutralization titers measured in the clinical trial to represent an average neutralization capacity. Samples were also selected with

attention to represent heterogeneity in a population, with specific attention to age and sex of the participants. All participants were considered generally healthy and had no documented history of CHIKV infection or arthralgia.

Endemic cohort participant samples collected after CHIKV infection in Puerto Rico

Individuals with CHIKV infection histories in this study were enrolled in a larger study of long-term immunity following infection with arthropod-borne viruses. Samples were provided by Dr. Vanessa Rivera-Amill (Ponce Health Sciences University, Ponce, Puerto Rico). Samples from participants in this study with either PCR-confirmed CHIKV infections or that had positive CHIKV IgG/IgM ELISA results were screened for CHIKV neutralizing antibodies. Nine samples had detectable neutralizing activity, and these were included in this study. Following informed consent, participants provided additional history including other known and suspected arboviral infections, lifetime travel histories, and vaccination histories. Samples were collected, processed, and shipped to Oregon Health & Science University for analysis.

3.5.3 Cells and viruses

Vero cells (ATCC CCL-81) were cultured in Dulbecco's Modified Eagle Medium (DMEM; Thermo Scientific) containing 5% fetal calf serum (FCS; Thermo Scientific) supplemented with 1X penicillin-streptomycin-glutamine (PSG; Life Technologies) (DMEM-5). *Aedes albopictus* C6/36 cells (ATCC CRL1660) were also cultured in DMEM-5. Vero cells were propagated at 37°C and 5% CO₂ and C6/36 cells were propagated at 28°C with 5% CO₂. Alphaviruses were sourced through the Biodefense and Emerging Infections Research Resources Repository (BEI Resources): MAYV_{BeAr505411} (BEI NR-49910), ONNV_{UgMP30} (BEI NR-51661), and RRV_{T-48} (BEI NR-51457). The infectious clone of CHIKV_{LR2006-OPY1} was provided by Steven Higgs (Kansas State University, Manhattan, KS). The infectious clone of CHIKV_{181/25} was provided by Terence Dermody (University of Pittsburgh, Pittsburgh, PA). The CHIKV_{Brazil-7124} infectious clone was engineered as described below. Viral stocks were generated from the two infectious CHIKV clones as previously described [112]. Alphaviruses were propagated in *Aedes albopictus* C6/36 cells. Cell culture supernatants were harvested and clarified 72 hours post-infection (hpi) then pelleted through a 10% sorbitol cushion by ultracentrifugation at 82,755 x g for 70 minutes. The viral

pellets were resuspended in PBS, frozen at -80°C , and titered by limiting dilution plaque assays using confluent monolayers of Vero cells. Infected cells were rocked continuously for 2 hours at 37°C with 5% CO_2 and overlaid with 2:1 mixture of DMEM-5 to 0.3% high / 0.3% low viscosity carboxymethyl cellulose (Sigma). Plaque assays were fixed with 3.7% formaldehyde and stained with 0.2% methylene blue at 48 hpi for CHIKV_{LR2006}, CHIKV_{Brazil-7124}, MAYV_{BeAr505411} and RRV_{T-48} or 72 hpi for CHIKV_{181/25} and ONNV_{UgMP30}. Plaques were visualized and enumerated using a dissecting microscope and the counts were used to calculate viral titers in plaque forming units per mL. Virus stocks used for all described experiments were either passage 1 or 2 and are sequence-validated as described below.

3.5.4 Construction of the CHIKV Brazil infectious clone

To assemble the infectious clone of chikungunya virus strain TO-UFT-7124 (CHIKV_{Brazil-7124}), seven genome fragments of approximately 1,700 bp, each with 20 bp of overlapping sequence, were synthesized by Twist Bioscience using the sequence originally reported [344]. The approximately 2,200 bp vector was amplified by PCR with 20 bp of overlapping sequence with fragment 1 and fragment 7 under standard PCR conditions. Each fragment (200 fmol) was combined with an equal volume of NEBuilder HiFi master mix (NEB) according to the manufacturer's instructions. Assembly was performed at 50°C for 60 minutes. TOP10 competent cells (Invitrogen) were transformed with 5 μL of the assembled PCR product. After DNA purification, the CHIKV_{Brazil-7124} infectious clone was verified by whole plasmid sequencing (Eurofins). The CHIKV_{Brazil-7124} plasmid was linearized with *Not* I digestion, and *in vitro* transcribed with the SP6 mMessage mMachine kit (Invitrogen). cDNA clone-derived RNA was purified using the RNeasy Mini Kit (Qiagen). Vero cells were transfected with 10 μg of RNA and 6 μL of Lipofectamine 2000 per well of a 6-well plate, according to the Invitrogen protocol. At 72 hours post-infection, supernatant was harvested and stored at -80°C . Virus stocks were propagated with 100 μL of resulting p0 per T-175 flask of C6/36 cells and purified as described above.

3.5.5 Next generation sequencing of viral stocks

Next generation sequencing (NGS) was used to sequence verify the viruses used in this study. Vero cells cultured in DMEM-5 were added to 6 well plates and incubated overnight at 37°C, 5% CO₂. For each viral infection, 100 µL of virus stock for CHIKV_{LR2006-OPY1} (accession DQ443544.2), CHIKV_{181/25} (accession MW473668.1), CHIKV_{Brazil-7124} (accession ON586955.1), MAYV_{BeAr505411} (accession KP842818.1), ONNV_{UgMP30} (accession M20303.1), and RRV_{T-48} (accession GQ433359.1) were added to 6 mL DMEM-5, mixed, and distributed between 3 wells of a 6 well plate. Cells were incubated at 37°C with 5% CO₂ and were allowed to infect for 24 hours. Cell supernatants were removed, cells were resuspended in 1 mL of Trizol reagent per well, incubated at room temperature for 5 minutes, and were collected with a cell scraper and transferred into new tubes for processing. RNA was extracted from Trizol-suspended samples following the manufacture's protocol and eluted in 20 µL of dH₂O. Concentration and quality of RNA was determined by OD using a Thermo Scientific Nanodrop instrument. NGS Sequencing libraries were produced with Illumina's Stranded mRNA Prep kit and qualified with Agilent's Bioanalyzer 2000. Viral reads from RNA sequencing data were compared to the corresponding GenBank reference viral sequences listed above using Geneious Prime software. Results listing nucleotide and amino acid changes and positions are shown in **Supplemental Table 1**. To construct the maximum likelihood phylogenetic tree in MEGA software, we first trimmed the sequences to focus on the structural proteins E1/6K/E2/E3, wherein the majority of the neutralizing antibody epitopes reside.

3.5.6 Neutralization assays (50% plaque reduction neutralization test, PRNT₅₀)

Neutralization assays were performed as previously described [59]. Briefly, serum samples from 30 human vaccinee participants at four timepoints (baseline and 1 month, 6 months, and 1-year post-vaccination with IXCHIQ) and from 9 CHIKV-immune individuals at ~8 and ~9 years post-infection were tested for neutralization activity against six viruses: CHIKV_{181/25}, CHIKV_{LR2006-OPY1}, CHIKV_{Brazil-7124}, MAYV_{BeAr505411}, ONNV_{UgMP30}, and RRV_{T-48}. Serum was heat-inactivated for 30 minutes at 56°C. Vero cells were cultured in 12-well plates in DMEM-5 plated one day prior to infection to reach confluency. The following day, serum was serially diluted in DMEM-5 starting at 1:10 in 96-well U-bottom plates, and further diluted for a total of 11 2-fold dilutions.

Each virus was diluted to a concentration that generated 50-200 plaques per well in DMEM-5 and added to 96-well round-bottom plates. Equivalent volumes of each diluted serum series were transferred and mixed in the plates containing diluted virus then rocked continuously and incubated at 37°C with 5% CO₂ for 2 hours. After 2 hours, 200 µL of each serum/virus mixture was used to infect each well of a 12-well plate. Plates were rocked continuously and incubated at 37°C with 5% CO₂ for 2 hours. Cells were overlaid with a 2:1 mixture of DMEM-5 to 0.3% high / 0.3% low viscosity carboxymethyl cellulose and incubated at 37°C for 48 hours (72 hours for CHIKV_{181/25} ONNV_{UGMP30}). After incubation, cells were fixed with 3.7% formaldehyde and stained with 0.2% methyl blue. Plaques were manually counted under a microscope or by eye to determine the percentage of plaques at each dilution relative to the number of plaques in virus only (no serum) control wells. Finally, 50% plaque reduction neutralization titers (PRNT₅₀) were calculated by variable slope non-linear regression in GraphPad Prism software. PRNT₅₀ values are reported as the inverse serum dilution. Baseline negative control human serum samples (Day 1) were run in every experiment.

3.5.7 Antigenic cartography

Antigenic cartography was used to visualize the serologic relationships between vaccinee and naturally infected patient samples and the profile of viruses neutralized based on 50% plaque reduction neutralization titers (PRNT₅₀) as previously described [329, 336]. Maps were constructed using the Racmacs package (<https://acorg.github.io/Racmacs/>, version 1.1.35.) in R (version 2023.12.1+402). For serum with neutralization under the limit of detection, the PRNT₅₀ was recorded as 10 for all calculations. The map was computed for 500 optimizations with two dimensions and the minimum column basis was set to none. The Bayesian method was used to perform 1,000 bootstrap repeats with 100 optimizations per repeat of the PRNT₅₀ data with the standard deviation of measurement noise set at 0.7 for both antigen and titer. Finally, blobs were added to the map using the “ks” algorithm method to represent the confidence levels of the viruses neutralized with the confidence level set at 0.68 and grid spacing set at 0.1. Each box of the grid is representative of a 2-fold difference in serum dilution.

3.5.8 Statistical analysis

All statistical analysis was completed using GraphPad Prism Version 10 software. Normalized variable slope non-linear regressions with upper and lower limits of 100 and 0, respectively, were used to calculate 50% plaque reduction neutralization titers (PRNT₅₀). For age and PRNT₅₀ correlations, both age and PRNT₅₀ were first log-transformed before applying Pearson correlation and simple linear regressions. For correlation of PRNT₅₀ and Dayhoff distance, Spearman correlation was used.

Section 3.6: Acknowledgements

The following reagents were obtained through BEI Resources, NIAID, NIH, as part of the WRCEVA program: MAYV_{BeAr505411} (NR-49910), ONNV_{UgMP30} (NR-51661), RRV_{T-48} (NR-51457) and VEEV_{TC-83} (NR-63). The authors thank Dr. Steven Higgs at Kansas State University, Manhattan, KS, for providing the CHIKV_{LR2006} infectious clone. The authors thank Dr. Terence Dermody at the University of Pittsburgh, Pittsburgh, PA, for providing the CHIKV_{181/25} infectious clone. The authors acknowledge Dr. Anders Lilja for editing and review of the manuscript.

Chapter 4: Non-reciprocity in CHIKV and MAYV vaccine-elicited protection

Status: Published in Vaccines, August 27th, 2024.

Whitney C. Weber^{1,2}, Takeshi F. Andoh¹, Craig N. Kreklywich¹, Zachary J. Streblow¹, Michael Denton¹, Magdalene M. Streblow¹, John M. Powers^{1#}, Gauthami Sulgey¹, Samuel Medica¹, Igor Dmitriev³, David T. Curiel³, Nicole N. Haese¹, and Daniel N. Streblow^{1,4*}

¹ Vaccine and Gene Therapy Institute, Oregon Health and Science University, Beaverton, Oregon, USA

² Department of Molecular Microbiology and Immunology, Oregon Health and Science University, Portland, Oregon, USA

³ Cancer Biology Division of the Department of Radiation Oncology, Washington University St. Louis, Missouri, USA

⁴ Division of Pathobiology and Immunology, Oregon National Primate Research Center, Beaverton, Oregon, USA

Current Address: Department of Epidemiology, University of North Carolina at Chapel Hill, Chapel Hill, North Carolina, USA

* Correspondence: streblow@ohsu.edu; Tel.: +1 (503)-418-2772

Publication info: *Vaccines*, **2024**, *12*(9), 970.

Doi: <https://doi.org/10.3390/vaccines12090970>

Author contributions: Conceptualization, D.N.S.; methodology, W.C.W., D.N.S.; validation, W.C.W., D.N.S.; formal analysis, W.C.W.; investigation, W.C.W., T.F.A., C.N.K., Z.J.S., M.D., M.M.S., J.M.P., N.N.H., G.S., S.M., I.G., D.T.C.; resources, D.N.S., D.T.C.; data curation, W.C.W.; writing—original draft preparation, W.C.W., D.N.S.; writing—review and editing, W.C.W., J.M.P., D.N.S.; visualization, W.C.W.; supervision, W.C.W. and D.N.S.; project administration, D.N.S.; funding acquisition, D.N.S. All authors have read and agreed to the published version of the manuscript.

Section 4.1: Abstract

Chikungunya virus (CHIKV) is a pathogenic arthritogenic alphavirus responsible for large-scale human epidemics for which a vaccine was recently approved for use. Mayaro virus (MAYV) is a related emerging alphavirus with epidemic potential with circulation overlap potential with CHIKV. We have previously reported the ability of a non-replicating human adenovirus (AdV) vectored vaccine expressing the MAYV structural polyprotein to protect against disease in mice following challenge with MAYV, CHIKV and UNAV. Herein, we evaluated mouse immunity and protective efficacy for an AdV-CHIKV full structural polyprotein vaccine in combination with heterologous AdV-MAYV prime/boost regimens versus vaccine coadministration. Heterologous prime/boost regimens skewed immunity toward the prime vaccine antigen, but allowed for boost of cross-neutralizing antibodies, while vaccine co-administration elicited robust, balanced responses capable of boosting. All immunization strategies protected against disease from homologous virus infection but reciprocal protective immunity differences were revealed upon challenge with heterologous viruses. *In vivo* passive transfer experiments reproduced the inequity in reciprocal cross-protection after heterologous MAYV challenge. We detected *in vitro* antibody-dependent enhancement of MAYV replication, suggesting a potential mechanism for the lack of cross-protection. Our findings provide important insights into rational alphavirus vaccine design that may have important implications for the evolving alphavirus vaccine landscape.

Section 4.2: Introduction

Chikungunya virus (CHIKV) is a mosquito-transmitted alphavirus that has caused numerous explosive epidemics since first emergence in 1952 and is actively causing outbreaks in Latin America, with over 320,000 cases reported so far in 2024 according to ECDC (as of May 31st). Mayaro virus (MAYV) is an emerging alphavirus first identified in 1954 that has caused outbreaks in Latin America and currently shares the potential for geographic co-circulation with CHIKV [352, 353]. In contrast to CHIKV, MAYV has caused only small outbreaks; however, the disease burden and seroprevalence is likely vastly underestimated due to neutralization and ELISA diagnostic assay cross-reactivity with CHIKV and overlap in circulation with other arboviruses [354]. Antibody cross-reactivity between CHIKV and MAYV and other Semliki Forest antigenic

complex alphaviruses has been observed in humans after infection [59, 75, 85] and vaccination [69, 274]. Due to overlap in viral circulation, cross-reactive herd immunity is one hypothesis of why MAYV cases are not more common. The currently utilized mosquito vectors for CHIKV and MAYV differ, as do their suitable habitats, providing an additional hypothesis for the restricted range of MAYV distribution. Nevertheless, MAYV has the potential to opportunistically emerge outside of the Amazon basin where it is currently endemic due to competence in additional mosquito vectors as demonstrated experimentally [196-198]. Old World alphavirus infections are typically characterized by fever, rash, arthritis, myalgia, headache, and fatigue with rare infections manifesting eye pain and encephalitis. There are currently no approved countermeasures to combat these symptoms with the only treatment available being supportive care, although several antivirals [355, 356] and monoclonal antibody therapies [357] are in pre-clinical development.

The landscape of CHIKV vaccines is rapidly evolving with the recent U.S. FDA, European Medicines Agency, and Health Canada approval of the live-attenuated IXCHIQ (VLA1553) vaccine, which is in ongoing clinical evaluation but was previously evaluated in mice [100, 101], NHP [99, 233], and in Phase I [265] and Phase III [264, 266-268] human clinical trials. Several additional inactivated, mRNA [284], viral-vectored [111, 358], and virus-like particle [273, 275] CHIKV vaccines are in clinical development [342]. MAYV vaccine development is not as advanced but approaches have included inactivated [286], live-attenuated [93, 287, 288], viral vectors [91, 92], VLP [289], and DNA/RNA [290] platforms. Despite the approval of IXCHIQ, the development of additional alphavirus vaccines is warranted, as is research to understand the impacts of differential alphavirus exposure history on vaccine efficacy and how vaccine administration strategies can balance cross-reactive immunity.

The specific correlates of protection from alphavirus infection are still frequently debated, especially following approval of the first CHIKV vaccine. Neutralizing antibodies are the generally agreed upon dominant correlate, although the magnitude of this response necessary to achieve protection from disease and/or infection is still disputed and dependent upon the vaccine type, animal model, challenge dose, and assay variability and lack of standardization. For example, CHIKV 50% plaque reduction neutralization titers (PRNT₅₀) as low as 10 [98] or 150 [99] and as high as an IgG titer of 10⁴ [100, 101] have been proposed to be the correlate of protective immunity. While these thresholds have been determined from various mouse and NHP studies, there are conflicts in translation to other studies. Protection from alphavirus infection and

pathogenesis relies on the cooperation of immune functions, and protective roles for binding/neutralizing antibodies, CD8⁺ T cells, macrophages, and other immune responses [98, 112, 357, 359]. One immune mechanism that challenges protection even in the presence of potent virus-specific antibodies is known as antibody-dependent enhancement (ADE). ADE of viral infectivity was first demonstrated in 1964 in chicken embryonic fibroblasts for replication of flaviviruses and the alphavirus, Getah virus (GETV) [116]. ADE of disease in the presence of sub-neutralizing antibody levels has been well documented for human dengue virus (DENV) infection and is generally thought to be a major clinical concern for flaviviruses only. ADE has been demonstrated for a diverse group of virus families including alphaviruses, which have implicated or hypothesized CHIKV [360, 361] and Ross River virus (RRV)[119-121] in *in vitro* or mouse studies. Direct evidence of CHIKV infection enhancement in humans has not been reported to date, but remains a topic warranting attention as to the impact it may have on disease outcomes. Two studies have provided encouraging evidence of the lack of risk of CHIKV-mediated ADE. One reported that pre-existing anti-CHIKV antibodies were shown to correlate with decreased symptomatic disease in a Philippine cohort [350]. Another study demonstrated that in context of pre-existing CHIKV immunity, individuals immunized with CHIKV VLP (PXVX0317) did not display increased adverse events relative to baseline seronegative immunized individuals [123]. In contrast, a few vaccine studies in mouse models have observed enhanced viral replication or disease after CHIKV challenge and hypothesized that ADE was the responsible mechanism [100-102, 362].

Considering the challenges associated with developing a protective alphavirus vaccine, especially in regions where multiple alphaviruses are endemic and/or reemerging causing the immune landscape to be in a general state of flux, we sought to evaluate different prime/boost vaccine regimens using a non-replicating human adenovirus (AdV) vaccine platform to express the structural polyproteins of MAYV or CHIKV. We have previously shown that homologous prime/boost using the AdV-MAYV vaccine is protective against MAYV, CHIKV, and UNAV-induced disease in mice [91]. Herein, using both AdV-MAYV and a newly developed AdV-CHIKV construct, we aimed to evaluate heterologous prime/boost and coadministration vaccine strategies to assess MAYV or CHIKV homotypic disease and heterotypic cross-protection. We found that all vaccine administration strategies elicited homologous immunity with variable levels of cross-neutralization against heterologous viruses that correlated with the prime antigen. In

addition, all of the vaccine strategies were capable of eliciting protection against footpad swelling disease but there were mixed cross-protective outcomes based upon quantification of viral dissemination in tissues. Passive transfer of immune sera from the various vaccine groups further demonstrated the lack of reciprocal cross-protection and showed that antibody-mediated immunity alone was insufficient to protect against disease, resulting in differential disease outcomes. Evaluation of antibody-dependent enhancement of infection in RAW264.7 cells demonstrated that diluted sera samples collected from each vaccine group had potential to enhance replication of both MAYV and UNAV but not CHIKV or RRV. Our findings shed light on potential differences in reciprocal cross-protective immunity for related alphaviruses, which may have implications on infection and vaccine coverage in populations with evolving alphavirus immunity.

Section 4.3: Results

4.3.1 Adenovirus-vectored alphavirus vaccines elicit virus-specific neutralizing antibodies and T cells in mice.

In previous studies, our group performed immunogenicity and protection studies in C57BL/6 mice using a non-replicating human adenovirus-vectored (AdV) AdV-MAYV vaccine construct expressing the entire MAYV structural protein [91]. In mice, vaccination with AdV-MAYV is protective against disease elicited by infection with MAYV and partially protective against CHIKV and UNAV, suggesting that this vaccine elicits immunity against a range of serologically related alphaviruses [91]. Herein we sought to determine: 1) if reciprocal protective immunity is elicited against MAYV and UNAV using an AdV-CHIKV vaccine that expresses the entire CHIKV₃₇₉₉₇ structural protein; and 2) whether cross-protective immunity could be improved by heterologous prime/boost or AdV co-administration strategies. To accomplish these goals, we vaccinated C57BL/6 mice with AdV-MAYV and/or AdV-CHIKV using homologous, heterologous, and coadministration immunization strategies and used vaccination with AdV-GFP as a vector control. **Figure 4.1A** depicts the vaccine strategy and bleeding schedule for this study. Mice were primed via intramuscular injection (i.m.) with 10^8 plaque forming units (PFU) of AdV, bled and then boosted at 28 days after receiving the priming vaccination. At 58 days post-prime, spleens and blood sera from three animals from each vaccine group were collected for the assessment of virus-specific T cell responses and passive transfer experiments, respectively. Sera were collected from the remaining animals (n= 10 or 8, depending upon the group) for use in 50%

plaque reduction neutralization tests (PRNT₅₀) against CHIKV (Figure 4.1B), MAYV (Figure 4.1C), and UNAV (Figure 4.1D) with results tabulated in Table 4.1. After homologous prime and boost regimens (C/C and M/M), the homotypic titers against their respective viruses were high but the titers against their heterotypic viruses were significantly lower, which demonstrates specificity against the homologous virus. Coadministration of AdV-CHIKV and AdV-MAYV (CM/CM) resulted in high serum neutralization dilution titers against all of the viruses including heterotypic UNAV. Neutralization titers for the heterologous prime boost groups (C/M and M/C) were significantly higher for the prime viral antigen and had limited boosting effect against CHIKV for the M/C group but titers against MAYV were boosted for the C/M group. Serum dilution titers against UNAV were similar for the heterologous prime boost groups. Together these findings suggest an interesting dichotomy in the responses generated by heterologous prime boost regimens and that the antibody responses are biased toward the priming vaccine antigen but can be overcome by vaccine co-administration. Prime and boost with only one AdV vaccine elicits limited cross-neutralization breadth. Additionally, we conducted an immunogenicity study in which a 2-week rather than 4-week interval between prime and boost was assessed and little differences in antibody responses were observed; this experiment also validated that mice were mounting viral antigen-specific antibody responses (Supplemental Figure 4.S1). Altogether, these data indicated that alphavirus AdV vaccine coadministration is a successful strategy for achieving balanced cross-neutralizing immunity against two pathogenic alphaviruses.

Figure 4.S1. Preliminary immunogenicity analysis.

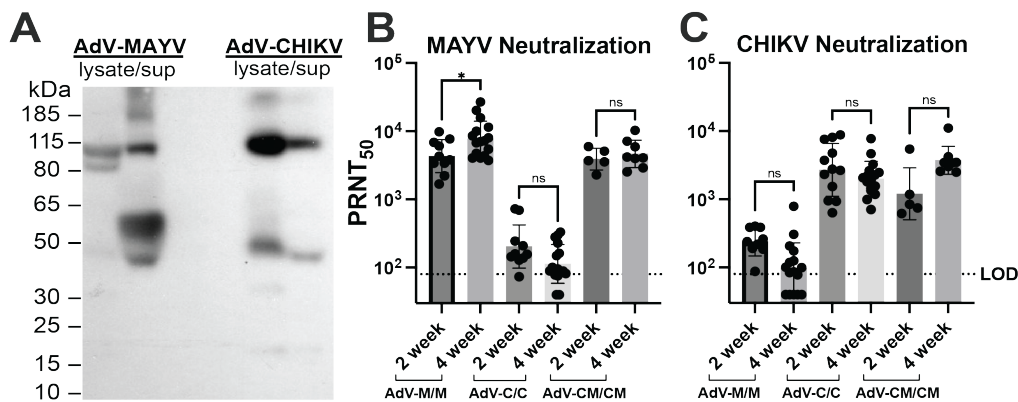


Figure 4.S1. In preliminary mouse studies, the virus-specific immune response was validated for the previously tested AdV-MAYV and new AdV-CHIKV vaccine constructs. (A) Confirmation of structural polyprotein expression within the supernatant and lysate of 293IQ cells by western blot. AdV-MAYV was probed with primary

mouse sera after AdV-MAYV homologous prime and boost (10^8 PFU i.m./dose) and AdV-CHIKV was probed with primary mouse sera after AdV-CHIKV homologous prime and boost (10^8 PFU i.m./dose). Neutralizing activity was assessed using 50% plaque reduction neutralization tests (PRNT₅₀) with Vero cells against (B) MAYV and (C) CHIKV. Neutralizing antibody titers at two and four weeks post-prime were compared using one-way ANOVA with Holm-Šídák's multiple comparisons where $*P = 0.0113$ and ns $P > 0.05$. The limit of detection for neutralization assays is 80. Bars are mean with SEM.

To examine T cell mediated vaccine-elicited immunity, virus-specific T cells were quantified in splenocytes collected at day 58 post-prime (30 days post-boost) in IFN- γ ELISPOT assays against a MAYV E2 peptide and CHIKV E1 peptide. The M/M vaccine group generated a robust homotypic MAYV T cell response at a mean of ~800 spot-forming units (SFU) per million splenocytes, the highest MAYV-specific response of any vaccine group (**Figure 4.1E**). While MAYV T cell responses in the M/C and CM/CM vaccine groups were not significantly lower than the M/M group (506 and 540 SFU, respectively), the numbers of MAYV specific T cells in the C/M group was 321 SFU and the heterotypic response for the C/C group was a mean of 169 SFU, which was significantly reduced ($P = 0.0190$) compared to the homotypic response of the M/M group (**Figure 4.1E**). For CHIKV-specific T cells, the highest response was evoked in the C/C vaccine group at a mean of >1300 SFU (**Figure 4.1E**) followed by the C/M and CM/CM groups (990 and 820, respectively), which were not statistically different when compared to the C/C group (**Figure 4.1E**). The CHIKV T cell response for the M/C group was significantly reduced compared to the homotypic response for the C/C group at a mean of 721 SFU ($P = 0.0143$) but a detectable cross-reactive T cell response for the M/M group was not generated against the CHIKV E1 peptide (**Figure 4.1E**). These data indicated that cross-reactive virus-specific T cells elicited by homologous vaccine administration strategies were limited and that cross-reactive responses could be achieved using heterologous and coadministration strategies. Together, these studies revealed limited cross-reactive alphavirus immunity elicited by the homologous vaccine administration strategies and supported that heterologous prime and boost or vaccine coadministration lead to greater antibody and T cell breadth. Additionally, we observed a bias for the virus-specific antibody and T cell immune response toward the priming vaccine antigen within the heterologous prime and boost groups.

Figure 4.1. Immunogenicity of adenovirus-vectored alphavirus vaccines in C57BL/6 mice.

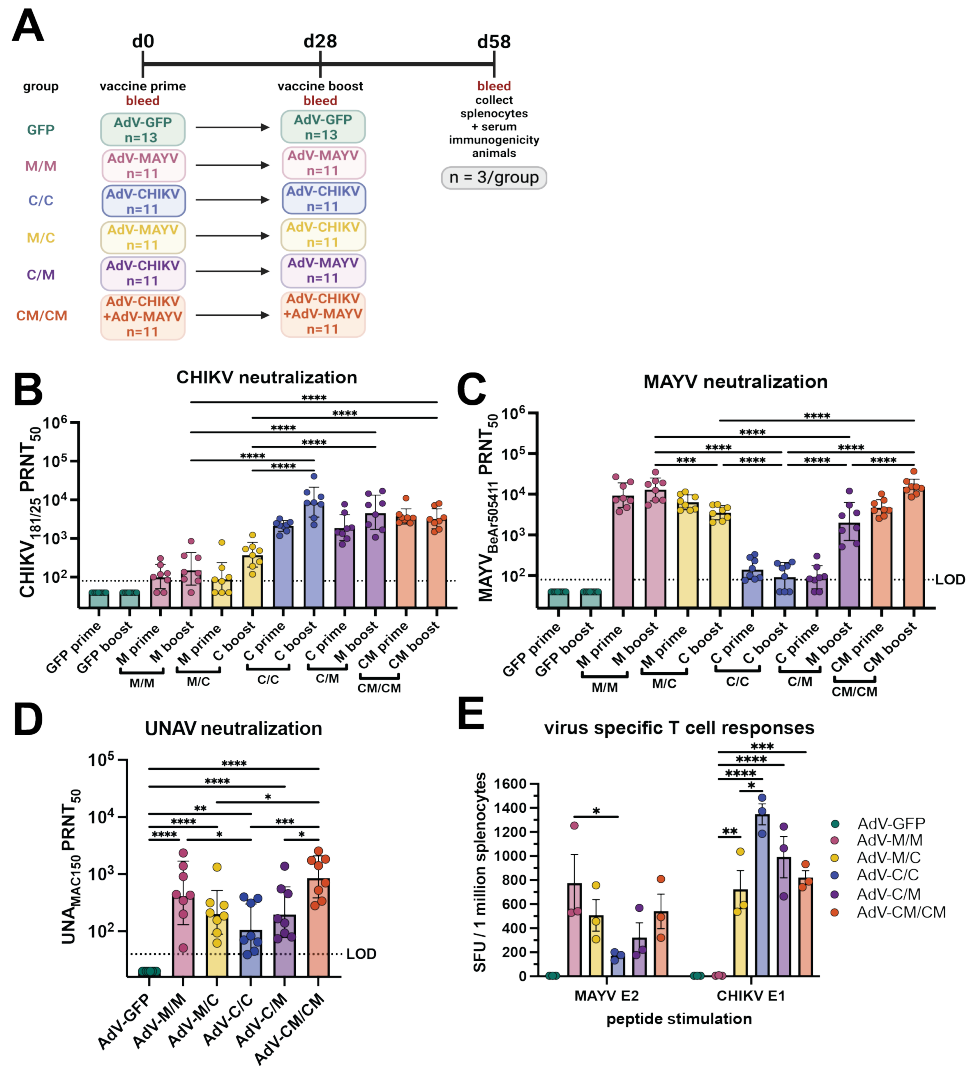


Figure 4.1. (A) Study design schematic. C57BL/6 mice were immunized by intramuscular injections in the left posterior thigh muscle with human adenovirus V (AdV) vaccines expressing CHIKV or MAYV structural proteins at a dose of 10^8 plaque-forming units (PFU) each. Animals were boosted at day 28 with the homologous or heterologous vaccine or both in equivalent concentrations. At 58 days post-prime, three animals from each group were humanely euthanized for serum and splenocyte isolation. Serum from each mouse was collected at days 0, 28, and 58 post-prime for assessment of neutralizing activity against (B) CHIKV_{181/25}, (C) MAYV_{BeAr505411}, and (D) UNAV_{MAC150} using 50% plaque reduction neutralization tests (PRNT₅₀) on confluent monolayers of Vero cells. In (B, C) the neutralization titer is shown at 28 days post-prime labeled as “prime” and 30 days post-boost labeled as “boost”. The neutralization titers were log-transformed and the boosted (day 58 post-prime) titers are analyzed by one-way ANOVA with Holm-Šidák’s multiple comparisons. In (D), neutralization titers against UNAV for 8 mice in each group at day 58 post-prime are shown. The day 58 post-prime titers are analyzed by one-way ANOVA

with Holm-Šidák's multiple comparisons. For all neutralization data (**B-D**), the geometric mean with geometric standard deviation is shown. The limit of detection (LOD) dilution titer for neutralization assays is 80 for CHIKV and MAYV and 40 for UNAV; samples with undetectable neutralizing activity are graphed as half of the LOD. In (**E**), splenocytes collected from each group of mice at day 58 post-prime were used to quantify virus-specific T cells against a MAYV E2 peptide and CHIKV E1 peptide using IFN- γ ELISPOT. The ELISPOT data reported as spot-forming units per 1 million splenocytes were background subtracted from wells without peptide stimulation and data were analyzed by two-way ANOVA with Tukey's multiple comparisons; mean with SEM is shown. For (**B, C, E**), only select, significant comparisons are shown for simplicity with comparisons to AdV-GFP excluded. In all panels, biological replicates are plotted. For all statistical analyses, * $P \leq 0.05$, ** $P \leq 0.01$, *** $P \leq 0.001$, **** $P \leq 0.0001$.

Table 4.1. Summary of alphavirus neutralizing antibody titer responses (n=8) and *in vitro* antibody-dependent enhancement activity in RAW264.7 at 58 days post-prime.

	CHIKV _{181/25}	MAYV _{BeAr505411}	UNAV _{MAC150}
<i>AdV-C/C</i>			
Min-Max PRNT ₅₀	2,257-40,820	40-217	40-358
GMT	8,690	95	116
Mean PRNT ₅₀	12,354	119	174
PRNT ₅₀ standard deviation	12,280	75	159
Observed ADE (≥ 10 -fold)	0/4	0/8	5/5
Serum dilution to maximum ADE	NE	NE	1:10-250
Maximum fold enhancement of viral titer	NE	NE	20-270
<i>AdV-M/M</i>			
Min-Max PRNT ₅₀	40-849	5,413-35,145	51-2,349
GMT	162	13,115	460
Mean PRNT ₅₀	250	15,658	764
PRNT ₅₀ standard deviation	268	9,877	769
Observed ADE (≥ 10 -fold)	0/4	8/8	6/6
Serum dilution to maximum ADE	NE	1:6,250-31,250	1:50-1,250
Maximum fold enhancement of viral titer	NE	10.7-233	16-372
<i>AdV-M/C</i>			
Min-Max PRNT ₅₀	119-1,235	2,043-5,597	62-1,333
GMT	377	3,526	214
Mean PRNT ₅₀	474	3,768	331
PRNT ₅₀ standard deviation	352	1,413	414
Observed ADE (≥ 10 -fold)	0/5	8/8	5/5
Serum dilution to maximum ADE	NE	1:1,250-6,250	1:10-50
Maximum fold enhancement of viral titer	NE	22-1,437	19-200
<i>AdV-C/M</i>			

Min-Max PRNT ₅₀	1,076-16,927	512-12,048	74-1,383
GMT	4,733	2,124	214
Mean PRNT ₅₀	7,008	3,481	368
PRNT ₅₀ standard deviation	5,970	3,837	449
Observed ADE (≥ 10 -fold)	0/5	7/8	5/5
Serum dilution to maximum ADE	NE	1:250-31,250	1:50-1,250
Maximum fold enhancement of viral titer	NE	15-86	32-567
<i>Adv-CM/CM</i>			
Min-Max PRNT ₅₀	1,491-8,074	8,568-36,537	282-2,540
GMT	3,231	15,154	892
Mean PRNT ₅₀	3,812	16,680	1,171
PRNT ₅₀ standard deviation	2,458	8,812	828
Observed ADE (≥ 10 -fold)	0/4	8/8	5/5
Serum dilution to maximum ADE	NE	1:6,250-31,250	1:50-1,250
Maximum fold enhancement of viral titer	NE	20-116	60-1,000

Geometric mean titer = GMT; Not enhanced = NE; enhancement is defined as ≥ 10 -fold increase in viral titer.

4.3.2 All vaccine regimens cross-protect against MAYV and CHIKV-induced disease.

To evaluate the ability of homologous, heterologous, and coadministration vaccine regimens to cross-protect against alphavirus infection and disease, we challenged the immunogenicity mice described in **Figure 4.1** with 10^4 PFU of MAYV_{BeAr505411} or 10^3 PFU of CHIKV_{SL15649} by subcutaneous injection in the footpad at day 63 post-prime (day 33 post-boost) (**Figure 4.2A**). Footpad swelling was measured daily, and the mice were humanely euthanized at 7 days post-infection (dpi) for quantification of tissue viral burden using qRT-PCR and limiting dilution plaque assays. After CHIKV challenge, vRNA (**Figure 4.2B**) and infectious virus (**Figure 4.2C**) were nearly undetectable in the left (contralateral) ankle, heart, quadriceps, or spleen of all alphavirus antigen immunized animals whereas AdV-GFP vaccinated controls had detectable CHIKV vRNA in all tissues that were tested (**Figure 4.2B**) and infectious virus in the ankles at 7 dpi (**Figure 4.2C**). The M/M and M/C vaccine groups had 10^3 - 10^5 copies/mL of CHIKV vRNA detected in the right ipsilateral ankle and the C/C, C/M, and CM/CM groups had near sterilizing immunity with except for one mouse in the C/C group and one mouse in the C/M group (**Figure 4.2B**). Compared to the AdV-GFP control, all groups of alphavirus vaccinated animals had significant reductions in CHIKV vRNA and infectious viral titers (**Figure 4.2B, 4.2C**). These results demonstrate that although the different vaccine groups had varying levels of CHIKV-

neutralizing antibodies and virus-specific T cells (**Figure 4.1B, 4.1E**), the antiviral immunity was sufficient to significantly reduce or prevent viral dissemination to tissues after CHIKV challenge. In vaccinated mice that were challenged with MAYV, there were significant reductions in MAYV vRNA (**Figure 4.2D**) in the right (ipsilateral) ankle and heart compared to the AdV-GFP control group. There was also a significant inhibition in the production of infectious virus in the ankles (**Figure 4.2E**) for all alphavirus vaccine groups relative to AdV-GFP controls. In the right (ipsilateral) quadriceps muscle and spleen, MAYV vRNA was significantly reduced compared to control mice for the M/M, C/M, and CM/CM vaccine groups (**Figure 4.2D**). However, the left (contralateral) ankle and left (contralateral) quadriceps muscle were two sites where the viral burden was generally not significantly reduced relative to controls, although vRNA levels trended lower in the left (contralateral) ankle for all vaccine groups except for the C/C group (**Figure 4.2D**). Despite the ability of the alphavirus vaccines to provide near-sterilizing protection against CHIKV infection, protection from MAYV infection was far from sterilizing, although significant reductions in MAYV vRNA in some tissues were observed and the infectious viral titers were inhibited, except for the C/C group (**Figure 4.2E**). There was no infectious virus detected in any mouse in the quadriceps, heart, or spleen, even for the AdV-GFP vaccinated controls, thus this data was excluded from graphical presentation. While there were differential outcomes in susceptibility of the alphavirus vaccinated mice to CHIKV and MAYV infection as evidenced by viral tissue dissemination, the ability of all the immunization strategies to protect against footpad swelling disease was striking. After CHIKV challenge, both homotypic and heterotypic protection from CHIKV-induced footpad swelling was observed for homologous, heterologous, and co-administration vaccine groups, which was statistically significant between 3 and 7 dpi (**Figure 4.2F**). Reciprocally after MAYV challenge, complete protection against MAYV-induced footpad swelling was observed for all alphavirus vaccinated mice, which was statistically significant at 6 and 7 dpi (**Figure 4.2G**). These studies demonstrated that homologous, heterologous, and coadministration immunization strategies could greatly reduce viral burden after challenge, in some cases providing sterilizing immunity, and cross-protect against inflammatory disease.

Figure 4.2. All CHIKV and MAYV vaccination strategies cross-protect against disease but protection is not sterilizing.

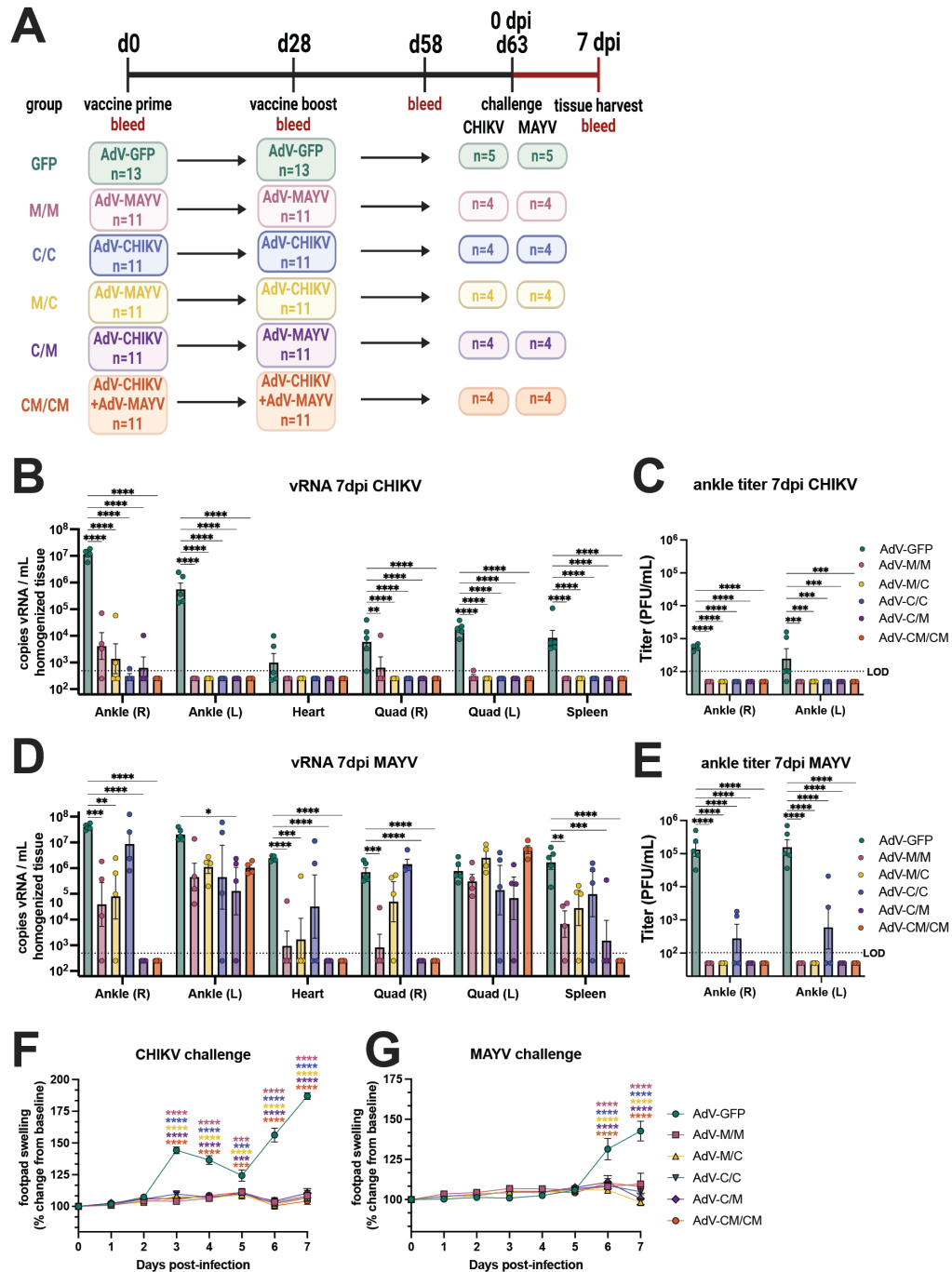


Figure 4.2. (A) Study immunogenicity and challenge efficacy study schematic. C57BL/6 mice were immunized with AdV vaccines by intramuscular injections in the left posterior thigh muscle. Animals were boosted at day 28 with the homologous or heterologous vaccine or both in equivalent concentrations. At 63 days post-prime, four animals per group were challenged by subcutaneous injection in the right footpad with 10^3 PFU of CHIKV_{SL15649}.

or 10^4 PFU of MAYV_{BeAr505411}. Ankles, heart, quadriceps, and spleen tissues as well as blood were harvested from animals at 7 days post-infection. CHIKV viral RNA (vRNA) was quantified in mouse tissue homogenates by (B) qRT-PCR and (C) infectious virus was quantified by limiting-dilution plaque assays. MAYV (D) vRNA levels and (E) infectious virus were also quantified in a similar manner. Infectious viral titers (C, E) are only shown for ankles as the quadriceps, heart, and spleen has no detectable titer at 7 days post-infection. Footpad swelling in the right (ipsilateral) rear footpad was measured daily after challenge for (F) CHIKV- and (G) MAYV-challenged mice. For all statistical analyses, two-way ANOVAs with Dunnett's multiple comparisons were performed using log-transformed data. Only significant comparisons are shown where ns $P > 0.05$, $*P \leq 0.05$, $**P \leq 0.01$, $***P \leq 0.001$, $****P \leq 0.0001$. The limit of detection (LOD) for vRNA detection by qRT-PCR was 500 copies/mL of tissue homogenate and 100 PFU/mL for infectious viral plaque assays. For all graphs, mean with SEM is plotted. In all panels, biological replicates are plotted.

To further examine the differences in tissue viral burden in vaccinated animals, we performed a related experiment where animals were primed and boosted using the C/C, M/M, and CM/CM vaccination regimens, challenged at 61 days post-prime, and euthanized at 5 dpi rather than 7 dpi (**Supplemental Figure 4.S2A**). Homologous prime boost resulted in high homotypic but low heterotypic antibody titers and similar to the previous experiment, vaccine coadministration resulted in high titers against both CHIKV and MAYV (**Supplemental Figure 4.S2B**). At 2 dpi, serum MAYV viremia was significantly reduced for all alphavirus vaccine groups compared to the AdV-GFP control group (**Supplemental Figure 4.S2C**). After CHIKV challenge, the infectious viral titers in the ankles revealed sterilizing protection elicited by the C/C and CM/CM vaccine groups but infectious virus was detected ($\sim 10^3$ PFU) in the right (ipsilateral) ankle for the M/M group (**Supplemental Figure 4.S2D**). CHIKV vRNA levels were significantly reduced at 5 dpi in the spleen, quadriceps, ankles, and heart in the C/C and CM/CM vaccine groups; and the M/M vaccine group also showed reduced levels of vRNA, although this was not significant for all tissues (**Supplemental Figure 4.S2F**). While a trend in reducing the viral burden after CHIKV infection at 5 dpi was observed, this contrasted with near-sterilizing immunity observed at 7 dpi (**Figure 4.2B**). A similar antiviral outcome profile was observed after MAYV challenge, where little to no infectious virus was detected at 5 dpi for M/M and CM/CM vaccine groups but 4 out of 5 mice in the C/C group had detectable infectious virus in the right ankle (**Supplemental Figure 4.S2E**). When examining vRNA levels after MAYV infection, significant reductions in vRNA in the spleen, right quadricep muscle, ankles, and heart were observed for each vaccine group relative to AdV-GFP controls (**Supplemental Figure 4.S2G**). Comparable to the results

observed in **Figure 4.2D**, the vaccine-elicited protection was not sterilizing against MAYV infection at 5 dpi (**Supplemental Figure 4.S2G**).

Figure 4.S2. Vaccine cross-protection at 5 dpi.

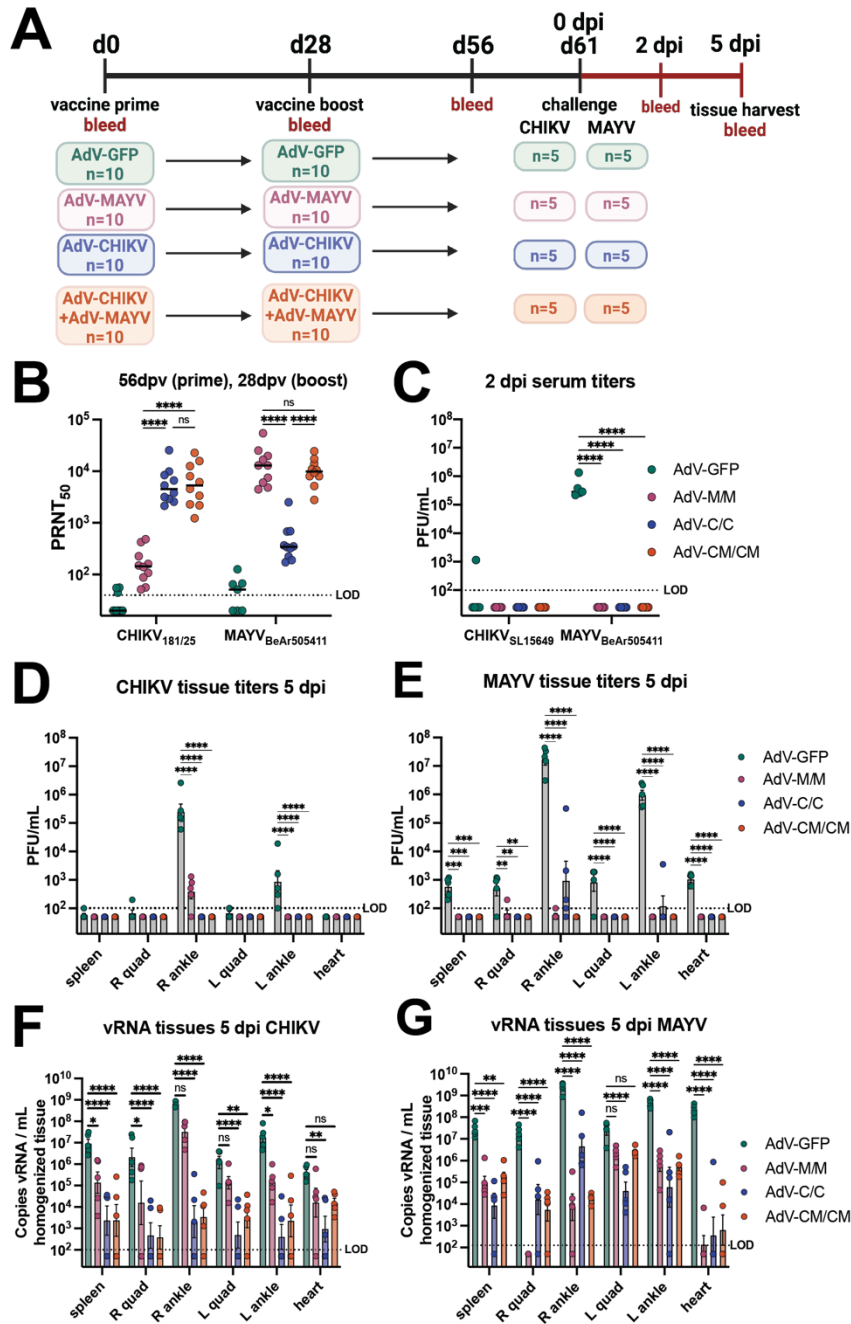


Figure 4.S2. (A) Study schematic. Ten C57BL/6 mice per adenovirus-vectored (AdV) vaccine group were immunized with intramuscular injections in the left posterior thigh muscle of 10⁸ PFU of AdV-CHIKV, AdV-

MAYV, or both. At 28 days post-prime, animals received a homologous boost via the same route and dose. Mice were challenged subcutaneously in the right footpad at 61 days post-prime (33 days post-boost) with 10^3 PFU of CHIKV_{SL15649} or 10^4 PFU of MAYV_{BeAr505411}. Animals were bled for quantification of serum viremia at 2 days post-infection (dpi) and at 5 dpi spleen, quadriceps, ankles, and heart were harvested for quantification of virus. **(B)** Neutralization data by 50% plaque reduction test (PRNT₅₀) against CHIKV_{181/25} and MAYV_{BeAr505411} using sera collected at 56 days post-prime (28 days post-boost). The limit of detection (LOD) for neutralization assays was 40. **(C)** Serum infectious virus detection by limiting-dilution plaque assay on Vero cells measured in PFU/mL. **(D)** Infectious virus isolation in tissue homogenates by plaque assay at 5 dpi for CHIKV and **(E)** MAYV. In **(C-E)**, the LOD is 100 PFU/mL of tissue homogenate. **(F)** Quantification of viral RNA (vRNA) by qRT-PCR in tissues at 5 dpi for CHIKV and **(G)** MAYV. The LOD for vRNA detection in **(F, G)** was 100 copies/ μ L of tissue homogenate. All statistical analyses are the result of log-transformed, two-way ANOVAs with Dunnett's multiple comparisons where ns $P > 0.05$, $*P \leq 0.05$, $**P \leq 0.01$, $***P \leq 0.001$, $****P \leq 0.0001$. For titer data in **(C-E)**, only significant comparisons $P < 0.05$ are shown. For neutralization titers, comparisons are not shown to the AdV-GFP group for clarity but every comparison was significant $P \leq 0.05$. For **(B, C)** the median is shown and in **(D-E)**, bars are mean with SEM.

4.3.3 Passive antibody transfer demonstrates that robust cross-neutralizing antibody responses are not sufficient to provide sterilizing cross-protection against infection or disease.

To investigate the impact that antibodies have on the non-reciprocal vaccine-induced cross-protection following viral challenge, passive transfer experiments using stored serum from the immunogenicity mice ($n=3$ /group; 58 days post-prime) for each of the five vaccine groups and AdV-GFP control were conducted (presented in **Figure 4.1**). One day before viral challenge with 10^3 PFU of CHIKV_{SL15649} or 10^4 PFU of MAYV_{BeAr505411}, 100 μ L of mouse vaccine immune serum was administered via intraperitoneal (i.p.) injection to naïve C57BL/6 mice (**Figure 4.3A**). Passive transfer of serum from M/M and M/C vaccine groups protected against MAYV viremia ($P \leq 0.05$), whereas two out of three mice in the C/M sera transfer group did not have detectable viremia (**Figure 4.3B**). In contrast, C/C sera provided little cross-protection against MAYV serum viremia with two of three mice developing similar serum viremia (mean $\sim 5 \times 10^4$ PFU/mL) to AdV-GFP passive transfer controls and the third mouse having a serum viremia equal to 9×10^2 PFU/mL (**Figure 4.3B**). For passive transfer of CM/CM vaccine sera (the vaccine group with similar MAYV-neutralizing antibody potency as the M/M homologous group as shown in **Figure 4.1C**),

two of three animals developed serum viremia ($\sim 2 \times 10^4$ PFU/mL) that was slightly reduced relative to AdV-GFP control animals (**Figure 4.3B**). A similar trend in tissue distribution was observed for both MAYV vRNA (**Figure 4.3C**) and infectious virus (**Figure 4.3D**): the C/C and CM/CM sera passive transfer groups did not show a reduction in viral loads and were similar to AdV-GFP control animals. The M/M, C/M, and M/C sera passive transfer groups had significant reductions in MAYV vRNA in the left (contralateral) ankle, quadriceps muscles, spleen, and heart (**Figure 4.3C**) as well as infectious viral titers in the ankles (**Figure 4.3D**). Viral burden across all tissues was similar in magnitude for the C/C and CM/CM sera passive transfer groups to the infected AdV-GFP control animals (**Figure 4.3C, 4.3D**). This revealed that antibody from M/M, M/C, or C/M vaccine administration strategies could substantially block MAYV replication in tissues whereas homologous C/C and co-administration CM/CM vaccine strategies resulted in antibody responses that had limited impacts on reducing MAYV viral dissemination. Together, these data indicate that robust neutralizing antibody potency alone in this context does not translate to complete protection from MAYV infection.

At 3 days post-CHIKV infection, all alphavirus vaccine passive transfer groups prevented serum viremia (**Figure 4.3B**). The homotypic C/C sera passive transfer group provided near-sterilizing protection (**Figure 4.3E and 4.3F**) except for low amounts of vRNA detected in heart, quadriceps muscles, and spleen subsets and at the right (ipsilateral) ankle challenge injection site. Although the other vaccine administration strategies (C/M, M/M, M/C and CM/CM) elicited near-sterilizing protection from CHIKV infection (**Figure 4.2B, 4.2C, 4.2F**), passive transfer experiments of sera from these groups were not sufficient to significantly reduce viral loads, with several mice actually displaying increased CHIKV vRNA levels in multiple tissues compared to those animals receiving the AdV-GFP control sera (**Figure 4.3E**).

Figure 4.3. Passive transfer of vaccine immune sera demonstrates that antibodies are not sufficient for sterilizing cross-protection against viral replication in tissues.

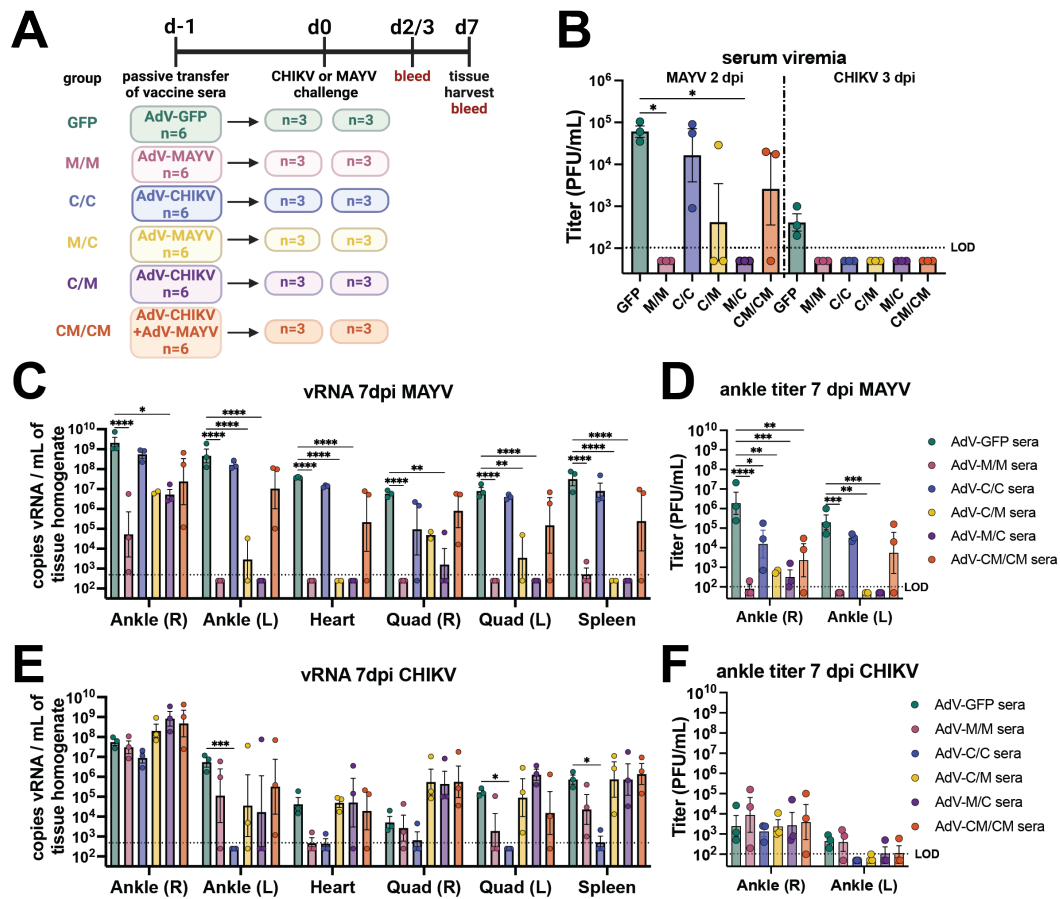


Figure 4.3. (A) Study schematic. Serum collected from three mice from each vaccine group described in Figure 1 was pooled and utilized for passive transfer by 100 μ L i.p. injection in each of six mice. The next day, three mice were challenged by subcutaneous right footpad injection with 10⁴ PFU of MAYV_{BeAr505411} and three mice were challenged with 10³ PFU of CHIKV_{SL15649}. MAYV infected animals were bled at 2 days post-infection (dpi) and 3 dpi following CHIKV infection. Limiting dilution titring was used to measure serum viremia and infectious viral loads in the ankle, quadriceps, heart, and spleen tissues collected at 7 dpi. (B) Serum titers quantified by limiting-dilution plaque assays measured in PFU/mL. (C) MAYV vRNA quantified by qRT-PCR in tissues and (D) MAYV infectious viral titers in ankles quantified by plaque assay at 7 dpi. (E) CHIKV vRNA quantified by qRT-PCR in tissues and (F) CHIKV infectious viral titers in ankles quantified by plaque assay at 7 dpi. All values are log-transformed in (B-F). Serum titers (B) are analyzed with a Kruskal-Wallis test with Dunn's multiple comparisons. Tissue titers and vRNA levels reported in (C-F) are analyzed by two-way ANOVA with the Dunnett's multiple comparisons test. For simplicity in all graphs, only comparisons of $p < 0.05$ are shown where * $P \leq 0.05$, ** $P \leq 0.01$, *** $P \leq 0.001$, **** $P \leq 0.0001$. For all graphs, mean with SEM are plotted. The limit of detection (LOD) for all plaque assays was 100 PFU/mL of serum or tissue homogenate with undetectable samples graphed as half of the LOD. The LOD for qRT-PCR assays was 500 vRNA copies/mL of tissue homogenate.

Footpad swelling outcomes for animals in the passive transfer experiments following infection with either MAYV or CHIKV are shown in **Figure 4.4**. All MAYV challenge mice receiving AdV-GFP sera developed footpad swelling peaking at 7 dpi (**Figure 4.4**). Consistent with our analysis of MAYV infected tissues, mice receiving sera from the M/M, M/C, and C/M vaccine groups were significantly protected from MAYV-induced footpad swelling (**Figure 4.4A, 4.4C, 4.4D**). In contrast, MAYV-induced footpad swelling was observed in mice receiving the serum from the C/C and CM/CM vaccine groups (**Figure 4.4B, 4.4E**). Interestingly, the mice in the C/C sera passive transfer group developed footpad swelling that was similar in magnitude to the AdV-GFP controls at 6 dpi, but the level was reduced at 7 dpi ($P \leq 0.0001$; compared to AdV-GFP) (**Figure 4.4B**). A similar footpad swelling phenotype was observed for the CM/CM sera passive transfer mice, with a reduction at 7 dpi ($P \leq 0.0001$; compared to AdV-GFP) (**Figure 4.4E**). Footpad swelling following CHIKV infection was reduced in animals receiving serum from the M/M, M/C, C/M, and CM/CM groups; however, for each group, two mice were fully protected and one mouse developed footpad swelling with similar kinetics to control mice (**Figure 4.4F, 4.4H, 4.4I, 4.4J**). The C/C sera passive transfer group was completely protected from footpad swelling, reaching statistical significance ($P \leq 0.0001$) (**Figure 4.4G**). These outcomes provide examples of differential disease outcomes in instances of varying levels of cross-neutralizing antibody potency based upon the vaccine antigen delivery regimen. These findings support observations of non-reciprocity in cross-protection for CHIKV and MAYV infection and suggested that other immune responses may also contribute to cross-protection.

Figure 4.4. Differential disease outcomes elicited by passive antibody transfer.

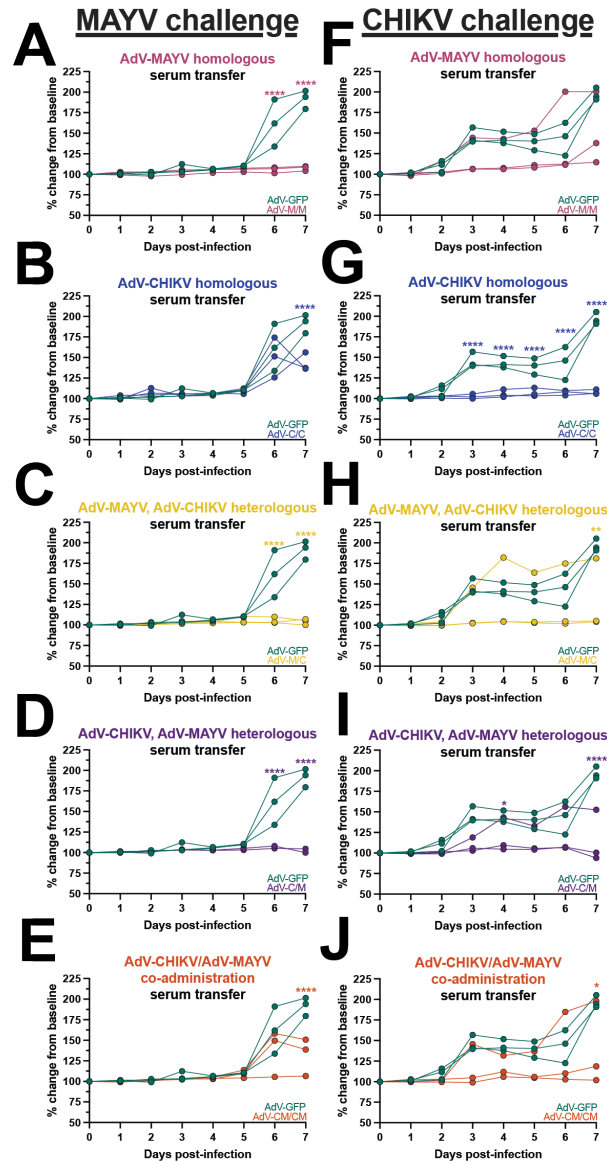


Figure 4.4. Naïve mice received mouse vaccine sera via passive antibody transfer and were challenged by subcutaneous injection into the footpad with CHIKV or MAYV. Footpad swelling was measured daily with digital calipers and mice were humanely euthanized at 7 days post-infection (dpi). Footpad swelling after MAYV challenge is plotted adjacent to control animals who received AdV-GFP sera or (A) AdV-MAYV homologous sera, (B) AdV-CHIKV homologous sera, (C) AdV-MAYV, AdV-CHIKV heterologous sera, (D) AdV-CHIKV, AdV-MAYV heterologous sera, or (E) AdV-CHIKV/AdV-MAYV co-administration sera transfer. Footpad swelling after CHIKV challenge is plotted adjacent to animals who received AdV-GFP sera for (F) AdV-MAYV homologous sera, (G) AdV-CHIKV homologous sera, (H) AdV-MAYV, AdV-CHIKV heterologous sera, (I) AdV-CHIKV, AdV-MAYV heterologous sera, and (J) AdV-CHIKV/AdV-MAYV co-administration sera transfer. Raw measurements were used to calculate percent change from baseline which is plotted for individual mice. These

values were compared to AdV-GFP serum-transferred controls and analyzed using a two-way ANOVA with the Šidák's multiple comparisons test where ns $P > 0.05$, * $P \leq 0.05$, ** $P \leq 0.01$, *** $P \leq 0.001$, **** $P \leq 0.0001$.

4.3.4 Serum from immunized mice exhibits antibody-dependent enhancement activity of MAYV and UNAV replication *in vitro*.

There are only a limited number of reports of antibody-dependent enhancement (ADE) of alphavirus infection but none, to date, have evaluated infection enhancement across different virus species. Since the vaccination and passive transfer experiments demonstrated an inequity in reciprocal cross-protection after heterologous MAYV challenge, we interrogated the *in vitro* ADE potential in macrophages for the adenovirus-vectored alphavirus vaccine-elicited antibodies. Using sera from each vaccine group collected from immunized mice shown in **Figure 4.1**, we first established ADE assays in which sera were serially diluted with MAYV or CHIKV and used to infect RAW264.7 cells (**Figure 4.5, Supplemental Figure 4.S3**). Viral supernatants were collected at 24 hours post-infection and titered by limiting dilution plaque assays. Fold enhancement of viral infection was calculated relative to wells of infected cells without sera and enhancement was defined as a ≥ 10 -fold increase in viral titer released from cells that were infected in the presence of diluted sera. Sera from AdV-GFP control vaccinated animals did not cause infection enhancement at any dilution. Similarly, dilution of the C/C sera did not lead to enhancement of MAYV infection (**Figure 4.5A**), which we hypothesized was also due to low levels of cross-neutralizing antibody titers with a GMT = 95 (**Table 4.1**). However, in the presence of M/M, M/C, C/M, and CM/CM diluted sera, increased infection of MAYV was observed for nearly all sera evaluated with the exception of one sample in the C/M group (**Figure 4.5B-4.5E**). The serum dilution to peak enhancement of MAYV replication varied between each vaccine group with the M/C group having the lowest dilution range to peak ADE of 1:1,250 to 1:6,250 (**Figure 4.5C**) while the M/M, C/M, and CM/CM groups (**Figure 4.5B, 4.5D, 4.5E**) had peak enhancing serum dilutions out to 1:31,250 (**Table 4.1**). In contrast, none of the sera samples from any vaccine group led to enhancement of CHIKV replication (**Figure 4.5F**). The MAYV neutralizing titer values directly correlated with the maximum enhancing serum dilution ($P < 0.0001$) (**Figure 4.5G**). The peak fold enhancement of MAYV titer for the M/C group was statistically significant relative to control wells at up to 1437-fold and was slightly reduced for the M/M, C/M, and CM/CM groups but ranged up to 233-, 86- and 116-fold, respectively (**Figure 4.5H, Table 4.1**).

These results demonstrated a range of vaccine-elicited neutralizing antibody potency that led to the enhancement of MAYV but not CHIKV replication in mouse macrophage cells. These findings also revealed the ability of both homotypic and heterotypic alphavirus-neutralizing antibodies to cause ADE in mouse macrophages.

Figure 4.5. Vaccine sera enhance MAYV but not CHIKV replication in mouse macrophages.

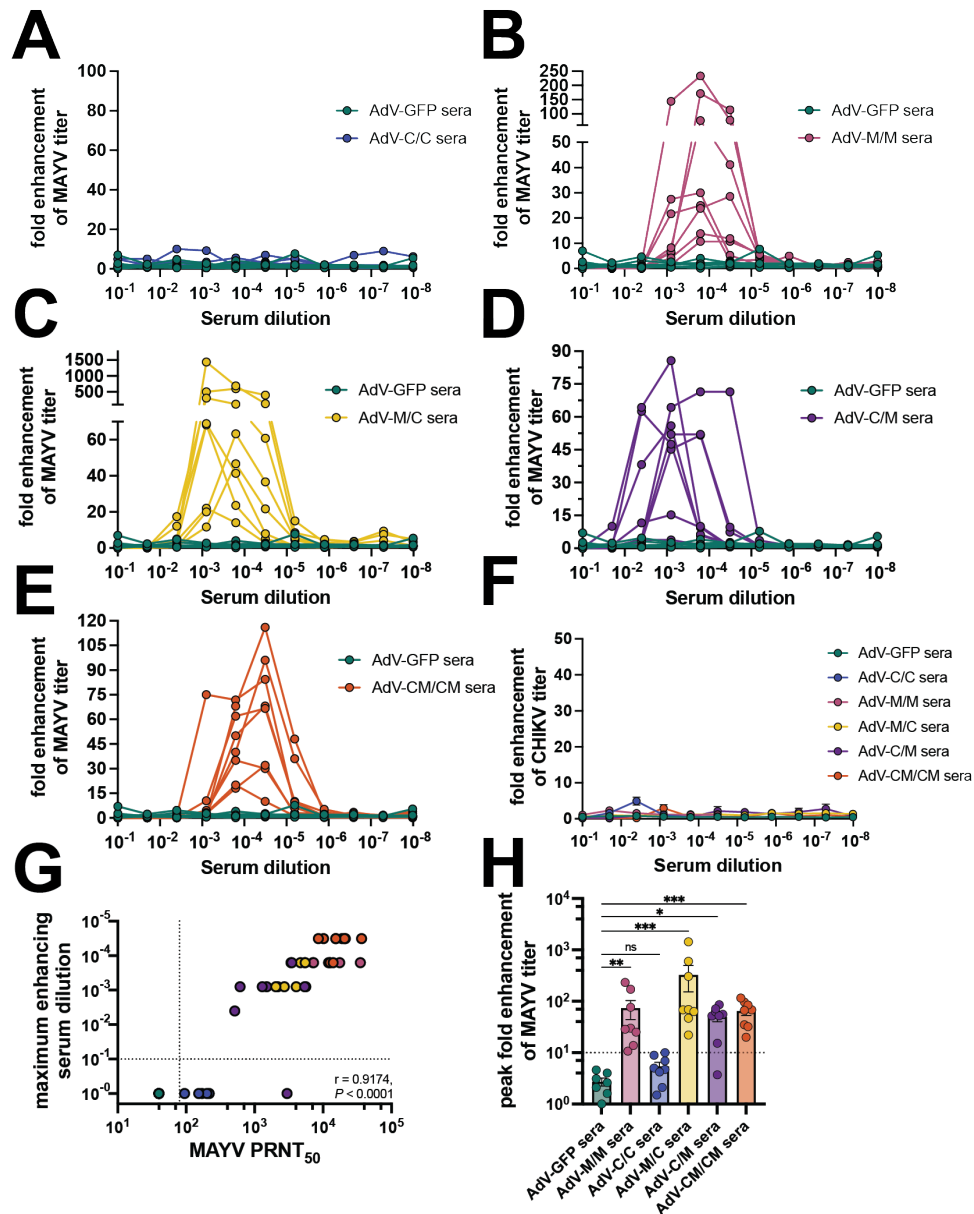


Figure 4.5. Mouse sera collected at 58 days post-prime as described in **Figure 1** was used in antibody-dependent enhancement (ADE) of infection assays in which 10^5 RAW264.7 cells per well were infected with 1:5 serial dilutions of mouse sera mixed with an MOI 1 of (A-E) MAYV_{BcAr505411} or (F) CHIKV_{I81/25}. Cells were incubated

with infection mixtures for 2 hours, media was replaced, and cells were incubated for 20-24 hours at 37°C. Viral supernatants from the RAW cells were collected and titered by limiting-dilution plaque assays. Fold enhancement of viral titer was calculated relative to wells infected with virus only without serum. ADE assays were performed for (A) AdV-C/C sera, (B) AdV-M/M sera, (C) AdV-M/C sera, (D) AdV-C/M sera, and (E) AdV-CM/CM sera all compared to AdV-GFP control sera. (G) Spearman's correlation of 58 days post-prime MAYV PRNT₅₀ (reported in Figure 4.1) versus maximum MAYV enhancing serum dilution in log scale. (H) Compilation of peak fold enhancement of MAYV titer values for each vaccine sera group analyzed by Kruskal Wallis test with Dunn's multiple comparisons where ns $P > 0.05$, * $P \leq 0.05$, ** $P \leq 0.01$, *** $P \leq 0.001$, **** $P \leq 0.0001$. All ADE assays were performed using 7 AdV-GFP and 8 AdV vaccine sera biological replicates for MAYV ADE assays or 4-5 AdV vaccine sera biological replicates for CHIKV assays. For (F, H), error bars are SEM. Supplemental Figure 4.S3 contains the raw titer values used to calculate fold enhancement of MAYV and CHIKV titer.

Figure 4.S3. Raw titer data for MAYV and CHIKV ADE assays.

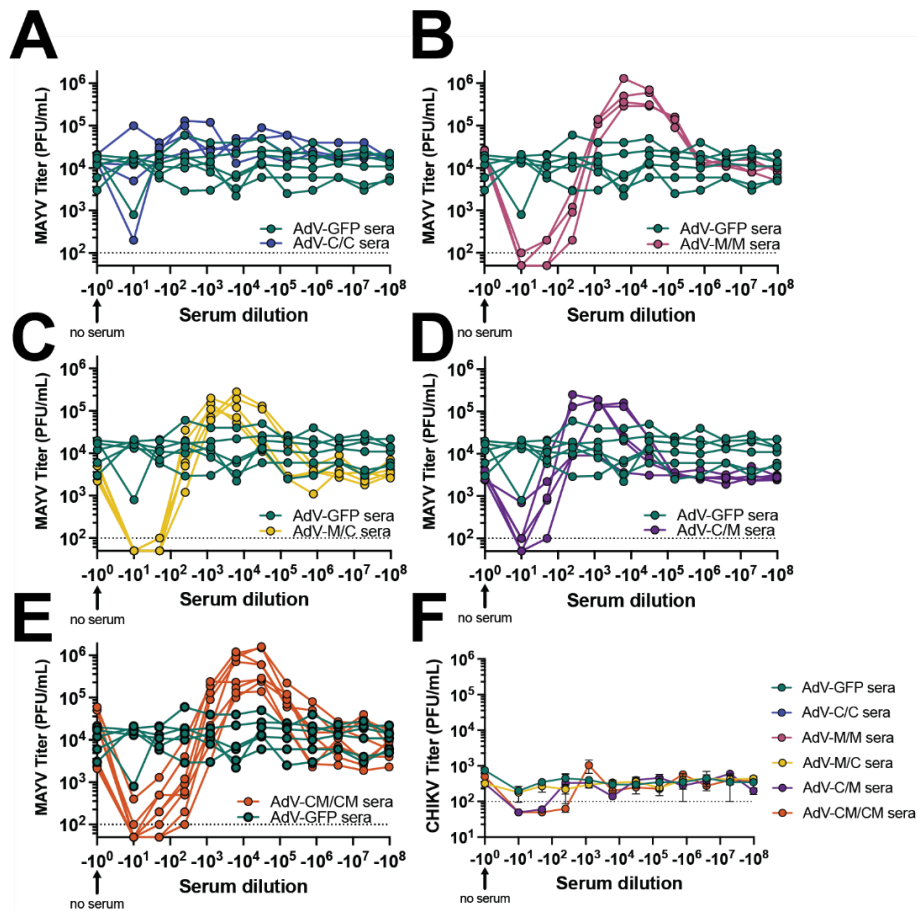


Figure 4.S3. Related to Figure 4.5. All graphs are in log-scale reporting raw viral titers (PFU/mL) of RAW264.7 cell supernatants titered in limiting-dilution plaque assays on Vero cells.

Antibody-mediated enhanced infection assays were extended to additional alphaviruses (UNAV and RRV) in RAW264.7 cells (**Figure 4.6, Supplemental Figure 4.S4**). In this case, where a higher potency of UNAV cross-neutralizing antibodies was present in the C/C group (**Table 4.1**), we observed enhancement of UNAV replication in the presence of diluted sera, reaching between 20- and 270-fold enhancement of viral titers for serum dilutions ranging 1:10 to 1:250 (**Figure 4.6A, Table 4.1**). Diluted vaccine sera from each of the tested samples in the M/M, M/C, C/M, and CM/CM groups also enhanced UNAV infection in macrophages (**Figure 4.6B-4.6E, Table 4.1**). The serum dilution to peak UNAV enhancement ranged from 1:10 dilution to 1:1,250 for M/M, M/C, C/M, and CM/CM vaccine groups (**Figure 4.6B-4.6E, Table 4.1**). We did not detect any substantial ADE activity for RRV using any of the sera samples (**Figure 4.6F**). For the UNAV ADE, we found that the UNAV PRNT₅₀ correlated with the dilution to maximum enhancement ($P < 0.001$) (**Figure 4.6G**). The peak fold enhancement of viral titer was statistically significant compared to AdV-GFP sera, ranging 16-1000-fold (**Figure 4.6H, Table 4.1**). These experiments demonstrate the ability of heterotypic alphavirus neutralizing antibodies to cause ADE of UNAV and MAYV in mouse macrophages, interestingly these two viruses are closely related, which may be important for their similar results but further studies will be required to fully understand this outcome.

Figure 4.6. Vaccine sera enhance UNAV replication in mouse macrophages.

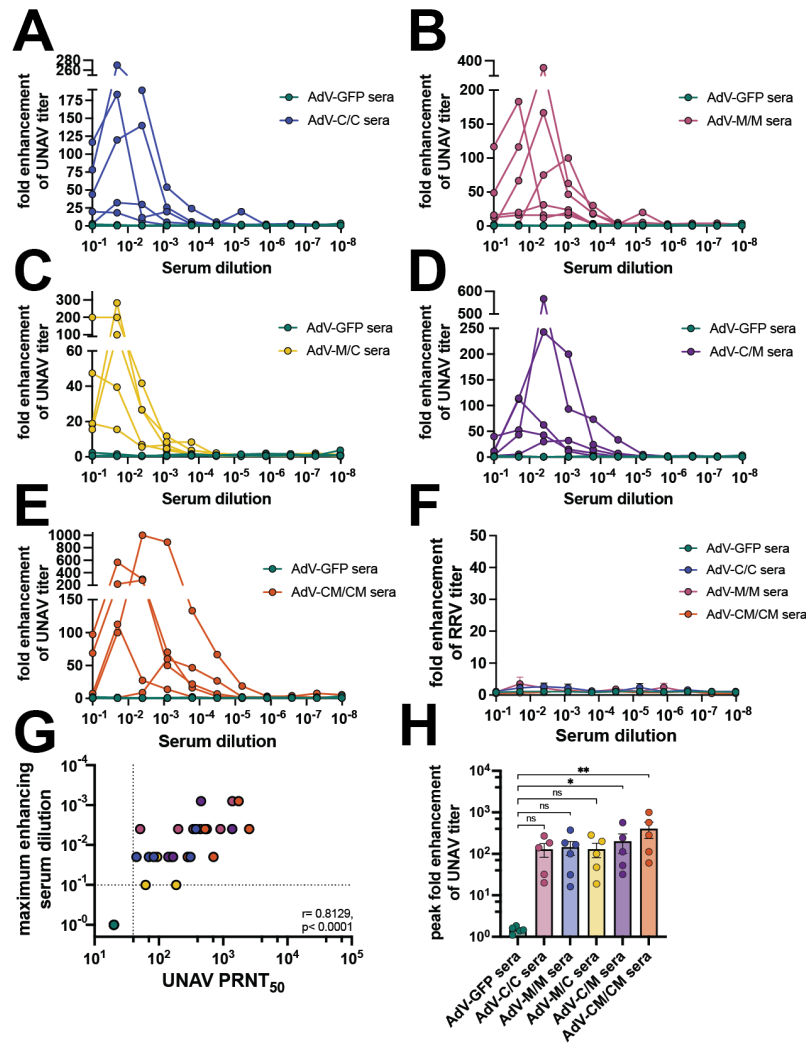


Figure 4.6. Mouse sera collected at 58 days post-prime (as described in **Figure 1**) was used in ADE of infection assays in which 10⁵ RAW264.7 cells per well were infected with 1:5 serial dilutions of mouse sera mixed with an MOI 1 of (A-E) UNAV_{MAC150} or (F) RRV_{T48}. Cells were incubated with infection mixtures for 2 hours, media was replaced, and cells were incubated for 20-24 hours at 37°C. Viral supernatants from the RAW cells were collected and titered by limiting-dilution plaque assays. Fold enhancement of viral titer was determined relative to wells infected with virus only without serum. ADE assays were performed for (A) AdV-C/C sera, (B) AdV-M/M sera, (C) AdV-M/C sera, (D) AdV-C/M sera, and (E) AdV-CM/CM sera all compared to AdV-GFP control sera. (G) Spearman's correlation of 58 days post-prime UNAV PRNT₅₀ (reported in **Figure 4.1**) versus maximum UNAV enhancing serum dilution in log scale. (H) Compilation of peak fold enhancement of UNAV titer values for each vaccine sera group analyzed by Kruskal Wallis test with Dunn's multiple comparisons where ns P > 0.05, *P ≤ 0.05, **P ≤ 0.01, ***P ≤ 0.001, ****P ≤ 0.0001. All assays were performed using 5 AdV-GFP and 5-6 AdV vaccine sera biological replicates. **Supplemental Figure 4.S4.** contains the raw titer values used to calculate fold enhancement of UNAV and RRV titer.

Figure 4.S4. Raw titer data for UNAV and RRV ADE assays.

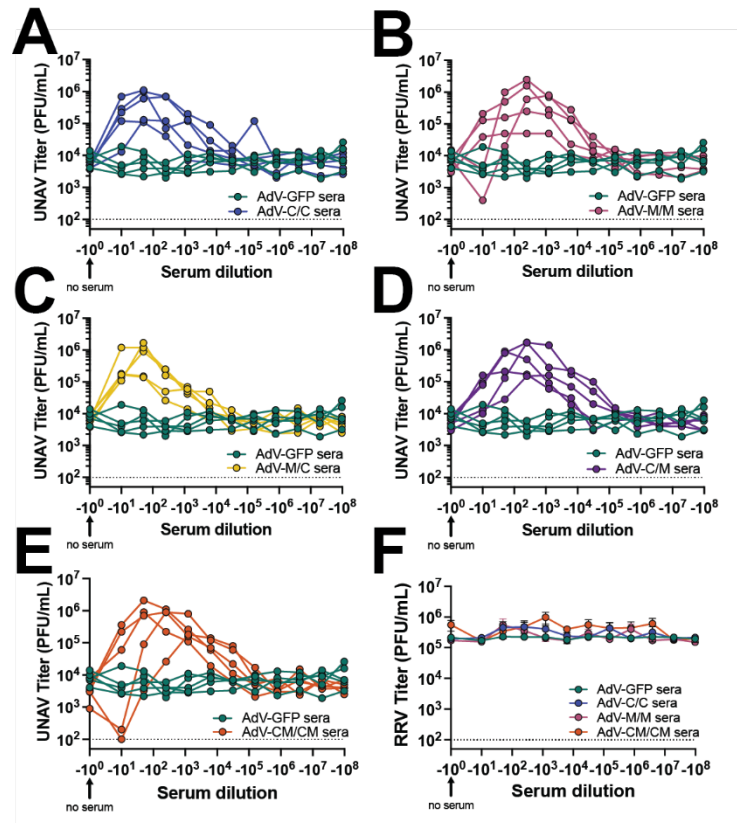


Figure 4.S4. Related to **Figure 4.6**. All graphs are in log-scale reporting raw viral titers (PFU/mL) of RAW264.7 cell supernatants titered in limiting-dilution plaque assays on Vero cells.

Section 4.4: Discussion

The ongoing CHIKV outbreak occurring in Latin America where other related alphaviruses are known to circulate has warranted studies to assess the cross-protective dynamics of prior infection or immunity imparted by vaccination. In this study, we evaluated immunization strategies in immunocompetent mice using our previously reported non-replicating human adenovirus-vectored (AdV) vaccine expressing the MAYV structural polyprotein and a similar AdV-CHIKV vaccine expressing the CHIKV structural polyprotein. We compared both the immunogenicity and protective capacity of these vaccines in C57BL/6 mice in homologous, heterologous and co-administration prime and boost strategies. Overall, our findings revealed that heterologous and coadministration immunization strategies are effective to achieve cross-reactive immunity but incompletely equate to balanced cross-protection. These observations have significance for multivalent alphavirus vaccine design and administration.

One of our major findings was non-reciprocity in CHIKV versus MAYV cross-protection. Passive transfer experiments revealed that antibody potency and other immune responses may have differential contributions to the threshold of protection against MAYV and CHIKV infection. One study demonstrated CHIKV infection elicited immunity can protect against MAYV infection and vice versa, but that vaccine-elicited cross-protective immunity is more complicated and harder to achieve [94]. Adenovirus-vectored vaccines have been previously developed for CHIKV [92, 358, 363-366] and for MAYV by our group [91] and others [92]. Partial cross-protection against MAYV afforded by CHIKV-specific vaccines has been reported using an adenovirus-vectored vaccine [92] and live-attenuated or chimeric vaccines [93]; our study corroborates these findings and shows how heterologous and coadministration immunization strategies are insufficient to fully prevent infection but can provide protection against disease. Consistent with our study, greater protection from infection was observed in context of MAYV immunization and CHIKV challenge compared to the reciprocal CHIKV vaccine with MAYV challenge [92]. In our previous study, we demonstrated near-sterilizing protection elicited by AdV-MAYV against lethal CHIKV and UNAV challenge in $IFN\alpha R1^{-/-}$ mice, a very stringent model [91]. The differential phenotypes in cross-protection observed in the literature also underscore the importance of utilizing a range of animal disease models to evaluate vaccine efficacy. Future studies should investigate the vaccine administration strategies presented in this manuscript in lethal challenge models of immunodeficiency to more definitively identify the necessary and sufficient immune players in cross-protection. Overall, our findings as well as these two published studies continue to suggest differences in CHIKV and MAYV reciprocal cross-protection [92, 93].

We also observed non-reciprocity in ADE assays with little to no enhancement for CHIKV or RRV but robust activity for MAYV and UNAV. Previous studies have shown that MAYV-neutralizing antibodies require Fc effector functions to be protective [77] and that non-neutralizing antibodies can also confer protection from alphavirus infection mediated by Fc effector functions and monocytes [72]. Especially given the range of neutralizing antibody potency resulting in ADE, a possibility is that the Fc effector functions elicited by the adenovirus-vectored vaccines in our study were not equal within or across vaccine groups, explaining both the partial protection phenotypes after passive transfer and range of the magnitude of ADE we observed. Although characterization of Fc effector functions was outside the scope of the current study, correlates of vaccine-elicited Fc effector functions and protection from infection and disease is an area that

warrants further investigation. The lack of evidence of *in vitro* ADE in mouse macrophages for CHIKV in our study remains an enigma. CHIKV replication is reduced in macrophages compared to other cell types, however, CHIKV is known to persist in activated macrophages [367] and infected macrophages are a source of arthritogenic inflammatory cytokines [368, 369]. The mechanisms of macrophage persistence of other alphaviruses like MAYV and UNAV has not been well characterized and may have some contribution to the virus-specific ADE phenotype we observed. Important limitations of our work for future consideration are the establishment of ADE assays in additional cell types, examination of viral RNA levels, and examination of viral output at later timepoints due to CHIKV persistence in macrophages. Our results here do not mean to exclude the possibility of CHIKV *in vitro* ADE, but rather to present an observed phenotype for MAYV and UNAV that was not recapitulated for CHIKV, which warrants further characterization. *In vitro* ADE studies of alphavirus infection to elucidate cell and virus-specific differences, as well as studies that examine translation of the findings *in vivo*, are areas that warrants further research.

Another major finding from our study was that the boosting of antibodies by heterologous vaccine regimens was more limited compared to coadministration or homologous boosting. Original antigenic sin is known to limit boosting to antigenic determinants that were recognized during the priming event and may be limiting increased breadth of our heterologous boosting regimen [370]. We and others have previously determined that cross-reactivity between human CHIKV antisera for recognition of MAYV, in large part, is driven by responses against the E2 B domain [59, 73, 75, 76, 79, 251, 274, 326, 331]. The similarity between these two viruses may focus immunity against the common epitopes found in this or other similar regions. Future studies should further characterize vaccine-elicited antibodies beyond binding and neutralizing functions to see if other antibody characteristics correlate with vaccine-elicited protection.

Our results from this study suggest important considerations for multivalent vaccine design and heterologous immunization strategies. Our conclusions highlight the need to characterize immunity and disease responses in those that have been infected with different but related alphaviruses as the ongoing CHIKV outbreak in Latin America continues to affect a large number of individuals that are also in regions susceptible to MAYV or other alphaviruses. Type-specific, balanced immune responses are very important for DENV vaccine efficacy and safety due to risk of enhanced disease mediated by ADE. Our findings suggested that while heterologous and

coadministration strategies can achieve balanced cross-reactive immunity, these responses do not translate to complete protection from infection or disease and these antibodies also have *in vitro* ADE potential that may or may not be translational *in vivo*. Balance of alphavirus cross-reactive immunity and translation to achieve protection without risk of ADE is a concept that should be carefully considered when developing alphavirus vaccines.

Section 4.5: Materials & Methods

4.5.1 Ethics statement

Mouse experiments were performed in an ABSL-3 facility, accredited by the Association for Accreditation and Assessment of Laboratory Animal Care (AALAC) International, in accordance with the animal protocols approved by the Oregon Health and Science University (OHSU) Institutional Animal Care and Use Committee (IACUC Protocol #0913). Mice were housed in the ABSL-3 laboratory at the OHSU Vaccine and Gene Therapy Institute (VGTI) in ventilated racks with access to food and water with a 12-hour light/dark cycle.

4.5.2 Cells, viruses, and viral vaccine vectors

Vero cells (ATCC CCL-81), 293IQ (Microbix), and RAW264.7 cells (provided by Dr. Victor DeFilippis, OHSU) were propagated at 37°C and 5% CO₂ in Dulbecco's Modified Eagle Medium (DMEM) supplemented with 5% fetal bovine serum (FBS) and 1% penicillin-streptomycin-glutamine (PSG) (DMEM-5). *Aedes albopictus* C6/36 cells (ATCC CRL1660) were propagated at 28°C with 5% CO₂ in DMEM containing 10% FBS and 1X PSG.

Mayaro virus (MAYV_{BeAr505411}, NR-49910), Una virus (UNAV_{MAC150}, NR-49912), and Ross River virus (RRV_{T-48}, NR-51457) were obtained through BEI Resources. Chikungunya virus (CHIKV_{181/25}) and CHIKV_{SL15649} were generated from infectious clones [112]. Alphaviruses were propagated in C6/36 cells by infection at MOI 0.1 and harvest of viral supernatant at 72 hours post-infection (hpi). Supernatants were clarified and virus purified over a 10% sorbitol gradient by ultracentrifugation at 82,755 x g for 70 minutes. Viral stocks were resuspended in 1X phosphate buffered saline (PBS), aliquoted, and frozen for later use at -80°C. Viral stocks were titered by limiting dilution plaque assays over confluent monolayers of Vero cells using a ten-fold dilution

series from 10^8 to 10^{-8} . Infected Vero cells were rocked for 2 hours at 37°C and overlaid with DMEM-5 containing 0.3% high / 0.3% low viscosity carboxymethylcellulose (CMC) (CMC-DMEM). Plaque assays for CHIKV_{SL15649}, MAYV_{BeAr505411}, UNAMAC150, and RRV_{T48} were fixed with 3.7% formaldehyde and stained with 0.2% methylene blue at 48 hpi. Plaque assays for CHIKV_{181/25} were fixed and stained at 72 hpi. Plaques were enumerated under a light microscope to determine viral stock titers. The limit of detection for plaque assays was 100 plaque forming units (PFU) per mL.

Adenovirus V (AdV) vaccine vectors were propagated in 293IQ cells. Construction of AdV-MAYV was previously described [91] and AdV-CHIKV was generated using similar techniques for the West African CHIKV₃₇₉₉₇ structural polyprotein sequence [91]. We chose CHIKV₃₇₉₉₇ as the vaccine strain because Akahata *et al.* showed CHIKV₃₇₉₉₇ produces nearly 100-fold higher levels of virus like particles compared to CHIKV_{LR2006} structural proteins, which we hypothesized to be an important feature for the generation of potent neutralizing antibody responses and subsequent protection [371].

4.5.3 Mouse experiments

C57BL/6 mice (4-6 weeks old) were purchased from Jackson laboratories. Animals were immunized with 50 μL containing 10^8 plaque forming units (PFU) of either AdV-MAYV and/or AdV-CHIKV diluted in 1X PBS injected in the left posterior thigh muscle. Animals were bled from saphenous veins at day 28 and 58 post-prime immunization for immunogenicity analysis. Serum was isolated from clotted blood following centrifugation for 5 minutes at 3,000 x g. For challenge experiments, female C57BL/6 mice were inoculated subcutaneously in the right footpad with 20 μL containing 10^4 plaque forming units (PFU) of MAYV_{BeAr505411} or 10^3 PFU of CHIKV_{SL15649}. Footpad thickness height was measured daily after infection in the right (ipsilateral) rear footpad using a digital caliper according to the established method [372]. Mice were bled at 2- or 3-days post-infection (dpi) to quantify the level of serum viremia and animals were euthanized using isoflurane overdose at 5 or 7 dpi to characterize viral infection. Mouse ankle, quad, spleen, and heart tissues were collected in 1mL of 1X PBS with approximately 250 μL of silica beads. Tissues were homogenized using a bead beater for three cycles of 45 seconds on and 30 seconds off. The tissue sample homogenates were centrifuged at 3,000 x g for 5 minutes to clear the debris. For the euthanized immunogenicity mice, splenocytes were isolated through a

70 μ M cell strainer and washed with RPMI 1640 medium supplemented with 10% FBS and 1% PSG. Splenocytes were pelleted at 650 x g for 10 minutes and the red blood cells were lysed with 1X BioLegend red blood cell lysis buffer for 3 minutes, washed, and frozen for later use.

4.5.4 Neutralization assays

Mouse serum was first heat inactivated by incubation for 30 minutes at 56°C and then diluted by serial 2-fold dilutions in DMEM-5. The diluted sera were mixed with media containing approximately 70–120 plaque forming units of MAYV_{BeAr505411}, CHIKV_{181/25}, or UNAV_{Mac150} and incubated for 2 hours at 37°C with 5% CO₂ with constant rocking. The mixtures were added to 12-well plates of confluent Vero cells and incubated for an additional 2 hours at 37°C with 5% CO₂ with continuous rocking. CMC-DMEM-5 was then added to each well to overlay. Cells were incubated for 48 hours for MAYV_{BeAr505411} and UNAV_{Mac150} or 72 hours for CHIKV_{181/25}. Plates were fixed and stained as described for the plaque assays above. Plaques were counted and the percent of plaques at each dilution relative to wells without serum were determined to calculate percent neutralization of infection. The 50% plaque reduction neutralization titers (PRNT₅₀) were calculated by non-linear regression analysis with variable slope using GraphPad Prism 9 software.

4.5.5 Viral RNA detection

Total nucleic acids were isolated from 300 μ L of each mouse tissue homogenate using the Promega Maxwell 48 sample RSC purification system with the Maxwell RSC Viral TNA extraction kit. Purified nucleic acids were resuspended in 70 μ L of RNase free water and each sample was diluted to 100ng/ μ L. ezDNase digestion was used to remove contaminating DNA. Single stranded cDNA was generated from 1 μ g of total RNA using random hexamers and reverse transcriptase Invitrogen Superscript IV, according to the manufacturer's protocol. Gene amplicons were used as quantification standards. The primers and probe used to detect MAYV RNA were Forward-CCATGCCGTAACGATTGC, Reverse-CTTCCAGGCTGCCCCGGCACCAT, and probe FAM-TGGACACCGTTCGATAC-MGB. The primers and probe used to detect CHIKV_{SL15649} RNA were Forward-CCGTCCCTTTCCTGCTTAGC, Reverse-AAAGGTTGCTGCTCGTTCCA, and Probe FAM-ACATACCAAGAGGCTGC. Quantitative RT-PCR was performed using a QuantStudio 7 Flex Real-Time PCR system in triplicate reactions. All data were analyzed using the Applied Biosystems QuantStudio 7 Flex Real-time PCR System software. The viral RNA

levels were normalized to a murine housekeeping gene, ribosomal protein RPS17, and reported in copies per mL of tissue homogenate.

4.5.6 Quantification of infectious virus

Infectious virus in mouse serum, tissue homogenate or RAW264.7 cell supernatants was quantified by limiting dilution plaque assays as described above. Briefly, 20 μ L of serum, tissue homogenate, or RAW264.7 cell supernatants were added to 180 μ L DMEM-5, which was serially diluted by ten-fold. Viral dilutions were added to confluent monolayers of Vero cells plated in 48-well plates and allowed to incubate for 2 hours at 37°C with 5% CO₂ with continuous rocking followed by addition of CMC-DMEM-5 overlay. Plaque assays were fixed and stained as described above.

4.5.7 ELISPOT

Splenocytes were added to mouse IFN- γ ELISPOT plates (Mabtech) at a density of 2.5x10⁵ cells in RPMI with 5% FBS and 1% PSG and treated with the CHIKV E1 18-mer peptide #451 (CAVHSMTNAVTIREAEIE) [112] or MAYV E2 15-mer peptide #2 (LAKCPPGEVISVSFV) [91] at a final concentration of 10 μ g/mL. A portion of the cells were stimulated with phorbol 12-myristate 13-acetate (PMA) at 25ng/mL plus ionomycin at 500ng/mL (positive control) or left untreated (negative control). Plates were wrapped in foil and incubated for 24 hours at 37°C with 5% CO₂. Plates were washed once with 1X PBS and incubated with anti-mouse IFN- γ biotin antibody for 2 hours. After a wash with 1x PBS, the plates were incubated with streptavidin-ALP antibody for 1 hour. Spots were visualized following addition of BCIP/NPT-plus substrate and washed a final time with 1X PBS before enumerating with an AID ELISPOT Reader Classic. The results were background subtracted using the number of spots calculated in the negative control wells and the data is reported in spot-forming units (SFU) per 1 million splenocytes.

4.5.8 Western blot analysis

Cell lysates were collected from 293IQ cells infected with AdV-MAYV or AdV-CHIKV at an MOI of 1. Lysates were loaded into 4–12% Bis/Tris polyacrylamide gels (ThermoFisher) and the samples were electrophoresed for 45 minutes at 170 volts. Proteins were transferred to activated PVDF membranes for 25 minutes at 25 volts using a semi-dry electro-blotter. To detect MAYV proteins, membranes were probed for 1 hour with serum diluted 1:500 from a mouse that was

primed and boosted (30 days post-boost) with 10^8 PFU of AdV-MAYV. To detect CHIKV proteins, membranes were probed for 1 hour with serum diluted 1:700 from a mouse that was primed and boosted (30 days post-boost) with 10^8 PFU of AdV-CHIKV. After extensive washing with TBS-Tween 20, the membranes were probed for 1 hour with anti-mouse IgG secondary antibody (Rockland) diluted 1:10,000. Membranes were washed and developed with SuperSignal West Pico Plus chemiluminescent substrate solution (ThermoFisher) and exposed onto X-ray film.

4.5.9 Antibody-dependent enhancement assays

RAW264.7 cells were seeded at a density of 10^5 cells per well in a 96 well plate the day prior to the assay. Serum samples collected from vaccinated mice at 58 days post-prime were serially diluted 1:5 after an initial 1:10 dilution for 11 total dilutions in DMEM-5 and then mixed with 1×10^5 PFU of MAYV_{BeAr505411}, CHIKV_{181/25}, UNAV_{MAC150}, or RRV_{T48}. A negative control well containing virus without serum was included as a baseline infection control. Media was removed from RAW264.7 cells and serum/virus dilutions were used to infect the cells by continuous rocking for 2 hours at 37°C with 5% CO₂. After 2 hours, infection media was removed and replaced with DMEM-5. At 24 hours post-infection, viral supernatants were titered by limiting dilution plaque assay using Vero cells as described above. Fold increase in release of infectious virus was calculated relative to wells containing virus and no serum.

4.5.10 Statistical analysis

All statistical analyses were performed using Graph Pad Prism 10 software. Nonlinear regressions with variable slope were used to calculate neutralization titers. Neutralizing antibody titers between vaccine groups were compared by one-way ANOVA. Viral loads in mouse tissues, virus-specific T cells, and footpad swelling were compared by two-way ANOVA. Correlations between PRNT₅₀ and dilution to maximum viral infection enhancement were compared by Spearman correlation. Peak fold viral infection enhancement data was compared by Kruskal Wallis test.

Section 4.6: Acknowledgements

The authors thank Dr. Victor DeFilippis at Oregon Health and Science University for providing the RAW264.7 cells. The following reagents were obtained through BEI Resources, NIAID, NIH,

as part of the WRCEVA program: MAYV_{BeAr505411} (NR-49910), UNAV_{MAC150} (NR-49912), and RRV_{T-48} (NR-51457). The authors thank Dr. Terence Dermody at the University of Pittsburgh, Pittsburgh, PA, for providing the CHIKV_{181/25} infectious clone.

Chapter 5: Development of a virulent O’nyong’nyong challenge model to evaluate heterologous protection mediated by a hydrogen peroxide-inactivated chikungunya virus vaccine

Status: In preparation for PLoS Neglected Tropical Diseases, October 2024.

Whitney C. Weber^{1,2*}, Zachary J. Streblow^{1,2*}, Takeshi F. Andoh^{1,2}, Michael Denton^{1,2}, Hans-Peter Raué³, Ian J. Amanna⁴, Dawn K. Slifka⁴, Craig N. Kreklywich^{1,2}, Irene Arduino⁵, Gauthami Sulgey^{1,2}, Magdalene M. Streblow^{1,2}, Mark Heise⁶, Mark K. Slifka³, and Daniel N. Streblow^{1,2#}

¹ Vaccine & Gene Therapy Institute, Oregon Health & Science University, Beaverton, Oregon, USA

² Division of Pathobiology & Immunology, Oregon National Primate Research Center, Beaverton, Oregon, USA

³ Division of Neurology, Oregon National Primate Research Center, Beaverton, Oregon, USA

⁴ Najit Technologies, Inc.; Beaverton, OR, 97006, USA

⁵ Department of Clinical and Biological Sciences, University of Turin, Orbassano, Italy

⁶ Department of Microbiology & Immunology, University of North Carolina at Chapel Hill, Chapel Hill, North Carolina, USA

*contributed equally

#Address correspondence to Daniel N. Streblow, streblow@ohsu.edu

Author contributions: Conceptualization: M.K.S, D.N.S; Data curation: W.C.W; Formal analysis: W.C.W; Investigation: W.C.W, Z.J.S, T.F.A, M.D, H.P.R, I.J.A, D.K.S, C.N.K, I.A, G.S, M.M.S, D.N.S; Methodology: W.C.W, Z.J.S, T.F.A, H.P.R, I.J.A, D.K.S, C.N.K, M.K.S, D.N.S; Validation: W.C.W, Z.J.S, T.F.A, H.P.R, I.J.A, D.K.S, C.N.K, M.K.S, D.N.S; Writing – original draft: W.C.W, Z.J.S, M.K.S, D.N.S; Writing – review & editing: W.C.W, I.J.A, M.K.S, D.N.S; Resources: M.H, M.K.S, D.N.S; Funding acquisition: D.N.S, M.K.S; Project administration: M.H, M.K.S, D.N.S; Supervision: M.H, M.K.S, D.N.S.

Section 5.1: Abstract

O'nyong-nyong virus (ONNV) is a mosquito-transmitted alphavirus identified in Uganda in 1959. The virus has potential for enzootic and urban transmission cycles, and in humans, ONNV infection manifests as fever, rash, and joint/muscle pain that can persist. There are currently no specific vaccines or antiviral treatments for ONNV. Since highly passaged alphaviruses often lose pathogenic features, we constructed an infectious clone for ONNV-UVRI0804 (ONNV₀₈₀₄), a 2017 isolate from a febrile patient in Uganda. Viral replication for ONNV₀₈₀₄ was compared to the highly passaged strain, ONNV_{UgMP30}, and ONNV_{UgMP30} replicated to higher levels in human dermal fibroblasts and Vero cells, but both viruses replicated similarly in C6/36 and mouse embryonic fibroblast cells. We performed a head-to-head comparison of *in vivo* virulence in both C57BL/6 mice and AG129 interferon deficient mice. In both mouse strains, ONNV₀₈₀₄ was more pathogenic than ONNV_{UgMP30}. In AG129 mice, ONNV₀₈₀₄ caused a more rapid onset of disease, higher viremia, and a >800-fold increase in virulence. In WT mice, ONNV₀₈₀₄ caused footpad swelling and the virus demonstrated broader tissue distribution and higher vRNA loads at both 5 and 43 days post-infection (dpi) relative to ONNV_{UgMP30}. This finding indicates that ONNV can persist in joint and muscle tissues for long periods of time, which has been associated with chronic arthritogenic human disease. Previous studies have shown that CHIKV infection or vaccination can provide cross-reactive immunity to ONNV. To determine if a CHIKV vaccine can protect against the more virulent ONNV₀₈₀₄ strain, we vaccinated mice with a hydrogen peroxide-inactivated CHIKV vaccine, HydroVax-CHIKV. Neutralizing antibody titers were determined against ONNV₀₈₀₄ and CHIKV and animals were challenged with ONNV₀₈₀₄. An optimized two-dose vaccination regimen of HydroVax-CHIKV protected against lethal infection and reduced virus-associated arthritogenic disease. These data indicate that HydroVax-CHIKV vaccination can protect against infection with a highly pathogenic contemporary strain of ONNV.

Section 5.2: Introduction

O'nyong-nyong virus (ONNV) is an enveloped, positive-sense, single-stranded alphavirus in the *Togaviridae* family with a high degree of similarity in genetics and clinical manifestation to

chikungunya virus (CHIKV). ONNV is a neglected, emerging and re-emerging virus first isolated in 1959 [172] that has been responsible for 3 major human epidemics. The first began around 1959 with over 2 million people infected in northwest Uganda. ONNV disappeared from detection between 1962 and 1996 then a second outbreak occurred where over 21,000 people were affected between 1996 and 1997 in southern Uganda [175-177]. Another smaller outbreak occurred in 2003 in Chad and a single case was reported in 2004 [178], further demonstrating potential for periodic re-emergence [373]. Although only three major outbreaks have been recognized, numerous studies have uncovered serological evidence of ONNV transmission, including in 2020, but there is potential that some of these reports may have been detecting cross-reactive antibodies elicited by CHIKV infection rather than ONNV infection [89, 374-376]. ONNV is transmitted by *Anopheles funestus* and *Anopheles gambiae* mosquitoes, nighttime biting mosquitos, which contrast with CHIKV transmission vectors. These mosquitoes also transmit malaria and are prevalent in many parts of Africa leading to outbreaks in West, East, and Central Africa [13]. Animal reservoirs of ONNV are currently undefined, but some serological evidence identifying antibodies in buffalo, duikers, and mandrills (non-human primates) within the Congo basin (Gabon, Democratic Republic of the Congo) and has been reported [179]. The primary clinical symptoms of ONNV include fever, arthralgia, myalgia, and rash but fatigue, headaches, and lymphadenopathy are also common [177], which resemble those of other arboviral diseases such as CHIKV, dengue virus (DENV) and Zika virus (ZIKV) complicating clinical diagnosis and likely leading to an underestimation of the number of infected individuals. The incubation period of ONNV is typically 4-7 days followed by the acute phase lasting one to two weeks, but joint pain and fatigue have been observed to persist for several weeks to years in some individuals [17-19]. Although ONNV strain-specific differences in clinical manifestation have not yet been identified, differences in pathogenicity in mice have been noted [249]. Despite a significant impact on public health during outbreaks, ONNV remains understudied, and therapeutics to treat infections and a vaccine to prevent them are currently unavailable.

ONNV is clinically and antigenically related to CHIKV and other viruses of the Semliki Forest antigenic complex such as Ross River virus (RRV), Mayaro virus (MAYV), and Una virus (UNAV). Due to shared antigenicity, it has been demonstrated that CHIKV infection can induce ONNV-neutralizing antibodies in humans (and vice versa) [59, 75, 377, 378] and that CHIKV infection can confer protection against ONNV challenge in mice [86]. Vaccines have been

developed for CHIKV with cross-reactivity against ONNV [69, 75, 102, 274] and some have been cross-protective [86, 106] but no vaccines specifically targeting ONNV have been developed. In this study, we generated a full-length infectious clone from the published genome sequence designated ONNV UVRI0804 isolated in 2017 [379] to compare pathogenic features to a highly passaged strain (ONNV_{UgMP30}) and to demonstrate cross-protective potential of our previously reported hydrogen peroxide inactivated HydroVax- CHIKV vaccine [102]. In line with extensive cell culture passage history, we observed modest replication advantages for ONNV_{UgMP30} *in vitro* but found ONNV₀₈₀₄ to be far more pathogenic *in vivo* in both immunocompetent and immunodeficient mice. Moreover, we found that HydroVax-CHIKV vaccination elicited ONNV₀₈₀₄ neutralizing antibodies that were cross-protective against lethal ONNV₀₈₀₄ infection and arthritogenic disease progression in mice.

Section 5.3: Results

5.3.1 Genetics and replication comparison of ONNV strains

While ONNV was first identified in Uganda in 1959 [1] and there have been numerous large outbreaks, relatively few viral isolates are available for research studies. In 2014, the U.S. Centers for Disease Control and Prevention and the Uganda Virus Research Institute initiated an outpatient study to identify causes of acute febrile disease in northwestern Uganda. In 2017, a sample collected from a febrile patient with fever, chills and joint pain was tested and found to cause cytopathic effect in Vero cells [379]. RNA was extracted, sequenced, and an 11kb genome aligned to the ONNV isolate, SG650, with a high degree of similarity (98.3% identical). To characterize this new isolate, named ONNV-UVRI0804, we first performed a phylogenetic analysis based on the structural proteins of the available ONNV strains with complete genomes and a selection of related Semliki Forest complex alphaviruses (**Figure 5.1A**). The ONNV strain cluster form two separate clades and are positioned between CHIKV_{SL15649} and MAYV₅₀₅₄₁₁. ONNV_{UgMP30}, which is one of the more common ONNV strains used in research studies, shares 98% amino acid identity with ONNV₀₈₀₄. Alignment of amino acids revealed multiple differences between the two strains, finding more conservation in the structural proteins than non-structural proteins, with highest divergence found in nonstructural protein 3 (nsP3) (**Figure 5.1B**). Of note, ONNV₀₈₀₄ contains the opal stop codon sequence directly preceding nsP4, which has been linked to infectivity conferring a fitness advantage whereas ONNV_{UgMP30} contains an arginine residue

instead [380]. To evaluate whether strain differences affect *in vitro* and *in vivo* viral replication, we used the published viral sequence for ONNV-UVRI0804 to construct a plasmid infectious clone containing the entire genome. RNA was synthesized by *in vitro* transcription, transfected into Vero cells, and the recovered recombinant virus (ONNV₀₈₀₄) was passaged in mosquito cells and sequenced by NGS to confirm genome integrity.

We compared the kinetics of viral replication for ONNV₀₈₀₄ and ONNV_{UgMP30} in four cell lines: mosquito cells (C6/36), mouse embryonic fibroblasts (MEF), African green monkey kidney epithelial cells (Vero), and primary human dermal fibroblasts (NHDF). The two viruses replicated similarly in C6/36 cells (**Figure 5.1C**) and MEFs (**Figure 5.1D**), but ONNV_{UgMP30} replicated to higher levels in Veros (**Figure 5.1E**) and NHDF cells (**Figure 5.1F**). We hypothesized that this tissue culture fitness advantage for ONNV_{UgMP30} is due to growth adaptation due to extensive prior passage history and potentially the loss of the opal codon between nsP3 and nsP4.

Figure 5.1. ONNV strain genetic comparison and growth characteristics in four cell lines.

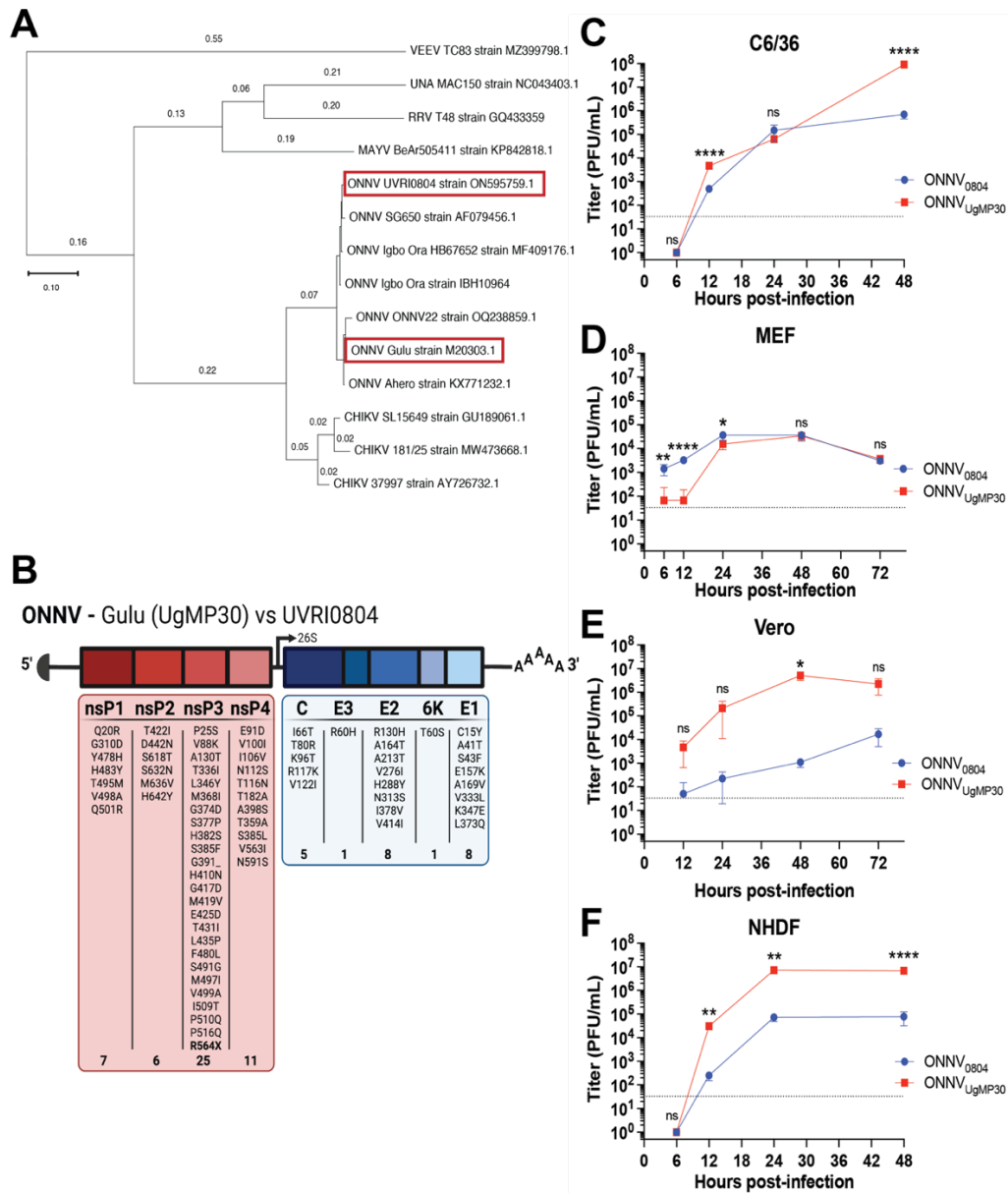


Figure 5.1. (A) Maximum likelihood phylogenetic tree constructed in MEGA software using the Dayhoff model and structural protein (C/E3/E2/6K/E1) amino acid sequences from all ONNV strains with available complete genomes and selected related alphaviruses of the Semliki Forest virus complex. ONNV₀₈₀₄ and ONNV_{UgMP30} strains are indicated in red outlined boxes. (B) Summary of amino acid differences between ONNV Gulu UgMP30 and UVRI0804 strains. The nsP3 opal stop codon is in bold lettering. Growth kinetics of ONNV_{UgMP30} (red) and ONNV₀₈₀₄ (blue) strains in (C) C6/36, (D) MEF, (E) Vero, and (F) NHDF cell lines. Cells were infected at a multiplicity of infection equal to 0.5 in triplicate wells. Viral supernatants were collected at the indicated timepoints and titered by plaque assays. Titers are reported in plaque forming units (PFU) per mL of viral supernatant. The dotted line represents the limit of detection at 33.3 PFU/mL. Mean and error bars with standard deviation are plotted

and analyzed by multiple paired t tests with Holm-Šidák's multiple comparisons where not significant (ns) $P > 0.05$, $*P \leq 0.05$, $**P \leq 0.01$, $***P \leq 0.001$, and $****P < 0.0001$.

5.3.2 ONNV₀₈₀₄ is more pathogenic than ONNV_{UgMP30} in immunocompetent mice

To compare strain pathogenesis *in vivo*, we challenged wild type (WT) C57BL/6 mice by subcutaneous footpad injection with two different dosages of ONNV₀₈₀₄ or ONNV_{UgMP30} (**Figure 5.2A**). Although body weight was not impacted following infection with either strain (**Figure 5.2B**), ONNV₀₈₀₄, at both dosages, caused footpad swelling in mice beginning at 2 dpi that was statistically significantly higher than for ONNV_{UgMP30}-challenged mice. The biphasic footpad swelling demonstrated peaks at 3 dpi and 7-8 dpi, depending upon initial infectious dose, and the swelling phenotype persisted until 14 dpi, the study endpoint (**Figure 5.2C**). In contrast, mice challenged with ONNV_{UgMP30}, at either infectious dose, did not develop footpad swelling. Histological analysis of the ipsilateral ankle was performed at 7 dpi for a second group of C57BL/6 mice that were infected with ONNV₀₈₀₄ and ONNV_{UgMP30}. Tendonitis, myositis, and arthritis with significant levels of inflammation were observed in ONNV₀₈₀₄-challenged animals with only minimal changes detected for mice infected with ONNV_{UgMP30} (**Figure 5.2D, 5.2E**). Tissue viral RNA (vRNA) was measured by quantitative RT-PCR using primers and probe specific for a region of genomic sequence common to both strains. Upon examination of viral dissemination, ONNV₀₈₀₄ demonstrated broader tissue distribution (joints, muscles, spleen, heart, and brain) and higher vRNA levels at 5 dpi relative to ONNV_{UgMP30} (**Figure 5.2F**). We also conducted a time course study to examine the kinetics of viral replication in the tissues in the first 5 days after infection (**Supplemental Figure 5.S1A**). ONNV vRNA was detected in serum samples for ONNV₀₈₀₄ at 1-4 dpi and peaked at 2 dpi, whereas vRNA was only detectable for ONNV_{UgMP30} at 4 dpi albeit at a lower level. (**Supplemental Figure 5.S1B**). Infectious virus was quantitated by plaque assays of tissue lysates from the ipsilateral ankles and both viruses followed similar growth kinetics between 1 and 4 dpi, but replication was elevated for ONNV_{UgMP30} at 5 dpi compared to ONNV₀₈₀₄ (**Supplemental Figure 5.S1C**). Between 1 and 5 dpi, ONNV₀₈₀₄ vRNA levels were elevated compared to ONNV_{UgMP30} at nearly all timepoints in the ankles, quadricep muscles, calf muscles, heart, and spleen (**Supplemental Figure 5.S1D-G**). Thus, our data confirm that the contemporary clinical isolate, ONNV₀₈₀₄, constructed using the viral sequence from a recent febrile patient, is

virulent *in vivo* when delivered by subcutaneous injection and this new infectious clone causes higher levels of pathogenesis relative to ONNV_{UgMP30}.

Figure 5.2. ONNV pathogenesis, disease, and viral persistence in immunocompetent mice.

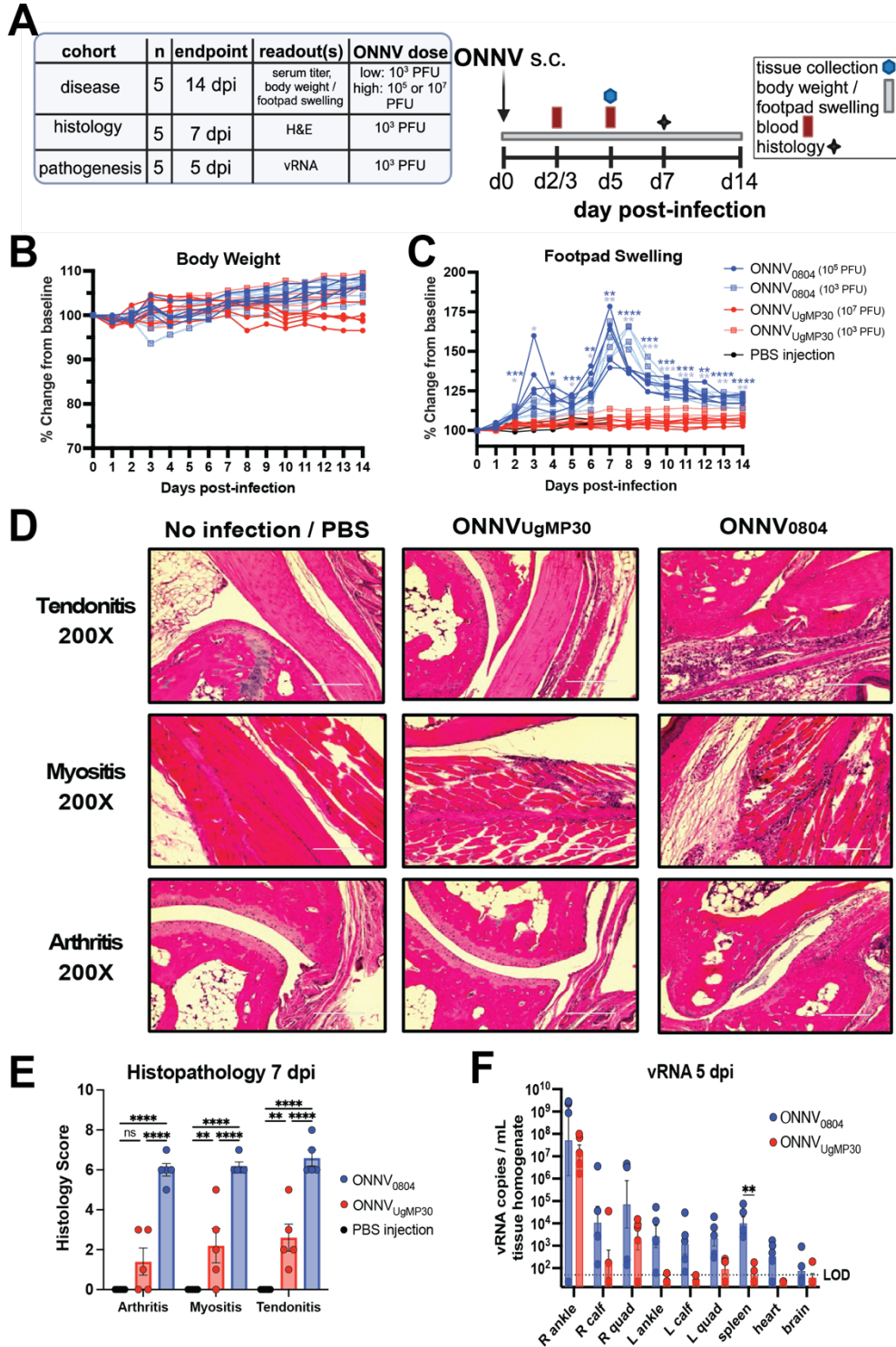


Figure 5.2. (A) Overview of study design. C57BL/6 mice ($n= 5/\text{group}$) were inoculated with a low or high dose of either ONNV strain in the right footpad (s.c.) then (B) body weight and (C) footpad swelling were monitored for 14 days. An additional group of mice ($n= 5/\text{group}$) were inoculated with 10^3 PFU of either ONNV strain or PBS, tissues were collected at 7 dpi and perfused with 4% PFA for (D) H&E histological staining and (E) inflammation grading on a scale of 0 to 10 with 0 indicating no inflammation and 10 indicating the most severe inflammation (see methods). Mean and SEM are plotted and analyzed by two-way ANOVA with Tukey's multiple comparisons. (F) For comparison of viral replication in tissues, mice ($n= 5/\text{group}$) were inoculated with 10^3 PFU of either ONNV strain and ankles, calf muscles, quadriceps muscles, spleen, heart, and brain were collected for vRNA quantification by qRT-PCR. Data in (F) are log-transformed, the mean and standard error are plotted, and data are analyzed by two-way ANOVA with Šidák's multiple comparisons where ns $P > 0.05$, $*P \leq 0.05$, $**P \leq 0.01$, $***P \leq 0.001$, and $****P < 0.0001$. Only significant comparisons are shown.

Figure 5.S1. ONNV pathogenesis in C57BL/6 mice between 1 and 5 days after viral challenge.

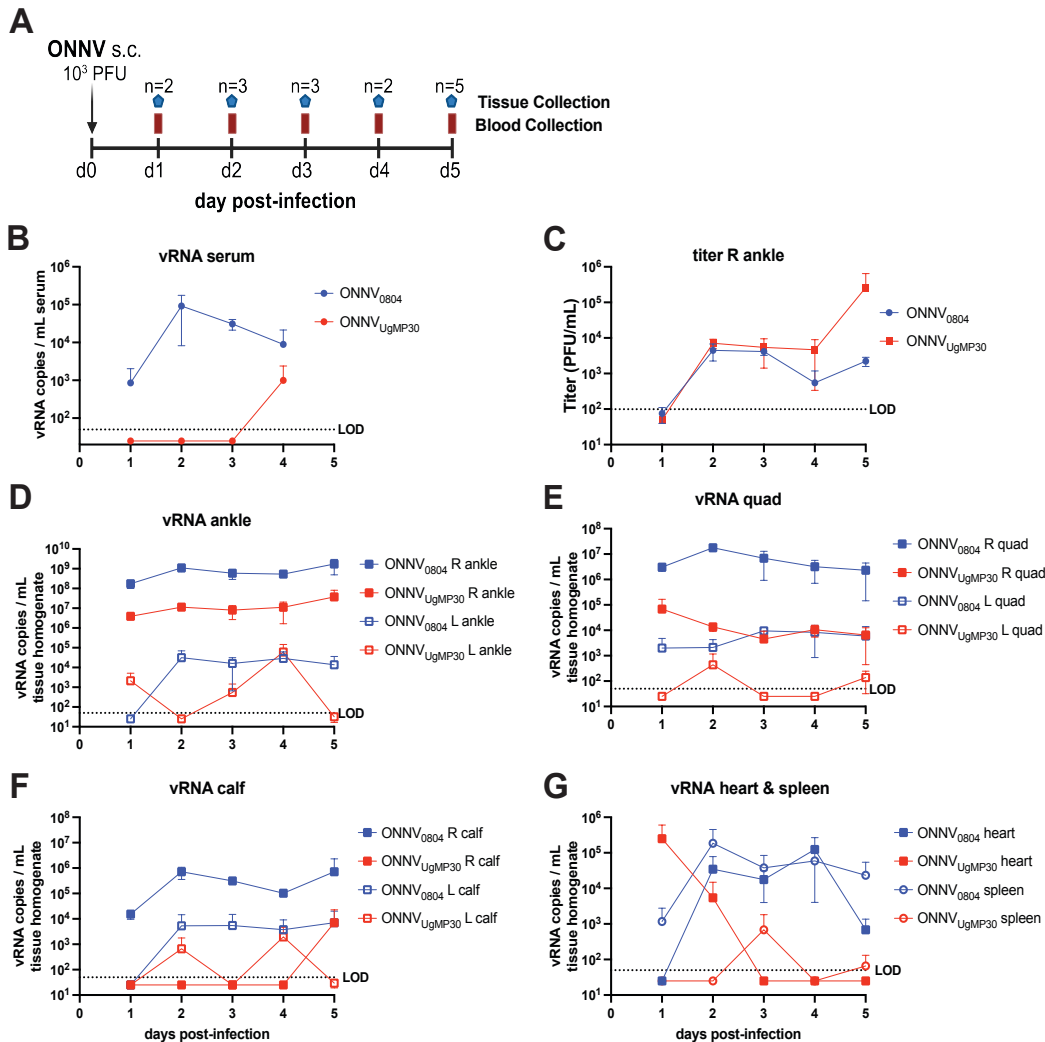


Figure 5.S1. (A) Study schematic. C57BL/6 mice were inoculated with 10^3 PFU of either ONNV strain and the indicated numbers of mice were euthanized for tissue harvest between 1 and 5 days after challenge. (B) Serum was collected and vRNA was quantified by qRT-PCR for 1-4 dpi. (C) Ankles, quadriceps, calves, heart, and spleen were collected and processed for titering by limiting dilution plaque assays and (D-G) quantifying vRNA by qRT-PCR for 1-5 dpi. Only right ankle titers are shown; no other tissues had detectable infectious virus.

5.3.3 ONNV₀₈₀₄ infection leads to persistence of viral RNA in muscle and joint tissues and potent neutralizing antibody levels and breadth

The ability of the ONNV strains to persist long term was determined at 43 dpi in mice challenged with two doses of ONNV₀₈₀₄ (10^3 or 10^5 PFU) or two doses of ONNV_{UgMP30} (10^5 or 10^7 PFU). Ankles, calf muscles, quadricep muscles, spleen, and heart tissues were collected and processed for vRNA detection by qRT-PCR (**Figure 5.3A**). The levels of persisting vRNA were readily detected (up to $\sim 100,000$ vRNA copies/mL) in the ipsilateral ankle for both ONNV strains but ONNV₀₈₀₄ was also detected in the ipsilateral and contralateral quadricep muscles as well as the spleen. Lower levels of vRNA (~ 100 - $1,000$ vRNA copies/mL) were detected in the calves and contralateral ankle for ONNV₀₈₀₄ but were below detection in ONNV_{UgMP30}-challenged mice at this time point. No vRNA was detected in the heart for any animal at 43 dpi. Overall, these results demonstrate that ONNV₀₈₀₄ persists in infected tissues much more effectively than ONNV_{UgMP30}, regardless of low or high dose challenge.

Serum 50% plaque reduction neutralization titer (PRNT₅₀) assays were performed against viruses within the Semliki Forest virus complex using sera collected at 43 dpi from mice challenged with 10^3 PFU of ONNV₀₈₀₄ or 10^7 PFU of ONNV_{UgMP30} (**Figure 5.3B**). The serum PRNT₅₀ values for mice infected with 10^3 PFU of ONNV₀₈₀₄ were significantly higher against ONNV₀₈₀₄ ($***P = 0.0005$), ONNV_{UgMP30} ($***P = 0.0009$), CHIKV_{SL15649} ($**P = 0.0027$), and UNAMAC150 ($***P = 0.0006$) compared to serum from mice challenged with a 1,000-fold higher dose (10^7 PFU) of ONNV_{UgMP30}. Despite a high degree of sequence similarity, we detected serological differences between the two strains that are likely due to the differences in the level of viral replication competence in WT mice. Although there were differences in neutralizing antibody potency and breadth, these results demonstrated the ability of ONNV infection, with either strain, to elicit cross-neutralizing antibodies against related alphaviruses. Together these findings indicate

that even in the presence of potent neutralizing antibody responses, ONNV can persist in joint and muscle tissues for long periods of time similarly to CHIKV, which has been associated with chronic arthritogenic disease [18].

Figure 5.3. ONNV RNA persistence at 43 dpi and the development of neutralizing antibodies in immunocompetent mice.

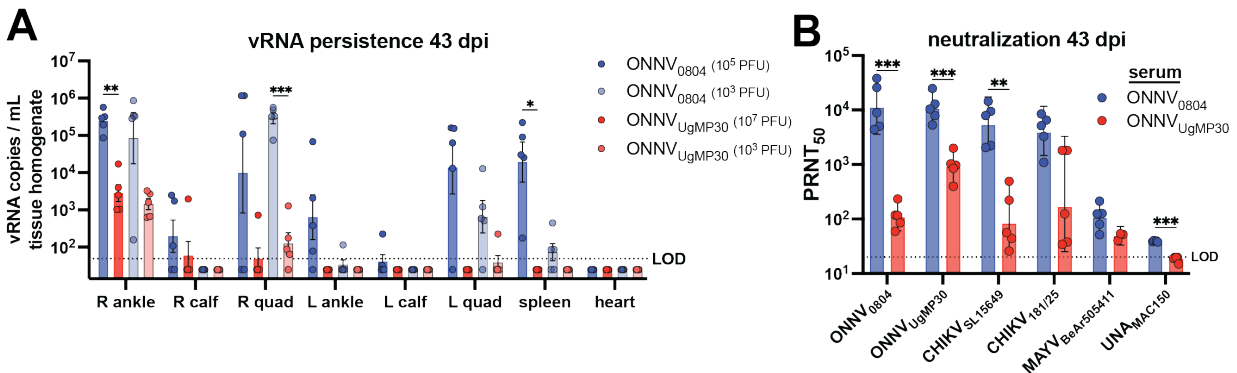


Figure 5.3. C57BL/6 mice ($n=5$ /group) were inoculated in the right footpad (s.c.) with a low (10^3) or high (10^5 or 10^7 PFU) dose of ONNV₀₈₀₄ or ONNV_{UgMP30}. The animals were humanely euthanized at 43 dpi for the detection of vRNA in tissues from mice challenged with each ONNV dose (A). Total RNA was processed from tissue lysates and vRNA data are log-transformed; the mean and standard error are plotted. Neutralizing antibodies against ONNV and related alphaviruses by 50% plaque reduction neutralization test (PRNT₅₀) in serum from mice challenged with the higher challenge doses only ($n=5$ per group except in assays intervals against MAYV ($n=3$) due to limited serum volume) (B). Geometric mean titers (GMT) are shown with error bars that represent 95% confidence intervals. The neutralization titers are analyzed by mixed-effects analysis two-way ANOVA with Šídák's multiple comparisons. The vRNA persistence data are analyzed by two-way ANOVA with Šídák's multiple comparisons. Only significant comparisons are shown in the figure (ns $P > 0.05$, * $P \leq 0.05$, ** $P \leq 0.01$, *** $P \leq 0.001$, **** $P < 0.0001$).

5.3.4 ONNV₀₈₀₄ is more pathogenic than ONNV_{UgMP30} in immunodeficient AG129 mice

To analyze differences in pathogenicity in a more stringent disease model, AG129 mice that are deficient in alpha, beta, and gamma interferon receptors were challenged with 10^5 PFU to 1 PFU of ONNV_{UgMP30} and 10^4 PFU to 0.0001 PFU of ONNV₀₈₀₄. Viremia was measured at 3 dpi, and footpad swelling and body weight were quantified daily during monitoring up to the study endpoint at 14 dpi. Mice challenged with the highest dose of ONNV_{UgMP30} (10^5 PFU) succumbed to infection between 6 and 9 dpi and the overall 50% humane endpoint (HE₅₀) dose was determined

to be 5 PFU (**Figure 5.4A**). Mice challenged with the highest dose of ONNV₀₈₀₄ (10⁴ PFU) succumbed to infection more rapidly and the HE₅₀ was calculated to be 0.006 PFU, representing a >800-fold increase in virus-associated lethality (**Figure 5.4B**). Animals challenged with ONNV_{UgMP30} lost body weight between 5 and 12 dpi depending on the challenge dose, and some animals recovered from infection despite weight loss (**Figure 5.4C**). Mice challenged with ONNV₀₈₀₄ generally reached humane endpoint before weight loss manifested (**Figure 5.4D**). The timing of peak footpad swelling in ONNV_{UgMP30}-challenged mice occurred in a dose-dependent manner, generally starting between 4 and 6 dpi (**Figure 5.4E**). Some of these animals that developed footpad swelling survived the infection. The development of footpad swelling in ONNV₀₈₀₄-challenged mice was more rapid, starting between 2 and 4 dpi, and peaked in a dose-dependent manner. Unlike ONNV_{UgMP30}, each mouse that developed footpad swelling also succumbed to infection (**Figure 5.4F**). Overall, the time to humane endpoint was significantly reduced for mice challenged with ONNV₀₈₀₄ compared to ONNV_{UgMP30} (**Figure 5.4G**). ONNV_{UgMP30} viremia was not consistently detected whereas viremias for ONNV₀₈₀₄-challenged mice were significantly higher at 10⁴ PFU ($P < 0.0001$), 10³ PFU ($P < 0.0007$), and 10² PFU ($P < 0.0001$) challenge doses. Viremia was consistently detected in all mice at 100-10,000 PFU ONNV₀₈₀₄ challenge doses. Overall, these findings affirmed that ONNV₀₈₀₄ is more virulent than ONNV_{UgMP30} *in vivo* in a susceptible mouse model of infection as evidenced by more severe disease, decreased time to humane endpoint, lower HE₅₀, and higher viremia.

Figure 5.4. ONNV₀₈₀₄ is more virulent than ONNV_{UgMP30} in AG129 immunodeficient mice.

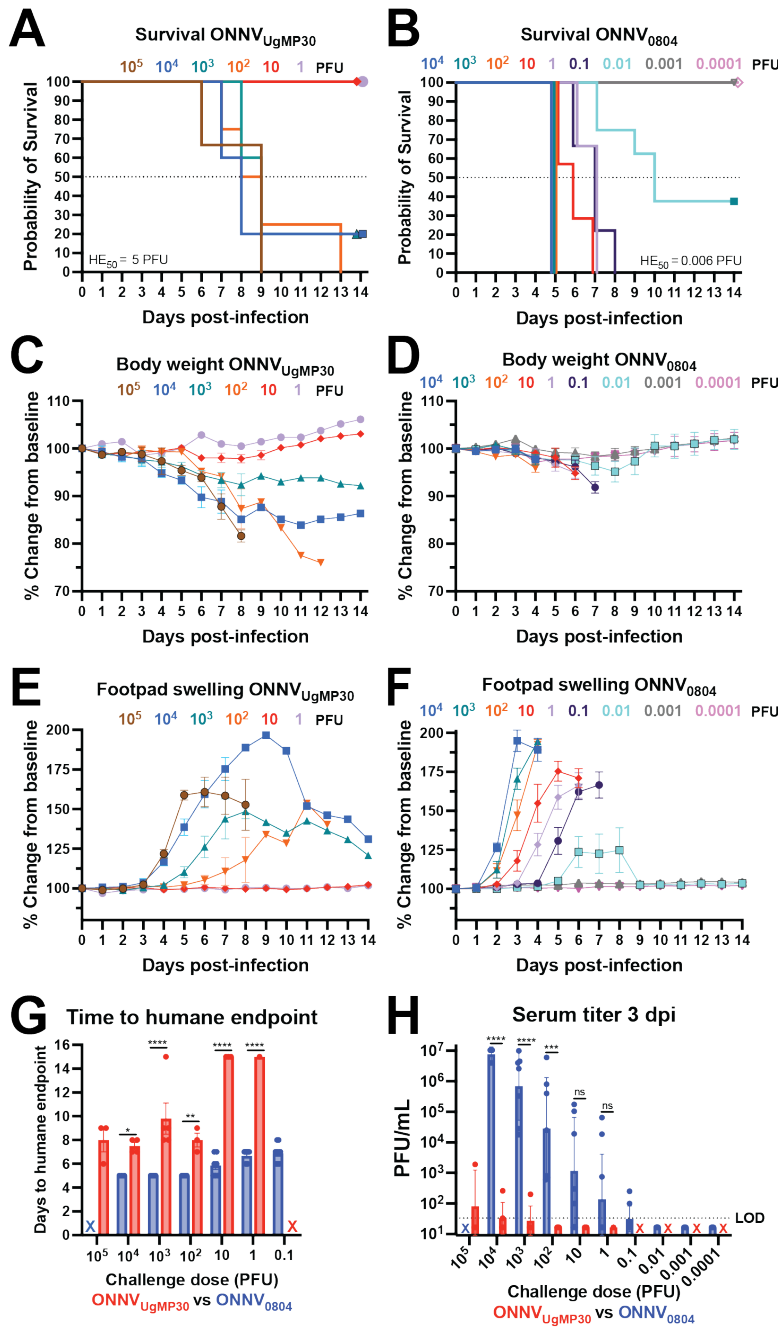


Figure 5.4. AG129 mice were infected with a range of doses of ONNV_{UgMP30} ($n = 3-5/\text{dose}$ except $n = 1$ at 1 PFU) or ONNV₀₈₀₄ ($n = 3-9/\text{dose}$) and monitored for 14 days after challenge. Kaplan-Meier survival curves for (A) ONNV_{UgMP30} and (B) ONNV₀₈₀₄ with the calculated 50% humane endpoint dose (HE₅₀). The humane endpoint was defined as loss of 25% of total body weight or observance of low body temperature or severe lethargy. Changes in body weight over 14 days for (C) ONNV_{UgMP30} and (D) ONNV₀₈₀₄. Changes in footpad swelling over 14 days for (E) ONNV_{UgMP30} and (F) ONNV₀₈₀₄. (G) Comparison of time to humane endpoint compared by two-way ANOVA with Šídák's multiple comparisons. Animals that survived infection are plotted at 15 days to humane endpoint. (H)

Serum collected at 3 dpi was titered in triplicate by plaque assays and mean values for each mouse are plotted. The LOD for this assay is 33.3 PFU/mL. Serum titers are log-transformed and analyzed by two-way ANOVA with Šidák's multiple comparisons where ns $P > 0.05$, * $P \leq 0.05$, ** $P \leq 0.01$, *** $P \leq 0.001$, and **** $P < 0.0001$.

5.3.5 HydroVax-CHIKV immunization elicits antibodies that cross-neutralize ONNV₀₈₀₄ and cross-protect against lethal arthritogenic disease in AG129 mice

Utilizing the susceptible AG129 mouse model of ONNV₀₈₀₄ infection, we evaluated cross-protection elicited by a hydrogen peroxide inactivated CHIKV vaccine (HydroVax-CHIKV) to determine whether vaccine-elicited immunity was sufficient to protect against lethal challenge with 10 PFU (1,700 HE₅₀) of the highly pathogenic contemporary ONNV₀₈₀₄ strain. Mice were immunized in the left leg with 5 µg of HydroVax-CHIKV adjuvanted with 0.1% Alum (Group 2) or mock vaccinated with 0.1% Alum alone as a vehicle control (Group 1). Another group of mice received two doses of HydroVax-CHIKV with a 28-day interval in a prime-boost regimen (Group 3). As indicated in the study schematic (**Figure 5.5A**), serum was obtained at two days prior to viral challenge for the assessment of neutralizing antibody titers. Animals were challenged in the right foot pad with ONNV₀₈₀₄, blood was drawn at 3 dpi, and footpad swelling and body weight were monitored daily for up to 14 dpi. Mice that survived through the study endpoint were humanely euthanized at 35 dpi and serum was collected to assess boosting in antibody response. Sera collected two days prior and 35 days after challenge were used in neutralization assays against CHIKV_{181/25} and ONNV₀₈₀₄ to quantify homotypic and heterotypic neutralizing antibodies. The prime/boost group displayed significantly higher CHIKV_{181/25} geometric mean titers (GMT 10,936) at -2 dpi (GMT) compared with the prime-only group (GMT 2168) ($P = 0.0014$); however, the titers of these groups equalized by 35 dpi (GMT 4916 vs 4525, respectively) demonstrating boosting of antibodies in the prime-only group after ONNV challenge (**Figure 5.5B**). Similar levels of cross-neutralization activity against the heterotypic ONNV₀₈₀₄ were observed for both vaccine groups, with no significant difference found between the two vaccine groups at either time point (**Figure 5.5C**). ONNV₀₈₀₄ neutralization titers were slightly reduced compared to CHIKV_{181/25} titers prior to challenge at -2 dpi (1.4-fold lower GMT for prime-only, 3.6-fold lower GMT for prime-boost group). Unvaccinated vehicle control mice succumbed to ONNV infection rapidly and reached a 50% survival rate by 7 dpi with all mice reaching humane endpoint by 8

days after challenge (**Figure 5.5D**). The vaccinated mice in both the prime-only and prime/boost groups were protected from lethal infection with ONNV₀₈₀₄, with only one animal succumbing to infection in the prime-only group at 11 dpi (i.e., 89% and 100% protection from lethal challenge, respectively). Footpad swelling developed rapidly in the vehicle control group with onset beginning at 3 dpi and continuing to increase in thickness until reaching a humane endpoint (**Figure 5.5E, 5.5H**). The prime-only group had a general increase in the time to peak footpad swelling post-infection relative to the vehicle control group and many of the prime-only animals demonstrated a significant reduction between 3 and 7 dpi (**Figure 5.5F, 5.5H**). Indeed, a major reduction in footpad swelling was observed in many of the mice in the prime-only group, and three of the nine mice did not develop footpad swelling, indicating that the level of immunity afforded to the HydroVax-CHIKV vaccine prime-only group may be near the protective threshold for ONNV. Prime/boost vaccination prevented footpad disease in all mice except one animal which developed footpad swelling at 13-14 dpi (**Figure 5.5G-5.5H**). The vehicle control mice challenged with ONNV₀₈₀₄ had decreasing body weights and succumbed to infection prior to reaching the humane endpoint of 25% total weight loss (**Figure 5.5I**) while both vaccination groups were protected from major changes in weight (**Figure 5.5J-5.5L**). Overall, a two-dose vaccination regimen with HydroVax-CHIKV afforded effective cross-protection against heterotypic challenge with the virulent ONNV₀₈₀₄ strain in the AG129 mouse model, resulting in protection from arthritogenic disease/footpad swelling and protection from lethal infection.

Figure 5.5. HydroVax-CHIKV immunization elicits antibodies that cross-neutralize ONNV₀₈₀₄ and cross-protect against lethal arthritogenic disease in AG129 mice.

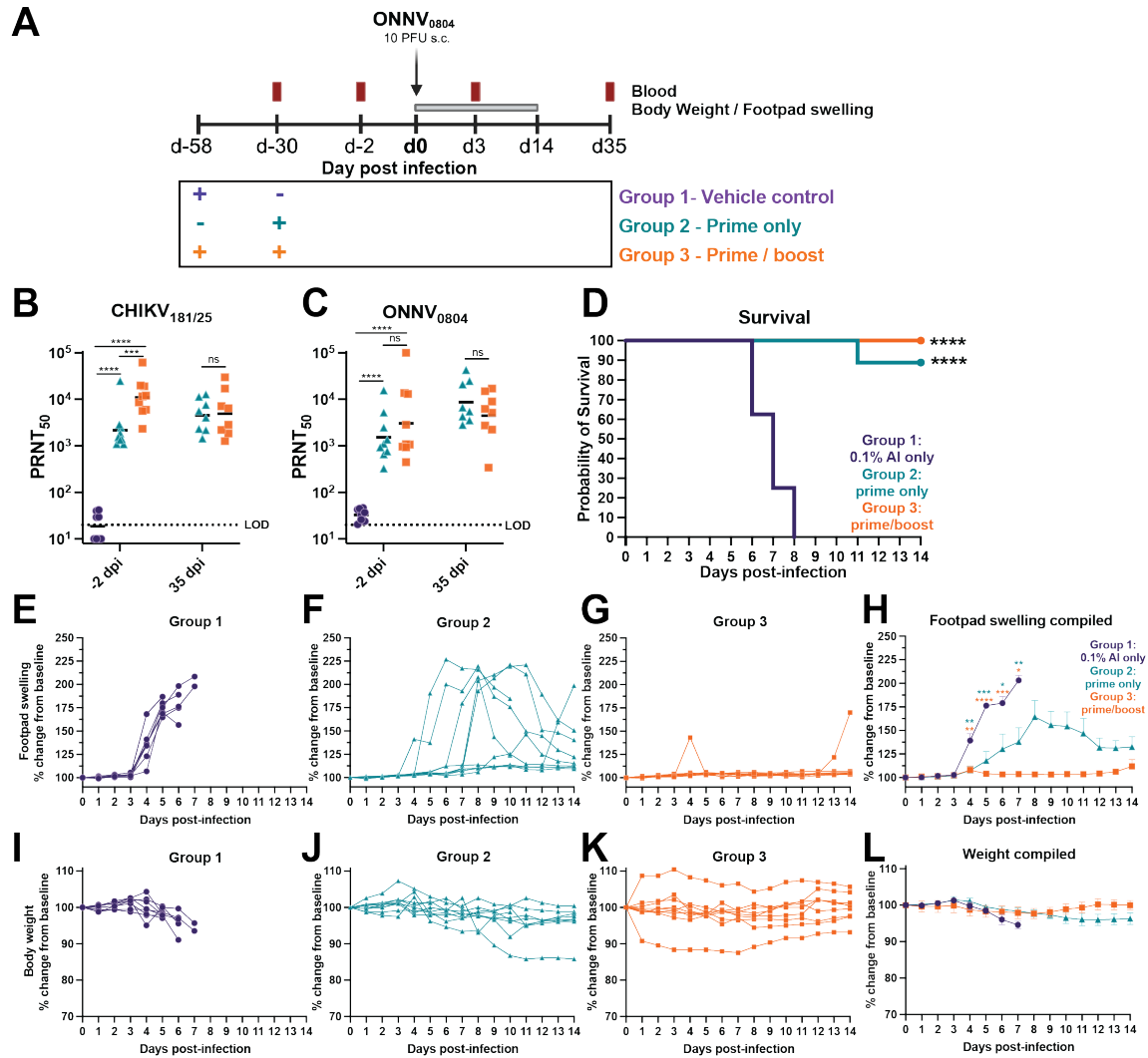


Figure 5.5. (A) Study schematic. AG129 mice aged 8-12 weeks old were immunized in the left leg with 0.1% Alum alone (Group 1, vehicle control, $n=8$) or 5 μg of HydroVax-CHIKV adjuvanted in 0.1% Alum (Group 2, Prime-only, $n=9$) at the indicated timepoints. Mice in Group 3 (Prime-boost, $n=9$) were boosted with the same dose 28 days later. Serum was isolated two days prior to viral challenge for assessment of neutralization titers. Animals (18-21 weeks old) were challenged in the right footpad with 1,700 HE₅₀ (10 PFU) of ONNV₀₈₀₄ then blood samples were drawn for quantification of viremia at 3 dpi by plaque assay. Animals were monitored daily for changes in footpad swelling and body weight with the humane endpoint defined as loss of 25% of total body weight or observance of low body temperature or severe lethargy. (B) Homotypic CHIKV_{181/25} neutralization titers and (C) heterotypic ONNV₀₈₀₄ neutralization titers by 50% plaque reduction neutralization test (PRNT₅₀). (D) Kaplan-Meier survival curve with log rank Mantel-Cox (**** $P < 0.0001$). Changes in (E-H) footpad swelling and (I-L) body weight for each group up to 14 dpi. Compiled footpad and body weight mean with SEM are plotted in (H) and (L),

respectively. Surviving animals were humanely euthanized at 35 dpi and serum was collected to determine **(B, C)** neutralizing antibody titers. Data in **(B, C)** are log-transformed and are analyzed by two-way ANOVA with Tukey's multiple comparisons where ns $P > 0.05$, $*P \leq 0.05$, $**P \leq 0.01$, $***P \leq 0.001$, and $****P < 0.0001$. Data in panels **(H)** and **(L)** were analyzed by mixed-effect analysis with Dunnett's multiple comparisons and only significant comparisons compared to group 1 controls are shown.

The HydroVax-CHIKV vaccine protected against lethal challenge with 10 PFU of the contemporary ONNV₀₈₀₄ strain. Next, the ability of this vaccination approach to protect against a high challenge dose of 1,000 PFU (170,000 HE₅₀) was tested in immunized AG129 mice. Animals received a single 5 µg dose of HydroVax-CHIKV vaccine either 30 days prior to challenge (Group 6) or 58 days prior to challenge (Group 5). Another group received a two-dose series of the same vaccine at 28 days apart (Group 7) and the animals were challenged at 30 days after their last vaccination (**Figure 5.6A**). Blood was drawn two days prior to challenge and was processed to test sera for neutralizing antibodies. Animals were challenged in the right footpad and blood was drawn at 3 dpi for quantification of viremia. Daily monitoring of footpad swelling and body weight measurements were conducted for all animals from 0 to 14 dpi. At 14 dpi, surviving animals were humanely euthanized for the quantification of vRNA in various tissues (**Figure 5.6A**). Sera collected two days prior to challenge were tested for homotypic and heterotypic neutralization of CHIKV_{181/25} and ONNV₀₈₀₄, respectively. The animals in prime/boost Group 7 developed a higher level of neutralizing antibodies against CHIKV_{181/25} with a geometric mean titer (GMT) of 4433 compared to the two prime only groups, Groups 5 and 6, with GMTs of 428 and 756, respectively (**Figure 5.6B**). The prime-only and prime/boost groups all developed similar levels of cross-neutralizing antibodies against ONNV₀₈₀₄ (GMT ~200-300) (**Figure 5.6C**). At 3 dpi, Group 5 had ~6500-fold lower levels of infectious ONNV₀₈₀₄ in the serum at a mean of 125 PFU/mL (ns, $P = 0.0895$) compared to Group 4 vehicle controls at mean viremia of 8×10^5 PFU/mL, whereas Group 6 ($**P = 0.0012$) and Group 7 ($**P = 0.0012$) were both below the limit of detection (**Figure 5.6D**). The mock-vaccinated Group 4 vehicle control animals succumbed to infection between 4 and 5 dpi, which was more rapid than the vehicle control animals that were challenged with 1700 HE₅₀ (6-8 dpi, **Figure 5.5D**). Although only 50% of Group 5 animals were protected from lethal infection ($**P = 0.0018$) (**Figure 5.6E**), all animals that received primary immunization at 28 days prior to challenge (Group 6) or the two-dose prime/boost regimen (Group 7) demonstrated 100% survival ($****P < 0.0001$) (**Figure 5.6E**). Although the vehicle control mice succumbed to

infection prior to the onset of body weight loss, all vaccinated animal groups displayed minimal weight changes with slight fluctuations occurring between 5 and 11 dpi (**Figure 5.6F-5.6J**). Footpad swelling was significantly reduced compared to controls in only the animals in prime/boost Group 7 at 2 dpi (** $P = 0.0048$), 3 dpi (** $P = 0.0097$), and 4 dpi (*** $P = 0.0004$) (**Figure 5.6K 5.6N, 5.6O**), whereas mice in prime-only (Group 6) initially developed footpad swelling similar to the controls but was later controlled by 9 dpi (**Figure 5.6M**). Remarkably, 50% of animals in Group 5 developed enhanced footpad swelling relative to control animals and did not survive infection, but 50% of the animals in the group developed disease that was later controlled by 8 dpi (**Figure 5.6K, 5.6L, 5.6O**). At 14 dpi, all surviving animals were humanely euthanized and vRNA was quantified in the spleen, quadricep muscles, calf muscles, ankles, and heart tissue (**Supplemental Figure 5.S2**). Although each of the vaccinated animals had controlled disease by 14 dpi, residual vRNA was detected in several tissues which trended higher for the Group 6 and 7 animals compared to Group 5. The caveat of this data was that a comparison could not be made to Group 4 vehicle control animals because they had all reached humane endpoint by 14 dpi. Overall, these findings indicate that the HydroVax-CHIKV prime/boost dose regimen reduced disease and confers protection in AG129 mice against a high challenge dose of ONNV₀₈₀₄.

Figure 5.6. HydroVax-CHIKV vaccination partially cross-protects against 170,000 HE₅₀ of ONNV₀₈₀₄ in AG129 mice.

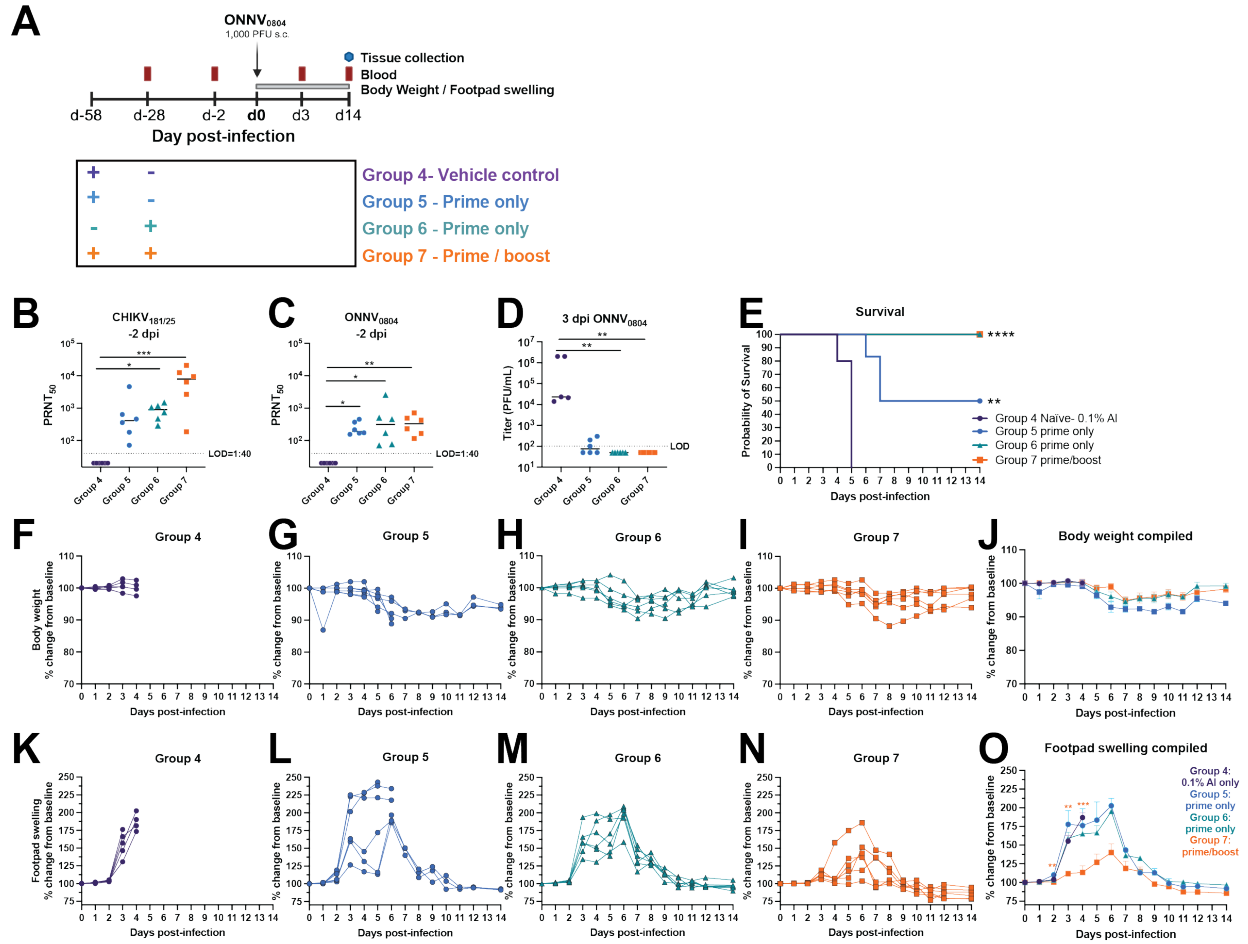


Figure 5.6. (A) Study schematic. AG129 mice aged 8-12 weeks old were immunized in the left leg with 0.1% Alum alone (Group 4, Vehicle control, $n = 5$) or $5 \mu\text{g}$ of HydroVax-CHIKV adjuvanted in 0.1% Alum (Groups 5 and 6, Prime-only, $n = 6$) at the indicated timepoints. Mice in Group 7 (Prime/boost, $n = 6$) were boosted with the same dose 30 days later. Serum was isolated two days prior to viral challenge for assessment of (B) homotypic CHIKV_{181/25} neutralization titers and (C) heterotypic ONNV₀₈₀₄ neutralization titers. Animals (18-21 weeks old) were challenged in the right footpad with 170,000 HE₅₀ (10^3 PFU) of ONNV₀₈₀₄ then blood samples were drawn for quantification of (D) viremia at 3 dpi by plaque assay. (E) Kaplan-Meier survival curve with log rank Mantel-Cox (** $P = 0.0018$, **** $P < 0.0001$). Animals were monitored daily for changes in (F-J) body weight and (K-O) footpad swelling with the humane endpoint defined as loss of 25% of total body weight or observance of low body temperature or severe lethargy. For (B-D), data are analyzed by Kruskal-Wallis test with Dunn's multiple comparisons and only significant comparisons are shown. In (J, O), data were analyzed by mixed-effect analysis with Dunnett's multiple comparisons and only significant comparisons compared to group 4 controls are shown. Only significant comparisons are shown: ns $P > 0.05$, * $P \leq 0.05$, ** $P \leq 0.01$, *** $P \leq 0.001$, and **** $P < 0.0001$.

Figure 5.S2. Viral loads in surviving animals at 14 dpi.

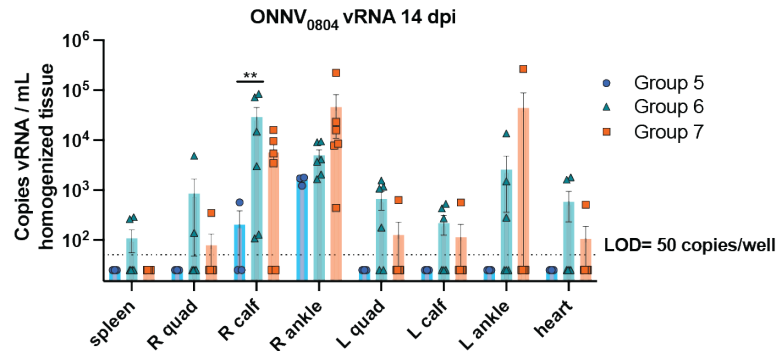


Figure 5.S2. Data relating to main Figure 5.6. At 14 dpi, surviving animals were humanely euthanized for quantification of vRNA in the spleen, ankles, quadricep muscles, calf muscles, and heart. Data are analyzed by two-way ANOVA with Tukey's multiple comparisons. Only significant comparisons are shown, ** $P=0.0088$.

Section 5.4: Discussion

ONNV is an arthritogenic alphavirus with striking similarity to CHIKV in circulation, genetics, pathogenesis, and clinical presentation. Pathogenesis of ONNV has been briefly explored *in vitro* [81] and *in vivo* in C57BL/6 [94, 250] and AG129 [106, 249] mouse models. Differential disease outcomes have generally not been observed in humans for different infecting ONNV strains but they have in mice [249]; although establishing a relevant infection model that has translation for human infection has been a challenge due to the minimal number of available virus stains. The UgMP30 strain has been passaged extensively in both mouse brains and Vero cells, potentially leading to reduced pathogenicity in mice. Studies have shown the SG650 [106, 249] and IMTSSA/5163 [86, 250] strains, both isolated from febrile patients, to be pathogenic in AG129 and C57BL/6 mice. However, these studies required very high challenge doses to achieve disease in their respective models. Here, we constructed an infectious clone using the sequence of the UVRI0804 strain isolated from a febrile patient in Uganda in 2017 and compared *in vitro* replication and *in vivo* pathogenesis to the highly passaged UgMP30 strain in both C57BL/6 and AG129 mice. The two strains replicated with comparable kinetics in fibroblasts, Vero cells, and mosquito cells, but ONNV_{UgMP30} generally replicated to higher titers. In immunocompetent mice, ONNV_{UgMP30} infection failed to induce appreciable disease, whereas ONNV₀₈₀₄ caused significant footpad swelling and moderate to severe arthritis, myositis, and tendonitis. ONNV₀₈₀₄ infection

led to greater viral distribution at 5 dpi and substantial levels of viral persistence at 43 dpi in several tissues including the ankle joints, quadricep muscles, and spleen. The viral persistence is consistent with what has been shown for CHIKV [43, 367] and has been linked to chronic arthralgia. This finding of persistence is also consistent with a study in C57BL/6 mice, which detected luciferase tagged-ONNV-IMTSSA/5163 at 40 dpi in the infected right ankle, the site of challenge [250]. Notably, this other study required a challenge dose of 10^6 PFU to achieve infection, disease, and viral persistence in their C57BL/6 model of ONNV infection whereas we observed these characteristics at a challenge dose of only 10^3 PFU. Altogether, ONNV_{UgMP30} pathogenesis was reduced compared to ONNV₀₈₀₄ in C57BL/6 mice, which is consistent with previous reports of an attenuated *in vivo* phenotype [249]. This study establishes the ONNV₀₈₀₄ strain as a reproducibly virulent model of ONNV infection in both AG129 and C57BL/6 mice that can be used to evaluate vaccines and therapeutics.

A reproducible trend in pathogenicity was observed in immunodeficient AG129 mice; compared to ONNV_{UgMP30}, the HE₅₀ for ONNV₀₈₀₄ was >800-fold higher and the time to death, or reaching humane endpoint, was significantly reduced. In addition, the development of disease was more rapid at lower doses for ONNV₀₈₀₄. One potential explanation for the differences in pathogenesis noted between these strains could be that the ONNV₀₈₀₄ strain contains the opal stop codon between nsP3 and nsP4 whereas ONNV_{UgMP30} does not, which has been previously linked to transmissibility and infectivity fitness advantages in mosquitos [380]. Interestingly, the SG650 strain of ONNV is the only other ONNV strain containing the opal stop codon and happens to be the strain with the most comparable pathogenicity in mice to the ONNV₀₈₀₄ strain. Overall, ONNV₀₈₀₄ caused similar pathogenesis in mice to what has been reported for the SG650 and IMTSSA/5163 strains but achieved this phenotype with a lower, more physiologically realistic challenge dose [249, 250]. These findings indicate that ONNV₀₈₀₄ is a more physiologically relevant isolate of ONNV in these infection models, making this virus best suited for challenge studies conducted for preventative or therapeutic evaluation.

We demonstrated in both our present and previous studies [102] that the HydroVax-CHIKV vaccine elicits antibodies that cross-neutralize ONNV. We and others have shown that CHIKV infection or vaccination elicits ONNV-neutralizing antibodies [59, 69, 75, 86, 102, 274, 378], but some studies have concluded that this is a one-way antigenic relationship [381, 382]. Our

work in the present study comparing serological differences in alphavirus neutralization after ONNV infection with either strain (**Figure 5.3B**) did not reveal a one-way antigenic relationship, however, significant differences in cross-neutralization of CHIKV and other alphaviruses were identified depending on the infecting ONNV strain. For example, ONNV₀₈₀₄ infection elicited antibodies that more potently cross-neutralized strains of CHIKV compared to ONNV_{UgMP30} infection, demonstrating antigenic differences between ONNV strains. These results are surprising given the genetic similarity of ONNV strains. The differences in the antigenic profile due to infection strain may have implications for individuals susceptible to CHIKV, ONNV, and other alphaviruses, such as the degree of potential cross-protective immunity afforded by infection. Additional studies are warranted to identify differential neutralization epitopes contributing to the antigenic profile of these strains.

With CHIKV and ONNV circulation overlapping throughout Africa [10, 13], in this study, we evaluated the cross-protective efficacy of a HydroVax-CHIKV [102] vaccine against ONNV₀₈₀₄ challenge in mice. We found that the HydroVax-CHIKV vaccine elicited ONNV-neutralizing antibodies in AG129 mice that were protective against the development of disease and increased survival following challenge with 10 or 1000 PFU. We demonstrated that a single dose of HydroVax-CHIKV provided 90% survival against ONNV challenge with 10 PFU but footpad swelling occurred in 67% of prime-only mice. Our second experiment, using a higher challenge dose, further validated this finding and revealed an impact of the prime vaccine timing on protection. In animals immunized with a single vaccine dose 58 days prior to challenge, cross-protection waned to 50% survival whereas 100% survival was observed in animals primed 28 days prior to challenge. In contrast, 100% of mice in the prime-boost group survived ONNV₀₈₀₄ challenge at both challenge doses and demonstrated significant reduction in footpad swelling, underscoring that a two-dose vaccine schedule with HydroVax-CHIKV provides effective protection against ONNV challenge. Overall, these results demonstrate the impact that cross-neutralizing antibody potency can have on cross-protection from disease, which should be carefully strategized in the design of cross-protective alphavirus vaccines.

Two studies have tested the cross-protective potential of a CHIKV-specific vaccine against ONNV. The first was reported by Partidos *et al.*, which demonstrated that one dose of an attenuated recombinant CHIKV vaccine reduced footpad swelling and weight loss and led to 100% survival

of AG129 mice after 10^4 or 10^5 PFU ONNV_{SG650} challenge [106]. In a second study, Nguyen *et al.* showed single dose protection of a CHIKV vaccine against 10^4 CCID₅₀ of ONNV-IMTSSA/5164 viremia between 1 and 6 dpi in C57BL/6, but data exploring protection from disease was not shown because ONNV-induced disease was reportedly not observed in their model, further underscoring the relevance of pathogenic ONNV strains [86]. Notably, in all comparable studies, development of a robust disease model was difficult and required use of high challenge dose. Our studies build upon these findings by establishing CHIKV vaccine-mediated cross-protection against a contemporary, highly virulent strain of ONNV and provide new insights into the pathogenesis of this virus in two mouse models. Following recent U.S. Food and Drug Administration [261], Health Canada, and European Medicines Agency [262] approval of the first CHIKV vaccine [383], there are several questions regarding how CHIKV vaccine rollout will shape CHIKV and related alphaviruses transmission and distribution. Future studies should explore HydroVax-CHIKV-mediated ONNV cross-protection from viral pathogenesis and viral persistence in additional mouse models and non-human primates to better understand the mechanisms mediating protection.

Section 5.5: Materials & Methods

5.5.1 Ethics Statement

Experiments that involved mice were performed in an Oregon Health and Science University (OHSU) ABSL-3 facility at the Vaccine and Gene Therapy Institute (VGTI). OHSU receives accreditation from the Association for Accreditation and Assessment of Laboratory Animal Care (AALAC) International. The experiments were performed in compliance with OHSU Institutional Biological Safety and the animal protocols were approved by the OHSU Institutional Animal Care and Use Committee (IACUC Protocols #0913 and 1181-02). Mice were housed in ventilated racks with access to food and water with a 12-hour light/dark cycle.

5.5.2 Cells

Normal human dermal fibroblasts (NHDF; ATCC PCS-201-012) and mouse embryonic fibroblasts (MEF; ATCC BL/6-1) were cultured at 37°C and 5% CO₂ in Dulbecco's modified Eagle medium

(DMEM; Corning), supplemented with 10% fetal bovine serum (FBS; HyClone) and 1% penicillin-streptomycin-glutamine (PSG; Life Technologies) (DMEM-10). Vero cells (ATCC CCL-81) were cultured at 37°C and 5% CO₂ in DMEM with 5% FBS and 1% PSG (DMEM-5). *Aedes albopictus* C6/36 cells (ATCC CRL-1660) were cultured at 28°C with 5% CO₂ in DMEM-10.

5.5.3 Viruses and the HydroVax-CHIKV Vaccine

O'nyong'nyong virus (ONNV_{UgMP30}; BEI NR-51661), Mayaro virus (MAYV_{BeAr505411}; BEI NR-49910), and Una virus (UNAV_{MAC150}; BEI NR-49912) were obtained from the Biodefense and Emerging Infectious Disease Research Resources Repository (BEI Resources). Chikungunya virus (CHIKV_{181/25}) and CHIKV_{SL15649} were generated from infectious clones as previously described [245, 384]. The O'nyong'nyong virus (ONNV₀₈₀₄) infectious clone was engineered as described below. Viral stocks were propagated in *Aedes albopictus* C6/36 cells. At 72 hours post-infection (hpi), supernatants were collected, clarified by centrifugation (Beckman CS-6, 900 x g, 15 minutes), and pelleted through a 10% sorbitol cushion by ultracentrifugation (82,755 x g for 70 minutes). Viral pellets were resuspended in phosphate buffered saline (PBS), frozen at -80°C, and titered on Vero cells using limiting dilution plaque assays in 48-well plates. Infected cells were incubated for 2 hours under continuous rocking at 37°C with 5% CO₂, then overlaid with a 2:1 mixture of DMEM-5 containing 0.3% high/low viscosity carboxymethyl cellulose (CMC-DMEM) (Sigma). Cells were fixed with 3.7% formaldehyde and stained with 0.2% methylene blue at 48 hpi for MAYV_{BeAr505411}, UNAV_{MAC150}, and CHIKV_{SL15649}, or at 72 hpi for ONNV_{UgMP30}, ONNV₀₈₀₄, and CHIKV_{181/25}. Plaques were visualized under a dissecting microscope, and counts were used to calculate viral titers in plaque-forming units (PFU) per mL. Virus stocks for all experiments were passaged 1 or 2 times and were sequence-validated as described below.

The HydroVax-CHIKV vaccine was produced as previously described [102]. Briefly, CHIKV_{181/25} was propagated on serum-free Vero cells, and harvests were clarified and treated with Benzonase to minimize host-cell DNA/RNA contamination prior to concentration and buffer exchange using tangential flow filtration (TFF) followed by CaptoCore 700 chromatography (Cytiva). HydroVax-based inactivation conditions were optimized for CHIKV_{181/25} and included 0.0003% H₂O₂, 2 µM CuCl₂, 20 µM methisazone, and 0.06% formaldehyde in a buffer matrix with 150 mM Na₂HPO₄

at pH 7.5, for 48 hours at room temperature. After inactivation, chemical components were removed using TFF. Complete inactivation was confirmed through cell culture-based residual live virus testing. HydroVax-CHIKV (5 µg/dose) was adjuvanted with 0.1% aluminum hydroxide (Alhydrogel, InvivoGen).

5.5.4 Cloning Strategy

To assemble the infectious clone of the O'nyong'nyong virus strain ONNV₀₈₀₄, seven genome fragments, each approximately 1700 base pairs (bp) with 20 bp of overlapping sequence, were synthesized by Twist Bioscience based on the sequence (accession number ON595759). The plasmid pSinRep5 (Invitrogen) was used as a template to generate a 2200 bp fragment using standard PCR conditions. We combined 200 femtomoles of each fragment with an equal volume of NEBuilder HiFi master mix (NEB) according to the manufacturer's instructions. Assembly was performed at 50°C for 60 minutes. TOP10 competent cells (Invitrogen) were then transformed with 5µL of the assembled product. After DNA purification, the infectious clone (ONNV₀₈₀₄ ic) was verified by whole plasmid sequencing (Eurofins). The ONNV₀₈₀₄ ic was linearized with *NotI* digestion and transcribed *in vitro* using the SP6 mMessage mMachine kit (Invitrogen) followed by purification with the RNeasy Mini Kit (Qiagen). Vero cells were transfected with 10µg of RNA and 6µL of Lipofectamine 2000 per well of a 6-well plate, following the Invitrogen protocol. After 3 days, supernatant was collected and stored at -80°C. Virus stocks were prepared using 100µL of the resulting p0 stock for each T-175 flask of C6/36 cells. Viral RNAs were confirmed by Next Generation Sequencing (NGS).

5.5.5 Growth Curves

C6/36, MEF, Vero, and NHDF cells were seeded into 48-well plates at 2×10^5 cells/well and incubated overnight at 37°C with 5% CO₂. Cells were infected with either ONNV_{UgMP30} or ONNV₀₈₀₄ at an MOI of 0.5. Infection occurred in 100µL of DMEM-5 with continuous rocking for 2 hours at 37°C with 5% CO₂. The infection media was then removed, and cells were washed twice with 500µL of PBS and resuspended in 250µL of DMEM-5. The supernatant was sampled for timepoints taken at 6, 12, 24, and 48 hours for PFU/mL quantification by plaque assays on Vero cells.

5.5.6 Mouse Experiments

C57BL/6 purchased from Jackson Laboratories and AG129 mice bred at OHSU were housed in ventilated racks with free access to food and water in a room with a 12 hour light/dark cycle. For viral challenge studies, mice were inoculated in the right posterior footpad with a 20 μ L subcutaneous (s.c.) injection of ONNV_{UgMP30} or ONNV₀₈₀₄ diluted in PBS. For AG129 mice, 50% humane endpoint dose (HE₅₀) was calculated used the methods of Reed and Muench [385]. Vaccination experiments were performed with challenge doses of 10 or 1000 PFU and all other challenge experiments were performed with various challenge doses as indicated. Animals at 8-12 weeks of age were vaccinated by intramuscular (i.m.) injection with 5 μ g of HydroVax-CHIKV or 0.1% Al adjuvant in TFF buffer alone in the left leg. Serum was isolated from the saphenous vein at the indicated timepoints for measurement of neutralizing antibodies or viremia. Serum was collected from clotted blood samples after centrifugation for 5 minutes at 9000 x g. Animals were challenged at 18-21 weeks of age and footpad swelling was measured with digital calipers and changes in body weight were recorded daily for up to 14 dpi. Humane endpoint was defined as 25% body weight loss but animals were also euthanized if they appeared severely lethargic. As indicated, ankles, quadricep muscles, calf muscles, heart, spleen, and brain were collected to assess viral dissemination.

5.5.7 Histopathological Analysis

At 7 dpi, PBS-control, ONNV_{UgMP30}, and ONNV_{UVRI0804} infected mice were sacrificed and perfused with 4% paraformaldehyde in PBS. Lower hind legs were collected, fixed in 4% paraformaldehyde, decalcified, embedded in paraffin, and sectioned into 5 micron thick slices. Sections of ipsilateral and contralateral legs were stained with H&E and evaluated for inflammation and tissue disease by light microscopy (Olympus VS120 Virtual Slide Microscope). Pathology specialists blindly scored the histological lesions, including necrosis, inflammation, fibrosis, edema, and vasculitis, using a 0-10 scoring system: 0 (no lesions), 1-2 (minimal, 1-10% affected), 3-4 (mild, 11-25% affected), 5-6 (moderate, 26-50% affected), 7-8 (marked, 51-75% affected), 9-10 (severe, >75% affected).

5.5.8 Viral RNA Detection

RNA was isolated from 300 μ L of each mouse tissue homogenate collected in 1mL of PBS. Total nucleic acids were extracted using the Promega Maxwell 48 sample RSC automated purification system and the Maxwell RSC Viral TNA extraction kit. RNA was resuspended in 70 μ L of RNase-free water and diluted to 100 ng/ μ L. Contaminating DNA was removed using ezDNase. Single-stranded cDNA was synthesized from 1 μ g of total RNA using random hexamers and reverse transcriptase (Invitrogen Superscript IV) following the manufacturer's protocol. Quantitative RT-PCR was performed on a QuantStudio 7 Flex system using the following primers and probe for ONNV RNA: Forward-CCCACAGCATGGCAAAGAAC, Reverse-CTGGCGGCATATGCACTTCT, and probe FAM-ACGTACGTCCATACCACAG-MGB. All reactions were performed in triplicate, and data were analyzed using Applied Biosystems software. Viral RNA levels were normalized to the murine housekeeping gene ribosomal protein RPS17 and reported per 1 mL of tissue homogenate.

5.5.9 Quantification and Isolation of Infectious Virus

Plaque assays were used to quantify infectious virus in mouse serum, tissue homogenate, or in growth curve cell supernatants. Briefly, 20 μ L of sample was added to 180 μ L DMEM-5 for 1:10 serial dilutions. Viral dilutions were added to confluent monolayers of Vero cells in 48-well plates and incubated for 2 hours at 37°C with 5% CO₂ with continuous rocking, followed by addition of CMC-DMEM-5 overlay. Plaque assays were fixed and stained as described above.

5.5.10 Neutralization Assays

Mouse serum was heat-inactivated for 30 minutes at 56°C and serially diluted 2-fold in DMEM-5. Diluted serum was mixed with media containing approximately 70-120 PFU of ONNV₀₈₀₄, ONNV_{UgMP30}, CHIKV_{SL15649}, CHIKV_{181/25}, MAYV_{BeAr505411}, or UNAV_{MAC150}. Mixtures were incubated for 2 hours at 37°C with 5% CO₂ with continuous rocking, then transferred to 12-well plates of confluent Vero cells. Cells were incubated for an additional 2 hours at 37°C with 5% CO₂ with continuous rocking, followed by addition of CMC-DMEM-5 overlay. Plates were incubated for 48 hours for CHIKV_{SL15649}, MAYV_{BeAr505411} and UNAV_{MAC150}, or 72 hours for ONNV_{UVRI0804}, ONNV_{UgMP30}, and CHIKV_{181/25}. Cells were fixed and stained as described for plaque assays.

Plaques were enumerated under a dissecting microscope or by eye depending on size and percent neutralization was determined at each dilution relative to control wells without serum.

5.5.11 Statistical Analysis

Data were analyzed using GraphPad Prism 10.2.3 software. Mixed-effects analyses were used to address instances of missing values. The 50% plaque reduction neutralization titers (PRNT₅₀) were calculated by variable slope, non-linear regression analysis. Kaplan-Meier survival curves were analyzed by log rank Mantel-Cox. Footpad swelling and body weight changes, vRNA levels, and neutralization titers at multiple timepoints were analyzed by two-way ANOVA with Šídák's or Tukey's multiple comparisons. The neutralization and serum infectious titer data presented for single timepoints in **Figure 5.6** are analyzed by Kruskal-Wallis test with Dunn's multiple comparisons.

Section 5.6: Acknowledgements

The following reagents were obtained through BEI Resources, NIAID, NIH, as part of the WRCEVA program: MAYV_{BeAr505411} (NR-49910), UNAV_{MAC150} (NR-49912), and ONNV_{UgMP30} (NR-51661). The funding sources of the study included NIH grant P51OD011092 (ONPRC operational grant), R44 AI128990, and Defense Threat Reduction Agency W15QKN-16-9-1002.

Chapter 6: Mayaro virus pathogenesis and immunity in rhesus macaques

Status: Published November 20th, 2023, in PLoS Neglected Tropical Diseases.

Whitney C. Weber^{1,2}, Caralyn S. Labriola^{1,3}, Craig N. Kreklywich¹, Karina Ray⁴, Nicole N. Haese¹, Takeshi F. Andoh¹, Michael Denton¹, Samuel Medica^{1,2}, Magdalene M. Streblow¹, Patricia P. Smith¹, Nobuyo Mizuno¹, Nina Frias¹, Miranda B. Fisher³, Aaron M. Barber-Axthelm³, Kimberly Chun³, Samantha Uttke³, Danika Whitcomb³, Victor DeFilippis¹, Shauna Rakshe⁴, Suzanne S. Fei⁴, Michael K. Axthelm^{1,3}, Jeremy V. Smedley^{1,3}, and Daniel N. Streblow^{1,3*}

¹ Vaccine and Gene Therapy Institute, Oregon Health and Science University, Beaverton, Oregon, USA

² Department of Molecular Microbiology and Immunology, Oregon Health and Science University, Portland, Oregon, United States of America

³ Division of Pathobiology and Immunology, Oregon National Primate Research Center, Beaverton, Oregon, United States of America

⁴ Bioinformatics & Biostatistics Core, Oregon National Primate Research Center, Oregon Health & Science University, Portland, Oregon, United States of America

*Correspondence: streblow@ohsu.edu

PLoS Neglected Tropical Diseases 17(11): e0011742. November 20th, 2023.

DOI: [10.1371/journal.pntd.0011742](https://doi.org/10.1371/journal.pntd.0011742)

Author contributions

Conceptualization: W.C.W, C.S.L, N.N.H, M.K.A, J.V.S, D.N.S; Data curation: W.C.W, C.S.L, K.R, S.M, S.R; Formal analysis: W.C.W, C.S.L, C.N.K, S.M, S.R, D.N.S; Investigation: W.C.W, C.S.L, C.N.K, K.R, N.N.H, T.F.A, M.D, S.M, M.M.S, P.P.S, N.M, N.F, M.B.F, A.M.B, K.C, S.U, D.W, M.K.A, J.V.S, D.N.S; Methodology: W.C.W, C.S.L, C.N.K, K.R, N.N.H, T.F.A, M.B.F, D.N.S; Validation: W.C.W; Writing – original draft: W.C.W, C.S.L, C.N.K, D.N.S; Writing – review & editing: W.C.W, K.R, M.D, S.R, S.S.F, D.N.S; Resources: V.D; Funding acquisition: D.N.S; Project administration: D.N.S; Supervision: D.N.S.

Section 6.1.1: Abstract

Mayaro virus (MAYV) is a mosquito-transmitted alphavirus that causes debilitating and persistent arthritogenic disease. While MAYV was previously reported to infect non-human primates (NHP), characterization of MAYV pathogenesis is currently lacking. Therefore, in this study we characterized MAYV infection and immunity in rhesus macaques. To inform the selection of a viral strain for NHP experiments, we evaluated five MAYV strains in C57BL/6 mice and showed that MAYV strain BeAr505411 induced robust tissue dissemination and disease. Three male rhesus macaques were subcutaneously challenged with 10^5 plaque-forming units of this strain into the arms. Peak plasma viremia occurred at 2 days post-infection (dpi). NHPs were taken to necropsy at 10 dpi to assess viral dissemination, which included the muscles and joints, lymphoid tissues, major organs, male reproductive tissues, as well as peripheral and central nervous system tissues. Histological examination demonstrated that MAYV infection was associated with appendicular joint and muscle inflammation as well as presence of perivascular inflammation in a wide variety of tissues. One animal developed a maculopapular rash and two NHP had viral RNA detected in upper torso skin samples, which was associated with the presence of perivascular and perifollicular lymphocytic aggregation. Analysis of longitudinal peripheral blood samples indicated a robust innate and adaptive immune activation, including the presence of anti-MAYV neutralizing antibodies with activity against related Una virus and chikungunya virus. Inflammatory cytokines and monocyte activation also peaked coincident with viremia, which was well supported by our transcriptomic analysis highlighting enrichment of interferon signaling and other antiviral processes at 2 days post MAYV infection. The rhesus macaque model of MAYV infection recapitulates many of the aspects of human infection and is poised to facilitate the evaluation of novel therapies and vaccines targeting this re-emerging virus.

Section 6.1.2: Author summary

Mayaro virus (MAYV) is an arbovirus capable of causing debilitating arthritis and myalgia in humans and the virus is currently circulating in Central and South America. With several factors supporting viral emergence, MAYV is a public health risk due to the lack of FDA-approved countermeasures. Although non-human primate (NHP) infection models are well established for chikungunya virus (CHIKV) and the equine encephalitic alphaviruses, there is currently no well-characterized NHP model of MAYV pathogenesis. With evidence of well-established mouse

models of MAYV infection and a report from 1967 demonstrating that MAYV infection of NHPs in a laboratory setting was feasible, we aimed to further characterize MAYV infection in three rhesus macaques. Following precursor studies in mice to identify an optimal viral strain for NHP infection, we subcutaneously challenged rhesus macaques and characterized viral pathogenesis and immunity over the course of 10 days. Our study establishes a framework for future evaluation of MAYV-specific treatments in this relevant animal model.

Section 6.2: Introduction

Mayaro virus (MAYV) is a re-emerging arthritogenic alphavirus responsible for numerous outbreaks that are increasing in frequency in the tropical regions of Latin America and the Caribbean. In 1954, MAYV was isolated from forest workers in Mayaro County, Trinidad and Tobago, but the virus is now endemic to 14 countries of Central and South America [183, 184, 386]. Travel-associated infections have occurred in these endemic regions and reported for people returning to the United States and Europe [65]. MAYV is related to and co-circulates with chikungunya virus (CHIKV), which is the most prevalent alphavirus contributing to several large outbreaks over the last several decades in over 110 countries [21]. In 2022, there were 383,357 reported cases and 76 deaths caused by CHIKV with Brazil bearing the brunt of the public health burden (265,289 cases and 75 deaths) [25]. Brazil is also home to the largest number of MAYV outbreaks and is continually faced with the threat of other arboviral infectious outbreaks including dengue fever and Zika [387]. MAYV is primarily transmitted by *Haemagogus* sp. mosquitoes dwelling in tropical forests, but experimental studies have shown other species to be capable of transmission [209, 388-392]. Transmission is maintained in sylvatic transmission cycles by non-human primate (NHP) primary hosts and by rodent or other secondary hosts [207]. Although evidence of urban transmission of MAYV has not been identified, in research settings, MAYV has been shown to be transmitted by urban-dwelling mosquito vectors [393] including *Aedes albopictus* and *Aedes aegypti*, causing concern for outbreaks outside of endemic regions [394-397]. While humans are only sporadically infected, some hypothesize that MAYV is poised to emerge more often due to tropical forest workers or travelers encountering more rural destinations [189, 398-400]. Currently, there are no approved vaccines or therapeutics for the treatment or

prevention of MAYV infections, presenting a major concern as MAYV continues to emerge in sporadic epidemics.

MAYV is an 11kb single-stranded, positive sense RNA member of the Semliki Forest antigenic complex that includes Una (UNAV), chikungunya (CHIKV), O'nyong'nyong (ONNV), Bebaru (BEBV), Getah (GETV), Semliki Forest (SFV), and Ross River (RRV) viruses [2]. Given the high degree of genetic and antigenic similarity within this serological complex, cross-reactive immune responses have been described for humans and in animal models [59, 86, 91, 106, 324, 325]. There may be a high level of cross-reactive herd immunity afforded by CHIKV-MAYV co-circulation, and cross-neutralization of MAYV by anti-CHIKV patient sera has been described by our group and others [85, 93, 401, 402]. Phylogenetically, there are three distinct genotypic strains of MAYV (D, L, and N) with only 17% nucleotide divergence between them [390]. Genotype D viruses are distributed in Venezuela, Peru, and Bolivia, the L genotype is primarily confined to Brazil and Haiti, and Genotype N only contains isolates from Peru [194]. Due to co-circulation with other arboviruses, clinical disease similarity, and alphavirus cross-reactivity, these infections can also be difficult to diagnose as differentiating diagnostics are limited. There are incidences of arboviral co-infections, including reports of MAYV and CHIKV co-infection [403] and *ex vivo* superinfection with MAYV and Zika (ZIKV) [397]. Co-infections with non-arboviruses like HIV have also been reported, but little research has been done to investigate the interplay of these co-infections or consequence of pre-existing immunodeficiency [404]. Altogether, these confounding factors may lead to an underestimation of MAYV human disease burden.

MAYV causes Mayaro fever in humans which was first described in 1957, detailing case reports of febrile forest workers infected in 1954 and their MAYV-seroconversion [183, 184]. Although disease is rarely fatal, it is estimated that 90% of MAYV infections are symptomatic and the incubation period is approximately 8 days [387]. Disease initially presents with a high fever that is concurrent with peak viremia at 1-2 days post-infection (dpi), and viremia has been reported to last at least 4 days [405]. Other disease symptoms include rash (inclusive of exanthema), headache, dizziness, retro-ocular pain, diarrhea, vomiting, inguinal lymphadenopathy, myalgia, and arthralgia [189]. These symptoms can last 5-7 days but myalgia and arthralgia can persist in >50% of patients for months to years following infection [405]. Acute phase infections can also present with mild leukopenia and thrombocytopenia [387]. Neurological complications associated

with more severe cases and myocarditis has been reported following CHIKV infection, thus cardiac involvement has been hypothesized for other arthritogenic alphavirus infections including MAYV [406-412].

MAYV infection in mice has been used to characterize viral pathogenesis and also to evaluate MAYV-specific countermeasures. Mouse models of MAYV infection have been reported for C57BL/6, Balb/c, CD-1, AG129, Rag1^{-/-}, and IFN α R^{-/-} mice utilizing different strains of the virus including: MAYV_{BeAr505411} [91], MAYV_{BeH407} [86, 251], MAYV_{TRVL} [248, 413, 414], MAYV_{IQT4235} [415] and MAYV_{CH} [77, 287]. Una virus (UNAV) is closely related to MAYV and has been used in a limited number of mouse infection studies [91]. To our knowledge, a comparison of MAYV strain pathogenicity in mice has not been published, however, the impact of genetic diversity on viral fitness was recently explored for three strains *in vitro* [416]. Vaccination strategies targeting MAYV have been reported for live-attenuated virus platforms [287, 288], virus-like particles [289], adenovirus vectors [91, 417], inactivated virus preparations [286], and DNA transfections [290]. Vaccines targeting CHIKV with cross-reactivity or cross-protective efficacy against MAYV have also been described [93, 102]. Monoclonal antibody treatments [77, 78, 418] and antiviral drugs [419-424] directed against MAYV are also in development. Despite promising MAYV treatments reported in the literature, evaluation of their efficacy in NHP infection models has been hindered by the absence of an established NHP model.

NHP models of CHIKV infection have been well established in cynomolgus macaques (*Macaca fascicularis*) [49, 425] and adult, aged, or pregnant rhesus macaques (*Macaca mulatta*) [224, 226, 227, 426]. These models have proven useful for evaluation of CHIKV-specific vaccines [99, 231, 427, 428] and monoclonal antibody therapies [40, 110, 235]. Additional NHP models of arthritogenic alphavirus disease have yet to be developed, although many have been established for the encephalitic alphaviruses. Indeed, Binn *et al.* established in 1967 that rhesus macaques could be infected with MAYV in a research setting, and the NHPs developed MAYV-neutralizing and CHIKV cross-neutralizing antibodies, which protected them from heterologous CHIKV challenge [224]. However, this study has left several unanswered questions pertaining to viral tissue tropism, persistence, viral strain-specific differences in pathogenicity, as well as a general lack of knowledge about the kinetics and durability of innate and adaptive immunity. Due to the potential emergence of MAYV and the active and ongoing development of alphavirus-specific

therapeutics and vaccines, we aimed to holistically characterize MAYV pathogenesis and immunity in adult rhesus macaques (RM).

Section 6.3: Results

6.3.1 Infection of mice with the MAYV BeAr505411 strain results in robust replication and viral dissemination.

To better inform strain selection for NHP experiments, we subcutaneously inoculated 4-week-old C57BL/6 mice (**Fig 6.1**) and 13-week-old IFN α R $^{-/-}$ mice (**6.S1 Fig**) in the right footpad with 10^4 PFU of genotype D and L MAYV strains including MAYV_{BeAr505411}, MAYV_{CH}, MAYV_{Guyane}, MAYV_{TRVL}, MAYV_{Uruma}, or UNAV_{MAC150} and compared viremia, tissue distribution and disease parameters for each of the strains. Infectious virus levels in serum collected at 2 days post-infection (dpi) from the female C57BL/6 mice were determined by limiting dilution plaque assays on Vero cells. Infection with MAYV_{BeAr505411} and MAYV_{CH} resulted in significantly higher serum viral titers compared to the three other MAYV strains tested (**Fig 6.1A**). Mice were euthanized at 5 dpi and MAYV vRNA levels were quantified using qRT-PCR for the RNA isolated from tissue homogenates of the contralateral and ipsilateral ankles, calves, and quads, as well as brain, spleen, and heart. Viral RNA levels generally trended significantly higher for MAYV_{BeAr505411} with infection in muscles (ranging 1-3 logs higher) and joints (ranging 2-5 logs higher) compared to the other strains (**Fig 6.1B-1G**). Across viral strains the levels of viral RNA in ipsilateral joints and muscles were equivalent to the levels detected in the contralateral samples indicating efficient viral spread. In spleen, brain, and heart tissue homogenates, vRNA levels trended significantly higher (ranging 1-3 logs greater) for MAYV_{BeAr505411} infection compared to the other MAYV strains (**Fig 6.1H-1J**). For many tissues, viral RNA levels in MAYV_{CH} and MAYV_{Guyane} infected C57BL/6 mice were similar to each other and higher than MAYV_{TRVL}, MAYV_{Uruma}, or UNAV_{MAC150}, but still lower relative to MAYV_{BeAr505411} (**Fig 6.1A-1H**). Interestingly, the MAYV strain differences observed in C57BL/6 mice were not as profound in IFN α R $^{-/-}$ mice as the five MAYV strains all lead to similar changes in weight loss (**6.S1D Fig**) and footpad swelling (**6.S1C Fig**) as well as survival time (**6.S1B Fig**). However, in these immunodeficient mice UNAV infection exhibited the highest viral titer at 1 dpi as well as the

quickest loss of body weight and time to death (6.S1A, 6.S1B, and 6.S1D Fig). In summary, MAYV_{BeAr505411} replicated to the highest levels in immunocompetent mouse tissues of expected viral tropism relative to other viral strains. Given these findings, we hypothesized that among the MAYV strains tested, MAYV_{BeAr505411} would replicate the most efficiently in rhesus macaques and potentially elicit better clinical disease.

Figure 6.1. Evaluation of MAYV strain pathogenesis in C57BL/6 mice.

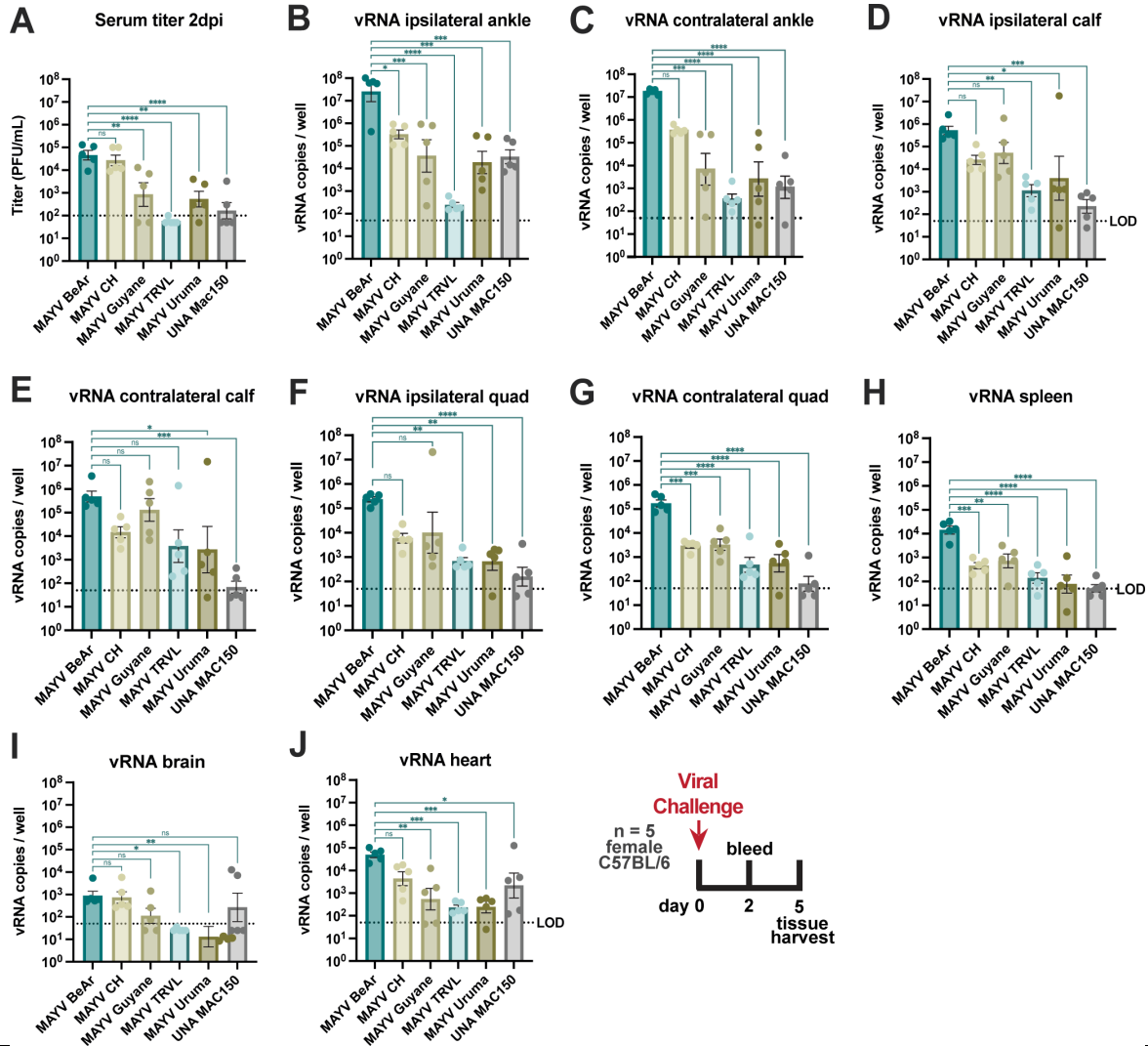


Figure 6.1. Five 4-week-old female C57BL/6 mice were infected with 10⁴ plaque forming units (PFU) with one of five MAYV strains or UNAV via a right foot pad 20μL injection. Blood was collected for serum isolation at 2 days post-infection (dpi) and tissues were harvested at 5 dpi. Titers of infectious virus in serum at 2 dpi are shown in (A) and viral RNA (vRNA) levels in tissues were quantified (B-J). Data points are mean with SEM error bars for n = 5 per group, measuring three replicates of log-transformed data. Serum was tittered on Vero cells by limiting dilution plaque assays and vRNA in tissues was measured in triplicate by qRT-PCR (vRNA copies per well were

normalized to the RsP17 house keeping gene.) The LOD in (A) was 100 PFU/mL with undetectable samples graphed as 50 PFU/mL. The LOD in (B-J) was 50 vRNA copies per well or per 200 μ L homogenate. Statistical analysis was completed using a one-way ANOVA with log-transformed data, where **** $p < 0.0001$, *** $p = 0.0001$, ** $p < 0.001$, * $p < 0.05$, ns $p > 0.05$.

Figure 6.S1. MAYV strains in IFN α R $^{-/-}$ mice.

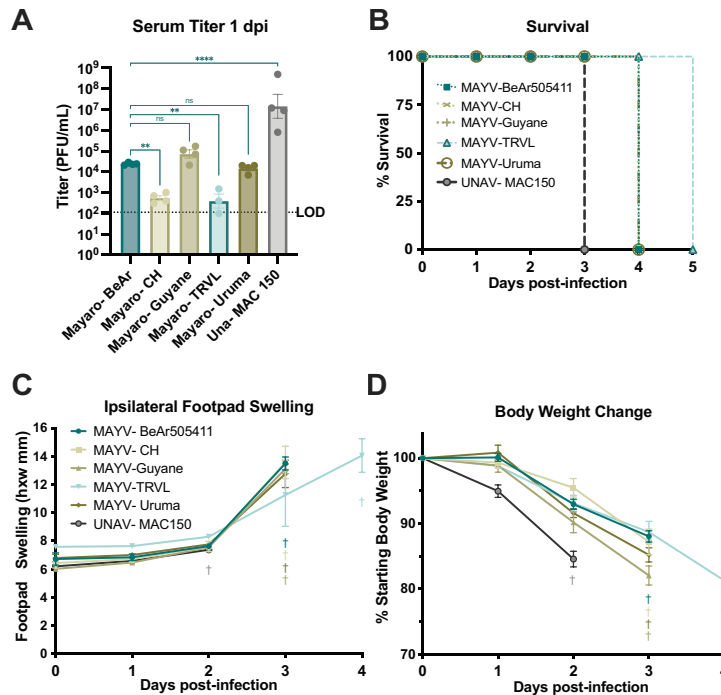


Figure 6.S1. Four 13-week-old IFN α R $^{-/-}$ mice per group received a subcutaneous right footpad injection of 10⁴ PFU of MAYV_{BeAr505411}, MAYV_{CH}, MAYV_{Guyane}, MAYV_{TRVL}, MAYV_{Uruma}, or UNAV_{MAC150}. Mice were bled at 1 dpi for peak serum viremia and body weights and footpad swelling were recorded daily until animals were euthanized due to excessive loss of body weight. Serum titer of infectious virus measured by plaque-forming units per mL (PFU/mL) is log-transformed and shown in (A). Statistical analysis for comparison of viral titers was completed using a one-way ANOVA with log transformed data, where **** $p < 0.0001$, *** $p = 0.0001$, ** $p < 0.001$, * $p < 0.05$, ns $p > 0.05$. The Kaplan-Meier survival curve is shown in (B) for the four-day monitoring period until mice succumbed to infection. A Kruskal-Wallis test was used to compare survival data for the groups of mice and the only significant comparison was survival of MAYV_{TRVL}-infected compared to UNAV_{MAC150}-infected mice, $p < 0.0001$. Footpad swelling (mm) in the ipsilateral footpad is shown in (C) and percent change from starting weight (%) is shown in (D). Error bars are SEM when included.

6.3.2 Kinetics of MAYV replication in rhesus macaques reveals peak viremia at 2 dpi.

To characterize MAYV pathogenesis in NHPs, we infected three male rhesus macaques (RM) ages 4, 10, and 13 years (**Fig 6.2**). At approximately one month prior to infection, we collected peripheral blood as well as spleen, axillary lymph node (LN) and mesenteric LN biopsies to provide baseline comparisons for immunological assays. Animals were inoculated subcutaneously in both hands and arms at five sites per arm (100 μ L per injection) in an attempt to mimic a mosquito bite with a total infectious dose of 1×10^5 PFU of MAYV_{BeAr505411}. Peripheral blood and urine samples were collected at 0, 1, 2, 3, 4, 5, 7, and 10 dpi (**Fig 6.2A**). RM were humanely euthanized at 10 dpi for extensive tissue collection that included lymphoid tissues, muscles, joints, heart, peripheral nerves, central nervous system, male reproductive tissues, and other major organs. The 10 dpi timepoint was chosen to maximize the characterization of viral dissemination and immune activation following MAYV infection. We quantified plasma viral RNA (vRNA) at all timepoints following infection and found that MAYV replicated up to 10^8 vRNA copies / mL of plasma, with peak viremia occurring at 2 dpi in all three animals (**Fig 6.2B**). Plasma infectious virus was consistently detected at 1-4 dpi but not at 5, 7 or 10 dpi. (**Table 6.1**). We were unable to detect MAYV vRNA in urine samples from any of the RM, at any timepoint. Complete blood counts and serum chemistry analyses of each macaque revealed few remarkable changes over the duration of the study, but one animal experienced minor anemia that coincided with peak viremia (**6.S2 and 6.S3 Figs**). One animal developed a fever of 104°F at 1 dpi, however, the animals were only monitored for temperature during procedures, making it impossible to know whether they were febrile at other times (**Fig 6.2C**). None of the three animals experienced weight loss over the duration of the 10-day infection study, although NHP 3 did experience 7% loss of body weight between the biopsy period and infection day. (**Fig 6.2D**). We did not observe additional signs of discomfort or disease in these three animals.

Figure 6.2. Study overview of MAYV infection of NHPs.

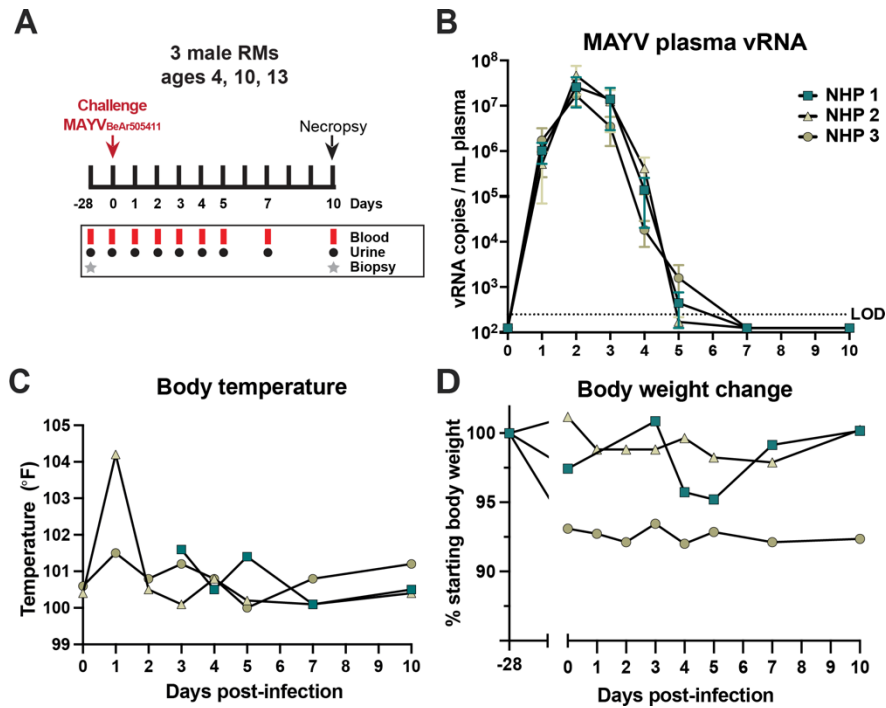


Figure 6.2. Schematic summarizing the MAYV macaque infection study (A). Pre-infection axillary, inguinal, and mesenteric lymph node and spleen biopsies as well as blood were collected one month prior to infection for three male rhesus macaques (RMs) ages 4, 10, and 13 years. Animals were inoculated with 10^5 plaque forming units (PFU) of MAYV_{BeAr505411} administered subcutaneously and spread evenly in both arms and hands. Blood was drawn for PBMC and plasma isolation as well as complete blood count (CBC) and serum chemistry at 0–5, 7, and 10 dpi. Animals were humanely euthanized at 10 dpi and extensive lymphoid, muscles, joints, nerves, lobes of the brain, heart, major organs, and male reproductive tissues were harvested. Plasma was isolated from blood collections at 0–5, 7, and 10 dpi for quantification of viral RNA in copies/mL of plasma by qRT-PCR in triplicate reactions (B). The qRT-PCR data is representative of three independent experiments. The LOD was 250 copies MAYV RNA per mL of plasma with undetectable samples graphed as 125 copies vRNA/mL plasma. Body temperatures (°F) (C) and change from starting body weight (%) (D) were recorded daily at all study timepoints.

Table 6.1. Isolation of infectious MAYV from RM plasma and tissue.

Plasma	NHP 1	NHP 2	NHP 3
1 dpi	1.00x10 ¹⁰ PFU	4.60x10 ¹⁰ PFU	5.00x10 ⁹ PFU
2 dpi	6.20x10 ¹⁰ PFU	4.66x10 ¹⁰ PFU	5.20x10 ¹⁰ PFU
3 dpi	2.90x10 ¹⁰ PFU	9.25x10 ¹⁰ PFU	2.40x10 ¹⁰ PFU
4 dpi	-	2.43x10 ⁶ PFU	3.40x10 ⁴ PFU
5 dpi	-	-	-
7 dpi	-	-	-
10 dpi	-	-	-
Tissue			
Ax LN	1.00x10 ² PFU	-	-
Ing LN	-	1.10x10 ⁴ PFU	3.30x10 ⁰ PFU
Submandibular LN	-	-	-
Finger	-	-	-
Wrist	1.43x10 ⁶ PFU	-	-
Elbow	-	-	3.10x10 ⁶ PFU
Toe	3.46x10 ⁴ PFU	-	1.36x10 ⁴ PFU
Ankle	1.96x10 ⁴ PFU	-	-
Bicep	-	-	-
Brachial radius	-	-	-
Knee	-	-	5.90x10 ⁶ PFU
Quad	-	-	-
Tricep	-	-	-
Soleus	-	-	-
Hamstring	-	-	-
Aorta	-	-	-
Heart left atrium	-	-	-
Heart right atrium	-	-	-
Heart left ventricle	-	-	-
Heart right ventricle	-	-	-
Kidney	-	-	-
Liver	-	-	-

<https://doi.org/10.1371/journal.pntd.0011742.t001>

Table 6.1. Using NHP tissue homogenates collected in PBS at 10 dpi, we infected C6/36 cells and harvested supernatants at 3 dpi to isolate infectious MAYV. Viral supernatants were tittered in triplicate by limiting dilution plaque assays on Vero cells to quantify infectious viral particles in cell supernatants. Viral titers are reported as plaque forming units per 1 mL of C6/36 viral supernatant. The LOD was 3.3 PFU/mL. Samples with titers below the LOD are labeled (-).

Figure 6.S2. Complete blood count (CBC) data for macaques over the duration of the study.

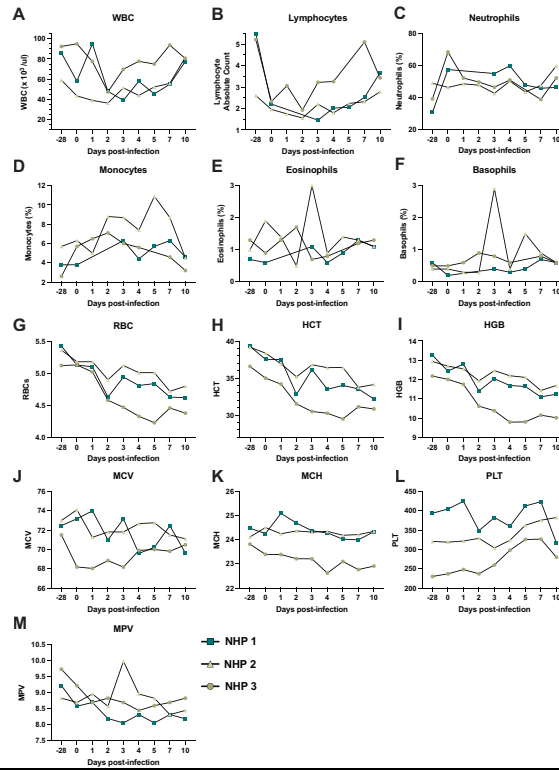


Figure 6.S2. CBC analytes from EDTA-treated whole blood: white blood cell count (A), lymphocytes (B), neutrophils (C), monocytes (D), eosinophils (E), basophils (F), red blood cells (G), hematocrit (H), hemoglobin (I), mean corpuscular volume (J), mean corpuscular hemoglobin (K), platelets (L), and mean platelet volume (M).

Figure 6.S3. Serum chemistry panel analytes for macaques during the study.

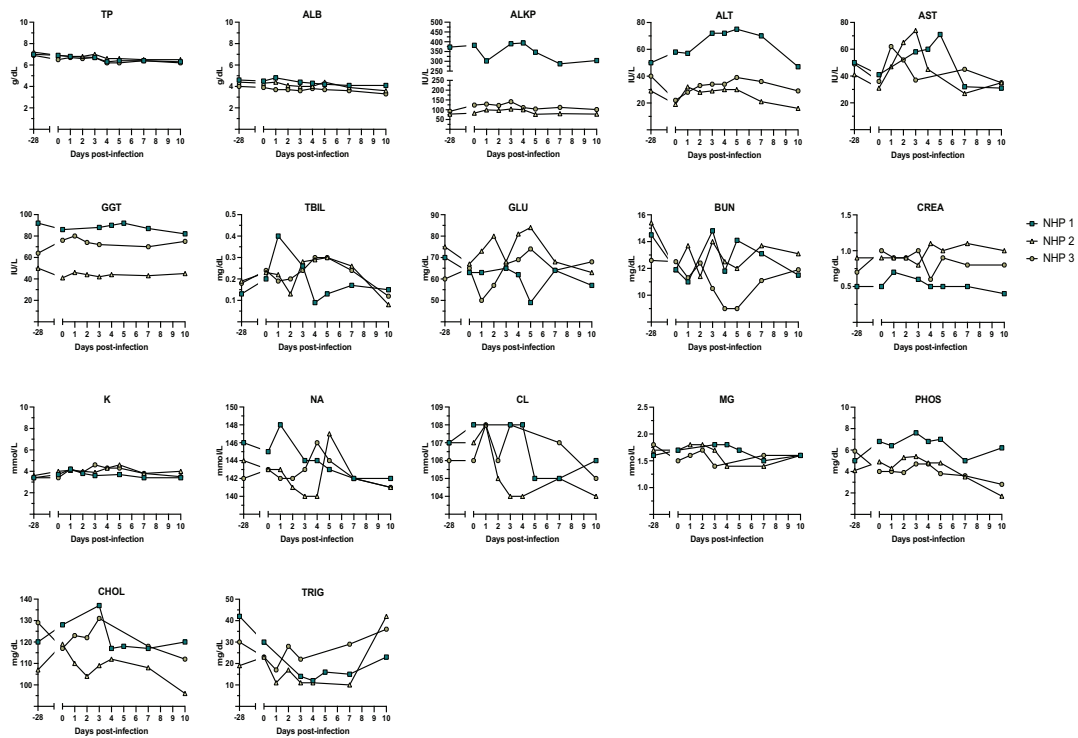


Figure 6.S3. Analytes for serum chemistry at all blood draw timepoints included total protein (TP), albumin (ALB), alkaline phosphatase (ALKP), alanine transaminase (ALT), aspartate transaminase (AST), gamma-glutamyl transferase (GGT), total bilirubin (TBIL), glucose (GLU), blood urea nitrogen (BUN), creatinine (CREA), potassium (K), sodium (NA), chloride (CL), magnesium (MG), phosphorus (PHOS), cholesterol (CHOL), and triglyceride (TRIG).

On the day of necropsy (10 dpi), a maculopapular rash was observed on the ventrum and flanks of one animal, without any observed pruritis, (**Fig 6.3A-3D** and **Table 6.2**) and these lesions were positive for MAYV RNA (**Fig 6.4E**). Erythematous macules, papules and xerotic plaques extended from the caudal thorax to the inguinal region with the most pronounced changes on the flanks. A bacterial culture revealed normal background dermatologic flora, and histologic screening for other etiologic causes such as measles virus was negative. Microscopic changes in the abdominal skin included multifocal acanthosis, mild dyskeratosis, and superficial edema which corresponded to grossly visible papules. Perivascular lymphocytic inflammation was within the superficial dermis, which increased in severity in areas accompanying epidermal lesions. In the absence of gross or histologic epidermal changes, perivascular inflammation extended to the thoracic skin in this animal, as well as one other in the cohort, where it also surrounded few hair follicles (**Fig 6.3E**). One of the three animals did not have lesions within the thoracic skin sample

that was collected, which was consistent with the negative viral detection as well (Fig 6.4E). Together, these data provide insight into the kinetics of MAYV viremia and disease symptoms.

Figure 6.3. Dermatologic pathology in MAYV-infected rhesus macaques.

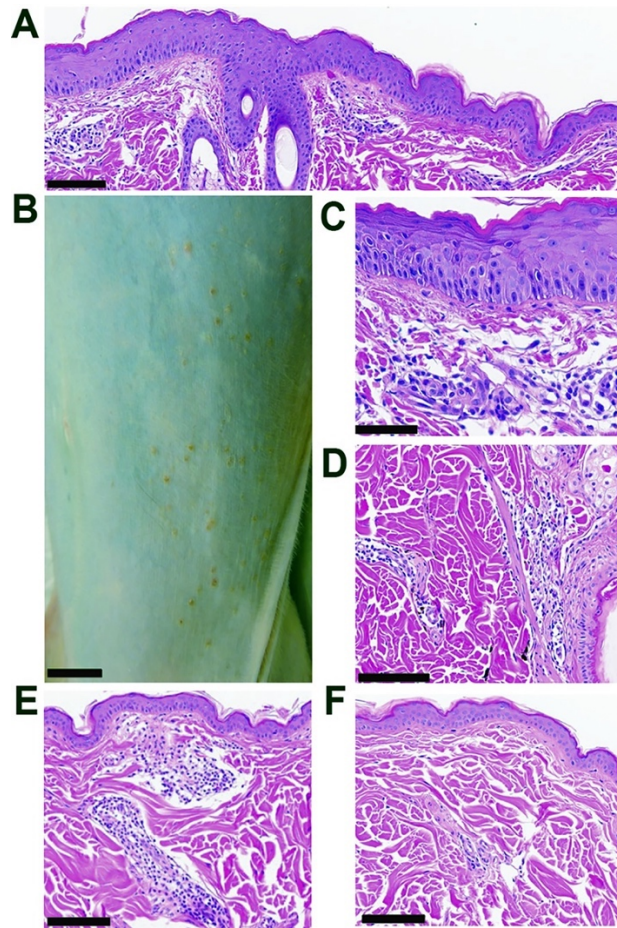


Figure 6.3. At 10 dpi with MAYV, macaque skin sections were collected during necropsy, fixed, paraffin embedded, sectioned and stained for examination with hematoxylin and eosin (HE). (**B**; Bar = 1 cm) A maculopapular rash extends from the ventral abdomen to the flanks and inguinal region of NHP 3. (**A**; Bar = 100 μ m. **C**; Bar = 50 μ m) Sections of a maculopapular rash in the abdominal skin displaying multifocal acanthosis, mild dyskeratosis, superficial dermal edema, and perivascular lymphocytic inflammation in the superficial dermis. (**D**; Bar = 100 μ m) The thoracic skin had similar perivascular and perifollicular lymphocytic aggregates. (**E**; Bar = 100 μ m) Thoracic skin from NHP 1 with mild perivascular lymphocytic inflammation in the superficial dermis. (**F**; Bar = 100 μ m) Normal thoracic skin from NHP 2.

Table 6.2. Perivascular lymphocytic inflammation in the musculoskeletal, nervous, cardiovascular, and integumentary tissues of MAYV-infected rhesus macaques at 10 dpi.

Tissue	NHP 2	NHP 3	NHP 1
Joints			
Elbow	-	++	-
Wrist/Fingers	+	+++	+
Knee	++	+	-
Ankle/Toes	+	+++	+++
Muscles			
Biceps brachii	-	-	-
Triceps brachii	-	-	-
Brachioradialis	-	-	+
Quadriceps femoris	-	- *	-
Biceps femoris (hamstring)	+	-	-
Soleus	-	-	-
Nervous Tissues			
Cerebrum	+	+	-
Cerebellum/brainstem	-	+	-
Trigeminal nerve	-	-	N
Spinal cord / dorsal root ganglia	-	+ (Lumbar)	+ (Cervical)
Brachial plexus	-	+	-
Femoral nerve	- **	-	-
Sciatic nerve	+	+	-
Eye	-	-	-
Cardiovascular Tissues			
Heart	+ ***	- ****	+
Aorta	-	- ****	-
Integument			
Abdominal skin (rash)	N	+++	N
Torso skin	-	+++	++

Tissues are scored for presence of lymphocytic inflammation by relative intensity (+ to +++) or absence (-) of pathology within sections using the following scale

+, one small aggregate of perivascular lymphocytes

++, multiple blood vessels within one or two areas of the tissue with small to moderate numbers of perivascular lymphocytes; and

+++ , perivascular lymphocytes affecting a majority of blood vessels in small to moderate numbers with or without infiltration of the surrounding tissue.

N, tissue not available for evaluation.

*, minor myocyte degeneration and regeneration

** , pre-existing fasciitis

*** , hypertrophic cardiomyopathy and valvular endocardiosis; and

**** , myxofibromatous degeneration of the mitral valve (endocardiosis) and aorta.

<https://doi.org/10.1371/journal.pntd.0011742.t002>

Table 6.2. Tissues are scored for presence of lymphocytic inflammation by relative intensity (+ to +++) or absence (-) of pathology within sections.

Figure 6.4. Detection of MAYV RNA in NHP tissues at 10 dpi.

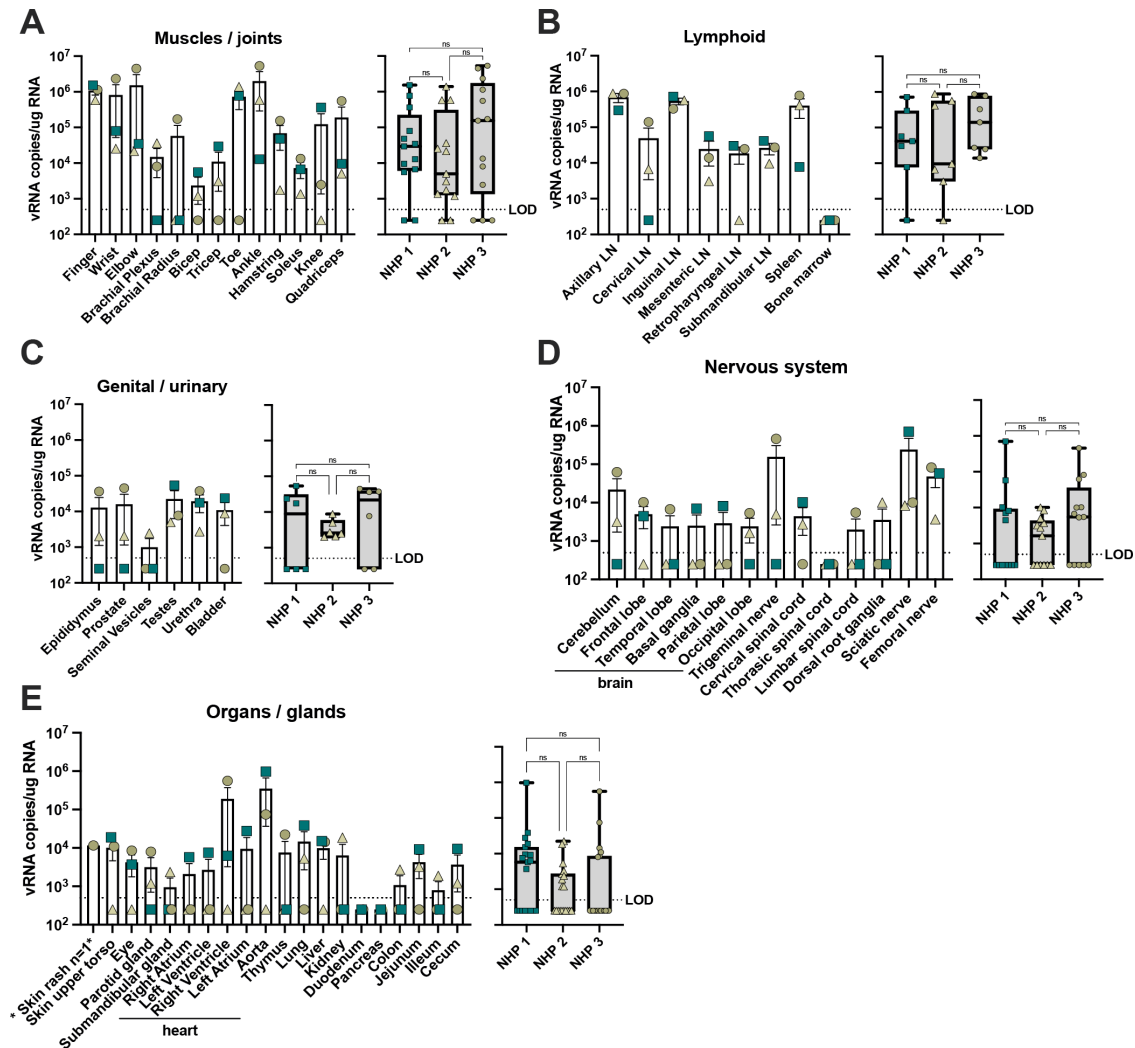


Figure 6.4. During necropsy extensive tissue subsets were collected from macaques and viral burden was determined through quantification of copies of viral RNA (vRNA) in qRT-PCR. Tissue subsets included muscles and joints (A), lymphoid tissues (B), genital and urinary (C), nervous system (D), and organs and glands (E). For all panels, the LOD was 500 copies per mL of tissue homogenate with undetectable samples graphed as 250 copies of vRNA/mL. Shown for each panel is a compilation and comparison of vRNA quantities for the tissue group, analyzed using a one-way ANOVA (ns = $p > 0.05$). All qRT-PCR reactions were performed in triplicate.

6.3.3 MAYV infects joint, muscle, lymphoid, cardiac, and nervous system tissues of rhesus macaques.

Next, we aimed to identify MAYV tissue distribution in the RMs at 10 dpi. Total RNA was isolated from muscle, joint, lymphoid, heart, brain, nerve, reproductive, and other major organs;

and vRNA was quantified for each sample using qRT-PCR (**Fig 6.4**). At the time of necropsy, we combined right and left muscle and joint tissues into one sample tube and detected high levels of vRNA in most subsets, notably the ankles, toes, elbows, fingers, and wrists for all three animals, indicating that the virus disseminated effectively throughout the body (**Fig 6.4A**). Consistent with this finding, we detected high levels of MAYV RNA for all three animals in several lymphoid tissues with the exception of bone marrow; viral loads were particularly high (nearly 10^6 copies of vRNA per μg of RNA) in the axillary and inguinal lymph nodes (LNs), which drain from the arms and legs, respectively (**Fig 6.4B**). Viral RNA was detected in the male reproductive tissues (**Fig 6.4C**). MAYV crosses the blood-brain barrier in NHPs, as we observed vRNA in all three animals in lobes of the brain and other major central nervous tissues, the thoracic spinal cord being the only subset sampled with no detection in any animal (**Fig 6.4D**). Although we detected MAYV vRNA in many nervous system tissues, we did not observe evidence of neurological disease in any of the macaques. Because we detected viral replication in cardiac compartments in our mouse strain selection study (**Fig 6.1J**), we separated the ventricles, atriums, and aorta of the heart for viral detection in the RMs. We detected vRNA in all cardiac compartments for one animal, in the right ventricle of two animals, but one animal had no detectable vRNA in the heart tissue samples (**Fig 6.4E**). The duodenum and pancreas were the only tissues that were undetectable for vRNA for all three animals (**Fig 6.4E**). We compared the pooled vRNA levels in each tissue group across the three animals in an attempt to identify any trends in quantity or distribution, but there were no significant differences (**Fig 6.4A-4E**). The presence of infectious virus was determined by coculture of tissue homogenates with C6/36 cells and subsequent titrating of culture supernatants. Infectious virus was recovered in several muscle and joint tissues as well as lymph nodes, which provides additional evidence of sustained viral replication (**Table 6.1**). These data provide valuable insights into MAYV tissue tropism, replication, and distribution with valuable translational impact for understanding human infection.

6.3.4 Immunopathologic changes associated with MAYV infection in rhesus macaques highlight variable tissue inflammation in joints, muscles, heart, and central nervous tissues.

Histological assessment revealed that each of the animals infected with MAYV exhibited variable degrees of perivascular inflammatory cell infiltration in several tissue types. For example, all three animals had minimal to moderate lymphocytic inflammation of the finger, wrist, ankle, and toe joints (**Fig 6.5A and 6.5B**). The degree of inflammatory infiltration varied from minimally affecting rare perivascular areas in the fascia to moderate tenosynovitis also involving the adjacent adipose tissues (**Table 6.2**), and vasculitis was present in the most affected tissues. Multifocally, synovial and endothelial cells were hypertrophic, indicative of cellular activation. Interestingly, the ankles and toes (secondary sites of infection) of NHP 1 had more involvement than the forelimb joints. A focus of perivascular lymphocytes was in the brachioradialis muscle of NHP 1, which was the muscle collected closest to the infection sites. The elbow of one animal (**Fig 6.5C**) and the knees of two animals showed similar minimal to mild findings. Lymphocytic inflammation in the joint tissues occurred without gross changes in the cartilage or bone and variations were absent macroscopically where present on sections stained with hematoxylin and eosin (H&E). These findings imply that any pre-existing osteoarthritic components were less likely, though this cannot be ultimately ruled out due to collection limitations on size of tissue samples. Additionally, these lesions would be unexpected in the juvenile NHP 1.

Aggregates of lymphocytes were also present surrounding rare blood vessels in multiple additional tissues, including the appendicular muscles, heart, and nervous system of all NHPs (**Figs 6.5D-5G and 6.S4, and Tables 6.2 and 6.S1**). The medullary sinuses of the axillary lymph nodes were expanded by histiocytes and hemophagocytes, which grossly presented as erythema and lymphadenopathy in all animals (**6.S5 Fig and 6.S2 Table**). Mild enlargement of many peripheral and visceral lymph nodes microscopically corresponded to sinus histiocytosis and varying levels of hemophagocytosis, particularly present in the medullary sinuses of mesenteric and sacral lymph nodes. A consistent finding between these animals was lesions within the red pulp of the spleen (**6.S5 Fig and 6.S2 Table**). At low magnification, a perifollicular pattern of congestion was evident (**6.S5D Fig**). At higher magnification, sinusoidal reticuloendothelial hyperplasia,

histiocytosis, erythrophagocytosis, increased neutrophils, and rare micro abscesses were evident (6.S5E-F Fig). Mentionable age-related or incidental lesions were chronic hepatic degeneration and valvular endocardiosis of NHP 3 and hypertrophic cardiomyopathy, valvular endocardiosis, and fasciitis near the femoral artery and nerve of animal NHP 2.

Figure 6.5. Lymphocytic inflammation in the musculoskeletal, cardiac, and nervous system of MAYV-infected rhesus macaques.

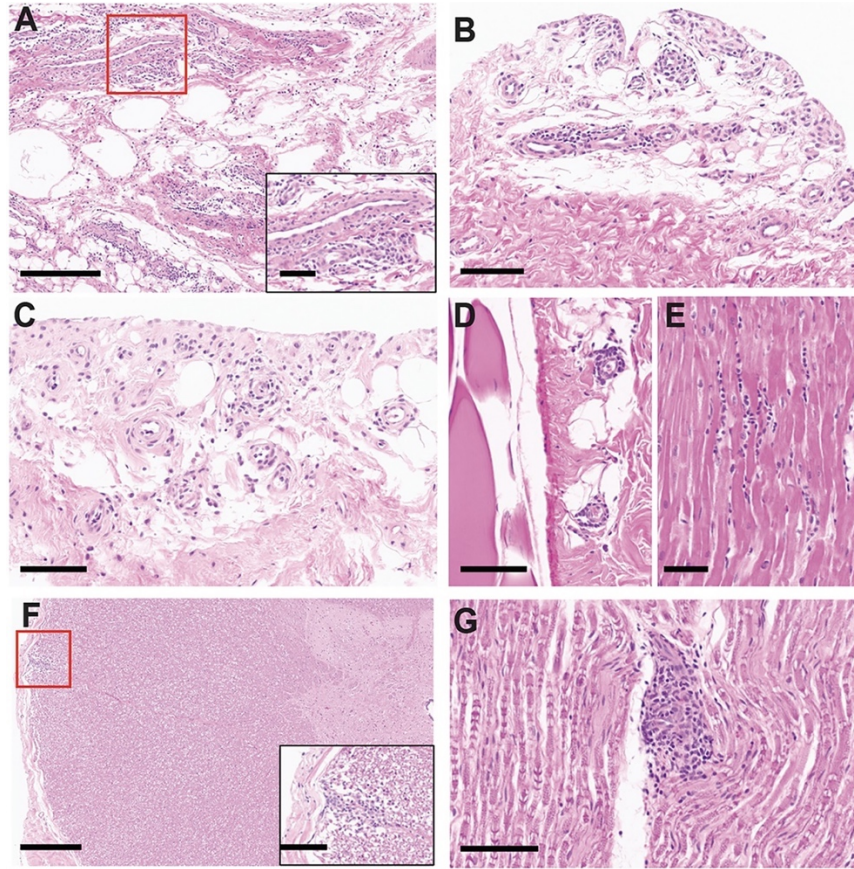


Figure 6.5. Macaque joint and muscle tissues were collected during necropsy, fixed, paraffin embedded, sectioned and stained with hematoxylin and eosin (HE). Extensive histology was examined, and select representative images are shown for the three animals. (A; Bar = 300 μm , inset 100 μm) Lymphocytic inflammation within the periarticular connective tissue of the wrist and fingers with a perivascular pattern. (B; Bar = 100 μm) Perivascular and synovial lymphocytic inflammation in the ankle and toes. (C; Bar = 100 μm) Similar lymphocytic inflammation affects the elbow. (D; Bar = 100 μm) Minor perivascular inflammation within the fascia adjacent to the hamstring. (E; Bar = 50 μm) A minor focal aggregate of lymphocytes within the interventricular septum of the heart. (F; Bars = 500 μm , inset 100 μm) A vessel within the dorsal funiculus of the cervical spinal cord surrounded by lymphocytes. (G; Bar = 100 μm) Minor lymphocytic inflammation in the perivascular space of a vessel in the sciatic nerve.

Figure 6.S4. Lymphoid pathology of MAYV-infected rhesus macaques.

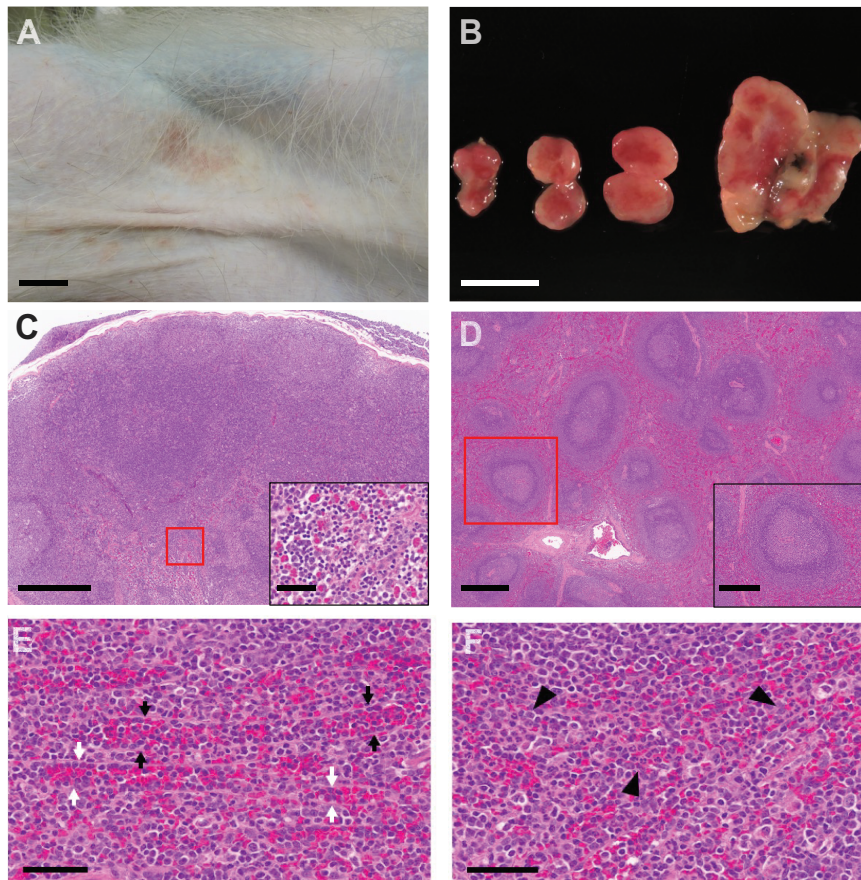


Figure 6.S4. Macaque lymphoid tissues were collected during necropsy, fixed, paraffin embedded, sectioned, and stained with hematoxylin and eosin (HE). Histology was examined, and select representative images are shown for the three animals. (A; Bar = 1 cm) The axillary skin of NHP 2 is discolored red-tan. (B; Bar = 1 cm) The axillary lymph nodes in all three animals were enlarged and erythematous. (C; Bars = 500 μ m, inset 50 μ m) The axillary lymph nodes have mild lymphofollicular hyperplasia and medullary sinus histiocytosis with hemophagocytosis. (D; Bars = 500 μ m, inset 300 μ m) Perifollicular sinusoids are congested. (E; Bar = 50 μ m) Perifollicular sinusoids (black and white arrows) have reticuloendothelial hypertrophy and are engorged with macrophages, lymphocytes, and erythrocytes. There is rare erythrophagocytosis. (F; Bar = 50 μ m) An increased number of neutrophils are within the red pulp (arrowheads).

Table 6.S1. Presence or absence of perivascular lymphocytic inflammation in endocrine, respiratory, alimentary, hepatobiliary and pancreatic, and genitourinary tissues in MAYV-infected rhesus macaques at 10 dpi.

Tissue	Animal 28472	Animal 30504	Animal 36647
Endocrine			
Thyroid gland	-	-	-

Respiratory			
Lungs	-	-	-
Alimentary			
Parotid salivary gland	-	-	-
Submandibular salivary gland	-	-	-
Duodenum	-	-	-
Jejunum	-	-	-
Ileum	-	-	-
Cecum	-	-	-
Colon	-	-	-
Hepatobiliary and pancreatic			
Liver	-	++ *	++
Gall bladder	-	-	-
Pancreas	-	-	-
Genitourinary			
Kidneys	+ **	-	-
Urinary bladder	-	-	-
Urethra	-	-	+++ ***
Prostate	-	+	-
Seminal vesicles	-	-	-
Epididymis	-	-	+
Testes	-	-	-

+, one small aggregate of perivascular lymphocytes; ++, multiple blood vessels within one or two areas of the tissue with small to moderate numbers of perivascular lymphocytes; +++, perivascular lymphocytes affecting a majority of blood vessels in small to moderate numbers with or without infiltration of the surrounding tissue.

*, Chronic hepatic degeneration and regeneration; **, Rare attenuated cortical tubules, scant cellular or proteinaceous casts with few associated lymphocytes; ***, diffuse chronic mild lymphocytic and neutrophilic urethritis.

Figure 6.S5. Lymphocytic inflammation in the nervous system of a MAYV-infected rhesus macaque.

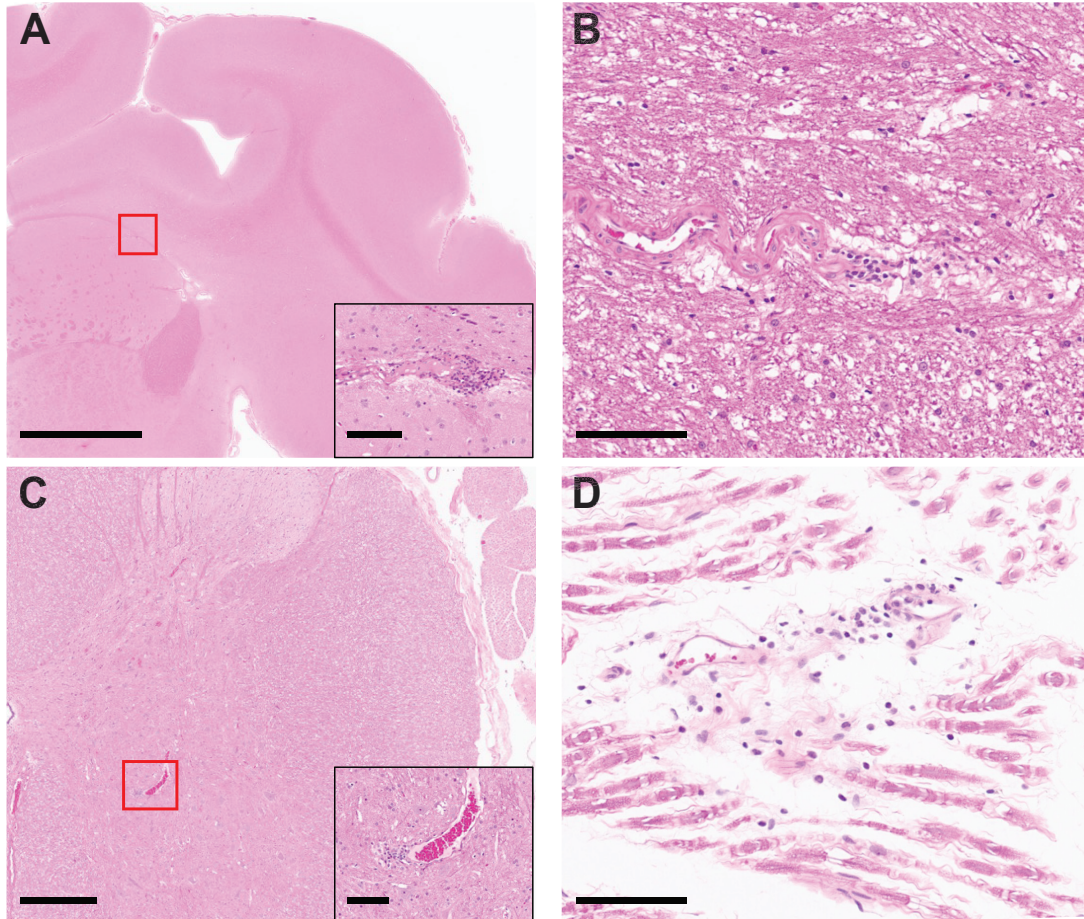


Figure 6.S5. At 10 dpi with MAYV, macaque hematopoietic tissues were collected, fixed, paraffin embedded, sectioned, and stained with hematoxylin and eosin (HE). Extensive histology was examined and select representative images are shown from NHP 3. (A; Bar = 5 mm, inset 200 μ m) Minor perivascular lymphocytic inflammation within the gray-white matter junction of the putamen, (B; Bar = 100 μ m) the brainstem, (C; Bar = 100 μ m, inset 50 μ m) the ventral horn of the lumbar spinal cord, (D; Bar = 100 μ m) and the brachial plexus.

Table 6.S2. Hematopoietic pathology in MAYV-infected rhesus macaques at 10 dpi.

Tissue	Animal 28472	Animal 30504	Animal 36647
Bone marrow	-	-	-
Thymus	-	-	-
Spleen	Perifollicular sinusoid congestion, sinusoidal reticuloendothelial hyperplasia, increased neutrophils within the red pulp	Perifollicular sinusoid congestion, sinusoidal reticuloendothelial hyperplasia, increased neutrophils within the red pulp	Perifollicular sinusoid congestion, sinusoidal reticuloendothelial hyperplasia, increased neutrophils within the red pulp

Cervical lymph node	Sinus histiocytosis with hemosiderophages, minimal	-	N
Submandibular lymph node	-	-	Sinus histiocytosis, mild
Axillary lymph node	Sinus histiocytosis and plasmacytosis, mild, with hemosiderophages	Follicular hyperplasia, minimal, axillary lymph node Sinus histiocytosis, with hemosiderophages, axillary lymph node	Lymphofollicular hyperplasia, moderate, with moderate sinus histiocytosis and plasmacytosis with hemosiderophages
Tracheobronchial lymph node	-	Follicular hyperplasia, mild	Follicular hyperplasia, multifocal, mild
Retroperitoneal lymph node	-	-	-
Mesenteric lymph node	Sinus histiocytosis and plasmacytosis, mild, with hemosiderophages	-	Sinus histiocytosis, moderate Follicular hyperplasia, mild
Iliosacral lymph node	Sinus histiocytosis, mild, with hemosiderophages	-	Sinus histiocytosis and plasmacytosis with hemosiderophages, mild
Inguinal lymph node	-	Sinus histiocytosis, mild	Sinus histiocytosis, mild

Table 6.S2. Table summarizes pathologic diagnoses in given lymphoid tissues. Absence of observed pathology within the tissue is denoted (-).

6.3.5 Cytokine and cellular innate immune signatures peak with MAYV viremia in rhesus macaques.

We analyzed the expression of 37 cytokines and chemokines in longitudinal plasma samples following MAYV infection. Previously, a number of different proinflammatory cytokines and chemokines have been reported to be activated following MAYV infection in mice and humans or CHIKV infection in NHPs, in a process that typically coincides with viremia and subsequent innate and adaptive immune activation [40, 226, 429, 430]. Studies with other arthritogenic alphavirus such as CHIKV and RRV have shown osteoblasts to be susceptible to infection, leading to secretion of MCP-1, IL-1, and IL-6 [431, 432]. Consistent with these findings, G-CSF, IL-RA, eotaxin, MCP-1, IFN- α , and IFN- γ were all elevated relative to baseline at 2 dpi, aligning with peak viremia in the MAYV-infected RMs (**Figs 6.6 and 6.S6**). Studies in mice following CHIKV infection have previously shown biphasic peaks in these inflammatory cytokines, and we captured sporadic secondary peaks for IL-4, IL-7, IL-8, IL-15, NGF- β , PDGP-BB, and SDF-1 (**6.S6 Fig**) [433]. Production of these cytokines and chemokines provide evidence

of monocyte recruitment and migration (i.e., eotaxin, MCP-1) during peak viremia, which have a prominent role in the control of infection.

Activation of monocytes, macrophages, and dendritic cells have been consistently shown to contribute to the innate immune response to help control alphavirus infection but are also capable of causing inflammatory damage [434-437]. To understand the kinetics of these innate immune responses in our MAYV-infected RMs, we quantified the frequency of total and activated (CD169+) monocytes, NK, and dendritic cells in longitudinal PBMC samples as well as lymphocytes isolated pre- and post-infection from lymphoid tissues (**Figs 6.7 and 6.S7**). All three key peripheral blood monocyte populations (classical, non-classical, and intermediate monocytes) were highly activated in a process that coincided with the kinetics of plasma viremia (**Fig 6.2B**), peaking between 2 and 4 dpi but returning to baseline by 10 dpi (**Fig 6.7A-7C**). The peak of activation of NK cells ($p=0.3139$), myeloid dendritic cells ($p=0.0460$), and plasmacytoid dendritic cells ($p=0.0767$) in PBMC also coincided with viremia (**Fig 6.7D-7F**), however, this trend was only statistically significant for myeloid dendritic cell activation (**Fig 6.7E**). While we detected increases in activation for monocyte, NK, and dendritic cell subsets, there were no significant changes in the total frequencies of any of these populations (**Fig 6.7A-7F**). Innate immune population activation in lymphoid tissues following infection varied by tissue and cell type. For example, after infection intermediate monocytes in the mesenteric LN were significantly activated ($p=0.0337$) and those from the spleen also trended towards increased activation ($p=0.2798$). However, other monocyte populations from these same tissues were not activated nor were they activated from axillary lymph node tissues (**Fig 6.7G-7I**). NK cell activation trended upwards following infection while not reaching statistical significance ($p=0.6650$, $p=0.1481$, $p=0.2022$, respectively) (**Fig 6.7J-7L**). There was a general trend for plasmacytoid DCs to express less CD169 following infection and this trend reached significance in cells isolated from the spleen ($p=0.0264$) (**Fig 6.7J-7L**).

Figure 6.6. Cytokine and chemokine profile following MAYV infection.

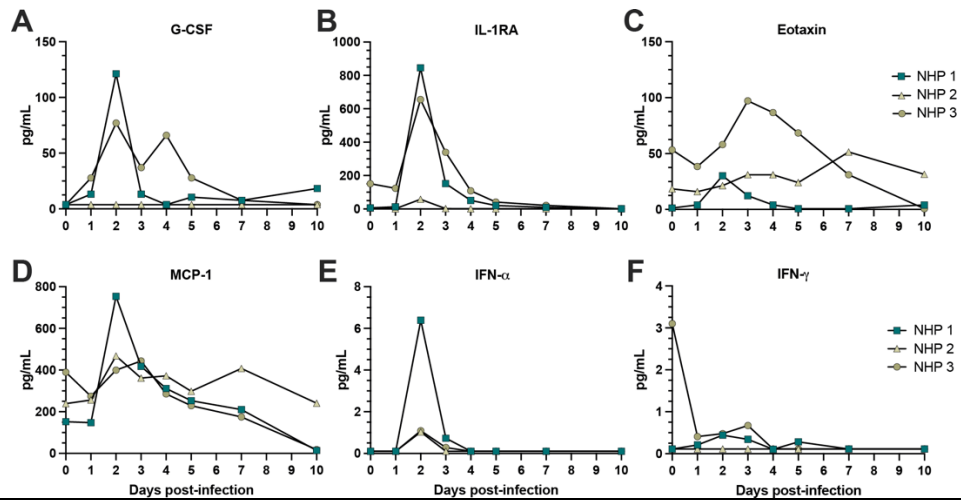


Figure 6.6. The inflammatory cytokine and chemokine profile following MAYV infection was characterized in macaque plasma at 0–5, 7, and 10 dpi using a Cytokine Monkey Magnetic 29-plex Panel for Luminex Platform Kit (Invitrogen) according to the manufacturer’s instructions. A full panel of 29 cytokine and chemokine levels (pg/mL of plasma) were quantified, but shown are G-CSF (A), IL-1RA (B), eotaxin (C), MCP-1 (D), IFN- α (E), and IFN- γ (F). The LOD was determined to be the lowest detectable value in the assay for each cytokine or chemokine. Paired t tests were used for statistical analysis where baseline (d0) was compared to each of the other timepoints but did not yield any statistically significant results ($p > 0.05$).

Figure 6.S6. Cytokine and chemokine profile following MAYV infection.

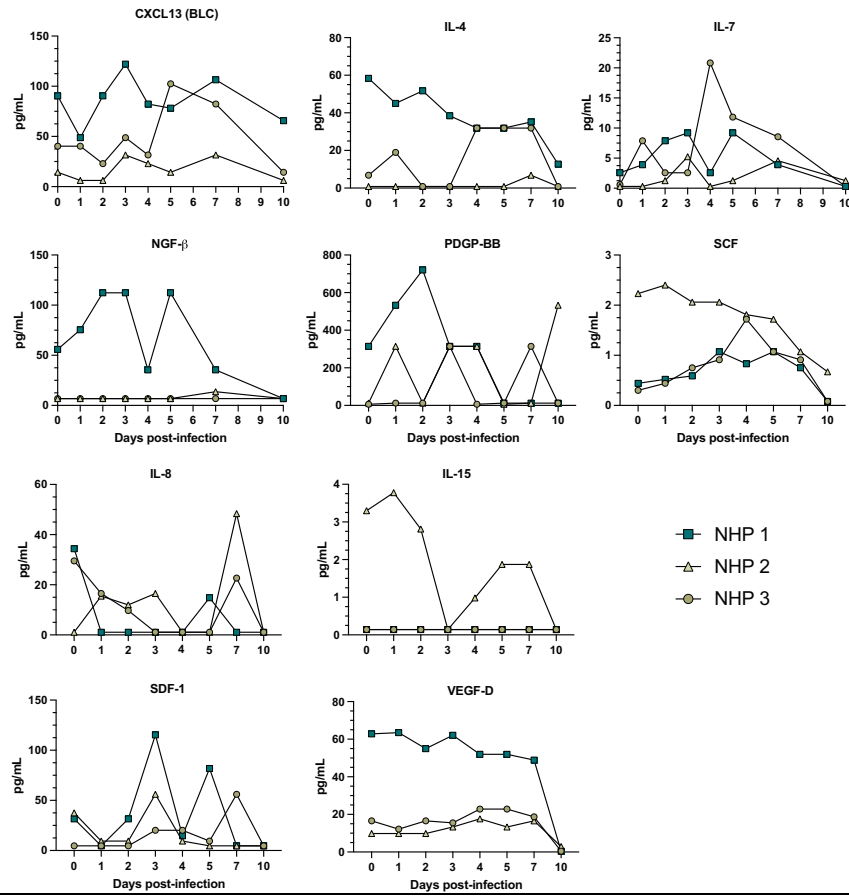


Figure 6.S6. Additional inflammatory cytokines and chemokines quantified in longitudinal macaque plasma that were included in the 29-plex Luminex panel. Select cytokines and chemokines are quantified in pg/mL at 0–5, 7, and 10 dpi. Paired t tests were used for statistical analysis where baseline (d0) was compared to each of the other timepoints but did not yield any statistically significant results ($p > 0.05$).

Figure 6.7. Longitudinal peripheral blood and lymphoid tissue cell phenotype activation of monocytes, dendritic cells, and NK cells following MAYV infection.

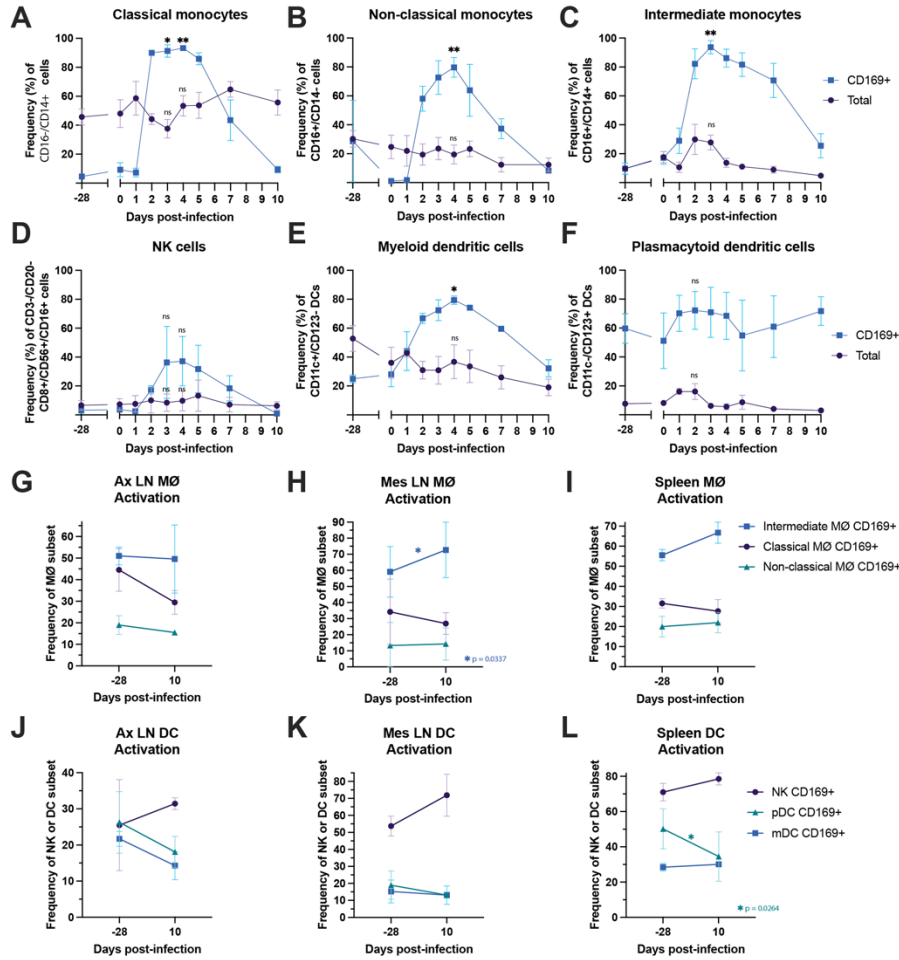


Figure 6.7. Macaque PBMC from -28, 0–5, 7, and 10 dpi (A–F) and lymphocytes isolated from three lymphoid tissues either one month prior to infection or 10 dpi (G–L) were analyzed for cell phenotype using flow cytometry. Changes in the longitudinal frequency of both total and activated (CD169+) classical monocytes (A), non-classical monocytes (B), intermediate monocytes (C), NK cells (D), myeloid dendritic cells (E), and plasmacytoid dendritic cells (F) are quantified. Comparison of the frequencies of intermediate, classical, and non-classical monocyte phenotype activation at pre- or post-infection are quantified for axillary (Ax) LN (G), mesenteric (Mes) LN (H), and spleen tissues (I). Frequency of NK cell and dendritic cell activation comparing pre- and post-infection is shown for axillary LN (J), mesenteric LN (K) and spleen tissues (L). Lines represent mean frequencies of the three animals and error bars represent the standard error of the mean. Longitudinal changes in total or activated (CD169+) cells in the peripheral blood (A–F) were analyzed using paired t tests where baseline (d0) was compared to the peak of the phenotype between 2 or 4 dpi; for this analysis, **** $p < 0.0001$, *** $p = 0.0001$, ** $p < 0.001$, * $p < 0.05$, ns $p > 0.05$. Statistical analyses for comparisons of baseline vs. 10 dpi cell phenotype frequencies in the lymphoid tissues (G–L) were completed using two-tailed paired t tests; only significant comparisons are shown, all other comparisons yielded ns p values > 0.05 .

Figure 6.S7. Flow cytometry gating strategy for monocyte/DC/NK panel.

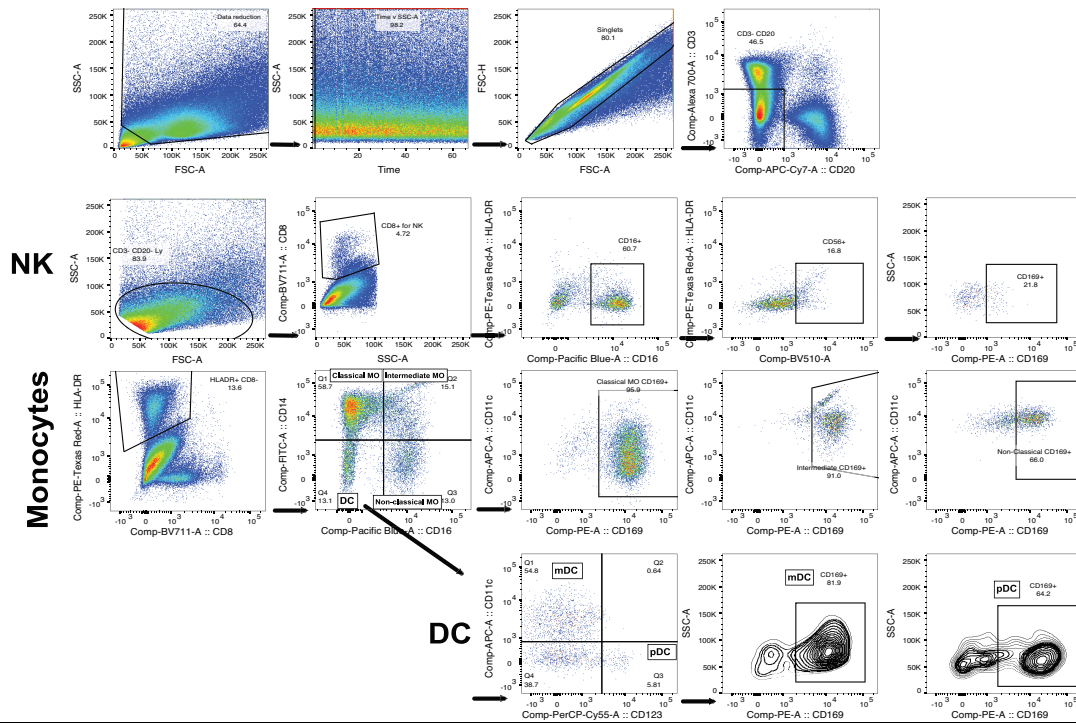


Figure 6.S7. Gating strategy for monocyte/DC/NK panel is shown. Monocytes and macrophages were defined as CD3-/CD20-/CD8-/HLA-DR+ with classical monocytes being CD16-/CD14+, intermediate monocytes being CD16+/CD14+, and non-classical monocytes being CD16+/CD14-. DCs were defined as CD3-/CD20-/CD8-/HLA-DR+/CD16-/CD14- with myeloid DCs being CD11c+/CD123- and plasmacytoid DCs being CD11c-/CD123+. Activated cells within each subset were defined as CD169+.

6.3.6 Proliferating T and B cell subsets dominate the early adaptive immune response to MAYV infection in rhesus macaques.

The adaptive arm of the immune system is activated during alphavirus infection leading to the production of functional antibodies and T cells. While T cells have been shown to control alphavirus-mediated infection and disease [438-440], anti-CHIKV CD4+ T cells have also been shown in mice to mediate joint disease [440, 441]. To characterize T cell frequency and phenotypic changes that occur in response to MAYV infection, we utilized flow cytometry for staining of longitudinal macaque PBMC from -28, 0-5, 7, and 10 dpi as well as lymphocyte preparations from lymph nodes and spleen collected at one month prior to infection and at 10 dpi (Figs 6.8 and 6.S8). Using a well-characterized panel of antibodies, we found that the overall frequencies of each of the CD4 and CD8 T cell subsets remained stable in the peripheral blood with no major changes

over time. While central memory (CM) CD4⁺ T cell proliferation (Ki67⁺) in peripheral blood increased at 2 dpi and again between 5 and 10 dpi (**Fig 6.8A**), only a slight increase in Ki67 staining was detected for the effector memory (EM) CD4⁺ T cells and less so for the naïve CD4⁺ T cell population. Proliferation of both CM and EM CD8⁺ T cell populations increased over time peaking at 7dpi (**Fig 6.8B**), which is consistent with previous published data for T cell proliferation in CHIKV-infected NHPs [40, 227]. Also in line with published data, there was a steady expansion of granzyme B positive EM CD4⁺ and CD8⁺ T cells with peak frequency values attained at 7 to 10 dpi (**Fig 6.8C and 6.8D**) [442]. In addition, the frequency of granzyme B positive naïve and CM CD4⁺ and CD8⁺ T cells also increased following MAYV infection with peak values detected between 7 and 10 dpi, depending upon the specific subtype (**Fig 6.8C and 6.8D**). In general, CD8⁺ CM and EM T cells isolated from the spleen, axillary LNs, and mesenteric LNs stained significantly higher for the proliferation marker Ki67 and for granzyme B at 10 dpi when compared with tissues from prior to infection (**Fig 6.8E-8J**). While CD4⁺ T cell granzyme B was lower than those observed for the CD8⁺ cells, the CD4⁺ CM and EM T cell populations also changed their frequency of Ki67 and granzyme B staining following infection but the responses were tissue and cell type specific with higher proliferation observed for cells derived from the axillary LN and spleen (**Fig 6.8E-8J**). Thus, these data demonstrate a robust cellular response following infection with MAYV.

Figure 6.8. Kinetics of T cell proliferation and granzyme B expression in peripheral blood and phenotype comparisons in lymphoid tissues pre- and post-MAYV infection.

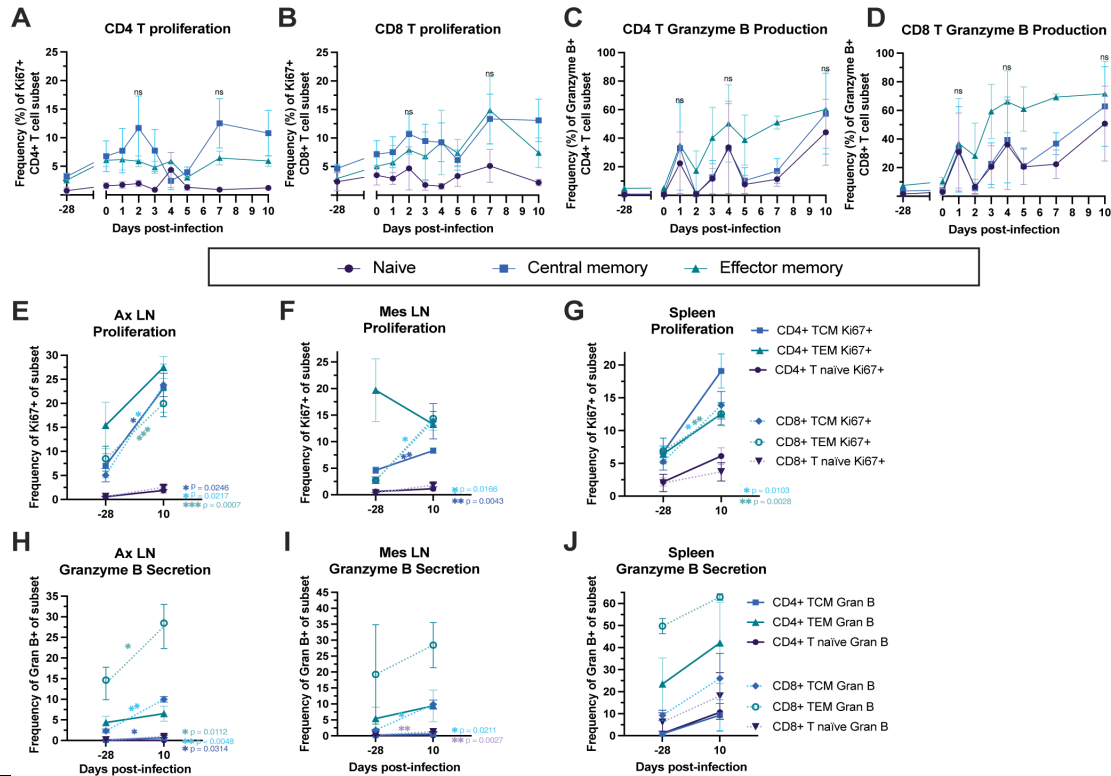


Figure 6.8. Macaque PBMC from -28, 0–5, 7, and 10 dpi (A–D) and lymphocytes isolated from three lymphoid tissues either one month prior to infection or 10 dpi (E–J) were analyzed for T cell phenotype using flow cytometry. Changes in the longitudinal frequency of proliferating naïve, central memory, and effector memory CD4+ T (A) and CD8+ T cells (B) as well as granzyme B expression (granzyme B+) by CD4+ T (C) and CD8+ T cells (D) are shown. We additionally compared proliferation of these same memory T cell subsets at baseline to 10 dpi in the axillary LN (E), mesenteric LN (F), and spleen (G). We finally compared frequencies of granzyme B positive CD4 and CD8 memory T cell subsets in the axillary LN (H), mesenteric LN (I) and spleen from baseline to 10 dpi as well (J). Lines represent mean frequencies of the three animals and error bars represent the standard error of the mean. Longitudinal changes in proliferating (Ki67+) or granzyme B+ T cell subsets in the peripheral blood (A–D) were analyzed using paired t tests where baseline (d0) was compared to the peak of the phenotype at 2–3 timepoints; for this analysis, ns (not significant) represents $p > 0.05$ for naïve, central memory, and effector memory T cell subsets. Statistical analyses for comparison of baseline to 10 dpi cell frequencies in the lymphoid tissues (E–J) were completed using two-tailed paired t tests; only significant comparisons are shown, all other comparisons yielded ns p values > 0.05 .

Flow cytometry was also used to characterize the B cell component of the adaptive immune response by measuring the kinetics of B cell subset expansion and proliferation (Ki67+) in peripheral blood and lymphoid tissues over the infection time course (6.S9 and 6.S8 Figs). Similar

to the T cell population frequency, no major changes in the total frequencies of naïve, marginal zone (MZ)-like, and memory B cell subsets were observed during the study period (6.S9A Fig) except for an expansion of proliferating MZ-like B cells that occurred between 5 and 10 dpi (6.S9B Fig). We did not detect major longitudinal changes in naïve or memory B cell proliferating subsets or proliferation of any B cell subsets in the axillary or mesenteric LNs (6.S9B-S9D Fig). However, we did identify an increase in proliferation of MZ-like B cells in axillary LN with a significant increase in cells from the spleen (Figs 6.9E and 6.S9C). Proliferation of memory B cells trended higher in the axillary LN and spleen following infection but not in cells from the mesenteric LN (6.S9C-S9E Fig). These data suggest that MZ-like B cells are activated and proliferating following MAYV infection in the peripheral blood and spleen, likely for preparation of downstream differentiation into antibody-secreting plasmablasts.

Figure 6.S8. Flow cytometry gating strategy for T and B cell panels.

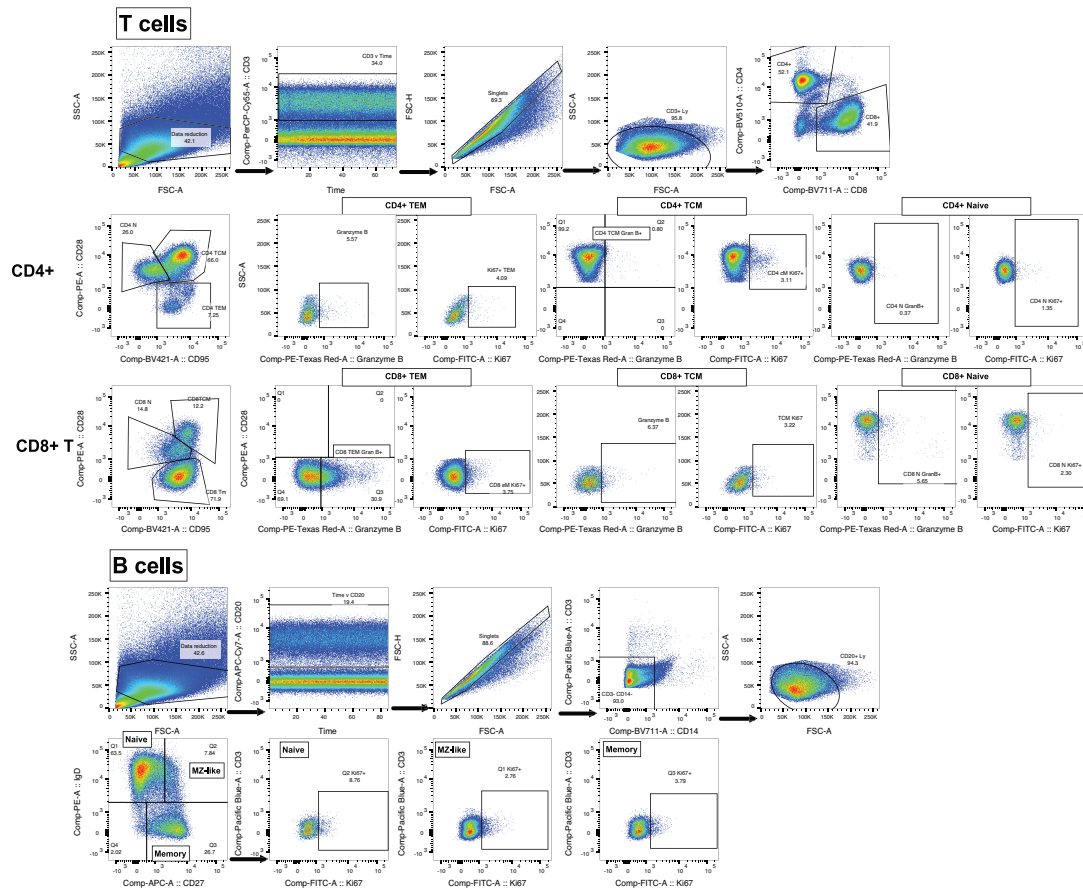


Figure 6.S8. Gating strategy for T and B cell panels are shown. Naïve CD4+ or CD8+ T cells were defined as CD28+/CD95-, central memory CD4+ or CD8+ T cells were defined as CD28+/CD95+, and effector memory

CD4+ or CD8+ T cells were defined as CD28-/CD95+. Naïve B cells were defined as IgD+/CD27-, MZ-like B cells were defined as IgD+/CD27+, and memory B cells were defined as IgD-/CD27+. Proliferating (Ki67+) T and B cells and granzyme B expressing (granzyme B+) T cells within each subset were also quantified using these gating schemes.

Figure 6.S9. B cell phenotype and proliferation in longitudinal peripheral blood and lymphoid tissues following MAYV infection.

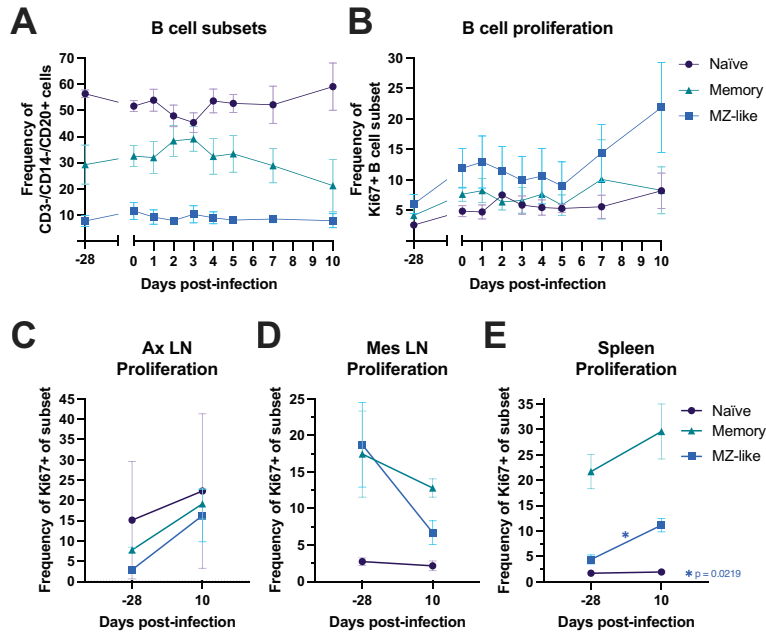


Figure 6.S9. Macaque PBMC from -28, 0–5, 7, and 10 dpi (A–B) and lymphocytes isolated from three lymphoid tissues either one month prior to infection or 10 dpi (C–E) were analyzed for B cell phenotype using flow cytometry. Changes in the total longitudinal frequency of naïve, memory, and MZ-like B cell subsets (A) as well as proliferation within these subsets (B) are quantified over time. B cell proliferation of these same subsets in the axillary LN (C), mesenteric LN (D), and spleen (E) is also compared at one month prior to and 10 dpi. Lines represent mean frequencies of the three animals and error bars represent the standard error of the mean. Longitudinal changes in total or proliferating (Ki67+) B cell subsets (A–B) relative to baseline (0 dpi) were compared to 7 or 10 dpi using paired t tests and yielded only p values > 0.05, ns, for naïve, marginal zone (MZ)-like, and memory B cell subsets. Statistical analyses for comparison of baseline to 10 dpi cell frequencies in the lymphoid tissues (C–E) were completed using two-tailed paired t tests; only significant comparisons are shown, all other comparisons yielded ns p values > 0.05.

To verify our immunology and pathogenesis findings at a global level, we performed RNAseq analysis of longitudinal PBMC samples. Differential expression (DE) analysis revealed that several genes involved in interferon signaling (i.e., IFI6, IFI44, ISG15), antiviral immunity (i.e., STAT2, PARP14, MX1), and negative regulation of viral replication (i.e., OAS1-3, RSAD2, MX1) were significantly upregulated at 2 dpi (**Fig 6.9A**), with $FDR_p < 0.05$ and $|FC| > 2$. If less stringent thresholds are used, other genes in these pathways such as IFIT1, IFNAR1, ISG15, and STAT1 are also differentially expressed ($FDR_p < 0.2$, $|FC| > 1.5$). The top 10 enriched DEGs between 0 and 2 dpi, all key players in the antiviral response, were PARP12, SLC38A5, DTX3L, OAS1/3, STAT2, DHX58, DDX60, AGRN, and SIGLEC1 ($FDR_p < 0.05$, $|FC| > 2$, ordered by FDR p-value) (**Fig 6.9B**). Similarly, Ingenuity Pathway Analysis (IPA) software identified changes in the enriched pathway signatures of both innate and adaptive immunity after MAYV infection. IPA also highlighted EIF2 signaling (translation modulation) to be tightly downregulated at 2 dpi while viral pathogenesis, interferon signaling, mTOR signaling, antiviral immune response, IL-12 signaling and production in macrophages, and B cell signaling pathways were among the top enriched upregulated pathways ($FDR_p < 0.2$, $|FC| > 1.5$) (**Fig 6.9C and 6.9D**). These conclusions were well supported when examining these aspects for the 0 and 3 dpi comparison as well (**6.S10 Fig**). Over-representation of these innate and adaptive immune pathways support our findings and suggest an important role for the interferon response and antiviral immune responses following MAYV infection (**Figs 6.6, 6.S6, 6.7, 6.8, and 6.S9**).

between 0 and 3 dpi (FDR p <0.2 and |FC|>1.5). Colors in all plots encode z-scores that are more upregulated in red/orange or more downregulated in blue.

6.3.7 Virus-specific antibodies are present as early as 5 dpi and expand in neutralization breadth by 10 dpi.

To interrogate humoral immune responses against MAYV, we measured the kinetics, magnitude, and breadth of antibody development following infection. Virus-specific IgM antibodies are typically present as early as 4 days post-infection but can persist for three months in humans [443-445]. In mice, evidence shows that CHIKV-specific IgM can be detected in serum as early as 2 dpi and CHIKV-specific IgG as early as 6 dpi, with both IgM and IgG anti-CHIKV antibodies having neutralizing abilities [53]. Consistent with these observations, we detected MAYV-specific IgM as well as IgG antibodies as early as 5 dpi in all three macaques (**Fig 6.10A**). Indeed, the IgM antibody response was more robust and initially increased more rapidly than IgG during this acute infection period, but the levels of antiviral IgG matched IgM by 10 dpi (**Fig 6.10A**). In a limiting dilution assay where we stimulated RM PBMC and screened supernatants by MAYV ELISAs, anti-MAYV antibody-secreting cells were detected with a similar frequency ($\sim 10^1$ cells / 10^6 PBMC) in all three animals at 10 dpi (**Fig 6.10B**). Furthermore, we utilized these same LDA supernatants in MAYV neutralization assays to compare the frequency of cells secreting MAYV-binding versus -neutralizing antibodies and found that these occur at about the same frequency (6 cells / 10^6 PBMC binding vs 10 cells / 10^6 PBMC neutralizing; $p=0.2703$) (**Fig 6.10B**). To interrogate the breadth of the MAYV-specific antibodies, we probed immunoblots of purified MAYV particle preparations with RM plasma from 0 and 10 dpi. Viral-envelope specific antibodies were detected in all RMs (**Fig 6.10C**). MAYV-neutralizing antibodies were detected as early as 5 dpi in all three macaques using plaque reduction neutralization assays (**Fig 6.10D**). These neutralizing antibody levels reached 50% plaque reduction neutralization titers (PRNT₅₀) of 3.5×10^3 - 4.6×10^4 by 10 dpi (**Fig 6.10D**). Finally, antiviral breadth of neutralizing antibodies was determined using plaque neutralization assays against additional Semliki Forest antigenic complex viruses including UNAV, CHIKV, O'nyong'nyong virus (ONNV), and Ross River virus (RRV) as well as Venezuelan equine encephalitis virus (VEEV) (**Fig 6.10E**). Pre-infection plasma was screened to ensure the absence of pre-existing cross-neutralizing antibodies, which were found to

be devoid of any neutralizing activity ($PRNT_{50} < 20$) against any of the viruses tested. At 10 dpi, cross-neutralizing antibodies were detected for UNA, CHIKV, ONNV, and RRV but not VEEV (Fig 6.10E). Cross-neutralization at 10 dpi was greatest against viruses more antigenically related to MAYV, which is visualized using antigenic cartography (Fig 6.10F). RM plasma clustered around MAYV due to highest neutralization potency with UNA, CHIKV, and ONNV positioned nearer to this cluster, but RRV and VEEV positioned further away due to little or no detectable neutralization against these viruses (Fig 6.10F). In summary, our findings indicate that MAYV-specific antibodies develop as early as 5 dpi and expand in both magnitude and breadth, with the capability to neutralize other related arthritogenic alphaviruses.

Figure 6.10. Characterization of MAYV-specific antibodies and analysis of cross-reactive breadth.

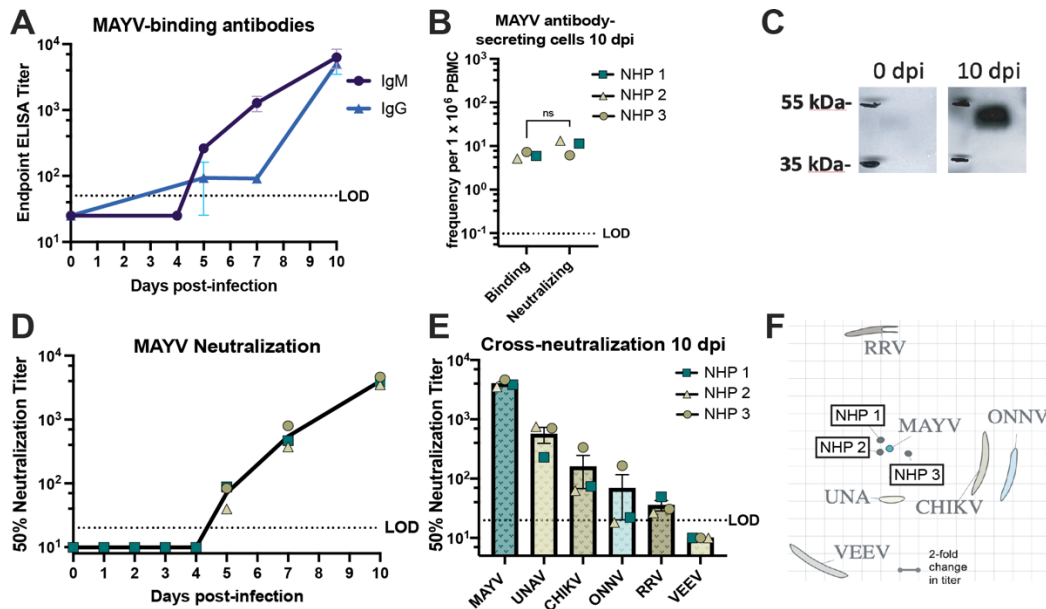


Figure 6.10. (A) The development of MAYV-binding, IgM and IgG isotype antibody titers were quantified in macaque plasma at 0, 5, 7, and 10 dpi in ELISA. The LOD was a 1:50 plasma dilution with undetectable values graphed as half the LOD. (B) The frequency of cells secreting MAYV binding or neutralizing antibodies were quantified in limiting dilution assays in which macaque PBMC from 10 dpi was stimulated with IL-2 and R848 and supernatants were screened in either MAYV ELISAs or MAYV neutralization assays. The LOD frequency was 0.01 cells per 1×10^6 PBMC. (C) The binding specificity of MAYV-specific antibodies was characterized in a western blot in which inactivated, purified MAYV was ran on a 4–12% Bis-Tris gel and probed with macaque plasma from 0 or 10 dpi. Blots from only one animal are shown but are representative for all three animals. (D) The longitudinal development of MAYV-neutralizing antibodies was quantified in MAYV neutralization assays using heat-inactivated macaque plasma at 0–5, 7, and 10 dpi. 50% plaque reduction neutralization titers ($PRNT_{50}$) were determined in non-linear regression. The LOD was a 1:20 plasma dilution and undetectable values were graphed as half of the LOD. (E) The breadth of antibodies that neutralized other relevant alphaviruses following MAYV

infection were characterized in cross-neutralization assays against UNAV, CHIKV, ONNV, RRV, and VEEV using heat-inactivated macaque plasma from 10 dpi. The LOD was a 1:20 plasma dilution and undetectable values were graphed as half of the LOD. (F) Antigenic cartography mapping the antigenic distances between viruses is used to visualize the cross-neutralization data. Error bars are SEM in (A) and (E). A paired t test was used to compare frequency of MBC secreting MAYV binding and neutralizing antibodies in (B).

Section 6.4: Discussion

MAYV is a virus endemic to Central and South America that is considered an emerging public health threat. While MAYV-specific therapeutics have been reported in the literature, their evaluation has been constricted to mouse models of infection due to lack of a fully defined NHP model. In this investigation, we characterized MAYV infection in rhesus macaques to better understand viral dissemination, pathogenesis and immunity. Before initiating our RM study, we compared the pathogenicity of MAYV strains and related UNAV in both immunocompetent and immunodeficient mice. While UNAV replicates more quickly in IFN α R^{-/-} mice leading to earlier demise when compared to the MAYV strains, we found that MAYV_{BeAr505411} infection resulted in the most robust viral replication in WT mice, which informed our strain selection for use in macaques. It should be noted that varying passage history of the MAYV strains used in our study may impact our conclusions regarding murine pathogenesis and strain selection. For example, MAYV_{TRVL} has been extensively passaged, which may have contributed to reduced virulence in mice. Nevertheless, our data supports increased pathogenesis of the MAYV_{BeAr505411} strain in mice relative to the other strains that were tested here. In 1967, MAYV-infected NHPs were reported to develop viremia lasting 4-5 days [224]. In our study, we explored the kinetics of MAYV viremia between 1 and 10 dpi, identifying the duration of viremia to be between 4 and 7 days with peak viral RNA levels occurring at 2 dpi. We isolated infectious virus from RM plasma from 1-4 dpi, suggesting that there is a brief window for blood-borne transmission. Future studies will be required to validate transmission potential and to evaluate disease presentation beyond the initial control of viremia.

In our study, we explored MAYV tissue tropism in a wide breadth of anatomical sites through quantification of viral genomes and qualification of inflammation via histopathology. Previously, the characterization of MAYV tissue tropism has been largely derived from infection in mouse models and mammalian cell lines [91, 289, 429, 446, 447]. Our study in NHPs indicated

that MAYV efficiently disseminated throughout major organ systems, infecting a broad range of muscles, joints, nerves, lobes of the brain, compartments of the heart, lymphoid tissues, and other primary organs. Our evidence of viral detection and lymphocyte aggregation near rare blood vessels of the heart and central nervous tissues is in agreement with experimental CHIKV infections CHIKV and clinical outcomes in patients infected with CHIKV [410, 411]. While we isolated infectious virus in multiple tissue types at 10 dpi, it is unclear whether this will lead to sustained viral replication in joints and muscles and/or be responsible for chronic disease symptoms in MAYV-infected humans. Robust MAYV viremia and widespread tissue distribution to the distal joints and muscles indicated that the virus is capable of causing disease in multiple tissues. While we did not detect overt clinical signs of arthritic or neurologic disease, there is potential for chronic disease development beyond 10 dpi in this model as evidenced by our viral detection data and pathological changes associated with infection.

A paucity of published data exists on the histopathology of MAYV in humans, presumably due to few cases causing mortality, difficulty in obtaining biopsy samples, and presence of other established diagnostics. This highlights the importance of elucidating the microscopic changes caused by MAYV in an animal model with high anatomic similarity to humans. Appurtenant to other techniques utilized, our study is the first to explore the pathology induced by MAYV infection in a broad range of rhesus macaque tissues, which has significant implications for understanding viral pathology in humans. Arenívar and colleagues have reported MAYV arthralgia to occur commonly in the hand, knee, ankle/foot, wrist, elbow, and shoulder in decreasing frequencies, which is a significant cause of disability in humans [448]. Equivalently, in the subacute period of infection, CHIKV frequently affects the distal joints of the limbs and may involve the elbows and knees [407]. Microscopic analysis of muscle and joint biopsies from alphavirus-infected patients has been employed for diagnosis in addition to molecular techniques. In CHIKV-infected humans, some of these microscopic findings have included synovial hyperplasia, muscle degeneration and necrosis, and mononuclear to mixed inflammation with indication of a change in cellular infiltration profiles between acute, subacute, and chronic infections [239, 449]. Of the extensive tissue sets sampled in our study, the fingers, wrists, ankles, and toes were the most consistent sites for inflammation and perivascular lymphocytic infiltration. Synovial and endothelial cell hyperplasia also occurred in these peripheral joints across the three animals. Similar findings were present in the knees of two animals and the elbows of one, which

is consistent with what has been noted for CHIKV infection in humans, NHPs, and mouse models [40]. Previous studies in multiple mouse strains have extensively characterized joint and muscle tissue inflammation following MAYV infection in the footpads [91, 289, 429]. Mimicking the results from our study, BALB/c mice displayed inflammatory infiltrates of the ligament, tendon, and muscle surrounding joints at 10 dpi [429]. Other studies have described vasculitis, mononuclear infiltration, polymorphonuclear cell infiltration, muscular necrosis and inflammation, and dermal edema [248] throughout the course of disease [415]. Despite investigation in only three animals, the consistent pathologic findings of inflammation in the peripheral joints of these rhesus macaques, in conjunction with viral detection, enhances our understanding of pathogenesis in an appropriate animal model. Taking into account alternative study designs with respect to timing, successive studies may supplement the musculoskeletal pathology information by inclusion of a larger subset of joints and muscles, including axial structures, to determine the extent of inflammation and screen for any potential tropism between appendicular versus axial structures.

Another discovery homologous with human MAYV infection was a maculopapular rash at 10 dpi spanning the caudal ventrum of NHP 3. In humans, papular to maculopapular rash described as variably pruritic typically presents on 5 dpi and generally lasts 3-7 days following onset [405]. Recorded spread of the rash is generally on the limbs and trunk [450, 451] and active replication of MAYV in human skin has been observed up to 4 days after infection [452]. In one macaque in our study, a rash was found at 10 dpi and was only able to be fully visualized with shaving, which would have precluded identification at any prior timepoints particularly given that pruritis was not a feature. The histologic picture matched the gross presentation with increased severity of lymphocytic dermatitis and epidermal hyperplasia in areas of macules and papules. Perivascular inflammation extended into distant areas of the integument on the thorax and were also found in one other animal. Maculopapular rash has not been reported in mice although it is possible it is missed without shaving the hair from these animals. Biopsies of human specimens are not widely conducted, potentially making the macaque a uniquely significant model for investigating dermatologic presentations of MAYV.

In our study, other sampled sites were recognized through the conjunction of histologic lesions and positive viral identification, which may offer promising insight into processes occurring in

humans. On routine microscopic evaluation, minimal to mild perivascular leukocytic aggregates spanned multiple organ systems. Influence of any potential age-related or incidental pre-existing lesions could not be definitively elucidated utilizing H&E-stained sections. However, in CHIKV infections in humans, it has been established that pre-existing chronic conditions are associated with increased inflammation and worsened disease [453, 454]. Future investigation into potential colocalization of viral particles and inflammatory or degenerative foci, which was not within the scope of this current study, would improve identification of lesion relevance.

The liver is a tissue of interest as it, along with the spleen, is considered a primary site of viral replication and the Pan American Health Organization recommends histologic and immunohistochemical analysis of both tissues [447, 455]. It was demonstrated that oxidative stress causes tissue damage in BALB/c mice, which manifests as polymorphonuclear hepatitis from 1 to 7 dpi [447]. As with other tissues, we observed a predominance of mononuclear inflammation in the liver of two rhesus macaques, with one having a pre-existing chronic hepatopathy. Though extensive determination of potential neurotropism in non-human primate species has yet to be carried out, MAYV possesses the ability to infect human neural cells with meningoencephalitis being described in rare human cases [456], and neurotropism has been demonstrated in both wild-type and immunocompromised mice [248]. We identified small leukocytic foci within different central and peripheral nervous system components between our experimental subjects, that was consistent with viral detection and these features bear additional probing as proposed for other tissues.

Coinciding with peak viremia at 2 dpi, we observed the elevation of proinflammatory cytokines and chemokines that have been associated with persistence of disease symptoms, although these responses could also play more of a protective role [11, 430]. It should be noted that we detected more limited levels of proinflammatory cytokine and chemokine responses in one animal (NHP 2) although other evidence of activation of innate immunity was present. In fact, a key component of innate immune activation that we characterized was the consistent activation of monocytes (classical, non-classical, intermediate), dendritic cells (myeloid and plasmacytoid) and NK cells between 2 and 4 dpi, which returned to baseline activation status by 10 dpi, closely mirroring viremia kinetics. To identify early adaptive immune responses, we used flow cytometry to detect changes in naïve and memory T cell population frequencies and capture their cytotoxic

and proliferative functions in response to MAYV infection. We identified CD4⁺ and CD8⁺ memory T cells with proliferative (Ki67⁺) and cytotoxic functions (granzyme B⁺) that expanded following infection, which makes it likely that they target MAYV-infected cells. However, we did not have access to a MAYV peptide library, but our future studies will characterize virus-specific T cell responses. Our transcriptomics data also indicates the robust activation of interferon responses coinciding with peak viremia as well as upregulation of pathways with antiviral effects, which is consistent with RNA-seq data for CHIKV infection comparing mouse and human gene expression profiles that showed similar signatures of immune activation [457-460]. Lastly, we characterized the timing of humoral immunity during acute infection, which indicated the presence of virus binding and neutralizing antibodies as early as 5 dpi, with breadth extending to similar arthritogenic alphaviruses as early as 10 dpi. We hypothesize that these cross-neutralizing antibody responses will expand in magnitude as the adaptive immune response develops beyond 10 dpi as we have observed in CHIKV-infected patients. Although antibody cross-reactivity within the SFV antigenic complex is well established, major questions remain regarding protective levels of cross-reactive antibody titers following infection and the duration of this immunity [59].

In this study, we were only able to explore MAYV pathogenesis and immunity in three macaques. With a small animal number, it is difficult to capture the spectrum of disease, although, many of our virologic, immunologic and histologic findings were consistent among all three animals. Limited tissue sampling could bias tissue viral load and histologic analyses as the whole tissue cannot be assayed in entirety, which is a limitation that should be considered when interpreting the tissue viral load and pathology data. Sex and age-related variation are two additional variables that were not addressed in this study due to small animal number but are variables that have been found to impact CHIKV disease [227, 461, 462]. Future MAYV NHP studies should explore both a shorter study duration to capture acute tissue viral loads and examine tissue-resident inflammatory immune responses as well as a longer study duration to understand long term kinetics and duration of homotypic and heterotypic adaptive immunity. This study establishes an MAYV infection model in NHP that contributes to our understanding of pathogenesis and immunity that could be used for the evaluation of MAYV-specific vaccines, monoclonal antibody therapies, and antivirals.

Section 6.5: Materials & Methods

6.5.1 Ethics statement

Mice were housed in the ABSL-3 facility at the Vaccine and Gene Therapy Institute (VGTI) of Oregon Health and Science University (OHSU) in ventilated racks with open access to food and water with a 12-hour light/dark cycle. Mouse experiments were performed in compliance with the Oregon Health and Science University (OHSU) Institutional Animal Care and Use Committee (IACUC Protocol #0913). Rhesus macaque studies were performed in an ABSL-2 facility at the Oregon National Primate Research Center (ONPRC) (IACUC #0993). Both facilities are accredited by the Association for Accreditation and Assessment of Laboratory Animal Care (AALAC) International. Mouse and macaque experiments were performed in compliance with good animal practices outlined by local and national welfare bodies and all efforts were made to reduce pain, distress, and discomfort experience by the animals when possible. When possible, rhesus macaques were housed in pairs with visual and auditory contact of other animals for social interaction and enrichment. Animals were fed standard chow supplemented with food enrichment. Animals were euthanized according to the recommendations of the American Veterinary Medical Association 2013 Panel on Euthanasia.

6.5.2 Cells and viruses

Vero cells (ATCC CCL-81) were propagated at 37°C and 5% CO₂ in Dulbecco's Modified Eagle Medium (DMEM; Thermo Scientific) containing 5% fetal calf serum (FCS; Thermo Scientific) supplemented with 1X penicillin-streptomycin-glutamine (PSG; Life Technologies). *Aedes albopictus* C6/36 cells (ATCC CRL1660) were grown at 28°C with 5% CO₂ in DMEM containing 5% FCS and 1X PSG. Alphaviruses MAYV_{BeAr505411} (NR-49910), MAYV_{Guyane} (NR-49911), MAYV_{TRVL4675} (NR-49913), MAYV_{Uruma} (NR-49914), UNAV_{MAC150} (NR-49912), ONNV_{UgMP30} (NR-51661), RRV_{T-48} (NR-51457) and VEEV_{TC-83} (NR-63) were obtained through BEI Resources. MAYV_{CH} was generated from an infectious clone provided by Dr. Thomas Morrison (University of Colorado Denver) and CHIKV_{181/25} was generated from an infectious clone as previously described [112]. Viruses were propagated in *Aedes albopictus* C6/36 cells. At 72 hours post-infection (hpi), clarified culture supernatants were pelleted through a 10% sorbitol cushion by ultracentrifugation at 82,755 x g for 70 minutes. The viral pellets were resuspended in PBS, aliquoted, and frozen at -80°C. Virus was tittered by limiting dilution plaque assays using

confluent monolayers of Vero E6 cells. Infected cells were rocked continuously for 2 hours at 37°C and overlaid with CMC-DMEM supplemented with 5% FBS, 1X PSG, and 0.3% high / 0.3% low viscosity carboxymethylcellulose (CMC; Sigma). Plaque assays for MAYV, UNA, RRV and VEEV were fixed with 3.7% formaldehyde and stained with 0.2% methylene blue at 48 hpi; and the plaque assays for CHIKV and ONNV were fixed and stained at 72 hpi. Plaques were enumerated under a light microscope and titers of viral stocks were determined. Virus stocks used for all lab experiments were either passage 1 or 2, although passage history at BEI prior to arrival in the lab does vary by strain and has been presented previously in a table for the MAYV strains by Powers 2006 *et al.* [315].

6.5.3 Mouse experiments

C57BL/6 mice were purchased from Jackson Laboratories and interferon alpha receptor knockout (IFN α R $^{-/-}$) mice originated from the OHSU/VGTI established breeding colony. MAYV and UNAV infections were performed in 4-week-old female C57BL/6 mice (n=5 per virus group) and 13-week-old male and female IFN α R $^{-/-}$ mice (n=4 per virus group). Mice were inoculated subcutaneously in the right footpad with 20 μ L containing 10⁴ plaque forming units (PFU) of MAYV_{BeAr505411} (NR-49910), MAYV_{CH}, MAYV_{Guyane} (NR-49911), MAYV_{TRVL4675} (NR-49913), MAYV_{Uruma} (NR-49914), or UNAV_{MAC150} (NR-49912). Infected C57BL/6 mice were bled at 2 days post-infection (dpi) to quantify the level of viremia in serum collected from clotted blood samples. These mice were euthanized by isoflurane overdose at 5 dpi to assess viral burden in ankle, calf, quad, spleen, brain, and heart tissues. IFN α R $^{-/-}$ mice were bled at 1 dpi to quantify the levels of serum viremia; body weight, survival, and ipsilateral footpad swelling measurements were recorded daily. IFN α R $^{-/-}$ mice were euthanized when 20% of body weight had been lost.

6.5.4 Nonhuman primate experiments

Three adult male rhesus macaques (*Macaca mulatta*) ages 4, 10 and 13 years were included in this study. Animals were sedated prior to any procedure. Lymphoid organ biopsies (axillary and mesenteric lymph nodes, and spleen) and blood were surgically collected at 28 days prior to infection [463-465]. Animals were infected with 10⁵ plaque forming units (PFU) of MAYV diluted in 1mL of PBS through 100 μ L subcutaneous injections in both of the arms and hands in an attempt to mimic virus inoculation through the bite of an infected mosquito. Animals were fed standard monkey chow with routine food supplements for enrichment. The animals were monitored daily

for clinical signs of disease and discomfort. Temperature and body weight were measured on the days on which peripheral blood and urine samples were collected (0, 1-5, 7, and 10 dpi). Blood was collected for monitoring by both complete blood count and serum chemistry analyses and analytes were compared to standard reference ranges [466]. Whole blood was layered over lymphocyte separation medium (Corning) and centrifuged for 30 minutes at 2,000 rpm for plasma and peripheral blood mononuclear cell (PBMC) isolation. PBMC were washed in RPMI medium (Fisher) supplemented with 5% FBS and 1X PSG. Rhesus macaques were humanely euthanized at 10 dpi and complete necropsies were performed. Representative tissue sections (~1cm³) from joint, muscle, lymphoid, major organs, nervous system, and reproductive tissue were collected into 1mL TRIzol reagent (Invitrogen) for RNA isolation or fixed in 10% formalin for histopathology. When appropriate, right and left tissues (i.e., fingers, toes, quadriceps, triceps, etc.) were combined for RNA analysis. An additional section from each tissue was preserved in RNAlater.

6.5.5 Histopathological analysis

A wide range of tissues were collected at necropsy for histologic analysis, which underwent fixation in 10% neutral buffered formalin for 24 hours and then 80% ethanol, stored at 4°C, for 24-72 hours followed by routine processing, sectioning at 5 µm, and staining with hematoxylin and eosin (HE). Slides were assessed on Leica DFV495 light microscopes by two board-certified veterinary pathologists and were scanned with a Leica Aperio AT2 slide scanner for creation of digital images. Presence and relative intensity of lymphocytic inflammation was graded based on a scale of - to +++ (**Tables 6.2 and 6.S1**) within all non-hematopoietic tissues. Lower scores (+) indicated one small aggregate of perivascular lymphocytes and ranged up to inflammation affecting the majority of blood vessels, in small to moderate numbers, with or without infiltration into the surrounding tissue (**Tables 6.2 and 6.S1**). Any additional pathologic diagnoses were included in these tables as well as separately for the hematopoietic tissues (**6.S2 Table**).

6.5.6 Viral RNA detection

Mouse tissues were homogenized in 1mL of 1X PBS with approximately 250µL of silica beads (VWR 48300-437) using a bead beater for three cycles of 45 seconds on and 30 seconds off (Precellys 24 homogenizer, Bertin Technologies). Samples were centrifuged at 5,000 rpm for 5 minutes in a microfuge to remove cellular debris, and 300µL of each homogenate was removed for RNA isolation. Nucleic acids from mouse tissues were isolated using the Promega Maxwell 48

sample RSC automated purification system and the Maxwell RSC Viral TNA extraction kit (Promega). Total nucleic acids were resuspended in 60µL of RNase free water. RM tissue samples were homogenized in 1mL of TRIzol reagent (Invitrogen) with approximately 250µL of silica beads using a Precellys 24 homogenizer bead beater as described above. Samples were centrifuged at 5,000 rpm for 5 minutes to remove cellular debris. Total RNA was isolated from either 200µL of homogenized tissue or 200µL of plasma or urine using a Direct-zol RNA Miniprep Plus kit (Zymo Research) following the manufacturer instructions. Total RNA was resuspended in 50µL of RNase-free water. Prepared RNA was quantified using a Nanodrop and diluted to 100ng/µL. Contaminating DNA was removed from all of the RNA samples by digestion with ezDNase (ThermoFisher). Single stranded cDNA was generated from 1µg of total RNA using random hexamers and reverse transcriptase Superscript IV (Invitrogen) following the manufacturer's protocol. Gene amplicons served as quantification standards. The following primers and probe were used to detect MAYV RNA: Forward- CCATGCCGTAACGATTGC, Reverse-CTTCCAGGCTGCCCGGCACCAT, and probe FAM- TGGACACCGTTCGATAC – MGB. The following primers and probe were used to detect UNAV RNA: Forward- GAAGCTTTTGTCTCCGGTGAA, Reverse-ATGACAATGGCCCGAATATGA, and Probe- FAM-TGAATGTCGCTGGGACT – MGB. Quantitative RT-PCR was performed on a QuantStudio 7 Flex Real-Time PCR system. All data was analyzed using Applied Biosystems QuantStudio 6 and 7 Flex Real-time PCR System software. For mouse tissues, viral RNA levels were normalized to a murine housekeeping gene, ribosomal protein RPS17. Viral RNA levels in RM tissues and blood were reported per µg of input RNA. All qRT-PCR reactions were performed in triplicate.

6.5.7 Quantification and isolation of infectious virus

Limiting dilution plaque assays were used to quantify viral loads in tissues and blood. For this assay, aliquots of 20µL of tissue homogenate, tissue culture supernatant, or mouse serum were serially diluted 10-fold in DMEM containing 5% FBS and 1X PSG, which was added to confluent monolayers of Vero cells in 48-well plates. The plates were rocked for 2 hours at 37°C and then CMC-DMEM was added to each well. At 2 dpi, the plates were fixed with 3.7% formaldehyde and stained with 0.2% methylene blue for microscopic visualization and enumeration of the plaques.

Isolation of MAYV from mouse tissues was carried out as previously described [91]. MAYV was isolated from NHP plasma and tissues as previously described for CHIKV [40]. Briefly, tissues were collected in 1mL of 1X PBS containing approximately 250µL of silica beads (VWR 48300-437) and homogenized using a bead beater for three cycles of 45 seconds on and 30 seconds off (Precellys 24 homogenizer, Bertin Technologies). Samples were centrifuged at 5,000 rpm for 5 minutes to remove cellular debris, sterile-filtered (0.22µM filter), and 400µL was used to infect a T25 flask of confluent C6/36 cells. At 3 dpi, supernatants were collected from C6/36 cultures and tittered in triplicate by limiting dilution plaque assays on Vero E6 cells as described above. Samples were considered positive for infectious virus if one or more plaques were detected, providing a limit of detection of 3.3 PFU/mL of cellular supernatant.

6.5.8 Transcriptomic analysis

Total RNA from rhesus macaque PBMC isolated using the TRIzol extraction method described above was prepared for transcriptomic analysis using the Illumina TruSeq Stranded mRNA Library Prep Kit (RS-122-2101, Illumina) as previously described [467]. The library was validated using an Agilent DNA 1000 kit on a bioanalyzer. Samples were sequenced by the OHSU Massively Parallel Sequencing Shared Resource using an Illumina NovaSeq.

Differential expression analysis was performed by the ONPRC Bioinformatics & Biostatistics Core. The quality of the raw sequencing files was evaluated using FastQC [468] combined with MultiQC [469] (<http://multiqc.info/>). Trimmomatic [470] was used to remove any remaining Illumina adapters. Reads were aligned to Ensembl's Mmul_10 genome along with its corresponding annotation, release 109. The program STAR [471] (v2.7.10b_alpha_220111) was used to align the reads to the genome. STAR has been shown to perform well compared to other RNA-seq aligners^[472]. Since STAR utilizes the gene annotation file, it also calculated the number of reads aligned to each gene. RNA-SeQC [473] and another round of MultiQC were utilized to ensure alignments were of sufficient quality.

Gene-level raw counts were filtered to remove genes with extremely low counts in many samples following the published guidelines [474], normalized using the trimmed mean of M-values method (TMM) [475], and transformed to log-counts per million with associated observational precision weights using the voom method [476]. Gene-wise linear models with primary variable day after

infection, and accounting for within subject correlation, were employed for differential expression analyses using limma with empirical Bayes moderation [477] and false discovery rate (FDR) adjustment [478]. Differential expression data were analyzed through the use of IPA (QIAGEN Inc., <https://www.qiagenbioinformatics.com/products/ingenuity-pathway-analysis>), using a stringent cutoff for significant molecules of $FDR_p < 0.2$ and $|FC| > 1.5$. The background reference set used was the dataset of all genes in the differential analysis.

6.5.9 Neutralization assays

RM plasma was heat inactivated for 30 minutes at 56°C and serially diluted in DMEM supplemented with 5% FBS and 1X PSG. Diluted plasma was mixed with media containing approximately 70-120 plaque forming units of MAYV_{BeAr505411}, CHIKV_{181/25}, UNAV_{Mac150}, ONNV_{UgMP30}, RRV_{T-48}, or VEEV_{TC-83}. Samples containing plasma and virus were incubated for 2 hours at 37°C with 5% CO₂ with continuous rocking and then transferred to 12-well plates of confluent Vero cells. Plates were incubated for an additional 2 hours at 37°C with continuous rocking followed by addition of a CMC-DMEM overlay. Plates were incubated 48 hours for MAYV, UNAV, RRV and VEEV or 72 hours for CHIKV and ONNV, then cells were fixed and stained as described above. The 50% plaque neutralization titers (PRNT₅₀) were calculated by non-linear regression analysis using GraphPad Prism 9 software after determining the percent of plaques at each dilution relative to control wells containing no plasma.

6.5.10 Antigenic cartography

The antigenic cartography plot to visualize alphavirus cross-neutralization following MAYV NHP infection was assembled as previously described [329, 336] and implemented using the Acmacs Web Cherry platform (<https://acmacs-web.antigenic-cartography.org/>). To ultimately construct the antigenic map, a table of calculated antigenic distances (D_{ij}) between each viral antigen (i) and plasma sample (j) using plasma titers for each plasma-titer pair (N_{ij}) is generated. To calculate table distance, the titer against the best neutralized virus for that plasma sample is defined as b_i and the distances from each virus for that plasma are calculated as $D_{ij} = \log_2(b_i) - \log(N_{ij})$. For the highest neutralization titer for a plasma sample, $N_{ij} = b_i$, and the distance will be equal to 0. For the remaining plasma-virus pairs, table distance D_{ij} is equivalent to the fold-difference in titer between b_{ij} and N_{ij} . Euclidean map distance (d_{ij}) for each plasma-virus pair is found by minimizing the error between the table distance D_{ij} and map distance, d_{ij} , using the error function $E =$

$\sum_{ij} e(D_{ij}, d_{ij})$, where $e(D_{ij}, d_{ij}) = (D_{ij} - d_{ij})^2$ when the neutralization titer is detectable or above 1:20. For instances where no detectable plasma neutralization titer is observed for a virus with neutralization titers <1:20, values of 19 are entered and the error is defined as $e(D_{ij}, d_{ij}) = (D_{ij} - 1 - d_{ij})^2 / (1 + e^{-10(D_{ij} - 1 - d_{ij})})$. To make a map and derive d_{ij} for each plasma-virus pair, viruses and plasma samples are assigned random starting coordinates and the error function is minimized using the conjugate gradient optimization method. Each square grid line on the antigenic map represents a two-fold change in plasma neutralization titer.

6.5.11 Enzyme-linked immunoassays (ELISA)

Purified MAYV_{BeAr505411} was inactivated at 56°C for 30 minutes, diluted in 1X PBS, and 5×10^8 plaque forming units (PFU) were added to each well of 96-well high binding plates (Corning) and incubated for 4 days at 4°C. To detect total IgG by ELISA for limiting dilution assays described below, a goat anti-human IgG (H+L) coating antibody (Jackson Immuno Research) was diluted in 1X PBS and added to the 96-well high binding plates at 1 µg/mL. Plates were washed with ELISA wash buffer (0.05% Tween-20, 1X PBS) and blocked for 1 hour with ELISA wash buffer containing 5% milk. The plates were washed with ELISA buffer and then 100 µL of 1:3 serial dilutions of heat-inactivated RM plasma were added and incubated for 1 hour. Plates were washed with ELISA wash buffer before secondary anti-monkey IgG or IgM (H+L) HRP-conjugated detection antibodies (Rockland) were diluted 1:5,000 and added to appropriate plates. Plates were washed, developed with OPD substrate buffer (0.05M citrate, 0.4 mg/mL o-phenylenediamine, 0.01% hydrogen peroxide, pH 5), and reactions were stopped with 1M HCl. A BioTek plate reader was used to read plates at 490nm. Log-log transformation of the linear portion of the curve was performed and 0.1 OD units was the cut-off point to calculate end point titers.

6.5.12 Limiting dilution assay for quantification of MAYV antibody-secreting cell frequency

Limiting dilution assays (LDA) to characterize the frequency of antibody-secreting cells, previously defined as memory B cells, were carried out as previously described [479]. Briefly, RM PBMC collected at 10 days post-infection (dpi) were resuspended in Roswell Park Memorial Institute (RPMI) 1640 medium supplemented with 5% FBS and 1X PSG. We chose not to refer to cells in our assay at 10 dpi as memory B cells because at this time following infection, this may

also include more premature plasmablasts. Two-fold serial dilutions of PBMC were added to a 96-well round-bottom plate; the top row contained 3-5x10⁵ PBMC per well. Next, 100µL of RPMI stimulation media containing 5% FBS, 1X PSG, 2.5 µg/mL R848 (InvivoGen), and 1000 U/mL IL-2 (Prospec) was added to each well with the exception of an unstimulated control column containing PBMC only. The 96-well plates were incubated for 7 days at 37°C with 5% CO₂, and then culture supernatants were collected for analysis by IgG ELISA detecting either total IgG (to determine the frequency of antibody producing cells) or MAYV proteins (to determine the frequency of viral antigen specific antibody producing cells) [335]. The supernatants from unstimulated PBMC served to normalize against background absorbance values. LDA supernatants were also collected for quantification of cells secreting MAYV-neutralizing antibodies. For these assays, remaining LDA supernatants were used in MAYV_{BeAr505411} neutralization assays as described above with approximately 80µL of supernatant serving in place of plasma. Neutralization in each individual well was calculated relative to a well containing MAYV only, with no LDA supernatant. Wells exhibiting 50% or greater neutralization relative to the control well were determined to be positive for neutralizing activity. The percentage of negative wells (below 50% neutralization) vs cell count in each row was graphed to calculate the frequency of cells secreting MAYV-neutralizing antibodies.

6.5.13 Plasma cytokine and chemokine analysis

The macaque inflammatory cytokine profile was characterized using a Cytokine Monkey Magnetic 29-plex Panel for Luminex Platform Kit (Invitrogen) according to the manufacturer's instructions using a 7-point standard curve. First, 25µL of RM plasma was incubated for 2 hours with beads and then washed and labeled with a biotinylated antibody for 1 hour. Beads were washed and incubated with R-Phycoerythrin conjugated to streptavidin for 30 minutes, then washed for a final time. Inflammatory cytokine levels were then quantified using a Luminex 200 Detection system (Luminex).

6.5.14 Lymphocyte phenotypic analysis

RM lymphocytes isolated from peripheral blood, spleen and lymph nodes and spleen were thawed and resuspended in RPMI medium supplemented with 10% FBS and 1X PSG. Cells were pelleted by centrifugation (2,000 rpm) and washed with 1X PBS and approximately one million cells were aliquoted for each of three panels for phenotypic analysis by flow cytometry. For T cell analysis,

cells were stained for cellular differentiation markers CD3, CD4, CD8, CD25, CD28, CD95, CD127, and intracellular Ki67 using fluorophore-conjugated antibodies. Naïve CD4⁺ or CD8⁺ T cells were defined as CD28⁺/CD95⁻, central memory CD4⁺ or CD8⁺ T cells were defined as CD28⁺/CD95⁺, and effector memory CD4⁺ or CD8⁺ T cells were defined as CD28⁻/CD95⁺. For B cell analysis, cells were stained with fluorophore-conjugated antibodies directed against CD3, CD20, CD27, CD14, IgD, and intracellular Ki67. Naïve B cells were defined as IgD⁺/CD27⁻, MZ-like B cells were defined as IgD⁺/CD27⁺, and memory B cells were defined as IgD⁻/CD27⁺. For innate immune cell analysis, cells were stained with CD3, CD8, CD14, CD16, CD11c, HLA-DR, CD56, CD123, and CD169 used as a marker for cellular activation. Monocytes and macrophages were defined as CD3⁻/CD20⁻/CD8⁻/HLA-DR⁺ with classical monocytes being CD16⁻/CD14⁺, intermediate monocytes being CD16⁺/CD14⁺, and non-classical monocytes being CD16⁺/CD14⁻. Dendritic cells (DCs) were defined as CD3⁻/CD20⁻/CD8⁻/HLA-DR⁺/CD16⁻/CD14⁻ with myeloid DCs being CD11c⁺/CD123⁻ and plasmacytoid DCs being CD11c⁻/CD123⁺. Sample analysis was performed using an LSRII instrument (BD Pharmingen) and analyzed with FlowJo Version 10 software.

6.5.15 Western blot analysis

Purified MAYV_{BeAr505411} proteins were separated by SDS-PAGE using 4-12% Bis-Tris polyacrylamide gels (Invitrogen) and loading (5×10^9 plaque forming units/lane). Proteins were transferred to an activated PVDF membrane (Millipore) using a semi-dry transfer system (30 minutes at 25V). Membranes were blocked with 3% BSA/TBST for 1 hour and probed with a 1:250 dilution of primary RM plasma from 0 or 10 dpi. Membranes were washed with TBST and probed with a secondary IgG anti-monkey, HRP conjugated antibody (Rockland) diluted 1:10,000. Membranes were washed a final time and developed in a Pico luminescence developer solution (ThermoFisher) and exposed on X-ray film.

6.5.16 Statistical analysis

Statistics and graphs were created with GraphPad Prism 9. A one-way ANOVA was used to compare means of viral RNA and viral titers levels between groups of mice infected with the different strains of MAYV. Neutralizing antibody titers were calculated using normalized variable slope non-linear regression with upper and lower limits of 100 and 0, respectively. Paired t tests

were used to compare cell phenotype changes and cytokine levels at various timepoints to baseline (0 dpi).

Section 6.6: Acknowledgements

The following reagents were obtained through BEI Resources, NIAID, NIH, as part of the WRCEVA program: MAYV_{BeAr505411} (NR-49910), MAYV_{Guyane} (NR-49911), MAYV_{TRVL4675} (NR-49913), MAYV_{Uruma} (NR-49914), UNAV_{MAC150} (NR-49912), ONNV_{UgMP30} (NR-51661), RRV_{T-48} (NR-51457) and VEEV_{TC-83} (NR-63). The authors thank Drs. Scott Hansen, David Morrow, Andrew Sylwester, and Eric McDonald for assistance with flow cytometry. The authors acknowledge the Integrated Pathology Core at the Oregon National Primate Research Center (ONPRC), which is supported by NIH Awards P51 OD 011092 and 1S10OD025002-01, for preparation and scanning of histologic slides. For contribution to the transcriptomics and RNAseq analysis, the authors acknowledge the support of the OHSU Massively Parallel Sequencing Shared Resource (MPSSR) as well as the ONPRC Bioinformatics & Biostatistics Core, which is funded in part by NIH grant OD P51 OD011092.

Appendix I: The alphavirus neutralizing antibody breadth is shaped by primary antigen exposure

Status: Ongoing collaboration with no immediate publication plans

Whitney C. Weber^{1,2}, Takeshi Andoh¹, Amy Morrison³, Lark Coffey³, and Daniel N. Streblow^{1,2#}

¹ Vaccine & Gene Therapy Institute, Oregon Health & Science University, Beaverton, Oregon, USA

² Division of Pathobiology & Immunology, Oregon National Primate Research Center, Beaverton, Oregon, USA

³ Division of Neurology, Oregon National Primate Research Center, Beaverton, Oregon, USA

#Address correspondence to Daniel N. Streblow, streblow@ohsu.edu

Section A1.1: Abstract

Alphaviruses and other arboviruses circulate in overlapping sylvatic transmission cycles in several regions around the world, leaving human populations at high risk and susceptibility to many viral infections due to spillover events. For example, ONNV and CHIKV overlap in circulation in Africa and CHIKV and RRV overlap in SE Asia. In the Amazon region of South America, MAYV, VEEV, CHIKV, and UNAV overlap in circulation. Although alphavirus cross-neutralization is well documented in the literature within the Semliki Forest complex, there are gaps in knowledge regarding the way the which the cross-neutralizing antibody breadth is shaped by alphavirus infection. To interrogate this question, we infected immunocompetent mice with five different arthritogenic alphaviruses then characterized the neutralizing antibody potency and breadth against homotypic and heterotypic alphaviruses in 50% plaque reduction neutralization assays (PRNT₅₀). Additionally, we utilized 30 human sera collected in Iquitos, Peru, in hopes of identifying seropositivity to more than one alphavirus. Iquitos is the largest urban center (~400,000 people) in the Peruvian Amazon, an epidemiological island only accessible by boat or air, nevertheless susceptible to circulation of multiple alphaviruses as well as other arboviruses. To characterize alphavirus circulation in and around Iquitos, we leveraged samples from a 2016-2018 community-based cohort study for *Aedes*-borne viruses (ABV). We identified one individual with evidence of experiencing both MAYV and VEEV infections due to equivalent PRNT₅₀s >1000 against each of these viruses as well as antibodies that cross-neutralized UNAV, CHIKV, RRV, and ONNV. Overall between the mouse experiments and characterization of human immune sera, we have

been able to reveal a collection of contexts in which the alphavirus cross-neutralizing antibody breadth is shaped by alphavirus infection exposure(s). These findings have applications for predicting how immunity may be shaped to related viruses after alphavirus infection or CHIKV vaccination.

Figure A1.1. Alphavirus infection in mice shapes the cross-neutralizing antibody breadth.

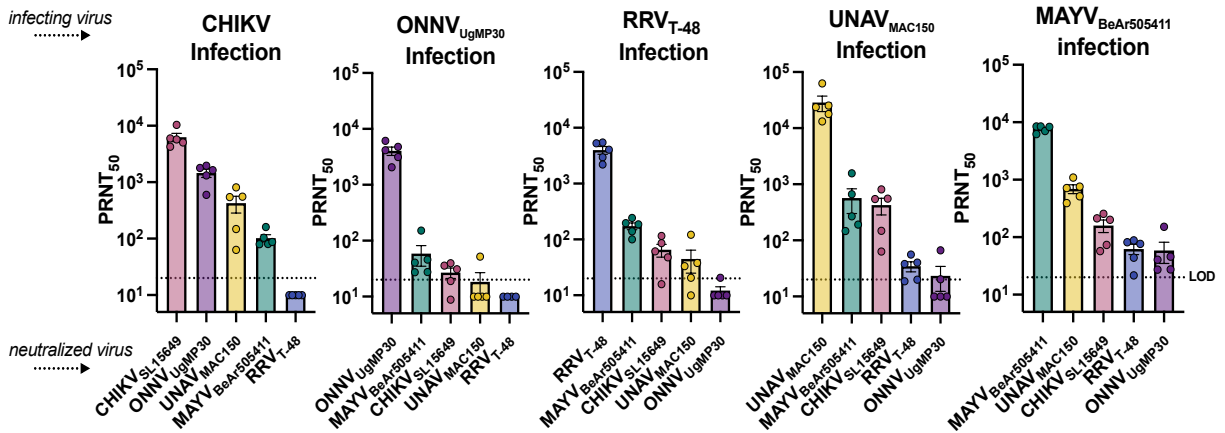


Figure A1.1. Female C57BL/6 mice ($n= 5/\text{group}$) were challenged in the right footpad (s.c.) with 10^4 PFU of MAYV, 10^4 PFU of UNAV, 10^3 PFU of CHIKV, 10^4 PFU of RRV, or 10^7 PFU of ONNV. At 43 days post-infection (dpi), serum was collected from these animals in used in both homotypic and heterotypic neutralization assays against CHIKV, ONNV, MAYV, UNAV, and RRV. Mice were challenged and euthanized by Takeshi Andoh. Serum samples were collected by Takeshi Andoh. Serum samples were processed and used in cross-neutralization assays, and data was analyzed (Whitney Weber).

Figure A1.2. Evidence of infection-elicited neutralizing antibodies against VEEV and MAYV and cross-neutralizing antibodies against related alphaviruses in an individual residing in Iquitos, Peru.

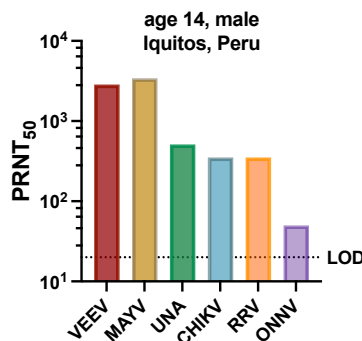


Figure A1.2. Patient serum collected in 2018 (Insect repellent trial in Iquitos, Peru) was tested for neutralization breadth by PRNT₅₀ assay and determined to be highly reactive against VEEV and MAYV with cross reactivity against UNA, CHIKV, RRV, and ONNV. Of the thirty samples screened for nAb in this batch of serum, this was the only positive sample for any alphavirus we screened against. Serum provided by Amy Morrison and Lark Coffey. Neutralization assays conducted and analyzed by Whitney Weber.

Section A1.2: Acknowledgements

Thank you to the study participants who volunteered their time and blood samples to be part of the study. Thank you to Amy Morrison, PhD, and her team for engaging in this community in Iquitos and collecting and processing blood samples. Thank you to Lark Coffey, PhD, and Adam Moore for coordinating sharing these samples with our lab at OHSU.

Appendix II: Development of mouse models of lethal arthritogenic alphavirus infection for evaluation of vaccine-elicited protection

Status: Ongoing collaboration with no immediate publication plans

Whitney C. Weber^{1,2}, Takeshi F. Andoh^{1,2}, Hans-Peter Raué³, Michael Denton^{1,2}, Mark K. Slifka³, and Daniel N. Streblow^{1,2#}

¹ Vaccine & Gene Therapy Institute, Oregon Health & Science University, Beaverton, Oregon, USA

² Division of Pathobiology & Immunology, Oregon National Primate Research Center, Beaverton, Oregon, USA

³ Division of Neurology, Oregon National Primate Research Center, Beaverton, Oregon, USA

#Address correspondence to Daniel N. Streblow, streblow@ohsu.edu

Section A2.1: Abstract

Alphaviruses are emerging viruses with epidemic potential and cause persistent polyarthralgia and myalgia in humans. Vaccine development is well underway for the pathogenic encephalitic alphaviruses, and a vaccine was recently approved for epidemic CHIKV. With plans to evaluate a pan-alphavirus vaccine candidate that is in development, we sought to optimize AG129 models of lethal infection to assess vaccine-elicited cross-protection against RRV and UNAV. Following RRV infection, animals challenged with 0.1 PFU developed footpad swelling disease and succumbed to infection by 5 dpi, but viremia at 1 dpi was only reliably detected in the 100 PFU challenge group. The 50% humane endpoint dose for RRV was determined to be 0.05 PFU using the Reed and Muench method of calculation. Following UNAV infection, we found that animals challenged with as low as 1 PFU reliably developed infectious viremia detectable at 2 dpi followed by footpad swelling and weight loss that caused mice to succumb to infection by 4 dpi. Some of the animals challenged with 0.1 PFU also developed disease and succumbed to infection but viremia was not consistently detected at 2 dpi. The 50% humane endpoint dose for UNAV was determined to be 0.06 PFU. These two models demonstrate highly stringent disease models of

alphavirus infection that are useful for analyzing the protective efficacy of alphavirus vaccine candidates and therapeutics or characterizing viral pathogenesis.

Figure A2.1. AG129 model of lethal RRV infection.

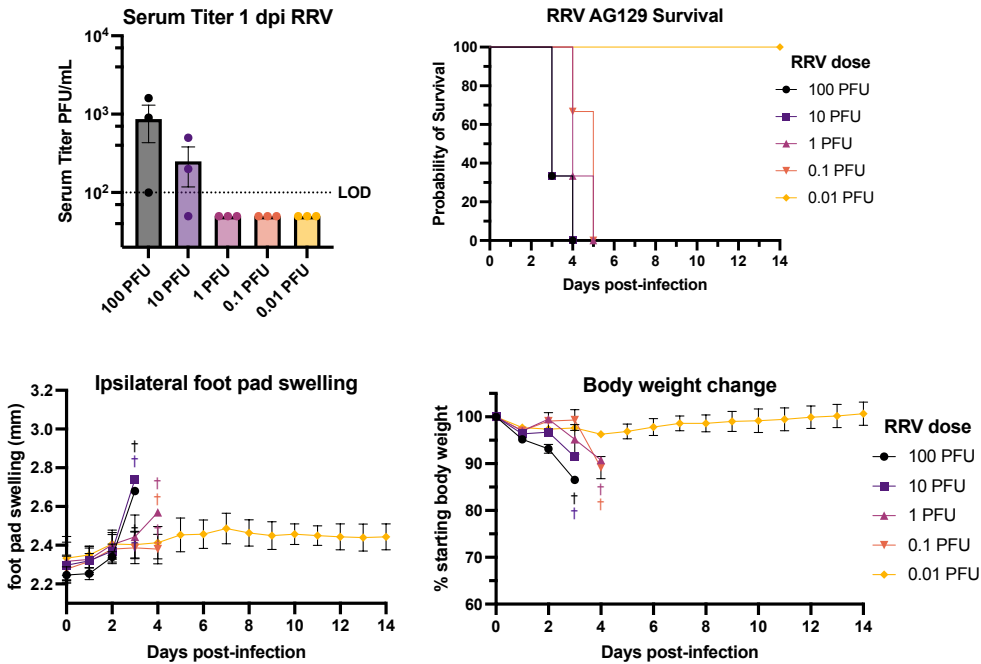
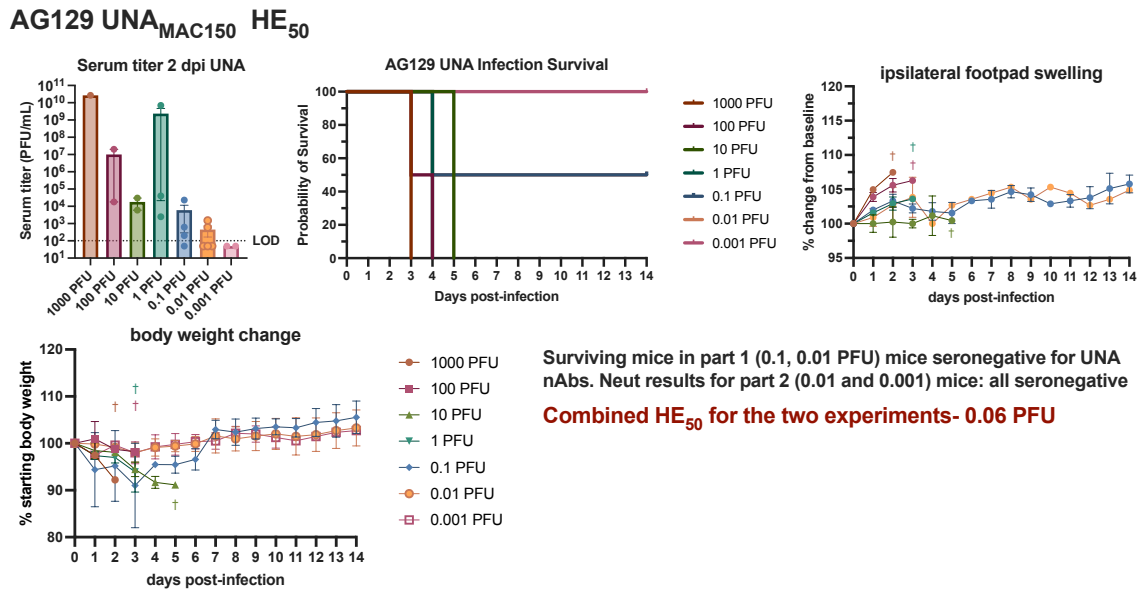


Figure A2.1. AG129 mice were challenged in the right footpad with the indicated doses of RRV_{T-48} and monitored for 14 days. Body weight changes and footpad swelling measured with calipers was recorded daily. Blood was collected from animals at 1 dpi via the saphenous vein for serum isolation for use in plaque assays to quantify infectious viremia. Mouse experiments were performed by Takeshi Andoh. Whitney Weber prepared virus for challenge, conducted plaques assays for analysis of viremia, and analyzed/curated and compiled the data.

Figure A2.2. AG129 model of lethal UNAV infection.



Infected 9 mice with 6.5 PFU (100X the HE₅₀) - 5 females, 4 males

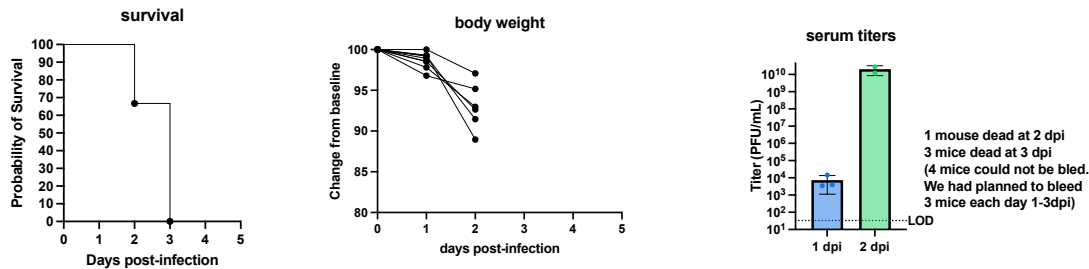


Figure A2.2. AG129 mice were challenged in the right footpad with the indicated doses of UNAV_{MAC150} and monitored for 14 days. Body weight changes and footpad swelling measured with calipers was recorded daily. Blood was collected from animals at 1 or 2 dpi via the saphenous vein for serum isolation for use in plaque assays to quantify infectious viremia. Mouse experiments were performed by Takeshi Andoh. Whitney Weber prepared virus for challenge, conducted plaques assays for analysis of viremia, and analyzed/curated the data.

Section A2.2: Acknowledgements

The funding source of these studies was a grant awarded by the Defense Threat Reduction Agency (DTRA) to Mark Slifka, PhD. Thank you to Hans-Peter Raué, PhD for breeding the AG129 mice used in these studies.

Appendix III: Chikungunya Virus Vaccines: A Review of IXCHIQ and PXVX0317 from Pre-Clinical Evaluation to Licensure

Status: Published in BioDrugs September 18th, 2024.

Whitney C. Weber^{1,2}, Daniel N. Streblow^{1,2}, Lark L. Coffey^{3#}

¹ Vaccine & Gene Therapy Institute, Oregon Health & Science University, Beaverton, Oregon, USA

² Division of Pathobiology & Immunology, Oregon National Primate Research Center, Beaverton, Oregon, USA

³ Department of Pathology, Microbiology, and Immunology, School of Veterinary Medicine, University of California, Davis, California, USA

#Address correspondence to Lark L. Coffey, lcoffey@ucdavis.edu

Author Contributions: WCW, DNS and LLC wrote the manuscript draft and generated figures. All authors read and approved the final manuscript.

Section A3.1: Abstract

Chikungunya virus is an emerging mosquito-borne alphavirus that causes febrile illness and arthritic disease. Chikungunya virus is endemic in 110 countries and the World Health Organization estimates that it has caused more than 2 million cases of crippling acute and chronic arthritis globally since it re-emerged in 2005. Chikungunya virus outbreaks have occurred in Africa, Asia, Indian Ocean islands, South Pacific islands, Europe, and the Americas. Until recently, no specific countermeasures to prevent or treat chikungunya disease were available. To address this need, multiple vaccines are in human trials. These vaccines use messenger RNA-lipid nanoparticles, inactivated virus, and viral vector approaches, with a live-attenuated vaccine VLA1553 and a virus-like particle PXVX0317 in phase III testing. In November 2023, the US Food and Drug Administration (FDA) approved the VLA1553 live-attenuated vaccine, which is marketed as IXCHIQ. In June 2024, Health Canada approved IXCHIQ, and in July 2024, IXCHIQ was approved by the European Commission. On August 13, 2024, the US FDA granted priority review for PXVX0317. The European Medicine Agency is considering accelerated assessment review of PXVX0317, with potential for approval by both agencies in 2025. In this review, we

summarize published data from pre-clinical and clinical trials for the IXCHIQ and PXVX0317 vaccines. We also discuss unanswered questions including potential impacts of pre-existing chikungunya virus immunity on vaccine safety and immunogenicity, whether long-term immunity can be achieved, safety in children, pregnant, and immunocompromised individuals, and vaccine efficacy in people with previous exposure to other emerging alphaviruses in addition to chikungunya virus.

Section A3.2.1: Chikungunya virus

Chikungunya virus (CHIKV) was first described in 1952 after an outbreak in people in Tanzania [145, 480, 481]. CHIKV is an alphavirus (*Togaviridae*, *Alphavirus chikungunya*) that comprises four major genetic lineages (West African, East Central South African [ECSA], Asian, and Indian Ocean Lineage). Despite this genetic diversity, CHIKV comprises a single serologic group. CHIKV is an enveloped, single-stranded, positive sense RNA virus. The viral RNA is translated from the full-length genomic RNA or a subgenomic RNA as two polyproteins; one encodes the four non-structural proteins (nsP1-4) to form a replication complex that synthesizes the genome, and the other encodes the structural proteins (capsid, 6K peptide, and E1, E2, and E3 envelope proteins). The envelope proteins are the dominant antibody targets of the host immune response with E1 conferring membrane fusion and E2 responsible for cell receptor (MXRA8) binding to target cells [482]. CHIKV is a member of the Semliki Forest virus antigenic complex that affords cross-reactive adaptive immunity to other emerging pathogenic alphaviruses including O'nyong nyong (ONNV), Mayaro (MAYV), Una (UNAV), and Ross River viruses (RRV) [483].

Section A3.2.2: Chikungunya disease and management

Chikungunya virus causes chikungunya (CHIK) disease. Chikungunya virus is transmitted to humans during blood feeding by infected *Aedes aegypti* or *Aedes albopictus* mosquitoes that are common in urban tropical and sub-tropical regions and spreading globally owing to various factors including climate change [484, 485]. After deposition by a mosquito, CHIKV spreads cell-free or in infected fibroblasts in the skin, leading to dissemination through the blood and infection

of and replication within liver, muscle, joint, lymphoid tissues including lymph nodes and spleen, and brain [15]. Although rarely fatal, CHIKV infection causes symptomatic disease in most infected people, presenting primarily as fever, myalgia, arthralgia, headache, stiffness, rash, and fatigue, with less frequent neurologic and ocular symptoms [486]. Many patients report chronic arthritic joint pain that persists 1 month or longer after acute disease [21]. Congenital infection also occurs, usually via intrapartum fetal infection [486], and infection of neonates can lead to severe and sometimes fatal disease. Acute CHIK disease is treated with rest, oral hydration, and pain mitigation using analgesics and non-steroidal anti-inflammatory drugs [487-489]. Chronic CHIK disease is treated with non-steroidal anti-inflammatory drugs or disease-modifying antirheumatic drugs [490-492]. A variety of antiviral and monoclonal antibody therapies have been tested in pre-clinical models for mitigation of disease, but none has been licensed for use in humans.

Section A3.2.3: Unmet need for CHIKV vaccine

Chikungunya disease presents a global health problem. The absence of CHIKV-specific therapies restricts treatment to supportive care. From 2010 to 2019, CHIK caused average annual loss of >100,000 disability-adjusted life-years in endemic areas, mostly due to chronic rheumatic manifestations [493]. Areas without prior CHIKV circulation are often especially affected, as evidenced by explosive and often unpredictable outbreaks that debilitated public health infrastructures in Reunion Island in 2005 [494], India in 2008–9 [495], and Paraguay in 2022–23 [496]. People more than 35 years of age and obese persons are also more prone to severe or atypical CHIK [497-499]. Chikungunya virus outbreaks present a clear need for licensed CHIKV vaccines. In the absence of vaccines, strategies to reduce CHIKV transmission focus on limiting exposure to mosquito vectors, which include removing standing water where immature mosquitoes develop, installing screens on buildings, wearing long clothing, using mosquito repellents, and aerosol insecticide applications.

Section A3.2.4: CHIKV vaccines in development

There are many CHIKV vaccines in development using various platforms. The nature of the platform and evaluation data has been extensively reviewed elsewhere [342, 481, 500-503]. This review focuses only on the two CHIKV vaccine candidates, the IXCHIQ live attenuated vaccine (LAV) and the PXVX0317 virus like particle (VLP), that have advanced farthest in human trials as of 2024.

Section A3.2.5: CHIKV-Specific Neutralizing Antibody as a Target for CHIKV Vaccine Development

Chikungunya virus-specific antibodies play an important protective role against CHIKV infection and disease [15, 104, 321, 349]. After a natural CHIKV infection, anti-CHIKV immunoglobulin M (IgM) antibody develops within 1 week and mediates early control of infection. An immunoglobulin G antibody (IgG), which develops after IgM, persists for months to years. A CHIKV-specific antibody recognizes viral components, especially the CHIKV structural envelope proteins E1 and E2. Passive transfer studies using serum or plasma containing CHIKV neutralizing antibody (NAb) from naturally infected or vaccinated people protects against CHIKV infection and disease in mice [231, 504], supporting a role for NAb in protection. These data are also used to support circulating NAb as a correlate of protection from CHIKV infection and disease that can be used in vaccine efficacy predictions.

Section A3.2.6: IXCHIQ

IXCHIQ (Valneva, Vienna, Austria), formerly called $\Delta 5\text{nsP3}$ and VLA1553, was created from an infectious clone of CHIKV strain LR2006-OPY1 that was isolated from a patient in 2006 in Reunion Island. This strain belongs to the ECSA CHIKV genotype. The clone was genetically modified by deleting 62 amino acids in the C terminal region of nsP3 that is part of the viral replication complex (Fig. A3.2.6) [101]. The rationale for this approach is that a LAV is immunostimulatory much like wild-type CHIKV, but mutations or deletions at specific locations in the alphavirus replication complex attenuate virulence by reducing viral replication efficiency

and fitness. The linker sequence AYRAAAG was inserted to replace the deleted nsP3 sequence. The deletion leads to decreased murine [101], macaque [233], and human virulence [264, 265], which will be discussed below, and forms the basis for attenuation of the LAV.

Figure A3.2.6 Design of the IXCHIQ live attenuated vaccine (LAV).

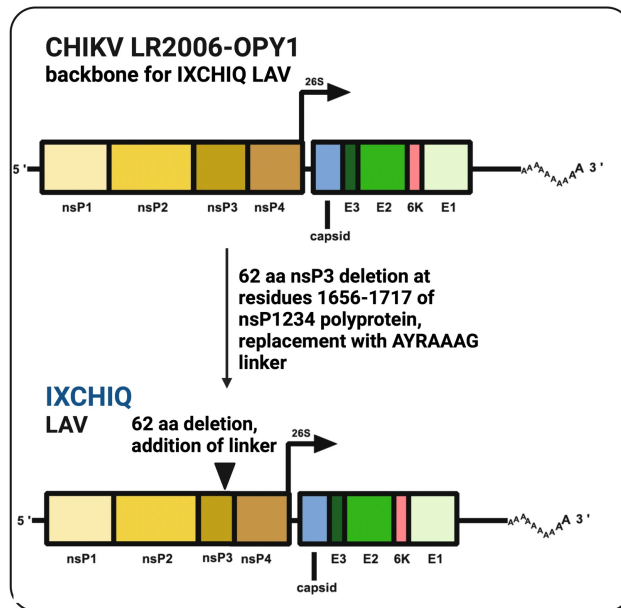


Figure A3.2.6. Design of the IXCHIQ live attenuated vaccine (LAV). A 62-amino acid (aa) deletion was made in the chikungunya virus (CHIKV) non-structural protein (nsP) 3. The deleted region was replaced by a linker. A publishing license was granted for the image created in Biorender.

Pre-Clinical Evaluations

Genetic Stability

In the first study after its generation, IXCHIQ, then identified as $\Delta 5\text{nsP3}$, was serially passaged at a low multiplicity of infection in Vero cells and then the genome region flanking the deletion was sequenced to assess genetic stability of the deletion over time [101]. No increases in titers were detected and the introduced deletions were genetically stable after five [101] or ten [233] passages.

Immunogenicity and Efficacy in Animal Models

Both humoral and cell-mediated immune responses protect against alphavirus-mediated disease. To evaluate immunogenicity and protective efficacy of CHIKV vaccines, mice and non-human primates (NHP) that each recapitulate features of human CHIK have been used.

Mice In the first studies evaluating IXCHIQ [101], then identified as $\Delta 5nsP3$, female inbred C57BL/6 mice aged 5–6 weeks were administered a single immunization of 10^4 or 10^5 Vero cell plaque forming units (PFU) of IXCHIQ subcutaneously in both upper thigh flanks. Mice vaccinated with 10^4 PFU did not develop detectable viremias 1 or 3 days after vaccination, but two of five mice vaccinated with 10^5 PFU developed detectable viremias. Footpad swelling, a proxy for arthritic disease in this model, was noted but it was suggested to not to occur at a significant level. Vaccinated mice developed IgG antibody responses measured by enzyme-linked immunosorbent assay, NAb titers assessed by 50% neutralization test (NT50) assays and CD8 T-cell responses measured by interferon- γ ELISPOT assays. Fifty percent neutralization dilution titers displayed a wide range, from less than 10^1 to $< 10^4$. Seven weeks after vaccination, mice were challenged in the feet with 10^6 PFU of the wild-type CHIKV LR2006-OPY1 strain that serves as the backbone for the vaccine. The challenged mice did not develop detectable viremias or footpad swelling. An inverse correlation was measured between IgG and NT50 titers and both viremia and footpad swelling, implicating both antibody measures as correlates of protection. Mice immunized with 10^5 PFU IXCHIQ challenged 8 or 20 weeks after immunization showed no detectable viremia and no differences in footpad swelling. Immunoglobulin G titers were not different at either post-immunization timepoint.

Non-Human Primates Following successful demonstration of immunogenicity and protection of the vaccine in mice, safety and efficacy studies in cynomolgus macaques were next performed [233], where the vaccine was then identified as $\Delta 5nsP3$. Adult cynomolgus macaques aged 3–4 years were vaccinated subcutaneously in the right upper backside with one injection of 1×10^5 PFU IXCHIQ. Vaccinated animals developed viremias between 1 and 9 days post-vaccination that peaked between days 2 and 4 at titers of 10^3 to $>10^6$ genomes/mL. These viremias were delayed in peak by 1–2 days, where macaques inoculated with wild-type CHIKV LR2006-OPY1 peaked 1 day after inoculation. The area under the viremia curve in vaccinated animals was also lower than in macaques that received wild-type CHIKV LR2006-OPY1. The vaccine induced high-titer CHIKV binding and NAb that did not decline between vaccination and challenge, 81 days later. The NAb responses against a heterologous strain of CHIKV representing a different

genetic lineage that was isolated from a patient in the Caribbean were similar to those for the homologous CHIKV LR2006-OPY1, suggesting vaccine-mediated cross-neutralization across different CHIKV genotypes. Each animal was challenged intravenously in the saphenous vein with 100 animal infectious dose 50%, corresponding to 7000–10,000 PFU of wild-type CHIKV. After challenge, none of the vaccinated animals developed detectable viremias, fever responses, lymphopenia, or monocytosis; these are disease signs that were observed in challenged animals that were not vaccinated. Further analyses showed that cytokines including interferons and tumor necrosis factor- α that correlate with disease in people and are upregulated in macaques infected with wild-type CHIKV were not increased after IXCHIQ vaccination.

Animal Toxicology

Toxicology of IXCHIQ is based on data from the Summary Basis for Regulatory Action [505]. Rabbits administered a human dose of IXCHIQ twice on days 1 and 15 showed no clinical signs including changes in body weight, temperature, dermal appearance, ophthalmic appearance, blood chemistry, coagulation, gross pathology, organ weight, and histopathology. Rabbits that received the vaccine showed mild hematologic changes including increased monocyte, eosinophil, and neutrophil counts compared with control rabbits that were not vaccinated. A three-fold to 5-fold increase in C-reactive protein was measured in vaccinated rabbits. Chikungunya virus antibody responses were detected in vaccinated rabbits. In rats, a human dose of IXCHIQ did not produce adverse effects on fetal development, fecundity, or pre- or post-natal infant development.

Clinical Trials

Based on the success of the vaccine in animals, safety and immunogenicity of IXCHIQ were next evaluated in two clinical trials that were conducted at vaccine trial sites across the USA with almost 3200 healthy participants aged 18 years and older. These data are reported in two publications [264, 265], which are detailed below.

Design and Protection from Disease

In the first study (ClinicalTrials.gov, NCT03382964), a phase I trial was conducted in 2018 in Illinois and Alabama, USA [265]. A total of 120 healthy volunteers between 18 and 45 years received one of three doses in a single shot intramuscular immunization of IXCHIQ, then identified as VLA1553, followed by re-vaccination with the highest dose 6 or 12 months later. The low dose

was 3.2×10^3 , the medium dose was 3.2×10^4 , and the high dose was 3.2×10^5 50% tissue culture infectious dose (TCID₅₀) per mL. Safety data and laboratory parameters were collected using the US FDA grading guidance [506]. Participants reported daily temperature, solicited injection, and systemic reactions for up to 14 days after vaccination. Participants were also monitored for signs of CHIKV-like disease that were recorded separately as adverse events of special interest (AESI) and included rapid-onset fever, myalgia, headache, back pain, rash, edema in the face and extremities, acute adenopathy, acute arthritis, tenosynovitis, neurological symptoms, or cardiac symptoms lasting for more than 3 days. The majority of adverse events across all dose groups were mild or moderate and occurred after the single vaccination. In the first 14 days after vaccination, 7% (4/59) in the high-dose group reported any local adverse event, which was most often injection-site tenderness. Systemic adverse events including short-term fever, fatigue, headache, and muscle pain were also reported. Severe fever exceeding 102.1 °F (38.9 °C) was reported in seven participants, all of whom were in the high-dose group, beginning 2–4 days after vaccination and lasted for 1–3 days. Systemic adverse events were less common in the low-dose and medium-dose groups compared with the high-dose group. Leukopenia, neutropenia, and lymphopenia were reported in one third of vaccinees after the single vaccination but not after revaccination. No CHIKV-like disease or vaccine-related serious events occurred in any vaccinee. Together, these metrics showed that the vaccine is safe and well tolerated for up to 12 months after the single vaccination in the low-dose and medium-dose groups, and safe in the high-dose group. Provided that a single vaccination induced antibody titers that plateaued in all dose groups, no phase II clinical trial was deemed necessary [507].

Building on the promising data from the phase I trial, another study (ClinicalTrials.gov, NCT04546724) was conducted in 2020–21 [264]. This study was a double-blind phase III trial performed at 43 sites in the USA in healthy volunteers aged 18 years and older. Based on the medium-dose safety and immunogenicity data from the phase I clinical trial in 2018, a final dose of 1×10^4 TCID₅₀ was selected. A total of 3082 participants received IXCHIQ, identified as VLA1553 in the study, and 1033 participants received the placebo. Participants were excluded if they were pregnant, had evidence of prior CHIKV infection, immunodeficiencies, or had received any inactivated vaccine within 2 weeks prior or any live vaccine within 4 weeks prior to receiving IXCHIQ. Adverse events to 180 days after vaccination were reported more frequently in vaccinated (63%) than placebo (45%) participants. Five of ten participants with AESI who

received IXCHIQ experienced CHIK-like disease in the form of a fever of 102.2 °F (39 °C) or higher for 2–4 days. Other adverse events in order of decreasing frequency reported in both vaccinated and placebo participants were headache (32% vaccinees, 16% placebo), fatigue (29%, 13%), myalgia (24%, 8%) and arthralgia (18%, 6%). Significant adverse events occurred in 1.5% of vaccinated and 0.8% of placebo participants. Two participants who received the vaccine were hospitalized but then recovered fully; one had myalgia and the other had high fever and atrial fibrillation and hyponatremia that was associated with a syndrome of inappropriate antidiuretic hormone secretion; both events were assessed as probably related to vaccination. Changes in hematologic parameters were not significant. The safety profile was similar in participants stratified by age in older (≥ 65 years) compared to the younger (18–64 years) groups. An independent Data Safety Monitoring Board did not raise major concerns about vaccine safety in the period after vaccination to 180 days.

Viremia and Urinary Shedding

In the phase I multi-dose trial, IXCHIQ produced viremias in study participants who received any of the vaccine doses. The mean viremia peak was 3 days after vaccination and viremia was detectable until 7 days. A caveat of this assessment is that blood was only collected 3, 7, and 14 days after vaccination, barring evaluation of whether the true peak was on day 3; NHP models with daily assessments show an earlier peak on day 2 [99]. The 3-day mean viremia titers were 2.3×10^5 in the high-dose group, 7.4×10^4 in the medium-dose group, and 8.9×10^4 genome copy equivalents/mL in the low-dose group. After re-vaccination, viremia above the 1087 genome copy equivalents/mL limit of detection was only detected 7 days after vaccination in the high-dose group. Urinary shedding was only detected in a single participant who received the low dose 7 days post-vaccination. Viremia and urinary shedding were not assessed in the phase III study.

Immunogenicity, Breadth, and Durability of Protection

In the phase I study, IXCHIQ was immunogenic and induced CHIKV-specific NAb titers in vaccinated study participants [265]. The micro plaque reduction neutralization test (μ PRNT) was performed with CHIKV strain 181/25, which represents a heterologous strain of CHIKV that belongs to the Asian genotype. One hundred percent (103/103) of participants seroconverted by 14 days and all 91 participants that were followed remained seropositive for up to 1 year. The mean peak micro neutralization antibody titer at day 28 ranged from 592 to 686 in the low-dose

and high-dose groups, respectively. Individuals that were revaccinated did not show anamnestic responses after revaccination and did not develop detectable viremias. In the phase III study [264], 98.9% of (263/266) participants vaccinated once with IXCHIQ developed μ PRNT₅₀ titers of ≥ 150 by day 28. The geometric mean titer (GMT) on day 29 was 3362. There was no difference in rates of seropositivity or magnitude of titers between participants aged 18–64 years versus participants aged older than 65 years. At 180 days, the GMT decreased to 752. There were no differences in GMT μ PRNT₅₀ based on sex, body mass index, ethnicity, or race [267]. One year after vaccination, 98.9% of participants had a μ PRNT₅₀ titer of ≥ 150 (the metric used to define seroprotection), and at two years, 96.8% of participants remained seroprotected [268]. In serum from 39 people in the Philippines who were naturally infected with the Asian genotype CHIKV, the GMT was 1341 (range: 170–5297) [349], which is similar to levels after IXCHIQ.

Neither of the clinical trials evaluated the breadth of NAb responses across genetically divergent CHIKV lineages or related alphaviruses. However, in studies we performed in the period since the IXCHIQ licensure, we detected cross-NAb using 50% plaque reduction neutralization test (PRNT₅₀) against divergent CHIKV lineages as well as related Semliki Forest virus antigenic complex alphaviruses ONNV, MAYV, and RRV viruses in participants from phase III trials [69]. There was little difference in NAb potency in vaccinees ($n = 30$) based on similar PRNT₅₀ titers for CHIKV LR2006-OPY1, 181/25, or a 2021 Brazilian isolate (ECSA genotype) up to 1 year post-vaccination. Neutralizing antibody responses against MAYV and ONNV were detected in 100% of vaccinees at 1-year post-vaccination. Neutralizing activity in participant sera was much lower against RRV but was present in $\sim 80\%$ of the participants. This cross-neutralizing activity in vaccinees was directly compared with CHIKV infection-elicited antibodies in serum collected from individuals 8–9 years post-infection living in endemic Puerto Rico, revealing consistency in potency and breadth of cross-NAb between these groups. These findings are consistent with our previous study that demonstrated the breadth and durability of CHIKV cross-NAb specific to the E2B domain in humans infected in Puerto Rico [59].

Serologic Correlates of Protective Efficacy

Late-stage vaccine evaluations typically require randomized controlled human efficacy trials in regions of virus endemicity with ongoing virus activity. However, CHIKV outbreaks are by nature unpredictable, sporadic, and explosive, with low case numbers during interepidemic

periods. This presents challenges to performing efficacy trials [508]. One approach to circumventing this hurdle is studies that establish a serologic surrogate of protection. For IXCHIQ, studies were performed where the protective efficacy of serum from IXCHIQ vaccinated humans passively transferred to NHP was evaluated, where the vaccine was identified as VLA1553 in that study [99]. Pooled human sera from IXCHIQ vaccinees in the phase I trial was passively transferred into cynomolgus macaques. One day later, animals were challenged with 100 animal infectious dose 50 wild-type CHIKV LR2006-OPY1 and protection from viremia, fever, and hematologic changes were assessed for 28 days and compared with control macaques that received human non-CHIKV immune sera. Serum from IXCHIQ vaccinated people reduced the magnitude of viremia by 3 to 5 log₁₀ genome copies/mL and delayed the peak and duration. None of the animals that received serum from IXCHIQ vaccinees developed fevers, lymphopenia, or neutropenia, and a μ PRNT₅₀ titer of ≥ 150 was defined as a surrogate of protection from viremia and development of fever.

Regulatory Agency Approvals for Human Use

On 9 November, 2023, the FDA approved IXCHIQ for use in people aged 18 years and older who are at risk of exposure to CHIKV [509]. On 28–29 February, 2024, the US Centers for Disease Control Advisory Committee on Immunization Practices recommended IXCHIQ for use in people aged ≥ 18 years traveling to a country or territory with a CHIKV outbreak or evidence of CHIKV transmission within the last 5 years. In addition, IXCHIQ may be considered in people aged >65 years with at least 2 weeks of mosquito exposure, and in travelers to CHIKV endemic areas who will be staying for cumulative periods of more than 6 months [510]. The Advisory Committee on Immunization Practices also recommended IXCHIQ for laboratory workers with potential exposure to CHIKV. On 24 June, 2024, Health Canada announced approval of IXCHIQ in Canada [511]. On 1 July, 2024, the European Commission granted marketing authorization of IXCHIQ in Europe [512].

Components and Storage

IXCHIQ is propagated in African green monkey kidney (Vero) cells in a growth medium that contains fetal bovine serum, amino acids, vitamins, and minerals. The LAV harvested from infected Vero cells is pooled, clarified, concentrated, purified by chromatography, and ultracentrifuged. The resulting vaccine is then mixed with formulation buffer and lyophilized.

Healthcare providers receive a vial of lyophilized IXCHIQ that should be stored in a refrigerator at 2–8 °C, prior to reconstitution for use in sterile water [513]. Each reconstituted 0.5-mL IXCHIQ dose contains at least 10^3 TCID₅₀ of CHIKV LAV.

Section A3.2.7: PXVX0317

PXVX0317 is a VLP vaccine that was initially developed by the US National Institutes of Health Vaccine Research Center. The vaccine (Fig. A3.2.7) contains recombinant CHIKV structural proteins capsid, E3, E2, 6K, and E1, which were derived from Senegalese CHIKV strain 37997, a member of the West African genotype. Following in vitro expression of the CHIKV structural gene cassette, the structural proteins self-assemble into a particle that is highly similar to wild-type CHIKV but that cannot replicate because of the absence of a viral genome [231]. The rationale for the VLP approach is that structural proteins enable attachment, entry, and fusion into host cells to resemble a CHIKV virion and induce NAb responses that are similar to wild-type CHIKV. In initial studies, NHP immunized with VLP-generated NAb and were protected from viremia after a wild-type CHIKV challenge [231]. These data served as the precedent for further development of this vaccine, discussed in detail below.

Figure A3.2.7 Design of the PXVX0317 virus-like particle (VLP) vaccine.

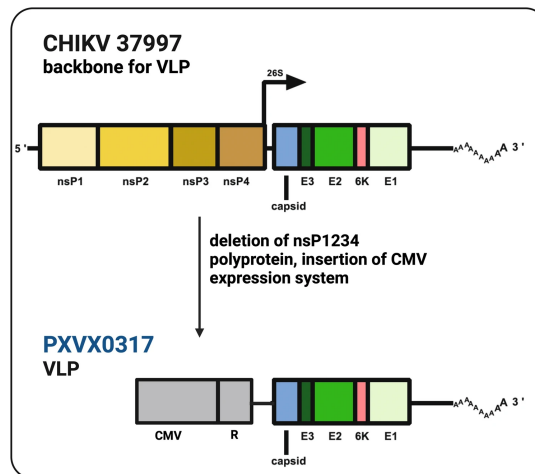


Figure A3.2.7. Design of the PXVX0317 virus-like particle (VLP) vaccine. The chikungunya virus (CHIKV) non-structural genes were removed and the structural proteins: capsid, E2 and E1, along with accessory proteins E3 and 6K, were expressed from a human cytomegalovirus (CMV) R vector that comprises the human CMV early

enhancer/promotor, a human T-cell leukemia virus-1 R region containing a splicing donor, a CMV immediate early-splicing acceptor, and a bovine growth hormone poly A signal. *nsP* is non-structural protein. A publishing license was granted for the image created in Biorender.

Pre-Clinical Evaluations

Immunogenicity and Efficacy in Animal Models

Mice Initial immunogenicity studies for PXVX0317 were performed in female BALB/C mice aged 6–8 weeks that were injected intramuscularly in the right and left quadricep muscles two times with a 1-month interval in between injections [231]. For some animals, the immune stimulatory adjuvant Ribi was also included together with PXVX0317. Compared with mice that received saline, mice administered adjuvanted PXVX0317 developed high titer NAb responses against the homologous 37997 strain and a heterologous CHIKV LR2006-OPY1 strain. Mice that received non-adjuvanted PXVX0317 also mounted NAb responses, although titers were lower than in mice that received adjuvanted vaccine.

Non-Human Primates Immunogenicity studies for PXVX0317 were performed in rhesus macaques [231]. Adult animals aged 3–4 years were administered PXVX0317 intramuscularly three times at weeks 0, 4, and 24. All developed NAb against homologous and heterologous CHIKV after the first immunization and titers increased with second and third immunizations. To assess protective efficacy, 15 weeks after the third immunization, animals were challenged intravenously with heterologous CHIKV LR2006-OPY1. Vaccinated animals did not develop detectable viremia 2 days post-inoculation, the time of peak viremia non-vaccinated rhesus macaques. Monocyte levels were also unchanged in vaccinated animals, contrasting with non-vaccinated controls, which showed increased levels. To evaluate the protective role of antibody after VLP vaccination, purified total IgG from immunized or control animals was passively transferred via an intravenous infusion into immunodeficient mice with defective type 1 interferon signaling (interferon- α/β receptor-1 knockout, *Ifnar1*^{-/-}), followed by a challenge with a lethal dose of CHIKV LR2006 OPY-1 1 day later. Mice that received IgG from vaccinated macaques did not develop detectable viremias and were protected from lethal disease, demonstrating the protective role of vaccine-stimulated IgG against CHIK.

Animal Toxicology

No publicly available data evaluate the toxicology of PXVX0317.

Clinical Trials

Design and Protection from Disease

Safety and immunogenicity of PXVX0317 were evaluated in three clinical trials that were conducted at vaccine trial sites across the USA comprising a combined total of nearly 1000 healthy participants aged 18 years and older. These data are reported in three publications describing the trials and three additional publications reporting on antibody responses, all of which are detailed below.

In the first study [271], a phase I dose-escalation, open-label clinical trial (ClinicalTrials.gov NCT04189358) was performed to evaluate the safety and tolerability of PXVX0317, which was named VRC-CHKVLP059-00-VP at the time. A total of 25 healthy adults aged 18–50 years were enrolled at the NIH Clinical Center, Bethesda, MD, USA in 2011–12. Participants received three sequential doses of 10 µg, 20 µg, or 40 µg administered intramuscularly in the deltoid on weeks 0, 4 and 20, and a follow-up at 44 weeks. Safety monitoring was similar to parameters used for IXCHIQ clinical trials and was performed via clinical and laboratory assessments. Vaccine injections were well tolerated with no serious adverse events. Thirty-six percent (9/25) of participants reported local reactogenicity and 40% (10/25) reported systemic reactogenicity at least once, usually manifest as malaise, headache, chills, nausea, fever, or joint pain.

Following success of the phase I trial, a phase II clinical trial for PXVX0317 (ClinicalTrials.gov NCT02562482) was performed next [273], in the period from 2015 to 2018. The trial was a randomized, placebo-controlled, double-blind study in male and female individuals at clinics in Dominican Republic, Guadeloupe, Haiti, Martinique, and Puerto Rico with 400 healthy adults aged 18–60 years as participants. The goal of the study was to evaluate the safety and tolerability of the vaccine in people in CHIKV endemic regions. Study participants received two intramuscular injections of VLP 20 µg 28 days apart ($N = 201$) or placebo ($N = 199$) and were followed for up to 72 weeks (1.5 years). Safety monitoring was similar to metrics from the phase I study and included laboratory parameters, adverse events, and tolerability based on local and

systemic reactogenicity. As the study was conducted in CHIKV endemic regions, CHIKV infection was also evaluated. Candidate subjects were excluded from the study if they showed CHIKV IgG/IgM antibodies prior to enrollment. Similar to the phase I study, PXVX0317 was well tolerated with no serious vaccine-related adverse events reported. Thirty two percent (64/201) of participants in the vaccine group reported local reactogenicity, including pain or tenderness and swelling, compared with 19% (37/199) in the placebo group. Solicited symptoms reported included malaise, headache, myalgia, chills, nausea, fever, and joint pain, with 44% (87/201) of vaccinees reporting at least one symptom, which was higher than in the placebo groups. Unsolicited adverse events included neutropenia, bradycardia, hypotension, viral infection, rash, chest pain, dry lips, light headedness, fever, myalgia, gastroenteritis, abdominal pain, anemia, increased alanine aminotransferase, and hematoma, and were more common in the vaccine group (75%, 12/16) compared with the placebo (25%, 4/16) group. Despite being in a CHIKV endemic area, CHIK was not reported in any study participants during the trial.

A second phase II trial [275] [(ClinicalTrials.gov NCT03483961)] was next performed for PXVX0317 from 2018 to 2020, with a goal of informing selection of dose, adjuvant formulation, and immunization schedule for phase III trials. Instead of using unadjuvanted PXVX0317 as in the prior two clinical trials, PXVX0317 was prepared in an aluminum hydroxide-adjuvanted formulation. Adjuvants are intended to produce higher, earlier, and longer lasting immune responses when added to vaccines compared with non-adjuvanted formulations; the specific adjuvant selected for this study was intended to increase the efficiency of antigen uptake and release at the injection site. The study consisted of a randomized, double-blinded, parallel-group trial and was conducted at three clinics in the USA in healthy male and female CHIKV-naïve adults aged between 18 and 45 years, with a 2-year timeline between the first vaccination and study end. Participants were assigned to one of eight vaccination groups: two doses of unadjuvanted PXVX0317 28 days apart ($2 \times 20 \mu\text{g}$; standard); adjuvanted PXVX0317 at two doses 28 days apart ($2 \times 6 \mu\text{g}$, $2 \times 10 \mu\text{g}$, or $2 \times 20 \mu\text{g}$); a booster dose 18 months after the first active injection ($40 \mu\text{g}$; standard plus booster); two doses 14 days apart ($2 \times 6 \mu\text{g}$, $2 \times 10 \mu\text{g}$, or $2 \times 20 \mu\text{g}$; accelerated); or one dose ($1 \times 40 \mu\text{g}$; single). Immunogenicity and safety were study endpoints. In most groups, the majority of vaccinated participants reported solicited adverse events including injection-site and systemic reactions, where events were more common after the first vaccination. The most common solicited adverse event was injection-site pain, reported in 15–49% of

participants, depending on the vaccine group. Common solicited adverse reactions were fatigue, headache, and myalgia across all dose groups and more common after the first vaccination. No treatment-related severe adverse events were reported. Significant differences in adverse events across vaccine groups were not reported.

A multi-center, randomized, double-blind, placebo-controlled, parallel-group phase III trial was performed next (ClinicalTrials.gov NCT05072080); some unpublished results are available [514]. Study subjects aged 12–64 years received VLP (2790 participants) or placebo (464 participants) as a single intramuscular injection. Ninety eight percent (2503/2559) of vaccinated participants achieved 80% neutralization test (NT₈₀) serum neutralizing antibody titers of ≥ 100 by 22 days after vaccination; by contrast, only 1% (5/424) of placebo-treated participants achieved this NT₈₀ serum neutralizing antibody level. Antibody responses were detected in all age groups. The most common adverse events were myalgia, fatigue, and headache.

Immunogenicity, Breadth, and Durability of Protection

In the phase I trial [271], immunogenicity was evaluated by measuring CHIKV-specific NAb titers using heterologous genotype CHIKV antigens or viruses at multiple intervals in the study timeline. Neutralizing antibodies were detected in all dose groups after the second vaccination and levels were boosted after the third. One month after the third vaccination, the GMT of the half-maximum inhibitory concentration was 8745 for participants who received 10 μg , 4525 for the 20- μg group, and 5390 for the 40- μg group. A second study [272] evaluated antibody responses generated by vaccinated participants in the phase I trial against nine CHIKV strains representing West African (homologous to PXVX0317 VLP strain 37997), ECSA, and Asian genotypes. The goal was to evaluate whether vaccination elicits cross-reactive NAb against all three genotypes (where the fourth genotype identified in the introduction of this review, Indian Ocean Lineage, is derived from the ECSA genotype), which would suggest that the vaccine cross-protects against all CHIKV across the globe. Serum from 12 study participants 44 weeks after enrollment and 24 weeks after the third vaccination was analyzed in cross-neutralization assays with several CHIKV strains from each of the three genotypes. Genotype-specific differences in neutralization potency were not measured, showing that the West African strain used in PXVX0317 produces a cross-reactive NAb response against the two other genotypes. Serum samples after the first and second vaccination were also evaluated and cross-neutralized CHIKV

strains from heterologous genotypes, indicating that three PXVX0317 immunizations were not necessary to achieve neutralization breadth.

In the Phase II PXVX0317 trial [273], CHIKV NAb responses were measured in serum from blood collected at intervals after vaccination using Asian genotype CHIKV strain 181/25. All but 1 of the 192 participants (99.5%) who received both vaccinations developed NAb. The GMT in the vaccine group increased from baseline to week 8 and was higher than in the placebo group. At the 72-week study endpoint, 88% of the participants in the vaccine group who were seronegative at baseline had at least a 4-fold increase in NAb titer, and 96% were seropositive as assessed by a neutralization assay. Even though the study attempted to pre-screen and exclude participants who were CHIKV seropositive, there were regional differences in baseline NAb titers, where participants from 2 of the sites (Dominican Republic and Haiti) had higher baseline levels. Baseline timepoints were up to 56 days prior to enrollment, and many were IgG and IgM positive by IgG/IgM enzyme-linked immunosorbent assay, suggestive of either failure to exclude CHIKV participants who were seropositive at enrollment or CHIKV infection in the interval between blood collection at enrollment and vaccination. In participants who were CHIKV seropositive when vaccinated, NAb responses increased 2-fold, showing immunogenicity in spite of prior CHIKV exposure. In additional post hoc analyses from the trial [123], antibody responses post-vaccination were compared between 39 study participants with CHIKV neutralizing antibodies and 155 baseline seronegative participants. Baseline seropositive vaccinees showed stronger post-vaccination neutralizing antibody responses (peak GMT of 3594) compared to seronegative participants (1728), which persisted for 17 months. CHIKV seropositive vaccinees more frequently reported vaccine injection site swelling (10%) compared to seronegative recipients (0.6%). These data suggest that although it more frequently causes reactogenicity after administration VLP vaccine is immunogenic in people previously infected with CHIKV.

Similar to the clinical trials that preceded it, the immunology endpoint in the second Phase II trial [275] with adjuvanted PXVX0317 was assessed by measuring the GMT of CHIKV NAb, which was evaluated 28 days after the last vaccination. Neutralizing antibody titers in all vaccine groups rose within 7 days after PXVX0317 vaccination and persisted to the study end, 2 years, and a booster dose administered 18 months after the first dose augmented NAb levels. The adjuvant enhanced the magnitude of GMT 28 days after the first vaccination, with titers significantly higher in participants who received adjuvant formulations of either $2 \times 10 \mu\text{g}$ or $2 \times 20 \mu\text{g}$ at a 28-day

interval, or $2 \times 20 \mu\text{g}$ at a 14-day interval, compared with the group that received $2 \times 20 \mu\text{g}$ at a 28-day interval without an adjuvant. The adjuvanted formulations showed no advantage over the non-adjuvanted formulation after the second dose was administered. Geometric mean NAb titers were higher in groups that received 28 day compared with 14-day dosing intervals. Based on the results of this study, a single 40- μg injection of adjuvanted PXVX0317 is being further investigated in two phase III clinical trials. In trial NCT05072080 that was completed on 30 April, 2023, a safety, immunogenicity, and lot-consistency trial of PXVX0317 in healthy adults and adolescents was performed, for which the results are not yet available as of 29 August, 2024.

Using samples from the phase II adjuvant PXVX0317 trial, another study [274] characterized the B-cell response to evaluate the breadth of neutralization for three genotypes of CHIKV and related arthritogenic alphaviruses. This study used serum collected 1, 29, and 57 days, corresponding to baseline before vaccination, 28 days after the first vaccination, and 28 days after the second vaccination, respectively, in 20 study participants who received $2 \times 20 \mu\text{g}$ adjuvant VLP at the 28 day interval. Beginning 29 days after vaccination, antibody in serum was strongly and equally neutralizing against CHIKV strains from all three genotypes. Some of the participant sera also showed >50% or 80% neutralization tests against related alphaviruses including ONNV, MAYV, and RRV, where the magnitude of PRNT₅₀ or PRNT₈₀ titers and rates of positivity in the 20 participants paralleled genetic distance from CHIKV in the order ONNV>MAYV>UNAV or RRV. To evaluate induction and persistence of humoral responses, CHIKV-specific B cells were isolated from peripheral blood mononuclear cells at the times above and also at 182 days, which was 153 days after the second vaccination. Chikungunya virus-specific B cells were detected in day 29, 57, and 182 sera, where cells at the last time indicate activation markers consistent with a memory phenotype.

The study also identified broadly neutralizing monoclonal antibodies (mAbs) that bind multiple sites on the E2 glycoprotein, which could reduce potential for viral escape via mutation(s) at just a single antigenic site. When passively transferred 1 day prior to challenge with CHIKV LR2006-OPY1, some of the mAbs with neutralizing activity also protected against lethal disease in *Ifnar1*^{-/-} mice; mAbs with reduced in vitro neutralizing capacity were less protective. A subset of the mAbs administered to C57BL/6 mice prophylactically reduced footpad swelling, virus levels in target tissues such as the ankle and calf, and histopathologic changes in myositis compared with isotype control mAbs. Using the same approach but for other alphaviruses, two of the mAbs that

showed the greatest breadth of binding and cross-neutralization reduced virus levels and swelling in joints of mice after MAYV but not RRV infection, indicating that a greater cross-neutralizing potency is needed to achieve cross-protection against RRV, which is not unexpected given RRV is more distantly related to CHIKV than MAYV.

Components and Storage

The PXVX0317 VLPs are produced by transfection of human embryonic kidney VRC293 cells with a DNA plasmid encoding the CHIKV structural genes. VRC293 cells are a suspension cell line adapted to grow without serum that were derived from HEK-293 cells, which derive from human embryonic kidneys. VRC293 cells do not contain adventitious agents and lack tumorigenicity, which are criteria for use for vaccine production based on FDA guidance [515]. After the enveloped VLPs self-assemble, they are released into the culture medium as particles. The VLPs are concentrated and purified using centrifugation, filtration, and chromatography, then formulated at the appropriate dosage and stored in sterile vials before administration. The VLP manufacturer has not published storage requirements but in prior studies [274] purified VLPs were stored at -80°C prior to use.

Section A3.2.8: Comparing IXCHIQ and PXVX0317

Although LAV and VLP represent fundamentally different approaches to CHIKV vaccine design, the data reviewed here show common features of both vaccines revealed through animal studies and clinical trials (Fig. A3.2.8). Both vaccines confer rapid and durable immune responses for 2 years, the longest study timepoint to date. As a LAV, IXCHIQ produces infection and viremias in vaccinees, while, as a virus like particle, PXVX0317 does not. The advantage of LAV is that replicating vaccines in general produce more robust immune responses than non-replicating vaccines. Although safety risks posed by LAV are typically considered greater than other vaccine platforms, the nsP3 deletion renders virulent reversion unlikely, although no published studies have directly addressed this possibility or elucidated the mechanism by which the deletion attenuates virulence. Given the LAV nature of IXCHIQ, use of this vaccine may be more limited in scope than PXVX0317, given that it is contraindicated in immunocompromised individuals and

people with a history of a severe allergic reaction such as anaphylaxis to components in IXCHIQ [513]. Contraindications for PXVX0317 have not been established.

Figure A3.2.8. Overview of IXCHIQ and PXVX0317 vaccines.

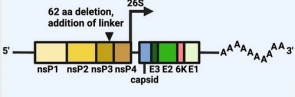
	IXCHIQ (VLA1553)	PXVX0317
 PHYSICAL STRUCTURE		
 GENETIC STRUCTURE		
 PLATFORM	Live-attenuated (LAV)	Virus-like particle (VLP)
 CHIKV STRAIN	LR2006-OPY1 (ECSA)	37997 (West African)
 DOSE STORAGE	10⁴ TCID₅₀ x 1 injection 2-8°C	20µg VLP x 2 injections 40µg VLP x 1 injection* not published
 APPROVAL STATUS	U.S. FDA ✓ Health Canada ✓ European Medicines Agency ✓ Pending: Brazil	Expected 2025
 ONGOING TRIALS	Phase III: Adolescents in Brazil Phase III: long-term safety / immunity in U.S.	Phase III: elderly adults in U.S. Phase III: adolescents + adults in U.S. Phase III: long-term safety / immunity in U.S.
 ANTIBODY POTENCY	10²-10³ GMT (1 year)	10²-10³ GMT (1 year)
 DURABILITY	2+ years	2+ years
 BREADTH	CHIKV genotypes, ONNV, MAYV, RRV	CHIKV genotypes, ONNV, MAYV, UNAV, RRV
 SYMPTOMS/SIDE EFFECTS	fever 13-24% joint pain 1-18% headache 24-40% muscle pain 15-25% chills 1.5% fatigue 17-39% serious adverse events 1.2-3.7%	fever 2-4% joint pain 10-12% headache 21-27% muscle pain 21-22% chills 6-7% fatigue 16% nausea 4-14% serious adverse events 0.5-4%
 VACCINE VIREMIA	Yes	No

Figure A3.2.8. Overview of IXCHIQ and PXVX0317 vaccines. Data are current as of August 30, 2024. Symptom ranges reported are compiled data for each level of symptom severity and vaccine dose across all reported clinical trials. *Indicates that the final dose has not yet been selected. *CHIKV* Chikungunya virus, *GMT* geometric mean titer, *ECSA* East Central South African, *MAYV* Mayaro virus, *ONNV* O’nyong nyong virus, *RRV* Ross River virus, *US FDA* US Food and Drug Administration. A publishing license was granted for the image created in Biorender.

PXVX0317 NAb titers were evaluated using a luciferase neutralizing antibody assay [273], where values reported use the stringent NT80. With this NT80 cut-off, 72–98% of PXVX0317 recipients were seropositive within 7 days after the first dose and all participants were seropositive 28 days after one or two doses, which was sustained for 2 years in all participants. The IXCHIQ studies [264, 265] used a μ PRNT test with a NT50 endpoint, which is less stringent than NT80. With NT50, IXCHIQ results in seropositivity in 30% of participants 7 days after vaccination, suggesting that the adjuvanted PXVX0317 leads to faster seroconversion. However, similar to the PXVX0317 data, NAb titers in participants who received IXCHIQ increased to 100% by day 14 and persisted for 2 years [265, 268]. Chikungunya virus 181/25, a different CHIKV LAV developed via serial passage of a wild-type strain, was evaluated in a prior clinical trial [230]. In that study, 8% (5/59) of participants developed transient arthralgia, which was noted with concern given that wild-type CHIKV infection frequently causes arthritic manifestations. In the phase I clinical trials reviewed here, IXCHIQ produced joint pain in 12% (14/120) participants within 14 days after vaccination, most frequently in the high-dose group. In part for these safety reasons, the medium dose (1×10^4 TCID₅₀) was used in the phase III study. In the phase III study only, 0.06% (2/3082) of participants had a serious adverse event considered related to IXCHIQ. The PXVX0317 studies also noted joint pain. Six percent of participants reported joint pain after the first injection of PXVX0317 and 5% after injection of placebo, and three transient but severe events were reported in the PXVX0317 group.

Section A3.2.9: Outstanding Unknowns

Licensure of IXCHIQ by US, Canadian, and European regulators and completion of phase III clinical trials for the VLP represent a significant step towards preventing CHIK. Furthermore, an agreement between Valneva and the Coalition for Epidemic Preparedness Innovations will aid in disseminating IXCHIQ to regions where outbreaks occur and will support WHO prequalification for widespread access in lower-income and middle-income countries [516]. Even with the licensure hurdle met or nearly met, unknown questions about both vaccines in context of endemic CHIKV circulation remain. Neither IXCHIQ clinical trial and only the phase II VLP study was conducted in a region with transmission of CHIKV or other alphaviruses (caveat: a subtype of Venezuelan equine encephalitis virus called Everglades virus is endemic to Florida

where some of the clinical trials were performed; seroprevalence is very low [517, 518]). As such, the effects of pre-existing immunity to CHIKV or other alphaviruses on IXCHIQ and PXVX0317 safety and immunogenicity remain unknown. In addition to CHIKV, at least seven other alphaviruses, including MAYV, VEEV, Eastern equine encephalitis and Western equine encephalitis, UNAV, ONNV, and RRV are considered significant emerging disease threats in regions that would be expected for CHIKV vaccine rollout.

Since 2005, the WHO estimates CHIKV has caused more than 2 million cases worldwide and is currently endemic in 110 countries [480]. The global spread of CHIKV extends into ranges of many of the other alphaviruses that threaten human health, especially in Latin America, where multiple alphavirus species share overlapping geographic distributions (Fig. A3.2.9) The shared range of CHIKV with other alphaviruses means that CHIKV vaccine delivery will be targeted to regions where people are exposed to other alphaviruses in addition to CHIKV. The impact of pre-existing alphavirus immunity on alphavirus cross-neutralization profiles has been examined in context of primary CHIKV infection [59, 75, 85], leaving open questions about how primary infection with other circulating alphaviruses shapes the neutralization breadth. Questions related to effects of pre-existing CHIKV or other alphavirus immunity and pan-alphavirus species protection can be initially addressed using experimental studies with existing animal models, where other human pathogenic alphaviruses that share geographic ranges with CHIKV also infect and cause disease in mice and NHP that model CHIKV.

Figure A3.2.9. Global distribution of medically important alphaviruses.

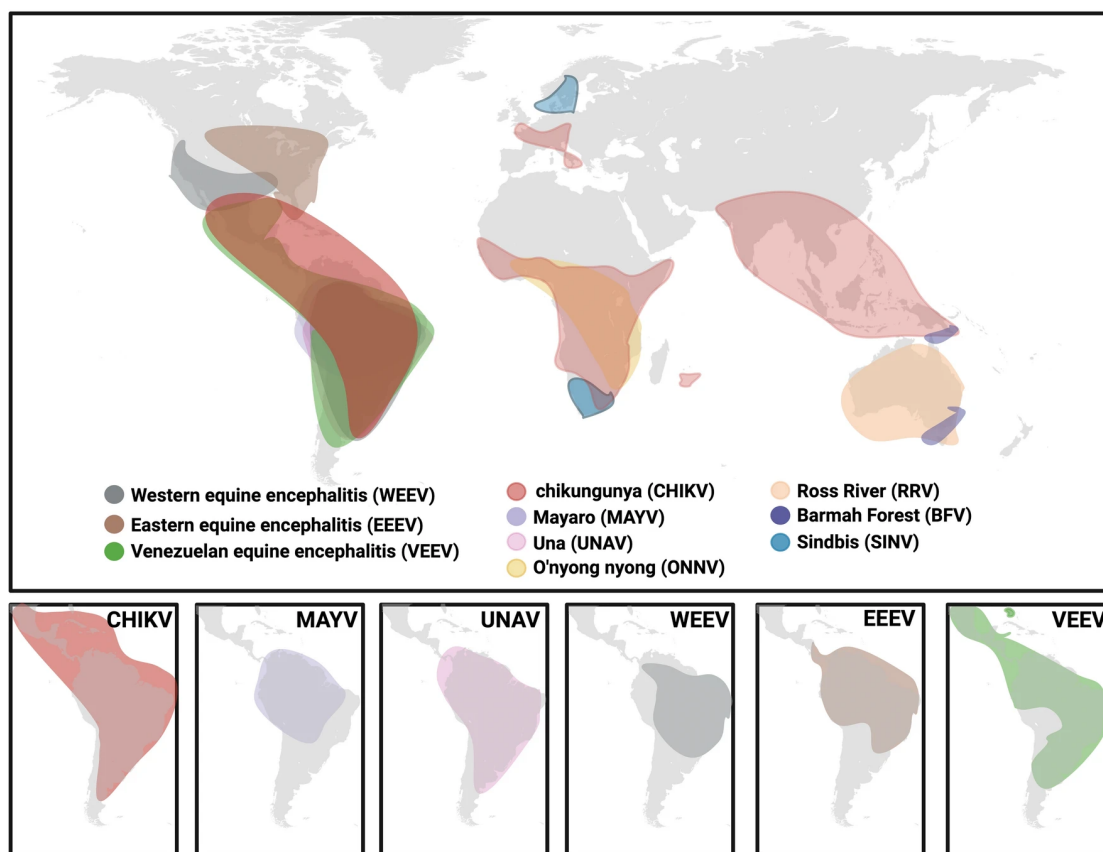


Figure A3.2.9. Global distribution of medically important alphaviruses, 2024. A publishing license was granted for the image created in Biorender.

As a LAV, IXCHIQ produces viremias of 3–5 log₁₀ genomes/mL in humans that peak at 3 days and usually last a week [265] but can extend up to 2 weeks [505]. These viremias exceed infection and transmission thresholds for CHIKV vector mosquito species *Aedes (Ae.) aegypti* and *Ae. albopictus* in laboratory studies we [519-521] and others [522] performed using the same or nearly identical CHIKV strains as the backbone used for IXCHIQ. However, no publicly available data have examined whether IXCHIQ is capable of transmission by mosquito vectors. It is not known whether the nsP3 deletion that attenuates vertebrate pathogenicity affects mosquito vector infection or transmission. Although regions of the C terminal portion of the CHIKV nsP3 that are required for mosquito infection and transmission have been defined [523], these are not in the region deleted in IXCHIQ. If vector infection and transmission are possible, even if only for a short period surrounding the viremia peak, IXCHIQ could be spread by mosquitoes from viremic vaccinees, producing mosquito-borne vaccine transmission in areas with

vaccine rollout, which could pose safety risks for populations for which the vaccine is not approved, adding another layer of complexity to dynamic population immunity. Infectiousness of IXCHIQ vaccinees to mosquito vectors could also lead to recommendations to protect recently vaccinated people from mosquito exposure. Experimental vector competence studies with IXCHIQ should be performed to address the possibility of IXCHIQ spread by CHIKV mosquito vectors.

Questions about the durability of IXCHIQ and PXVX0317 protection also remain. Although CHIKV antibody and memory B cells after natural infection in humans persist for several years [20, 59, 69], it is currently unknown whether long-term immunity beyond 2 years for both vaccines can be achieved. To address this question for IXCHIQ, a 5-year antibody persistence and long-term safety trial (ClinicalTrials.gov NCT04838444) that started in April 2021 is currently underway in the same participants in the phase III trial.

IXCHIQ and PXVX0317 safety and immunogenicity in children, elderly, immunocompromised individuals, and pregnant people are also not known. To study IXCHIQ in children, a prospective, double-blinded, multicenter, randomized phase III trial of 750 participants aged 12 to < 18 years was initiated in 2022 in Brazil (ClinicalTrials.gov NCT04650399). The goal of this study is to evaluate the safety and immunogenicity of the adult dose of IXCHIQ, 1×10^4 TCID₅₀, up to 180 days after a single immunization. On 13 May, 2024, Valneva reported positive immunogenicity and safety data where 99% (232/234) of juvenile study participants were seroresponsive 180 days after vaccination and GMT antibody titers exceeded the seroresponse threshold of a μ PRNT₅₀ titer of ≥ 150 and study participants reported mild or moderate solicited adverse events [524]. To evaluate PXVX0317 in elderly persons, a phase III, randomized, double-blind, placebo-controlled trial (ClinicalTrials.gov NCT05349617) to evaluate the safety and immunogenicity of in adults aged ≥ 65 years in the USA was completed on 8 August, 2023.

Absent efficacy trials in CHIKV endemic countries, vaccine licensing is based on NAb titers in human trials, animal studies, and serologic studies in areas with CHIKV. Some of these studies show apparently contradictory μ PRNT₅₀ titers necessary to confer protection. Passive transfer of sera from IXCHIQ vaccinated humans into macaques established the μ PRNT₅₀ titer of ≥ 150 as the threshold [99], but a human serosurveillance study indicated the protective titer against re-infection may be as low as 10 [349]. In an attempt to resolve this disparity, a WHO Expert

Committee on Biological Standardization has established a WHO International Standard for CHIKV NAb that will allow for more direct comparisons of NAb titers between studies [525].

While NAbs play a key role in protection from disease, additional research is also warranted to understand the protective role of other contributing immune responses that mediate protection from infection and disease, especially in the context of pre-existing vaccine-elicited and/or natural infection-elicited alphavirus immunity.

Section A3.2.10: Conclusions

Two CHIKV vaccines have recently reached or are approaching regulatory approvals in 2024. One vaccine is a LAV, VLA1553, marketed as IXCHIQ, and the other is a VLP, PXVX0317. Pre-clinical and clinical data reviewed here support the safety, immunogenicity, and protective efficacy of the two vaccines. Outstanding questions for both vaccines include impacts of pre-existing CHIKV immunity on vaccine safety and immunogenicity, long-term immunity, safety in young, pregnant, and immunocompromised people, and efficacy in individuals previously exposed to other alphaviruses in addition to chikungunya virus. Although many questions remain about how CHIKV vaccine coverage will shift the landscape of population-level alphavirus immunity and circulation, vaccine licensure represents a promising leap forward in global CHIKV disease prevention.

Section A3.3: Acknowledgements

This work was supported by the University of California Davis School of Veterinary Medicine and the US National Institute of Health grants R01AI125902 to LLC, U19AI142790 to DNS, and T32GM142619 to WCW. DNS received funding through a sponsored research grant from Valneva Inc.

Chapter 7: Summary and final perspectives

Section 7.1: Highlights and future directions

7.1.1 Chapter 1 highlights: Alphaviruses

1. Alphaviruses have global distribution and epidemic potential, and these pathogens have the ability to cause disease in human hosts.
2. Established transmission cycles, hosts, and vectors differ amongst the alphaviruses but natural transmission is between mosquitos and non-human primates for the arthritogenic alphaviruses.
3. The magnitude of the antibody response to alphavirus infection is highly potent, durable, and cross-reactive with related alphaviruses.
4. Extensive characterization has been done to study immunity, pathogenesis, and to establish disease models of infection for the arthritogenic alphaviruses in mice as well as NHP models for CHIKV.
5. A number of vaccines have been evaluated in NHP prior to advancement to clinical development, demonstrating appropriate use of the model.
6. Emerging work has characterized MAYV pathogenesis and immunity in NHP models and shown that key characteristics of human infection are recapitulated.
7. Alphavirus vaccine development is most advanced for CHIKV, the most expansively distributed alphavirus, and the first vaccine was recently licensed (IXCHIQ).
8. A number of alphavirus vaccines have also been developed for MAYV and a great number of vaccines with cross-reactive or cross-protective immunity have been reported.

7.1.2 Chapter 2 highlights: Infection with chikungunya virus confers heterotypic cross-neutralizing antibodies and memory B cells against other arthritogenic alphaviruses predominantly through the B domain of the E2 glycoprotein

1. Infection with CHIKV elicits antibodies that cross-neutralize additional alphaviruses in the Semliki Forest Virus complex such as ONNV, MAYV, UNA, RRV, and VEEV. These responses are durable for several years after infection.

2. Depletion of E2B-binding antibodies resulted in the ablation of the cross-reactive antibody response, implicating E2B as a major epitope of cross-neutralizing antibodies.
3. CHIKV infection induces the development of memory B cells that, when stimulated, secrete antibodies that bind to CHIKV, MAYV, and the E2B domain and are functional several years after infection.

In collaboration with Dr. William Messer's laboratory and Ponce Health Sciences University in Puerto Rico, we characterized both neutralizing antibody and memory B cell responses in convalescent blood samples of both non-endemic travelers and individuals living in endemic Puerto Rico 1-24 years after chikungunya virus (CHIKV) infection. Our data revealed that CHIKV infection elicits antibody breadth extending to related Semliki Forest complex alphaviruses which remains durable for years after infection. Our studies emphasized the contribution of the E2B domain as a cross-neutralizing antibody epitope and provided insights into the neutralizing antibody potency and breadth induced by CHIKV infection. These new insights into cross-reactive alphavirus immunity may even offer an explanation as to why related alphaviruses have not yet emerged on the same scale as CHIKV.

7.1.3 Chapter 3 highlights: The approved live-attenuated chikungunya virus vaccine (IXCHIQ[®]) elicits cross-neutralizing antibody breadth extending to multiple arthritogenic alphaviruses similar to the antibody breadth following natural infection

1. The first licensed vaccine for CHIKV elicits antibodies that neutralize heterotypic CHIKV strains, ONNV, MAYV, and RRV.
2. The cross-neutralizing antibodies are detectable at one-month post-vaccination and persist at one-year post-vaccination, although their potency is reduced.
3. The potency of these vaccine-elicited cross-neutralizing antibodies decreases with increasing phylogenetic distance from the attenuated vaccine virus.
4. The potency and breadth of the alphavirus cross-neutralizing antibodies in vaccinees is similar in individuals at >8 years post- CHIKV infection.

In collaboration with the French biotech company, Valneva, we similarly characterized the human cross-neutralizing antibody potency and breadth elicited by vaccination with the first approved vaccine for CHIKV, the live-attenuated IXCHIQ vaccine. In collaboration with Dr. William Messer's laboratory and Ponce Health Sciences University in Puerto Rico, we utilized convalescent blood samples from individuals living in Puerto Rico collected 8-9 years after infection to directly compare the CHIKV infection-elicited and vaccine-elicited antibody potency and breadth. We found that IXCHIQ immunization elicits antibodies that neutralize multiple CHIKV genotypes, O'nyong-nyong virus (ONNV), MAYV, and Ross River virus (RRV) with potency that decreases with increasing phylogenetic distance but responses that retain durability at one-year post-vaccination. Importantly, IXCHIQ vaccination elicits a neutralizing antibody profile that is nearly indistinguishable from natural CHIKV infection. These translational findings have valuable implications for CHIKV disease prevention as vaccine access increases globally and may even offer protective immunity against related arthritogenic alphaviruses. Evolving population immunity following CHIKV vaccine roll out also has potential to alter existing CHIKV transmission.

7.1.4 Chapter 4 highlights: Nonreciprocity in CHIKV and MAYV vaccine-elicited protection

1. Non-replicating human adenovirus V (AdV)-vectored CHIKV and MAYV vaccines elicit cross-neutralizing antibodies against CHIKV, MAYV, and UNAV in mice that are achieved in heterologous prime-boost or coadministration prime-boost regimens.
2. Coadministration and heterologous prime-boost vaccine regimens in mice elicit cross-reactive CHIKV and MAYV-specific T-cells that recognize epitopes in the E1 and E2 glycoproteins.
3. Homologous, heterologous, and coadministration vaccination with AdV-MAYV and AdV-CHIKV elicits complete protection against the development of footpad swelling disease after homotypic and heterotypic viral challenge.
4. Homologous, heterologous, and coadministration vaccination strategies followed by homotypic and heterotypic challenge reveal differences in reciprocal cross-protection evidenced by viral replication in arthrotropic tissues.

5. Passive transfer experiments of vaccine-immune sera in mice reproduce trends in nonreciprocity in CHIKV and MAYV vaccine-elicited cross-protection.
6. Dilution of mouse vaccine-immune sera in *in vitro* antibody dependent enhancement assays demonstrates evidence of enhanced infectious virus production of MAYV and UNAV but not CHIKV or RRV in a mouse macrophage cell line.

In an effort to broaden cross-reactive immunity after adenovirus V (AdV)-vectored alphavirus vaccination, we completed several studies exploring homologous, heterologous, and coadministration immunization strategies with AdV-CHIKV and AdV-MAYV vaccines followed by homotypic and heterotypic challenge in mice. A key finding was that vaccine coadministration circumvented skewing of the antibody response as seen with a heterologous prime-boost approach and offered protective immunity against CHIKV and MAYV infection. We demonstrated evidence of non-reciprocity in CHIKV and MAYV vaccine-elicited protection wherein vaccination against CHIKV did not protect against MAYV but vaccination against MAYV elicited protective immunity against CHIKV. This study also generated evidence of *in vitro* antibody-mediated enhancement (ADE) of viral replication for MAYV and Una virus (UNAV) infection using mouse sera collected after vaccination. This is the first report of vaccine-elicited alphavirus *in vitro* ADE, and reports of infection-elicited alphavirus ADE have been restricted to limited *in vitro* findings. These results revealed potential for ADE due to cross-reactive antibodies, highlighting potential for enhancement of infection of a related alphavirus in context of pre-existing immunity to CHIKV or MAYV. This is important amidst CHIKV vaccine roll out and ongoing clinical trials, especially in endemic areas where other alphaviruses like MAYV are circulating.

7.1.5 Chapter 5 highlights: Heterologous protection of contemporary O'nyong-nyong virus strain UVRI0804 by a hydrogen peroxide inactivated chikungunya virus vaccine

1. A contemporary strain of ONNV isolated from a febrile patient (ONNV₀₈₀₄) is comparatively more pathogenic in C57BL/6 and AG129 mice than a highly passaged strain, ONNV_{UgMP30}.
2. ONNV₀₈₀₄ causes footpad swelling disease in C57BL/6 mice, a model that has very limited reports of capacity for ONNV pathogenesis.

3. A hydrogen peroxide-inactivated vaccine against CHIKV elicits ONNV-neutralizing antibodies that protect against disease following high dose challenge with ONNV₀₈₀₄.

In collaboration with Dr. Mark Slifka's laboratory, we conducted a comparative pathogenesis project comparing pathogenesis of a contemporary ONNV strain to a highly passaged strain both *in vitro* and *in vivo* in immunocompetent and immunodeficient mouse models. There are limited pathogenic ONNV strains available for research, and therefore limited translational models of ONNV disease. These studies highlight increased pathogenicity of a recent clinical isolate in mice, presenting a potential public health threat. Utilizing the hydrogen peroxide-inactivated HydroVax-CHIKV vaccine for which we had previously demonstrated homologous protection, we demonstrated vaccine-elicited heterologous protection against the contemporary pathogenic ONNV strain. These studies both established an improved lethal model of ONNV infection and revealed cross-protective efficacy of a CHIKV vaccine.

7.1.6 Chapter 6 highlights: Mayaro virus pathogenesis and immunity in rhesus macaques

1. Rhesus macaques challenged with MAYV develop viremia that peaks at 2 dpi and in one animal, a rash containing viral RNA.
2. MAYV infects joint, muscle, lymphoid, skin, major organs, central nervous tissues, and reproductive tissues which is detectable at 10 dpi.
3. Pro-inflammatory cytokines peak in MAYV-infected macaques at 2 dpi, coinciding with peak viremia.
4. Gene signatures of antiviral immunity and the inflammatory response are highly upregulated at 2 dpi.
5. Activation of monocyte and dendritic cell subsets occurs between 2 and 5 dpi, coinciding with the peak and decline of viremia.
6. Central and effector memory CD4 and CD8 T cell subset are actively proliferating and secreting granzyme B, concurrent with viremia.
7. Binding and neutralizing virus specific antibodies are identifiable as early as 5 dpi that expand in potency at 10 dpi and cross-react with related alphaviruses.

We developed a non-human primate (NHP) model of MAYV infection in rhesus macaques. Previous research seeking to understand MAYV infection in NHP had been limited to a single study published in 1967. This early study demonstrated that MAYV can infect rhesus macaques but did not define the virus used nor did it fully characterize immunity. We characterized viral pathogenesis and tropism, progression of arthritogenic disease, and innate and adaptive immunity in response to infection. We provided evidence of how the alphavirus cross-neutralizing antibody profile is shaped by MAYV infection, and how this contrasts responses following CHIKV primary infection. Our model expands what is known about MAYV pathogenesis in a physiologically relevant model and illustrates the kinetics of antiviral immunity in the acute phase after infection.

7.1.7 Appendix I highlights: The alphavirus neutralizing antibody breadth is shaped by the primary antigen exposure

1. Primary alphavirus infection shapes the neutralizing antibody breadth against antigenically related alphaviruses.
2. Antigenic relationships among the alphaviruses are not reciprocal in potency.
3. The way that multi-alphavirus exposure profiles and hybrid immunity influence the cross-reactive neutralizing antibody potency, breadth, and response hierarchy warrant further investigation.

7.1.8 Appendix II highlights: Development of mouse models of lethal arthritogenic alphavirus infection for evaluation of vaccine-elicited protection

1. UNAV and RRV cause lethal infection in AG129 mice with similar 50% humane endpoint doses.
2. UNAV and RRV infection in AG129 mice represent appropriate disease models for the analysis of therapeutics.

Section 7.2: Cross-reactive alphavirus immunity

In every chapter, this dissertation explored several contexts by which the potency and breadth of cross-reactive alphavirus immunity can be shaped by infection or vaccination, making this the central theme of this dissertation. Cross-reactive immunity is very intriguing to me for its ability to cross-protect against infection or disease at an individual level, or the ability to slow transmission or emergence of related viruses through herd immunity at the population level. Cross-reactivity is a product of the brilliantly diverse vertebrate immune response to counteract antigenically diverse pathogens, which some may even argue is an evolutionary adaptation. Alike other pathogens, I think it is a very intriguing time in alphavirus emergence. CHIKV has swept through many regions of the world, seroconverting large populations, yet leaving numerous pockets still naïve and susceptible to future outbreaks. I am interested to see if other alphaviruses like MAYV or the encephalitic viruses such as VEEV are capable of broader emergence in both areas of CHIKV seroconversion and CHIKV-naïve populations. Vice versa, I think further studies are warranted to understand the factors contributing to why CHIKV has not emerged in certain regions, which could be due to population immunity to a related alphavirus or related to vector distribution. The urban center of the Amazon, Iquitos, Peru, is a prime example of a population that has been sheltered from CHIKV emergence yet seroprevalence to MAYV and VEEV are high in the community. It will also be interesting to see if increasing CHIKV vaccine coverage is able to halt CHIKV transmission or if this will impose selective pressure that promotes the emergence of divergent strains. Some examples of future studies that are influenced or related to the theme of cross-reactive immunity that I believe would advance the field are listed below. Nevertheless, I enjoy the mysteries of studying emerging and reemerging viruses.

- Phase IV efficacy/surveillance trials to assess protection elicited by IXCHIQ in real world settings of CHIKV or related alphavirus exposure (heterologous challenge could be examined in animal studies)
- Phase III/IV trials or animal studies that examine the impact of prior alphavirus immunity on the protective efficacy of IXCHIQ (these are underway for prior CHIKV immunity)

- Examination of the impact of dual alphavirus infection exposure history on the cross-reactive immune breadth and response hierarchy, as well as the impact this has on vaccine safety, immunogenicity and efficacy
- Surveillance in human, animal, and vector hosts in CHIKV outbreak settings of CHIKV vaccine coverage to examine vaccine efficacy, changes in viral transmission, viral evolution (on both sides of the transmission cycle), and potential for spillover/spillback of CHIKV and other alphaviruses.

Section 7.3: Strategies for developing cross-protective alphavirus vaccines

Design of innovative cross-protective vaccines

With the recent approval of the first CHIKV vaccine, a new focus of alphavirus vaccine development pursuits may be vaccines that cross-protect against related alphaviruses, or the design of vaccines targeting both flaviviruses and alphaviruses. A vaccine targeting yellow fever, CHIKV, ZIKV, and Japanese encephalitis was evaluated for immunogenicity in a preclinical setting, which is an excellent strategic approach for mitigation of cocirculating viruses [302]. My dissertation presented alphavirus vaccine strategies for improving cross-protection and cross-reactive immunity in **Chapter 4**, which included two strategies that have not yet been reported in the alphavirus vaccine literature, heterologous prime/boost and vaccine co-administration targeting two alphaviruses. Expansion of these kinds of vaccine approaches would advance the prevention of multiple pathogenic alphaviruses and have a positive impact on public health. Development of robust type-specific immunity and consideration of safety concerns such as ADE will be important for the success of these kinds of platforms. Future studies that I anticipate are on the horizon that would advance the field are further development of multivalent alphavirus vaccines and perhaps even the careful development and evaluation of more pan-arbovirus-like vaccines.

Barriers to vaccine access

Although the first CHIKV vaccine has been licensed, additional hurdles exist for CHIKV disease prevention. With the licensure of any new vaccine, delivery to a target population is complicated for several reasons in today's world- political and economic obstacles as well as

vaccine hesitancy are a few. One of the most devastating things about infectious disease is that the majority of the burden is placed on marginalized communities in resource-limited parts of the world, and these countries don't have easy access to vaccines despite being the populations that need them the most. Paired with lack of access is lack of education around vaccines in these populations, promoting lack of awareness and vaccine hesitancy. To overcome these barriers that are perhaps more significant than designing an effective vaccine in itself, public and private partners should be called to invest in bringing vaccines to these groups and a significant investment needs to be made in scientific communication by today's scientists at the community, state, country, and international level. This is one of the biggest and most consequential lessons learned following the SARS-CoV-2 pandemic.

Section 7.4: Developing new infection and disease animal models

This dissertation provided examples of studies where new disease models were developed in mice and NHPs. Developing relevant alphavirus models of disease is important for gaining a clearer understanding of pathogenesis and immunity during host infection with the downstream goal being to evaluate virus-specific therapies. **Chapter 6** highlighted a study in which we conducted a comparative pathogenesis study of various MAYV strains in C57BL/6 and IFNAR mice to inform selection of the most pathogenic strain for the NHP study. Infection of these strains had been demonstrated in previous studies, but not a head to head comparison where these strains were evaluated in the same study for comparison of disease, tissue replication, and viremia. Prior studies of MAYV infection in NHP had been limited in characterization of pathogenesis and immunity and many conclusions about MAYV infection in humans had been translated from what has been illustrated for CHIKV. Comprehensive studies of viral pathogenesis and immunity for emerging viruses like MAYV are crucial for the understanding of the translation of disease in humans and for the evaluation of therapeutics. In **Chapter 5**, we developed two new mouse models of infection and disease for a contemporary strain of ONNV, ONNV₀₈₀₄. Developing disease models of contemporary strains is important to ensure that therapeutics are being tested in the most stringent and realistic models that are recapitulating virulent circulating strains that humans are

exposed to. This study demonstrated that pathogenicity of ONNV isolates has changed over time, which has not been demonstrated in the literature. We went on to test cross-protection against ONNV elicited by a CHIKV vaccine candidate in this model to evaluate the vaccine under stringent conditions, illustrating appropriate use of this model. Studies like this highlight why it is important to continue studying the pathogenesis of emerging viral strains and building new models to evaluate therapeutics in development. Gaps I see in the field that I envision will be addressed in the coming years in terms of new infection and disease models include:

- Development of new mouse models using contemporary clinical isolates of CHIKV, MAYV, and RRV and use of these models to evaluate therapeutics
- Evaluation of vector competence using these new models
- Characterization of antigenic relationships and the impact on potency, breadth, and response hierarchy for infection of with these new strains in these new models
- ONNV and RRV NHP models of infection and exploration of pathogenesis and immunity

Section 7.5: Final Thoughts

Progress in the alphavirus vaccine landscape and the spark of an inspiring new era for vaccine development

I find it very interesting to think about how the alphavirus field has evolved since I started my PhD four years ago and can only imagine what it feels like to devote your career to one area of research and look back at how the field has changed at retirement. From my perspective as a viral immunologist, the biggest advancement has been the licensure of the first vaccine against CHIKV, IXCHIQ. When I started my PhD, there were no licensed vaccines or therapeutics available for any alphavirus. The licensure of the IXCHIQ vaccine was over ten years in the making, as the initial pre-clinical evaluation of the licensed vaccine was published in 2014 [100, 101]. The efficacy of the vaccine in non-human primates was reported in 2017 [233] and the first Phase I clinical trial results were published in 2020 [265]. Altogether, ten years of development from pre-clinical evaluation to licensure seems standard, although outbreaks and early vaccine development has been ongoing since original viral emergence in the 1950s, over 70 years ago.

I started my PhD in 2020 and I've witnessed the fastest vaccine development timeline in history. For SARS-CoV-2 the first mRNA vaccine was evaluated in a Phase I clinical trial starting just 66 days after the sequence of the virus was released [526]. This was by far the fastest vaccine development and deployment timeline in history, which has sparked an exciting and inspiring era for vaccine development. I cannot overstate how inspiring it has been for me to work on my PhD amidst these discoveries. I recognize that CHIKV and SARS-CoV-2 cause different disease and emerged in very different ways, but I can't help but wonder how vaccine development (pace, platforms, etc.) will be influenced in the future. The first CHIKV vaccine was licensed amidst this new era of vaccine development and it will be interesting to see how this process continues to evolve in the best interest of pandemic preparedness.

References

1. Koerich, L. B.; Sant'Anna, M. R. V.; Huits, R., Recent Technological Advances and Strategies for Arbovirus Vector Control. *Tropical Medicine and Infectious Disease* **2022**, 7, (9), 204.
2. Chapter 28 - Togaviridae. In *Fenner's Veterinary Virology (Fifth Edition)*, MacLachlan, N. J.; Dubovi, E. J., Eds. Academic Press: Boston, 2017; pp 511-524.
3. La Linn, M.; Gardner, J.; Warrilow, D.; Darnell, G. A.; McMahon, C. R.; Field, I.; Hyatt, A. D.; Slade, R. W.; Suhrbier, A., Arbovirus of marine mammals: a new alphavirus isolated from the elephant seal louse, *Lepidophthirus macrorhini*. *J Virol* **2001**, 75, (9), 4103-9.
4. Chowdhury, A.; Modahl, C. M.; Missé, D.; Kini, R. M.; Pompon, J., High resolution proteomics of *Aedes aegypti* salivary glands infected with either dengue, Zika or chikungunya viruses identify new virus specific and broad antiviral factors. *Sci Rep* **2021**, 11, (1), 23696.
5. Chowdhury, A.; Modahl, C. M.; Tan, S. T.; Wong Wei Xiang, B.; Missé, D.; Vial, T.; Kini, R. M.; Pompon, J. F., JNK pathway restricts DENV2, ZIKV and CHIKV infection by

activating complement and apoptosis in mosquito salivary glands. *PLoS Pathog* **2020**, 16, (8), e1008754.

6. Tjaden, N. B.; Suk, J. E.; Fischer, D.; Thomas, S. M.; Beierkuhnlein, C.; Semenza, J. C., Modelling the effects of global climate change on Chikungunya transmission in the 21st century. *Scientific reports* **2017**, 7, (1), 3813.

7. Leta, S.; Beyene, T. J.; De Clercq, E. M.; Amenu, K.; Kraemer, M. U.; Revie, C. W., Global risk mapping for major diseases transmitted by *Aedes aegypti* and *Aedes albopictus*. *International journal of infectious diseases* **2018**, 67, 25-35.

8. Kraemer, M. U. G.; Reiner, R. C.; Brady, O. J.; Messina, J. P.; Gilbert, M.; Pigott, D. M.; Yi, D.; Johnson, K.; Earl, L.; Marczak, L. B.; Shirude, S.; Davis Weaver, N.; Bisanzio, D.; Perkins, T. A.; Lai, S.; Lu, X.; Jones, P.; Coelho, G. E.; Carvalho, R. G.; Van Bortel, W.; Marsboom, C.; Hendrickx, G.; Schaffner, F.; Moore, C. G.; Nax, H. H.; Bengtsson, L.; Wetter, E.; Tatem, A. J.; Brownstein, J. S.; Smith, D. L.; Lambrechts, L.; Cauchemez, S.; Linard, C.; Faria, N. R.; Pybus, O. G.; Scott, T. W.; Liu, Q.; Yu, H.; Wint, G. R. W.; Hay, S. I.; Golding, N., Past and future spread of the arbovirus vectors *Aedes aegypti* and *Aedes albopictus*. *Nature Microbiology* **2019**, 4, (5), 854-863.

9. Hou, W.; Zhou, Y.; Luo, W.; Wang, L.; Kwan, M.-P.; Cook, A. R., Mapping environmental suitability changes for arbovirus mosquitoes in Southeast Asia: 1960–2020. *iScience* **2024**, 27, (8), 110498.

10. Weber, W. C.; Streblow, D. N.; Coffey, L. L., Chikungunya Virus Vaccines: A Review of IXCHIQ and PXVX0317 from Pre-Clinical Evaluation to Licensure. *BioDrugs* **2024**.

11. Baxter, V. K.; Heise, M. T., Chapter Nine - Immunopathogenesis of alphaviruses. In *Advances in Virus Research*, Carr, J. P.; Roossinck, M. J., Eds. Academic Press: 2020; Vol. 107, pp 315-382.

12. Zaid, A.; Burt, F. J.; Liu, X.; Poo, Y. S.; Zandi, K.; Suhrbier, A.; Weaver, S. C.; Texeira, M. M.; Mahalingam, S., Arthritogenic alphaviruses: epidemiological and clinical perspective on emerging arboviruses. *Lancet Infect Dis* **2021**, 21, (5), e123-e133.

13. Tong Jia Ming, S.; Tan Yi Jun, K.; Carissimo, G., Pathogenicity and virulence of O'nyong-nyong virus: A less studied Togaviridae with pandemic potential. *Virulence* **2024**, *15*, (1), 2355201.
14. Powers, A. M.; Brault, A. C.; Shirako, Y.; Strauss, E. G.; Kang, W.; Strauss, J. H.; Weaver, S. C., Evolutionary Relationships and Systematics of the Alphaviruses. *Journal of Virology* **2001**, *75*, (21), 10118-10131.
15. Schwartz, O.; Albert, M. L., Biology and pathogenesis of chikungunya virus. *Nature Reviews Microbiology* **2010**, *8*, (7), 491-500.
16. Borgherini, G.; Poubeau, P.; Jossaume, A.; Gouix, A.; Cotte, L.; Michault, A.; Arvin-Berod, C.; Paganin, F., Persistent arthralgia associated with chikungunya virus: a study of 88 adult patients on reunion island. *Clin Infect Dis* **2008**, *47*, (4), 469-75.
17. Hayd, R. L. N.; Moreno, M. R.; Naveca, F.; Amdur, R.; Suchowiecki, K.; Watson, H.; Firestein, G. S.; Simon, G.; Chang, A. Y., Persistent chikungunya arthritis in Roraima, Brazil. *Clinical Rheumatology* **2020**, *39*, (9), 2781-2787.
18. Yodtaweeponnanan, P.; Pongsittisak, W.; Satpanich, P., Incidence and factors associated with chronic chikungunya arthritis following chikungunya virus infection. *Trop Med Int Health* **2023**, *28*, (8), 653-659.
19. Tritsch, S. R.; Encinales, L.; Pacheco, N.; Cadena, A.; Cure, C.; McMahon, E.; Watson, H.; Porras Ramirez, A.; Mendoza, A. R.; Li, G.; Khurana, K.; Jaller-Raad, J. J.; Castillo, S. M.; Barrios Taborda, O.; Jaller-Char, J. J.; Echavez, L. A.; Jiménez, D.; Gonzalez Coba, A.; Alarcon Gomez, M.; Ariza Orozco, D.; Bravo, E.; Martinez, V.; Guerra, B.; Simon, G.; Firestein, G. S.; Chang, A. Y., Chronic Joint Pain 3 Years after Chikungunya Virus Infection Largely Characterized by Relapsing-remitting Symptoms. *The Journal of Rheumatology* **2020**, *47*, (8), 1267.
20. Ninla-Aesong, P.; Mitarnun, W.; Noipha, K., Long-term persistence of chikungunya virus-associated manifestations and anti-chikungunya virus antibody in southern Thailand: 5 years after an outbreak in 2008–2009. *Viral Immunology* **2020**, *33*, (2), 86-93.

21. Suhrbier, A., Rheumatic manifestations of chikungunya: emerging concepts and interventions. *Nature Reviews Rheumatology* **2019**, 15, (10), 597-611.
22. Pinheiro, F. P.; Freitas, R. B.; Travassos da Rosa, J.; Gabbay, Y. B.; Mello, W. A.; LeDuc, J. W., An outbreak of Mayaro virus disease in Belterra, Brazil. I. Clinical and virological findings. *The American journal of tropical medicine and hygiene* **1981**, 30, (3), 674-681.
23. Appassakij, H.; Khuntikij, P.; Kemapunmanus, M.; Wutthananarungsan, R.; Silpapojakul, K., Viremic profiles in asymptomatic and symptomatic chikungunya fever: a blood transfusion threat? *Transfusion* **2013**, 53, (10pt2), 2567-2574.
24. Pinheiro, T. J.; Guimarães, L. F.; Silva, M. T. T.; Soares, C. N., Neurological manifestations of Chikungunya and Zika infections. *Arquivos de neuro-psiquiatria* **2016**, 74, 937-943.
25. de Souza, W. M.; de Lima, S. T. S.; Simões Mello, L. M.; Candido, D. S.; Buss, L.; Whittaker, C.; Claro, I. M.; Chandradeva, N.; Granja, F.; de Jesus, R.; Lemos, P. S.; Toledo-Teixeira, D. A.; Barbosa, P. P.; Firmino, A. C. L.; Amorim, M. R.; Duarte, L. M. F.; Pessoa, I. B., Jr.; Forato, J.; Vasconcelos, I. L.; Maximo, A.; Araújo, E. L. L.; Perdigo Mello, L.; Sabino, E. C.; Proença-Módena, J. L.; Faria, N. R.; Weaver, S. C., Spatiotemporal dynamics and recurrence of chikungunya virus in Brazil: an epidemiological study. *Lancet Microbe* **2023**, 4, (5), e319-e329.
26. de Souza, W. M.; Fumagalli, M. J.; de Lima, S. T. S.; Parise, P. L.; Carvalho, D. C. M.; Hernandez, C.; de Jesus, R.; Delafiori, J.; Candido, D. S.; Carregari, V. C.; Muraro, S. P.; Souza, G. F.; Simões Mello, L. M.; Claro, I. M.; Díaz, Y.; Kato, R. B.; Trentin, L. N.; Costa, C. H. S.; Maximo, A. C. B. M.; Cavalcante, K. F.; Fiuza, T. S.; Viana, V. A. F.; Melo, M. E. L.; Ferraz, C. P. M.; Silva, D. B.; Duarte, L. M. F.; Barbosa, P. P.; Amorim, M. R.; Judice, C. C.; Toledo-Teixeira, D. A.; Ramundo, M. S.; Aguilar, P. V.; Araújo, E. L. L.; Costa, F. T. M.; Cerqueira-Silva, T.; Khouri, R.; Boaventura, V. S.; Figueiredo, L. T. M.; Fang, R.; Moreno, B.; López-Vergès, S.; Mello, L. P.; Skaf, M. S.; Catharino, R. R.; Granja, F.; Martins-de-Souza, D.; Plante, J. A.; Plante, K. S.; Sabino, E. C.; Diamond, M. S.; Eugenin, E.; Proença-Módena, J. L.; Faria,

- N. R.; Weaver, S. C., Pathophysiology of chikungunya virus infection associated with fatal outcomes. *Cell Host & Microbe* **2024**, 32, (4), 606-622.e8.
27. Dramé, M.; Kanagaratnam, L.; Hentzien, M.; Fanon, J.-L.; Bartholet, S.; Godaert, L., Clinical forms of chikungunya virus infection: the challenge and utility of a consensus definition. *The American Journal of Tropical Medicine and Hygiene* **2018**, 99, (2), 552.
28. de Paula, H. H. S.; Martins, A. F.; das Chagas, R. R.; Moreira, J.; de Aguiar, R. S.; da Cruz Lamas, C.; Cardozo, S. V., Chikungunya fever: How accurate is the clinical-epidemiological diagnosis compared to the gold standard of molecular and serological laboratory diagnosis? *Journal of Clinical Virology* **2020**, 133, 104679.
29. Ronca, S. E.; Dineley, K. T.; Paessler, S., Neurological sequelae resulting from encephalitic alphavirus infection. *Frontiers in microbiology* **2016**, 7, 959.
30. Zacks, M. A.; Paessler, S., Encephalitic alphaviruses. *Veterinary Microbiology* **2010**, 140, (3), 281-286.
31. Henderson Sousa, F.; Ghaisani Komarudin, A.; Findlay-Greene, F.; Bowolaksono, A.; Sasmono, R. T.; Stevens, C.; Barlow, P. G., Evolution and immunopathology of chikungunya virus informs therapeutic development. *Dis Model Mech* **2023**, 16, (4).
32. Priya, R.; Patro, I.; Parida, M., TLR3 mediated innate immune response in mice brain following infection with Chikungunya virus. *Virus research* **2014**, 189, 194-205.
33. Onomoto, K.; Onoguchi, K.; Yoneyama, M., Regulation of RIG-I-like receptor-mediated signaling: interaction between host and viral factors. *Cellular & molecular immunology* **2021**, 18, (3), 539-555.
34. Rudd, P. A.; Wilson, J.; Gardner, J.; Larcher, T.; Babarit, C.; Le, T. T.; Anraku, I.; Kumagai, Y.; Loo, Y. M.; Gale, M., Jr.; Akira, S.; Khromykh, A. A.; Suhrbier, A., Interferon response factors 3 and 7 protect against Chikungunya virus hemorrhagic fever and shock. *J Virol* **2012**, 86, (18), 9888-98.

35. Tan, Y. B.; Chmielewski, D.; Law, M. C. Y.; Zhang, K.; He, Y.; Chen, M.; Jin, J.; Luo, D., Molecular architecture of the Chikungunya virus replication complex. *Sci Adv* **2022**, 8, (48), eadd2536.
36. Hoarau, J. J.; Jaffar Bandjee, M. C.; Krejbich Trotot, P.; Das, T.; Li-Pat-Yuen, G.; Dassa, B.; Denizot, M.; Guichard, E.; Ribera, A.; Henni, T.; Tallet, F.; Moiton, M. P.; Gauzère, B. A.; Bruniquet, S.; Jaffar Bandjee, Z.; Morbidelli, P.; Martigny, G.; Jolivet, M.; Gay, F.; Grandadam, M.; Tolou, H.; Vieillard, V.; Debré, P.; Autran, B.; Gasque, P., Persistent chronic inflammation and infection by Chikungunya arthritogenic alphavirus in spite of a robust host immune response. *J Immunol* **2010**, 184, (10), 5914-27.
37. Wauquier, N.; Becquart, P.; Nkoghe, D.; Padilla, C.; Ndjoyi-Mbiguino, A.; Leroy, E. M., The Acute Phase of Chikungunya Virus Infection in Humans Is Associated With Strong Innate Immunity and T CD8 Cell Activation. *The Journal of Infectious Diseases* **2010**, 204, (1), 115-123.
38. Teng, T.-S.; Kam, Y.-W.; Lee, B.; Hapuarachchi, H. C.; Wimal, A.; Ng, L.-C.; Ng, L. F., A systematic meta-analysis of immune signatures in patients with acute chikungunya virus infection. *The Journal of infectious diseases* **2015**, 211, (12), 1925-1935.
39. Weber, W. C.; Labriola, C. S.; Kreklywich, C. N.; Ray, K.; Haese, N. N.; Andoh, T. F.; Denton, M.; Medica, S.; Streblow, M. M.; Smith, P. P.; Mizuno, N.; Frias, N.; Fisher, M. B.; Barber-Axthelm, A. M.; Chun, K.; Uttke, S.; Whitcomb, D.; DeFilippis, V.; Rakshe, S.; Fei, S. S.; Axthelm, M. K.; Smedley, J. V.; Streblow, D. N., Mayaro virus pathogenesis and immunity in rhesus macaques. *PLoS Negl Trop Dis* **2023**, 17, (11), e0011742.
40. Broeckel, R.; Fox, J. M.; Haese, N.; Kreklywich, C. N.; Sukulpovi-Petty, S.; Legasse, A.; Smith, P. P.; Denton, M.; Corvey, C.; Krishnan, S.; Colgin, L. M. A.; Ducore, R. M.; Lewis, A. D.; Axthelm, M. K.; Mandron, M.; Cortez, P.; Rothblatt, J.; Rao, E.; Focken, I.; Carter, K.; Sapparapau, G.; Crowe, J. E., Jr.; Diamond, M. S.; Streblow, D. N., Therapeutic administration of a recombinant human monoclonal antibody reduces the severity of chikungunya virus disease in rhesus macaques. *PLoS Negl Trop Dis* **2017**, 11, (6), e0005637.

41. Dias, C. N. d. S.; Gois, B. M.; Lima, V. S.; Guerra-Gomes, I. C.; Araújo, J. M. G.; Gomes, J. d. A. S.; Araújo, D. A. M.; Medeiros, I. A.; Azevedo, F. d. L. A. A. d.; Veras, R. C., Human CD 8 T-cell activation in acute and chronic chikungunya infection. *Immunology* **2018**, 155, (4), 499-504.
42. Poo, Y. S.; Rudd, P. A.; Gardner, J.; Wilson, J. A.; Larcher, T.; Colle, M.-A.; Le, T. T.; Nakaya, H. I.; Warrilow, D.; Allcock, R., Multiple immune factors are involved in controlling acute and chronic chikungunya virus infection. *PLoS neglected tropical diseases* **2014**, 8, (12), e3354.
43. Teo, T. H.; Lum, F. M.; Claser, C.; Lulla, V.; Lulla, A.; Merits, A.; Rénia, L.; Ng, L. F., A pathogenic role for CD4+ T cells during Chikungunya virus infection in mice. *J Immunol* **2013**, 190, (1), 259-69.
44. Broeckel, R.; Haese, N.; Ando, T.; Dmitriev, I.; Kreklywich, C.; Powers, J. *Vaccine-induced skewing of T cell responses protects against chikungunya virus disease. Front Immunol. 2019; 10: 2563*; Epub 2019/11/19. <https://doi.org/10.3389/fimmu.2019.02563> PMID: 31736977: 2019.
45. Hoarau, J. J.; Gay, F.; Pellé, O.; Samri, A.; Jaffar-Bandjee, M. C.; Gasque, P.; Autran, B., Identical strength of the T cell responses against E2, nsP1 and capsid CHIKV proteins in recovered and chronic patients after the epidemics of 2005-2006 in La Reunion Island. *PLoS One* **2013**, 8, (12), e84695.
46. Weger-Lucarelli, J.; Chu, H.; Aliota, M. T.; Partidos, C. D.; Osorio, J. E., A Novel MVA Vectored Chikungunya Virus Vaccine Elicits Protective Immunity in Mice. *PLOS Neglected Tropical Diseases* **2014**, 8, (7), e2970.
47. Poh, C. M.; Chan, Y.-H.; Ng, L. F., Role of T cells in Chikungunya virus infection and utilizing their potential in anti-viral immunity. *Frontiers in Immunology* **2020**, 11, 287.
48. Ikeda, N.; Asano, K.; Kikuchi, K.; Uchida, Y.; Ikegami, H.; Takagi, R.; Yotsumoto, S.; Shibuya, T.; Makino-Okamura, C.; Fukuyama, H., Emergence of immunoregulatory Ym1+

Ly6Chi monocytes during recovery phase of tissue injury. *Science immunology* **2018**, 3, (28), eaat0207.

49. Labadie, K.; Larcher, T.; Joubert, C.; Mannioui, A.; Delache, B.; Brochard, P.; Guigand, L.; Dubreil, L.; Lebon, P.; Verrier, B., Chikungunya disease in nonhuman primates involves long-term viral persistence in macrophages. *The Journal of clinical investigation* **2010**, 120, (3), 894-906.

50. Song, L.; Dong, G.; Guo, L.; Graves, D. T., The function of dendritic cells in modulating the host response. *Mol Oral Microbiol* **2018**, 33, (1), 13-21.

51. Shabman, R. S.; Morrison, T. E.; Moore, C.; White, L.; Suthar, M. S.; Hueston, L.; Rulli, N.; Lidbury, B.; Ting, J. P.; Mahalingam, S.; Heise, M. T., Differential induction of type I interferon responses in myeloid dendritic cells by mosquito and mammalian-cell-derived alphaviruses. *J Virol* **2007**, 81, (1), 237-47.

52. Swiecki, M.; Colonna, M., The multifaceted biology of plasmacytoid dendritic cells. *Nature Reviews Immunology* **2015**, 15, (8), 471-485.

53. Lum, F.-M.; Teo, T.-H.; Lee, W. W. L.; Kam, Y.-W.; Rénia, L.; Ng, L. F. P., An Essential Role of Antibodies in the Control of Chikungunya Virus Infection. *The Journal of Immunology* **2013**, 190, (12), 6295-6302.

54. Dal Porto, J. M.; Haberman, A. M.; Shlomchik, M. J.; Kelsoe, G., Antigen drives very low affinity B cells to become plasmacytes and enter germinal centers. *The Journal of Immunology* **1998**, 161, (10), 5373-5381.

55. Slifka, M. K.; Antia, R.; Whitmire, J. K.; Ahmed, R., Humoral immunity due to long-lived plasma cells. *Immunity* **1998**, 8, (3), 363-372.

56. Lam, J. H.; Smith, F. L.; Baumgarth, N., B cell activation and response regulation during viral infections. *Viral immunology* **2020**, 33, (4), 294-306.

57. McHeyzer-Williams, L. J.; Driver, D. J.; McHeyzer-Williams, M. G., Germinal center reaction. *Current opinion in hematology* **2001**, 8, (1), 52-59.

58. Calame, K. L., Plasma cells: finding new light at the end of B cell development. *Nature Immunology* **2001**, 2, (12), 1103-1108.
59. Powers, J. M.; Lyski, Z. L.; Weber, W. C.; Denton, M.; Streblow, M. M.; Mayo, A. T.; Haese, N. N.; Nix, C. D.; Rodríguez-Santiago, R.; Alvarado, L. I.; Rivera-Amill, V.; Messer, W. B.; Streblow, D. N., Infection with chikungunya virus confers heterotypic cross-neutralizing antibodies and memory B-cells against other arthritogenic alphaviruses predominantly through the B domain of the E2 glycoprotein. *PLoS Negl Trop Dis* **2023**, 17, (3), e0011154.
60. Adam, A.; Luo, H.; Osman, S. R.; Wang, B.; Roundy, C. M.; Auguste, A. J.; Plante, K. S.; Peng, B. H.; Thangamani, S.; Frolova, E. I.; Frolov, I.; Weaver, S. C.; Wang, T., Optimized production and immunogenicity of an insect virus-based chikungunya virus candidate vaccine in cell culture and animal models. *Emerg Microbes Infect* **2021**, 10, (1), 305-316.
61. Crowe, J. E., Jr., Human Antibodies for Viral Infections. *Annu Rev Immunol* **2022**, 40, 349-386.
62. Chua, C.-L.; Sam, I.-C.; Chiam, C.-W.; Chan, Y.-F., The neutralizing role of IgM during early Chikungunya virus infection. *PloS one* **2017**, 12, (2), e0171989.
63. Panning, M.; Grywna, K.; Van Esbroeck, M.; Emmerich, P.; Drosten, C., Chikungunya fever in travelers returning to Europe from the Indian Ocean region, 2006. *Emerging infectious diseases* **2008**, 14, (3), 416.
64. Bozza, F. A.; Moreira-Soto, A.; Rockstroh, A.; Fischer, C.; Nascimento, A. D.; Calheiros, A. S.; Drosten, C.; Bozza, P. T.; Souza, T. M. L.; Ulbert, S., Differential shedding and antibody kinetics of Zika and Chikungunya viruses, Brazil. *Emerging infectious diseases* **2019**, 25, (2), 311.
65. Diagne, C. T.; Bengue, M.; Choumet, V.; Hamel, R.; Pompon, J.; Missé, D., Mayaro Virus Pathogenesis and Transmission Mechanisms. *Pathogens* **2020**, 9, (9).
66. Farmer, J. F.; Suhrbier, A., Interpreting paired serology for Ross River virus and Barmah Forest virus diseases. *Aust J Gen Pract* **2019**, 48, (9), 645-649.

67. Malvy, D.; Ezzedine, K.; Mamani-Matsuda, M.; Autran, B.; Tolou, H.; Receveur, M.-C.; Pistone, T.; Rambert, J.; Moynet, D.; Mossalayi, D., Destructive arthritis in a patient with chikungunya virus infection with persistent specific IgM antibodies. *BMC infectious diseases* **2009**, *9*, 1-7.
68. Costa, D.; Coêlho, M.; Gouveia, P.; Bezerra, L. A.; Marques, C. D. L.; Duarte, A.; Valente, L. M.; Magalhães, V., Long-Term Persistence of Serum-Specific Anti-Chikungunya IgM Antibody - A Case Series of Brazilian Patients. *Rev Soc Bras Med Trop* **2021**, *54*, e0855.
69. Weber, W. C.; Streblow, Z. J.; Kreklywich, C. N.; Denton, M.; Sulgey, G.; Streblow, M. M.; Marcano, D.; Flores, P. N.; Rodriguez-Santiago, R. M.; Alvarado, L. I.; Rivera-Amill, V.; Messer, W. B.; Hochreiter, R.; Kosulin, K.; Dubischar, K.; Buerger, V.; Streblow, D. N., The Approved Live-Attenuated Chikungunya Virus Vaccine (IXCHIQ®) Elicits Cross-Neutralizing Antibody Breadth Extending to Multiple Arthritogenic Alphaviruses Similar to the Antibody Breadth Following Natural Infection. *Vaccines* **2024**, *12*, (8), 893.
70. Voss, J. E.; Vaney, M.-C.; Duquerroy, S.; Vonnrhein, C.; Girard-Blanc, C.; Crublet, E.; Thompson, A.; Bricogne, G.; Rey, F. A., Glycoprotein organization of Chikungunya virus particles revealed by X-ray crystallography. *Nature* **2010**, *468*, (7324), 709-712.
71. Porta, J.; Jose, J.; Roehrig, J. T.; Blair, C. D.; Kuhn, R. J.; Rossmann, M. G., Locking and blocking the viral landscape of an alphavirus with neutralizing antibodies. *J Virol* **2014**, *88*, (17), 9616-23.
72. Earnest, J. T.; Holmes, A. C.; Basore, K.; Mack, M.; Fremont, D. H.; Diamond, M. S., The mechanistic basis of protection by non-neutralizing anti-alphavirus antibodies. *Cell Rep* **2021**, *35*, (1), 108962.
73. Weber, C.; Büchner, S. M.; Schnierle, B. S., A small antigenic determinant of the Chikungunya virus E2 protein is sufficient to induce neutralizing antibodies which are partially protective in mice. *PLoS Negl Trop Dis* **2015**, *9*, (4), e0003684.
74. Torres-Ruesta, A.; Chee, R. S.-L.; Ng, L. F. P., Insights into Antibody-Mediated Alphavirus Immunity and Vaccine Development Landscape. *Microorganisms* **2021**, *9*, (5), 899.

75. Henss, L.; Yue, C.; Von Rhein, C.; Tschismarov, R.; Lewis-Ximenez, L. L.; Dölle, A.; Baylis, S. A.; Schnierle, B. S., Analysis of Humoral Immune Responses in Chikungunya Virus (CHIKV)-Infected Patients and Individuals Vaccinated With a Candidate CHIKV Vaccine. *The Journal of Infectious Diseases* **2019**, 221, (10), 1713-1723.
76. Malonis, R. J.; Earnest, J. T.; Kim, A. S.; Angeliadis, M.; Holtsberg, F. W.; Aman, M. J.; Jangra, R. K.; Chandran, K.; Daily, J. P.; Diamond, M. S.; Kielian, M.; Lai, J. R., Near-germline human monoclonal antibodies neutralize and protect against multiple arthritogenic alphaviruses. *Proceedings of the National Academy of Sciences* **2021**, 118, (37), e2100104118.
77. Earnest, J. T.; Basore, K.; Roy, V.; Bailey, A. L.; Wang, D.; Alter, G.; Fremont, D. H.; Diamond, M. S., Neutralizing antibodies against Mayaro virus require Fc effector functions for protective activity. *J Exp Med* **2019**, 216, (10), 2282-2301.
78. Kim, A. S.; Kafai, N. M.; Winkler, E. S.; Gilliland, T. C.; Cottle, E. L.; Earnest, J. T.; Jethva, P. N.; Kaplonek, P.; Shah, A. P.; Fong, R. H.; Davidson, E.; Malonis, R. J.; Quiroz, J. A.; Williamson, L. E.; Vang, L.; Mack, M.; Crowe, J. E.; Doranz, B. J.; Lai, J. R.; Alter, G.; Gross, M. L.; Klimstra, W. B.; Fremont, D. H.; Diamond, M. S., Pan-protective anti-alphavirus human antibodies target a conserved E1 protein epitope. *Cell* **2021**, 184, (17), 4414-4429.e19.
79. Zhou, Q. F.; Fox, J. M.; Earnest, J. T.; Ng, T. S.; Kim, A. S.; Fibriansah, G.; Kostyuchenko, V. A.; Shi, J.; Shu, B.; Diamond, M. S.; Lok, S. M., Structural basis of Chikungunya virus inhibition by monoclonal antibodies. *Proc Natl Acad Sci U S A* **2020**, 117, (44), 27637-27645.
80. Kasbe, R.; Tripathy, A. S.; Wani, M. R.; Mullick, J., Elevated Complement Activation Fragments and C1q-Binding Circulating Immune Complexes in Varied Phases of Chikungunya Virus Infection. *Current Microbiology* **2024**, 81, (8), 242.
81. Bedoui, Y.; De Larichaudy, D.; Daniel, M.; Ah-Pine, F.; Selambarom, J.; Guiraud, P.; Gasque, P., Deciphering the Role of Schwann Cells in Inflammatory Peripheral Neuropathies Post Alphavirus Infection. *Cells* **2022**, 12, (1).

82. Morrison, T. E.; Simmons, J. D.; Heise, M. T., Complement receptor 3 promotes severe Ross River virus-induced disease. *Journal of virology* **2008**, 82, (22), 11263-11272.
83. Morrison, T. E.; Fraser, R. J.; Smith, P. N.; Mahalingam, S.; Heise, M. T., Complement contributes to inflammatory tissue destruction in a mouse model of Ross River virus-induced disease. *Journal of virology* **2007**, 81, (10), 5132-5143.
84. Pereira-Filho, A. A.; Mateus Pereira, R. H.; da Silva, N. C. S.; Ferreira Malta, L. G.; Serravite, A. M.; Carvalho de Almeida, C. G.; Fujiwara, R. T.; Bartholomeu, D. C.; Giunchetti, R. C.; D'Ávila Pessoa, G. C.; Koerich, L. B.; Pereira, M. H.; Araujo, R. N.; Gontijo, N. F.; Viana Sant'Anna, M. R., The gut anti-complement activity of *Aedes aegypti*: Investigating new ways to control the major human arboviruses vector in the Americas. *Insect Biochem Mol Biol* **2020**, 120, 103338.
85. Martins, K. A.; Gregory, M. K.; Valdez, S. M.; Sprague, T. R.; Encinales, L.; Pacheco, N.; Cure, C.; Porras-Ramirez, A.; Rico-Mendoza, A.; Chang, A.; Pitt, M. L.; Nasar, F., Neutralizing Antibodies from Convalescent Chikungunya Virus Patients Can Cross-Neutralize Mayaro and Una Viruses. *Am J Trop Med Hyg* **2019**, 100, (6), 1541-1544.
86. Nguyen, W.; Nakayama, E.; Yan, K.; Tang, B.; Le, T. T.; Liu, L.; Cooper, T. H.; Hayball, J. D.; Faddy, H. M.; Warrilow, D.; Allcock, R. J. N.; Hobson-Peters, J.; Hall, R. A.; Rawle, D. J.; Lutzky, V. P.; Young, P.; Oliveira, N. M.; Hartel, G.; Howley, P. M.; Prow, N. A.; Suhrbier, A., Arthritogenic Alphavirus Vaccines: Serogrouping Versus Cross-Protection in Mouse Models. *Vaccines (Basel)* **2020**, 8, (2).
87. Bopp, N. E.; Jencks, K. J.; Siles, C.; Guevara, C.; Vilcarromero, S.; Fernández, D.; Halsey, E. S.; Ampuero, J. S.; Aguilar, P. V., Serological Responses in Patients Infected with Mayaro Virus and Evaluation of Cross-Protective Responses against Chikungunya Virus. *Am J Trop Med Hyg* **2021**, 106, (2), 607-609.
88. Zini, N.; Ávila, M. H. T.; Cezarotti, N. M.; Parra, M. C. P.; Banho, C. A.; Sacchetto, L.; Negri, A. F.; Araújo, E.; Bittar, C.; Milhin, B.; Miranda Hernandez, V.; Dutra, K. R.; Trigo, L. A.; Cecílio da Rocha, L.; Alves da Silva, R.; Celestino Dutra da Silva, G.; Fernanda Pereira Dos Santos, T.; de Carvalho Marques, B.; Lopes Dos Santos, A.; Augusto, M. T.; Mistrão, N. F. B.;

Ribeiro, M. R.; Pinheiro, T. M.; Maria Izabel Lopes Dos Santos, T.; Avilla, C. M. S.; Bernardi, V.; Freitas, C.; Gandolfi, F. A.; Ferraz Júnior, H. C.; Perim, G. C.; Gomes, M. C.; Garcia, P. H. C.; Rocha, R. S.; Galvão, T. M.; Fávoro, E. A.; Scamardi, S. N.; Rogovski, K. S.; Peixoto, R. L.; Benfatti, L.; Cruz, L. T.; Chama, P. P. F.; Oliveira, M. T.; Watanabe, A. S. A.; Terzian, A. C. B.; de Freitas Versiani, A.; Dibo, M. R.; Chiaravalotti-Neto, F.; Weaver, S. C.; Estofolete, C. F.; Vasilakis, N.; Nogueira, M. L., Cryptic circulation of chikungunya virus in São Jose do Rio Preto, Brazil, 2015-2019. *PLoS Negl Trop Dis* **2024**, 18, (3), e0012013.

89. Hozé, N.; Diarra, I.; Sangaré, A. K.; Pastorino, B.; Pezzi, L.; Kouriba, B.; Sagara, I.; Dabo, A.; Djimé, A.; Thera, M. A., Model-based assessment of Chikungunya and O'nyong-nyong virus circulation in Mali in a serological cross-reactivity context. *Nature communications* **2021**, 12, (1), 6735.

90. Weber, W. C.; Andoh, T. F.; Kreklywich, C. N.; Streblow, Z. J.; Denton, M.; Streblow, M. M.; Powers, J. M.; Sulgey, G.; Medica, S.; Dmitriev, I.; Curiel, D. T.; Haese, N. N.; Streblow, D. N., Nonreciprocity in CHIKV and MAYV Vaccine-Elicited Protection. *Vaccines* **2024**, 12, (9), 970.

91. Powers, J. M.; Haese, N. N.; Denton, M.; Ando, T.; Kreklywich, C.; Bonin, K.; Streblow, C. E.; Kreklywich, N.; Smith, P.; Broeckel, R.; DeFilippis, V.; Morrison, T. E.; Heise, M. T.; Streblow, D. N., Non-replicating adenovirus based Mayaro virus vaccine elicits protective immune responses and cross protects against other alphaviruses. *PLoS Negl Trop Dis* **2021**, 15, (4), e0009308.

92. Campos, R. K.; Preciado-Llanes, L.; Azar, S. R.; Kim, Y. C.; Brandon, O.; López-Camacho, C.; Reyes-Sandoval, A.; Rossi, S. L., Adenoviral-Vectored Mayaro and Chikungunya Virus Vaccine Candidates Afford Partial Cross-Protection From Lethal Challenge in A129 Mouse Model. *Front Immunol* **2020**, 11, 591885.

93. Webb, E. M.; Azar, S. R.; Haller, S. L.; Langsjoen, R. M.; Cuthbert, C. E.; Ramjag, A. T.; Luo, H.; Plante, K.; Wang, T.; Simmons, G.; Carrington, C. V. F.; Weaver, S. C.; Rossi, S. L.; Auguste, A. J., Effects of Chikungunya virus immunity on Mayaro virus disease and epidemic potential. *Scientific Reports* **2019**, 9, (1), 20399.

94. Nguyen, W.; Nakayama, E.; Yan, K.; Tang, B.; Le, T. T.; Liu, L.; Cooper, T. H.; Hayball, J. D.; Faddy, H. M.; Warrilow, D., Arthritogenic alphavirus vaccines: serogrouping versus cross-protection in mouse models. *Vaccines* **2020**, *8*, (2), 209.
95. Walton, T. E.; Jochim, M. M.; Barber, T. L.; Thompson, L. H., Cross-protective immunity between equine encephalomyelitis viruses in equids. *Am J Vet Res* **1989**, *50*, (9), 1442-6.
96. Linn, M. L.; Mateo, L.; Gardner, J.; Suhrbier, A., Alphavirus-specific cytotoxic T lymphocytes recognize a cross-reactive epitope from the capsid protein and can eliminate virus from persistently infected macrophages. *J Virol* **1998**, *72*, (6), 5146-53.
97. Plotkin, S. A., Correlates of protection induced by vaccination. *Clinical and vaccine immunology* **2010**, *17*, (7), 1055-1065.
98. Milligan, G. N.; Schnierle, B. S.; McAuley, A. J.; Beasley, D. W. C., Defining a correlate of protection for chikungunya virus vaccines. *Vaccine* **2019**, *37*, (50), 7427-7436.
99. Roques, P.; Fritzer, A.; Dereuddre-Bosquet, N.; Wressnigg, N.; Hochreiter, R.; Bossevoit, L.; Pascal, Q.; Guehenneux, F.; Bitzer, A.; Corbic Ramljak, I.; Le Grand, R.; Lundberg, U.; Meinke, A., Effectiveness of CHIKV vaccine VLA1553 demonstrated by passive transfer of human sera. *JCI Insight* **2022**, *7*, (14).
100. Hallengård, D.; Lum, F.-M.; Kümmerer, B. M.; Lulla, A.; Lulla, V.; García-Arriaza, J.; Fazakerley, J. K.; Roques, P.; Grand, R. L.; Merits, A.; Ng, L. F. P.; Esteban, M.; Liljeström, P., Prime-Boost Immunization Strategies against Chikungunya Virus. *Journal of Virology* **2014**, *88*, (22), 13333-13343.
101. Hallengård, D.; Kakoulidou, M.; Lulla, A.; Kümmerer, B. M.; Johansson, D. X.; Mutso, M.; Lulla, V.; Fazakerley, J. K.; Roques, P.; Le Grand, R.; Merits, A.; Liljeström, P., Novel attenuated Chikungunya vaccine candidates elicit protective immunity in C57BL/6 mice. *J Virol* **2014**, *88*, (5), 2858-66.
102. Slifka, D. K.; Raué, H. P.; Weber, W. C.; Andoh, T. F.; Kreklywich, C. N.; DeFilippis, V. R.; Streblow, D. N.; Slifka, M. K.; Amanna, I. J., Development of a next-generation

chikungunya virus vaccine based on the HydroVax platform. *PLoS Pathog* **2022**, 18, (7), e1010695.

103. Brandler, S.; Ruffié, C.; Combredet, C.; Brault, J. B.; Najburg, V.; Prevost, M. C.; Habel, A.; Tauber, E.; Desprès, P.; Tangy, F., A recombinant measles vaccine expressing chikungunya virus-like particles is strongly immunogenic and protects mice from lethal challenge with chikungunya virus. *Vaccine* **2013**, 31, (36), 3718-25.

104. Chu, H.; Das, S. C.; Fuchs, J. F.; Suresh, M.; Weaver, S. C.; Stinchcomb, D. T.; Partidos, C. D.; Osorio, J. E., Deciphering the protective role of adaptive immunity to CHIKV/IRES a novel candidate vaccine against Chikungunya in the A129 mouse model. *Vaccine* **2013**, 31, (33), 3353-60.

105. Holzer, G. W.; Coulibaly, S.; Aichinger, G.; Savidis-Dacho, H.; Mayrhofer, J.; Brunner, S.; Schmid, K.; Kistner, O.; Aaskov, J. G.; Falkner, F. G., Evaluation of an inactivated Ross River virus vaccine in active and passive mouse immunization models and establishment of a correlate of protection. *Vaccine* **2011**, 29, (24), 4132-4141.

106. Partidos, C. D.; Paykel, J.; Weger, J.; Borland, E. M.; Powers, A. M.; Seymour, R.; Weaver, S. C.; Stinchcomb, D. T.; Osorio, J. E., Cross-protective immunity against o 'nyong-nyong virus afforded by a novel recombinant chikungunya vaccine. *Vaccine* **2012**, 30, (31), 4638-4643.

107. Williamson, L. E.; Reeder, K. M.; Bailey, K.; Tran, M. H.; Roy, V.; Fouch, M. E.; Kose, N.; Trivette, A.; Nargi, R. S.; Winkler, E. S.; Kim, A. S.; Gainza, C.; Rodriguez, J.; Armstrong, E.; Sutton, R. E.; Reidy, J.; Carnahan, R. H.; McDonald, W. H.; Schoeder, C. T.; Klimstra, W. B.; Davidson, E.; Doranz, B. J.; Alter, G.; Meiler, J.; Schey, K. L.; Julander, J. G.; Diamond, M. S.; Crowe, J. E., Therapeutic alphavirus cross-reactive E1 human antibodies inhibit viral egress. *Cell* **2021**, 184, (17), 4430-4446.e22.

108. Julander, J. G.; Anderson, N.; Haese, N.; Andoh, T.; Streblow, D. N.; Cortez, P.; Carter, K.; Marniquet, X.; Watson, H.; Mandron, M., Therapeutic and prophylactic treatment with a virus-specific antibody is highly effective in rodent models of Chikungunya infection and disease. *Antiviral Research* **2022**, 202, 105295.

109. Pal, P.; Dowd, K. A.; Brien, J. D.; Edeling, M. A.; Gorlatov, S.; Johnson, S.; Lee, I.; Akahata, W.; Nabel, G. J.; Richter, M. K.; Smit, J. M.; Fremont, D. H.; Pierson, T. C.; Heise, M. T.; Diamond, M. S., Development of a highly protective combination monoclonal antibody therapy against Chikungunya virus. *PLoS Pathog* **2013**, *9*, (4), e1003312.
110. Pal, P.; Fox, J. M.; Hawman, D. W.; Huang, Y. J.; Messaoudi, I.; Kreklywich, C.; Denton, M.; Legasse, A. W.; Smith, P. P.; Johnson, S.; Axthelm, M. K.; Vanlandingham, D. L.; Streblow, D. N.; Higgs, S.; Morrison, T. E.; Diamond, M. S., Chikungunya viruses that escape monoclonal antibody therapy are clinically attenuated, stable, and not purified in mosquitoes. *J Virol* **2014**, *88*, (15), 8213-26.
111. Schmitz, K. S.; Comvalius, A. D.; Nieuwkoop, N. J.; Geers, D.; Weiskopf, D.; Ramsauer, K.; Sette, A.; Tschismarov, R.; de Vries, R. D.; de Swart, R. L., A measles virus-based vaccine induces robust chikungunya virus-specific CD4(+) T-cell responses in a phase II clinical trial. *Vaccine* **2023**, *41*, (43), 6495-6504.
112. Broeckel, R. M.; Haese, N.; Ando, T.; Dmitriev, I.; Kreklywich, C. N.; Powers, J.; Denton, M.; Smith, P.; Morrison, T. E.; Heise, M.; DeFilippis, V.; Messaoudi, I.; Curiel, D. T.; Streblow, D. N., Vaccine-Induced Skewing of T Cell Responses Protects Against Chikungunya Virus Disease. *Front Immunol* **2019**, *10*, 2563.
113. Choi, H.; Kudchodkar, S. B.; Reuschel, E. L.; Asija, K.; Borole, P.; Ho, M.; Wojtak, K.; Reed, C.; Ramos, S.; Bopp, N. E., Protective immunity by an engineered DNA vaccine for Mayaro virus. *PLoS neglected tropical diseases* **2019**, *13*, (2), e0007042.
114. Halstead, S. B., Neutralization and antibody-dependent enhancement of dengue viruses. **2003**.
115. Taylor, A.; Foo, S. S.; Bruzzone, R.; Vu Dinh, L.; King, N. J.; Mahalingam, S., Fc receptors in antibody-dependent enhancement of viral infections. *Immunological reviews* **2015**, *268*, (1), 340-364.

116. Hawkes, R. A., ENHANCEMENT OF THE INFECTIVITY OF ARBOVIRUSES BY SPECIFIC ANTISERA PRODUCED IN DOMESTIC FOWLS. *Aust J Exp Biol Med Sci* **1964**, 42, 465-82.
117. Peiris, J.; Porterfield, J., Antibody-dependent plaque enhancement: its antigenic specificity in relation to Togaviridae. *Journal of General Virology* **1982**, 58, (2), 291-296.
118. Chanas, A.; Gould, E.; Clegg, J.; Varma, M., Monoclonal antibodies to Sindbis virus glycoprotein E1 can neutralize, enhance infectivity, and independently inhibit haemagglutination or haemolysis. *Journal of General Virology* **1982**, 58, (1), 37-46.
119. Linn, M. L.; Aaskov, J. G.; Suhrbier, A., Antibody-dependent enhancement and persistence in macrophages of an arbovirus associated with arthritis. *J Gen Virol* **1996**, 77 (Pt 3), 407-11.
120. Lidbury, B. A.; Mahalingam, S., Specific ablation of antiviral gene expression in macrophages by antibody-dependent enhancement of Ross River virus infection. *J Virol* **2000**, 74, (18), 8376-81.
121. Mahalingam, S.; Lidbury, B. A., Suppression of lipopolysaccharide-induced antiviral transcription factor (STAT-1 and NF-kappa B) complexes by antibody-dependent enhancement of macrophage infection by Ross River virus. *Proc Natl Acad Sci U S A* **2002**, 99, (21), 13819-24.
122. Lum, F.-M.; Couderc, T.; Chia, B.-S.; Ong, R.-Y.; Her, Z.; Chow, A.; Leo, Y.-S.; Kam, Y.-W.; Rénia, L.; Lecuit, M., Antibody-mediated enhancement aggravates chikungunya virus infection and disease severity. *Scientific reports* **2018**, 8, (1), 1860.
123. McCarty, J. M.; Bedell, L.; Mendy, J.; Coates, E. E.; Chen, G. L.; Ledgerwood, J. E.; Tredo, S. R.; Warfield, K. L.; Richardson, J. S., Chikungunya virus virus-like particle vaccine is well tolerated and immunogenic in chikungunya seropositive individuals. *Vaccine* **2023**, 41, (42), 6146-6149.
124. Buerger, V.; Hadl, S.; Schneider, M.; Schaden, M.; Hochreiter, R.; Bitzer, A.; Kosulin, K.; Mader, R.; Zoihsel, O.; Pfeiffer, A.; Loch, A. P.; Morandi, E., Jr.; Nogueira, M. L.; de Brito,

C. A. A.; Croda, J.; Teixeira, M. M.; Coelho, I. C.-B.; Gurgel, R.; da Fonseca, A. J.; de Lacerda, M. V. G.; Moreira, E. D., Jr.; Veiga, A. P. R.; Dubischar, K.; Wressnigg, N.; Eder-Lingelbach, S.; Jaramillo, J. C., Safety and immunogenicity of a live-attenuated chikungunya virus vaccine in endemic areas of Brazil: interim results of a double-blind, randomised, placebo-controlled phase 3 trial in adolescents. *The Lancet Infectious Diseases*.

125. Kim, A. S.; Diamond, M. S., A molecular understanding of alphavirus entry and antibody protection. *Nature Reviews Microbiology* **2023**, 21, (6), 396-407.

126. Zhang, R.; Kim, A. S.; Fox, J. M.; Nair, S.; Basore, K.; Klimstra, W. B.; Rimkunas, R.; Fong, R. H.; Lin, H.; Poddar, S., Mxra8 is a receptor for multiple arthritogenic alphaviruses. *Nature* **2018**, 557, (7706), 570-574.

127. Basore, K.; Kim, A. S.; Nelson, C. A.; Zhang, R.; Smith, B. K.; Uranga, C.; Vang, L.; Cheng, M.; Gross, M. L.; Smith, J., Cryo-EM structure of chikungunya virus in complex with the Mxra8 receptor. *Cell* **2019**, 177, (7), 1725-1737. e16.

128. Zhang, K.; Law, M. C. Y.; Nguyen, T. M.; Tan, Y. B.; Wirawan, M.; Law, Y.-S.; Jeong, L. S.; Luo, D., Molecular basis of specific viral RNA recognition and 5'-end capping by the Chikungunya virus nsP1. *Cell Reports* **2022**, 40, (4).

129. Nowee, G.; Bakker, J. W.; Geertsema, C.; Ros, V. I. D.; Göertz, G. P.; Fros, J. J.; Pijlman, G. P., A Tale of 20 Alphaviruses; Inter-species Diversity and Conserved Interactions Between Viral Non-structural Protein 3 and Stress Granule Proteins. *Front Cell Dev Biol* **2021**, 9, 625711.

130. Gao, Y.; Goonawardane, N.; Ward, J.; Tuplin, A.; Harris, M., Multiple roles of the non-structural protein 3 (nsP3) alphavirus unique domain (AUD) during Chikungunya virus genome replication and transcription. *PLoS Pathog* **2019**, 15, (1), e1007239.

131. Frolova, E. I.; Palchevska, O.; Dominguez, F.; Frolov, I., Alphavirus-induced transcriptional and translational shutoffs play major roles in blocking the formation of stress granules. *J Virol* **2023**, 97, (11), e0097923.

132. Wang, Y.-F.; Sawicki, S. G.; Sawicki, D. L., Alphavirus nsP3 functions to form replication complexes transcribing negative-strand RNA. *Journal of virology* **1994**, 68, (10), 6466-6475.
133. Tomar, S.; Hardy, R. W.; Smith, J. L.; Kuhn, R. J., Catalytic core of alphavirus nonstructural protein nsP4 possesses terminal adenylyltransferase activity. *Journal of virology* **2006**, 80, (20), 9962-9969.
134. Tsetsarkin, K.; Higgs, S.; McGee, C. E.; De Lamballerie, X.; Charrel, R. N.; Vanlandingham, D. L., Infectious clones of Chikungunya virus (La Réunion isolate) for vector competence studies. *Vector Borne Zoonotic Dis* **2006**, 6, (4), 325-37.
135. Suzuki, Y.; Tanaka, A.; Maeda, Y.; Emi, A.; Fujioka, Y.; Sakaguchi, S.; Vasudevan, S. G.; Kobayashi, T.; Lim, C. K.; Takasaki, T.; Wu, H.; Nakano, T., Construction and characterization of an infectious clone generated from Chikungunya virus SL11131 strain. *Virology* **2021**, 552, 52-62.
136. Scholte, F. E.; Tas, A.; Martina, B. E.; Cordioli, P.; Narayanan, K.; Makino, S.; Snijder, E. J.; van Hemert, M. J., Characterization of synthetic Chikungunya viruses based on the consensus sequence of recent E1-226V isolates. *PLoS One* **2013**, 8, (8), e71047.
137. Phuektes, P.; Chu, J. J., Reverse Genetics Approaches for Chikungunya Virus. *Methods Mol Biol* **2016**, 1426, 283-95.
138. Jones, J. E.; Long, K. M.; Whitmore, A. C.; Sanders, W.; Thurlow, L. R.; Brown, J. A.; Morrison, C. R.; Vincent, H.; Peck, K. M.; Browning, C.; Moorman, N.; Lim, J. K.; Heise, M. T., Disruption of the Opal Stop Codon Attenuates Chikungunya Virus-Induced Arthritis and Pathology. *mBio* **2017**, 8, (6).
139. Dickson, S. H., *On dengue: its history, pathology, and treatment*. Haswell, Barrington, and Haswell: 1839.
140. Dickson, S. H., *Elements of Medicine: A Compendious View of Pathology and Therapeutics, Or the History and Treatment of Diseases*. Blanchard and Lea: 1855.

141. Christie, J., Remarks on “Kidinga Pepo”: a peculiar form of exanthematous disease. *British medical journal* **1872**, 1, (596), 577.
142. Christie, J., On epidemics of dengue fever: their diffusion and etiology. *Glasgow Medical Journal* **1881**, 16, (3), 161.
143. Halstead, S. B., Reappearance of chikungunya, formerly called dengue, in the Americas. *Emerg Infect Dis* **2015**, 21, (4), 557-61.
144. Lumsden, W. H. R., An epidemic of virus disease in Southern Province, Tanganyika territory, in 1952–1953 II. General description and epidemiology. *Transactions of The Royal Society of Tropical Medicine and Hygiene* **1955**, 49, (1), 33-57.
145. Robinson, M. C., An epidemic of virus disease in Southern Province, Tanganyika territory, in 1952–1953. *Transactions of the royal society of tropical medicine and hygiene* **1955**, 49, (1), 28-32.
146. Halstead, S. B.; Scanlon, J. E.; Umpaivit, P.; Udomsakdi, S., Dengue and chikungunya virus infection in man in Thailand, 1962-1964. IV. Epidemiologic studies in the Bangkok Metropolitan area. **1969**.
147. Halstead, S. B.; Udomsakdi, S.; Scanlon, J. E.; Rohitayodhin, S., Dengue and chikungunya virus infection in man in Thailand, 1962-1964. V. Epidemiologic observations outside Bangkok. *Am J Trop Med Hyg* **1969**, 18, (6), 1022-33.
148. Padbidri, V. S.; Gnaneswar, T. T., Epidemiological investigations of chikungunya epidemic at Barsi, Maharashtra state, India. *J Hyg Epidemiol Microbiol Immunol* **1979**, 23, (4), 445-51.
149. Khongwichit, S.; Chansaenroj, J.; Chirathaworn, C.; Poovorawan, Y., Chikungunya virus infection: molecular biology, clinical characteristics, and epidemiology in Asian countries. *Journal of Biomedical Science* **2021**, 28, (1), 84.
150. Lahariya, C.; Pradhan, S. K., Emergence of chikungunya virus in Indian subcontinent after 32 years: A review. *J Vector Borne Dis* **2006**, 43, (4), 151-60.

151. Sergon, K.; Njuguna, C.; Kalani, R.; Ofula, V.; Onyango, C.; Konongoi, L. S.; Bedno, S.; Burke, H.; Dumilla, A. M.; Konde, J., Seroprevalence of chikungunya virus (CHIKV) infection on Lamu Island, Kenya, October 2004. *American Journal of Tropical Medicine and Hygiene* **2008**, 78, (2), 333-337.
152. Sergon, K.; Yahaya, A. A.; Brown, J.; Bedja, S. A.; Mlindasse, M.; Agata, N.; Allaranger, Y.; Ball, M. D.; Powers, A. M.; Ofula, V.; Onyango, C.; Konongoi, L. S.; Sang, R.; Njenga, M. K.; Breiman, R. F., Seroprevalence of Chikungunya virus infection on Grande Comore Island, union of the Comoros, 2005. *Am J Trop Med Hyg* **2007**, 76, (6), 1189-93.
153. Jossieran, L.; Paquet, C.; Zehgnoun, A.; Caillere, N.; Le Tertre, A.; Solet, J.-L.; Ledrans, M., Chikungunya disease outbreak, Reunion island. *Emerging infectious diseases* **2006**, 12, (12), 1994.
154. Renault, P.; Solet, J. L.; Sissoko, D.; Balleydier, E.; Larrieu, S.; Filleul, L.; Lassalle, C.; Thiria, J.; Rachou, E.; de Valk, H.; Ilef, D.; Ledrans, M.; Quatresous, I.; Quenel, P.; Pierre, V., A major epidemic of chikungunya virus infection on Reunion Island, France, 2005-2006. *Am J Trop Med Hyg* **2007**, 77, (4), 727-31.
155. Tsetsarkin, K. A.; Vanlandingham, D. L.; McGee, C. E.; Higgs, S., A single mutation in chikungunya virus affects vector specificity and epidemic potential. *PLoS Pathog* **2007**, 3, (12), e201.
156. Schuffenecker, I.; Iteman, I.; Michault, A.; Murri, S.; Frangeul, L.; Vaney, M.-C.; Lavenir, R.; Pardigon, N.; Reynes, J.-M.; Pettinelli, F., Genome microevolution of chikungunya viruses causing the Indian Ocean outbreak. *PLoS medicine* **2006**, 3, (7), e263.
157. Krishnamoorthy, K.; Harichandrakumar, K.; Kumari, A. K.; Das, L., Burden of chikungunya in India: estimates of disability adjusted life years (DALY) lost in 2006 epidemic. *Journal of vector borne diseases* **2009**, 46, (1), 26.
158. Rezza, G.; Nicoletti, L.; Angelini, R.; Romi, R.; Finarelli, A. C.; Panning, M.; Cordioli, P.; Fortuna, C.; Boros, S.; Magurano, F.; Silvi, G.; Angelini, P.; Dottori, M.; Ciufolini, M. G.;

Majori, G. C.; Cassone, A., Infection with chikungunya virus in Italy: an outbreak in a temperate region. *Lancet* **2007**, 370, (9602), 1840-6.

159. Leparc-Goffart, I.; Nougairede, A.; Cassadou, S.; Prat, C.; De Lamballerie, X., Chikungunya in the Americas. *The Lancet* **2014**, 383, (9916), 514.

160. Teixeira, M. G.; Andrade, A. M.; Costa Mda, C.; Castro, J. N.; Oliveira, F. L.; Goes, C. S.; Maia, M.; Santana, E. B.; Nunes, B. T.; Vasconcelos, P. F., East/Central/South African genotype chikungunya virus, Brazil, 2014. *Emerg Infect Dis* **2015**, 21, (5), 906-7.

161. Petersen, L. R.; Powers, A. M., Chikungunya: epidemiology. *F1000Research* **2016**, 5.

162. de Souza, W. M.; Ribeiro, G. S.; de Lima, S. T. S.; de Jesus, R.; Moreira, F. R. R.; Whittaker, C.; Sallum, M. A. M.; Carrington, C. V. F.; Sabino, E. C.; Kitron, U.; Faria, N. R.; Weaver, S. C., Chikungunya: a decade of burden in the Americas. *Lancet Reg Health Am* **2024**, 30, 100673.

163. Weaver, S. C.; Chen, R.; Diallo, M., Chikungunya virus: role of vectors in emergence from enzootic cycles. *Annual Review of Entomology* **2020**, 65, (1), 313-332.

164. Althouse, B. M.; Guerbois, M.; Cummings, D. A. T.; Diop, O. M.; Faye, O.; Faye, A.; Diallo, D.; Sadio, B. D.; Sow, A.; Faye, O.; Sall, A. A.; Diallo, M.; Benefit, B.; Simons, E.; Watts, D. M.; Weaver, S. C.; Hanley, K. A., Role of monkeys in the sylvatic cycle of chikungunya virus in Senegal. *Nature Communications* **2018**, 9, (1), 1046.

165. Tsetsarkin, K. A.; Chen, R.; Weaver, S. C., Interspecies transmission and chikungunya virus emergence. *Current Opinion in Virology* **2016**, 16, 143-150.

166. Diallo, M.; Thonnon, J.; Traore-Lamizana, M.; Fontenille, D., Vectors of Chikungunya virus in Senegal: current data and transmission cycles. *The American journal of tropical medicine and hygiene* **1999**, 60, (2), 281-286.

167. Bosco-Lauth, A. M.; Nemeth, N. M.; Kohler, D. J.; Bowen, R. A., Viremia in North American Mammals and Birds After Experimental Infection with Chikungunya Viruses. *Am J Trop Med Hyg* **2016**, 94, (3), 504-6.

168. de Souza, W. M.; Gaye, A.; Ndiaye, E. H.; Morgan, A. L.; Sylla, E. H. D.; Sy, F. A.; Diallo, M.; Weaver, S. C., Serosurvey of Chikungunya Virus in Old World Fruit Bats, Senegal, 2020-2022. *Emerg Infect Dis* **2024**, 30, (7), 1490-1492.
169. Moreira-Soto, A.; Carneiro, I. d. O.; Fischer, C.; Feldmann, M.; Kümmerer, B. M.; Silva, N. S.; Santos, U. G.; Souza, B. F. d. C. D.; Liborio, F. d. A.; Valença-Montenegro, M. M.; Laroque, P. d. O.; Fontoura, F. R. d.; Oliveira, A. V. D.; Drosten, C.; Lamballerie, X. d.; Franke, C. R.; Drexler, J. F., Limited Evidence for Infection of Urban and Peri-urban Nonhuman Primates with Zika and Chikungunya Viruses in Brazil. *mSphere* **2018**, 3, (1), 10.1128/msphere.00523-17.
170. Diallo, D.; Sall, A. A.; Buenemann, M.; Chen, R.; Faye, O.; Diagne, C. T.; Faye, O.; Ba, Y.; Dia, I.; Watts, D., Landscape ecology of sylvatic chikungunya virus and mosquito vectors in southeastern Senegal. *PLoS neglected tropical diseases* **2012**, 6, (6), e1649.
171. Hakim, M. S.; Annisa, L.; Gazali, F. M.; Aman, A. T., The origin and continuing adaptive evolution of chikungunya virus. *Archives of Virology* **2022**, 167, (12), 2443-2455.
172. Haddow, A. J.; Davies, C. W.; Walker, A. J., O'nyong-nyong fever: An epidemic virus disease in East Africa 1. Introduction. *Transactions of The Royal Society of Tropical Medicine and Hygiene* **1960**, 54, (6), 517-522.
173. Williams, M. C.; Woodall, J. P.; Corbet, P. S.; Gillett, J. D., O'NYONG-NYONG FEVER: AN EPIDEMIC VIRUS DISEASE IN EAST AFRICA. 8. VIRUS ISOLATIONS FROM ANOPHELES MOSQUITOES. *Trans R Soc Trop Med Hyg* **1965**, 59, 300-6.
174. Williams, M. C.; Woodall, J. P.; Gillett, J. D., O'NYONG-NYONG FEVER: AN EPIDEMIC VIRUS DIESEASE IN EAST AFRICA. VII. VIRUS ISOLATIONS FROM MAN AND SEROLOGICAL STUDIES UP TO JULY 1961. *Trans R Soc Trop Med Hyg* **1965**, 59, 186-97.
175. Lanciotti, R. S.; Ludwig, M. L.; Rwiguma, E. B.; Lutwama, J. J.; Kram, T. M.; Karabatsos, N.; Cropp, B. C.; Miller, B. R., Emergence of epidemic O'nyong-nyong fever in

Uganda after a 35-year absence: genetic characterization of the virus. *Virology* **1998**, 252, (1), 258-268.

176. Sanders, E. J.; Rwaguma, E. B.; Kawamata, J.; Kiwanuka, N.; Lutwama, J. J.; Ssengooba, F. P.; Lamunu, M.; Najjemba, R.; Were, W. A.; Bagambisa, G., O'nyong-nyong fever in south-central Uganda, 1996–1997: description of the epidemic and results of a household-based seroprevalence survey. *The Journal of infectious diseases* **1999**, 180, (5), 1436-1443.

177. Kiwanuka, N.; Sanders, E. J.; Rwaguma, E. B.; Kawamata, J.; Ssengooba, F. P.; Najjemba, R.; Were, W. A.; Lamunu, M.; Bagambisa, G.; Burkot, T. R.; Dunster, L.; Lutwama, J. J.; Martin, D. A.; Cropp, C. B.; Karabatsos, N.; Lanciotti, R. S.; Tsai, T. F.; Campbell, G. L., O'Nyong-Nyong Fever in South-Central Uganda, 1996—1997: Clinical Features and Validation of a Clinical Case Definition for Surveillance Purposes. *Clinical Infectious Diseases* **1999**, 29, (5), 1243-1250.

178. Bessaud, M.; Peyrefitte, C. N.; Pastorino, B. A.; Gravier, P.; Tock, F.; Boete, F.; Tolou, H. J.; Grandadam, M., O'nyong-nyong Virus, Chad. *Emerg Infect Dis* **2006**, 12, (8), 1248-50.

179. Kading, R. C.; Borland, E. M.; Cranfield, M.; Powers, A. M., Prevalence of antibodies to alphaviruses and flaviviruses in free-ranging game animals and nonhuman primates in the greater Congo basin. *J Wildl Dis* **2013**, 49, (3), 587-99.

180. Vanlandingham, D. L.; Hong, C.; Klingler, K.; Tsetsarkin, K.; McElroy, K. L.; Powers, A. M.; Lehane, M. J.; Higgs, S., Differential infectivities of o'nyong-nyong and chikungunya virus isolates in *Anopheles gambiae* and *Aedes aegypti* mosquitoes. *American Journal of Tropical Medicine and Hygiene* **2005**, 72, (5), 616-621.

181. De Zulueta, J.; Woodall, J. P.; Cullen, J.; Williams, M. C.; Kafuko, G.; Gillett, J. D., An observation on the possible effect of o'nyong-nyong fever on malaria. *Bulletin of the World Health Organization* **1962**, 26, (1), 135.

182. Mala, W.; Wilairatana, P.; Kotepui, K. U.; Kotepui, M., Prevalence of malaria and chikungunya co-infection in febrile patients: A systematic review and meta-analysis. *Tropical Medicine and Infectious Disease* **2021**, 6, (3), 119.
183. Casals, J.; Whitman, L., Mayaro virus: a new human disease agent. I. Relationship to other arbor viruses. *Am J Trop Med Hyg* **1957**, 6, (6), 1004-11.
184. Anderson, C. R.; Downs, W. G.; Wattley, G. H.; Ahin, N. W.; Reese, A. A., Mayaro virus: a new human disease agent. II. Isolation from blood of patients in Trinidad, B.W.I. *Am J Trop Med Hyg* **1957**, 6, (6), 1012-6.
185. Blohm, G.; Elbadry, M. A.; Mavian, C.; Stephenson, C.; Loeb, J.; White, S.; Telisma, T.; Chavannes, S.; De Rochar, V. M. B.; Salemi, M., Mayaro as a Caribbean traveler: Evidence for multiple introductions and transmission of the virus into Haiti. *International Journal of Infectious Diseases* **2019**, 87, 151-153.
186. Lednicky, J.; De Rochars, V. M. B.; Elbadry, M.; Loeb, J.; Telisma, T.; Chavannes, S.; Anilis, G.; Cella, E.; Ciccozzi, M.; Okech, B., Mayaro virus in child with acute febrile illness, Haiti, 2015. *Emerging infectious diseases* **2016**, 22, (11), 2000.
187. White, S. K.; Mavian, C.; Elbadry, M. A.; Beau De Rochars, V. M.; Paisie, T.; Telisma, T.; Salemi, M.; Lednicky, J. A.; Morris Jr, J. G., Detection and phylogenetic characterization of arbovirus dual-infections among persons during a chikungunya fever outbreak, Haiti 2014. *PLoS Neglected Tropical Diseases* **2018**, 12, (5), e0006505.
188. Navarrete-Espinosa, J.; Gómez-Dantés, H., Arbovirus causing hemorrhagic fever at IMSS. *Revista médica del Instituto Mexicano del Seguro Social* **2006**, 44, (4), 347-353.
189. Acosta-Ampudia, Y.; Monsalve, D. M.; Rodríguez, Y.; Pacheco, Y.; Anaya, J. M.; Ramírez-Santana, C., Mayaro: an emerging viral threat? *Emerg Microbes Infect* **2018**, 7, (1), 163.
190. Wei, L. L. L.; Tom, R.; Kim, Y. C., Mayaro Virus: An Emerging Alphavirus in the Americas. *Viruses* **2024**, 16, (8), 1297.

191. Ganjian, N.; Riviere-Cinnamond, A., Mayaro virus in Latin America and the Caribbean. *Rev Panam Salud Publica* **2020**, *44*, e14.
192. Pujhari, S.; Brustolin, M.; Heu, C. C.; Smithwick, R.; Larrosa, M.; Hafenstein, S.; Rasgon, J. L., Characterization of Mayaro virus (strain BeAn343102) biology in vertebrate and invertebrate cellular backgrounds. *J Gen Virol* **2022**, *103*, (10).
193. Hoch, A. L.; Peterson, N. E.; LeDuc, J. W.; Pinheiro, F. P., An outbreak of Mayaro virus disease in Belterra, Brazil. III. Entomological and ecological studies. *The American journal of tropical medicine and hygiene* **1981**, *30*, (3), 689-698.
194. Auguste, A. J.; Liria, J.; Forrester, N. L.; Giambalvo, D.; Moncada, M.; Long, K. C.; Morón, D.; de Manzione, N.; Tesh, R. B.; Halsey, E. S.; Kochel, T. J.; Hernandez, R.; Navarro, J. C.; Weaver, S. C., Evolutionary and Ecological Characterization of Mayaro Virus Strains Isolated during an Outbreak, Venezuela, 2010. *Emerg Infect Dis* **2015**, *21*, (10), 1742-50.
195. Pérez, J. G.; Carrera, J. P.; Serrano, E.; Pittí, Y.; Maguiña, J. L.; Mentaberre, G.; Lescano, A. G.; Valderrama, A.; Mayor, P., Serologic Evidence of Zoonotic Alphaviruses in Humans from an Indigenous Community in the Peruvian Amazon. *Am J Trop Med Hyg* **2019**, *101*, (6), 1212-1218.
196. Wiggins, K.; Eastmond, B.; Alto, B. W., Transmission potential of Mayaro virus in Florida *Aedes aegypti* and *Aedes albopictus* mosquitoes. *Med Vet Entomol* **2018**, *32*, (4), 436-442.
197. Krovovsky, L.; Lins, C. R. B.; Guedes, D. R. D.; Wallau, G. D. L.; Ayres, C. F. J.; Paiva, M. H. S., Dynamic of Mayaro Virus Transmission in *Aedes aegypti*, *Culex quinquefasciatus* Mosquitoes, and a Mice Model. *Viruses* **2023**, *15*, (3).
198. Long, K. C.; Ziegler, S. A.; Thangamani, S.; Hausser, N. L.; Kochel, T. J.; Higgs, S.; Tesh, R. B., Experimental transmission of Mayaro virus by *Aedes aegypti*. *The American journal of tropical medicine and hygiene* **2011**, *85*, (4), 750.

199. Mourão, M. P.; Bastos Mde, S.; de Figueiredo, R. P.; Gimaque, J. B.; Galusso Edos, S.; Kramer, V. M.; de Oliveira, C. M.; Naveca, F. G.; Figueiredo, L. T., Mayaro fever in the city of Manaus, Brazil, 2007-2008. *Vector Borne Zoonotic Dis* **2012**, 12, (1), 42-6.
200. de Paula Silveira-Lacerda, E.; Laschuk Herlinger, A.; Tanuri, A.; Rezza, G.; Anunciação, C. E.; Ribeiro, J. P.; Tannous, I. P.; Abrantes, G. R.; da Silva, E. G.; Arruda, K. F.; de Sousa, A. R. V.; Romero Rebello Moreira, F.; Santana Aguiar, R.; Corrêa, J. F.; Dos Santos, M. M.; Silva, H. D.; Garcia-Zapata, M. T. A.; do Nascimento, N. S.; Talon de Menezes, M.; Araujo Maia, R.; Ferreira, C. O.; Barbosa, R.; Brindeiro, R.; Cardoso, C.; Brunini, S. M., Molecular epidemiological investigation of Mayaro virus in febrile patients from Goiania City, 2017-2018. *Infect Genet Evol* **2021**, 95, 104981.
201. Vieira, C. J. d. S. P.; da Silva, D. J. F.; Barreto, E. S.; Siqueira, C. E. H.; Colombo, T. E.; Ozanic, K.; Schmidt, D. J.; Drumond, B. P.; Mondini, A.; Nogueira, M. L., Detection of Mayaro virus infections during a dengue outbreak in Mato Grosso, Brazil. *Acta tropica* **2015**, 147, 12-16.
202. Saatkamp, C. J.; Rodrigues, L. R. R.; Pereira, A. M. N.; Coelho, J. A.; Marques, R. G. B.; Souza, V. C. d.; Nascimento, V. A. d.; Saatkamp, J. G. d. S.; Naveca, F. G.; Figueiredo, R. M. P. d., Mayaro virus detection in the western region of Pará state, Brazil. *Revista da Sociedade Brasileira de Medicina Tropical* **2021**, 54, e0055-2020.
203. Taylor, R. M., *Catalogue of arthropod-borne viruses of the world: a collection of data on registered arthropod-borne animal viruses*. US Public Health Service: 1967.
204. Calisher, C. H.; Gutiérrez, E.; Maness, K.; Lord, R. D., Isolation of Mayaro virus from a migrating bird captured in Louisiana in 1967. *Bulletin of the Pan American Health Organization (PAHO)*; 8 (3), 1974 **1974**.
205. Izurieta, R. O.; Macaluso, M.; Watts, D. M.; Tesh, R. B.; Guerra, B.; Cruz, L. M.; Galwankar, S.; Vermund, S. H., Hunting in the Rainforest and Mayaro Virus Infection: An emerging Alphavirus in Ecuador. *J Glob Infect Dis* **2011**, 3, (4), 317-23.

206. Talarmin, A.; Chandler, L. J.; Kazanji, M.; de Thoisy, B.; Debon, P.; Lelarge, J.; Labeau, B.; Bourreau, E.; Vié, J. C.; Shope, R. E.; Sarthou, J. L., Mayaro virus fever in French Guiana: isolation, identification, and seroprevalence. *Am J Trop Med Hyg* **1998**, 59, (3), 452-6.
207. de Thoisy, B.; Gardon, J.; Salas, R. A.; Morvan, J.; Kazanji, M., Mayaro Virus in Wild Mammals, French Guiana. *Emerging Infectious Disease journal* **2003**, 9, (10), 1326.
208. Dias, H. G.; Familiar-Macedo, D.; Garrido, I. O.; Dos Santos, F. B.; Pauvolid-Corrêa, A., Exposure of domestic animals to Mayaro and Oropouche viruses in urban and peri-urban areas of West-Central Brazil. *One Health Outlook* **2024**, 6, (1), 12.
209. Cereghino, C.; Roesch, F.; Carrau, L.; Hardy, A.; Ribeiro-Filho, H. V.; Henrion-Lacritick, A.; Koh, C.; Marano, J. M.; Bates, T. A.; Rai, P.; Chuong, C.; Akter, S.; Vallet, T.; Blanc, H.; Elliott, T. J.; Brown, A. M.; Michalak, P.; LeRoith, T.; Bloom, J. D.; Marques, R. E.; Saleh, M. C.; Vignuzzi, M.; Weger-Lucarelli, J., The E2 glycoprotein holds key residues for Mayaro virus adaptation to the urban *Aedes aegypti* mosquito. *PLoS Pathog* **2023**, 19, (4), e1010491.
210. Doherty, R. L.; Whitehead, R. H.; Gorman, B. M.; apos, O.; Gower, A., The Isolation of a Third Group A Arbovirus in Australia, with Preliminary Observations on its Relationship to Epidemic Polyarthritis. *The Australian journal of science* **1963**, 26, 183-184.
211. Kumar, P.; Kaur, Y.; Apostolopoulos, V.; Pant, M.; Gaidhane, A. M.; Zahiruddin, Q. S.; Singh, M. P.; Sah, S., The rising threat of Ross River virus: Climate change and its implications on public health in Australia. *New Microbes New Infect* **2024**, 60-61, 101451.
212. Scrimgeour, E. M.; Aaskov, J. G.; Matz, L. R., Ross River virus arthritis in Papua New Guinea. *Transactions of the Royal Society of Tropical Medicine and Hygiene* **1987**, 81, (5), 833-834.
213. Tesh, R. B.; Gajdusek, D. C.; Garruto, R. M.; Cross, J. H.; Rosen, L., The distribution and prevalence of group A arbovirus neutralizing antibodies among human populations in Southeast Asia and the Pacific islands. *The American journal of tropical medicine and hygiene* **1975**, 24, (4), 664-675.

214. Aaskov, J.; Mataika, J.; Lawrence, G.; Rabukawaqa, V.; Tucker, M.; Miles, J.; Dalglish, D., An epidemic of Ross River virus infection in Fiji, 1979. *The American journal of tropical medicine and hygiene* **1981**, 30, (5), 1053-1059.
215. Tesh, R. B.; McLean, R. G.; Shroyer, D. A.; Calisher, C. H.; Rosen, L., Ross river virus (togaviridae: Alphavirus) infection (epidemic polyarthritits) in American Samoa. *Transactions of the Royal Society of Tropical Medicine and Hygiene* **1981**, 75, (3), 426-431.
216. Rosen, L.; Gubler, D. J.; Bennett, P. H., Epidemic polyarthritits (Ross River) virus infection in the Cook Islands. *The American journal of tropical medicine and hygiene* **1981**, 30, (6), 1294-1302.
217. Fauran, P.; Donaldson, M.; Harper, J.; Oseni, R.; Aaskov, J., Characterization of Ross River viruses isolated from patients with polyarthritits in New Caledonia and Wallis and Futuna Islands. *The American journal of tropical medicine and hygiene* **1984**, 33, (6), 1228-1231.
218. Stephenson, E. B.; Peel, A. J.; Reid, S. A.; Jansen, C. C.; McCallum, H., The non-human reservoirs of Ross River virus: a systematic review of the evidence. *Parasites & Vectors* **2018**, 11, (1), 188.
219. Yuen, K. Y.; Bielefeldt-Ohmann, H., Ross River Virus Infection: A Cross-Disciplinary Review with a Veterinary Perspective. *Pathogens* **2021**, 10, (3).
220. Kay, B. H.; Boyd, A. M.; Ryan, P. A.; Hall, R. A., Mosquito feeding patterns and natural infection of vertebrates with Ross River and Barmah Forest viruses in Brisbane, Australia. *American Journal of Tropical Medicine and Hygiene* **2007**, 76, (3), 417.
221. Liu, W.; Kizu, J. R.; Le Grand, L. R.; Moller, C. G.; Carthew, T. L.; Mitchell, I. R.; Gubala, A. J.; Aaskov, J. G., Localized outbreaks of epidemic polyarthritits among military personnel caused by different sublineages of Ross River virus, northeastern Australia, 2016–2017. *Emerging Infectious Diseases* **2019**, 25, (10), 1793.
222. Weaver, S. C.; Ferro, C.; Barrera, R.; Boshell, J.; Navarro, J.-C., Venezuelan equine encephalitis. *Annual Reviews in Entomology* **2004**, 49, (1), 141-174.

223. Ross, R., The Newala epidemic: III. The virus: isolation, pathogenic properties and relationship to the epidemic. *Epidemiology & Infection* **1956**, 54, (2), 177-191.
224. Binn, L. N.; Harrison, V. R.; Randall, R., Patterns of viremia and antibody observed in rhesus monkeys inoculated with chikungunya and other serologically related group A arboviruses. *Am J Trop Med Hyg* **1967**, 16, (6), 782-5.
225. Broeckel, R.; Haese, N.; Messaoudi, I.; Streblow, D. N., Nonhuman Primate Models of Chikungunya Virus Infection and Disease (CHIKV NHP Model). *Pathogens* **2015**, 4, (3), 662-681.
226. Chen, C. I.; Clark, D. C.; Pesavento, P.; Lerche, N. W.; Luciw, P. A.; Reisen, W. K.; Brault, A. C., Comparative pathogenesis of epidemic and enzootic Chikungunya viruses in a pregnant Rhesus macaque model. *Am J Trop Med Hyg* **2010**, 83, (6), 1249-58.
227. Messaoudi, I.; Vomazke, J.; Totonchy, T.; Kreklywich, C. N.; Haberthur, K.; Springgay, L.; Brien, J. D.; Diamond, M. S.; Defilippis, V. R.; Streblow, D. N., Chikungunya virus infection results in higher and persistent viral replication in aged rhesus macaques due to defects in anti-viral immunity. *PLoS Negl Trop Dis* **2013**, 7, (7), e2343.
228. Chen, H.; Shi, J.; Tang, C.; Xu, J.; Li, B.; Wang, J.; Zhou, Y.; Yang, Y.; Yang, H.; Huang, Q.; Yu, W.; Wang, H.; Wu, D.; Hu, Y.; Zhou, H.; Sun, Q.; Lu, S., CHIKV infection drives shifts in the gastrointestinal microbiome and metabolites in rhesus monkeys. *Microbiome* **2024**, 12, (1), 161.
229. Levitt, N. H.; Ramsburg, H. H.; Hasty, S. E.; Repik, P. M.; Cole Jr, F. E.; Lupton, H. W., Development of an attenuated strain of chikungunya virus for use in vaccine production. *Vaccine* **1986**, 4, (3), 157-162.
230. Edelman, R.; Tacket, C. O.; Wasserman, S. S.; Bodison, S. A.; Perry, J. G.; Mangiafico, J. A., Phase II safety and immunogenicity study of live chikungunya virus vaccine TSI-GSD-218. *Am J Trop Med Hyg* **2000**, 62, (6), 681-5.
231. Akahata, W.; Yang, Z.-Y.; Andersen, H.; Sun, S.; Holdaway, H. A.; Kong, W.-P.; Lewis, M. G.; Higgs, S.; Rossmann, M. G.; Rao, S.; Nabel, G. J., A virus-like particle vaccine for

epidemic Chikungunya virus protects nonhuman primates against infection. *Nature Medicine* **2010**, 16, (3), 334-338.

232. Rossi, S. L.; Comer, J. E.; Wang, E.; Azar, S. R.; Lawrence, W. S.; Plante, J. A.; Ramsauer, K.; Schrauf, S.; Weaver, S. C., Immunogenicity and efficacy of a measles virus-vectored chikungunya vaccine in nonhuman primates. *The Journal of infectious diseases* **2019**, 220, (5), 735-742.

233. Roques, P.; Ljungberg, K.; Kümmerer, B. M.; Gosse, L.; Dereuddre-Bosquet, N.; Tchitchek, N.; Hallengård, D.; García-Arriaza, J.; Meinke, A.; Esteban, M.; Merits, A.; Le Grand, R.; Liljeström, P., Attenuated and vectored vaccines protect nonhuman primates against Chikungunya virus. *JCI Insight* **2017**, 2, (6), e83527.

234. Mallilankaraman, K.; Shedlock, D. J.; Bao, H.; Kawalekar, O. U.; Fagone, P.; Ramanathan, A. A.; Ferraro, B.; Stabenow, J.; Vijayachari, P.; Sundaram, S. G., A DNA vaccine against chikungunya virus is protective in mice and induces neutralizing antibodies in mice and nonhuman primates. *PLoS neglected tropical diseases* **2011**, 5, (1), e928.

235. Kose, N.; Fox, J. M.; Sapparapu, G.; Bombardi, R.; Tennekoon, R. N.; de Silva, A. D.; Elbashir, S. M.; Theisen, M. A.; Humphris-Narayanan, E.; Ciaramella, G.; Himansu, S.; Diamond, M. S.; Crowe, J. E., Jr., A lipid-encapsulated mRNA encoding a potently neutralizing human monoclonal antibody protects against chikungunya infection. *Sci Immunol* **2019**, 4, (35).

236. Roques, P.; Thiberville, S. D.; Dupuis-Maguiraga, L.; Lum, F. M.; Labadie, K.; Martinon, F.; Gras, G.; Lebon, P.; Ng, L. F. P.; de Lamballerie, X.; Le Grand, R., Paradoxical Effect of Chloroquine Treatment in Enhancing Chikungunya Virus Infection. *Viruses* **2018**, 10, (5).

237. Hamilton, M. M.; Webb, E. M.; Peterson, M. C.; Patel, G.; Porto, M.; Orekov, T.; Erasmus, J. H.; Finneyfrock, B.; Cook, A.; Auguste, A. J.; Kar, S., Comparative pathogenesis of three Mayaro virus genotypes in the cynomolgus macaque. *Journal of General Virology* **2024**, 105, (7).

238. Labrada, L.; Liang, X. H.; Zheng, W.; Johnston, C.; Levine, B., Age-dependent resistance to lethal alphavirus encephalitis in mice: analysis of gene expression in the central nervous system and identification of a novel interferon-inducible protective gene, mouse ISG12. *Journal of virology* **2002**, 76, (22), 11688-11703.
239. Lucas, C. J.; Morrison, T. E., Animal models of alphavirus infection and human disease. *Adv Virus Res* **2022**, 113, 25-88.
240. Haese, N. N.; Broeckel, R. M.; Hawman, D. W.; Heise, M. T.; Morrison, T. E.; Streblow, D. N., Animal Models of Chikungunya Virus Infection and Disease. *J Infect Dis* **2016**, 214, (suppl 5), S482-s487.
241. Rosa, R. B.; de Castro, E. F.; de Oliveira Santos, D.; da Silva, M. V.; Pena, L. J., Mouse Models of Mayaro Virus. *Viruses* **2023**, 15, (9), 1803.
242. Rulli, N. E.; Suhrbier, A.; Hueston, L.; Heise, M. T.; Tupanceska, D.; Zaid, A.; Wilmes, A.; Gilmore, K.; Lidbury, B. A.; Mahalingam, S., Ross River virus: Molecular and cellular aspects of disease pathogenesis. *Pharmacology & Therapeutics* **2005**, 107, (3), 329-342.
243. Couderc, T.; Chrétien, F.; Schilte, C.; Disson, O.; Brigitte, M.; Guivel-Benhassine, F.; Touret, Y.; Barau, G.; Cayet, N.; Schuffenecker, I., A mouse model for Chikungunya: young age and inefficient type-I interferon signaling are risk factors for severe disease. *PLoS pathogens* **2008**, 4, (2), e29.
244. Gardner, C. L.; Burke, C. W.; Higgs, S. T.; Klimstra, W. B.; Ryman, K. D., Interferon-alpha/beta deficiency greatly exacerbates arthritogenic disease in mice infected with wild-type chikungunya virus but not with the cell culture-adapted live-attenuated 181/25 vaccine candidate. *Virology* **2012**, 425, (2), 103-112.
245. Morrison, T. E.; Oko, L.; Montgomery, S. A.; Whitmore, A. C.; Lotstein, A. R.; Gunn, B. M.; Elmore, S. A.; Heise, M. T., A mouse model of chikungunya virus-induced musculoskeletal inflammatory disease: evidence of arthritis, tenosynovitis, myositis, and persistence. *Am J Pathol* **2011**, 178, (1), 32-40.

246. Ferguson, M. C.; Saul, S.; Fragkoudis, R.; Weisheit, S.; Cox, J.; Patabendige, A.; Sherwood, K.; Watson, M.; Merits, A.; Fazakerley, J. K., Ability of the Encephalitic Arbovirus Semliki Forest Virus To Cross the Blood-Brain Barrier Is Determined by the Charge of the E2 Glycoprotein. *J Virol* **2015**, *89*, (15), 7536-49.
247. Arpino, C.; Curatolo, P.; Rezza, G., Chikungunya and the nervous system: what we do and do not know. *Rev Med Virol* **2009**, *19*, (3), 121-9.
248. Figueiredo, C. M.; Neris, R. L. d. S.; Gavino-Leopoldino, D.; da Silva, M. O. L.; Almeida, J. S.; Dos-Santos, J. S.; Figueiredo, C. P.; Bellio, M.; Bozza, M. T.; Assunção-Miranda, I., Mayaro virus replication restriction and induction of muscular inflammation in mice are dependent on age, type-I interferon response, and adaptive immunity. *Frontiers in Microbiology* **2019**, *10*, 2246.
249. Seymour, R. L.; Rossi, S. L.; Bergren, N. A.; Plante, K. S.; Weaver, S. C., The role of innate versus adaptive immune responses in a mouse model of O'nyong-nyong virus infection. *Am J Trop Med Hyg* **2013**, *88*, (6), 1170-9.
250. Chan, Y. H.; Teo, T. H.; Torres-Ruesta, A.; Hartimath, S. V.; Chee, R. S.; Khanapur, S.; Yong, F. F.; Ramasamy, B.; Cheng, P.; Rajarethinam, R.; Robins, E. G.; Goggi, J. L.; Lum, F. M.; Carissimo, G.; Rénia, L.; Ng, L. F. P., Longitudinal [18F]FB-IL-2 PET Imaging to Assess the Immunopathogenicity of O'nyong-nyong Virus Infection. *Front Immunol* **2020**, *11*, 894.
251. Fox, J. M.; Long, F.; Edeling, M. A.; Lin, H.; van Duijl-Richter, M. K. S.; Fong, R. H.; Kahle, K. M.; Smit, J. M.; Jin, J.; Simmons, G.; Doranz, B. J.; Crowe, J. E., Jr.; Fremont, D. H.; Rossmann, M. G.; Diamond, M. S., Broadly Neutralizing Alphavirus Antibodies Bind an Epitope on E2 and Inhibit Entry and Egress. *Cell* **2015**, *163*, (5), 1095-1107.
252. Albe, J. R.; Ma, H.; Gilliland, T. H.; McMillen, C. M.; Gardner, C. L.; Boyles, D. A.; Cottle, E. L.; Dunn, M. D.; Lundy, J. D.; O'Malley, K. J., Physiological and immunological changes in the brain associated with lethal eastern equine encephalitis virus in macaques. *PLoS Pathogens* **2021**, *17*, (2), e1009308.

253. Smith, D. R.; Schmaljohn, C. S.; Badger, C.; Ostrowski, K.; Zeng, X.; Grimes, S. D.; Rayner, J. O., Comparative pathology study of Venezuelan, eastern, and western equine encephalitis viruses in non-human primates. *Antiviral research* **2020**, 182, 104875.
254. Reed, D. S.; Lackemeyer, M. G.; Garza, N. L.; Norris, S.; Gamble, S.; Sullivan, L. J.; Lind, C. M.; Raymond, J. L., Severe encephalitis in cynomolgus macaques exposed to aerosolized Eastern equine encephalitis virus. *The Journal of infectious diseases* **2007**, 196, (3), 441-450.
255. Ma, H.; Lundy, J. D.; O'Malley, K. J.; Klimstra, W. B.; Hartman, A. L.; Reed, D. S., Electrocardiography Abnormalities in Macaques after Infection with Encephalitic Alphaviruses. *Pathogens* **2019**, 8, (4).
256. Ma, H.; Lundy, J. D.; Cottle, E. L.; O'Malley, K. J.; Trichel, A. M.; Klimstra, W. B.; Hartman, A. L.; Reed, D. S.; Teichert, T., Applications of minimally invasive multimodal telemetry for continuous monitoring of brain function and intracranial pressure in macaques with acute viral encephalitis. *PLoS One* **2020**, 15, (6), e0232381.
257. Reed, D. S.; Lind, C. M.; Sullivan, L. J.; Pratt, W. D.; Parker, M. D., Aerosol infection of cynomolgus macaques with enzootic strains of Venezuelan equine encephalitis viruses. *The Journal of infectious diseases* **2004**, 189, (6), 1013-1017.
258. Ma, H.; Albe, J. R.; Gilliland, T.; McMillen, C. M.; Gardner, C. L.; Boyles, D. A.; Cottle, E. L.; Dunn, M. D.; Lundy, J. D.; Salama, N.; O'Malley, K. J.; Pandrea, I.; Teichert, T.; Barrick, S.; Klimstra, W. B.; Hartman, A. L.; Reed, D. S., Long-term persistence of viral RNA and inflammation in the CNS of macaques exposed to aerosolized Venezuelan equine encephalitis virus. *PLoS Pathog* **2022**, 18, (6), e1009946.
259. Reed, D. S.; Larsen, T.; Sullivan, L. J.; Lind, C. M.; Lackemeyer, M. G.; Pratt, W. D.; Parker, M. D., Aerosol exposure to western equine encephalitis virus causes fever and encephalitis in cynomolgus macaques. *The Journal of infectious diseases* **2005**, 192, (7), 1173-1182.

260. Ko, S.-Y.; Akahata, W.; Yang, E. S.; Kong, W.-P.; Burke, C. W.; Honnold, S. P.; Nichols, D. K.; Huang, Y.-J. S.; Schieber, G. L.; Carlton, K., A virus-like particle vaccine prevents equine encephalitis virus infection in nonhuman primates. *Science Translational Medicine* **2019**, 11, (492), eaav3113.
261. Food, U.; Administration, D., FDA approves first vaccine to prevent disease caused by chikungunya virus. *FDA News Release. Available at: <https://www.fda.gov/news-events/press-announcements/fda-approves-first-vaccine-prevent-disease-caused-chikungunya-virus> (Accessed 15 November 2023)* **2023**.
262. European Medicines Agency. First vaccine to protect adults from Chikungunya. 2024. <https://www.ema.europa.eu/en/news/first-vaccine-protect-adults-chikungunya> (5 July 2024),
263. Hallengård, D.; Lum, F. M.; Kümmerer, B. M.; Lulla, A.; Lulla, V.; García-Arriaza, J.; Fazakerley, J. K.; Roques, P.; Le Grand, R.; Merits, A.; Ng, L. F.; Esteban, M.; Liljeström, P., Prime-boost immunization strategies against Chikungunya virus. *J Virol* **2014**, 88, (22), 13333-43.
264. Schneider, M.; Narciso-Abraham, M.; Hadl, S.; McMahon, R.; Toepfer, S.; Fuchs, U.; Hochreiter, R.; Bitzer, A.; Kosulin, K.; Larcher-Senn, J.; Mader, R.; Dubischar, K.; Zoihs, O.; Jaramillo, J. C.; Eder-Lingelbach, S.; Buerger, V.; Wressnigg, N., Safety and immunogenicity of a single-shot live-attenuated chikungunya vaccine: a double-blind, multicentre, randomised, placebo-controlled, phase 3 trial. *Lancet* **2023**, 401, (10394), 2138-2147.
265. Wressnigg, N.; Hochreiter, R.; Zoihs, O.; Fritzer, A.; Bézay, N.; Klingler, A.; Lingnau, K.; Schneider, M.; Lundberg, U.; Meinke, A.; Larcher-Senn, J.; Čorbic-Ramljak, I.; Eder-Lingelbach, S.; Dubischar, K.; Bender, W., Single-shot live-attenuated chikungunya vaccine in healthy adults: a phase 1, randomised controlled trial. *Lancet Infect Dis* **2020**, 20, (10), 1193-1203.
266. McMahon, R.; Fuchs, U.; Schneider, M.; Hadl, S.; Hochreiter, R.; Bitzer, A.; Kosulin, K.; Koren, M.; Mader, R.; Zoihs, O.; Wressnigg, N.; Dubischar, K.; Buerger, V.; Eder-Lingelbach, S.; Jaramillo, J. C., A randomized, double-blinded Phase 3 study to demonstrate lot-

to-lot consistency and to confirm immunogenicity and safety of the live-attenuated chikungunya virus vaccine candidate VLA1553 in healthy adults†. *Journal of Travel Medicine* **2023**, 31, (2).

267. Buerger, V.; Maurer, G.; Kosulin, K.; Hochreiter, R.; Larcher-Senn, J.; Dubischar, K.; Eder-Lingelbach, S., Combined immunogenicity evaluation for a new single-dose live-attenuated chikungunya vaccine. *J Travel Med* **2024**.

268. McMahon, R.; Toepfer, S.; Sattler, N.; Schneider, M.; Narciso-Abraham, M.; Hadl, S.; Hochreiter, R.; Kosulin, K.; Mader, R.; Zoihsel, O.; Wressnigg, N.; Dubischar, K.; Buerger, V.; Eder-Lingelbach, S.; Jaramillo, J.-C., Antibody persistence and safety of a live-attenuated chikungunya virus vaccine up to 2 years after single-dose administration in adults in the USA: a single-arm, multicentre, phase 3b study. *The Lancet Infectious Diseases* **2024**.

269. Halstead, S. B., Dengvaxia sensitizes seronegatives to vaccine enhanced disease regardless of age. *Vaccine* **2017**, 35, (47), 6355-6358.

270. Pintado Silva, J.; Fernandez-Sesma, A., Challenges on the development of a dengue vaccine: a comprehensive review of the state of the art. *J Gen Virol* **2023**, 104, (3).

271. Chang, L.-J.; Dowd, K. A.; Mendoza, F. H.; Saunders, J. G.; Sitar, S.; Plummer, S. H.; Yamshchikov, G.; Sarwar, U. N.; Hu, Z.; Enama, M. E., Safety and tolerability of chikungunya virus-like particle vaccine in healthy adults: a phase 1 dose-escalation trial. *The Lancet* **2014**, 384, (9959), 2046-2052.

272. Goo, L.; Dowd, K. A.; Lin, T.-Y.; Mascola, J. R.; Graham, B. S.; Ledgerwood, J. E.; Pierson, T. C., A virus-like particle vaccine elicits broad neutralizing antibody responses in humans to all chikungunya virus genotypes. *The Journal of infectious diseases* **2016**, 214, (10), 1487-1491.

273. Chen, G. L.; Coates, E. E.; Plummer, S. H.; Carter, C. A.; Berkowitz, N.; Conan-Cibotti, M.; Cox, J. H.; Beck, A.; O'Callahan, M.; Andrews, C.; Gordon, I. J.; Larkin, B.; Lamplé, R.; Kaltovich, F.; Gall, J.; Carlton, K.; Mendy, J.; Haney, D.; May, J.; Bray, A.; Bailer, R. T.; Dowd, K. A.; Brockett, B.; Gordon, D.; Koup, R. A.; Schwartz, R.; Mascola, J. R.; Graham, B. S.; Pierson, T. C.; Donastorg, Y.; Rosario, N.; Pape, J. W.; Hoen, B.; Cabié, A.; Diaz, C.;

Ledgerwood, J. E., Effect of a Chikungunya Virus-Like Particle Vaccine on Safety and Tolerability Outcomes: A Randomized Clinical Trial. *Jama* **2020**, 323, (14), 1369-1377.

274. Raju, S.; Adams, L. J.; Earnest, J. T.; Warfield, K.; Vang, L.; Crowe, J. E., Jr.; Fremont, D. H.; Diamond, M. S., A chikungunya virus-like particle vaccine induces broadly neutralizing and protective antibodies against alphaviruses in humans. *Sci Transl Med* **2023**, 15, (696), eade8273.

275. Bennett, S. R.; McCarty, J. M.; Ramanathan, R.; Mendy, J.; Richardson, J. S.; Smith, J.; Alexander, J.; Ledgerwood, J. E.; de Lame, P. A.; Royalty Tredo, S.; Warfield, K. L.; Bedell, L., Safety and immunogenicity of PXVX0317, an aluminium hydroxide-adjuvanted chikungunya virus-like particle vaccine: a randomised, double-blind, parallel-group, phase 2 trial. *Lancet Infect Dis* **2022**, 22, (9), 1343-1355.

276. Kumar, M.; Sudeep, A. B.; Arankalle, V. A., Evaluation of recombinant E2 protein-based and whole-virus inactivated candidate vaccines against chikungunya virus. *Vaccine* **2012**, 30, (43), 6142-6149.

277. Gorchakov, R.; Wang, E.; Leal, G.; Forrester, N. L.; Plante, K.; Rossi, S. L.; Partidos, C. D.; Adams, A. P.; Seymour, R. L.; Weger, J.; Borland, E. M.; Sherman, M. B.; Powers, A. M.; Osorio, J. E.; Weaver, S. C., Attenuation of Chikungunya virus vaccine strain 181/clone 25 is determined by two amino acid substitutions in the E2 envelope glycoprotein. *J Virol* **2012**, 86, (11), 6084-96.

278. Reisinger, E. C.; Tschismarov, R.; Beubler, E.; Wiedermann, U.; Firbas, C.; Loebermann, M.; Pfeiffer, A.; Muellner, M.; Tauber, E.; Ramsauer, K., Immunogenicity, safety, and tolerability of the measles-vectored chikungunya virus vaccine MV-CHIK: a double-blind, randomised, placebo-controlled and active-controlled phase 2 trial. *Lancet* **2019**, 392, (10165), 2718-2727.

279. Ramsauer, K.; Schwameis, M.; Firbas, C.; Müllner, M.; Putnak, R. J.; Thomas, S. J.; Desprès, P.; Tauber, E.; Jilma, B.; Tangy, F., Immunogenicity, safety, and tolerability of a recombinant measles-virus-based chikungunya vaccine: a randomised, double-blind, placebo-controlled, active-comparator, first-in-man trial. *Lancet Infect Dis* **2015**, 15, (5), 519-27.

280. López-Camacho, C.; Chan Kim, Y.; Blight, J.; Lazaro Moreli, M.; Montoya-Diaz, E.; T Huiskonen, J.; Mareike Kümmerer, B.; Reyes-Sandoval, A., Assessment of immunogenicity and neutralisation efficacy of viral-vectored vaccines against chikungunya virus. *Viruses* **2019**, *11*, (4), 322.
281. Campos, R. K.; Preciado-Llanes, L.; Azar, S. R.; Lopez-Camacho, C.; Reyes-Sandoval, A.; Rossi, S. L., A single and un-adjuvanted dose of a chimpanzee adenovirus-vectored vaccine against chikungunya virus fully protects mice from lethal disease. *Pathogens* **2019**, *8*, (4), 231.
282. Folegatti, P. M.; Harrison, K.; Preciado-Llanes, L.; Lopez, F. R.; Bittaye, M.; Kim, Y. C.; Flaxman, A.; Bellamy, D.; Makinson, R.; Sheridan, J., A single dose of ChAdOx1 Chik vaccine induces neutralizing antibodies against four chikungunya virus lineages in a phase 1 clinical trial. *Nature communications* **2021**, *12*, (1), 4636.
283. August, A.; Attarwala, H. Z.; Himansu, S.; Kalidindi, S.; Lu, S.; Pajon, R.; Han, S.; Lecerf, J.-M.; Tomassini, J. E.; Hard, M., A phase 1 trial of lipid-encapsulated mRNA encoding a monoclonal antibody with neutralizing activity against Chikungunya virus. *Nature medicine* **2021**, *27*, (12), 2224-2233.
284. Shaw, C. A.; August, A.; Bart, S.; Booth, P. J.; Knightly, C.; Brasel, T.; Weaver, S. C.; Zhou, H.; Panther, L., A phase 1, randomized, placebo-controlled, dose-ranging study to evaluate the safety and immunogenicity of an mRNA-based chikungunya virus vaccine in healthy adults. *Vaccine* **2023**, *41*, (26), 3898-3906.
285. Shaw, C.; Panther, L.; August, A.; Zaks, T.; Smolenov, I.; Bart, S.; Watson, M., Safety and immunogenicity of a mRNA-based chikungunya vaccine in a phase 1 dose-ranging trial. *International Journal of Infectious Diseases* **2019**, *79*, 17.
286. Robinson, D. M.; Cole, F. E., Jr.; McManus, A. T.; Pedersen, C. E., Jr., Inactivated Mayaro vaccine produced in human diploid cell cultures. *Mil Med* **1976**, *141*, (3), 163-6.
287. Weise, W. J.; Hermance, M. E.; Forrester, N.; Adams, A. P.; Langsjoen, R.; Gorchakov, R.; Wang, E.; Alcorn, M. D.; Tsetsarkin, K.; Weaver, S. C., A novel live-attenuated vaccine candidate for mayaro Fever. *PLoS Negl Trop Dis* **2014**, *8*, (8), e2969.

288. Mota, M. T. O.; Costa, V. V.; Sugimoto, M. A.; Guimarães, G. F.; Queiroz-Junior, C. M.; Moreira, T. P.; de Sousa, C. D.; Santos, F. M.; Queiroz, V. F.; Passos, I.; Hubner, J.; Souza, D. G.; Weaver, S. C.; Teixeira, M. M.; Nogueira, M. L., In-depth characterization of a novel live-attenuated Mayaro virus vaccine candidate using an immunocompetent mouse model of Mayaro disease. *Sci Rep* **2020**, 10, (1), 5306.
289. Abbo, S. R.; Nguyen, W.; Abma-Henkens, M. H. C.; van de Kamer, D.; Savelkoul, N. H. A.; Geertsema, C.; Le, T. T. T.; Tang, B.; Yan, K.; Dumenil, T.; van Oers, M. M.; Suhrbier, A.; Pijlman, G. P., Comparative Efficacy of Mayaro Virus-Like Particle Vaccines Produced in Insect or Mammalian Cells. *J Virol* **2023**, e0160122.
290. Choi, H.; Kudchodkar, S. B.; Reuschel, E. L.; Asija, K.; Borole, P.; Ho, M.; Wojtak, K.; Reed, C.; Ramos, S.; Bopp, N. E.; Aguilar, P. V.; Weaver, S. C.; Kim, J. J.; Humeau, L.; Tebas, P.; Weiner, D. B.; Muthumani, K., Protective immunity by an engineered DNA vaccine for Mayaro virus. *PLoS Negl Trop Dis* **2019**, 13, (2), e0007042.
291. Wressnigg, N.; van der Velden, M. V.; Portsmouth, D.; Draxler, W.; O'Rourke, M.; Richmond, P.; Hall, S.; McBride, W. J.; Redfern, A.; Aaskov, J., An inactivated Ross River virus vaccine is well tolerated and immunogenic in an adult population in a randomized phase 3 trial. *Clinical and Vaccine Immunology* **2015**, 22, (3), 267-273.
292. Kistner, O.; Barrett, N.; Brühmann, A.; Reiter, M.; Mundt, W.; Savidis-Dacho, H.; Schober-Bendixen, S.; Dorner, F.; Aaskov, J., The preclinical testing of a formaldehyde inactivated Ross River virus vaccine designed for use in humans. *Vaccine* **2007**, 25, (25), 4845-4852.
293. Aichinger, G.; Ehrlich, H. J.; Aaskov, J. G.; Fritsch, S.; Thomasser, C.; Draxler, W.; Wolzt, M.; Müller, M.; Pinl, F.; Van Damme, P., Safety and immunogenicity of an inactivated whole virus Vero cell-derived Ross River virus vaccine: a randomized trial. *Vaccine* **2011**, 29, (50), 9376-9384.
294. Miao, Q.; Nguyen, W.; Zhu, J.; Liu, G.; van Oers, M. M.; Tang, B.; Yan, K.; Larcher, T.; Suhrbier, A.; Pijlman, G. P., A getah virus-like-particle vaccine provides complete protection from viremia and arthritis in wild-type mice. *Vaccine* **2024**.

295. Phillpotts, R. J.; Wright, A. J., TC-83 vaccine protects against airborne or subcutaneous challenge with heterologous mouse-virulent strains of Venezuelan equine encephalitis virus. *Vaccine* **1999**, 17, (7), 982-988.
296. Alevizatos, A. C.; McKinney, R. W.; Feigin, R. D.; Jaeger, R., Live, attenuated Venezuelan equine encephalomyelitis virus vaccine. I. Clinical effects in man. **1967**.
297. Mckinney, R. W.; Berge, T. O.; Sawyer, W.; Tigertt, W.; Crozier, D., Use of an attenuated strain of Venezuelan equine encephalomyelitis virus for immunization in man. *The American journal of tropical medicine and hygiene* **1963**, 12, 597-603.
298. Casamassima, A. C.; Hess, L. W.; Marty, A., TC-83 Venezuelan equine encephalitis vaccine exposure during pregnancy. *Teratology* **1987**, 36, (3), 287-289.
299. Slifka, M. K.; Amanna, I. J., Role of Multivalency and Antigenic Threshold in Generating Protective Antibody Responses. *Front Immunol* **2019**, 10, 956.
300. Irvine, D. J.; Read, B. J., Shaping humoral immunity to vaccines through antigen-displaying nanoparticles. *Curr Opin Immunol* **2020**, 65, 1-6.
301. Schmidt, C.; Hastert, F. D.; Gerbeth, J.; Beissert, T.; Sahin, U.; Perkovic, M.; Schnierle, B. S., A Bivalent Trans-Amplifying RNA Vaccine Candidate Induces Potent Chikungunya and Ross River Virus Specific Immune Responses. *Vaccines* **2022**, 10, (9), 1374.
302. Garg, H.; Mehmetoglu-Gurbuz, T.; Joshi, A., Virus Like Particles (VLP) as multivalent vaccine candidate against Chikungunya, Japanese Encephalitis, Yellow Fever and Zika Virus. *Scientific Reports* **2020**, 10, (1), 4017.
303. Coates, E. E.; Edupuganti, S.; Chen, G. L.; Happe, M.; Strom, L.; Widge, A.; Florez, M. B.; Cox, J. H.; Gordon, I.; Plummer, S.; Ola, A.; Yamshchikov, G.; Andrews, C.; Curate-Ingram, S.; Morgan, P.; Nagar, S.; Collins, M. H.; Bray, A.; Nguyen, T.; Stein, J.; Case, C. L.; Kaltovich, F.; Wycuff, D.; Liang, C. J.; Carlton, K.; Vazquez, S.; Mascola, J. R.; Ledgerwood, J. E., Safety and immunogenicity of a trivalent virus-like particle vaccine against western, eastern, and Venezuelan equine encephalitis viruses: a phase 1, open-label, dose-escalation, randomised clinical trial. *Lancet Infect Dis* **2022**, 22, (8), 1210-1220.

304. Dupuy, L. C.; Richards, M. J.; Livingston, B. D.; Hannaman, D.; Schmaljohn, C. S., A Multiagent Alphavirus DNA Vaccine Delivered by Intramuscular Electroporation Elicits Robust and Durable Virus-Specific Immune Responses in Mice and Rabbits and Completely Protects Mice against Lethal Venezuelan, Western, and Eastern Equine Encephalitis Virus Aerosol Challenges. *Journal of immunology research* **2018**, 2018, (1), 8521060.
305. Auerswald, H.; Boussioux, C.; In, S.; Mao, S.; Ong, S.; Huy, R.; Leang, R.; Chan, M.; Duong, V.; Ly, S.; Tarantola, A.; Dussart, P., Broad and long-lasting immune protection against various Chikungunya genotypes demonstrated by participants in a cross-sectional study in a Cambodian rural community. *Emerging Microbes & Infections* **2018**, 7, (1), 1-13.
306. Buerger, V.; Hadl, S.; Schneider, M.; Schaden, M.; Hochreiter, R.; Bitzer, A.; Kosulin, K.; Mader, R.; Zoihs, O.; Pfeiffer, A.; Loch, A. P.; Morandi, E., Jr.; Nogueira, M. L.; de Brito, C. A. A.; Croda, J.; Teixeira, M. M.; Coelho, I. C.; Gurgel, R.; da Fonseca, A. J.; de Lacerda, M. V. G.; Moreira, E. D., Jr.; Veiga, A. P. R.; Dubischar, K.; Wressnigg, N.; Eder-Lingelbach, S.; Jaramillo, J. C., Safety and immunogenicity of a live-attenuated chikungunya virus vaccine in endemic areas of Brazil: interim results of a double-blind, randomised, placebo-controlled phase 3 trial in adolescents. *Lancet Infect Dis* **2024**.
307. Chen, R.; Mukhopadhyay, S.; Merits, A.; Bolling, B.; Nasar, F.; Coffey, L. L.; Powers, A.; Weaver, S. C.; Ictv Report, C., ICTV Virus Taxonomy Profile: Togaviridae. *J Gen Virol* **2018**, 99, (6), 761-762.
308. Weston, J.; Villoing, S.; Brémont, M.; Castric, J.; Pfeffer, M.; Jewhurst, V.; McLoughlin, M.; Rødseth, O.; Christie, K. E.; Koumans, J.; Todd, D., Comparison of two aquatic alphaviruses, salmon pancreas disease virus and sleeping disease virus, by using genome sequence analysis, monoclonal reactivity, and cross-infection. *J Virol* **2002**, 76, (12), 6155-63.
309. Howley, P. M.; Knipe, D. M., *Fields virology: Emerging viruses*. Lippincott Williams & Wilkins: 2020.
310. Bettis, A. A.; L'Azou Jackson, M.; Yoon, I.-K.; Breugelmans, J. G.; Goios, A.; Gubler, D. J.; Powers, A. M., The global epidemiology of chikungunya from 1999 to 2020: A systematic

literature review to inform the development and introduction of vaccines. *PLoS neglected tropical diseases* **2022**, 16, (1), e0010069.

311. Yactayo, S.; Staples, J. E.; Millot, V.; Cibrelus, L.; Ramon-Pardo, P., Epidemiology of Chikungunya in the Americas. *The Journal of infectious diseases* **2016**, 214, (suppl_5), S441-S445.
312. Freitas, A. R. R.; Donalisio, M. R.; Alarcón-Elbal, P. M., Excess Mortality and Causes Associated with Chikungunya, Puerto Rico, 2014-2015. *Emerg Infect Dis* **2018**, 24, (12), 2352-2355.
313. Rezza, G., Chapter 12 - Chikungunya Fever. In *Emerging Infectious Diseases*, Ergönül, Ö.; Can, F.; Madoff, L.; Akova, M., Eds. Academic Press: Amsterdam, 2014; pp 163-174.
314. Weaver, S. C.; Lecuit, M., Chikungunya virus and the global spread of a mosquito-borne disease. *N Engl J Med* **2015**, 372, (13), 1231-9.
315. Powers, A. M.; Aguilar, P. V.; Chandler, L. J.; Brault, A. C.; Meakins, T. A.; Watts, D.; Russell, K. L.; Olson, J.; Vasconcelos, P. F.; Da Rosa, A. T.; Weaver, S. C.; Tesh, R. B., Genetic relationships among Mayaro and Una viruses suggest distinct patterns of transmission. *Am J Trop Med Hyg* **2006**, 75, (3), 461-9.
316. Caspar, D. L.; Klug, A., Physical principles in the construction of regular viruses. *Cold Spring Harb Symp Quant Biol* **1962**, 27, 1-24.
317. Jose, J.; Snyder, J. E.; Kuhn, R. J., A structural and functional perspective of alphavirus replication and assembly. *Future Microbiol* **2009**, 4, (7), 837-56.
318. Zheng, Y.; Kielian, M., Imaging of the alphavirus capsid protein during virus replication. *J Virol* **2013**, 87, (17), 9579-89.
319. Kim, D. Y.; Reynaud, J. M.; Rasaloukaya, A.; Akhrymuk, I.; Mobley, J. A.; Frolov, I.; Frolova, E. I., New World and Old World Alphaviruses Have Evolved to Exploit Different Components of Stress Granules, FXR and G3BP Proteins, for Assembly of Viral Replication Complexes. *PLoS Pathog* **2016**, 12, (8), e1005810.

320. Leung, J. Y.; Ng, M. M.; Chu, J. J., Replication of alphaviruses: a review on the entry process of alphaviruses into cells. *Adv Virol* **2011**, 2011, 249640.
321. Kam, Y.-W.; Lee, W. W.; Simarmata, D.; Harjanto, S.; Teng, T.-S.; Tolou, H.; Chow, A.; Lin, R. T.; Leo, Y.-S.; Rénia, L., Longitudinal analysis of the human antibody response to Chikungunya virus infection: implications for serodiagnosis and vaccine development. *Journal of virology* **2012**, 86, (23), 13005-13015.
322. Smith, S. A.; Silva, L. A.; Fox, J. M.; Flyak, A. I.; Kose, N.; Sapparapu, G.; Khomandiak, S.; Ashbrook, A. W.; Kahle, K. M.; Fong, R. H., Isolation and characterization of broad and ultrapotent human monoclonal antibodies with therapeutic activity against chikungunya virus. *Cell host & microbe* **2015**, 18, (1), 86-95.
323. Weger-Lucarelli, J.; Aliota, M. T.; Wlodarchak, N.; Kamlangdee, A.; Swanson, R.; Osorio, J. E., Dissecting the Role of E2 Protein Domains in Alphavirus Pathogenicity. *Journal of Virology* **2016**, 90, (5), 2418-2433.
324. Fox, J. M.; Huang, L.; Tahan, S.; Powell, L. A.; Crowe Jr, J. E.; Wang, D.; Diamond, M. S., A cross-reactive antibody protects against Ross River virus musculoskeletal disease despite rapid neutralization escape in mice. *PLoS pathogens* **2020**, 16, (8), e1008743.
325. Martins, K. A.; Gregory, M. K.; Valdez, S. M.; Sprague, T. R.; Encinales, L.; Pacheco, N.; Cure, C.; Porrás-Ramírez, A.; Rico-Mendoza, A.; Chang, A., Neutralizing antibodies from convalescent Chikungunya virus patients can cross-neutralize Mayaro and Una viruses. *The American journal of tropical medicine and hygiene* **2019**, 100, (6), 1541.
326. Powell, L. A.; Miller, A.; Fox, J. M.; Kose, N.; Klose, T.; Kim, A. S.; Bombardi, R.; Tennekoon, R. N.; Dharshan de Silva, A.; Carnahan, R. H.; Diamond, M. S.; Rossmann, M. G.; Kuhn, R. J.; Crowe, J. E., Jr., Human mAbs Broadly Protect against Arthritogenic Alphaviruses by Recognizing Conserved Elements of the Mxra8 Receptor-Binding Site. *Cell Host Microbe* **2020**, 28, (5), 699-711.e7.

327. Purtha, W. E.; Tedder, T. F.; Johnson, S.; Bhattacharya, D.; Diamond, M. S., Memory B cells, but not long-lived plasma cells, possess antigen specificities for viral escape mutants. *Journal of Experimental Medicine* **2011**, 208, (13), 2599-2606.
328. Wong, R.; Belk, J. A.; Govero, J.; Uhrlaub, J. L.; Reinartz, D.; Zhao, H.; Errico, J. M.; D'Souza, L.; Ripperger, T. J.; Nikolich-Zugich, J.; Shlomchik, M. J.; Satpathy, A. T.; Fremont, D. H.; Diamond, M. S.; Bhattacharya, D., Affinity-Restricted Memory B Cells Dominate Recall Responses to Heterologous Flaviviruses. *Immunity* **2020**, 53, (5), 1078-1094.e7.
329. Katzelnick, L. C.; Fonville, J. M.; Gromowski, G. D.; Bustos Arriaga, J.; Green, A.; James, S. L.; Lau, L.; Montoya, M.; Wang, C.; VanBlargan, L. A.; Russell, C. A.; Thu, H. M.; Pierson, T. C.; Buchy, P.; Aaskov, J. G.; Muñoz-Jordán, J. L.; Vasilakis, N.; Gibbons, R. V.; Tesh, R. B.; Osterhaus, A. D.; Fouchier, R. A.; Durbin, A.; Simmons, C. P.; Holmes, E. C.; Harris, E.; Whitehead, S. S.; Smith, D. J., Dengue viruses cluster antigenically but not as discrete serotypes. *Science* **2015**, 349, (6254), 1338-43.
330. Smith, D. J.; Lapedes, A. S.; De Jong, J. C.; Bestebroer, T. M.; Rimmelzwaan, G. F.; Osterhaus, A. D.; Fouchier, R. A., Mapping the antigenic and genetic evolution of influenza virus. *science* **2004**, 305, (5682), 371-376.
331. Quiroz, J. A.; Malonis, R. J.; Thackray, L. B.; Cohen, C. A.; Pallesen, J.; Jangra, R. K.; Brown, R. S.; Hofmann, D.; Holtsberg, F. W.; Shulenin, S.; Nyakatura, E. K.; Durnell, L. A.; Rayannavar, V.; Daily, J. P.; Ward, A. B.; Aman, M. J.; Dye, J. M.; Chandran, K.; Diamond, M. S.; Kielian, M.; Lai, J. R., Human monoclonal antibodies against chikungunya virus target multiple distinct epitopes in the E1 and E2 glycoproteins. *PLoS Pathog* **2019**, 15, (11), e1008061.
332. Lyski, Z. L.; Brunton, A. E.; Strnad, M. I.; Sullivan, P. E.; Siegel, S. A. R.; Tafesse, F. G.; Slifka, M. K.; Messer, W. B., SARS-CoV-2 specific memory B-cells from individuals with diverse disease severities recognize SARS-CoV-2 variants of concern. *medRxiv* **2021**.
333. Berman, H. M.; Westbrook, J.; Feng, Z.; Gilliland, G.; Bhat, T. N.; Weissig, H.; Shindyalov, I. N.; Bourne, P. E., The protein data bank. *Nucleic acids research* **2000**, 28, (1), 235-242.

334. Pinna, D.; Corti, D.; Jarrossay, D.; Sallusto, F.; Lanzavecchia, A., Clonal dissection of the human memory B-cell repertoire following infection and vaccination. *Eur J Immunol* **2009**, 39, (5), 1260-70.
335. Amanna, I. J.; Slifka, M. K., Quantitation of rare memory B cell populations by two independent and complementary approaches. *J Immunol Methods* **2006**, 317, (1-2), 175-85.
336. Smith, D. J.; Lapedes, A. S.; de Jong, J. C.; Bestebroer, T. M.; Rimmelzwaan, G. F.; Osterhaus, A. D.; Fouchier, R. A., Mapping the antigenic and genetic evolution of influenza virus. *Science* **2004**, 305, (5682), 371-6.
337. Sumathy, K.; Ella, K. M., Genetic diversity of Chikungunya virus, India 2006-2010: evolutionary dynamics and serotype analyses. *J Med Virol* **2012**, 84, (3), 462-70.
338. Kizu, J. G.; Graham, M.; Grant, R.; McCallum, F.; McPherson, B.; Auliff, A.; Kaminiel, P.; Liu, W., Prevalence of Barmah Forest Virus, Chikungunya Virus and Ross River Virus Antibodies among Papua New Guinea Military Personnel before 2019. *Viruses* **2023**, 15, (2).
339. dos Santos Souza Marinho, R.; Duro, R. L. S.; Bellini Caldeira, D.; Galinskas, J.; Oliveira Mota, M. T.; Hunter, J.; Rodrigues Teles, M. d. A.; de Pádua Milagres, F. A.; Sobhie Diaz, R.; Shinji Kawakubo, F.; Vasconcelos Komninakis, S., Re-emergence of mayaro virus and coinfection with chikungunya during an outbreak in the state of Tocantins/Brazil. *BMC Research Notes* **2022**, 15, (1), 271.
340. Abdoullah, B.; Durand, G. A.; Basco, L. K.; El Bara, A.; Bollahi, M. A.; Bosio, L.; Geulen, M.; Briolant, S.; Boukhary, A. O. M. S., Seroprevalence of Alphaviruses (Togaviridae) among Urban Population in Nouakchott, Mauritania, West Africa. *Viruses* **2023**, 15, (7), 1588.
341. Carrillo-Hernández, M. Y.; Ruiz-Saenz, J.; Villamizar, L. J.; Gómez-Rangel, S. Y.; Martínez-Gutierrez, M., Co-circulation and simultaneous co-infection of dengue, chikungunya, and zika viruses in patients with febrile syndrome at the Colombian-Venezuelan border. *BMC Infectious Diseases* **2018**, 18, (1), 61.

342. Rao, S.; Erku, D.; Mahalingam, S.; Taylor, A., Immunogenicity, safety and duration of protection afforded by chikungunya virus vaccines undergoing human clinical trials. *J Gen Virol* **2024**, 105, (2).
343. National Health Surveillance Agency - Anvisa. Chikungunya: Anvisa and European agency evaluate vaccine from Butantan Institute. 2023. <https://www.gov.br/anvisa/pt-br/assuntos/noticias-anvisa/2023/chikungunya-anvisa-e-agencia-europeia-avaliam-vacina-do-instituto-butantan>
344. Souza, U. J. B. d.; Santos, R. N. d.; Giovanetti, M.; Alcantara, L. C. J.; Galvão, J. D.; Cardoso, F. D. P.; Brito, F. C. S.; Franco, A. C.; Roehe, P. M.; Ribeiro, B. M.; Spilki, F. R.; Campos, F. S., Genomic Epidemiology Reveals the Circulation of the Chikungunya Virus East/Central/South African Lineage in Tocantins State, North Brazil. *Viruses* **2022**, 14, (10), 2311.
345. Sharp, T. M.; Ryff, K. R.; Alvarado, L.; Shieh, W. J.; Zaki, S. R.; Margolis, H. S.; Rivera-Garcia, B., Surveillance for Chikungunya and Dengue During the First Year of Chikungunya Virus Circulation in Puerto Rico. *J Infect Dis* **2016**, 214, (suppl 5), S475-s481.
346. Gallian, P.; de Lamballerie, X.; Salez, N.; Piorkowski, G.; Richard, P.; Paturel, L.; Djoudi, R.; Leparc-Goffart, I.; Tiberghien, P.; Chiaroni, J.; Charrel, R. N., Prospective detection of chikungunya virus in blood donors, Caribbean 2014. *Blood* **2014**, 123, (23), 3679-3681.
347. Rossini, G.; Gaibani, P.; Vocale, C.; Finarelli, A. C.; Landini, M. P., Increased number of cases of Chikungunya virus (CHIKV) infection imported from the Caribbean and Central America to northern Italy, 2014. *Epidemiology and Infection* **2016**, 144, (9), 1912-1916.
348. Kizu, J.; Graham, M.; Liu, W., Potential Serological Misdiagnosis of Barmah Forest Virus and Ross River Virus Diseases as Chikungunya Virus Infections in Australia: Comparison of ELISA with Neutralization Assay Results. *Viruses* **2024**, 16, (3), 384.
349. Yoon, I. K.; Alera, M. T.; Lago, C. B.; Tac-An, I. A.; Villa, D.; Fernandez, S.; Thaisomboonsuk, B.; Klungthong, C.; Levy, J. W.; Velasco, J. M.; Roque, V. G., Jr.; Salje, H.; Macareo, L. R.; Hermann, L. L.; Nisalak, A.; Srikiatkachorn, A., High rate of subclinical

chikungunya virus infection and association of neutralizing antibody with protection in a prospective cohort in the Philippines. *PLoS Negl Trop Dis* **2015**, 9, (5), e0003764.

350. Yoon, I. K.; Srikiatkachorn, A.; Alera, M. T.; Fernandez, S.; Cummings, D. A. T.; Salje, H., Pre-existing chikungunya virus neutralizing antibodies correlate with risk of symptomatic infection and subclinical seroconversion in a Philippine cohort. *Int J Infect Dis* **2020**, 95, 167-173.

351. Chua, C. L.; Sam, I. C.; Merits, A.; Chan, Y. F., Antigenic Variation of East/Central/South African and Asian Chikungunya Virus Genotypes in Neutralization by Immune Sera. *PLoS Negl Trop Dis* **2016**, 10, (8), e0004960.

352. Forato, J.; Meira, C. A.; Claro, I. M.; Amorim, M. R.; de Souza, G. F.; Muraro, S. P.; Toledo-Teixeira, D. A.; Dias, M. F.; Meneses, C. A. R.; Angerami, R. N.; Lalwani, P.; Weaver, S. C.; Sabino, E. C.; Faria, N. R.; de Souza, W. M.; Granja, F.; Proenca-Modena, J. L., Molecular Epidemiology of Mayaro Virus among Febrile Patients, Roraima State, Brazil, 2018-2021. *Emerg Infect Dis* **2024**, 30, (5), 1013-1016.

353. Brustolin, M.; Bartholomeeusen, K.; Rezende, T.; Ariën, K. K.; Müller, R., Mayaro virus, a potential threat for Europe: vector competence of autochthonous vector species. *Parasites & Vectors* **2024**, 17, (1), 200.

354. da Silva, S. J. R.; Krokovsky, L., Clinical and laboratory diagnosis of Mayaro virus (MAYV): Current status and opportunities for further development. *Rev Med Virol* **2024**, 34, (2), e2528.

355. Wang, M.; Wang, L.; Leng, P.; Guo, J.; Zhou, H., Drugs targeting structural and nonstructural proteins of the chikungunya virus: A review. *Int J Biol Macromol* **2024**, 262, (Pt 2), 129949.

356. Haese, N.; Powers, J.; Streblow, D. N., Small Molecule Inhibitors Targeting Chikungunya Virus. *Curr Top Microbiol Immunol* **2022**, 435, 107-139.

357. Chandley, P.; Lukose, A.; Kumar, R.; Rohatgi, S., An overview of anti-Chikungunya antibody response in natural infection and vaccine-mediated immunity, including anti-CHIKV

vaccine candidates and monoclonal antibodies targeting diverse epitopes on the viral envelope. *The Microbe* **2023**, 1, 100018.

358. Folegatti, P. M.; Harrison, K.; Preciado-Llanes, L.; Lopez, F. R.; Bittaye, M.; Kim, Y. C.; Flaxman, A.; Bellamy, D.; Makinson, R.; Sheridan, J.; Azar, S. R.; Campos, R. K.; Tilley, M.; Tran, N.; Jenkin, D.; Poulton, I.; Lawrie, A.; Roberts, R.; Berrie, E.; Rossi, S. L.; Hill, A.; Ewer, K. J.; Reyes-Sandoval, A., A single dose of ChAdOx1 Chik vaccine induces neutralizing antibodies against four chikungunya virus lineages in a phase I clinical trial. *Nat Commun* **2021**, 12, (1), 4636.

359. Atella, M. O.; Carvalho, A. S.; Da Poian, A. T., Role of macrophages in the onset, maintenance, or control of arthritis caused by alphaviruses. *Exp Biol Med (Maywood)* **2023**, 248, (22), 2039-2044.

360. Lum, F. M.; Couderc, T.; Chia, B. S.; Ong, R. Y.; Her, Z.; Chow, A.; Leo, Y. S.; Kam, Y. W.; Rénia, L.; Lecuit, M.; Ng, L. F. P., Antibody-mediated enhancement aggravates chikungunya virus infection and disease severity. *Sci Rep* **2018**, 8, (1), 1860.

361. Taraphdar, D.; Singh, B.; Pattanayak, S.; Kiran, A.; Kokavalla, P.; Alam, M. F.; Syed, G. H., Comodulation of Dengue and Chikungunya Virus Infection During a Coinfection Scenario in Human Cell Lines. *Front Cell Infect Microbiol* **2022**, 12, 821061.

362. Abeyratne, E.; Tharmarajah, K.; Freitas, J. R.; Mostafavi, H.; Mahalingam, S.; Zaid, A.; Zaman, M.; Taylor, A., Liposomal Delivery of the RNA Genome of a Live-Attenuated Chikungunya Virus Vaccine Candidate Provides Local, but Not Systemic Protection After One Dose. *Front Immunol* **2020**, 11, 304.

363. Cao, L.; Wang, W.; Sun, W.; Zhang, J.; Han, J.; Xie, C.; Ha, Z.; Xie, Y.; Zhang, H.; Jin, N.; Lu, H., Construction and Evaluation of Recombinant Adenovirus Candidate Vaccines for Chikungunya Virus. *Viruses* **2022**, 14, (8).

364. Wang, D.; Suhrbier, A.; Penn-Nicholson, A.; Woraratanadharm, J.; Gardner, J.; Luo, M.; Le, T. T.; Anraku, I.; Sakalian, M.; Einfeld, D.; Dong, J. Y., A complex adenovirus vaccine

against chikungunya virus provides complete protection against viraemia and arthritis. *Vaccine* **2011**, 29, (15), 2803-9.

365. Dora, E. G.; Rossi, S. L.; Weaver, S. C.; Tucker, S. N.; Mateo, R., An adjuvanted adenovirus 5-based vaccine elicits neutralizing antibodies and protects mice against chikungunya virus-induced footpad swelling. *Vaccine* **2019**, 37, (24), 3146-3150.

366. Campos, R. K.; Preciado-Llanes, L.; Azar, S. R.; Lopez-Camacho, C.; Reyes-Sandoval, A.; Rossi, S. L., A Single and Un-Adjuvanted Dose of a Chimpanzee Adenovirus-Vectored Vaccine against Chikungunya Virus Fully Protects Mice from Lethal Disease. *Pathogens* **2019**, 8, (4).

367. Labadie, K.; Larcher, T.; Joubert, C.; Mannioui, A.; Delache, B.; Brochard, P.; Guigand, L.; Dubreil, L.; Lebon, P.; Verrier, B.; de Lamballerie, X.; Suhrbier, A.; Cherel, Y.; Le Grand, R.; Roques, P., Chikungunya disease in nonhuman primates involves long-term viral persistence in macrophages. *J Clin Invest* **2010**, 120, (3), 894-906.

368. Nayak, T. K.; Mamidi, P.; Sahoo, S. S.; Kumar, P. S.; Mahish, C.; Chatterjee, S.; Subudhi, B. B.; Chattopadhyay, S.; Chattopadhyay, S., P38 and JNK mitogen-activated protein kinases interact with chikungunya virus non-structural protein-2 and regulate TNF induction during viral infection in macrophages. *Frontiers in Immunology* **2019**, 10, 786.

369. Assunção-Miranda, I.; Cruz-Oliveira, C.; Da Poian, A. T., Molecular mechanisms involved in the pathogenesis of alphavirus-induced arthritis. *Biomed Res Int* **2013**, 2013, 973516.

370. Francis, T., On the doctrine of original antigenic sin. *Proceedings of the American Philosophical Society* **1960**, 104, (6), 572-578.

371. Akahata, W.; Yang, Z. Y.; Andersen, H.; Sun, S.; Holdaway, H. A.; Kong, W. P.; Lewis, M. G.; Higgs, S.; Rossmann, M. G.; Rao, S.; Nabel, G. J., A virus-like particle vaccine for epidemic Chikungunya virus protects nonhuman primates against infection. *Nat Med* **2010**, 16, (3), 334-8.

372. Dagley, A.; Julander, J. G., A Mouse Model of Chikungunya Virus with Utility in Antiviral Studies. In *Antiviral Methods and Protocols*, Gong, E. Y., Ed. Humana Press: Totowa, NJ, 2013; pp 439-448.
373. Posey, D. L.; O'Rourke, T.; Roehrig, J. T.; Lanciotti, R. S.; Weinberg, M.; Maloney, S., O'Nyong-nyong fever in West Africa. *Am J Trop Med Hyg* **2005**, 73, (1), 32.
374. Tinto, B.; Bicaba, B.; Kagoné, T. S.; Kayiwa, J.; Rabe, I.; Merle, C. S. C.; Zango, A.; Ayouba, A.; Salinas, S.; Kania, D.; Simonin, Y., Co-circulation of two Alphaviruses in Burkina Faso: Chikungunya and O'nyong nyong viruses. *PLoS Negl Trop Dis* **2024**, 18, (6), e0011712.
375. LaBeaud, A. D.; Banda, T.; Brichard, J.; Muchiri, E. M.; Mungai, P. L.; Mutuku, F. M.; Borland, E.; Gildengorin, G.; Pfeil, S.; Teng, C. Y., High rates of o'nyong nyong and Chikungunya virus transmission in coastal Kenya. *PLoS neglected tropical diseases* **2015**, 9, (2), e0003436.
376. Masika, M. M.; Korhonen, E. M.; Smura, T.; Uusitalo, R.; Ogola, J.; Mwaengo, D.; Jääskeläinen, A. J.; Alburkat, H.; Gwon, Y.-D.; Evander, M., Serological evidence of exposure to Onyong-Nyong and chikungunya viruses in febrile patients of rural Taita-Taveta County and urban kibera informal settlement in Nairobi, Kenya. *Viruses* **2022**, 14, (6), 1286.
377. Williams, M. C.; Woodall, J. P.; Porterfield, J. S., O'nyong-nyong fever; an epidemic virus disease in East Africa. V Human antibody studies by plaque inhibition and other serological tests. *Trans R Soc Trop Med Hyg* **1962**, 56, 166-72.
378. Powell, L. A.; Miller, A.; Fox, J. M.; Kose, N.; Klose, T.; Kim, A. S.; Bombardi, R.; Tennekoon, R. N.; de Silva, A. D.; Carnahan, R. H., Human mAbs broadly protect against arthritogenic alphaviruses by recognizing conserved elements of the Mxra8 receptor-binding site. *Cell host & microbe* **2020**, 28, (5), 699-711. e7.
379. Ledermann Jeremy, P.; Kayiwa John, T.; Perinet Lara, C.; Apangu, T.; Acayo, S.; Lutwama Julius, J.; Powers Ann, M.; Mossel Eric, C., Complete Genome Sequence of O'nyong Nyong Virus Isolated from a Febrile Patient in 2017 in Uganda. *Microbiology Resource Announcements* **2022**, 11, (12), e00692-22.

380. Myles, K. M.; Kelly, C. L.; Ledermann, J. P.; Powers, A. M., Effects of an opal termination codon preceding the nsP4 gene sequence in the O'Nyong-Nyong virus genome on *Anopheles gambiae* infectivity. *J Virol* **2006**, 80, (10), 4992-7.
381. Blackburn, N. K.; Besselaar, T. G.; Gibson, G., Antigenic relationship between chikungunya virus strains and o'nyong nyong virus using monoclonal antibodies. *Research in Virology* **1995**, 146, (1), 69-73.
382. Chanas, A. C.; Hubalek, Z.; Johnson, B. K.; Simpson, D. I. H., A comparative study of O'nyong nyong virus with Chikungunya virus and plaque variants. *Archives of Virology* **1979**, 59, (3), 231-238.
383. Ng, L. F. P.; Rénia, L., Live-attenuated chikungunya virus vaccine. *Cell* **2024**, 187, (4), 813-813.e1.
384. Broeckel, R.; Sarkar, S.; May, N. A.; Totonchy, J.; Kreklywich, C. N.; Smith, P.; Graves, L.; DeFilippis, V. R.; Heise, M. T.; Morrison, T. E.; Moorman, N.; Streblow, D. N., Src Family Kinase Inhibitors Block Translation of Alphavirus Subgenomic mRNAs. *Antimicrob Agents Chemother* **2019**, 63, (4).
385. Reed, L. J.; Muench, H., A simple method of estimating fifty per cent endpoints. **1938**.
386. Caicedo, E.-Y.; Charniga, K.; Rueda, A.; Dorigatti, I.; Mendez, Y.; Hamlet, A.; Carrera, J.-P.; Cucunubá, Z. M., The epidemiology of Mayaro virus in the Americas: A systematic review and key parameter estimates for outbreak modelling. *PLOS Neglected Tropical Diseases* **2021**, 15, (6), e0009418.
387. Lopes Marques, C. D.; Ranzolin, A.; Cavalcanti, N. G.; Branco Pinto Duarte, A. L., Arboviruses related with chronic musculoskeletal symptoms. *Best Pract Res Clin Rheumatol* **2020**, 34, (4), 101502.
388. Celone, M.; Pecor, D. B.; Potter, A.; Richardson, A.; Dunford, J.; Pollett, S., An ecological niche model to predict the geographic distribution of *Haemagogus janthinomys*, Dyar, 1921 a yellow fever and Mayaro virus vector, in South America. *PLoS Negl Trop Dis* **2022**, 16, (7), e0010564.

389. Suchowiecki, K.; Reid, S. P.; Simon, G. L.; Firestein, G. S.; Chang, A., Persistent Joint Pain Following Arthropod Virus Infections. *Curr Rheumatol Rep* **2021**, *23*, (4), 26.
390. Pezzi, L.; Rodriguez-Morales, A. J.; Reusken, C. B.; Ribeiro, G. S.; LaBeaud, A. D.; Lourenço-de-Oliveira, R.; Brasil, P.; Lecuit, M.; Failloux, A. B.; Gallian, P.; Jaenisch, T.; Simon, F.; Siqueira, A. M.; Rosa-Freitas, M. G.; Vega Rua, A.; Weaver, S. C.; Drexler, J. F.; Vasilakis, N.; de Lamballerie, X.; Boyer, S.; Busch, M.; Diallo, M.; Diamond, M. S.; Drebot, M. A.; Kohl, A.; Neyts, J.; Ng, L. F. P.; Rios, M.; Sall, A.; Simmons, G., GloPID-R report on chikungunya, o'nyong-nyong and Mayaro virus, part 3: Epidemiological distribution of Mayaro virus. *Antiviral Research* **2019**, *172*, 104610.
391. Martins, M. M.; Prata-Barbosa, A.; Cunha, A., Arboviral diseases in pediatrics. *J Pediatr (Rio J)* **2020**, *96* Suppl 1, (Suppl 1), 2-11.
392. Pereira, T. N.; Carvalho, F. D.; De Mendonça, S. F.; Rocha, M. N.; Moreira, L. A., Vector competence of *Aedes aegypti*, *Aedes albopictus*, and *Culex quinquefasciatus* mosquitoes for Mayaro virus. *PLoS Negl Trop Dis* **2020**, *14*, (4), e0007518.
393. Caicedo, E. Y.; Charniga, K.; Rueda, A.; Dorigatti, I.; Mendez, Y.; Hamlet, A.; Carrera, J. P.; Cucunubá, Z. M., The epidemiology of Mayaro virus in the Americas: A systematic review and key parameter estimates for outbreak modelling. *PLoS Negl Trop Dis* **2021**, *15*, (6), e0009418.
394. Dieme, C.; Ciota, A. T.; Kramer, L. D., Transmission potential of Mayaro virus by *Aedes albopictus*, and *Anopheles quadrimaculatus* from the USA. *Parasit Vectors* **2020**, *13*, (1), 613.
395. Long, K. C.; Ziegler, S. A.; Thangamani, S.; Hausser, N. L.; Kochel, T. J.; Higgs, S.; Tesh, R. B., Experimental transmission of Mayaro virus by *Aedes aegypti*. *Am J Trop Med Hyg* **2011**, *85*, (4), 750-7.
396. Pereira, T. N.; Carvalho, F. D.; De Mendonça, S. F.; Rocha, M. N.; Moreira, L. A., Vector competence of *Aedes aegypti*, *Aedes albopictus*, and *Culex quinquefasciatus* mosquitoes for Mayaro virus. *PLOS Neglected Tropical Diseases* **2020**, *14*, (4), e0007518.

397. Brustolin, M.; Pujhari, S.; Terradas, G.; Werling, K.; Asad, S.; Metz, H. C.; Henderson, C. A.; Kim, D.; Rasgon, J. L., In Vitro and In Vivo Coinfection and Superinfection Dynamics of Mayaro and Zika Viruses in Mosquito and Vertebrate Backgrounds. *J Virol* **2023**, *97*, (1), e0177822.
398. Esposito, D. L. A.; Fonseca, B., Will Mayaro virus be responsible for the next outbreak of an arthropod-borne virus in Brazil? *Braz J Infect Dis* **2017**, *21*, (5), 540-544.
399. Mackay, I. M.; Arden, K. E., Mayaro virus: a forest virus primed for a trip to the city? *Microbes and Infection* **2016**, *18*, (12), 724-734.
400. Kraemer, M. U. G.; Sinka, M. E.; Duda, K. A.; Mylne, A. Q. N.; Shearer, F. M.; Barker, C. M.; Moore, C. G.; Carvalho, R. G.; Coelho, G. E.; Van Bortel, W.; Hendrickx, G.; Schaffner, F.; Elyazar, I. R. F.; Teng, H.-J.; Brady, O. J.; Messina, J. P.; Pigott, D. M.; Scott, T. W.; Smith, D. L.; Wint, G. R. W.; Golding, N.; Hay, S. I., The global distribution of the arbovirus vectors *Aedes aegypti* and *Ae. albopictus*. *eLife* **2015**, *4*, e08347.
401. Fumagalli, M. J.; de Souza, W. M.; de Castro-Jorge, L. A.; de Carvalho, R. V. H.; Castro Í, A.; de Almeida, L. G. N.; Consonni, S. R.; Zamboni, D. S.; Figueiredo, L. T. M., Chikungunya Virus Exposure Partially Cross-Protects against Mayaro Virus Infection in Mice. *J Virol* **2021**, *95*, (23), e0112221.
402. Powers, J. M.; Lyski, Z. L.; Weber, W. C.; Denton, M.; Streblow, M. M.; Mayo, A. T.; Haese, N. N.; Nix, C. D.; Rodríguez-Santiago, R.; Alvarado, L. I.; Rivera-Amill, V.; Messer, W. B.; Streblow, D. N., Infection with chikungunya virus confers heterotypic cross-neutralizing antibodies and memory B-cells against other arthritogenic alphaviruses predominantly through the B domain of the E2 glycoprotein. *PLOS Neglected Tropical Diseases* **2023**, *17*, (3), e0011154.
403. Dos Santos Souza Marinho, R.; Duro, R. L. S.; Bellini Caldeira, D.; Galinskas, J.; Oliveira Mota, M. T.; Hunter, J.; Rodrigues Teles, M. D. A.; de Pádua Milagres, F. A.; Sobhie Diaz, R.; Shinji Kawakubo, F.; Vasconcelos Komninakis, S., Re-emergence of mayaro virus and coinfection with chikungunya during an outbreak in the state of Tocantins/Brazil. *BMC Res Notes* **2022**, *15*, (1), 271.

404. Estofolete, C. F.; Mota, M. T.; Vedovello, D.; Góngora, D. V.; Maia, I. L.; Nogueira, M. L., Mayaro fever in an HIV-infected patient suspected of having Chikungunya fever. *Rev Soc Bras Med Trop* **2016**, 49, (5), 648-652.
405. Pinheiro, F. P.; Freitas, R. B.; Travassos da Rosa, J. F.; Gabbay, Y. B.; Mello, W. A.; LeDuc, J. W., An outbreak of Mayaro virus disease in Belterra, Brazil. I. Clinical and virological findings. *Am J Trop Med Hyg* **1981**, 30, (3), 674-81.
406. Chen, Z.; Lang, D., The effectiveness of disease management interventions on health-related quality of life of patients with established arthritogenic alphavirus infections: a systematic review protocol. *JBI Evidence Synthesis* **2013**, 11, (9).
407. Kucharz, E. J.; Cebula-Byrska, I., Chikungunya fever. *Eur J Intern Med* **2012**, 23, (4), 325-9.
408. Pialoux, G.; Gaüzère, B. A.; Strobel, M., [Chikungunya virus infection: review through an epidemic]. *Med Mal Infect* **2006**, 36, (5), 253-63.
409. Gear, J. H., Hemorrhagic fevers, with special reference to recent outbreaks in southern Africa. *Rev Infect Dis* **1979**, 1, (4), 571-91.
410. de Lima, S. T. S.; de Souza, W. M.; Cavalcante, J. W.; da Silva Candido, D.; Fumagalli, M. J.; Carrera, J.-P.; Simões Mello, L. M.; De Carvalho Araújo, F. M.; Cavalcante Ramalho, I. L.; de Almeida Barreto, F. K.; de Melo Braga, D. N.; Simião, A. R.; Miranda da Silva, M. J.; Alves Barbosa Oliveira, R. d. M.; Lima, C. P. S.; de Sousa Lins, C.; Barata, R. R.; Pereira Melo, M. N.; Caldas de Souza, M. P.; Franco, L. M.; Fernandes Távora, F. R.; Queiroz Lemos, D. R.; de Alencar, C. H. M.; de Jesus, R.; de Souza Fonseca, V.; Dutra, L. H.; de Abreu, A. L.; Lima Araújo, E. L.; Ribas Freitas, A. R.; Vianez Júnior, J. L. d. S. G.; Pybus, O. G.; Figueiredo, L. T. M.; Faria, N. R.; Nunes, M. R. T.; Cavalcanti, L. P. d. G.; Miyajima, F., Fatal Outcome of Chikungunya Virus Infection in Brazil. *Clinical Infectious Diseases* **2020**, 73, (7), e2436-e2443.
411. Noval, M. G.; Spector, S. N.; Bartnicki, E.; Izzo, F.; Narula, N.; Yeung, S. T.; Damani-Yokota, P.; Dewan, M. Z.; Mezzano, V.; Rodriguez-Rodriguez, B. A.; Loomis, C.; Khanna, K.

- M.; Stapleford, K. A., MAVS signaling is required for preventing persistent chikungunya heart infection and chronic vascular tissue inflammation. *Nature Communications* **2023**, 14, (1), 4668.
412. Langsjoen, R. M.; Zhou, Y.; Holcomb, R. J.; Routh, A. L., Chikungunya Virus Infects the Heart and Induces Heart-Specific Transcriptional Changes in an Immunodeficient Mouse Model of Infection. *Am J Trop Med Hyg* **2021**, 106, (1), 99-104.
413. Baldon, L. V. R.; de Mendonça, S. F.; Ferreira, F. V.; Rezende, F. O.; Amadou, S. C. G.; Leite, T.; Rocha, M. N.; Marques, J. T.; Moreira, L. A.; Ferreira, A. G. A., AG129 Mice as a Comprehensive Model for the Experimental Assessment of Mosquito Vector Competence for Arboviruses. *Pathogens* **2022**, 11, (8).
414. Chuong, C.; Bates, T. A.; Weger-Lucarelli, J., Infectious cDNA clones of two strains of Mayaro virus for studies on viral pathogenesis and vaccine development. *Virology* **2019**, 535, 227-231.
415. de Carvalho, A. C.; Dias, C. S. B.; Coimbra, L. D.; Rocha, R. P. F.; Borin, A.; Fontoura, M. A.; Carvalho, M.; Proost, P.; Nogueira, M. L.; Consonni, S. R.; Sesti-Costa, R.; Marques, R. E., Characterization of Systemic Disease Development and Paw Inflammation in a Susceptible Mouse Model of Mayaro Virus Infection and Validation Using X-ray Synchrotron Microtomography. *Int J Mol Sci* **2023**, 24, (5).
416. Patel, A. R.; Dulcey, M.; Abid, N.; Cash, M. N.; Dailey, J.; Salemi, M.; Mavian, C.; Vittor, A. Y., Infectivity of three Mayaro Virus geographic isolates in human cell lines. *Acta Tropica* **2023**, 242, 106894.
417. Rafael, K. C.; Preciado-Llanes, L.; Azar, S. R.; Kim, Y. C.; Brandon, O.; López-Camacho, C.; Reyes-Sandoval, A.; Rossi, S. L., Adenoviral-Vectored Mayaro and Chikungunya Virus Vaccine Candidates Afford Partial Cross-Protection From Lethal Challenge in A129 Mouse Model. *Front Immunol* **2020**, 11, 591885.
418. Malonis, R. J.; Earnest, J. T.; Kim, A. S.; Angeliadis, M.; Holtsberg, F. W.; Aman, M. J.; Jangra, R. K.; Chandran, K.; Daily, J. P.; Diamond, M. S.; Kielian, M.; Lai, J. R., Near-germline

human monoclonal antibodies neutralize and protect against multiple arthritogenic alphaviruses. *Proc Natl Acad Sci U S A* **2021**, 118, (37).

419. Neris, R. L. S.; Figueiredo, C. M.; Higa, L. M.; Araujo, D. F.; Carvalho, C. A. M.; Verçoza, B. R. F.; Silva, M. O. L.; Carneiro, F. A.; Tanuri, A.; Gomes, A. M. O.; Bozza, M. T.; Da Poian, A. T.; Cruz-Oliveira, C.; Assunção-Miranda, I., Co-protoporphyrin IX and Sn-protoporphyrin IX inactivate Zika, Chikungunya and other arboviruses by targeting the viral envelope. *Scientific Reports* **2018**, 8, (1), 9805.

420. Campos, D.; Navarro, S.; Llamas-González, Y. Y.; Sugasti, M.; González-Santamaría, J., Broad antiviral activity of ginkgolic acid against chikungunya, Mayaro, una, and Zika viruses. *Viruses* **2020**, 12, (4), 449.

421. Bakhache, W.; Neyret, A.; McKellar, J.; Clop, C.; Bernard, E.; Weger-Lucarelli, J.; Briant, L., Fatty acid synthase and stearyl-CoA desaturase-1 are conserved druggable cofactors of Old World Alphavirus genome replication. *Antiviral Research* **2019**, 172, 104642.

422. Llamas-González, Y. Y.; Campos, D.; Pascale, J. M.; Arbiza, J.; González-Santamaría, J., A functional ubiquitin-proteasome system is required for efficient replication of new world mayaro and una alphaviruses. *Viruses* **2019**, 11, (4), 370.

423. Broeckel, R.; Sarkar, S.; May, N. A.; Totonchy, J.; Kreklywich, C. N.; Smith, P.; Graves, L.; DeFilippis, V. R.; Heise, M. T.; Morrison, T. E., Src family kinase inhibitors block translation of alphavirus subgenomic mRNAs. *Antimicrobial agents and chemotherapy* **2019**, 63, (4), e02325-18.

424. Carvalho, C. A.; Sousa Jr, I. P.; Silva, J. L.; Oliveira, A. C.; Gonçalves, R. B.; Gomes, A. M., Inhibition of Mayaro virus infection by bovine lactoferrin. *Virology* **2014**, 452, 297-302.

425. Cirimotich, C. M.; Vela, E. M.; Garver, J.; Barnewall, R. E.; Miller, B. D.; Meister, G. T.; Rogers, J. V., Chikungunya virus infection in Cynomolgus macaques following Intradermal and aerosol exposure. *Virology Journal* **2017**, 14, (1), 135.

426. Ross, R. W., The Newala epidemic. III. The virus: isolation, pathogenic properties and relationship to the epidemic. *J Hyg (Lond)* **1956**, 54, (2), 177-91.

427. Roy, C. J.; Adams, A. P.; Wang, E.; Plante, K.; Gorchakov, R.; Seymour, R. L.; Vinet-Oliphant, H.; Weaver, S. C., Chikungunya Vaccine Candidate Is Highly Attenuated and Protects Nonhuman Primates Against Telemetrically Monitored Disease Following a Single Dose. *The Journal of Infectious Diseases* **2014**, 209, (12), 1891-1899.
428. Roques, P.; Ljungberg, K.; Kümmerer, B. M.; Gosse, L.; Dereuddre-Bosquet, N.; Tchitchek, N.; Hallengård, D.; García-Arriaza, J.; Meinke, A.; Esteban, M.; Merits, A.; Le Grand, R.; Liljeström, P., Attenuated and vectored vaccines protect nonhuman primates against Chikungunya virus. *JCI Insight* **2017**, 2, (6).
429. Santos, F. M.; Dias, R. S.; de Oliveira, M. D.; Costa, I. C. T. A.; Fernandes, L. d. S.; Pessoa, C. R.; da Matta, S. L. P.; Costa, V. V.; Souza, D. G.; da Silva, C. C.; de Paula, S. O., Animal model of arthritis and myositis induced by the Mayaro virus. *PLOS Neglected Tropical Diseases* **2019**, 13, (5), e0007375.
430. Santiago, F. W.; Halsey, E. S.; Siles, C.; Vilcarrromero, S.; Guevara, C.; Silvas, J. A.; Ramal, C.; Ampuero, J. S.; Aguilar, P. V., Long-Term Arthralgia after Mayaro Virus Infection Correlates with Sustained Pro-inflammatory Cytokine Response. *PLOS Neglected Tropical Diseases* **2015**, 9, (10), e0004104.
431. Chen, W.; Foo, S.-S.; Rulli, N. E.; Taylor, A.; Sheng, K.-C.; Herrero, L. J.; Herring, B. L.; Lidbury, B. A.; Li, R. W.; Walsh, N. C., Arthritogenic alphaviral infection perturbs osteoblast function and triggers pathologic bone loss. *Proceedings of the National Academy of Sciences* **2014**, 111, (16), 6040-6045.
432. Rulli, N. E.; Rolph, M. S.; Srikiatkachorn, A.; Anantapreecha, S.; Guglielmotti, A.; Mahalingam, S., Protection From Arthritis and Myositis in a Mouse Model of Acute Chikungunya Virus Disease by Bindarit, an Inhibitor of Monocyte Chemotactic Protein-1 Synthesis. *The Journal of Infectious Diseases* **2011**, 204, (7), 1026-1030.
433. Dagley, A.; Ennis, J.; Turner, J. D.; Rood, K. A.; Van Wettere, A. J.; Gowen, B. B.; Julander, J. G., Protection against Chikungunya virus induced arthralgia following prophylactic treatment with adenovirus vectored interferon (mDEF201). *Antiviral Res* **2014**, 108, 1-9.

434. Haist, K. C.; Burrack, K. S.; Davenport, B. J.; Morrison, T. E., Inflammatory monocytes mediate control of acute alphavirus infection in mice. *PLOS Pathogens* **2017**, 13, (12), e1006748.
435. Lidbury, B. A.; Simeonovic, C.; Maxwell, G. E.; Marshall, I. D.; Hapel, A. J., Macrophage-induced muscle pathology results in morbidity and mortality for Ross River virus-infected mice. *The Journal of infectious diseases* **2000**, 181, (1), 27-34.
436. Hoarau, J.-J.; Jaffar Bandjee, M.-C.; Krejbich Trotot, P.; Das, T.; Li-Pat-Yuen, G.; Dassa, B.; Denizot, M.; Guichard, E.; Ribera, A.; Henni, T., Persistent chronic inflammation and infection by Chikungunya arthritogenic alphavirus in spite of a robust host immune response. *The Journal of Immunology* **2010**, 184, (10), 5914-5927.
437. Her, Z.; Malleret, B.; Chan, M.; Ong, E. K.; Wong, S. C.; Kwek, D. J.; Tolou, H.; Lin, R. T.; Tambyah, P. A.; Rénia, L.; Ng, L. F., Active infection of human blood monocytes by Chikungunya virus triggers an innate immune response. *J Immunol* **2010**, 184, (10), 5903-13.
438. Hawman, D. W.; Stoermer, K. A.; Montgomery, S. A.; Pal, P.; Oko, L.; Diamond, M. S.; Morrison, T. E., Chronic joint disease caused by persistent Chikungunya virus infection is controlled by the adaptive immune response. *Journal of virology* **2013**, 87, (24), 13878-13888.
439. Teo, T.-H.; Chan, Y.-H.; Lee, W. W.; Lum, F.-M.; Amrun, S. N.; Her, Z.; Rajarethinam, R.; Merits, A.; Röttschke, O.; Rénia, L., Fingolimod treatment abrogates chikungunya virus-induced arthralgia. *Science Translational Medicine* **2017**, 9, (375), eaal1333.
440. Broeckel, R. M.; Haese, N.; Ando, T.; Dmitriev, I.; Kreklywich, C. N.; Powers, J.; Denton, M.; Smith, P.; Morrison, T. E.; Heise, M.; DeFilippis, V.; Messaoudi, I.; Curiel, D. T.; Streblow, D. N., Vaccine-Induced Skewing of T Cell Responses Protects Against Chikungunya Virus Disease. *Frontiers in Immunology* **2019**, 10.
441. Morrison, T. E.; Oko, L.; Montgomery, S. A.; Whitmore, A. C.; Lotstein, A. R.; Gunn, B. M.; Elmore, S. A.; Heise, M. T., A mouse model of chikungunya virus-induced musculoskeletal inflammatory disease: Evidence of arthritis, tenosynovitis, myositis, and persistence. *The American journal of pathology* **2011**, 178, (1), 32-40.

442. Baxter, V. K.; Griffin, D. E., Interferon-Gamma Modulation of the Local T Cell Response to Alphavirus Encephalomyelitis. *Viruses* **2020**, 12, (1), 113.
443. Mourão, M. P. G.; Bastos, M. d. S.; de Figueiredo, R. P.; Gimaque, J. B. L.; dos Santos Galusso, E.; Kramer, V. M.; de Oliveira, C. M. C.; Naveca, F. G.; Figueiredo, L. T. M., Mayaro fever in the city of Manaus, Brazil, 2007–2008. *Vector-Borne and Zoonotic Diseases* **2012**, 12, (1), 42-46.
444. Figueiredo, L. T. M.; Nogueira, R. M. R.; Cavalcanti, S. M. B.; Schatzmayr, H.; Rosa, A. T. d., Study of two different enzyme immunoassays for the detection of Mayaro virus antibodies. *Memórias do Instituto Oswaldo Cruz* **1989**, 84, 303-307.
445. Torres, J. R.; Russell, K. L.; Vasquez, C.; Tesh, R. B.; Salas, R.; Watts, D. M., Family cluster of Mayaro fever, Venezuela. *Emerging infectious diseases* **2004**, 10, (7), 1304.
446. Bengue, M.; Ferraris, P.; Baronti, C.; Diagne, C. T.; Talignani, L.; Wichit, S.; Liegeois, F.; Bisbal, C.; Nougairède, A.; Missé, D., Mayaro Virus Infects Human Chondrocytes and Induces the Expression of Arthritis-Related Genes Associated with Joint Degradation. *Viruses* **2019**, 11, (9), 797.
447. da Silva Caetano, C. C.; Camini, F. C.; Almeida, L. T.; Ferraz, A. C.; da Silva, T. F.; Lima, R. L. S.; de Freitas Carvalho, M. M.; de Freitas Castro, T.; Carneiro, C. M.; de Mello Silva, B.; de Queiroz Silva, S.; de Magalhães, J. C.; de Brito Magalhães, C. L., Mayaro Virus Induction of Oxidative Stress is Associated With Liver Pathology in a Non-Lethal Mouse Model. *Sci Rep* **2019**, 9, (1), 15289.
448. Arenívar, C.; Rodríguez, Y.; Rodríguez-Morales, A. J.; Anaya, J. M., Osteoarticular manifestations of Mayaro virus infection. *Curr Opin Rheumatol* **2019**, 31, (5), 512-516.
449. Ozden, S.; Huerre, M.; Riviere, J. P.; Coffey, L. L.; Afonso, P. V.; Mouly, V.; de Monredon, J.; Roger, J. C.; El Amrani, M.; Yvin, J. L.; Jaffar, M. C.; Frenkiel, M. P.; Sourisseau, M.; Schwartz, O.; Butler-Browne, G.; Desprès, P.; Gessain, A.; Ceccaldi, P. E., Human muscle satellite cells as targets of Chikungunya virus infection. *PLoS One* **2007**, 2, (6), e527.

450. Blohm, G. M.; Márquez-Colmenarez, M. C.; Lednicky, J. A.; Bonny, T. S.; Mavian, C.; Salemi, M.; Delgado-Noguera, L.; Morris, J. G.; Paniz-Mondolfi, A. E., Isolation of Mayaro Virus from a Venezuelan Patient with Febrile Illness, Arthralgias, and Rash: Further Evidence of Regional Strain Circulation and Possible Long-Term Endemicity. *Am J Trop Med Hyg* **2019**, 101, (6), 1219-1225.
451. Neumayr, A.; Gabriel, M.; Fritz, J.; Günther, S.; Hatz, C.; Schmidt-Chanasit, J.; Blum, J., Mayaro virus infection in traveler returning from Amazon Basin, northern Peru. *Emerg Infect Dis* **2012**, 18, (4), 695-6.
452. Esterly, A. T.; Lloyd, M. G.; Upadhyaya, P.; Moffat, J. F.; Thangamani, S., A Human Skin Model for Assessing Arboviral Infections. *JID Innovations* **2022**, 2, (4), 100128.
453. Segura-Charry, J. S.; Parada-Martinez, M. A.; Segura-Puello, H. R.; Muñoz-Forero, D. M.; Nieto-Mosquera, D. L.; Villamil-Ballesteros, A. C.; Cortés-Muñoz, A. J., Musculoskeletal disorders due to chikungunya virus: A real experience in a rheumatology department in Neiva, Huila. *Reumatol Clin (Engl Ed)* **2021**, 17, (8), 456-460.
454. Sissoko, D.; Malvy, D.; Ezzedine, K.; Renault, P.; Moschetti, F.; Ledrans, M.; Pierre, V., Post-Epidemic Chikungunya Disease on Reunion Island: Course of Rheumatic Manifestations and Associated Factors over a 15-Month Period. *PLOS Neglected Tropical Diseases* **2009**, 3, (3), e389.
455. (PAHO), P. A. H. O. Mayaro virus laboratory diagnosis as Chikungunya differential diagnosis. <https://www.paho.org/en/documents/mayaro-virus-laboratory-diagnosis-chikungunya-differential-diagnosis-2019>
456. Bengue, M.; Ferraris, P.; Barthelemy, J.; Diagne, C. T.; Hamel, R.; Liégeois, F.; Nougairède, A.; de Lamballerie, X.; Simonin, Y.; Pompon, J.; Salinas, S.; Missé, D., Mayaro Virus Infects Human Brain Cells and Induces a Potent Antiviral Response in Human Astrocytes. *Viruses* **2021**, 13, (3).

457. Bishop, C. R.; Caten, F. T.; Nakaya, H. I.; Suhrbier, A., Chikungunya patient transcriptional signatures faithfully recapitulated in a C57BL/6J mouse model. *Front Immunol* **2022**, 13, 1092370.
458. Soares-Schanoski, A.; Baptista Cruz, N.; de Castro-Jorge, L. A.; de Carvalho, R. V. H.; Santos, C. A. D.; Rós, N. D.; Oliveira, Ú.; Costa, D. D.; Santos, C.; Cunha, M. D. P.; Oliveira, M. L. S.; Alves, J. C.; Océa, R.; Ribeiro, D. R.; Gonçalves, A. N. A.; Gonzalez-Dias, P.; Suhrbier, A.; Zanotto, P. M. A.; Azevedo, I. J.; Zamboni, D. S.; Almeida, R. P.; Ho, P. L.; Kalil, J.; Nishiyama, M. Y. J.; Nakaya, H. I., Systems analysis of subjects acutely infected with the Chikungunya virus. *PLoS Pathog* **2019**, 15, (6), e1007880.
459. Michlmayr, D.; Pak, T. R.; Rahman, A. H.; Amir, E. D.; Kim, E. Y.; Kim-Schulze, S.; Suprun, M.; Stewart, M. G.; Thomas, G. P.; Balmaseda, A.; Wang, L.; Zhu, J.; Suárez-Fariñas, M.; Wolinsky, S. M.; Kasarskis, A.; Harris, E., Comprehensive innate immune profiling of chikungunya virus infection in pediatric cases. *Mol Syst Biol* **2018**, 14, (8), e7862.
460. Wilson, J. A.; Prow, N. A.; Schroder, W. A.; Ellis, J. J.; Cumming, H. E.; Gearing, L. J.; Poo, Y. S.; Taylor, A.; Hertzog, P. J.; Di Giallonardo, F., RNA-Seq analysis of chikungunya virus infection and identification of granzyme A as a major promoter of arthritic inflammation. *PLoS pathogens* **2017**, 13, (2), e1006155.
461. Gérardin, P.; Fianu, A.; Michault, A.; Mussard, C.; Boussaïd, K.; Rollot, O.; Grivard, P.; Kassab, S.; Bouquillard, E.; Borgherini, G.; Gaüzère, B.-A.; Malvy, D.; Bréart, G.; Favier, F., Predictors of Chikungunya rheumatism: a prognostic survey ancillary to the TELECHIK cohort study. *Arthritis Research & Therapy* **2013**, 15, (1), R9.
462. Huits, R.; De Kort, J.; Van Den Berg, R.; Chong, L.; Tsoumanis, A.; Eggermont, K.; Bartholomeeusen, K.; Ariën, K. K.; Jacobs, J.; Van Esbroeck, M.; Bottieau, E.; Cnops, L., Chikungunya virus infection in Aruba: Diagnosis, clinical features and predictors of post-chikungunya chronic polyarthralgia. *PLOS ONE* **2018**, 13, (4), e0196630.
463. Smedley, J.; Macalister, R.; Wangari, S.; Gathuka, M.; Ahrens, J.; Iwayama, N.; May, D.; Bratt, D.; O'Connor, M.; Munson, P.; Koday, M.; Lifson, J.; Fuller, D. H., Laparoscopic

Technique for Serial Collection of Para-Colonic, Left Colic, and Inferior Mesenteric Lymph Nodes in Macaques. *PLOS ONE* **2016**, 11, (6), e0157535.

464. Zevin, A. S.; Moats, C.; May, D.; Wangari, S.; Miller, C.; Ahrens, J.; Iwayama, N.; Brown, M.; Bratt, D.; Klatt, N. R.; Smedley, J., Laparoscopic Technique for Serial Collection of Liver and Mesenteric Lymph Nodes in Macaques. *J Vis Exp* **2017**, (123).

465. Moats, C.; Cook, K.; Armantrout, K.; Crank, H.; Uttke, S.; Maher, K.; Bochart, R. M.; Lawrence, G.; Axthelm, M. K.; Smedley, J. V., Antimicrobial prophylaxis does not improve post-surgical outcomes in SIV/SHIV-uninfected or SIV/SHIV-infected macaques (*Macaca mulatta* and *Macaca fascicularis*) based on a retrospective analysis. *PLoS One* **2022**, 17, (4), e0266616.

466. Koo, B. S.; Lee, D. H.; Kang, P.; Jeong, K. J.; Lee, S.; Kim, K.; Lee, Y.; Huh, J. W.; Kim, Y. H.; Park, S. J.; Jin, Y. B.; Kim, S. U.; Kim, J. S.; Son, Y.; Lee, S. R., Reference values of hematological and biochemical parameters in young-adult cynomolgus monkey (*Macaca fascicularis*) and rhesus monkey (*Macaca mulatta*) anesthetized with ketamine hydrochloride. *Lab Anim Res* **2019**, 35, 7.

467. Haese, N. N.; Burg, J. M.; Andoh, T. F.; Jones, I. K. A.; Kreklywich, C. N.; Smith, P. P.; Orloff, S. L.; Streblow, D. N., Macrophage depletion of CMV latently infected donor hearts ameliorates recipient accelerated chronic rejection. *Transpl Infect Dis* **2021**, 23, (2), e13514.

468. Andrews, S. *FastQC: A quality control tool for high throughput sequence data*.

469. Ewels, P.; Magnusson, M.; Lundin, S.; Källner, M., MultiQC: summarize analysis results for multiple tools and samples in a single report. *Bioinformatics* **2016**, 32, (19), 3047-3048.

470. Bolger, A. M.; Lohse, M.; Usadel, B., Trimmomatic: a flexible trimmer for Illumina sequence data. *Bioinformatics* **2014**, 30, (15), 2114-2120.

471. Dobin, A.; Davis, C. A.; Schlesinger, F.; Drenkow, J.; Zaleski, C.; Jha, S.; Batut, P.; Chaisson, M.; Gingeras, T. R., STAR: ultrafast universal RNA-seq aligner. *Bioinformatics* **2012**, 29, (1), 15-21.

472. Engström, P. G.; Steijger, T.; Sipos, B.; Grant, G. R.; Kahles, A.; Alioto, T.; Behr, J.; Bertone, P.; Bohnert, R.; Campagna, D.; Davis, C. A.; Dobin, A.; Engström, P. G.; Gingeras, T. R.; Goldman, N.; Grant, G. R.; Guigó, R.; Harrow, J.; Hubbard, T. J.; Jean, G.; Kahles, A.; Kosarev, P.; Li, S.; Liu, J.; Mason, C. E.; Molodtsov, V.; Ning, Z.; Ponstingl, H.; Prins, J. F.; Räscher, G.; Ribeca, P.; Seledtsov, I.; Sipos, B.; Solovyev, V.; Steijger, T.; Valle, G.; Vitulo, N.; Wang, K.; Wu, T. D.; Zeller, G.; Räscher, G.; Goldman, N.; Hubbard, T. J.; Harrow, J.; Guigó, R.; Bertone, P.; The, R. C., Systematic evaluation of spliced alignment programs for RNA-seq data. *Nature Methods* **2013**, 10, (12), 1185-1191.
473. DeLuca, D. S.; Levin, J. Z.; Sivachenko, A.; Fennell, T.; Nazaire, M.-D.; Williams, C.; Reich, M.; Winckler, W.; Getz, G., RNA-SeQC: RNA-seq metrics for quality control and process optimization. *Bioinformatics* **2012**, 28, (11), 1530-1532.
474. Chen, Y.; Lun, A. T.; Smyth, G. K., From reads to genes to pathways: differential expression analysis of RNA-Seq experiments using Rsubread and the edgeR quasi-likelihood pipeline. *F1000Res* **2016**, 5, 1438.
475. Robinson, M. D.; Oshlack, A., A scaling normalization method for differential expression analysis of RNA-seq data. *Genome Biol* **2010**, 11, (3), R25.
476. Law, C. W.; Chen, Y.; Shi, W.; Smyth, G. K., voom: Precision weights unlock linear model analysis tools for RNA-seq read counts. *Genome Biol* **2014**, 15, (2), R29.
477. Ritchie, M. E.; Phipson, B.; Wu, D.; Hu, Y.; Law, C. W.; Shi, W.; Smyth, G. K., limma powers differential expression analyses for RNA-sequencing and microarray studies. *Nucleic Acids Res* **2015**, 43, (7), e47.
478. Benjamini, Y.; Hochberg, Y., Controlling the False Discovery Rate: A Practical and Powerful Approach to Multiple Testing. *Journal of the Royal Statistical Society: Series B (Methodological)* **1995**, 57, (1), 289-300.
479. Lyski, Z. L.; Brunton, A. E.; Strnad, M. I.; Sullivan, P. E.; Siegel, S. A. R.; Tafesse, F. G.; Slifka, M. K.; Messer, W. B., Severe Acute Respiratory Syndrome Coronavirus 2 (SARS-

CoV-2)-Specific Memory B Cells From Individuals With Diverse Disease Severities Recognize SARS-CoV-2 Variants of Concern. *J Infect Dis* **2022**, 225, (6), 947-956.

480. Chikungunya virus. https://www.who.int/health-topics/chikungunya#tab=tab_1 (19 July 2024),

481. de Lima Cavalcanti, T. Y. V.; Pereira, M. R.; de Paula, S. O.; Franca, R. F. d. O., A Review on Chikungunya Virus Epidemiology, Pathogenesis and Current Vaccine Development. *Viruses* **2022**, 14, (5), 969.

482. Raju, S.; Adams, L. J.; Diamond, M. S., The many ways in which alphaviruses bind to cells. *Trends in Immunology* **2024**, 45, (2), 85-93.

483. Kuhn, R., Togaviridae: the viruses and their replication. *Fields virology* **2007**, 1, 1001-1022.

484. Khan, S. U.; Ogden, N. H.; Fazil, A. A.; Gachon, P. H.; Dueymes, G. U.; Greer, A. L.; Ng, V., Current and Projected Distributions of *Aedes aegypti* and *Ae. albopictus* in Canada and the US. *Environmental health perspectives* **2020**, 128, (5), 057007.

485. Kraemer, M. U.; Sinka, M. E.; Duda, K. A.; Mylne, A.; Shearer, F. M.; Brady, O. J.; Messina, J. P.; Barker, C. M.; Moore, C. G.; Carvalho, R. G., The global compendium of *Aedes aegypti* and *Ae. albopictus* occurrence. *Scientific data* **2015**, 2, (1), 1-8.

486. Bartholomeeusen, K.; Daniel, M.; LaBeaud, D. A.; Gasque, P.; Peeling, R. W.; Stephenson, K. E.; Ng, L. F.; Ariën, K. K., Chikungunya fever. *Nature Reviews Disease Primers* **2023**, 9, (1), 17.

487. Simon, F.; Javelle, E.; Cabie, A.; Bouquillard, E.; Troisgros, O.; Gentile, G.; Leparco-Goffart, I.; Hoen, B.; Gandjbakhch, F.; Rene-Corail, P.; Franco, J. M.; Caumes, E.; Combe, B.; Poiraudau, S.; Gane-Troplent, F.; Djossou, F.; Schaerverbeke, T.; Criquet-Hayot, A.; Carrere, P.; Malvy, D.; Gaillard, P.; Wendling, D., French guidelines for the management of chikungunya (acute and persistent presentations). November 2014. *Médecine et Maladies Infectieuses* **2015**, 45, (7), 243-263.

488. Brito, C. A. A. d.; Sohsten, A. K. A. v.; Leitão, C. C. d. S.; Brito, R. d. C. C. M. d.; Valadares, L. D. D. A.; Fonte, C. A. M. d.; Mesquita, Z. B. d.; Cunha, R. V.; Luz, K.; Leão, H. M. C., Pharmacologic management of pain in patients with Chikungunya: a guideline. *Revista da Sociedade Brasileira de Medicina Tropical* **2016**, 49, (06), 668-679.
489. Webb, E.; Michelen, M.; Rigby, I.; Dagens, A.; Dahmash, D.; Cheng, V.; Joseph, R.; Lipworth, S.; Harriss, E.; Cai, E., An evaluation of global Chikungunya clinical management guidelines: a systematic review. *EClinicalMedicine* **2022**, 54.
490. Vairo, F.; Haider, N.; Kock, R.; Ntoumi, F.; Ippolito, G.; Zumla, A., Chikungunya: epidemiology, pathogenesis, clinical features, management, and prevention. *Infectious Disease Clinics* **2019**, 33, (4), 1003-1025.
491. Sales, G. M. P. G.; Barbosa, I. C. P.; Canejo, L. M. S.; Melo, P. L. d.; Leitão, R. d. A.; Melo, H. M. d. A., Treatment of chikungunya chronic arthritis: A systematic review. *Revista da Associação Médica Brasileira* **2018**, 64, (1), 63-70.
492. Kumar, R.; Ahmed, S.; Parray, H. A.; Das, S., Chikungunya and arthritis: An overview. *Travel medicine and infectious disease* **2021**, 44, 102168.
493. Puntasecca, C. J.; King, C. H.; LaBeaud, A. D., Measuring the global burden of chikungunya and Zika viruses: A systematic review. *PLoS neglected tropical diseases* **2021**, 15, (3), e0009055.
494. Flahault, A.; Aumont, G.; Boisson, V.; de Lamballerile, X.; Favier, F.; Fontenille, D.; Gaüzère, B. A.; Journeaux, S.; Lotteau, V.; Paupy, C.; Sanquer, M. A.; Setbon, M., [Chikungunya, La Réunion and Mayotte, 2005-2006: an epidemic without a story?]. *Sante Publique* **2007**, 19 Suppl 3, S165-95.
495. Chhabra, M.; Mittal, V.; Bhattacharya, D.; Rana, U.; Lal, S., Chikungunya fever: a re-emerging viral infection. *Indian journal of medical microbiology* **2008**, 26, (1), 5-12.
496. Torales, M., Notes from the field: Chikungunya outbreak—Paraguay, 2022–2023. *MMWR. Morbidity and Mortality Weekly Report* **2023**, 72.

497. Fred, A.; Fianu, A.; Béral, M.; Guernier, V.; Sissoko, D.; Méchain, M.; Michault, A.; Boisson, V.; Gaüzère, B.-A.; Favier, F., Individual and contextual risk factors for chikungunya virus infection: the SEROCHIK cross-sectional population-based study. *Epidemiology & Infection* **2018**, 146, (8), 1056-1064.
498. González-Sánchez, J. A.; Ramírez-Arroyo, G. F., Chikungunya virus: history, geographic distribution, clinical picture, and treatment. *Puerto Rico Health Sciences Journal* **2018**, 37, (4), 187-194.
499. van Aalst, M.; Nelen, C. M.; Goorhuis, A.; Stijnis, C.; Grobusch, M. P., Long-term sequelae of chikungunya virus disease: A systematic review. *Travel medicine and infectious disease* **2017**, 15, 8-22.
500. Cherian, N.; Bettis, A.; Deol, A.; Kumar, A.; Di Fabio, J. L.; Chaudhari, A.; Yimer, S.; Fahim, R.; Endy, T., Strategic considerations on developing a CHIKV vaccine and ensuring equitable access for countries in need. *npj Vaccines* **2023**, 8, (1), 123.
501. Roongaraya, P.; Boonyasuppayakorn, S., Chikungunya vaccines: An update in 2023. *Asian Pacific Journal of Allergy and Immunology* **2023**, 41, (1), 1-11.
502. Schmidt, C.; Schnierle, B. S., Chikungunya vaccine candidates: current landscape and future prospects. *Drug Design, Development and Therapy* **2022**, 3663-3673.
503. Flandes, X.; Hansen, C. A.; Palani, S.; Abbas, K.; Bennett, C.; Caro, W. P.; Hutubessy, R.; Khazhidinov, K.; Lambach, P.; Maure, C., Vaccine value profile for Chikungunya. *Vaccine* **2024**, 42, (19), S9-S24.
504. Couderc, T.; Khandoudi, N.; Grandadam, M.; Visse, C.; Gangneux, N.; Bagot, S.; Prost, J.-F.; Lecuit, M., Prophylaxis and therapy for Chikungunya virus infection. *The Journal of infectious diseases* **2009**, 200, (4), 516-523.
505. US FDA, A. S. SBRA-IXCHIQ. Report no.: 125777. <https://www.fda.gov/media/174693/download>. (19 July 2024),

506. FDA, U. Toxicology grading scale for healthy adult and adolescent volunteers enrolled in preventative vaccine clinical trials. <https://www.fda.gov/regulatory-information/search-fda-guidance-documents/toxicity-grading-scale-healthy-adult-and-adolescent-volunteers-enrolled-preventive-vaccine-clinical>. (19 July 2024),
507. CDC VLA1553 Chikungunya vaccine candidate. <https://stacks.cdc.gov/view/cdc/122361> (19 July 2024),
508. Rezza, G.; Weaver, S. C., Chikungunya as a paradigm for emerging viral diseases: Evaluating disease impact and hurdles to vaccine development. *PLoS neglected tropical diseases* **2019**, 13, (1), e0006919.
509. FDA, U. FDA approves first vaccine to prevent disease caused by Chikungunya virus. <https://www.fda.gov/news-events/press-announcements/fda-approves-first-vaccine-prevent-disease-caused-chikungunya-virus>. (19 July 2024),
510. CDC Advisory Committee on Immunization Practices recommendations. <https://www.cdc.gov/vaccines/acip/recommendations.html> (19 July 2024),
511. Valneva Valneva announces Health Canada approval of the world's first Chikungunya vaccine, IXCHIQ®. <https://valneva.com/press-release/valneva-announces-health-canada-approval-of-the-worlds-first-chikungunya-vaccine-ixchiq/> (19 July 2024),
512. Valneva Valneva receives marketing authorization in Europe for the world's first Chikungunya vaccine, IXCHIQ®. <https://valneva.com/press-release/valneva-receives-marketing-authorization-in-europe-for-the-worlds-first-chikungunya-vaccine-ixchiq/>. (19 July 2024),
513. FDA, U. Valneva: highlights of prescribing information for IXCHIQ. <https://www.fda.gov/media/173758/download?attachment> (19 July 2024),
514. Gache HRJ, M. J., Muhammad S, Lauren T, Tobi L, Royalty Trendero S, et al. Positive immunogenicity and safety profile for a virus-like particle (VLP) based Chikungunya virus (CHIKV) vaccine: results from a pivotal phase III trial. <https://escmid.reg.key4events.com/AbstractList.aspx?e=21&preview=1&aig=-1&ai=19663> (29 August 2024),

515. FDA, U. US Department of Health and Human Services. Points to consider in the characterization of cell lines used to produce biologicals (1993). <https://www.fda.gov/media/76255/download> (19 July 2024),
516. CEPI CEPI awards up to US\$23.4 million to Valneva for late-stage development of a single-dose Chikungunya vaccine. [https://cepi.net/cepi-awards-us234-million-valneva-late-stage-development-single-dose-chikungunya-vaccine#:~:text=With%20support%20from%20the%20European,vaccine%20\(VLA1553\)%20against%20Chikungunya](https://cepi.net/cepi-awards-us234-million-valneva-late-stage-development-single-dose-chikungunya-vaccine#:~:text=With%20support%20from%20the%20European,vaccine%20(VLA1553)%20against%20Chikungunya) (19 July 2024),
517. Burkett-Cadena, N. D.; Fish, D.; Weaver, S.; Vittor, A. Y., Everglades virus: an underrecognized disease-causing subtype of Venezuelan equine encephalitis virus endemic to Florida, USA. *Journal of medical entomology* **2023**, 60, (6), 1149-1164.
518. Work, T. H., Serological evidence of arbovirus infection in the Seminole Indians of southern Florida. *Science* **1964**, 145, (3629), 270-272.
519. Coffey, L. L.; Beeharry, Y.; Bordería, A. V.; Blanc, H.; Vignuzzi, M., Arbovirus high fidelity variant loses fitness in mosquitoes and mice. *Proceedings of the National Academy of Sciences* **2011**, 108, (38), 16038-16043.
520. Riemersma, K. K.; Coffey, L. L., Chikungunya virus populations experience diversity-dependent attenuation and purifying intra-vector selection in Californian *Aedes aegypti* mosquitoes. *PLoS Neglected Tropical Diseases* **2019**, 13, (11), e0007853.
521. Stapleford, K. A.; Coffey, L. L.; Lay, S.; Bordería, A. V.; Duong, V.; Isakov, O.; Rozen-Gagnon, K.; Arias-Goeta, C.; Blanc, H.; Beaucourt, S., Emergence and transmission of arbovirus evolutionary intermediates with epidemic potential. *Cell host & microbe* **2014**, 15, (6), 706-716.
522. Coffey, L. L.; Failloux, A.-B.; Weaver, S. C., Chikungunya virus–vector interactions. *Viruses* **2014**, 6, (11), 4628-4663.
523. Göertz, G. P.; Lingemann, M.; Geertsema, C.; Abma-Henkens, M. H.; Vogels, C. B.; Koenraadt, C. J.; van Oers, M. M.; Pijlman, G. P., Conserved motifs in the hypervariable domain

of chikungunya virus nsP3 required for transmission by *Aedes aegypti* mosquitoes. *PLoS Neglected Tropical Diseases* **2018**, 12, (11), e0006958.

524. Valneva Valneva reports further positive pivotal phase 3 data in adolescents for its single-shot Chikungunya vaccine. https://valneva.com/press-release/valneva-reports-further-positive-pivotal-phase-3-data-in-adolescents-for-its-single-shot-chikungunya-vaccine/#_ftn3 (19 July 2024),

525. Baylis, S. A.; Knezevic, I.; Almond, N. M., Harmonising the measurement of neutralising antibodies against chikungunya virus: a path forward for licensing of new vaccines? *The Lancet Microbe* **2024**.

526. Corbett, K. S.; Edwards, D. K.; Leist, S. R.; Abiona, O. M.; Boyoglu-Barnum, S.; Gillespie, R. A.; Himansu, S.; Schäfer, A.; Ziwawo, C. T.; DiPiazza, A. T.; Dinnon, K. H.; Elbashir, S. M.; Shaw, C. A.; Woods, A.; Fritch, E. J.; Martinez, D. R.; Bock, K. W.; Minai, M.; Nagata, B. M.; Hutchinson, G. B.; Wu, K.; Henry, C.; Bahl, K.; Garcia-Dominguez, D.; Ma, L.; Renzi, I.; Kong, W.-P.; Schmidt, S. D.; Wang, L.; Zhang, Y.; Phung, E.; Chang, L. A.; Loomis, R. J.; Altaras, N. E.; Narayanan, E.; Metkar, M.; Presnyak, V.; Liu, C.; Louder, M. K.; Shi, W.; Leung, K.; Yang, E. S.; West, A.; Gully, K. L.; Stevens, L. J.; Wang, N.; Wrapp, D.; Doria-Rose, N. A.; Stewart-Jones, G.; Bennett, H.; Alvarado, G. S.; Nason, M. C.; Ruckwardt, T. J.; McLellan, J. S.; Denison, M. R.; Chappell, J. D.; Moore, I. N.; Morabito, K. M.; Mascola, J. R.; Baric, R. S.; Carfi, A.; Graham, B. S., SARS-CoV-2 mRNA vaccine design enabled by prototype pathogen preparedness. *Nature* **2020**, 586, (7830), 567-571.